THE EMERGING ROLE OF SPECT FUNCTIONAL NEUROIMAGING IN PSYCHIATRY & NEUROLOGY

EDITED BY: Theodore A. Henderson, Joe Cardaci, Philip Frank Cohen, Catherine Faget and Jean-Luc Urbain

PUBLISHED IN: Frontiers in Psychiatry and Frontiers in Neurology

frontiers Research Topics

ISSN 1664-8714
ISBN 978-2-88976-655-0
DOI 10.3389/978-2-88976-655-0

About Frontiers

Frontiers is more than just an open-access publisher of scholarly articles: it is a pioneering approach to the world of academia, radically improving the way scholarly research is managed. The grand vision of Frontiers is a world where all people have an equal opportunity to seek, share and generate knowledge. Frontiers provides immediate and permanent online open access to all its publications, but this alone is not enough to realize our grand goals.

Frontiers Journal Series

The Frontiers Journal Series is a multi-tier and interdisciplinary set of open-access, online journals, promising a paradigm shift from the current review, selection and dissemination processes in academic publishing. All Frontiers journals are driven by researchers for researchers; therefore, they constitute a service to the scholarly community. At the same time, the Frontiers Journal Series operates on a revolutionary invention, the tiered publishing system, initially addressing specific communities of scholars, and gradually climbing up to broader public understanding, thus serving the interests of the lay society, too.

Dedication to Quality

Each Frontiers article is a landmark of the highest quality, thanks to genuinely collaborative interactions between authors and review editors, who include some of the world's best academicians. Research must be certified by peers before entering a stream of knowledge that may eventually reach the public - and shape society; therefore, Frontiers only applies the most rigorous and unbiased reviews.
Frontiers revolutionizes research publishing by freely delivering the most outstanding research, evaluated with no bias from both the academic and social point of view. By applying the most advanced information technologies, Frontiers is catapulting scholarly publishing into a new generation.

What are Frontiers Research Topics?

Frontiers Research Topics are very popular trademarks of the Frontiers Journals Series: they are collections of at least ten articles, all centered on a particular subject. With their unique mix of varied contributions from Original Research to Review Articles, Frontiers Research Topics unify the most influential researchers, the latest key findings and historical advances in a hot research area! Find out more on how to host your own Frontiers Research Topic or contribute to one as an author by contacting the Frontiers Editorial Office: frontiersin.org/about/contact

THE EMERGING ROLE OF SPECT FUNCTIONAL NEUROIMAGING IN PSYCHIATRY & NEUROLOGY

Topic Editors:
Theodore A. Henderson, Consultant
Joe Cardaci, University of Notre Dame Australia, Australia
Philip Frank Cohen, University of British Columbia, Canada
Catherine Faget, Assistance Publique Hôpitaux de Marseille, France
Jean-Luc Urbain, Wake Forest University, United States

Citation: Henderson, T. A., Cardaci, J., Cohen, P. F., Faget, C., Urbain, J.-L., eds. (2022). The Emerging Role of SPECT Functional Neuroimaging in Psychiatry & Neurology. Lausanne: Frontiers Media SA. doi: 10.3389/978-2-88976-655-0

Table of Contents

05 ***Editorial: The Emerging Role of SPECT Functional Neuroimaging in Psychiatry & Neurology***
Theodore A. Henderson, Philip F. Cohen, Giuseppe Cardaci and Jean-Luc C. Urbain

09 ***The Role of Frontal Assessment Battery and Frontal Lobe Single-Photon Emission Computed Tomography in the Differential Diagnosis of Progressive Supranuclear Palsy Variants and Corticobasal Syndrome—A Pilot Study***
Piotr Alster, Bartosz Migda, Natalia Madetko, Karolina Duszyńska-Wąs, Agnieszka Drzewińska, Ingeborga Charzyńska, Miłosz Starczyński, Ada Szepelska, Leszek Królicki and Andrzej Friedman

18 ***Utility of SPECT Functional Neuroimaging of Pain***
Mohammed Bermo, Mohammed Saqr, Hunter Hoffman, David Patterson, Sam Sharar, Satoshi Minoshima and David H. Lewis

25 ***Regional Cerebral Blood Flow Abnormalities in Neurosyphilis: A Pilot SPECT Study***
Jooyeon J. Im, Hyeonseok Jeong, Young Do Kim, Kyung-Sool Jang, In-Uk Song and Yong-An Chung

30 ***SPECT Functional Neuroimaging Distinguishes Adult Attention Deficit Hyperactivity Disorder From Healthy Controls in Big Data Imaging Cohorts***
Daniel G. Amen, Theodore A. Henderson and Andrew Newberg

43 ***A New Way Forward: How Brain SPECT Imaging Can Improve Outcomes and Transform Mental Health Care Into Brain Health Care***
Daniel G. Amen and Michael Easton

60 ***The Emerging Role of SPECT Functional Neuroimaging in Schizophrenia and Depression***
Anil Kalyoncu and Ali Saffet Gonul

68 ***Brain SPECT as an Imaging Biomarker for Evaluating Effects of Novel Treatments in Psychiatry–A Case Series***
Steven R. D. Best, Natalie Haustrup and Dan G. Pavel

81 ***Longitudinal Single Photon Emission Computed Tomography Neuroimaging as an Indication of Improvement in Psychiatric Disorders in a Community Psychiatric Practice***
John F. Thornton, Howard Schneider, Philip F. Cohen, Simon DeBruin, John Michael Uszler, Yin-Hui Siow, Mary K. McLean, Muriel J. van Lierop, Dan G. Pavel and Theodore A. Henderson

90 ***The Legacy of the TTASAAN Report—Premature Conclusions and Forgotten Promises: A Review of Policy and Practice Part I***
Dan G. Pavel, Theodore A. Henderson and Simon DeBruin

124 ***Using Single-Photon Emission Computerized Tomography on Patients With Positive Quantitative Electroencephalogram to Evaluate Chronic Mild Traumatic Brain Injury With Persistent Symptoms***
Alexi Gosset, Hayley Wagman, Dan Pavel, Philip Frank Cohen, Robert Tarzwell, Simon de Bruin, Yin Hui Siow, Leonard Numerow, John Uszler, John F. Rossiter-Thornton, Mary McLean, Muriel van Lierop, Zohar Waisman, Stephen Brown, Behzad Mansouri, Vincenzo Santo Basile, Navjot Chaudhary and Manu Mehdiratta

132 ***Increased Asymmetric Perfusion of the Cerebral Cortices and Thalamus Indicates Individuals at Risk for Bipolar Disorder: A Family Cohort Single Photon Emission Computed Tomography Neuroimaging Study***
Mary McLean, Theodore A. Henderson, Dan G. Pavel and Phil Cohen

156 ***The Legacy of the TTASAAN Report – Premature Conclusions and Forgotten Promises About SPECT Neuroimaging: A Review of Policy and Practice Part II***
Dan G. Pavel, Theodore A. Henderson, Simon DeBruin and Philip F. Cohen

frontiers | Frontiers in Psychiatry

EDITORIAL
published: 04 July 2022
doi: 10.3389/fpsyt.2022.928653

Editorial: The Emerging Role of SPECT Functional Neuroimaging in Psychiatry & Neurology

Theodore A. Henderson[1,2,3,4,5]*, *Philip F. Cohen*[1,6,7], *Giuseppe Cardaci*[1,8] and *Jean-Luc C. Urbain*[9,10]

[1] The International Society of Applied Neuroimaging (ISAN), Denver, CO, United States, [2] The Synaptic Space, Inc., Denver, CO, United States, [3] Neuro-Luminance, Inc., Denver, CO, United States, [4] Dr. Theodore Henderson, Inc., Denver, CO, United States, [5] Neuro-Laser Foundation, Denver, CO, United States, [6] Nuclear Medicine, Lions Gate Hospital, Vancouver, BC, Canada, [7] Department of Radiology, University of British Columbia, Vancouver, BC, Canada, [8] University of Notre Dame, Fremantle, WA, Australia, [9] Department of Radiology, Wake Forest School of Medicine, Winston-Salem, NC, United States, [10] Department of Nuclear Medicine, Wake Forest School of Medicine, Winston-Salem, NC, United States

Keywords: traumatic brain injury, dementia, bipolar disorder, biomarker, ADHD, Parkinson's disease, psychiatric comorbidity, fMRI

Editorial on the Research Topic

The Emerging Role of SPECT Functional Neuroimaging in Psychiatry & Neurology

OPEN ACCESS

Edited and reviewed by:
Thomas Nickl-Jockschat, The University of Iowa, United States

***Correspondence:**
Theodore A. Henderson
thesynapticspace7@gmail.com

Specialty section:
This article was submitted to Neuroimaging and Stimulation, a section of the journal Frontiers in Psychiatry

Received: *26 April 2022*
Accepted: *16 May 2022*
Published: *04 July 2022*

Citation:
Henderson TA, Cohen PF, Cardaci G and Urbain J-LC (2022) Editorial: The Emerging Role of SPECT Functional Neuroimaging in Psychiatry & Neurology. Front. Psychiatry 13:928653. doi: 10.3389/fpsyt.2022.928653

"Emerging" is somewhat of a misnomer when used to describe the role of perfusion single photon emission computed tomography (SPECT) neuroimaging in Neurology and Psychiatry. More appropriate terms that come to mind are "misunderstood" or "ignored and undervalued". The description which most springs to mind based on the comprehensive review by Pavel et al. (A) is "well-established, but overlooked and underutilized". Perfusion SPECT neuroimaging has been available for a long time—over 40 years, using current tracers—still the field has not stagnated. New technology, processing techniques, normative databases, and statistical analysis algorithms have been refining the field on an ongoing basis. Amen and Easton, Pavel et al. (A) and Pavel et al. (B) provide in-depth looks at the technological advances. SPECT scans are not the Rorschach-like blobs of the 1980's, but detailed examinations of activity patterns within the human brain (using the one-off metric of perfusion), which provide a certain level of anatomical accuracy and can be compared to normative databases for differential diagnoses with high sensitivity and specificity [Pavel et al. (A)].

Yet, SPECT neuroimaging meets with sustained resistance from the fields of Neurology and Psychiatry. While the American Psychiatric Association (APA) initially embraced SPECT neuroimaging (holding seminars and workshops on its use per, Amen and Easton), now the APA and psychiatrists, in general, vilify SPECT and clinicians who utilize it (1). The untenable position of the APA (2), mired in the committee-created artificial diagnostic constructs of the Diagnostic and Statistical Manual (DSM) system (3), cannot be reconciled with the current level of neurophysiological evidence of the underpinnings of psychiatric conditions, as revealed by perfusion SPECT, quantitative electroencephalographalogram (qEEG), arterial spin echo, and functional MRI (fMRI) studies [(4, 5); Pavel et al. (A)]. Neurology as a field has

taken a similar position, rejecting perfusion SPECT neuroimaging as "old", "inaccurate", or "experimental". For example, they maintain that there is insufficient proof that SPECT is diagnostic or even contributory in the evaluation of traumatic brain injury (TBI). However, the sensitivity and specificity of SPECT scans in the evaluation of TBI has been studied in over 23,944 subjects [Pavel et al. (A)] and SPECT meets the criteria set forth by the American Academy of Neurology (AAN) for a Type A Recommendation based on Class II evidence from multiple large N clinical studies with control groups [Pavel et al. (A)]. Note that Class I evidence is ethically impossible in the study of TBI. Similarly, thousands of subjects have been studied using SPECT in epilepsy (over 8,500 in 10 years), and dementia (over 18,000). Perfusion SPECT is diagnostic for Alzheimer's disease with comparison to histopathology with a sensitivity of 96% and a specificity of 89% (6). Moreover, SPECT can predict the conversion from mild cognitive impairment (MCI) to Alzheimer's disease with a sensitivity of 89–97% and a specificity of 89–100%, which is arguably better than ^{18}F-fluorodeoxyglucose-positron emission tomography (FDG-PET) (70–90% sensitivity/82–90% specificity) [Pavel et al. (A)].

A theme which emerged among the articles in this Research Topic was the concept of a perfusion SPECT "biomarker". While biomarker was defined in a number of ways, the definition provided by Food and Drug Administration is rigorous: "a defined characteristic that is measured as an indicator of normal biological processes, pathogenic processes, or responses to an exposure or intervention, including therapeutic interventions." (7). Given that biomarkers are defined as a characteristic that can indicate change, as well as a condition, ample evidence was presented for the use of perfusion SPECT neuroimaging as a biomarker. Im et al. demonstrated frontal, insular and posterior cingulate hypoperfusion in four cases of neurosyphilis. While frontal and posterior cingulate hypoperfusion are also found in Alzheimer's disease, the additional finding of insular hypoperfusion may be a unique marker. McLean et al. presented a unique "clinical pearl" of a family of five—all of whom have been diagnosed with bipolar disorder using DSM criteria. This situation provides control for many socioeconomical, genetic, and family dynamic variables. All members of this family showed similar perfusion SPECT findings—specifically increased asymmetrical perfusion of the thalamus and increased asymmetrical perfusion of the cerebral cortices—which may serve as a biomarker for bipolar disorder (McLean et al.). Amen et al. described a potential biomarker for ADHD in a large population ($N = 1{,}006$) defined by DSM-IV criteria, detailed clinical history, and the Structure Clinical Interview for Diagnosis (SCID) who were compared to a control group that did not meet DSM-IV criteria for any psychiatric disorder. They found that hypoperfusion in the medial anterior prefrontal (orbitofrontal) cortices, anterior cingulate gyri, bilateral temporal cortices, and cerebellar subregions 8 and 9 were highly predictive of ADHD with a sensitivity of 100% and specificity of 100% (Amen et al.). Both Alster et al. and Pavel et al. (B) described SPECT findings or biomarkers which served to differentiate forms of Parkinsonian syndromes including Progressive Supranuclear Palsy, Idiopathic Parkinson's disease, Multiple System Atrophy, and Corticobasal Syndrome. Gosset et al. examined patients with both perfusion SPECT and qEEG evidence of brain injury following head trauma. Both visual read and quantitative analysis revealed frontal lobe and temporal lobe hypoperfusion in over 90% of cases with positive qEEG findings for TBI. Indeed, perfusion SPECT found cerebral changes in 100% of cases with electroencephalographic evidence of TBI, while CT and/or MRI were negative in all but one case (Gosset et al.). This finding of a potential marker for TBI replicates and reinforces the findings described in Amen and Easton, detailed extensively in Pavel et al. (B) and identified in Best et al.. Furthermore, prior studies and reviews (4, 5, 8–14) support the use of SPECT in the evaluation of TBI.

Another aspect of biomarker utility is the demonstration of change. Perfusion SPECT scans have been utilized to demonstrate response to a number of novel treatments (15–18). Best et al. revealed two additional novel treatments effective in complex, treatment-resistant cases of depression, dementia, and TBI. They used ketamine anesthesia to facilitate more powerful transcranial magnetic stimulation than would normally be tolerated to successfully treat unipolar or bipolar depression which was unresponsive to other treatments (Best et al.). In addition, they used hyperbaric oxygen therapy combined with paraspinal injection of etanercept (a tumor necrosis factor inhibitor purported to reduce inflammation) to treat TBI and dementia. In all cases, they demonstrated improvement in clinical symptoms and neurophysiological function based on pre- and post-treatment SPECT scans. Thornton et al. illustrated the neurophysiological evidence for standard community psychiatric treatment in a large open cohort of 72 patients using pre- and post-treatment SPECT scans. These studies support the use of perfusion SPECT scans as a tool to guide treatment and improve clinical outcomes by neurophysiological assessment in psychiatric disorders. The concept that SPECT scans can guide treatment and lead to improved clinical outcome is extensively discussed by Amen and Easton, Pavel et al. (B) McLean et al., and others (4, 5, 12–14, 19–21).

One final point emerged in the articles of this Research Topic. Perfusion SPECT occupies a unique niche in neuroimaging. While much maligned for its anatomical resolution, perfusion SPECT scan offers superior temporal resolution and much higher contrast sensitivity compared to anatomical MRI, functional MRI, FDG-PET, and X-ray computed tomography (CT). Contrast is the ability to discern an abnormal signal from background. The sensitivity of CT for detecting contrast agents is in the millimolar range, while that of MRI is in the micromolar range. The sensitivity of SPECT neuroimaging for detecting a radiopharmaceutical is in the nanomolar range, exceeding MRI by a thousand-fold and exceeding CT by a million-fold. Functional MRI is an area of widespread research but suffers from low signal-to-noise ratios. Temporal resolution relates to the uptake of radiopharmaceutical. The uptake of FDG in FDG-PET imaging extends over 20 min. In contrast, the uptake of perfusion SPECT radiopharmaceuticals occurs

over 40–50 s. Thus, rapid events can be captured by SPECT, including seizures, attention tasks (in ADHD), pain episodes (Bermo et al.), psychotic episodes (Kalyoncu and Gonul), and other transient events. Yet, anatomical resolution is a concern in SPECT imaging and new processing techniques [McLean et al.; Best et al.; Pavel et al. (B)] and new cadmium-zinc-telluride (CZT) camera detector technologies [Pavel et al. (B)] will lead to a dramatic improvement in anatomical resolution. Nevertheless, a Pubmed search for terms "MRI brain death" yields 4,524 references. None of them specify MRI diagnostic criteria for brain death. Now, this is partly due to the incompatibility of life support equipment with the magnetic field. Nonetheless, the MRI of a dead brain can be indistinguishable for the MRI of a live brain. Ironically, the AAN practice guidelines (22, 23) specify perfusion SPECT as a diagnostic tool to prove and support the clinical diagnosis of brain death (24). While the AAN recognizes that perfusion SPECT is more sensitive than MRI in the diagnosis of brain death, the Academy fails to recognize that perfusion SPECT is more sensitive than MRI for the more subtle brain dysfunction associated with TBI, dementia, neurotoxicity, and psychiatric illnesses. The irony is striking.

DISCLOSURE

TH, PC, and GC are members of the International Society of Applied Neuroimaging (ISAN), a volunteer organization devoted to the understanding and appropriate clinical utilization of SPECT brain imaging. All authors volunteered their time in the research and writing of this manuscript.

AUTHOR CONTRIBUTIONS

The first draft was prepared by TH. All authors contributed to the conceptualization and editing of the manuscript.

ACKNOWLEDGMENTS

We would like to acknowledge the entire International Society of Applied Neuroimaging.

REFERENCES

1. Tucker, N. *Daniel Amen is the most popular psychiatrist in America. To most researchers and scientists, that's a bad thing*. Washington Post. (2012). Available online at: https://www.washingtonpost.com/lifestyle/magazine/daniel-amen-is-the-most-popular-psychiatrist-in-america-to-most-researchers-and-scientists-thats-a-very-bad-thing/2012/08/07/467ed52c-c540-11e1-8c16-5080b717c13e_story.html?noredirect=on&utm_term=.47ca50ea5098 (accessed January 21, 2019).
2. First MB, Drevets WC, Carter C, Dickerstein DP, Kasoff L, Kim KL, et al. Clinical applications of neuroimaging in psychiatric disorders. *Am J Psychiatry*. (2018) 175:915–6. doi: 10.1176/appi.ajp.2018.1750701
3. American Psychiatric Association. *Diagnostic and Statistical Manual of Mental Disorders. 5th ed*. Arlington VA: American Psychiatric Association. (2013). doi: 10.1176/appi.books.9780890425596
4. Henderson TA, Uszler JM, Rossiter-Thornton JF, Siow Y-H, Pavel DG, McLean M, et al. The American Psychiatric Association fails to recognize the value of neuroimaging in psychiatry. *Interv Med Clin Imaging*. (2019) 1:1–8.
5. Henderson TA, van Lierop MJ, McLean M, Uszler JM, Thornton JF, Siow YH, et al. Functional neuroimaging in psychiatry-aiding in diagnosis and guiding treatment. What the American Psychiatric Association does not know. *Front Psychiatry*. (2020) 11:276. doi: 10.3389/fpsyt.2020.00276
6. Henderson TA. The diagnosis and evaluation of dementia and mild cognitive impairment with emphasis on SPECT perfusion neuroimaging. *CNS Spectr*. (2012) 17:176–206. doi: 10.1017/S1092852912000636
7. Food and Drug Administration. *About Biomarkers and Qualification webpage*. Available online at: https://www.fda.gov/drugs/biomarker-qualification-program/about-biomarkers-and-qualification (accessed April 3, 2022).
8. Kapucu OL, Nobili F, Varrone A, Booij J, Vander Borght T, Någren K, et al. Procedure guideline for brain perfusion SPECT using 99mTc-labelled radiopharmaceuticals, version 2. *Eur J Nucl Med Mol Imaging*. (2009) 36:2093–102. doi: 10.1007/s00259-009-1266-y
9. Cohen PF, Tarzwell R, Numerow L, Siow Y-H, Uszler JM, Pavel DG, et al. *CANM Guidelines for Brain Perfusion Single Photon Emission Computed Tomography (SPECT)*. Available online at: https://wwwcanm-acmnca/guidelines (accessed April 3, 2022).
10. Stamatakis EA, Wilson JT, Hadley DM, Wyper DJ, SPECT. imaging in head injury interpreted with statistical parametric mapping. *J Nucl Med*. (2002) 43:476–83.
11. Raji CA, Tarzwell R, Pavel D, Schneider H, Uszler M, Thornton J, et al. Clinical utility of SPECT neuroimaging in the diagnosis and treatment of traumatic brain injury: a systematic review. *PLoS ONE*. (2014) 9:e91088. doi: 10.1371/journal.pone.0091088
12. Raji CA, Willeumier K, Taylor D, Tarzwell R, Newberg A, Henderson TA, et al. Functional neuroimaging with default mode network regions distinguishes PTSD from TBI in a military veteran population. *Brain Imaging Behav*. (2015) 9:527–34. doi: 10.1007/s11682-015-9385-5
13. Amen DG, Raji CA, Willeumier K, Taylor D, Tarzwell R, Newberg A, et al. Functional neuroimaging distinguishes posttraumatic stress disorder from traumatic brain injury in focused and large community datasets. *PLoS ONE*. (2015) 10:e0129659. doi: 10.1371/journal.pone.0129659
14. Henderson TA. Brain SPECT imaging in neuropsychiatric diagnosis and monitoring. *EPatient*. (2018) 1:40–7. Available online at: http://nmpangea.com/2018/10/09/738/
15. Lansing K, Amen DG, Hanks C, Rudy L. High-resolution brain SPECT imaging and eye movement desensitization and reprocessing in police officers with PTSD. *J Neuropsychiatry Clin Neurosci*. (2005) 17:526–32. doi: 10.1176/jnp.17.4.526
16. Amen DG, Wu JC, Taylor D, Willeumier K. Reversing brain damage in former NFL players: implications for traumatic brain injury and substance abuse rehabilitation. *J Psychoactive Drugs*. (2011) 43:1–5. doi: 10.1080/02791072.2011.566489
17. Henderson TA, Morries LD. SPECT perfusion imaging demonstrates improvement of traumatic brain injury with transcranial near-infrared laser phototherapy. *Adv Mind Body Med*. (2015) 29:27–33. doi: 10.2147/NDT.S65809
18. Boussi-Gross R, Golan H, Fishlev G, Bechor Y, Volkov O, Bergan J, et al. Hyperbaric oxygen therapy can improve post concussion syndrome years after mild traumatic brain injury - randomized prospective trial. *PLoS ONE*. (2013) 8:e79995. doi: 10.1371/journal.pone.0079995
19. Amen DG, Jourdain M, Taylor DV, Pigott HE, Willeumier K. Multi-site six month outcome study of complex psychiatric patients evaluated with addition of brain SPECT imaging. *Adv Mind Body Med Spring*. (2013) 27:6–16.
20. Amen DG, Highum D, Licata R, Annibali JA, Somner L, Pigott HE, et al. Specific ways brain SPECT imaging enhances clinical psychiatric practice. *J Psychoactive Drugs*. (2012) 44:96–106. doi: 10.1080/02791072.2012.684615
21. Thornton JF, Schneider H, McLean MK, van Lierop MJ, Tarzwell R. Improved outcomes using brain SPECT-guided treatment versus treatment-as-usual in community psychiatric outpatients: a retrospective case-control study. *J Neuropsychiatry Clin Neurosci*. (2014) 26:51–6. doi: 10.1176/appi.neuropsych.12100238

22. Practice parameters for determining brain death in adults (summary statement). The Quality Standards Subcommittee of the American Academy of Neurology. *Neurology*. (1995) 45:1012–4. doi: 10.1212/WNL.45.5.1012
23. American Academy of Neurology. *Policy & Guidelines. Update: Determining Bran Death in Adults.* Available online at: https://www.aan.com/Guidelines/home/GuidelineDetail/431 (accessed April 17, 2022).
24. Donohoe KJ, Agrawal G, Frey KA, Gerbaudo VH, Mariani G, Nagel JS, et al. SNM practice guideline for brain death scintigraphy 20. *J Nuc Med Tech.* (2012) 40:198–203. doi: 10.2967/jnmt.112.105130

Conflict of Interest: TH is the president and principal owner of The Synaptic Space, a neuroimaging consulting firm, CEO and Chairman of the Board of Neuro-Luminance Corporation, a medical service company, president and principal owner of Dr. Theodore Henderson, Inc, a medical service company, President of the Neuro-Laser Foundation, a non-profit organization, and member of and a former officer of the Brain Imaging Council Board of the Society of Nuclear Medicine and Molecular Imaging (SNMMI). Since 2017, TH has served in the SNMMI Brain Imaging Outreach Working Group. Currently, TH serves as president of the International Society of Applied Neuroimaging. TH has no ownership in, and receives no remuneration from, any neuroimaging company. No more than 5% of his income is derived from neuroimaging.

The remaining authors declare that the research was conducted in the absence of any commercial or financial relationships that could be construed as a potential conflict of interest.

Publisher's Note: All claims expressed in this article are solely those of the authors and do not necessarily represent those of their affiliated organizations, or those of the publisher, the editors and the reviewers. Any product that may be evaluated in this article, or claim that may be made by its manufacturer, is not guaranteed or endorsed by the publisher.

frontiers in Neurology

ORIGINAL RESEARCH
published: 04 February 2021
doi: 10.3389/fneur.2021.630153

The Role of Frontal Assessment Battery and Frontal Lobe Single-Photon Emission Computed Tomography in the Differential Diagnosis of Progressive Supranuclear Palsy Variants and Corticobasal Syndrome—A Pilot Study

Piotr Alster[1], Bartosz Migda[2], Natalia Madetko[1], Karolina Duszyńska-Waś[1], Agnieszka Drzewińska[1], Ingeborga Charzyńska[3], Miłosz Starczyński[1], Ada Szepelska[1], Leszek Królicki[4] and Andrzej Friedman[1]*

[1] Department of Neurology, Medical University of Warsaw, Warsaw, Poland, [2] Ultrasound Diagnostic Department, Faculty of Medical Sciences, Medical University of Warsaw, Warsaw, Poland, [3] Department of Nuclear Medicine and Magnetic Resonance, Mazowiecki Hospital Brodnowski, Warsaw, Poland, [4] Department of Nuclear Medicine, University Clinical Center, Medical University of Warsaw, Warsaw, Poland

OPEN ACCESS

Edited by:
Theodore A. Henderson, Consultant, Denver, CO, United States

Reviewed by:
Philip Frank Cohen, University of British Columbia, Canada
Yashar Zeighami, McGill University, Canada

***Correspondence:**
Piotr Alster
piotr.alster@gmail.com

Specialty section:
This article was submitted to Applied Neuroimaging, a section of the journal Frontiers in Neurology

Received: *17 November 2020*
Accepted: *05 January 2021*
Published: *04 February 2021*

Citation:
Alster P, Migda B, Madetko N, Duszyńska-Waś K, Drzewińska A, Charzyńska I, Starczyński M, Szepelska A, Królicki L and Friedman A (2021) The Role of Frontal Assessment Battery and Frontal Lobe Single-Photon Emission Computed Tomography in the Differential Diagnosis of Progressive Supranuclear Palsy Variants and Corticobasal Syndrome—A Pilot Study. Front. Neurol. 12:630153. doi: 10.3389/fneur.2021.630153

Progressive supranuclear palsy (PSP) and corticobasal syndrome (CBS) are clinical syndromes classified as atypical parkinsonism. Due to their overlapping symptomatology, recent research shows the necessity of finding new methods of examination of these clinical entities. PSP is a heterogenic disease. PSP Richardson-Steele Syndrome (PSP-RS) and parkinsonism predominant (PSP-P) are the most common clinical variants of progressive supranuclear palsy syndrome. The different clinical course and life expectancy of PSP-RS and PSP-P stress the need of efficient examination in the early stages. The aim of the study was to evaluate the possible feasibility of the combined use of frontal assessment battery (FAB) and single-photon emission computed tomography (SPECT) in the differentiation of PSP-RS, PSP-P, and CBS. The findings show that FAB may be interpreted as a possible supplementary tool in the differential diagnosis of PSP-P and PSP-RS. The differences in SPECT are less pronounced. The study does not show any advantages of performing combined frontal SPECT and FAB in the differential examination of PSP and CBS. Moreover, PSP-RS and CBS, in a detailed evaluation of the frontal lobe, do not show any significant differences. This is a relatively small study which, however, highlights the relevant features of clinical examination of these rare entities.

Keywords: SPECT, tauopathies, parkinsonism, progressive supranuclear palsy, frontal lobe

INTRODUCTION

The examination of tauopathic atypical parkinsonism remains a difficult issue. The differentiation of progressive supranuclear palsy syndrome and corticobasal syndrome (CBS) is affected by significant overlaps in the diseases' symptomatology. Growing interest is associated with the search for effective tools in the assessment of four-repeat tauopathies and their clinical manifestations (1). The recent criteria of diagnosis of PSP show four critical axes of diagnosis—akinesia, postural instability, cognitive and language deficiencies, and oculomotor dysfunction—and stress the necessity of discriminating variants (2). Among the variants of PSP, the most common—PSP-Richardson–Steele syndrome and PSP-parkinsonism predominant—should be primarily indicated as they are related with up to 90% cases of PSP (about 60% of PSP-RS and about 30% of PSP-P)[3]. Additionally, recent literature highlights the boundaries between PSP and CBS and stresses the need for finding examination tools, which may be supplemental to neurological examination and most common additional assessments such as magnetic resonance imaging (MRI) (1, 3–5). The contemporary criteria of diagnosis of CBS were released in 2013 and do not explore the field of evolving supplementary examinations (3). The studies based on positron emission tomography (PET) showed various limitations as off-binding of radiotracer observed in [^{18}F]-AV1451-PET, non-specific radiotracers as [^{18}F]-FDG-PET[7], or unfortunate economical aspect. The second-generation tau radiotracers such as [^{18}F]-PI2620-PET seem to play a possibly beneficial role; however, they are not accessible in everyday clinical practice. Single-photon emission computed tomography (SPECT), with its various radiotracers such as ^{99m}Tc-HMPAO, is more accessible which, however, is affected by low specificity. Previous studies with SPECT-^{99m}Tc-HMPAO conducted on patients with tauopathic atypical parkinsonism showed thalamic hypoperfusion in PSP which, however, did not confirm any significant differences of perfusion between PSP and CBS (6, 7). A combined assessment using dopamine transporter and perfusion SPECT was evaluated in a paper by Van Laere et al. where the authors attempted to define the role of this assessment in the differential diagnosis of parkinsonism (8). The study examined patients with diagnosis of idiopathic Parkinson's disease, essential tremor, PSP, multiple-system atrophy, and dementia with Lewy bodies. The singular dopamine transporter evaluation enabled 58.8% effective differentiation. Perfusion examination presented effectiveness in 67.6% of differential diagnoses. The combined examination showed 82.4% efficacy. The study was based on the examination of small groups−12 PSP patients (8). The authors did not discuss PSP phenotypes as separate entities. The issue of combined perfusion, metabolism, and dopaminergic evaluation was earlier evaluated in PET. Striatal abnormalities in metabolic PET were found to be sensitive in the examination of multiple system atrophy (MSA); however, dopaminergic evaluation was not found to be feasible in the differential examination of parkinsonian syndrome (9). Another work presented the differentiation of parkinsonism using technetium-99m ethyl cysteinate dimer. It confirmed a potentially beneficial role in the differential diagnosis of MSA and idiopathic Parkinson's disease (PD) (10). An examination performed using simultaneous ^{99m}Tc-ECD/^{123}I-FP-CIT revealed higher striatal binding in MSA when compared to PD. Asymmetry was more prominent in PD[13]. A study evaluating Tc-99m ethylene cysteinate in the SPECT examination of PD and MSA showed elevated perfusion in the lentiform, cerebellum, and thalamus among patients with PD (11).

The diagnosis of PSP-P was not stressed in any of the studies. Regarding the limited feasibility of SPECT in the examination of tauopathic parkinsonism, the authors of this study intended to verify the usefulness of combined examination using assessment of frontal lobe in perfusion and neuropsychological assessment using frontal assessment battery (FAB), a short screening test that evaluates the executive functions.

According to the most recent theories, frontal lobes are responsible for the control of complex functions, such as abstract reasoning, self-regulation, motor programming, mental flexibility, inhibitory control, and environmental autonomy (12). Assessing these functions and being able to identify the dysexecutive syndrome are helpful for the diagnosis of brain diseases, such as frontotemporal dementia, parkinsonian dementia, and vascular dementia.

Deficits in executive functioning may be observed in PD and also in all atypical parkinsonisms (13–15). The severity of the dysexecutive syndrome in these diseases may vary from mild deterioration to a highly pronounced executive dysfunction being one of the main symptoms (PSP-RS). It may also coexist with other cognitive deficits (as in some manifestations of CBS) (15). However, as present in almost all patients with parkinsonism, the dysexecutive syndrome should be always neuropsychologically assessed. Several neuropsychological tests and clinical trials were designed to assess the frontal lobe functions. The most known and widely used are The Wisconsin Card Sorting Test (WCST), the Stroop Test, the Tower of London, Brixton Spatial Anticipation Test, and the Behavioral Assessment of the Disexecutive Syndrome (BADS) (13). All of them are tests of confirmed sensitivity to the disexecutive syndrome; however, they assess just some several aspects of executive functioning (WCST and Stroop), take quite a lot of time, and require some more complex preparations and use of test tools (BADS) or the results depend on the time of performance (ToL).

FAB is designed to be administered at bedside in about 10 min. It consists of six tasks, each of which was designed to assess one of the main frontal lobe functions (abstract reasoning, mental flexibility, motor programming, inhibitory control, sensitivity to interference, environmental autonomy)[15]. It is possible to receive zero to three points for each of the test items, giving a maximal total score of 18 points. None of the tasks requires any tools. There is no need for the patient to be able to perform complex movements (which is particularly important while assessing patients with movement disorders, such as Parkinson's Disease or atypical parkinsonian syndromes) (13). The FAB has been found

to highly correlate with the results of other neuropsychological tests measuring executive functions (e.g., WCST) and is known for its sensitivity to executive dysfunctions in parkinsonism (14), which makes it a useful tool for clinical practice.

MATERIALS AND METHODS

In this prospective study, all patients gave informed consent to participate in this research. The bioethical committee of the Medical University of Warsaw approved this study. From May 2017 to September 2020, 58 patients, in total, were enrolled. The neurological examination and diagnosis were based on the recent criteria and conducted in the Department of Neurology of the Medical University of Warsaw in all of the cases. The neuropsychological examination was performed by two neuropsychologists working (9 years of experience) in the Department of Neurology at the Medical University of Warsaw and experienced in the assessment of psychological deficiencies in atypical parkinsonism.

Due to the fact that certain patients did not accomplish the examination for various reasons, the authors of this study were forced to exclude about 29.3% of the cases primarily planned for further evaluation. Finally, the research group was based on 41 participants with clinical diagnosis of probable PSP-P, CBS, and PSP-RS and consisted of 18 patients with PSP-RS (11 male, seven female), 11 patients with PSP (six male, five female), and 12 patients with CBS (one male, 11 female). All patients were right-handed, and the duration of the disease varied from 2 to 5 years. Out of the 41 study participants, 23 (56.1%) were female and 18 (43.9%) were male. The mean age was 70.2 years (range, 54–85 years) (**Table 1**).

The final research group underwent neuropsychological examination with FAB testing and perfusion assessment using SPECT ^{99m}Tc-HMPAO. Due to the fact that the software used in the study to assess perfusion in SPECT shows the results of patients compared to 20 healthy volunteers, due to ethical reasons, SPECT was not additionally conducted on the controls in this study. In order to avoid examining the controls only in neuropsychological examination, the results of the FAB test were compared with the standard results of healthy volunteers from the literature.

Frontal Assessment Battery

In this study, FAB was used due to the relevant role of frontal lobe syndrome in the symptomatology of PSP. The frontal lobe syndrome is generally associated with the Richardson–Steele variant of PSP, as patients affected by this disease often present rapidly progressing changes in behavior. In this context, FAB, regarding its simplicity and possible screening value, may be interpreted as a valuable supplement in the examination of PSP. As growing interest is related to boundaries between parkinsonian syndromes based on four-repeat tauopathies, in the opinion of the authors of the study, extended evaluation of similarities and differences regarding the frontal lobe in PSP-RS, PSP-P, and CBS seem to be an intriguing issue.

Single-Photon Emission Computed Tomography

SPECT, with technetium-99m hexamethylpropyleneamine oxime (^{99m}Tc-HMPAO) as a radiotracer, was used for the evaluation of regional cerebral blood flow. Then, 740 MBq of radiotracer was administered in patients placed in a quiet, dimly lit room in supine position. Examinations were performed with SPECT/CT scan (Symbia T6, Siemens) on dual-head gamma camera with low-energy high-resolution parallel-hole collimator. Step and shoot acquisition mode was used, and sequences of 128 frames on a 128 × 128 matrix were obtained (64 projections per head, 30 s per projection). The photopeak was set at 140 keV with 10% window on either site of the photopeak. Iterative reconstruction (eight iterations, eight subsets, 7 mm Gauss filter), scatter correction, and CT attenuation correction were performed. Post-processing analysis was performed with Scenium software (Siemens Medical Solutions USA, Inc.). The regions of interest (ROIs) were predefined on a high-resolution T1 MRI volume scan. Perfusion in the basal ganglia, frontal lobes, hemispheres of cerebella, and thalami was subsequently examined among all patients. Values of variances from ROIs in individual parts of the frontal lobe on both sides (right and left separately) were taken for statistical analysis.

Statistical Analysis

Statistical analyses were performed using Statistica software (version 13.1, Dell, Inc. Statsoft). The presented data were expressed as means with 95% confidence interval. Data distributions were assessed by Shapiro–Wilk W test. For comparison of parametric and non-parametric variables, Student's t test and Mann–Whitney U test were used, respectively. Frequencies of nominal variables were compared using χ^2 test. In case of small group counts, Yates correction was used. We performed receiver operating characteristic (ROC) curves to evaluate the diagnostic performance of SPECT parameters and FAB as predictors of PSP-RS, PSP-P, and CBS analyzing sensitivity and specificity for each possible threshold/cutoff, and we used area under the ROC curve (AUC) to express the overall diagnostic accuracy of the index criterion and for comparison between significant parameters. Analysis was made in search of the parameters that best differentiate particular subgroups against each other. We have reported 95% confidence interval for calculated AUC p-value. Based on the ROC curves, we have determined the cutoff point for each parameter and reported its positive predictive value (PPV), negative predictive value (NPV), and accuracy (ACC). Those results were used in next-step multivariable analysis. For this purpose, we have used logistic regression to answer a question if any combination of SPECT parameters and FAB has greater overall performance in relation to single-variable analysis in differentiating PSP-RS, PSP-P, and CBS with a report of OR and its 95% confidence interval, accuracy, and level of significance (p-value). $P < 0.05$ was considered as indicative of a statistically significant difference. In the logistic regression part of the analysis, we have made an effort to build a multivariate model characterizing each

TABLE 1 | Basic characteristics of research group and subgroups: progressive supranuclear palsy-Richardson–Steele syndrome (PSP-RS), progressive supranuclear palsy-parkinsonism predominant (PSP-P), and corticobasal syndrome (CBS) in relation to single-photon emission computed tomography parameters, frontal assessment battery, and subgroups comparison.

	All *N* = 41					PSP–RS *N* = 18					PSP–P *N* = 11					CBS *N* = 12					*p* PSP–RS vs. PSP–P	*p* PSP–RS vs. CBS	*p* PSP–P vs. CBS
	F/M	Mean	Min	Max	SD (95% CI)	F/M	Mean	Min	Max	SD (95% CI)	F/M	Mean	Min	Max	SD (95% CI)	F/M	Mean	Min	Max	SD (95% CI)			
Gender	23/18					7/11					6/5					11/1					0.7276c	0.0121cy	0.0509cy
Age		70.2	54.0	85.0	6.8 (5.6–8.7)		71.1	59	80	5.7 (4.3–8.5)		70.2	57	77	6.9 (4.8–12.1)		68.9	54	85	8.5 (6–14.5)	0.713t	0.4151t	0.7009t
FAB		12.3	6.0	18.0	2.9 (2.4–3.7)		11.4	6	18	2.9 (2.2–4.3)		13.9	11	17	1.9 (1.3–3.4)		12.3	7	16	3.2 (2.2–5.4)	0.0165t	0.4481t	0.1481t
(1) Frontal lobe		−1.7	−6.9	2.6	1.8 (1.5–2.4)		−1.8	−6.9	1.5	1.9 (1.4–2.8)		−0.7	−3.5	2.6	2.1 (1.5–3.7)		−2.4	−3.9	0.4	1.2 (0.9–2.1)	0.1765t	0.2718t	0.0231t
(2) Frontal lobe (AAL)		−1.6	−7.2	2.5	1.8 (1.5–2.3)		−1.8	−7.2	1.4	1.9 (1.4–2.8)		−0.6	−3.4	2.5	2 (1.4–3.5)		−2.3	−3.7	0.7	1.2 (0.8–2)	0.107t	0.433t	0.0202t
(16) Frontal lobe (AAL) (L)		−1.5	−6.1	2.6	1.8 (1.5–2.3)		−1.7	−6.1	2	1.8 (1.4–2.8)		−0.4	−3	2.6	1.9 (1.4–3.4)		−2.3	−3.8	0.9	1.2 (0.9–2.1)	0.1056u	0.1624u	0.0138u
(3) Frontal lobe (AAL) (R)		−1.7	−8.1	3.1	2 (1.6–2.5)		−1.9	−8.1	1.6	2.1 (1.5–3.1)		−0.8	−3.6	3.1	2.2 (1.5–3.8)		−2.2	−5.1	0.4	1.5 (1.1–2.6)	0.3012u	0.5117u	0.1962u
(4) Frontal lobe-Atlas 2		−2.8	−9.6	2.3	2.3 (1.9–3)		−2.7	−9.6	1.6	2.5 (1.8–3.7)		−1.9	−5.2	2.3	2.5 (1.7–4.3)		−3.6	−6.1	0.7	1.8 (1.2–3)	0.417t	0.252t	0.0634t
(5) Frontal lobe-Atlas 1		−1.3	−9.4	2.8	2.3 (1.9–2.9)		−1.2	−9.4	1.8	2.6 (2–3.9)		−0.4	−4.5	2.8	2.3 (1.6–4)		−2.1	−4	1	1.6 (1.1–2.7)	0.4448u	0.049u	0.0694u
(17) Frontal lobe-Atlas 3		−2.4	−9.3	2.2	2.2 (1.8–2.8)		−2.5	−9.3	1.2	2.4 (1.8–3.5)		−1.4	−5.1	2.2	2.4 (1.7–4.3)		−3.3	−5.2	0.1	1.4 (1–2.3)	0.236t	0.3317t	0.0338t
(6) Inferior frontal gyrus, opercular part (AAL) (L)		−2.6	−6.0	5.2	2.2 (1.8–2.9)		−2.4	−5.8	0.5	1.9 (1.4–2.8)		−1.9	−4.3	1.7	1.9 (1.3–3.3)		−3.4	−6	5.2	2.9 (2.1–5)	0.6531u	0.0515u	0.0228u
(7) Inferior frontal gyrus, opercular part (AAL) (R)		−1.5	−5.6	4.8	2.2 (1.8–2.8)		−1.5	−5.1	2.1	2 (1.5–3)		−1.2	−5	4.8	2.6 (1.8–4.6)		−1.7	−5.6	3.1	2.2 (1.5–3.7)	0.7487t	0.8227t	0.6556t
(8) Inferior frontal gyrus, orbital part (AAL) (L)		−2.1	−6.4	3.1	2.4 (2–3.1)		−2.4	−6	1.7	2.2 (1.6–3.3)		−1.7	−5.7	1	1.9 (1.3–3.4)		−2	−6.4	3.1	3.1 (2.2–5.3)	0.3903t	0.7089t	0.764t
(9) Inferior frontal gyrus, orbital part (AAL) (R)		−1,0	−5.4	4.6	2.1 (1.7–2.7)		−1.2	−5.4	3.2	2.1 (1.6–3.2)		−1.1	−5.1	1.6	2 (1.4–3.4)		−0.7	−4.2	4.6	2.2 (1.6–3.8)	0.8667t	0.5015t	0.6415t
(10) Inferior frontal gyrus, triangular part (AAL) (L)		−1.4	−5.5	2.5	2.3 (1.9–2.9)		−1.1	−5.5	2.5	2.6 (1.9–3.8)		−1.5	−3.9	1.7	1.9 (1.3–3.4)		−1.8	−5.3	2.1	2.3 (1.7–4)	0.7112t	0.4566t	0.6913t
(18) Inferior frontal gyrus, triangular part (AAL) (R)		−0.5	−5.3	4.4	2.3 (1.9–2.9)		−0.3	−2.9	4.2	1.9 (1.5–2.9)		−0.9	−5.3	3.4	2.9 (2–5.1)		−0.5	−4.7	4.4	2.3 (1.6–3.9)	0.5684t	0.8298t	0.7528t
(11) Middle frontal gyrus (AAL) (L)		−1,0	−3.7	3.6	1.7 (1.4–2.1)		−0.8	−3.6	3.6	1.9 (1.4–2.8)		−0.4	−2.7	2.6	1.5 (1.1–2.7)		−1.9	−3.7	0.4	1.1 (0.8–1.9)	0.5015t	0.075t	0.0106t
(12) Middle frontal gyrus (AAL) (R)		−1.7	−8.5	3.9	2.4 (1.9–3)		−1.5	−8.5	1.2	2.2 (1.7–3.4)		−0.9	−3.3	3.9	2.4 (1.7–4.3)		−2.7	−6.5	0.4	2.3 (1.6–3.9)	0.9105u	0.1384u	0.1569u
(13) Middle frontal gyrus, orbital part (AAL) (L)		−1.3	−5.7	3.4	2.3 (1.9–2.9)		−0.8	−5.7	3.4	2.6 (2–3.9)		−1.2	−4.1	1.8	1.9 (1.3–3.3)		−2.3	−5.3	1.9	1.9 (1.4–3.3)	0.6958t	0.111t	0.1822t
(14) Middle frontal gyrus, orbital part (AAL) (R)		−1.8	−5.2	3.1	2.1 (1.8–2.7)		−1.9	−5.2	3.1	2.4 (1.8–3.6)		−1.3	−3.9	2.5	1.8 (1.3–3.2)		−2	−4.1	3.1	2.1 (1.5–3.5)	0.486u	0.8989u	0.1481u
(15) Superior frontal gyrus, dorsolateral (AAL) (L)		−1.1	−5.7	3.3	2 (1.7–2.6)		−1.1	−5.1	2.9	2 (1.5–3)		0.3	−3.4	3.3	2 (1.4–3.5)		−2.2	−5.7	−0.3	1.4 (1–2.4)	0.0803t	0.1344t	0.0027t
(5) Superior frontal gyrus, dorsolateral (AAL) (R)		−1.2	−6.2	3.1	1.8 (1.5–2.4)		−1.4	−6.2	0.9	1.8 (1.3–2.7)		−0.2	−3.9	3.1	2 (1.4–3.5)		−1.9	−4.4	0.1	1.4 (1–2.4)	0.0953t	0.4544t	0.0268t
(19) Superior frontal gyrus, medial (AAL) (L)		−1.1	−3.9	1.5	1.3 (1–1.6)		−1.5	−3.9	0.5	1.2 (0.9–1.8)		−0.2	−1.8	1.5	1.1 (0.8–1.9)		−1.4	−2.9	1.1	1.2 (0.8–2)	0.0091t	0.9354t	0.0171t
(20) Superior frontal gyrus, medial (AAL) (R)		−1.2	−6.9	2.2	1.7 (1.4–2.2)		−1.6	−6.9	0.4	1.7 (1.3–2.6)		−0.3	−3.7	2.2	1.9 (1.3–3.3)		−1.3	−2.9	1.7	1.4 (1–2.3)	0.1009u	0.9325u	0.1397u
(21) Superior frontal gyrus, medial orbital (AAL) (L)		−1.2	−10.4	2.6	2.5 (2–3.1)		−1	−10.4	2.2	2.9 (2.2–4.3)		−0.6	−4.3	2.6	1.9 (1.3–3.3)		−2.1	−5.1	2.6	2.1 (1.5–3.6)	0.8047u	0.072u	0.0489u
(22) Superior frontal gyrus, medial orbital (AAL) (R)		−0.7	−8.3	3.4	2.2 (1.8–2.9)		−0.6	−8.3	2	2.4 (1.8–3.6)		−0.3	−3.5	3.4	2.1 (1.4–3.6)		−1.3	−4	2.7	2.2 (1.6–3.7)	0.9105u	0.0904u	0.2184u
(23) Superior frontal gyrus, orbital part (AAL) (L)		−0.7	−8.1	3.1	2 (1.7–2.6)		−0.7	−8.1	2.9	2.3 (1.8–3.5)		−0.4	−4.5	2.3	1.7 (1.2–3)		−1.1	−3.2	3.1	2 (1.4–3.3)	0.7192u	0.2276u	0.1569u
(24) Superior frontal gyrus, orbital part (AAL) (R)		−1.5	−11.6	2.6	2.3 (1.9–3)		−1.6	−11.6	2.2	3.1 (2.3–4.6)		−1.2	−4	1	1.4 (1–2.4)		−1.4	−3.5	2.6	1.9 (1.3–3.2)	0.9642u	0.6567u	0.5588u

SD, standard deviation; CI, confidence interval.

For p-value: "t" for Student's t test, "u" for Mann–Whitney U test, "c" for χ^2 test, "cy" for χ^2 square test with Yates correction.

TABLE 2 | Receiver operating characteristic curve analysis of single-photon emission computed tomography parameters and frontal assessment battery (FAB).

		S/D	Cutoff	AUC	95% CI	*p*	Se	Sp	PPV	NPV	ACC
FAB	PSP-RS	D	12	0.691	0.522–0.86	0.027	72.2	65.2	61.9	75	68.3
FAB	PSP-P	S	12	0.726	0.568–0.883	0.0049	90.9	43.3	37	92.9	56.1
(16) Frontal lobe (AAL) (L)		S	−1.4	0.73	0.552–0.909	0.0115	72.7	70	47.1	87.5	70.7
(15) Superior frontal gyrus, dorsolateral (AAL) (L)		S	0	0.748	0.567–0.93	0.0073	63.6	83.3	58.3	86.2	78
(1) Frontal lobe	CBS	D	−1.2	0.704	0.536–0.872	0.0171	91.7	44.8	40.7	92.9	58.5
(16) Frontal lobe (AAL) (L)		D	−2.2	0.71	0.542–0.878	0.0145	75	95.7	90	88	88.6
(5) Frontal lobe—Atlas 1		D	−2.5	0.718	0.552–0.885	0.0103	66.7	75.9	53.3	84.6	73.2
(6) Inferior frontal gyrus, opercular part (AAL) (L)		D	−3.5	0.739	0.557–0.92	0.0102	75	75.9	56.3	88	75.6
(11) Middle frontal gyrus (AAL) (L)		D	−1.4	0.728	0.566–0.891	0.0058	83.3	69	52.6	90.9	73.2
(15) Superior frontal gyrus, dorsolateral (AAL) (L)		D	−1	0.749	0.601–0.896	0.001	91.7	65.5	52.4	95	73.2

S/D, stimulant/destimulant; AUC, area under the ROC curve; CI, confidence interval; p, p value for AUC; Se, sensitivity; Sp, specificity; PPV, positive predictive value; NPV, negative predictive value; ACC, accuracy.

of the subgroups separately using logistic regression and taking into account previous results.

RESULTS

Basic Characteristics

The mean, maximal, minimal, and standard deviation with 95% confidence interval values of age, frontal assessment battery, and SPECT parameters [divided into right (R) and left (L) sides] are listed in **Table 1**. A comparison of PSP-P and PSP-RS revealed significantly higher values of FAB for PSP-P (13.9 vs. 11.4; $p = 0.0165$) and higher values of SPECT variances [superior frontal gyrus, medial (AAL) on the left side] for PSP-P (−0.2 vs. −1.5; $p = 0.0091$; **Table 1**). Higher values of SPECT variances were also obtained for PSP-P in relation to CBS in several regions: frontal lobe, −0.7 vs. −2.4 ($p = 0.023$); frontal lobe (AAL), −0.6 vs. −2.3 ($p = 0.0202$); frontal lobe (AAL) (L), −0.4 vs. −2.3 ($p = 0.0138$); frontal lobe (flutemetamol), −1.4 vs. −3.3 ($p = 0.0338$); inferior frontal gyrus opercular part (AAL) (L), −1.9 vs. −3.4 ($p = 0.0228$); middle frontal gyrus (AAL) (L), −0.4 vs. −1.9 ($p = 0.0106$); superior frontal gyrus, dorsolateral (AAL) (L), 0.3 vs. −2.2 ($p = 0.0027$); superior frontal gyrus, dorsolateral (AAL) (R), −0.2 vs. −1.9 ($p = 0.0268$); superior frontal gyrus, medial (AAL) (L), −0.2 vs. −1.4 ($p = 0.0171$); and superior frontal gyrus, medial orbital (AAL) (L), −0.6 vs. −2.1 ($p = 0.0489$) (**Table 1**). Assessment of SPECT parameters in relation to PSP-RS and CBS revealed significant differences only in one region, frontal lobe—Atlas 1, with higher values of SPECT variances in the case of PSP-RS, −1.2 vs. −2.1 ($p = 0.049$) (**Table 1**).

ROC Curve Analysis

In the case of PSP-RS, only the FAB turned out to be a significant parameter differentiating this subgroup from the others with AUC of 0.691 (95% CI, 0.522–0.86; $p = 0.027$) and cutoff of 12, with sensitivity, specificity, PPV, NPV, and ACC at 72.2, 65.2, 61.9, 75, and 68.3%, respectively (**Table 2** and **Figure 1**). Similarly, for PSP-P, among others, FAB turned out to be a significant parameter, with AUC of 0.726 (95% CI, 0.568–0.883; $p = 0.0049$) and the same cutoff of 12 and with higher values of sensitivity at 90.9% and NPV at 92.9% but lower specificity, PPV, and ACC at 43.3, 37, and 56.1%, respectively (**Figure 2A**). The other parameters include frontal lobe (AAL) L (**Figure 2B**) and superior frontal gyrus dorsolateral (AAL) L (**Figure 2C**), with higher values of AUC at 0.73 (95% CI, 0.552–0.909; $p = 0.0115$) and 0.748 (95% CI, 0.567–0.93; $p = 0.0073$), respectively, and a slightly better overall performance (**Table 2**). For CBS, the essential parameters occurred to be six SPECT parameters as listed in **Table 1** and **Figures 3A–F**. The best overall performance revealed frontal lobe (AAL) L with AUC = 0.71 (95% CI, 0.542–0.878; $p = 0.0145$) and

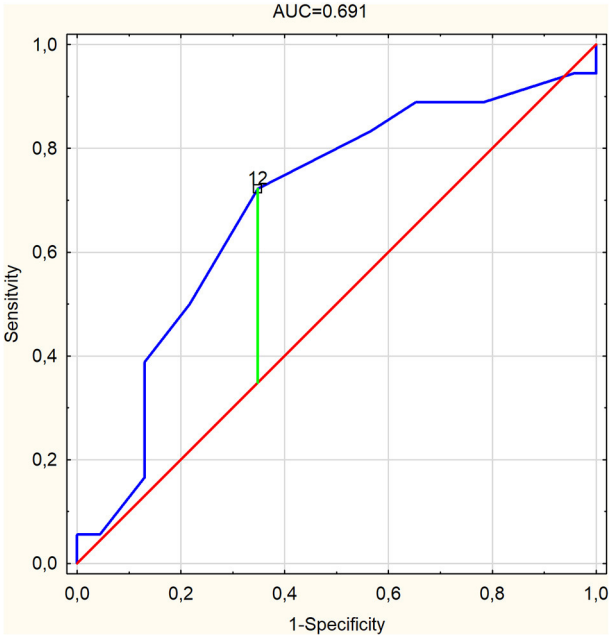

FIGURE 1 | Receiver operating characteristic curve graph of frontal assessment battery (area under the ROC curve = 0.691) as a predictor for progressive supranuclear palsy-Richardson–Steele syndrome with marked cutoff value.

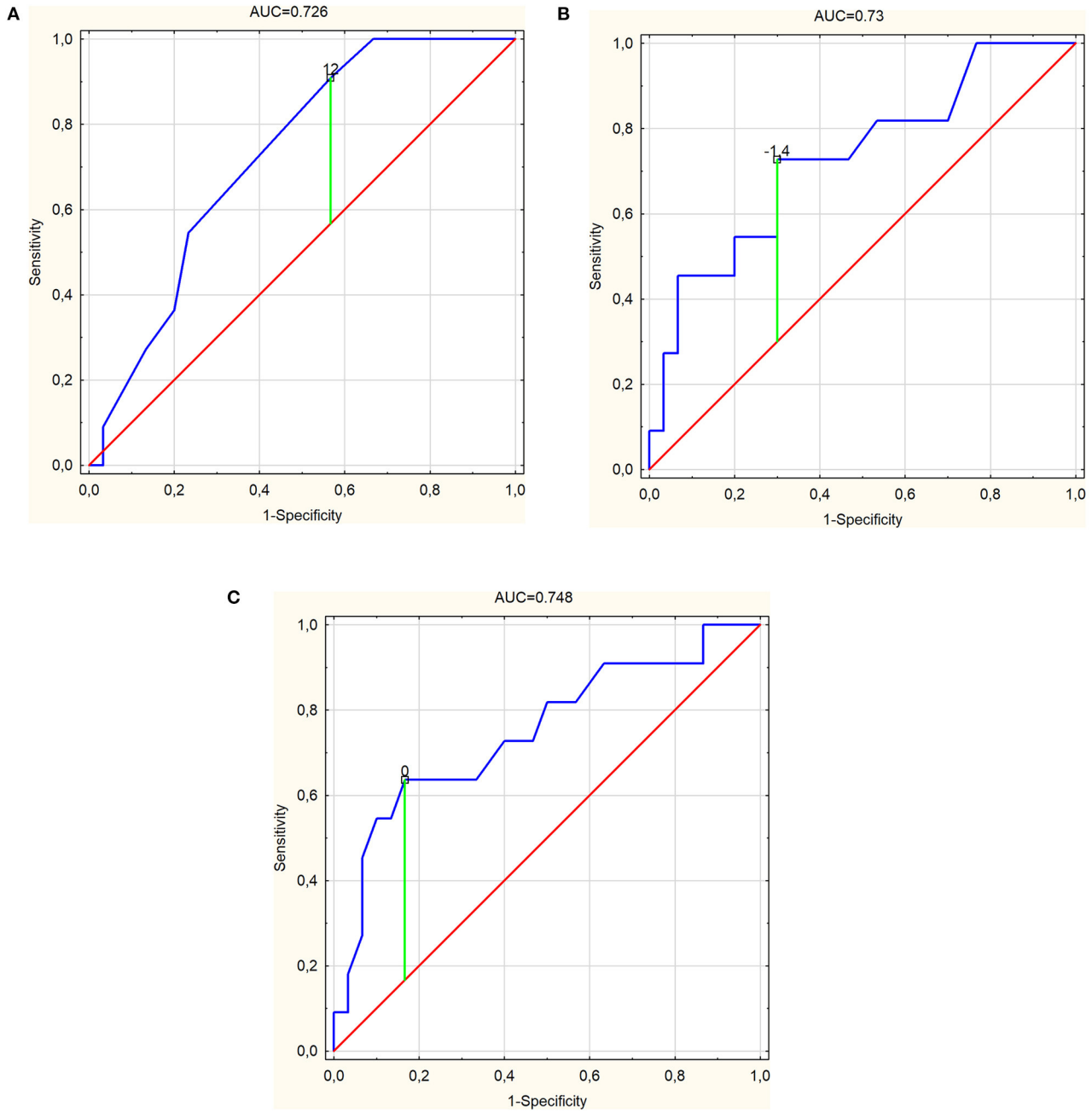

FIGURE 2 | Receiver operating characteristic curve graphs of **(A)** frontal assessment battery [area under the ROC curve (AUC) = 0.726], **(B)** frontal lobe (AAL) (L) (AUC = 0.73), and **(C)** superior frontal gyrus, dorsolateral (AAL) (L) (AUC = 0.748) as independent predictors for progressive supranuclear palsy-parkinsonism predominant with marked cutoff values.

with cutoff value equal to −2.2 and sensitivity, specificity, PPV, NPV, and ACC at 75, 95.7, 90, 88, and 88.6%, respectively (**Figure 3B**). The highest value of AUC (0.749; 95% CI, 0.601–0.896; $p = 0.001$) was calculated for superior frontal gyrus dorsolateral (AAL) L (**Figure 3F**), with slightly higher values of sensitivity and NPV but with lower values of specificity, PPV, and ACC (**Table 2**).

Logistic Regression

Unfortunately, for PSP-RS, it was not possible to build a model based on logistic regression in any combination of the available variables. In the case of PSP-P and CBS, models were successfully built, but only based on single variables. Any other combination and adding of the next variables did not bring any statistically significant changes. For PSP-P, the FAB turned out to be an

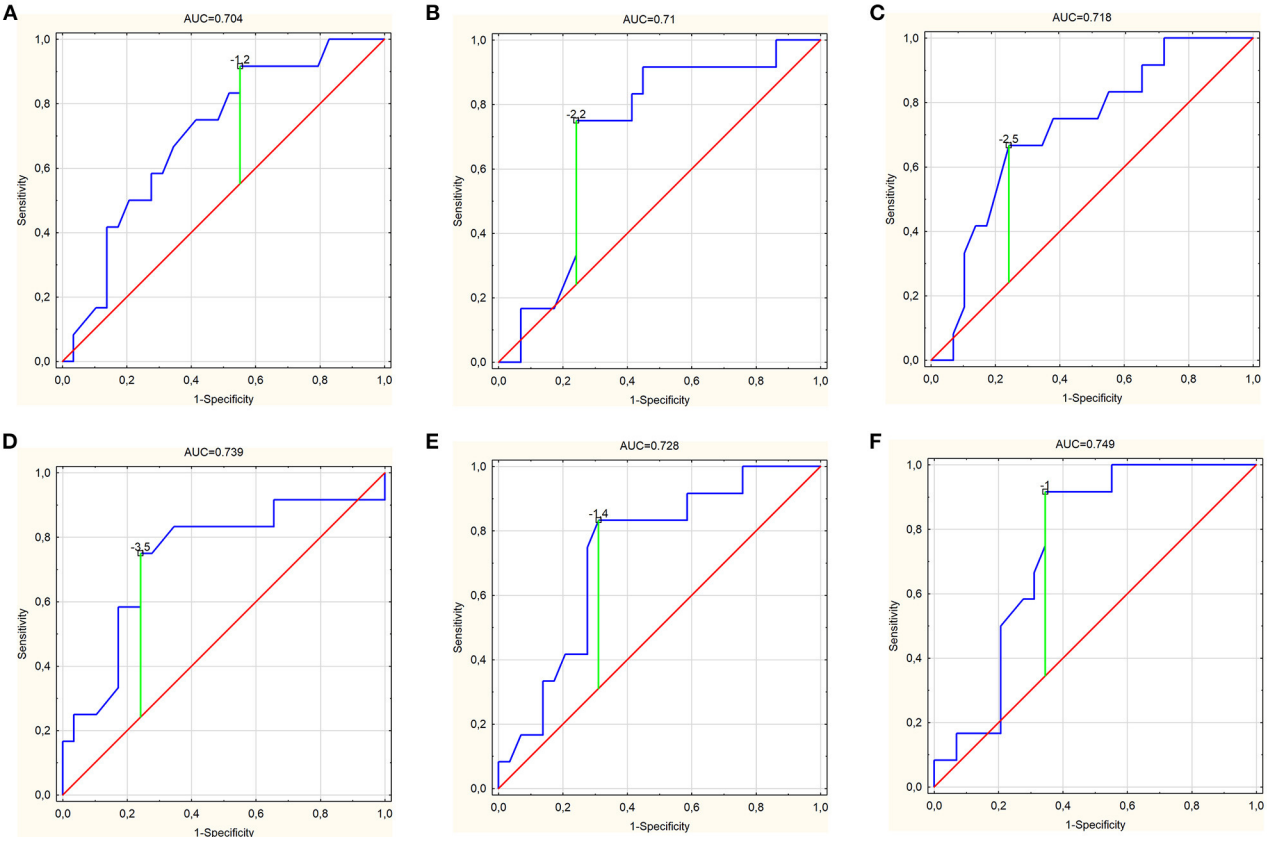

FIGURE 3 | Receiver operating characteristic curve graphs of **(A)** frontal lobe [area under the ROC curve (AUC) = 0.704], **(B)** frontal lobe (AAL) (L) (AUC = 0.71), **(C)** frontal lobe—Atlas 1 (AUC = 0.718), **(D)** inferior frontal gyrus, opercular part (AAL) (L) (AUC = 0.739), **(E)** middle frontal gyrus (AAL) (L) (AUC = 0.728), and **(F)** superior frontal gyrus, dorsolateral (AAL) (L) (AUC = 0.749) as independent predictors for corticobasal syndrome with marked cutoff values.

important parameter, with OR of 29.3 (95% CI, 2.6–336.4; $p = 0.0311$) and with diagnostic accuracy of 72.4%. On the other hand, superior frontal gyrus dorsolateral (AAL) L was an important parameter for CBS with OR of 6.0 (95% CI, 1.1–33.4; $p = 0.0218$) and with diagnostic accuracy of 82.6% (**Table 3**).

TABLE 3 | Logistic regression analysis of progressive supranuclear palsy-parkinsonism predominant (PSP-P) and corticobasal syndrome (CBS) in relation to single-photon emission computed tomography and frontal assessment battery parameters.

		OR	95% CI	*p*	ACC
FAB	PSP-P	29.3	2.6–336.4	0.0311	72.4
(15) Superior frontal gyrus, dorsolateral (AAL) (L)	CBS	6.0	1.1–33.4	0.0218	82.6

p for logistic regression.
OR, odds ratio; CI, confidence interval; ACC, accuracy.

DISCUSSION

PSP-P as an Important Entity in Differential Diagnosis

To the best of our knowledge, this is the first study to evaluate the examination of frontal lobe as a possible factor differentiating variants of PSP in a combined neuropsychological and perfusion assessment perspective. Our data confirm the clinical variability among patients with the two main subtypes of PSP. As the obtained results show, the impairment in executive functions could be a significant factor in the differential diagnosis of PSP variants. The analysis of the results indicate that the dysexecutive syndrome in the parkinsonian variant (PSP-P) might be less severe than in PSP-RS, with the FAB scores oscillating rather above 12 in the first and under 12 in the latter. Such differences could be correlated to distinct tau distribution in the course of PSP in each of its variants (5). Our findings are congruent with observations made by Pellicano et al. who reported some significant differences in executive functioning in PSP-P vs. PSP-RS patients (19). The lack of additional role of combined examination in FAB and SPECT seems to be a consequence of the limited specificity of the methods and the assessment being limited to the frontal lobe rather than the lack of differences between these two entities. Previous studies showed more severe volume loss in PSP-RS within the frontal pole and inferior frontal gyrus in the volumetric analysis (5). In our study, significant differences between PSP-P and PSP-RS were observed within the superior frontal gyrus medial

of the dominant hemisphere. It should also be stressed that, in the majority of works, the abnormalities in PSP-P were rarely observed within the frontal lobe (16). Additionally, more differences were observed in the comparison of perfusion of PSP-P and CBS. This observation, in association with the lack of significant differences between PSP-RS and CBS, shows that perfusion in PSP-P is least deteriorated when evaluating all three entities. The results comparing PSP-P and PSP-RS, on one hand, come up with the findings showing a more beneficial course of the disease and the necessity of evaluating these variants as separate entities (20). The obtained results show that more research in the field involving larger groups of patients should be conducted. Previous studies of SPECT in PSP-P and PSP-RS did not highlight the issue of perfusion; however, an analysis concerning the dopaminergic degeneration in both entities was conducted. In a study evaluating groups of patients with PSP-P—four patients, PSP-RS—six patients, and PD−10 patients, the authors used alternative sets of SPECT—dopamine transporter and I-iodobenzamide D2 receptor radiotracer in each case. The first radiotracer showed significant differences in the putamen-to-caudate ratio between PD and PSP groups (without discriminating variants of PSP). The radiotracer indicating D2 receptor was found to be feasible in the differentiation of PSP-RS and PSP-P as the striatal uptake was reduced in PSP-RS and mildly increased in PSP-P (21). The obtained results, though based on relatively small groups of patients, show that assessment in executive functions using FAB is possibly useful in the differential diagnosis of PSP-P and PSP-RS with similar durations.

The Boundaries Between PSP-RS and CBS

This study, though presenting minor differences between PSP-RS and CBS, shows that FAB and assessments of perfusion in SPECT present slightly more severe deterioration in CBS. The differences cannot be interpreted as evident as the significant differences in SPECT were observed only in one of the parameters, frontal lobe—Atlas 1 (an area automatically indicated by Scenium software). All other evaluations of the frontal lobe in SPECT did not provide significant differences. This difference does not significantly impact the clinical manifestation and the doubtful boundaries between PSP-RS and CBS. This could be partially explained by similarities of perfusion in the vast majority of ROIs. The combined assessment using FAB and SPECT examination of frontal perfusion does not provide an additional tool in differential diagnosis. The finding confirms the questionable boundaries between the clinical syndromes (1, 7).

However, considering the variety of possible manifestations of CBS, a further research considering the use of other neuropsychological assessment methods should be done. The frontal–executive variant may, in fact, be hardly distinguished from PSP-RS. The other variants of CBS though (the variants with apraxia, aphasia, or visuospatial deficits dominating the clinical manifestation) (13, 15) should be distinguished.

Earlier evaluations of PSP and CBS generally did not discriminate the variant PSP-RS, which could deviate possible findings. In a study analyzing iodine-123-labeled FP-CIT SPECT, the authors indicated high sensitivity in the examination of PSP (22). The work did not take into account the heterogeneity of PSP. A work examining patients with PD, MSA-P, and PSP showed no significant differences between PD and PSP (23). The utility of dopamine transporter SCAN (DaTSCAN) is interpreted as limited in the examination of PSP. The limitations of DaTSCAN in the examination of PSP are related with the lack of differential impact in the examination of Parkinson's disease and atypical parkinsonism (24). The DaTSCAN of a patient with PSP and CBS was also found to lack differences with that of a patient affected by progressive apraxia of speech (25).

Limitations

This study is based on the examination of relatively small groups of patients, which is a result of examining rare entities in a single department. The authors of this study are aware that the methods used in the study are non-specific, should be interpreted as possible supplementary tools, and cannot be evaluated independently when making the diagnosis. The disproportion of the number of males and females in the CBS group is a result of the need to exclude patients who did not fulfill all of the examinations planned in the study. Another limitation associated with this investigation is that the increase in familywise error rate across the reported statistical analyses was not controlled. Overall, we consider this research as a pilot study and encourage replication. The aim of the study was to choose tools which could be accessible in everyday practice.

CONCLUSIONS

1. Neuropsychological examinations of patients based on the FAB tool is important and can be helpful in the diagnosis of the subtypes of PSP: PSP-RS and PSP-P.
2. For CBS, SPECT shows greater differences of mean variance values from the neutral level in comparison to PSP-RS and PSP-P. This may be related to a more severe clinical course compared to PSP.
3. Currently, basing on the study group, the multiparametric assessment of patients with PSP-RS, PSP-P, and CBS based on SPECT features and FAB has not achieved greater overall performance than the single-parameter assessment. This implies a need for discerning clinical evaluation of the patient by an experienced clinician during the diagnostic process and use of SPECT and FAB as accessory tools.

DATA AVAILABILITY STATEMENT

The raw data supporting the conclusions of this article will be made available by the authors, without undue reservation.

ETHICS STATEMENT

The studies involving human participants were reviewed and approved by Ethical Committee of the Medical University of Warsaw. The patients/participants provided their written informed consent to participate in this study.

AUTHOR CONTRIBUTIONS

PA study design, data analysis, review of literature, and discussion. BM data analysis, statistical analysis, and discussion. NM data analysis, review of literature, and discussion. KD-W, AD, LK, and AF data analysis and discussion. IC, AS, and MS data analysis. All authors contributed to the article and approved the submitted version.

REFERENCES

1. Respondek G, Grimm MJ, Piot I, Arzberger T, Compta Y, Englund E, et al. Movement disorder society-endorsed progressive supranuclear palsy study group. validation of the movement disorder society criteria for the diagnosis of 4-repeat tauopathies. *Mov Disord.* (2020) 35:171–6. doi: 10.1002/mds.27872
2. Höglinger GU, Respondek G, Stamelou M, Kurz C, Josephs KA, Lang AE, et al. Clinical diagnosis of progressive supranuclear palsy: the movement disorder society criteria. *Mov Disord.* (2017) 32:853–64. doi: 10.1002/mds.26987
3. Armstrong MJ, Litvan I, Lang AE, Bak TH, Bhatia KP, Borroni B, et al. Criteria for the diagnosis of corticobasal degeneration. *Neurology*. (2013) 80:496–503. doi: 10.1212/WNL.0b013e31827f0fd1
4. Dabrowska M, Schinwelski M, Sitek EJ, Muraszko-Klaudel A, Brockhuis B, Jamrozik Z, et al. The role of neuroimaging in the diagnosis of the atypical parkinsonian syndromes in clinical practice. *Neurol Neurochir Pol.* (2015) 49:421–31. doi: 10.1016/j.pjnns.2015.10.002
5. Schofield EC,Hodges JR, Macdonald V, Cordato NJ, Kril JJ, Halliday GM. Cortical atrophy differentiates Richardson's syndrome from the parkinsonian form of progressive supranuclear palsy. *Mov Disord*. (2011) 26:256–63. doi: 10.1002/mds.23295
6. Alster P, Nieciecki M, Koziorowski DM, Cacko A, Charzyńska I, Królicki L, et al. Thalamic and cerebellar hypoperfusion in single photon emission computed tomography may differentiate multiple system atrophy and progressive supranuclear palsy. *Medicine.* (2019) 98:e16603. doi: 10.1097/MD.0000000000016603
7. Alster P, Nieciecki M, Koziorowski D, Cacko A, Charzyńska I, Królicki L, et al. Is brain perfusion a differentiating feature in the comparison of Progressive Supranuclear Palsy Syndrome (PSPS) and Corticobasal Syndrome (CBS)? *J Clin Neurosci.* (2020) 77:123–7. doi: 10.1016/j.jocn.2020.05.005
8. Van Laere K, Casteels C, De Ceuninck L, Vanbilloen B, Maes A, Mortelmans L, et al. Dual-tracer dopamine transporter and perfusion SPECT in differential diagnosis of parkinsonism using template-based discriminant analysis. *J Nucl Med.* (2006) 47:384–92.
9. Antonini A, Leenders KL, Vontobel P, Maguire RP, Missimer J, Psylla M, et al. Complementary PET studies of striatal neuronal function in the differential diagnosis between multiple system atrophy and Parkinson's disease. *Brain*. (1997) 120(Pt 12):2187–95. doi: 10.1093/brain/120.12.2187
10. Bosman T, Van Laere K, Santens P. Anatomically standardised 99mTc-ECD brain perfusion SPET allows accurate differentiation between healthy volunteers, multiple system atrophy and idiopathic Parkinson's disease. *Eur J Nucl Med Mol Imaging*. (2003) 30:16–24. doi: 10.1007/s00259-002-1009-9
11. Feigin A, Antonini A, Fukuda M, De Notaris R, Benti R, Pezzoli G, et al. Tc-99m ethylene cysteinate dimer SPECT in the differential diagnosis of parkinsonism. *Mov Disord*. (2002) 17:1265–70. doi: 10.1002/mds.10270
12. Dubois B, Slachevsky A, Litvan I, Pillon B. The FAB. A frontal assessment battery at bedside. *Neurology*. (2000) 55:1621–6. doi: 10.1212/WNL.55.11.1621
13. Sitek E, Wójcik J, Barczak A, Sławek J. Diagnostyka neuropsychologiczna w atypowych zespołach parkinsonowskich. *Pol Przeg Neurol.* (2015) 11:21–32.
14. Cohen OS, Vakil E, Tanne D, Molshatzki N, Nitsan Z, Hassin-Baer S. The frontal assessment battery as a tool for evaluation of frontal lobe dysfunction in patients with parkinson disease. *J Geriatr Psychiatr Neurol.* (2012) 25:71–7. doi: 10.1177/0891988712445087
15. Drzewińska A. Zaburzenia poznawcze i emocjonalne" in Choroba Parkinsona. Od mechanizmów do leczenia., ed. A. Friedman (Warszawa: PZWL) (2019). p. 71–91.
16. Alster P, Madetko N, Koziorowski D, Friedman A. Progressive supranuclear palsy-parkinsonism predominant (PSP-P)-a clinical challenge at the boundaries of PSP and Parkinson's Disease (PD). *Front Neurol.* (2020) 11:180. doi: 10.3389/fneur.2020.00180
17. Alster P, Madetko NK, Koziorowski DM, Królicki L, Budrewicz S, Friedman A. Accumulation of tau protein, metabolism and perfusion-application and efficacy of positron emission tomography (PET) and single photon emission computed tomography (SPECT) Imaging in the examination of progressive supranuclear palsy (PSP) and corticobasal syndrome (CBS). *Front Neurol.* (2019) 10:101. doi: 10.3389/fneur.2019.00101
18. El Fakhri G, Habert MO, Maksud P, Kas A, Malek Z, Kijewski MF, et al. Quantitative simultaneous (99m)Tc-ECD/123I-FP-CIT SPECT in Parkinson's disease and multiple system atrophy. *Eur J Nucl Med Mol Imaging.* (2006) 33:87–92. doi: 10.1007/s00259-005-1920-y
19. Pellicano C, Assogna F, Cellupica N, Piras F, Pierantozzi M, Stefani A, et al. Neuropsychiatric and cognitive profile of early Richardson's syndrome, Progressive Supranuclear Palsy-parkinsonism and Parkinson's disease. *Parkinson Related Disord.* (2017) 45:50–56. doi: 10.1016/j.parkreldis.2017.10.002
20. Shoeibi A, Litvan I, Tolosa E, Ser TD, Lee E, TAUROS Investigators. Progression of two progressive supranuclear palsy phenotypes with comparable initial disability. *Parkinsonism Relat Disord.* (2019) 66:87–93. doi: 10.1016/j.parkreldis.2019.07.010
21. Lin WY, Lin KJ, Weng YH, Yen TC, Shen LH, Liao MH, et al. Preliminary studies of differential impairments of the dopaminergic system in subtypes of progressive supranuclear palsy. *Nucl Med Commun.* (2010) 31:974–80. doi: 10.1097/MNM.0b013e32833e5f90
22. Sakamoto F, Shiraishi S, Kitajima M, Ogasawara K, Tsuda N, Tomiguchi S, et al. Diagnostic performance of ^{123}I-FPCIT SPECT specific binding ratio in progressive supranuclear palsy: use of core clinical features and MRI for comparison. *AJR Am J Roentgenol.* (2020) 6:1–6. doi: 10.2214/AJR.19.22436
23. Murakami N, Sako W, Haji S, Furukawa T, Otomi Y, Otsuka H, et al. Differences in cerebellar perfusion between Parkinson's disease and multiple system atrophy. *J Neurol Sci.* (2020) 409:116627. doi: 10.1016/j.jns.2019.116627
24. Shigekiyo T, Arawaka S. Laterality of specific binding ratios on DAT-SPECT for differential diagnosis of degenerative parkinsonian syndromes. *Sci Rep.* (2020) 10:15761. doi: 10.1038/s41598-020-72321-y
25. Seckin ZI, Whitwell JL, Utianski RL, Botha H, Ali F, Duffy JR, et al. Ioflupane 123I (DAT scan) SPECT identifies dopamine receptor dysfunction early in the disease course in progressive apraxia of speech. *J Neurol.* (2020) 267: 2603–11. doi: 10.1007/s00415-020-09883-4

Conflict of Interest: The authors declare that the research was conducted in the absence of any commercial or financial relationships that could be construed as a potential conflict of interest.

frontiers in Psychiatry

PERSPECTIVE
published: 29 July 2021
doi: 10.3389/fpsyt.2021.705242

Utility of SPECT Functional Neuroimaging of Pain

Mohammed Bermo[1], Mohammed Saqr[2,3], Hunter Hoffman[4], David Patterson[4], Sam Sharar[4], Satoshi Minoshima[5] and David H. Lewis[4]*

[1] Virginia Tech Carilion School of Medicine, Roanoke, VA, United States, [2] School of Computing, University of Eastern Finland, Joensuu Campus, Joensuu, Finland, [3] EECS - School of Electrical Engineering and Computer Science, Media Technology & Interaction Design, KTH Royal Institute of Technology, Stockholm, Sweden, [4] University of Washington, Seattle, WA, United States, [5] The University of Utah, Salt Lake City, UT, United States

Functional neuroimaging modalities vary in spatial and temporal resolution. One major limitation of most functional neuroimaging modalities is that only neural activation taking place inside the scanner can be imaged. This limitation makes functional neuroimaging in many clinical scenarios extremely difficult or impossible. The most commonly used radiopharmaceutical in Single Photon Emission Tomography (SPECT) functional brain imaging is Technetium 99 m-labeled Ethyl Cysteinate Dimer (ECD). ECD is a lipophilic compound with unique pharmacodynamics. It crosses the blood brain barrier and has high first pass extraction by the neurons proportional to regional brain perfusion at the time of injection. It reaches peak activity in the brain 1 min after injection and is then slowly cleared from the brain following a biexponential mode. This allows for a practical imaging window of 1 or 2 h after injection. In other words, it freezes a snapshot of brain perfusion at the time of injection that is kept and can be imaged later. This unique feature allows for designing functional brain imaging studies that do not require the patient to be inside the scanner at the time of brain activation. Functional brain imaging during severe burn wound care is an example that has been extensively studied using this technique. Not only does SPECT allow for imaging of brain activity under extreme pain conditions in clinical settings, but it also allows for imaging of brain activity modulation in response to analgesic maneuvers whether pharmacologic or non-traditional such as using virtual reality analgesia. Together with its utility in extreme situations, SPECTS is also helpful in investigating brain activation under typical pain conditions such as experimental controlled pain and chronic pain syndromes.

Keywords: SPECT, pain, ECD, brain, functional imaging

OPEN ACCESS

Edited by:
Theodore A. Henderson, Consultant, Denver, CO, United States

Reviewed by:
Eric Guedj, Aix-Marseille Université, France
Catherine Faget, Assistance Publique Hôpitaux de Marseille, France

****Correspondence:***
Mohammed Bermo
Mohammed.bermo@gmail.com

Specialty section:
This article was submitted to Neuroimaging and Stimulation, a section of the journal Frontiers in Psychiatry

Received: *04 May 2021*
Accepted: *30 June 2021*
Published: *29 July 2021*

Citation:
Bermo M, Saqr M, Hoffman H, Patterson D, Sharar S, Minoshima S and Lewis DH (2021) Utility of SPECT Functional Neuroimaging of Pain. Front. Psychiatry 12:705242. doi: 10.3389/fpsyt.2021.705242

INTRODUCTION

Pain is one of the most challenging clinical entities in medicine. Developments in non-invasive functional brain imaging techniques in the last few decades such as Single Photon Emission Computed Tomography (SPECT), Positron Emission Tomography (PET) and functional Magnetic Resonance Imaging (fMRI) have significantly added to the scientific knowledge about the mechanism of brain processing of pain signals and how it is modulated by different analgesic interventions (1, 2).

Functional brain imaging studies vary in design and investigated target. Receptor imaging studies such as Serotonin and Nicotinic Receptors do not provide temporal information.

Fluorodeoxyglucose (FDG) PET utilizes glucose metabolism as a surrogate of neuronal activity. FDG is continuously taken in by the neurons during the uptake time (time between injection and scanning, typically 30–90 min) and does not provide useful temporal information for shorter-lived events such as acute pain or epilepsy. The majority of functional neuroimaging techniques focus on detecting changes in regional blood flow as a surrogate of neuronal activation. fMRI measures/images changes in brain activation while the subject is inside the scanner. fMRI allows real time imaging of brain functional changes during minor or experimental pain experiences with a relatively good temporal resolution. But has limited utility for imaging of severe clinical pain that occurs when the patient is not in the brain scanner, (e.g., during painful medical procedures). It would be difficult or unethical to have the patient inside the scanner during the event. For example, you cannot perform painful wound debridement on a severe burn patient that is in the fMRI borehole (and the patient would have trouble keeping their head very still during the scan, as required to avoid motion artifacts). Similarly, it is difficult to obtain good fMRI brain scans of an epilepsy patient while they are having a seizure due to timing challenges and motion artifacts.

Brain perfusion SPECT using commercially available radiotracers has a unique characteristic that allows freezing an image of brain activation at the time of injection, which can be done in virtually any clinical scenario (e.g., during painful medical procedures conducted outside of the brain scanner, or they can get injected during unpredictable onset epileptic seizures as they are laying in their hospital beds, and the snapshot of brain perfusion at the time of injection is temporarily stored in their brain and can be imaged 1 or 2 h later. This brain activation pattern can be converted into a computer image after the painful event is over, when the patient can be transported and can stay still in the scanner. The concept of freezing an image of pain-related brain activity that can be imaged later is clinically useful in designing functional brain imaging studies where fMRI is not possible due to MRI unfriendly or incompatible clinical circumstances (3), e.g., all virtual reality equipment used in the fMRI scanner must be non-ferrous and non-conductive.

Brain SPECT is a simple technique with minimal stress to the patients. It involves only intravenous administration of a radioisotope during the painful event (e.g., the medical procedure, seizure, or spike in chronic pain) then later laying still in a relatively quiet scanner. Radiation dose varies depending on the radiotracer used and whether an additional low dose CT is used for anatomic localization and attenuation correction to facilitate quantification (4).

Multiple radiotracers have been developed with different purposes; to understand normal brain physiology, to detect static or slowly dynamic brain changes in pathologic conditions, and to investigate brain functional changes at selected time points under natural or experimental pathologic conditions with and without medical interventions. The aim of these studies is to improve our understanding of normal brain function and physiopathological mechanisms of neuropsychiatric diseases. Interpretation of these studies can be either purely qualitative or can provide quantitative/semi-quantitative information (5–7).

SPECT VS. PET

Compared to PET, SPECT images suffer from limited spatial resolution. This is partially inherent in the physics of the technique, however there have been significant improvements in SPECT spatial resolution with the introduction of high sensitivity solid state detectors such as Cadmium zinc telluride (CTZ) and Cesium Iodide (CsI) as compared to a conventional Anger camera (8).

Temporal resolution is an important factor in designing functional brain studies. Temporal characteristics of functional brain imaging with PET varies with the radiotracer used and the image acquisition technique. Oxygen-15 (^{15}O) gas inhalation or labeled water (^{15}O-water) infusion has been used as perfusion agents to study experimental brain activation. ^{15}O has a very short half-life (∼2 min) requiring onsite cyclotron, a complicated imaging setup, and is limited to brain activity that can take place inside the PET scanner only. The most commonly used isotope in PET imaging, Fluorine-18(^{18}F) is commercially available with a half-life of about 110 min, eliminating the requirement for an onsite cyclotron. In traditional FDG-PET imaging, using the most popular tracer paralleling glucose metabolism (^{18}F-labeled FDG), there is continuous uptake of the tracer by the neurons during the time between radiotracer injection and imaging (the uptake time, typically 30–90 min), which limits its utility to imaging of prolonged brain activity experiences such as interictal imaging of epilepsy, prolonged pain, or placing the patient into a predesigned activation status such as virtual reality (9), walking (10), or prolonged olfactory stimulation (11) during the uptake time. Ripp et al. (12) tested dual time point acquisition of baseline brain metabolism and metabolism with predesigned activation after single FDG injection. There have been recent reports for redesigned FDG-PET functional brain imaging studies with constant infusion of the radiotracer while the patient is inside the scanner and acquiring dynamic images, a technique called functional PET (fPET) (13–15). fPET might gain popularity with the introduction of new high efficiency total body PET scanners and improved time resolution of the camera. The major limitations of fPET are the radiation dose penalty -compared to fMRI which does not use ionizing radiation- and the "activation in the scanner" requirement (16, 17).

SPECT RADIOPHARMACEUTICALS

The two most commonly used radiotracers to evaluate brain perfusion using SPECT are Technetium-99 m (^{99m}Tc) labeled Hexamethylpropylene Amine Oxime (HMPAO) and Ethyl Cysteinate Dimer (ECD). Both agents have very similar imaging characteristics, however ECD is more popular due its longer shelf life that is very helpful in designing studies when the patient cannot be inside the scanner at the expected time of brain activation, and more importantly when the time of desired brain activity when radiotracer injection is required cannot be predicted, such as ictal epilepsy or migraine studies.

ECD is a lipophilic compound that moves across the blood-brain barrier efficiently and has a high first pass uptake by a normal brain proportional to regional cerebral blood flow

with the maximum peak activity reached within 1–2 min after intravenous injection. No significant further radiotracer uptake by the brain takes place a few minutes after intravenous injection. Once taken in by the neurons, it is rapidly de-esterified to a polar metabolite that does not cross the blood brain barrier back and is retained within the brain. ECD does not undergo redistribution within the brain and the gray/white matter activity ratio remains consistently high within the imaging window as measured from multiple sequential SPECT studies. ECD clearance from the brain is relatively so slow that the intracerebral distribution is almost fixed during the time period required inside the scanner. Clearance of ECD from the brain follows a biexponential mode: 40% percent of the brain activity is cleared with a biological half-life of 1.3 h while the remaining activity is cleared slowly with a biological half-life of 42.3 h. There is an additional exponential decay of radiotracer activity with a physical half-life of 6 h. Blood pool activity is cleared rapidly, resulting in high target to background ratio that leads to good quality images starting shortly after injection. ECD demonstrates rapid clearance from facial muscles and salivary glands, further improving image quality. Rapid lung clearance further reduces background activity and improves the brain to soft tissue ratio. The main route of excretion is through the kidneys with a small fraction cleared through hepatobiliary system. The critical organ is the urinary bladder wall (18–23).

IMAGE RECONSTRUCTION

There is no standardized technique for SPECT image reconstruction and viewing. The most commonly used steps involve normalizing measured activity to global brain activity and spatially registering each individual brain to a standard space to eliminate individual differences in the configuration of the brain. Statistical analysis is then performed via voxel by voxel comparison to a normal database. The two most commonly used software packages for image processing and display are Statistical Parametric Mapping (SPM) and Three-Dimensional Stereotactic Surface Projection (3D-SSP). SPM utilizes the *t*-test for analysis of results in high specificity but low sensitivity. 3D-SSP analyzes blood flow to the brain surface (1, 24).

IMAGING OF PAIN

Functional brain studies allow non-invasive assessment of regional brain activity, generally using blood flow or metabolism as a surrogate of neuronal activity. Advances in functional brain imaging in the last few decades has provided cumulative knowledge about the central mechanisms involved in perception of pain and modulation of this activity by different pharmacologic and non-pharmacologic analgesic interventions (25–27).

Pain is a basic human sensation and an important warning tool against serious conditions. Pain is generally induced by tissue damage or neural pathway abnormality (neuropathic pain). Pain can be acute, chronic, or episodic. Pain is also a complex experience that does not include merely nociception of a stimulus causing sensory input, but is further modified by genetic factors, cultural and environmental factors, memory, circumstantial expectations, anticipation, emotional background, empathy, alertness, motivation, degree of attention vs. distraction, cognitive interpretation and active attempts at modulation of pain perception. Given the diverse nature of human pains and the difficulty to design a study paradigm that completely accommodates for the emotional, cognitive and sensorimotor changes usually associated with the pain experience, it is expected that not all pain experiments will demonstrate the same pattern of brain activation (28–34).

The full anatomic and physiologic process of pain signal processing is not completely understood. The process involves a large network including cortical and subcortical regions. The regions reported to be most consistently activated in functional brain studies during acute pain include the midbrain, thalamus, hypothalamus, amygdala, anterior cingulate cortex, prefrontal region, insula, orbito-frontal cortex, and primary and secondary somatosensory cortices. The term "pain matrix" is commonly used to refer to these regions collectively. Increased regional blood flow in these regions is correlated with the subjective rating of the painful stimuli. The subjective pain experience is further influenced by contextual cortical modulations and the descending pain modulatory system, which can exert inhibitory control at the dorsal horn of the spinal cord to modulate nociceptive input. In other words, the brain can send signals down to the spinal cord, which reduce (or in some cases increase) the amount of nociceptive signals allowed to travel from the spinal cord to the brain. This control system has a cortical component at the anterior cingulate and prefrontal cortex and subcortical components at certain brainstem nuclei (3, 25, 34–39). A small but important study in two subjects who are "pain-free" due to SCN9A mutation, showed activation of the pain matrix during laboratory mechanical pain applied to the dorsum of their hand, similar to response in 4 normal control subjects (40). Further study in this area of understanding the "pain-matrix" for acute pain is needed.

A pain processing network model by Garcia et al. (29) suggested that pain is processed at three levels, at an unconscious level processed in peri-Rolandic cortex and limbic system receiving afferent spinothalamic pain signals, at an intermediate awareness level processed at fronto-cingulate-parietal networks in addition to the sensorimotor cortices, and at a higher conscious extended level which includes adding input from memories and self-awareness. The comprehensive pain experience processing network appears to include more regions with contribution from other cortical and subcortical cerebral regions such as the brain stem and the cerebellum (3, 29).

CHRONIC PAIN

Chronic pain syndrome is a difficult clinical entity that is not completely understood. Some studies suggested that dysfunctional coordination between ascending and descending pain pathways plays a major role in the pathophysiology of

chronic pain syndrome. Brain activation appears to be different in chronic pain compared to acute pain (25, 41).

Nakamura et al. (4), recruited low back pain patients with no significant abnormalities in the lumbar spine detected during MRI and reported significantly decreased blood flow in the bilateral prefrontal cortex in patients with chronic low back pain compared to patients with acute low back pain. In a controlled study of 12 patients with chronic pain using ECD SPECT, Nakabeppu et al. (41) reported a significant decrease in blood perfusion in the thalamus bilaterally in chronic pain patients compared to their control counterparts. Honda et al. (1) studied 15 chronic pain patients using SPECT and reported reduction in rCBF in several brain areas (e.g., prefrontal area, right orbitofrontal cortex, anterior cingulate gyrus).

FIBROMYALGIA (FM)

Several studies have demonstrated the role of ECD brain perfusion SPECT in imaging of brain activity changes in Fibromyalgia (FM) patients before and after therapy (42–50). Chen et al. studied 91 patients with FM and reported reduction in blood flow in the temporoparietal and frontal regions in addition to the thalamus and basal ganglia (42). In a study of fibromyalgia patients, baseline thalamic blood flow was decreased below normal age matched database. Thalamic blood flow improved after electroconvulsive therapy (ECT), this improvement was correlated with subjective reporting of improved level of pain (47).

In a controlled study of 18 hyperalgesic FM female patients, Guedj et al. reported significant hypoperfusion in the somatosensory cortex as well as frontal, cingulate, medial temporal and cerebellar cortices (50). In another study of 20 Fibromyalgia patients, the same group studied the correlation between cerebral blood flow and pain using several self-reported pain measurement as well as depression and anxiety scales. They reported that the clinical severity of the disease was correlated with abnormalities of blood flow (43). The authors suggested that SPECT can guide therapeutic strategies for patients as an objective measure. In two other studies, the same group reported that SPECT predicted analgesic response to ketamine in hyperalgesic FM patients. The authors showed a significant hyperperfusion in midbrain periaqueductal gray in patients reporting reduction in subjective pain after Ketamine (responders) vs. non-responders (49) while non-responders exhibited a significant hypoperfusion in bilateral medial frontal gyri (50).

Usui et al. reported rCBF abnormalities in FM patients compared to their control counterparts including decreased perfusion at the left culmen and increased perfusion in the right posterior cingulate, precentral, superior occipital, and middle temporal gyri and right cuneus, and increased perfusion at the left superior and inferior parietal lobules and postcentral gyrus. Furthermore, patients with good response to gabapentin demonstrated significant hypoperfusion in the right medial frontal gyrus, left insula, left inferior frontal gyrus, and left culmen and increased perfusion in the left superior frontal and postcentral gyri while poor responders demonstrated significant decreased perfusion to the left orbital gyrus and hyperperfusion in the right precentral and postcentral, posterior cingulate, and superior temporal gyri, right precuneus, right inferior parietal lobule, and left middle frontal and middle occipital gyri (48).

Episodic Pain

Ictal perfusion SPECT imaging has been used for presurgical evaluation of epilepsy patients for decades. Subtracting interictal from ictal SPECT perfusion studies and overlying the subtraction results on structural imaging, particularly MRI, is the most accurate functional imaging technique for localizing the seizure onset zone in patient with epilepsy (51, 52). A rare form of seizure is Ictal pain. While epileptic pain is usually associated with other seizure symptoms, sometimes pain is the only symptom of epilepsy. It can be unilateral or bilateral, pain location varies, most commonly in the head and neck or abdomen (53).

The unique characteristic of SPECT tracers makes it feasible to study regional perfusion changes in other episodic pain syndromes such as migraine during the attack (ictal) and between the attacks (interictal). Similar to epilepsy ictal SPECT studies, ictal migraine study setup is challenging and requires patient hospitalization and exposure to potential migraine triggers with a trained nurse available by the patient's side ready to inject the radiotracer as soon as the patient starts to experience the migraine aura. The longer shelf life of the ECD compound compared to HMPAO is very helpful in these situations as the waiting time is unpredictable. Significantly reduced rCBF at the thalamus on SPECT has been reported in two patients with ophthalmoplegic migraine (54) and in a child with hemiplegic migraine (55). It is not clear, however, if the changes in regional blood flow associated at the ictal phase of migraine is related to the primary etiology or is a secondary phenomenon (56).

Response to Therapy

Brain perfusion SPECT has been used to study not only brain activation with pain, but also modulation of this activity under pharmacologic and non-pharmacologic analgesic interventions. In addition to the previously discussed studies demonstrating blood flow changes in response to therapy in FM patients, Trucco et al. (57) demonstrated reversal of perfusion abnormality on brain perfusion SPECT in migraine patients under pharmacologic therapy. Newberg et al. (58) reported asymmetric thalamic blood flow in acute postoperative dental pain, this perfusion abnormality improved in patients receiving successful analgesic treatment (**Figure 1**). A study of brain perfusion SPECT in the setting of severe clinical pain during burn wound cleaning/debridement demonstrated intense activation of the cerebellum, this activation was reversed in the same patients when using immersive virtual reality analgesia in a different session (59).

A study evaluating the effect of analgesic acupuncture on regional blood flow demonstrated a significant asymmetric uptake in the thalami in pain patients compared to controls. This abnormal thalamic flow was normalized in the post acupuncture therapy scan (60).

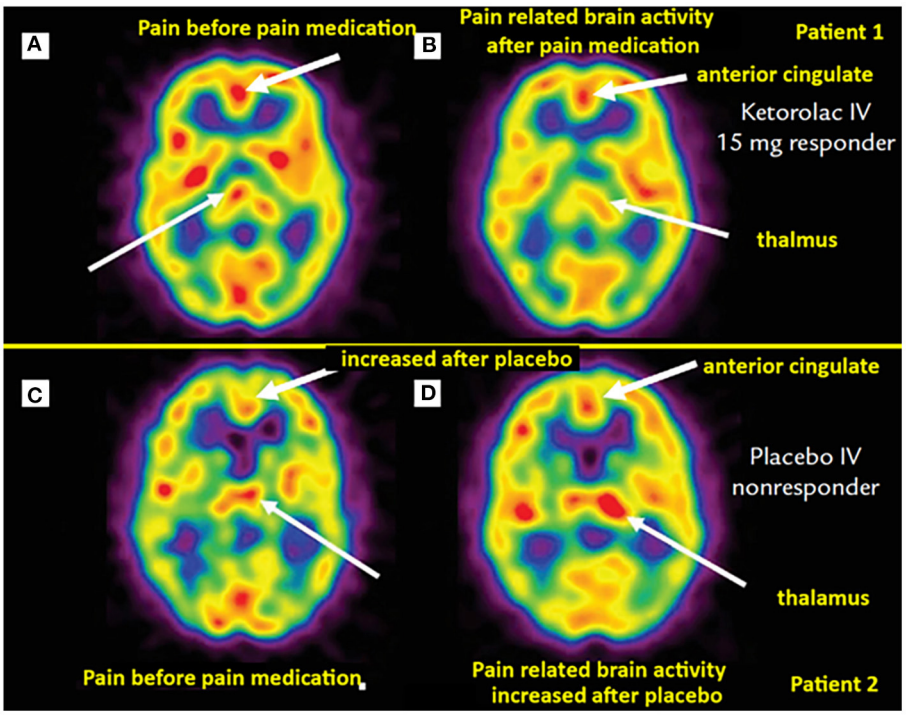

FIGURE 1 | Brain perfusion SPECT of dental pain patients receiving analgesia (top row) vs. placebo (bottom row). **(A)** Asymmetric thalamic activity, more on the right (thin arrow). Post IV ketorolac, the post-interventional scan **(B)** of the same patient exhibits a slight "switch" in thalamic asymmetry, with mildly greater perfusion on the left (thin arrow). Noted also decreased perfusion in the anterior cingulate region with pain relief [thick arrows in **(A)** and **(B)**]. **(C)** Scan from another patient demonstrating mild asymmetric increased activity in the left thalamus (thin arrow). **(D)** Same patient with worsening pain after receiving IV placebo, the scan demonstrates more asymmetrically increased perfusion in the left thalamus (thin arrow). Not also increased perfusion in the anterior cingulate cortex compared to **(C)** (thick arrows). [Images by Newberg et al. (58), reproduced here with permission].

Fukui et al. (61) demonstrated normalization of the thalamic hypoperfusion in complex regional pain syndrome patients after ECT. Changes in rCBF have also been reported following deep brain stimulation for chronic pain (62). Tamura et al. studied seven normal subjects and reported a significant correlation between improved subjective pain and rCBF changes measured by SPECT after repetitive transcranial magnetic stimulation on acute pain induced by capsaicin (63).

Limitations

The brain perfusion SPECT technique has its limitations: the technique utilizes ionizing radiation, mainly from the injected radiotracer and additionally from the optional low dose CT sometimes used for rough localization and attenuation correction. Software fusion of SPECT and MRI images instead provides significantly better anatomical details and avoids the radiation penalty associated with CT. Multiple conditions typically cannot be evaluated during the same session. The ability to repeat the study to investigate multiple variables or time evolution of one variable is also limited due to the irradiation dose, cost, and the complexity of the SPECT procedure. The technique is more complex compared to fMRI as additional steps related to the handling and injection of the radiopharmaceuticals are involved. While temporal characteristics are unique in one aspect, it is still limited, because it is basically a summed 1–2 min of brain activation with less temporal resolution than fMRI. The control study is typically performed on a separate day. Data processing and image display are not standardized. There are also problems related to differences in interpretation of results according to the experience of the radiologist so reproducibility and interobserver agreement is not high (64–67).

In summary, despite these limitations, one of the great advantages of SPECT is that unlike most neuroimaging modalities, with the SPECT technique, the patient does not need to be in the scanner at the time of brain activation. SPECT freezes a snapshot of brain activity at the time of injection that is kept and can be imaged later (after wound care is completed). The SPECT technique allows researchers to measure brain activity in much wider range of clinical settings, increasing the ecological validity of clinical pain research and potentially increasing our understanding of pain-related brain activity during painful medical procedures, and during painful spikes in chronic pain. Additional research and development of brain perfusion SPECT technique is recommended.

AUTHOR CONTRIBUTIONS

MB and DL: conception and design. MB and HH: collection and assembly of figures. MB, MS, HH, DP, SS, SM, and DL: manuscript writing and final approval of manuscript. All authors contributed to the article and approved the submitted version.

FUNDING

This work reported here was supported in part by National Institutes of Health award R01 GM042725 to DP, R01 DA026438 to SS, and from the Mayday Fund to HH.

REFERENCES

1. Honda T, Maruta T, Takahashi K. Brain perfusion abnormality in patients with chronic pain. *Keio J Med.* (2007) 56:48–52. doi: 10.2302/kjm.56.48
2. Apkarian AV, Bushnell MC, Treede RD, Zubieta JK. Human brain mechanisms of pain perception and regulation in health and disease. *Eur J Pain.* (2005) 9:463–84. doi: 10.1016/j.ejpain.2004.11.001
3. Bermo MS, Patterson D, Sharar SR, Hoffman H, Lewis DH. Virtual reality to relieve pain in burn patients undergoing imaging and treatment. *Top Magn Reson Imaging.* (2020) 29:203–8. doi: 10.1097/RMR.0000000000000248
4. Nakamura Y, Nojiri K, Yoshihara H, Takahata T, Honda-Takahashi K, Kubo S, et al. Significant differences of brain blood flow in patients with chronic low back pain and acute low back pain detected by brain SPECT. *J Orthop Sci.* (2014) 19:384–9. doi: 10.1007/s00776-014-0534-2
5. D'Elia A, Schiavi S, Soluri A, Massari R, Soluri A, Trezza V. Role of nuclear imaging to understand the neural substrates of brain disorders in laboratory animals: current status and future prospects. *Front Behav Neurosci.* (2020) 14:596509. doi: 10.3389/fnbeh.2020.596509
6. Kim JH, Marton J, Ametamey SM, Cumming P. A review of molecular imaging of glutamate receptors. *Molecules.* (2020) 25. doi: 10.3390/molecules25204749
7. Beaurain M, Salabert AS, Ribeiro MJ, Arlicot N, Damier P, Le Jeune F, et al. Innovative molecular imaging for clinical research, therapeutic stratification, and nosography in neuroscience. *Front Med (Lausanne).* (2019) 6:268. doi: 10.3389/fmed.2019.00268
8. Bordonne M, Chawki MB, Marie PY, Zaragori T, Roch V, Grignon R, et al. High-quality brain perfusion SPECT images may be achieved with a high-speed recording using 360 degrees CZT camera. *EJNMMI Phys.* (2020) 7:65. doi: 10.1186/s40658-020-00334-7
9. Rousseau PF, Malbos E, Verger A, Nicolas F, Lancon C, Khalfa S, et al. Increase of precuneus metabolism correlates with reduction of PTSD symptoms after EMDR therapy in military veterans: an 18F-FDG PET study during virtual reality exposure to war. *Eur J Nucl Med Mol Imaging.* (2019) 46:1817–21. doi: 10.1007/s00259-019-04360-1
10. la Fougere C, Zwergal A, Rominger A, Forster S, Fesl G, Dieterich M, et al. Real versus imagined locomotion: a [18F]-FDG PET-fMRI comparison. *Neuroimage.* (2010) 50:1589–98. doi: 10.1016/j.neuroimage.2009.12.060
11. Chiaravalloti A, Pagani M, Micarelli A, Di Pietro B, Genovesi G, Alessandrini M, et al. Cortical activity during olfactory stimulation in multiple chemical sensitivity: a (18)F-FDG PET/CT study. *Eur J Nucl Med Mol Imaging.* (2015) 42:733–40. doi: 10.1007/s00259-014-2969-2
12. Ripp I, Wallenwein LA, Wu Q, Emch M, Koch K, Cumming P, et al. Working memory task induced neural activation: A simultaneous PET/fMRI study. *Neuroimage.* (2021) 237:118131. doi: 10.1016/j.neuroimage.2021.118131
13. Villien M, Wey HY, Mandeville JB, Catana C, Polimeni JR, Sander CY, et al. Dynamic functional imaging of brain glucose utilization using fPET-FDG. *Neuroimage.* (2014) 100:192–9. doi: 10.1016/j.neuroimage.2014.06.025
14. Hahn A, Gryglewski G, Nics L, Hienert M, Rischka L, Vraka C, et al. Quantification of task-specific glucose metabolism with constant infusion of 18F-FDG. *J Nucl Med.* (2016) 57:1933–40. doi: 10.2967/jnumed.116.176156
15. Rischka L, Gryglewski G, Pfaff S, Vanicek T, Hienert M, Klobl M, et al. Reduced task durations in functional PET imaging with [(18)F]FDG approaching that of functional MRI. *Neuroimage.* (2018) 181:323–30. doi: 10.1016/j.neuroimage.2018.06.079
16. Verger A, Guedj E. The renaissance of functional (18)F-FDG PET brain activation imaging. *Eur J Nucl Med Mol Imaging.* (2018) 45:2338–41. doi: 10.1007/s00259-018-4165-2
17. Pagani M, Carletto S, Ostacoli L. PET. and SPECT in psychiatry: the past and the future. *Eur J Nucl Med Mol Imaging.* (2019) 46:1985–7. doi: 10.1007/s00259-019-04451-z
18. Holman BL, Hellman RS, Goldsmith SJ, Mena IG, Leveille J, Gherardi PG, et al. Biodistribution, dosimetry, and clinical evaluation of technetium-99m ethyl cysteinate dimer in normal subjects and in patients with chronic cerebral infarction. *J Nucl Med.* (1989) 30:1018–24.
19. Walovitch RC, Hill TC, Garrity ST, Cheesman EH, Burgess BA, O'Leary DH, et al. Characterization of technetium-99m-L,L-ECD for brain perfusion imaging, Part 1: Pharmacology of technetium-99m ECD in nonhuman primates. *J Nucl Med.* (1989) 30:1892–901.
20. Matsuda H, Yagishita A, Tsuji S, Hisada K. A quantitative approach to technetium-99m ethyl cysteinate dimer: a comparison with technetium-99m hexamethylpropylene amine oxime. *Eur J Nucl Med.* (1995) 22:633–7. doi: 10.1007/BF01254564
21. Leveille J, Demonceau G, De Roo M, Rigo P, Taillefer R, Morgan RA, et al. Characterization of technetium-99m-L,L-ECD for brain perfusion imaging, Part 2: Biodistribution and brain imaging in humans. *J Nucl Med.* (1989) 30:1902–10.
22. Walovitch RC, Franceschi M, Picard M, Cheesman EH, Hall KM, Makuch J, et al. Metabolism of 99mTc-L,L-ethyl cysteinate dimer in healthy volunteers. *Neuropharmacology.* (1991) 30:283–92. doi: 10.1016/0028-3908(91)90156-6
23. Vallabhajosula S, Zimmerman RE, Picard M, Stritzke P, Mena I, Hellman RS, et al. Technetium-99m ECD: a new brain imaging agent: in vivo kinetics and biodistribution studies in normal human subjects. *J Nucl Med.* (1989) 30:599–604.
24. Minoshima S, Koeppe RA, Frey KA, Kuhl DE. Anatomic standardization: linear scaling and nonlinear warping of functional brain images. *J Nucl Med.* (1994) 35:1528–37.
25. Somborski K, Bingel U. Functional imaging in pain research. *Schmerz.* (2010) 24:385–400. doi: 10.1007/s00482-010-0917-z
26. Hoffman HG, Richards TL, Coda B, Bills AR, Blough D, Richards AL, et al. Modulation of thermal pain-related brain activity with virtual reality: evidence from fMRI. *Neuroreport.* (2004) 15:1245–8. doi: 10.1097/01.wnr.0000127826.73576.91
27. Hoffman HG, Richards TL, Van Oostrom T, Coda BA, Jensen MP, Blough DK, et al. The analgesic effects of opioids and immersive virtual reality distraction: evidence from subjective and functional brain imaging assessments. *Anesth Analg.* (2007) 105:1776–83. doi: 10.1213/01.ane.0000270205.45146.db
28. Price DD. Central neural mechanisms that interrelate sensory and affective dimensions of pain. *Mol Interv.* (2002) 2:392–403. doi: 10.1124/mi.2.6.392
29. Garcia-Larrea L, Bastuji H. Pain and consciousness. *Prog Neuropsychopharmacol Biol Psychiatry.* (2018) 87:193–9. doi: 10.1016/j.pnpbp.2017.10.007
30. Coombes SA, Misra G. Pain and motor processing in the human cerebellum. *Pain.* (2016) 157:117–27. doi: 10.1097/j.pain.0000000000000337
31. Stohler CS, Zubieta JK. Pain imaging in the emerging era of molecular medicine. *Methods Mol Biol.* (2010) 617:517–37. doi: 10.1007/978-1-60327-323-7_38
32. Rainville P, Duncan GH, Price DD, Carrier B, Bushnell MC. Pain affect encoded in human anterior cingulate but not somatosensory cortex. *Science.* (1997) 277:968–71. doi: 10.1126/science.277.5328.968
33. Ploghaus A, Tracey I, Gati JS, Clare S, Menon RS, Matthews PM, et al. Dissociating pain from its anticipation in the human brain. *Science.* (1999) 284:1979–81. doi: 10.1126/science.284.5422.1979
34. Karibe H, Arakawa R, Tateno A, Mizumura S, Okada T, Ishii T, et al. Regional cerebral blood flow in patients with orally localized somatoform pain disorder: a single photon emission computed tomography study. *Psychiatry Clin Neurosci.* (2010) 64:476–82. doi: 10.1111/j.1440-1819.2010.02119.x

35. Coghill RC, McHaffie JG, Yen YF. Neural correlates of interindividual differences in the subjective experience of pain. *Proc Natl Acad Sci U S A.* (2003) 100:8538–42. doi: 10.1073/pnas.1430684100
36. Scott DJ, Stohler CS, Egnatuk CM, Wang H, Koeppe RA, Zubieta JK. Placebo and nocebo effects are defined by opposite opioid and dopaminergic responses. *Arch Gen Psychiatry.* (2008) 65:220–31. doi: 10.1001/archgenpsychiatry.2007.34
37. Lorenz J, Minoshima S, Casey KL. Keeping pain out of mind: the role of the dorsolateral prefrontal cortex in pain modulation. *Brain.* (2003) 126:1079–91. doi: 10.1093/brain/awg102
38. Iadarola MJ, Coghill RC. Imaging of pain: recent developments. *Curr Opin Anaesthesiol.* (1999) 12:583–9. doi: 10.1097/00001503-199910000-00016
39. Melzack R, Wall PD. Pain mechanisms: a new theory. *Science.* (1965) 150:971–9. doi: 10.1126/science.150.3699.971
40. Salomons TV, Iannetti GD, Liang M, Wood JN. The "pain matrix" in pain-free individuals. *JAMA Neurol.* (2016) 73:755–6. doi: 10.1001/jamaneurol.2016.0653
41. Nakabeppu Y, Nakajo M, Gushiken T, Tsuchimochi S, Tani A, Kanmura Y. Decreased perfusion of the bilateral thalami in patients with chronic pain detected by Tc-99m-ECD SPECT with statistical parametric mapping. *Ann Nucl Med.* (2001) 15:459–63. doi: 10.1007/BF02988354
42. Chen JJH, Wang JY, Chang YM, Su SY, Chang CT, Sun SS, et al. Regional cerebral blood flow between primary and concomitant fibromyalgia patients: A possible way to differentiate concomitant fibromyalgia from the primary disease. *Scand J Rheumatol.* (2007) 36:226–32. doi: 10.1080/03009740601153790
43. Guedj E, Cammilleri S, Niboyet J, Dupont P, Vidal E, Dropinski J-P, et al. Clinical correlate of brain {SPECT} perfusion abnormalities in fibromyalgia. *J Nucl Med.* (2008) 49:1798–803. doi: 10.2967/jnumed.108.053264
44. Guedj E, Cammilleri S, Niboyet J, Mundler O. Clinical image: brain perfusion single-photon-emission computed tomography findings in a patient with an asymmetric fibromyalgia syndrome. *Arthritis and Rheumatism.* (2009) 60:298. doi: 10.1002/art.24252
45. Guedj E, Taieb D, Cammilleri S, Lussato D, de Laforte C, Niboyet J, et al. Voxel-by-voxel analysis of brain {SPECT} perfusion in Fibromyalgia. *Nucl Instrum Methods Phys Res A.* (2007) 571:85–8. doi: 10.1016/j.nima.2006.10.035
46. Guedj E, Taieb D, Cammilleri S, Lussato D, De Laforte C, Niboyet J, et al. 99mTc-ECD brain perfusion SPECT in hyperalgesic fibromyalgia. *Eur J Nucl Med Mol Imaging.* (2007) 34:130–4. doi: 10.1007/s00259-006-0174-7
47. Usui C, Doi N, Nishioka M, Komatsu H, Yamamoto R, Ohkubo T, et al. Electroconvulsive therapy improves severe pain associated with fibromyalgia. *Pain.* (2006) 121:276–80. doi: 10.1016/j.pain.2005.12.025
48. Usui C, Hatta K, Doi N, Nakanishi A, Nakamura H, Nishioka K, et al. Brain perfusion in fibromyalgia patients and its differences between responders and poor responders to gabapentin. *Arthritis Res Ther.* (2010) 12. doi: 10.1186/ar2980
49. Guedj E, Cammilleri S, Colavolpe C, de Laforte C, Niboyet J, Mundler O. Follow-up of pain processing recovery after ketamine in hyperalgesic fibromyalgia patients using brain perfusion ECD-SPECT. *Eur J Nucl Med Mol Imaging.* (2007) 34:2115–9. doi: 10.1007/s00259-007-0589-9
50. Guedj E, Cammilleri S, Colavolpe C, Taieb D, de Laforte C, Niboyet J, et al. Predictive value of brain perfusion SPECT for ketamine response in hyperalgesic fibromyalgia. *Eur J Nucl Med Mol Imaging.* (2007) 34:1274–9. doi: 10.1007/s00259-007-0392-7
51. Goffin K, Dedeurwaerdere S, Van Laere K, Van Paesschen W. Neuronuclear assessment of patients with epilepsy. *Semin Nucl Med.* (2008) 38:227–39. doi: 10.1053/j.semnuclmed.2008.02.004
52. Lancman ME, Morris HH. 3rd, Raja S, Sullivan MJ, Saha G, Go R. Usefulness of ictal and interictal 99mTc ethyl cysteinate dimer single photon emission computed tomography in patients with refractory partial epilepsy. *Epilepsia.* (1997) 38:466–71. doi: 10.1111/j.1528-1157.1997.tb01737.x
53. Siegel AM, Williamson PD, Roberts DW, Thadani VM, Darcey TM. Localized pain associated with seizures originating in the parietal lobe. *Epilepsia.* (1999) 40:845–55. doi: 10.1111/j.1528-1157.1999.tb00790.x
54. Shin D-J, Kim J-H, Kang S-S. Ophthalmoplegic migraine with reversible thalamic ischemia. shown by brain {SPECT}. (2002) 132–5. doi: 10.1046/j.1526-4610.2002.02029.x
55. Koyano K, Konishi Y, Okada H, Kusaka T, Itoh S. Changes in ({99m)Tc-ECD} {SPECT} and magnetic resonance angiography with sporadic hemiplegic migraine in a child. *Clin Nucl Med.* (2014) 39:483–4. doi: 10.1097/RLU.0000000000000401
56. Soriani S, Feggi L, Battistella PA, Arnaldi C, De Carlo L, Stipa S. Interictal and ictal phase study with Tc 99m HMPAO brain SPECT in juvenile migraine with aura. *Headache.* (1997) 37:31–6. doi: 10.1046/j.1526-4610.1997.3701031.x
57. Trucco M, Cananzi C, Salvadori PR, Badino R. Piroxicam-beta-cyclodextrin in induced migraine attacks: a SPECT study with Tc-99m HM-PAO split-dose method. *Funct Neurol.* (1994) 9:247–57.
58. Newberg AB, Hersh EV, Levin LM, Giannakopoulos H, Secreto SA, Wintering NA, et al. Double-blind, placebo-controlled, randomized pilot study of cerebral blood flow patterns employing SPECT imaging in dental postsurgical pain patients with and without pain relief. *Clin Ther.* (2011) 33:1894–903. doi: 10.1016/j.clinthera.2011.10.013
59. Bermo MS, Zacharias C, Patterson D, Wilson A, Sharar S, Minoshima S, et al. The Role of the Cerebellum in Pain Perception: A Brain SPECT Perfusion Study in Patients with Burn Injuries. *J Neuroimaging.* (2020) 30:815–21. doi: 10.1111/jon.12759
60. Newberg AB, Lariccia PJ, Lee BY, Farrar JT, Lee L, Alavi A. Cerebral blood flow effects of pain and acupuncture: a preliminary single-photon emission computed tomography imaging study. *J Neuroimaging.* (2005) 15:43–9. doi: 10.1111/j.1552-6569.2005.tb00284.x
61. Fukui S, Shigemori S, Nosaka S. Changes in regional cerebral blood flow in the thalamus after electroconvulsive therapy for patients with complex regional pain syndrome type 1 (preliminary case series). *Reg Anesth Pain Med.* (2002) 27:529–32. doi: 10.1053/rapm.2002.34330
62. Pereira EAC, Green AL, Bradley KM, Soper N, Moir L, Stein JF, et al. Regional cerebral perfusion differences between periventricular grey, thalamic and dual target deep brain stimulation for chronic neuropathic pain. *Stereotact Funct Neurosurg.* (2007) 85:175–83. doi: 10.1159/000101296
63. Tamura Y, Okabe S, Ohnishi TN, Saito D, Arai N, Mochio S, et al. Effects of 1-Hz repetitive transcranial magnetic stimulation on acute pain induced by capsaicin. *Pain.* (2004) 107:107–15. doi: 10.1016/j.pain.2003.10.011
64. Ito S, Takaki A, Inoue S, Tomiguchi S, Shiraishi S, Akiyama Y, et al. Improvement of the (99m)Tc-ECD brain uptake ratio (BUR) method for measurement of cerebral blood flow. *Ann Nucl Med.* (2012) 26:351–8. doi: 10.1007/s12149-012-0582-7
65. Fu P, Zhang F, Gao J, Jing J, Pan L, Li D, et al. NeuroGam software analysis in epilepsy diagnosis using 99mTc-ECD brain perfusion SPECT imaging. *Med Sci Monit.* (2015) 21:2801–8. doi: 10.12659/MSM.894566
66. Cheng MF, Wu YW, Tang SC. Cerebral perfusion changes in hemiplegic migraine: illustrated by Tc-99m ECD brain perfusion scan. *Clin Nucl Med.* (2010) 35:456–8. doi: 10.1097/RLU.0b013e3181db4ba5
67. Stockbridge HL, Lewis D, Eisenberg B, Lee M, Schacher S, van Belle G, et al. Brain SPECT: a controlled, blinded assessment of intra-reader and inter-reader agreement. *Nucl Med Commun.* (2002) 23:537–44. doi: 10.1097/00006231-200206000-00005

Conflict of Interest: The authors declare that the research was conducted in the absence of any commercial or financial relationships that could be construed as a potential conflict of interest.

frontiers in Neurology

ORIGINAL RESEARCH
published: 10 November 2021
doi: 10.3389/fneur.2021.726006

Regional Cerebral Blood Flow Abnormalities in Neurosyphilis: A Pilot SPECT Study

Jooyeon J. Im[1†], Hyeonseok Jeong[1,2†], Young Do Kim[3], Kyung-Sool Jang[4], In-Uk Song[3] and Yong-An Chung[1,2*]*

[1] Department of Nuclear Medicine, Incheon St. Mary's Hospital, College of Medicine, The Catholic University of Korea, Seoul, South Korea, [2] Department of Radiology, Incheon St. Mary's Hospital, College of Medicine, The Catholic University of Korea, Seoul, South Korea, [3] Department of Neurology, Incheon St. Mary's Hospital, College of Medicine, The Catholic University of Korea, Seoul, South Korea, [4] Department of Neurosurgery, Incheon St. Mary's Hospital, College of Medicine, The Catholic University of Korea, Seoul, South Korea

Objective: Clinical and radiological findings on neurosyphilis are fairly non-specific and there is a paucity of functional neuroimaging studies on neurosyphilis other than case reports and case series. The purpose of this study was to investigate brain perfusion abnormalities in patients with neurosyphilis.

Methods: Four HIV-negative neurosyphilis patients and 4 healthy controls underwent clinical evaluation, brain technetium-99m ethyl cysteinate dimer (99mTc-ECD) single-photon emission computed tomography (SPECT) imaging, and neuropsychological assessments which included the Mini-Mental State Examination (MMSE), Clinical Dementia Rating (CDR), Clinical Dementia Rating—Sum of Boxes (CDR-SOB), and Global Deterioration Scale (GDS). Voxel-wise differences in regional cerebral blood flow were compared between the two groups.

Results: Neuropsychological test results indicated cognitive impairment in all patients. SPECT analysis revealed multifocal hypoperfusion predominantly in the frontal, insular, and posterior cingulate regions in neurosyphilis patients compared with healthy controls (family-wise error corrected $p < 0.05$).

Conclusions: Together with previous findings, our results suggest that the hypoperfusion in the frontal, insular, and posterior cingulate regions may reflect cognitive impairments observed in neurosyphilis patients. Further studies with larger samples are needed to confirm our findings.

Keywords: neurosyphilis, single-photon emission computed tomography, regional cerebral blood flow, cognitive function, neuroimaging

OPEN ACCESS

Edited by:
Philip Frank Cohen, University of British Columbia, Canada

Reviewed by:
Theodore A. Henderson, Independent Researcher, Denver, CO, United States
Sonia Neubauer, Clinica Las Condes, Chile

***Correspondence:**
In-Uk Song
siuy@catholic.ac.kr
Yong-An Chung
yongan@catholic.ac.kr

† These authors have contributed equally to this work

Specialty section:
This article was submitted to Applied Neuroimaging, a section of the journal Frontiers in Neurology

Received: *16 June 2021*
Accepted: *07 October 2021*
Published: *10 November 2021*

Citation:
Im JJ, Jeong H, Kim YD, Jang K-S, Song I-U and Chung Y-A (2021) Regional Cerebral Blood Flow Abnormalities in Neurosyphilis: A Pilot SPECT Study. Front. Neurol. 12:726006. doi: 10.3389/fneur.2021.726006

INTRODUCTION

Neurosyphilis is an infection of the central nervous system by Treponema pallidum (1). Neurosyphilis has been reported to develop in up to 5–10% of patients with untreated syphilis and can occur at any stage of syphilis, which is divided into primary, secondary, latent, and tertiary syphilis (1, 2). The incidence of syphilis has varied over time with a marked decrease after the introduction of penicillin and a surge in the era of HIV/AIDS pandemic followed by another

TABLE 1 | Demographic and clinical characteristics of the participants.

Participant	Age	Sex	MMSE	CDR	CDR-SOB	GDS
Patient 1	43	Male	20	1	4.5	4
Patient 2	37	Male	28	0.5	0.5	3
Patient 3	53	Male	22	1	4.5	4
Patient 4	52	Male	23	1	6	5
Control 1	48	Male	30	0	0	1
Control 2	54	Male	28	0	0	1
Control 3	44	Male	30	0	0	1
Control 4	39	Male	29	0	0	1

CDR, Clinical Dementia Rating; CDR-SOB, Clinical Dementia Rating—Sum of Boxes; GDS, Global Deterioration Scale; MMSE, Mini-Mental State Examination.

decline due to engaging in safe sexual practices. However, the rates of syphilis began to increase again since 2000 (3). Despite the relative success in controlling syphilis in the post-penicillin era, syphilis remains an important public health issue with an estimated annual global incidence of 12 million (4).

Neurosyphilis is classified into early forms of neurosyphilis which includes asymptomatic neurosyphilis, syphilitic meningitis, and syphilitic meningovasculitis and late forms of neurosyphilis which includes general paresis and tabes dorsalis (5). Early forms of neurosyphilis primarily affects the meninges, cerebrospinal fluid (CSF), and vasculature, and late forms of neurosyphilis affects the brain and spinal cord parenchyma. The clinical manifestations of symptomatic neurosyphilis are diverse and usually non-specific including meningitis, stroke, seizures, headache, hearing loss, vision loss, personality changes, cognitive decline, dementia, or sensory and gait abnormalities (5, 6). The diagnosis of symptomatic neurosyphilis is based on the serological testing, CSF examination, and clinical findings (5). However, diagnosis of neurosyphilis is often difficult because many patients present either non-specific symptoms or are asymptomatic.

Identifying radiological features of neurosyphilis may be useful in aiding the diagnosis and distinguishing the disease from other conditions. Previous neuroimaging studies have reported generalized cerebral atrophy, non-specific white matter lesions, meningeal and CSF enhancement, and signal changes in the frontotemporal lobes as well as some normal findings in neurosyphilis patients (7–9). However, apart from case reports and case series, no prospective studies have been published investigating the cerebral perfusion in neurosyphilis patients. The purpose of this study was to investigate the differences in regional cerebral blood flow (rCBF) between neurosyphilis patients and healthy controls using single-photon emission computed tomography (SPECT).

METHODS

Participants

Neurosyphilis patients and healthy controls were recruited at the Incheon St. Mary's Hospital (Incheon, South Korea). The diagnosis of neurosyphilis is based on a CSF WBC count of 5 cells/microL or more, CSF protein 45 mg/dl or more and a reactive CSF VDRL. All patients in this study showed a reactive serum FTA-ABS and cognitive impairment including neuropsychiatric symptoms. All patients were HIV-negative. This study excluded patients with following past history: head trauma, existing dementia diagnosis, stroke, brain tumor, epilepsy, sexually transmitted diseases except for syphilis, and other neurological or psychiatric disorders. Healthy controls were age- and sex-matched volunteers who met the same exclusion criteria and inclusion criteria, except for the presence of neurosyphilis. The study was approved by the Institutional Review Board of the Incheon St. Mary's Hospital, and all participants provided written consent form.

Clinical Assessment

Screening tests included a medical history interview, physical and neurological examinations by a neurologist, routine blood biochemistry and blood count, 12-lead electrocardiogram, chest x-ray, and CSF study including counts of WBC and RBC, protein, glucose, and CSF VDRL. We performed brain magnetic resonance imaging, SPECT scans, and neuropsychological tests before medical treatment. Neuropsychological assessments consisted of the Mini-Mental State Examination (MMSE) (10), Clinical Dementia Rating (CDR) (11), Clinical Dementia Rating—Sum of Boxes (CDR-SOB) (11), and Global Deterioration Scale (GDS) (12).

Brain SPECT Imaging

Brain SPECT scans were performed using a dual-headed gamma camera (Discovery NM630; GE Healthcare, Milwaukee, WI, USA) equipped with a low-energy fan-beam collimator. Patients were injected with 555–740 MBq of technetium-99m ethyl cysteinate dimer (99mTc-ECD) and rested for ∼40 min prior to scanning. Images were taken by rotating the camera a total of 720° at 6-degree intervals at a rate of 12 s per frame (average counts = 1.50 kcts/s). Images were corrected for attenuation using a standard commercial correction routine provided by the scanner vendor and reconstructed into a 128 × 128 matrix with a pixel size of 1.95 × 1.95 × 2.08 mm and a 20% symmetric energy window at 140 keV using the ordered-subset expectation maximization (OSEM) algorithm (6 iterations and 10 subsets) and a Butterworth filter (cut-off frequency of 0.5 cycles/pixel and power of 10.0) to reduce noise.

All SPECT images were pre-processed and analyzed using Statistical Parametric Mapping 12 (SPM; Wellcome Center for Human Neuroimaging, London, UK) implemented in MATLAB R2017b (MathWorks, Natick, MA, USA). The images were spatially normalized to the standard SPECT template provided by SPM. After spatial normalization, the count of each voxel was standardized to the mean voxel count of the whole brain using proportional scaling. The normalized images were then smoothed using a 16-mm full-width half-maximum Gaussian kernel.

A two-sample *t*-test was performed to compare the rCBF between the groups. The voxel-wise significance threshold was set at $p < 0.001$ with a cluster-level family-wise error (FWE) correction at $p < 0.05$.

TABLE 2 | Differences in regional cerebral blood flow between patients with neurosyphilis and healthy controls.

Region	*z*	*p*	Coordinates* (x, y, z)	Cluster size (voxels)
Neurosyphilis group < control group				
R inferior/middle frontal gyrus, anterior insula	4.89	<0.001	40, 28, −8	1,489
R medial frontal cortex, middle cingulate gyrus	4.65	<0.001	2, 58, −14	8,453
R central operculum, posterior insula	4.09	<0.001	40, −16, 14	669
R posterior cingulate gyrus	4.08	<0.001	4, −36, 28	533
L anterior insula, superior temporal gyrus	3.87	<0.001	−40, 12, 0	302
L inferior/middle frontal gyrus	3.74	<0.001	−50, 10, 26	313
Neurosyphilis group > control group				
None				

**The coordinates refer to the Montreal Neurological Institute coordinate system. L, left; R, right.*

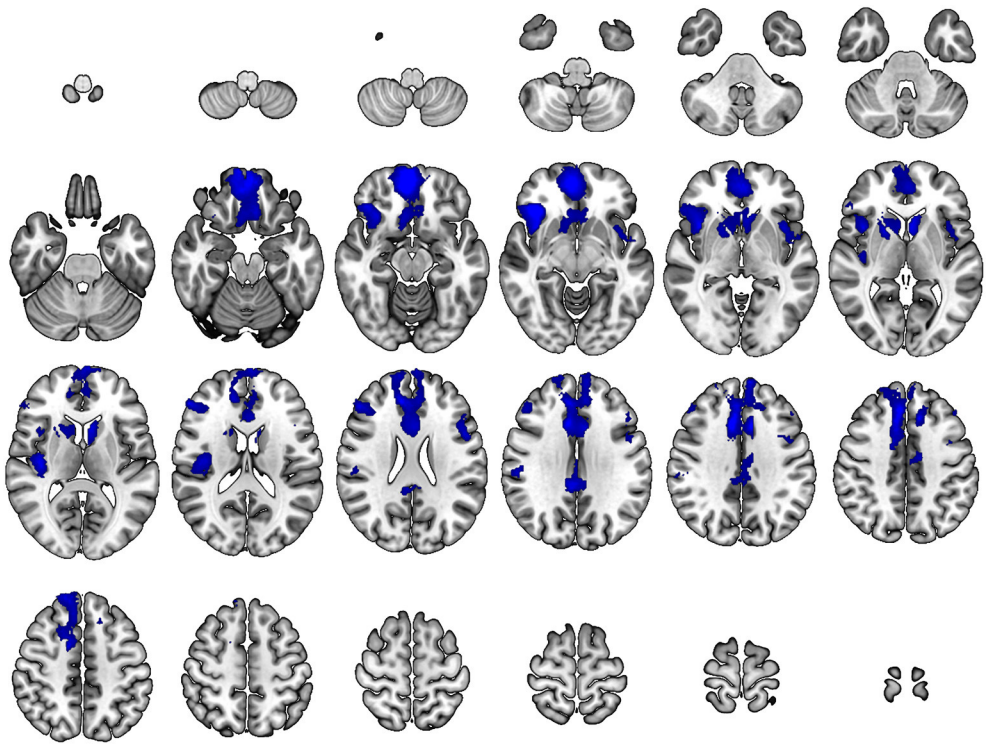

FIGURE 1 | Differences in regional cerebral blood flow between patients with neurosyphilis and healthy controls. At each voxel, decreases in brain perfusion in neurosyphilis patients compared with healthy controls appear in blue. The height threshold is $p < 0.001$ with a cluster-level family-wise error correction at $p < 0.05$. Images are shown in radiological convention.

To assess individual patterns of abnormalities in rCBF, separate two-sample *t*-tests were conducted to compare each patient with the control group. The voxel-level threshold of $p < 0.005$ with cluster-level FWE corrected $p < 0.05$ was applied for the individual analysis.

Statistical Analysis

Mann-Whitney *U* test was used to compare age between the groups. The significance level was set at $p < 0.05$ (two-tailed). All statistical analyses were performed using Stata/MP 16.0 (Stata Corp., College Station, TX, USA).

RESULTS

Demographic and Clinical Characteristics

Four patients with neurosyphilis and four healthy controls were enrolled in the study. Demographic and clinical characteristics are summarized in **Table 1**. All participants were male, and age

did not significantly differ between the neurosyphilis (mean ± standard deviation = 46.3 ± 7.6) and control groups (46.3 ± 6.3, $p = 0.77$). Scores of MMSE, CDR, CDR-SOB, GDS indicated cognitive impairment in patients with neurosyphilis.

Brain SPECT Imaging Results

As compared with controls, neurosyphilis patients showed reduced rCBF in six clusters including the (1) right inferior/middle frontal gyrus and anterior insula ($z = 4.89$, $p < 0.001$), (2) right medial frontal cortex and middle cingulate gyrus ($z = 4.65$, $p < 0.001$), (3) right central operculum and posterior insula ($z = 4.09$, $p < 0.001$), (4) right posterior cingulate gyrus ($z = 4.08$, $p < 0.001$), (5) left anterior insula and superior temporal gyrus ($z = 3.87$, $p < 0.001$), and (6) left inferior/middle frontal gyrus ($z = 3.74$, $p < 0.001$) (**Table 2** and **Figure 1**). No significant clusters of increased rCBF were detected.

For each patient, the SPECT images and the results of individual analysis are demonstrated in **Supplementary Figures 1–4**. Despite some differences of rCBF patterns among patients, frontal and insular hypoperfusion was observed in all patients.

DISCUSSION

In the current study, HIV-negative neurosyphilis patients showed multifocal hypoperfusion predominantly in the frontal, insular, and posterior cingulate regions compared to healthy controls. Although diffuse hypoperfusion has been found in various central nervous system infections and neurotoxicity such as HIV and alcohol-related dementia (13, 14), the regional pattern of our findings may be associated with cognitive decline found in patients with neurosyphilis.

Our results are in agreement with previous SPECT findings of decreased rCBF in the frontal regions in patients with general paresis (15–18), which is the most common form of neurosyphilis presenting with cognitive impairment and psychiatric symptoms (19). These cases also reported decreased rCBF in the temporal regions (15–18), which was less prominent in our study. In contrast, there are single-case reports that showed increased rCBF in the temporal lobe (20) and frontal and temporo-occipital regions (21). Moreover, in a SPECT study which included 32 patients with early syphilis, a general and patchy hypoperfusion was found in the frontal, temporal, parietal, occipital lobes as well as the basal ganglia, cerebellum, and nerve nucleus (22).

These inconsistencies may be partially attributed to differences in disease stage at diagnosis as hyperperfusion may reflect inflammatory changes in the early phase and hypoperfusion may reflect neural death and decreased metabolism in the late phase (21). Besides that, the uncontrolled nature of case reports and bias from visual inspection might have contributed to the discrepancies as well. In spite of these differences, previous reports consistently showed improved rCBF after successful treatment, suggesting that SPECT may be a useful method in detecting subtle changes in neurosyphilis patients receiving antisyphilitic treatment (15–17, 20, 21).

In the present study, the neurosyphilis patients demonstrated hypoperfusion in multiple frontal regions, particularly in the medial frontal regions. Numerous studies have been published on the role of the medial frontal cortex in a wide range of high-level cognition and its involvement in neurological and psychiatric disorders (23). The medial frontal cortex has been implicated in performance monitoring, motivation, decision making, and social cognition (24–27). Moreover, it has been proposed that the medial frontal cortex is part of a dual hierarchical system for the prefrontal executive function that extends from the posterior to anterior regions in the medial frontal cortex and lateral frontal cortex (26).

We also found hypoperfusion in the insula and posterior cingulate gyrus. In addition to its well-established role in processing interoceptive information, growing evidence suggests that the insula is also involved in cognitive and emotional processing (28). The insula has bidirectional connections with the critical brain areas for cognition such as the orbitofrontal cortex and anterior cingulate cortex, and impairment in the insula has been linked with cognitive impairment across all neuropsychological domains (28). Abnormalities in the posterior cingulate cortex are often associated with impairments in cognitive functions including memory and attention (29). Notably, atrophy and reduced metabolism in the posterior cingulate cortex are seen in Alzheimer's disease (29).

CONCLUSION

In conclusion, the present study found the perfusion abnormalities in the frontal, insular, and posterior cingulate regions among HIV-negative neurosyphilis patients. These results, together with previous findings, suggest that the hypoperfusion in these areas may reflect cognitive impairments observed in neurosyphilis patients. Further studies with larger samples are needed to confirm our findings. In addition, multi-modal neuroimaging studies may be useful to evaluate potential associations between structural and functional deficits in these patients.

DATA AVAILABILITY STATEMENT

The datasets presented in this article are not readily available because the IRB has restrictions on sharing datasets. Requests to access the datasets should be directed to Yong-An Chung, yongan@catholic.ac.kr.

ETHICS STATEMENT

The studies involving human participants were reviewed and approved by Institutional Review Board of the Incheon St. Mary's Hospital. The patients/participants provided their written informed consent to participate in this study.

AUTHOR CONTRIBUTIONS

JI and HJ contributed to analysis, interpretation of data, and original draft preparation. YK and K-SJ contributed to data acquisition. I-US and Y-AC contributed to study concept, design,

and interpretation of data. All authors contributed to the article and approved the submitted version.

FUNDING

This research was supported by the Korea Health Industry Development Institute (KHIDI) and Korea Dementia Research Center (KDRC) (HU21C0081) and the National Research Foundation of Korea (NRF) funded by the Korean government (2020R1C1C1007254).

SUPPLEMENTARY MATERIAL

The Supplementary Material for this article can be found online at: https://www.frontiersin.org/articles/10.3389/fneur.2021.726006/full#supplementary-material

REFERENCES

1. Berger JR, Dean D. Neurosyphilis. *Handb Clin Neurol.* (2014) 121:1461–72. doi: 10.1016/B978-0-7020-4088-7.00098-5
2. Clark EG, Danbolt N. The Oslo study of the natural course of untreated syphilis: an epidemiologic investigation based on a re-study of the Boeck-Bruusgaard material. *Med Clin North Am.* (1964) 48:613–23. doi: 10.1016/S0025-7125(16)33445-9
3. Ropper AH. Neurosyphilis. *N Engl J Med.* (2019) 381:1358–63. doi: 10.1056/NEJMra1906228
4. Fenton KA, Breban R, Vardavas R, Okano JT, Martin T, Aral S, et al. Infectious syphilis in high-income settings in the 21st century. *Lancet Infect Dis.* (2008) 8:244–53. doi: 10.1016/S1473-3099(08)70065-3
5. Marra CM. Update on neurosyphilis. *Curr Infect Dis Rep.* (2009) 11:127–34. doi: 10.1007/s11908-009-0019-1
6. Brown DL, Frank JE. Diagnosis and management of syphilis. *Am Fam Physician.* (2003) 68:283–90.
7. Nagappa M, Sinha S, Taly AB, Rao SL, Nagarathna S, Bindu PS, et al. Neurosyphilis: MRI features and their phenotypic correlation in a cohort of 35 patients from a tertiary care university hospital. *Neuroradiology.* (2013) 55:379–88. doi: 10.1007/s00234-012-1017-9
8. Peng F, Hu X, Zhong X, Wei Q, Jiang Y, Bao J, et al. CT and MR findings in HIV-negative neurosyphilis. *Eur J Radiol.* (2008) 66:1–6. doi: 10.1016/j.ejrad.2007.05.018
9. Russouw HG, Roberts MC, Emsley RA, Truter R. Psychiatric manifestations and magnetic resonance imaging in HIV-negative neurosyphilis. *Biol Psychiatry.* (1997) 41:467–73. doi: 10.1016/S0006-3223(96)00060-1
10. Kang Y, Na DL, Hahn S. A validity study on the Korean Mini-Mental State Examination (K-MMSE) in dementia patients. *J Korean Neurol Assoc.* (1997) 15:300–8.
11. Morris JC. The Clinical Dementia Rating (CDR): current version and scoring rules. *Neurology.* (1993) 43:2412–4. doi: 10.1212/WNL.43.11.2412-a
12. Reisberg B, Ferris SH, de Leon MJ, Crook T. The Global Deterioration Scale for assessment of primary degenerative dementia. *Am J Psychiatry.* (1982) 139:1136–9. doi: 10.1176/ajp.139.9.1136
13. Su T, Mutsaerts HJ, Caan MW, Wit FW, Schouten J, Geurtsen GJ, et al. Cerebral blood flow and cognitive function in HIV-infected men with sustained suppressed viremia on combination antiretroviral therapy. *AIDS.* (2017) 31:847–56. doi: 10.1097/QAD.0000000000001414
14. Chung YA, Choi SW, Joe KH, Jeong J, Cheon Y, Kim DJ. Regional cerebral blood flow in patients with alcohol-related dementia: a SPECT study. *Int J Neurosci.* (2009) 119:2100–11. doi: 10.1080/00207450903170338
15. Kawai N, Baba A, Mizukami K, Sakai T, Shiraishi H, Koizumi J. CT, MR, and SPECT findings in a general paresis. *Comput Med Imaging Graph.* (1994) 18:461–5. doi: 10.1016/0895-6111(94)90084-1
16. Lee CH, Lin WC, Lu CH, Liu JW. Initially unrecognized dementia in a young man with neurosyphilis. *Neurologist.* (2009) 15:95–7. doi: 10.1097/NRL.0b013e31817781c9
17. Morikawa M, Kosaka J, Imai T, Ohsawa H, Iida J, Kishimoto T. A case of general paresis showing marked treatment-associated improvement of cerebellar blood flow by quantitative imaging analysis. *Ann Nucl Med.* (2002) 16:71–4. doi: 10.1007/BF02995296
18. Stefani A, Riello M, Rossini F, Mariotto S, Fenzi F, Gambina G, et al. Neurosyphilis manifesting with rapidly progressive dementia: report of three cases. *Neurol Sci.* (2013) 34:2027–30. doi: 10.1007/s10072-013-1531-5
19. Drago F, Merlo G, Ciccarese G, Agnoletti AF, Cozzani E, Rebora A, et al. Changes in neurosyphilis presentation: a survey on 286 patients. *J Eur Acad Dermatol Venereol.* (2016) 30:1886–900. doi: 10.1111/jdv.13753
20. Denays R, Collier A, Rubinstein M, Atsama P. A 51-year-old woman with disorientation and amnesia. *Lancet.* (1999) 354:1786. doi: 10.1016/S0140-6736(99)09151-5
21. Ide M, Mizukami K, Fujita T, Ashizawa Y, Asada T. A case of neurosyphilis showing a marked improvement of clinical symptoms and cerebral blood flow on single photon emission computed tomography with quantitative penicillin treatment. *Prog Neuropsychopharmacol Biol Psychiatry.* (2004) 28:417–20. doi: 10.1016/j.pnpbp.2003.11.021
22. Shi X, Wu J, Liu Z, Tang J, Su Y. Single photon emission CT perfusion imaging of cerebral blood flow of early syphilis patients. *Chin Med J.* (2003) 116:1051–4.
23. Nachev P. Cognition and medial frontal cortex in health and disease. *Curr Opin Neurol.* (2006) 19:586–92. doi: 10.1097/01.wco.0000247609.36482.ae
24. Amodio DM, Frith CD. Meeting of minds: the medial frontal cortex and social cognition. *Nat Rev Neurosci.* (2006) 7:268–77. doi: 10.1038/nrn1884
25. Bechara A, Damasio H, Damasio AR. Emotion, decision making and the orbitofrontal cortex. *Cereb Cortex.* (2000) 10:295–307. doi: 10.1093/cercor/10.3.295
26. Kouneiher F, Charron S, Koechlin E. Motivation and cognitive control in the human prefrontal cortex. *Nat Neurosci.* (2009) 12:939–45. doi: 10.1038/nn.2321
27. Ridderinkhof KR, Nieuwenhuis S, Braver TS. Medial frontal cortex function: an introduction and overview. *Cogn Affect Behav Neurosci.* (2007) 7:261–5. doi: 10.3758/CABN.7.4.261
28. Gasquoine PG. Contributions of the insula to cognition and emotion. *Neuropsychol Rev.* (2014) 24:77–87. doi: 10.1007/s11065-014-9246-9
29. Leech R, Sharp DJ. The role of the posterior cingulate cortex in cognition and disease. *Brain.* (2014) 137(Pt 1):12–32. doi: 10.1093/brain/awt162

Conflict of Interest: The authors declare that the research was conducted in the absence of any commercial or financial relationships that could be construed as a potential conflict of interest.

Publisher's Note: All claims expressed in this article are solely those of the authors and do not necessarily represent those of their affiliated organizations, or those of the publisher, the editors and the reviewers. Any product that may be evaluated in this article, or claim that may be made by its manufacturer, is not guaranteed or endorsed by the publisher.

frontiers in Psychiatry

ORIGINAL RESEARCH
published: 24 November 2021
doi: 10.3389/fpsyt.2021.725788

SPECT Functional Neuroimaging Distinguishes Adult Attention Deficit Hyperactivity Disorder From Healthy Controls in Big Data Imaging Cohorts

Daniel G. Amen[1*†], *Theodore A. Henderson*[2,3,4,5†] *and Andrew Newberg*[6]

[1] Amen Clinics, Inc., Costa Mesa, CA, United States, [2] The Synaptic Space, Denver, CO, United States, [3] The International Society of Applied Neuroimaging, Denver, CO, United States, [4] Neuro-Luminance, Inc., Denver, CO, United States, [5] Dr. Theodore Henderson, Inc., Denver, CO, United States, [6] Marcus Institute of Integrative Health, Thomas Jefferson University, Philadelphia, PA, United States

Background: The diagnosis of attention deficit hyperactivity disorder (ADHD) relies on history and observation, as no reliable biomarkers have been identified. In this study, we compared a large single diagnosis group of patients with ADHD (combined, inattentive, and hyperactive) to healthy controls using brain perfusion single-photon emission computed tomography (SPECT) imaging to determine specific brain regions which could serve as potential biomarkers to reliably distinguish ADHD.

Methods: In a retrospective analysis, subjects (n = 1,135) were obtained from a large multisite psychiatric database, where resting state (baseline) and on-task SPECT scans were obtained. Only baseline scans were analyzed in the present study. Subjects were separated into two groups – Group 1 (n = 1,006) was composed of patients who only met criteria for ADHD with no comorbid diagnoses, while a control group (n = 129) composed of individuals who did not meet criteria for any psychiatric diagnosis, brain injury, or substance use served as a non-matched control. SPECT regions of interests (ROIs) and visual readings were analyzed using binary logistic regression. Predicted probabilities from this analysis were inputted into a Receiver Operating Characteristic analysis to identify sensitivity, specificity, and accuracy.

Results: The baseline ROIs and visual readings show significant separations from healthy controls. Sensitivity of the visual reads was 100% while specificity was >97%. The sensitivity and specificity of the *post-hoc* ROI analysis were both 100%. Decreased perfusion was primarily seen in the orbitofrontal cortices, anterior cingulate gyri, areas of the prefrontal cortices, basal ganglia, and temporal lobes. In addition, ROI analysis revealed some unexpected areas with predictive value in distinguishing ADHD, such as cerebellar subregions and portions of the temporal lobes.

Conclusions: Brain perfusion SPECT distinguishes adult ADHD patients without comorbidities from healthy controls. Areas which were highly significantly different from control and thus may serve as biomarkers in baseline SPECT scans included: medial anterior prefrontal cortex, left anterior temporal lobe, and right insular cortex. Future studies of these potential biomarkers in ADHD patients with comorbidities are warranted.

Keywords: brain SPECT, ADHD, comorbidity, single photon emission computed tomography, inattention

Edited by:
Wenbin Guo,
Central South University, China

Reviewed by:
Paul T. Fillmore,
Baylor University, United States
Richard Bruce Bolster,
University of Winnipeg, Canada

****Correspondence:***
Daniel G. Amen
daniel@amenclinic.com

†These authors have contributed equally to this work and share first authorship

Specialty section:
This article was submitted to Neuroimaging and Stimulation, a section of the journal Frontiers in Psychiatry

Received: *15 June 2021*
Accepted: *18 October 2021*
Published: *24 November 2021*

Citation:
Amen DG, Henderson TA and Newberg A (2021) SPECT Functional Neuroimaging Distinguishes Adult Attention Deficit Hyperactivity Disorder From Healthy Controls in Big Data Imaging Cohorts. Front. Psychiatry 12:725788. doi: 10.3389/fpsyt.2021.725788

INTRODUCTION

Attention deficit hyperactivity disorder (ADHD) is one the most costly psychiatric disorders, conservatively estimated to be around 42.5 billion USD annually (1). ADHD is also one of the most prevalent disorders in the USA with ∼5.29–10% of school-aged children estimated to suffer from the disorder (1). Despite these enormous costs and the issues of administering stimulant medication to children, there remains no empirically validated means by which ADHD can be diagnosed. Objective markers of ADHD would not only improve reliability of the diagnosis but might also allow for precision medicine treatments (2). Problems associated with the use of subjective criteria for diagnosing ADHD are extensive (3). Subjective diagnostic criteria and related diagnostic processes are highly vulnerable to variability by different clinics and by different clinicians within the same clinic (4, 5). Moreover, even when clinicians strictly adhere to the DSM method for diagnosing ADHD, there is also significant variation in the rates of ADHD secondary to the DSM versions utilized by a clinician (6). The problem does not become easier with adult ADHD patients with whom confounds of coping strategies, substance use, and comorbidities cloud the diagnostic picture (7).

Furthermore, the cardinal symptom of ADHD—inattention—is a non-specific symptom. Inattention is found not only in ADHD, mania, anxiety, and depression, but it is also found in traumatic brain injury, carbon monoxide poisoning, cadmium toxicity, lead toxicity, schizophrenia, post-traumatic stress disorder (PTSD), post-coronary bypass syndrome, multiple sclerosis, substance abuse, space-occupying lesions, CNS infections, dementia, and a litany of other conditions which alter frontal lobe functioning. Distinguishing among these alternatives by interview alone is challenging, because, for instance, there is no specific question that will reveal lead toxicity or cadmium toxicity. Similarly, an interview may or may not uncover a history of brain injury, depending on the degree of anterograde amnesia or how the patient has trivialized the impact of a concussive event. The authors have seen numerous cases of drowning, toxicity, post-pediatric surgery, hypomania, and irritable depression which were misdiagnosed clinically as ADHD. An additional challenge in diagnosing ADHD, regardless of age, is that comorbidity is the rule, rather than the exception in ADHD.

DIAGNOSTIC EVALUATION OF ADHD

The base level of precision in the diagnostic evaluation of ADHD is the use of rating scales. Measures such as the Vanderbilt Rating Scale (6), and the Conners Parent Rating Scales (8) are quantifiable, but lack diagnostic precision. Scales are dependent upon the subjective opinion of parents and/or teachers. Symptom overlap of scale items across multiple DSM diagnoses is the rule rather than the exception (9, 10).

A higher level of accuracy can be derived by the use of computerized tests of attention. While there is perception that continuous performance tests are the "objective standard" for ADHD diagnosis, the research demonstrates a distinct gap between the computerized diagnosis and the clinical presentation. For example, correlation between the Conners Continuous Performance Test (CPT) results and results of parent or teacher symptom rating scales is low to moderate (11, 12). The Test of Variables of Attention (TOVA) has a sensitivity of ∼85% and a false positive rate of 30% (11, 13). In contrast, the CPT has a high false negative rate (14). Combining the continuous performance test with an infrared motion sensor (McLean Motion Attention Test or Quotient ADHD System) has been FDA-cleared as a diagnostic tool for ADHD. Using this system, Teicher et al. found that boys with ADHD moved their heads 2.3 times more often than boys without ADHD (15). However, this system is less effective in the diagnosis of inattentive-type ADHD and of adult ADHD.

BIOMARKERS FOR ADHD

The Food and Drug Administration's (FDA) Biomarkers, EndpointS and other Tools (BEST) glossary defines a biomarker as: "a defined characteristic that is measured as an indicator of normal biological processes, pathogenic processes, or responses to an exposure or intervention, including therapeutic interventions" (16). Note that the BEST definition does not limit the nature of the characteristic to a molecule. Any characteristic can serve as an indicator of pathology or response to therapeutic intervention. A significant need remains for identifying biomarkers for psychiatric conditions, including ADHD, to provide more accurate diagnosis and to foster efforts to develop more effective treatments. While there is widespread agreement that fronto-striatal-thalamic pathways are altered in ADHD (17, 18), it has been difficult to identify a reliable neuroimaging biomarker, regardless of the neuroimaging technique.

Quantitative EEG

Quantitative electroencephalogram (qEEG) has been FDA-approved as a diagnostic tool for ADHD and purported to serve as a biomarker. However, the marker of elevated theta/beta wave ratio is not reliably diagnostic. The pivotal study on the ratio reported a 20% false negative rate (19). Moreover, Arns et al. analyzed the collective data of more than 1,750 children and concluded that the elevated theta/beta ratio was not a reliable diagnostic measure for ADHD (20). Elevated theta/beta ratio has not proven to be the endophenotype or biomarker that was initially hoped.

Anatomical MRI

Anatomical magnetic resonance imaging (MRI) studies have found a small number of consistent findings across the age-range of ADHD (21). Multiple meta-analyses of case-control studies have shown reduced volume of the striatum in children with ADHD (22–25); however, the reduced striatal volume in ADHD appears to correct itself with age (24, 26). Notably, reduced striatal volume is also found in children with autism spectrum disorders (27). The ENIGMA-ADHD project examined the volumes of subcortical structures in a large sample of 1,713 cases of ADHD compared to 1,529 controls (28). In children, slight, but significant, decreases in volume were found in the

caudate, putamen, and amygdala, as well as the hippocampus and nucleus accumbens. However, these differences were not found in the adult subjects, confirming the results of some meta-analyses (24, 26). Similarly, the ENIGMA-ADHD analysis of cortical thickness found smaller surface areas in the frontal, cingulate, and temporal cortices in children, but not in adults (29). Further analysis of the ENIGMA data including 2,271 cases of ADHD and 5,827 controls found cortical thickness was smaller in orbital frontal, inferior frontal and cingulate cortices across all age ranges, including adults.

One limitation of this anatomical MRI research is that a majority of the studies do not control for comorbidities or medication use. Also, the relative paucity of longitudinal studies precludes determining if the brain volume changes represent a persisting difference or a delay in maturation. An additional limitation of this work is the high degree of variability within groups for any given metric (27). Lastly, while the ENIGMA-ADHD database represents an impressive feat of cross-site coordination and data collection, the ADHD population captured therein is incompletely characterized. For example, comorbidities are known in only 58% of the population and stimulant use is documented for only about half of all cases (27).

Functional MRI

ADHD has been the subject of intense study using functional MRI over the past 24 years, yet the results have been highly divergent (30–32). Multiple meta-analyses have yielded mixed results. To quote the authors of a recent meta-analysis of 96 studies with over 1,914 subjects which found no statistically significant functional abnormalities in ADHD:

> "*The overall findings indicate a lack of regional convergence in children/adolescents with ADHD, which might be due to heterogenous clinical populations, various experimental design, preprocessing, (or) statistical procedures in individual publications.*" (32)

Despite the harsh criticism of the heterogeneity in the field, these authors did find a marginally significant decrease in left inferior frontal cortex activity in male children only (32). Others have found similar task-dependent inferior frontal cortex deficits, although it varies whether the right or left side is more involved (32–36). For example, Pliszka et al. found that adolescents with ADHD ($N = 17$; age 13.4 $\pm$ 1.9 yrs) failed to show increased perfusion in the anterior cingulate bilaterally and in the left orbitofrontal prefrontal cortex during an inhibitory task (Stop Signal Task) compared to 15 age-matched controls (age 13.2 $\pm$ 1.9). These authors further analyzed the ADHD subjects by comparing children who were medication-naïve and those who were not. These two subgroups did not differ in performance or functional neuroimaging findings (37). Smith et al. described similar findings in a small group of 19 medication-naïve patients (age 12.9 $\pm$ 1.9 yrs) compared to 27 healthy controls (age 14.1 $\pm$ 2.0 yrs). They found decreased perfusion in the left rostral mesial frontal cortex during one interference-type concentration task and decreased perfusion in the bilateral inferior prefrontal (right more significant than left) and temporal lobes during a switch task (34).

Efforts to explore networks either via the default mode network (DMN) or using selected kernels to identify networks of activation, have suggested that ADHD is not a disorder of isolated brain regions, but more of a connectivity disorder (38). Nevertheless, in a recent meta-analysis involving 30 studies with 1,094 subjects with ADHD and 884 Controls, no significant functional networks or areas were found to distinguish ADHD from Controls (38).

In addition, multiple areas of the cerebral cortex, including parietal and temporal regions, as well as the cerebellum, have shown decreased activity during concentration tasks in subjects with ADHD (17). Thus, in addition to the technical discrepancies in fMRI studies, the effects of age, medication use, comorbidities, and recruitment or suppression of activity in multiple areas of the brain have hampered the ability of fMRI to reveal a consistent biomarker.

Machine Learning – Multimodal Imaging

Machine learning or artificial intelligence (AI) techniques have been applied to neuroimaging in an effort to detect patterns and findings not evident from simple statistical analysis. Numerous AI techniques, such as support vector machine, multiple kernel learning, deep belief network, convolutional neural network and others have been applied to fMRI and anatomical MRI data (39). For example, a group of 36 adults with ADHD and 36 controls underwent anatomical MRI, fMRI using a cued attention task, and diffusion tensor imaging. Twenty features were chosen from this multimodal dataset and processed in a meta-algorithm referred to as "ensemble learning techniques" (ELT). A series of training and validation algorithms followed by multiple ELT-based models yielded a number of parameters with favorable sensitivity and specificity (18). Notably, decreased activity of the right inferior frontal gyrus stood out as a strong predictor of ADHD status. The limitation of the AI work to date has been the relatively small sample sizes, the lack of consistent findings across studies (18, 39, 40) and the need for multiple time-consuming scans.

Functional SPECT

Functional neuroimaging studies of ADHD utilizing single-photon emission computed tomography (SPECT) in children and adults have included baseline studies, cognitive challenge studies, and medication effect studies. The controlled clinical trials have been small with a range of 6–54 subjects (reviewed in Discussion). Our earliest study in this area included 54 children who met DSM-III-R criteria for ADHD compared to a clinical group of 18 children who did not meet those criteria (41). Visual, semi-quantitative reads revealed areas of increased perfusion in dorsal frontal cortices, while areas of decreased perfusion were noted in the orbitofrontal/inferior prefrontal cortices in baseline SPECT scans. SPECT scans during intellectual challenge also revealed decreased inferior prefrontal cortical perfusion (41). A smaller study by our group in 27 older adults (>50 years) who met DSM-IV criteria for ADHD, but not for major depression, revealed a similar decrease of perfusion in the

orbitofrontal cortices at baseline (42). Recently, a larger, open retrospective case series of 170 patients ranging in age from adolescent to adult utilized visual reads of SPECT scans found that visual read to assess ADHD using 3D renderings yielded 83% sensitivity and 77% specificity in the diagnosis of ADHD based predominately on the finding of decreased orbitofrontal perfusion (43).

Findings across multiple studies are consistent but are they reliable and can they be used on an individual basis to predict the diagnosis of ADHD? This question is central to the ability to use a SPECT neuroimaging finding as a biomarker. Herein, we describe the first step in an analysis of a community dataset totaling over 100,000 patients. We describe the analysis of adults with ADHD free of comorbidity compared to a control group who lack any psychiatric or neurological diagnoses. Future steps will include comparisons of comorbid ADHD across age groups and predictive modeling utilizing machine learning algorithms involving iterative comparisons of data subsets to assess the predictive value of specific biomarker candidates.

MATERIALS AND METHODS

Study Subjects

This study adhered to the STAR-D guidelines (44) (see **Supplementary Material** for table). This retrospective review was approved by an accredited institutional review board, IntegReview (http://www.integreview.com/). In this retrospective analysis, all study subjects were patients at Amen Clinics, Incorporated (ACI), a multidisciplinary group of psychiatric clinics that incorporates SPECT neuroimaging into diagnostic assessment and treatment (45). Methods of clinical assessment, gamma camera equipment, scan analysis software, and interpretation protocols are unified throughout the group of clinics. All subjects were drawn from the following ACI branches: Newport Beach, CA; Brisbane, CA; Fairfield, CA; Tacoma, WA; Bellevue, WA; Reston, VA; New York, NY; Atlanta, GA. Group 1 included patients seen from April 1996 to November 2013. Informed consent was obtained at the time of patient evaluation from all patients or legal guardians to allow their anonymous clinical data to be utilized for future research purposes. We identified from this clinical cohort, Group 1 (n = 1,006) which included persons that met the DSM-IV criteria for ADHD (46) and no other diagnoses (**Table 1**). The diagnosis of ADHD (inattentive, impulsive-hyperactive, combined) was determined by DSM-IV guided clinical interview, internal DSM-IV-guided symptom checklists, and a Conners Continuous Performance Test (47). The ADHD-only group was compared to a Control group who did not meet criteria for any psychiatric condition and had no history of traumatic or toxic brain injury (n = 129). The Control group was recruited using local advertisements in newspapers and local colleges. Each subject met the clinical criteria for a healthy brain subject based on our criteria that included the absence of current medical illnesses, brain trauma, family history of psychiatric illness, drug/alcohol abuse and no current or past evidence of behavioral or psychiatric issues as measured by a detailed clinical history, Minnesota Multiphasic Personality Inventory (MMPI) and Structured Clinical Interview for Diagnosis (SCID) for DSM-IV. The Control group recruitment and scanning study protocol was approved by Western IRB (WIRB # 20021714). All subjects were fully informed and gave their written consent.

TABLE 1 | Demographic characteristics of Group 1.

Variable	ADHD (n = 1,006)	Control (n = 129)	Statistical comparison (t, p)
Age	37.7 ± 15.5	45.4 ± 16.9	2.9, 0.004
Gender (% female)	34	44	30.6, <0.001
Race (% non-Caucasian)	31	33	48.9, <0.001
Bipolar disorder	0	0	NA
Depression	0	0	NA
Dementia	0	0	NA
Brain trauma	0	0	NA
PTSD	0	0	NA
Substance disorder	0	0	NA
Schizophrenia	0	0	NA

SPECT Neuroimaging

Brain SPECT was applied as previously described in published work using standard methods (48). To review, all patients were instructed to refrain from the use of stimulants, caffeine, ephedrine, bupropion, atomoxetine, nicotine, alcohol, illicit drugs, opiates, benzodiazepines, guarana, or steroids for 48 h prior to scanning. Other medications including psychotropic medications were not restricted. For each scan, an age- and weight-appropriate dose of technetium Tc99m-HMPAO (commercially available as Ceretec) was administered intravenously. At all clinic sites, photon emission was captured using a high-resolution Picker (Phillips) Prism 3000 triple-headed gamma camera with fan beam collimator with data collected in 128 × 128 matrices, yielding 120 images per scan with each image separated by three degrees spanning 360 degrees. A low pass filter was applied with a high cutoff. A Chang attenuation correction was performed using linear methods (49).

All images were processed using Odyssey software (Picker), with transaxial slices oriented horizontal to the AC-PC line. Coronal, sagittal, and transaxial slice images (6.6 mm apart, unsmoothed) were then rendered in the Odyssey step-20 scale, a commercial scale included in the Odyssey software package, which scales all voxels to the brain maximum and assigns each a color gradient based on its percentile of activity. Each color step represents a (not necessarily linear) five-percentile-point change in rCBF.

Baseline images were acquired in the following manner, adapted from the Society of Nuclear Medicine and Molecular Imaging Procedure Guideline for Brain Perfusion SPECT (50). Patients sat upright in a quiet, dimly lit room with open eyes, and the bolus was injected after 10 min. Patients sat for an

additional 10 min post-injection. While concentration-task scans were obtained for all patients, they are not included in the current analysis and will be subject of future studies.

Clinician Visual Rating of Regions of Interest

Methods for clinical interpretation of SPECT scans by visual read have not changed during the 17 years of patient evaluations from which these data are drawn. These methods have already been fully described in prior peer reviewed work (42). To review, 14 gross general cortical regions of interest (ROIs) in orthogonal planes were visually inspected and rated using the Mai Atlas of the Human Brain (51): the left and right prefrontal poles [medial aspect of Brodmann area (BA) 10, anterior rostral aspect of BA 12]; the left and right inferior orbitofrontal (BA 11); the left and right anterior/lateral PFC (comprised of BAs 45, 46, 47, the anterior aspect of area 9, the lateral aspect of area 10); the left and right midlateral PFC (BAs 8 and 44, and the posterior aspect of area 9); the left and right posterior frontal region (BAs 4, 6, and the anterior aspect of area 43); the left and right parietal lobes (BAs 1, 2, 3, 5, 7, 39, and 40, and the posterior aspect of area 43); and the left and right occipital lobes (BAs 17, 18, and 19). In like manner, we rated both the left and right cerebellum. In addition, seven gross subcortical ROIs were rated: the anterior cingulate gyrus (BAs 25, 32, 33, and the anterior aspect of BA 24); the left and right insula; the left and right thalami; the left and right caudate nuclei; and the left and right putamina. The following non-linear scheme was used to visually rate rCBF: activity rated above the top 95% was assigned a score of +4; 91–95% was scored +3; 86–90% was scored +2; 81–85% was scored +1; 61–80% was scored 0; 56–60% was scored −1; 51–55% was scored −2; 46–50% was scored −3; and 41–45% was scored −4. Because of the non-uniform nature of perfusion within any given ROI, each area was rated for its highest and lowest activity, and the average of the two was taken as a given ROI's final rating, resulting in a rating scale ranging from +4 to −4 in half-point intervals. Raters had minimal clinical information. Interrater reliability was not assessed for these particular groups; however, prior studies have found a kappa of 0.79 or above for all visually-read regions (42).

Post-hoc ROI Analysis

All baseline scans in the two groups were subjected to *post-hoc* ROI analysis. ROI counts were derived from the anatomical regions in the AAL atlas (52), different, but closely aligned with the regions in the atlas used for visual reads. ROI included in this study were as follows: anterior cingulate, mid-orbital frontal, insula, anterior inferior temporal, middle inferior temporal, posterior inferior temporal, temporal pole, superior parietal, hippocampus, thalamus, caudate, pallidum, cerebellar regions 7b,8,9, cerebellar crus1, and cerebellar vermis. To account for outliers, T-score derived ROI count measurements were derived using trimmed means that are calculated using all scores within the 98% confidence interval ($-2.58 < Z < -2.58$). The ROI mean for each subject and the trimmed mean for the sample are used to calculate with the following formula:

$$T = 10^{*}((subject\ \ roi\_mean - trimmed\ \ regional\_avg)/ trimmed\ \ regional\_stdev) + 50$$

Statistical Analyses

All analyses were performed using Statistical Package for Social Science (SPSS) (53). In Group 1, a receiver operating characteristic (ROC) curve analysis was done using DSM-IV diagnosis for ADHD as ground truth. The first step of this analysis was constructing logistic regression models with age, gender, and race as co-variates. Separate models were constructed with the following independent variables: (i) Baseline visual reads, and (ii) T-score ROI counts from baseline scans. From each of these logistic regression models, odds ratios and predicted probabilities were computed and then inputted into an ROC analysis to determine area under the curve, or accuracy of the given methods used. For ROI data, one way ANOVA with Least Square Differences (LSD) for correcting for multiple comparisons was done to assess group differences. Automated linear regression was used for feature selection. Correction for multiple comparisons were performed in each logistic regression model.

RESULTS

The total sample of 1,135 subjects were separated into two groups. Group 1 consisted of patients who met the DSM-IV criteria for ADHD, and it contained 1,006 subjects (see **Table 1**). The mean age was 37.7 ± 15.5, making it somewhat younger than the control group ($n = 129$) with a mean age of 45.4 ± 16.9 ($p \leq 0.001$). Group 1 was 34% female and 31% non-Caucasian, while the control group was 44% female and 33% non-Caucasian ($p < 0.001$ in age group and non-significant for non-Caucasian). Group 1 did not meet criteria for any other psychiatric disorder, substance abuse, or brain injury based on a detailed clinical history, the Minnesota Multiphasic Personality Inventory (MMPI) and the Structured Clinical Interview for Diagnosis (SCID) for DSM-IV.

The results of the logistic regression models with age, gender, and race as co-variates, computation of odds ratios and predicted probabilities with correction for multiple comparisons were input for a ROC analysis which yielded area under the curve (AUC) calculations. The AUC for Visually Read ROI's of the Baseline scan was 97.6%. The AUC for the *post-hoc* ROI analysis of the Baseline scan was 100%. Sensitivity of the visual reads was 100% while specificity was >97%. The sensitivity and specificity of the *post-hoc* ROI analysis were both 100%. **Figure 1** is a typical baseline tomogram presentation of the SPECT scan data from a control case. **Figure 2** is a typical baseline tomogram of the SPECT scan data from a patient in Group 1 illustrating hypoperfusion by visual interpretation in the medial anterior prefrontal (orbitofrontal) cortex, bilateral temporal lobes, and the anterior cingulate gyri. These findings proved strongly predictive of the diagnosis of ADHD, as illustrated in **Table 2**. Areas identified by visual read as having highly significant Odds Ratio ($p < 0.001$) for discriminating ADHD from control included:

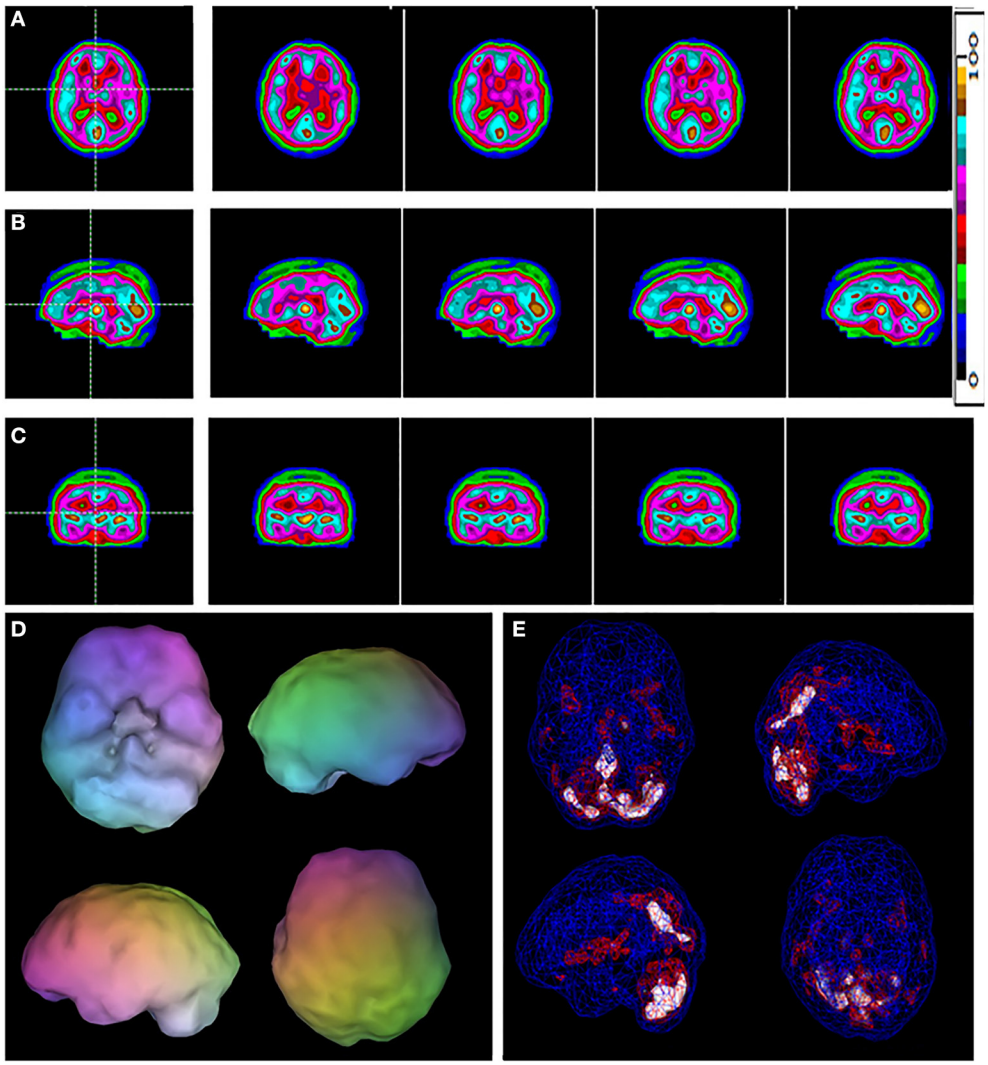

FIGURE 1 | A typical example of a control case. Selected tomograms in horizontal **(A)**, sagittal **(B)**, and coronal **(C)** orientation are provided. The color scale for the tomograms is provided. All voxels are scaled to the brain maximum and assigned each a color gradient based on its percentile of activity. Each color step represents a (not necessarily linear) five-percentile-point change in rCBF. **(D)** A 3-D representation of the scan data is shown. The surface is set at 60% of brain maximum. Areas which fall below 55% are represented as indentations or holes depending on how far below 55% the activity falls. **(E)** A wireframe brain representation is shown, wherein the areas of brain with activity at 85% of maximum or greater are shown in red and areas of 92% or greater are shown in white.

medial anterior prefrontal cortex, left anterior temporal lobe, and right insular cortex. Areas with moderately significant Odds Ratio ($p < 0.03$) included: right lateral middle temporal lobe, right medial temporal lobe, dorsal anterior cingulate gyrus, the genu of the anterior cingulate gyrus, and the left parietal cortex (see **Table 2**).

Table 3 shows the *post-hoc* quantified ROI regions that were most predictive in distinguishing cases of ADHD in Group 1 from controls. In particular, cerebellar subregions were very predictive ($p < 0.001$), along with the bilateral anterior inferior temporal lobe, bilateral middle temporal pole, and the bilateral inferior occipital lobe. Areas with significant predictive findings ($p < 0.03$) included: bilateral anterior cingulate gyri, bilateral mid orbital frontal cortices, right superior orbital frontal cortex, bilateral hippocampi, right middle occipital cortex, bilateral thalamus, and bilateral pallidum. Some left/right differences were observed. The left anterior cingulate showed a higher odds ratio than the right, while the right orbital frontal cortical areas had higher odds ratios than the corresponding areas on the left.

DISCUSSION

In the adult population, there was high separation between non-comorbid ADHD patients vs. healthy controls using this method. The ROC characteristics were similar for the baseline scan data whether using visual or quantitative analysis. Since the *post-hoc* ROIs were not used in any way to initially establish the clinical diagnoses, they serve as a particularly rigorous independent

TABLE 2 | Predictive visually interpreted ROIs from Group 1.

Brain region Baseline	Statistical output Odds ratio of increased probability for ADHD, *p*-value
Medial anterior prefrontal cortex	5.4, 0.001
Left anterior temporal lobe	4.7, 0.001
Right insular cortex	4.3, 0.001
Right lateral middle temporal lobe	3, 0.01
Right medial temporal lobe	3.6, 0.02
Dorsal anterior cingulate gyrus	2.8, 0.02
Genu anterior cingulate gyrus	4.5, 0.03
Left parietal lobe	4.4, 0.03

predictor of diagnostic category. However, it is emphasized that nuclear medicine physicians and radiologists typically use visual analysis for readings SPECT scans in a clinical setting; thus the high sensitivity and specificity of the identified areas serve as promising steps for the translation of SPECT markers for ADHD more widely into clinical practice.

To guide the relevance of these results as possible ADHD biomarkers we use the term *biomarker* as defined by the FDA BEST criteria (16) - "a defined characteristic that is measured as an indicator of normal biological processes, pathogenic processes, or responses to an exposure or intervention, including therapeutic interventions." A safe and effective biomarker for ADHD could guide diagnosis and treatment. Treating ADHD based solely on clinical indications is not without risk. For example, the differentiation of ADHD from incipient bipolar disorder is challenging. Clinical experience and research data have shown that stimulant medications can precipitate a manic episode, exacerbate mood instability, and/or increase rapid cycling. Some (54) hypothesize that stimulant medication exposure can permanently alter the course of bipolar disorder in some children. In addition, atomoxetine, FDA-approved for the treatment of ADHD, has been clinically found to be a potent mood destabilizer. A large open-label naturalistic case series (55) found that roughly 33% of patients became mood dysregulated on atomoxetine. Symptoms of aggression, hypomania, agitation, and frank mania were reported in patients, some of whom lacked any previous history of mood symptoms. Thus, correctly differentiating ADHD from incipient bipolar disorder and/or possible variants of ADHD who show adverse reactions to stimulants and/or atomoxetine would mitigate serious patient harm.

Prior SPECT neuroimaging studies of ADHD in children and adults have varied in quality considerably, but have consistently pointed in the direction of potential biomarkers. The first baseline investigations by Lou et al. (56, 57) utilized Xenon-133, which provides a single-pass perfusion scan and absolute quantification of perfusion in units of ml/min/100 g of tissue, albeit with limited resolution. In addition, confounds of methodology and diagnostics further limit the validity of these studies. Nevertheless, a later study by the same group with better technology replicated the findings of decreased perfusion of the striatum based on Xenon-133 quantitative perfusion (58). Gustafsson et al. (59) compared baseline SPECT scan data to EEG and neurological examination in a group of 28 children with broadly defined ADHD (based on Conners Parent Rating Scale and Wechsler Intelligence Scale for Children). While this study lacked a control group, it is notable for its correlation of EEG findings, symptoms, soft neurological signs, and functional neuroimaging. The key findings were that patients

TABLE 3 | Group 1 ROI differences between ADHD and normal.

Region	Control	ADHD	*F*, *p*-value
Baseline			
L caudate	55.6 ± 8.2	53.4 ± 8.1	3.9, 0.04
R caudate	55.7 ± 8.1	53.5 ± 8	4.2, 0.04
L cerebellum 7b	47.6 ± 6.9	54.8 ± 9.4	33.2, <0.001
R cerebellum 7b	47.7 ± 8.1	54.2 ± 10.1	23.5, <0.001
L cerebellum 8	49.2 ± 7.8	55.7 ± 9.1	27.3, <0.001
R cerebellum 8	49 ± 8	55.2 ± 8.9	26.3, <0.001
L cerebellum 9	51.4 ± 8.5	56 ±8.6	15.5, <0.001
R cerebellum 9	51.4 ± 8.2	55.9 ± 8.6	14.9, <0.001
L cerebellum crus1	51.3 ± 8	54.6 ± 8.1	8.7, 0.003
R cerebellum crus1	50.7 ± 8.3	54.6 ± 8.4	11.2, 0.001
L cerebellum crus2	47.1 ± 7.8	54.3 ± 9.5	32.2, <0.001
R cerebellum crus2	47.2 ± 7.8	54.1 ± 9.8	27.3, <0.001
L anterior cingulate gyrus	56.1 ± 8.7	53.1 ± 8.2	7.1, 0.008
R anterior cingulate gyrus	55.7 ± 8.7	53.1 ± 8.2	5.4, 0.02
L mid orbital frontal 9	51.3 ± 9.2	54.2 ± 8.2	6.1, 0.01
R mid orbital frontal 10	50.3 ± 9.3	54.1 ± 8.5	10.1, 0.002
R superior orbital frontal lobe 10	51.8 ± 9.2	54.3 ± 7.9	5.1, 0.02
L hippocampus	56.2 ± 8.6	53.7 ± 8.1	4.9, 0.02
R hippocampus	56.2 ± 8.5	53.7 ± 7.8	5.5, 0.01
R insula	55.6 ± 8.2	53.3 ± 7.9	4.3, 0.04
L inferior occipital lobe	49.9 ± 8.5	54.7 ± 8.6	16.2, <0.001
R inferior occipital lobe	48.6 ± 9.3	54.9 ± 8.8	26.8, <0.001
R middle occipital lobe	51.1 ± 8.7	54.7 ± 8.3	10.3, 0.001
L superior occipital lobe	51.9 ± 8.5	54.4 ± 8.2	4.6, 0.03
R superior occipital lobe	52.1 ± 8.2	54.5 ± 8.1	4.3, 0.04
L pallidum	56.2 ± 8.6	53.5 ± 8.2	5.6, 0.01
R pallidum	56.3 ± 8.7	53.8 ± 8.1	4.6, 0.03
R superior parietal	49.6 ± 8.4	52.4 ± 8.7	5.3, 0.02
L anterior inferior temporal lobe	47.9 ± 9.2	53.4 ± 9.3	18.3, <0.001
R anterior inferior temporal lobe	48 ± 7.6	53.4 ± 9.7	17.1, <0.001
L mid inferior temporal lobe	51 ± 8.3	54.1 ± 8.4	7.5, 0.006
R mid inferior temporal lobe	50.5 ± 7.6	53.9 ± 8.2	9.3, 0.002
L posterior inferior temporal lobe	51.5 ± 7.8	54.3 ± 8.1	6.4, 0.01
R posterior inferior temporal lobe	51 ± 8.5	54.6 ± 8.2	9.5, 0.002
L mid temporal pole	49.7 ± 9.1	53.7 ± 9.2	10.2, 0.001
R mid temporal pole	48.6 ± 9.2	53.9 ± 9.3	17.1, <0.001
L thalamus	55.1 ± 6.4	53.1 ± 7.9	5.1, 0.02
R thalamus	54.9 ± 7.1	53.4 ± 7.8	5.2, 0.02
Vermis 10	56.5 ± 6.9	53 ± 8.1	10.3, 0.001
Vermis 8	51 ± 7.1	55.2 ± 8.2	11.2, 0.001

This table shows the quantified statistically significant ROI differences between ADHD and normal controls in Group 1 on baseline and concentration scans.

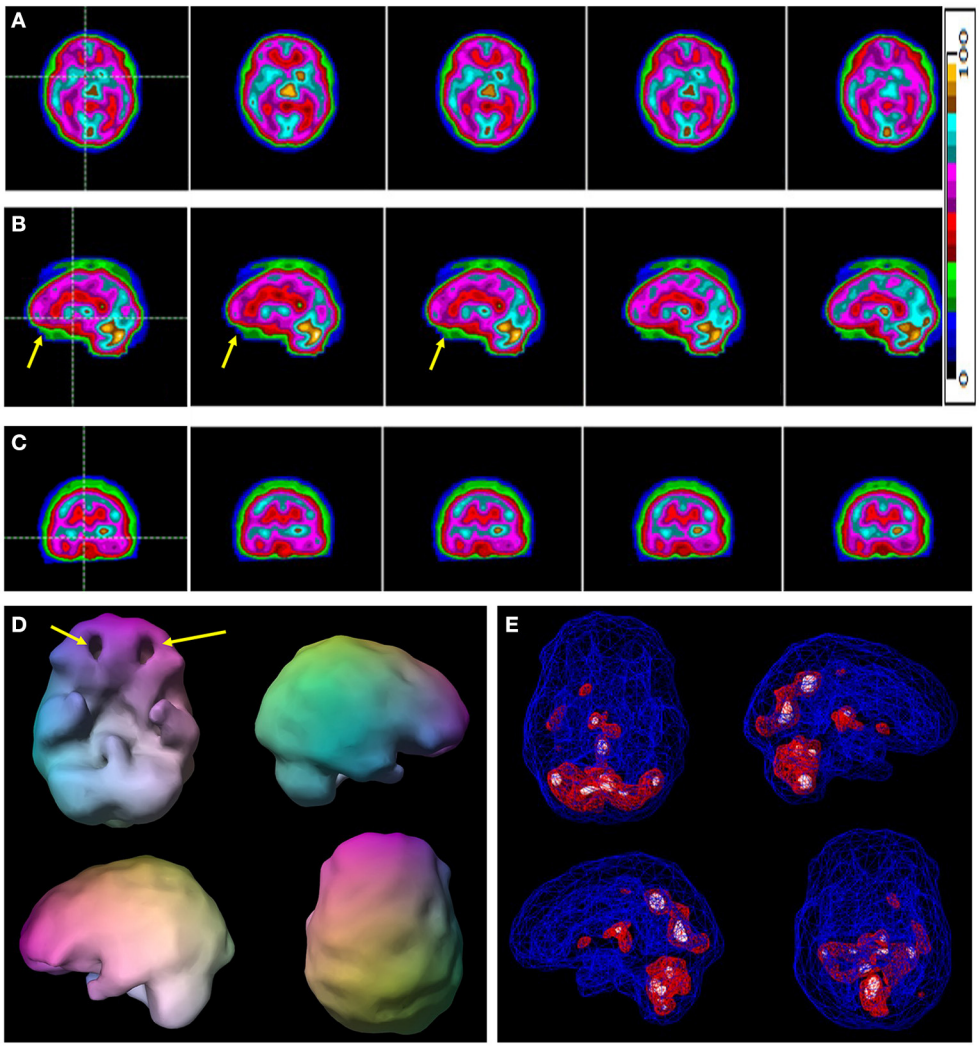

FIGURE 2 | A typical example of a case of ADHD without comorbidity. Selected tomograms in horizontal **(A)**, sagittal **(B)**, and coronal **(C)** orientation are provided. The color scale is the same as **Figure 1** for the tomograms is provided. All voxels are scaled to the brain maximum and assigned each a color gradient based on its percentile of activity. Each color step represents a (not necessarily linear) five-percentile-point change in rCBF. Yellow arrows indicate areas of hypoperfusion in the orbitofrontal cortices. **(D)** A 3-D representation of the scan data is shown. The surface setting is the same as in **Figure 1**. Yellow arrows point to the areas of decreased perfusion in the orbitofrontal cortices. **(E)** A wireframe brain representation is shown with setting the same as in **Figure 1**.

with ADHD showed decreased frontal lobe perfusion and the degree of symptoms correlated with the degree of hypoperfusion (decreased activity) in the frontal lobes (59). In addition, patients with ADHD had a number of soft neurological signs and physical anomalies. Similarly, Spalletta et al. (60) found a correlation between symptoms of ADHD and frontal lobe perfusion. In a carefully screened group of 8 children (inclusion criteria were medication-naïve, normal MRI scan, no comorbid psychiatric diagnoses, IQ > 80, and ADHD diagnosis based on Stroop Test and neurometric data), baseline scans done under sedation showed decreased perfusion of the left dorsolateral prefrontal cortex and orbital frontal cortex. Relatively increased perfusion in the right prefrontal cortex and relatively decreased perfusion in the left prefrontal cortex were correlated with worse clinical symptomatology (60). Given that the radiopharmaceuticals HMPAO and ECD are distributed and relatively fixed within 2 min of injection and a waiting period of roughly 15–30 min was allowed after tracer injection, sedation during the scan would have no significant effect on the distribution of radiotracer and scan results.

Cognitive challenge tasks highlight the deficits in task-specific function that characterize ADHD. A response inhibition task was administered to 20 children with ADHD and 4 controls (61). The authors concluded that children with ADHD exhibited a right prefrontal cortex dysfunction based on an exaggerated left-to-right asymmetry of perfusion.

Medication response trials using SPECT or fMRI can also point toward areas which may serve as candidate imaging biomarkers. In general, control patients showed equivocal differences in perfusion in the frontal lobes whether they were

on- and off-stimulant medications. In contrast, children with ADHD demonstrate decreased perfusion at baseline (which equates to decreased activity) in the frontal cortices and often the temporal lobes and cerebellum (42, 61–66) that increased with stimulant medication (61, 63, 64, 67).

Kim et al. (68) conducted an elegant treatment effect study involving 40 medication-naïve children with ADHD (who were evaluated with ADHD assessment scales, structured clinical interviews, and neuropsychological testing, and had normal MRI or CT scans) and who were compared to 17 controls using statistical parametric analysis before and after treatment with methylphenidate (68). Baseline HMPAO SPECT scans were obtained in 40 children (age 9.7 ± 2.1 years) diagnosed with ADHD. Strict exclusion criteria eliminated subjects with IQ below 90, learning disorders, neurological disorders, or comorbid psychiatric diagnoses of mood, anxiety, or conduct. These baseline scans were then compared statistically to baseline scans of 17 similar strictly screened controls (age 10.5 ± 2.2 years). Then, ADHD subjects were started on methylphenidate at standard doses (0.3–1.0 mg/kg/day). After 4–5 weeks of stimulant treatment, ADHD subjects underwent a second baseline SPECT scan while taking methylphenidate. The second scan was again compared statistically to the control scans and differences between the pre- and post-medication scans were identified. All ADHD subjects showed significant improvement in symptoms based on psychometric testing while taking methylphenidate. Pre-treatment scans of subjects with ADHD showed decreased perfusion of the prefrontal cortex and middle temporal gyri but showed increased perfusion in the somatosensory cortex and anterior cingulate gyri, compared to controls. After treatment with methylphenidate, ADHD subjects showed increased perfusion of the prefrontal cortex relative to their own pre-medication scans. Perfusion in the somatosensory cortex and striatum was reduced (68). 3D SPECT images in ADHD have also been used by Schneider et al. (43, 69) to show orbitofrontal cortex hypoperfusion in patients with ADHD.

Lorberboym et al. (70) examined ADHD with and without comorbid learning or behavioral diagnoses (oppositional defiant disorder, conduct disorder, learning disorder, mood disorder). After psychometric testing and structured clinical interview, a group of 8 children with simple ADHD, a group of 11 children with ADHD comorbid for one or more of the above diagnoses, and a group of 9 age-matched controls underwent SPECT scanning, and the scans were compared. Using a semi-quantitative analysis of selected regions of baseline scans, ∼50% of cases showed decreased frontal lobe perfusion, but all of the cases who were comorbid demonstrated decreased temporal lobe perfusion (70). These findings were largely confirmed in a study of 19 children with specific learning disorders compared to 12 children with ADHD (71). Unfortunately, no control group was included in this confirmatory study. Children with learning disorders showed relatively decreased perfusion in the temporal lobes and the right parietal lobe, but also in the bilateral basal ganglia.

Recently, these neuroimaging findings have been replicated using a newer technique of infrared spectroscopy (72). A sample of 150 children with ADHD were compared to 51 controls in a series of concentration tasks. Children with ADHD demonstrated low activation of the medial prefrontal (orbitofrontal) cortex during vigilance and concentration tasks.

COMORBIDITY IS THE RULE, NOT THE EXCEPTION

Unfortunately, comorbidity is the rule, rather than the exception, in cases of ADHD. Therefore, a study of pure ADHD is not sufficient to identify a clinically useful imaging biomarker for ADHD. Children with ADHD frequently have comorbid anxiety, oppositional disorders, or learning disorders (73, 74). For example, learning disorders are highly prevalent among those with ADHD, ranging from 10 to 90% comorbidity (75, 76). The prevalence of anxiety disorders among those with ADHD ranges from 15 to 35% (77, 78). Depressive disorders occur in 12–59% of children with ADHD (79, 80). The prevalence of conduct disorder and oppositional defiant disorder among those with ADHD ranges from 30 to 50% (76, 81). The comprehensive Multimodal Treatment Study of Children with Attention-Deficit/Hyperactivity Disorder (MTA) study similarly found 29 % of children diagnosed with ADHD were comorbid for either conduct disorder or oppositional defiant disorder (78). These comorbidities profoundly alter the clinical picture of ADHD and undoubtedly alter the response to pharmacological interventions. Current diagnostic methods fail to fully assess the presence and impact of comorbidities.

ADHD in adults was largely unrecognized prior to 2002 (82, 83). Comorbidity clouds the diagnosis in adults, as well. An estimated 65–89% of adult patients with ADHD also have anxiety disorders, depressive disorders, bipolar disorder, personality disorders, drug abuse, and alcohol abuse (84). Comorbidity of ADHD and depressive disorders ranges from 18.6 to 53% (85). Anxiety disorders are quite common in adults with ADHD, approaching 50% comorbidity (86). An estimated 20–47% of adults with ADHD are comorbid for bipolar disorder (87, 88). Comorbid substance abuse is estimated at 23.3% based on a systematic review (89). Although not well-studied, at least one analysis of insurance data indicates that ADHD leads to an increased risk of TBI. The risk for receiving any form of TBI was 9.8% for those with ADHD compared to 2.2% for those without ADHD, representing a 4.5-fold increase in risk (90).

NEXT STEPS

Herein, we have analyzed baseline SPECT scans of adult patients with pure ADHD compared to an age-matched control group. Interesting potential candidate neuroimaging biomarkers have been identified. Next, it will be vital to expand these analyses to patients with ADHD comorbid for diagnoses such as anxiety, depression, bipolar disorder, addictions, gender-based differences, and/or brain trauma (among others). Going forward, we will also implement machine learning algorithms to rigorously test the candidate biomarkers utilizing our large-N dataset. These algorithms will be applied to our adolescent

datasets to explicitly address the complex diagnostic picture of ADHD symptomatology in the adolescent patient.

CONCLUSIONS

Strengths of this study include the large sample size of non-comorbid ADHD compared to a well-characterized control group, the consistent methods of visual interpretation of rest (or baseline) scans with a well-validated functional imaging modality, and detailed quantitative analysis. The study is further enhanced by a *post-hoc* ROI analysis which had similar findings. That said, several caveats of the study must be addressed. First, the data are retrospective, and higher levels of evidence can be derived from either prospective studies or randomized clinical trials. However, the large sample size and diverse multi-site study optimizes the generalizability of our results. Second, this dataset does not have associated structural imaging data. Such information would have been useful in characterizing any atrophy associated hypoperfusion. However, the use of functional neuroimaging is essential in characterizing subtle abnormalities that may not be apparent on even quantitative structural neuroimaging. Third, in such a large retrospective database, there are many patients who were on one or more medications for medical and psychiatric indications. While known stimulants and depressants of brain function were withheld prior to scanning, the confounding effects of medical and psychiatric medications cannot be completely eliminated.

Using the method described above we consistently distinguished adult ADHD patients from healthy controls. Given the wide availability of brain SPECT imaging and the need for accurate diagnosis in ADHD, this test, with appropriate reader training, could provide valuable information in clinical practice.

DATA AVAILABILITY STATEMENT

The original contributions presented in the study are included in the article/**Supplementary Material**. Further inquiries can be directed to the corresponding author/s.

ETHICS STATEMENT

The studies involving human participants were reviewed and approved by IntegReview (http://www.integreview.com/) and Western IRB (WIRB # 20021714). The patients/participants provided their written informed consent to participate in this study.

AUTHOR CONTRIBUTIONS

All authors listed have made a substantial, direct, and intellectual contribution to the work and approved it for publication.

SUPPLEMENTARY MATERIAL

The Supplementary Material for this article can be found online at: https://www.frontiersin.org/articles/10.3389/fpsyt.2021.725788/full#supplementary-material

REFERENCES

1. Wallis D. The search for biomarkers for attention deficit/hyperactivity disorder. *Drug News Perspect.* (2010) 23:438–49. doi: 10.1358/dnp.2010.23.7.1472296
2. Kam H, Jeong H. Pharmacogenomic biomarkers and their applications in psychiatry. *Genes.* (2020) 11:1445. doi: 10.3390/genes11121445
3. Gualtieri CT, Johnson LG. ADHD: is objective diagnosis possible? *Psychiatry.* (2005) 2:44–53.
4. Faraone SV, Sergeant J, Gillberg C, Biederman J. The worldwide prevalence of ADHD: is it an American condition? *World Psychiatry.* (2003) 2:104.
5. Hinshaw SP, Scheffler RM, Fulton BD, Aase H, Banaschewski T, Cheng W, et al. International variation in treatment procedures for ADHD: social context and recent trends. *Psychiatr Serv.* (2011) 62:459–64. doi: 10.1176/ps.62.5.pss6205_0459
6. Wolraich ML, Lambert W, Doffing MA, Bickman L, Simmons T, Worley K. Psychometric properties of the Vanderbilt ADHD Diagnostic Parent Rating Scale in a referred population. *J Pediatr Psychol.* (2003) 28:559–67. doi: 10.1093/jpepsy/jsg046
7. Jain R, Jain S, Montano CB. Addressing diagnosis and treatment gaps in adults with attention-deficit/hyperactivity disorder. *Prim Care Companion CNS Disord.* (2017) 19:17nr02153. doi: 10.4088/PCC.17nr02153
8. Cohen ML, Kelly PC, Atkinson AW. Parent, teacher, child: a trilateral approach to attention deficit disorder. *Am J Dis Child.* (1989) 143:1229–33. doi: 10.1001/archpedi.1989.02150220137034
9. Furman L. What is attention-deficit hyperactivity disorder (ADHD)? *J Child Neurol.* (2005) 20:994–1002. doi: 10.1177/08830738050200121301
10. Ghanizadeh A. Overlap of ADHD and oppositional defiant disorder DSM-IV derived criteria. *Arch Iran Med.* (2011) 14:179–82.
11. Forbes GB. Clinical utility of the test of variables of attention (TOVA) in the diagnosis of attention-deficit/hyperactivity disorder. *J Clin Psychol.* (1998) 54:461–76. doi: 10.1002/(SICI)1097-4679(199806)54:4<461::AID-JCLP8>3.0.CO;2-Q
12. McGee RA, Clark SE, Symons DK. Does the conners continuous performance test aid in ADHD diagnosis? *J Abnorm Child Psychol.* (2000) 28:415–24. doi: 10.1023/a:1005127504982
13. Schatz AM, Ballantyne AO, Trauner DA. Sensitivity and specificity of a computerized test of attention in the diagnosis of attention-deficit/hyperactivity disorder. *Assessment.* (2001) 8:357–65. doi: 10.1177/107319110100800401
14. Suhr JA, Sullivan BK, Rodriguez JL. The relationship of noncredible performance to continuous performance test scores in adults referred for attention-deficit/hyperactivity disorder evaluation. *Arch Clin Neuropsychol.* (2011) 26:1–7. doi: 10.1093/arclin/acq094
15. Teicher MH, Ito Y, Glod CA, Barber NI. Objective measurement of hyperactivity and attentional problems in ADHD. *J Am Acad Child Adolesc Psychiatry.* (1996) 35:334–42. doi: 10.1097/00004583-199603000-00015
16. *Food and Drug Administration website – About Biomarkers and Qualification webpage*. Available online at: https://www.fda.gov/drugs/biomarker-qualification-program/about-biomarkers-and-qualification (accessed August 22, 2021).
17. Cherkasova MV, Hechtman L. Neuroimaging in attention-deficit hyperactivity disorder: beyond the frontostriatal circuitry. *Can J Psychiatry.* (2009) 54:651–64. doi: 10.1177/070674370905401002
18. Luo Y, Alvarez TL, Halperin JM, Li X. Multimodal neuroimaging-based prediction of adult outcomes in childhood-onset ADHD using ensemble learning techniques. *Neuroimage Clin.* (2020) 26:102238. doi: 10.1016/j.nicl.2020.102238

19. Neba Health, LLC. *De Novo Classification Request for Neuropsychiatric EEG-Based Assessment Aid for ADHD (NEBA) System*. (2017). Available online at: https://www.accessdata.fda.gov/cdrh_docs/reviews/K112711.pdf (accessed December 20, 2017).
20. Arns M, Conners CK, Kraemer HC. A decade of EEG theta/beta ratio research in ADHD: a meta-analysis. *J Atten Disord*. (2013) 17:374–83. doi: 10.1177/1087054712460087
21. Vieira de Melo BB, Trigueiro MJ, Rodrigues PP. Systematic overview of neuroanatomical differences in ADHD: definitive evidence. *Dev Neuropsychol*. (2018) 43:52–68. doi: 10.1080/87565641.2017.1414821
22. Valera EM, Faraone SV, Murray KE, Seidman LJ. Meta-analysis of structural imaging findings in attention-deficit/hyperactivity disorder. *Biol Psychiatry*. (2007) 61:1361–9. doi: 10.1016/j.biopsych.2006.06.011
23. Ellison-Wright I, Ellison-Wright Z, Bullmore E. Structural brain change in attention deficit hyperactivity disorder identified by meta-analysis. *BMC Psychiatry*. (2008) 8:51. doi: 10.1186/1471-244X-8-51
24. Frodl T, Skokauskas N. Meta-analysis of structural MRI studies in children and adults with attention deficit hyperactivity disorder indicates treatment effects. *Acta Psychiatr Scand*. (2012) 125:114–26. doi: 10.1111/j.1600-0447.2011.01786.x
25. Norman LJ, Carlisi C, Lukito S, Hart H, Mataix-Cols D, Radua J, et al. Structural and functional brain abnormalities in attention-deficit/hyperactivity disorder and obsessive-compulsive disorder: a comparative meta-analysis. *JAMA Psychiatry*. (2016) 73:815–25. doi: 10.1001/jamapsychiatry.2016.0700
26. Nakao T, Radua J, Rubia K, Mataix-Cols D. Gray matter volume abnormalities in ADHD: voxel-based meta-analysis exploring the effects of age and stimulant medication. *Am J Psychiatry*. (2011) 168:1154–63. doi: 10.1176/appi.ajp.2011.11020281
27. Hoogman M, van Rooij D, Klein M, Boedhoe P, Ilioska I, Li T, et al. Consortium neuroscience of attention deficit/hyperactivity disorder and autism spectrum disorder: the ENIGMA adventure. *Hum Brain Mapp*. (2020) 1–19. doi: 10.1002/hbm.25029
28. Hoogman M, Bralten J, Hibar DP, Mennes M, Zwiers MP, Schweren LSJ, et al. Subcortical brain volume differences in participants with attention deficit hyperactivity disorder in children and adults: a cross-sectional mega-analysis. *Lancet Psychiatry*. (2017) 4:310–9. doi: 10.1016/S2215-0366(17)30160-8
29. Hoogman M, Muetzel R, Guimaraes JP, Shumskaya E, Mennes M, Zwiers MP, et al. Brain imaging of the cortex in ADHD: a coordinated analysis of large-scale clinical and population-based samples. *Am J Psychiatry*. (2019) 176:531–42. doi: 10.1176/appi.ajp.2019.18091033
30. McCarthy H, Skokauskas N, Frodl T. Identifying a consistent pattern of neural function in attention deficit hyperactivity disorder: a meta-analysis. *Psychol Med*. (2014) 44:869–80. doi: 10.1017/S0033291713001037
31. Lei D, Du M, Wu M, Chen T, Huang X, Du X, et al. Functional MRI reveals different response inhibition between adults and children with ADHD. *Neuropsychology*. (2015) 29:874–81. doi: 10.1037/neu0000200
32. Samea F, Soluki S, Nejati V, Zarei M, Cortese S, Eickhoff SB, et al. Brain alterations in children/adolescents with ADHD revisited: a neuroimaging meta-analysis of 96 structural and functional studies. *Neurosci Biobehav Rev*. (2019) 100:1–8. doi: 10.1016/j.neubiorev.2019.02.011
33. Rubia K, Smith AB, Brammer MJ, Toone B, Taylor E. Abnormal brain activation during inhibition and error detection in medication-naive adolescents with ADHD. *Am J Psychiatry*. (2005) 162:1067–75. doi: 10.1176/appi.ajp.162.6.1067
34. Smith AB, Taylor E, Brammer M, Toone B, Rubia K. Task-specific hypoactivation in prefrontal and temporoparietal brain regions during motor inhibition and task switching in medication-naive children and adolescents with attention deficit hyperactivity disorder. *Am J Psychiatry*. (2006) 163:1044–51. doi: 10.1176/ajp.2006.163.6.1044
35. Rubia K, Cubillo A, Smith AB, Woolley J, Heyman I, Brammer MJ. Disorder-specific dysfunction in right inferior prefrontal cortex during two inhibition tasks in boys with attention-deficit hyperactivity disorder compared to boys with obsessive-compulsive disorder. *Hum Brain Mapp*. (2010) 31:287–99. doi: 10.1002/hbm.20864
36. Hart H, Radua J, Nakao T, Mataix-Cols D, Rubia K. Meta-analysis of functional magnetic resonance imaging studies of inhibition and attention in attention-deficit/hyperactivity disorder: exploring task-specific, stimulant medication, and age effects. *JAMA Psychiatry*. (2013) 70:185–98. doi: 10.1001/jamapsychiatry.2013.277
37. Pliszka SR, Glahn DC, Semrud-Clikeman M, Franklin C, Perez R, Xiong J, et al. Neuroimaging of inhibitory control areas in children with attention deficit hyperactivity disorder who were treatment naive or in long-term treatment. *Am J Psychiatry*. (2006) 163:1052–60. doi: 10.1176/ajp.2006.163.6.1052
38. Cortese S, Aoki YY, Itahashi T, Castellanos FX, Eickhoff SB. Systematic review and meta-analysis: resting-state functional magnetic resonance imaging studies of attention-deficit/hyperactivity disorder. *J Am Acad Child Adolesc Psychiatry*. (2021) 60:61–75. doi: 10.1016/j.jaac.2020.08.014
39. Zhang Z, Li G, Xu Y, Tang X. Application of artificial intelligence in the MRI classification task of human brain neurological and psychiatric diseases: a scoping review. *Diagnostics*. (2021) 11:1402. doi: 10.3390/diagnostics11081402
40. Riaz A, Asad M, Alonso E, Slabaugh G. DeepFMRI: End-to-end deep learning for functional connectivity and classification of ADHD using fMRI. *J Neurosci Methods*. (2020) 335:108506. doi: 10.1016/j.jneumeth.2019.108506
41. Amen DG, Carmichael BD. High-resolution brain SPECT imaging in ADHD. *Ann Clin Psychiatry*. (1997) 9:81–6. doi: 10.3109/10401239709147778
42. Amen DG, Hanks C, Prunella J. Predicting positive and negative treatment responses to stimulants with brain SPECT imaging. *J Psychoactive Drugs*. (2008) 40:131–8. doi: 10.1080/02791072.2008.10400622
43. Schneider H, Thornton JF, Freeman MA, McLean MK, van Lierop MJ, Schneider J. Conventional SPECT versus 3D thresholded SPECT imaging in the diagnosis of ADHD: a retrospective study. *J Neuropsychiatry Clin Neurosci*. (2014) 26:335–43. doi: 10.1176/appi.neuropsych.12110280
44. Cohen JF, Korevaar DA, Altman DG, Bruns DE, Gatsonis CA, Hooft L, et al. STARD 2015 guidelines for reporting diagnostic accuracy studies: explanation and elaboration. *BMJ Open*. (2016) 6:e012799. doi: 10.1136/bmjopen-2016-012799
45. Amen DA, Willeumier K. Brain SPECT imaging: a powerful, evidence-based tool for transforming clinical psychiatric practice. *Minerva Psichiatr*. (2011) 52:109–23.
46. American Psychiatric Association. *Diagnostic and Statistical Manual of Mental Disorders*. 5th ed. Arlington, VA. American Psychiatric Association.
47. Conners CK, Sitarenios G. Conners' Continuous Performance Test (CPT). In: Kreutzer JS, editor. *Encyclopedia of Clinical Neuropsychology*. New York, NY: Springer (2011). p. 681–3.
48. Amen DG, Raji CA, Willeumier K, Taylor D, Tarzwell R, Newberg N, et al. Functional neuroimaging distinguishes posttraumatic stress disorder from traumatic brain injury in focused and large community datasets. *PLoS ONE*. (2015) 10:e0129659. doi: 10.1371/journal.pone.0129659
49. Chang LT. A method for attenuation correction in radionuclide computed tomography. *IEEE Trans Nucl Sci*. (1977) 25:638–43. doi: 10.1109/TNS.1978.4329385
50. Juni JE, Waxman AD, Devous MD Sr, Tifosky RS, Ichise M, Van Heertum RL, et al. Procedure guideline for brain perfusion SPECT using (99m)Tc radiopharmaceuticals 3.0. *J Nucl Med Technol*. (2009) 37:191–5. doi: 10.2967/jnmt.109.067850
51. Mai JK, Assheuer J, Paxinos G. *Atlas of the Human Brain*. San Diego, CA: Academic Press (1997).
52. Tzourio-Mazoyer N, Landeau B, Papathanassiou D, Crivello F, Etard O, Delcroix N, et al. Automated anatomical labeling of activations in SPM using a macroscopic anatomical parcellation of the MNI MRI single-subject brain. *Neuroimage*. (2002) 15:273–89. doi: 10.1006/nimg.2001.0978
53. *Statistical Package for Social Science (SPSS), Version 24.0*. Armonk, NY: IBM Corp. (2016).
54. Ross R. Psychotic and manic-like symptoms during stimulant treatment of attention deficit hyperactivity disorder. *Am J Psychiatry*. (2006) 163:1149. doi: 10.1176/ajp.2006.163.7.1149
55. Henderson TA, Hartman K. Aggression, mania, and hypomania induction associated with atomoxetine. *Pediatrics*. (2004) 114:895–6. doi: 10.1542/peds.2004-1140
56. Lou HC, Henriksen L, Bruhn P. Focal cerebral hypoperfusion in children with dysphasia and/or attention deficit disorder. *Arch Neurol*. (1984) 41:825–9. doi: 10.1001/archneur.1984.04050190031010

57. Lou HC, Henriksen L, Bruhn P, Børner H, Nielsen JB. Striatal dysfunction in attention deficit and hyperkinetic disorder. *Arch Neurol.* (1989) 46:48–52. doi: 10.1001/archneur.1989.00520370050018
58. Lou HC, Henriksen L, Bruhn P. Focal cerebral dysfunction in developmental learning disabilities. *Lancet Lond Engl.* (1990) 335:8–11. doi: 10.1016/0140-6736(90)90136-S
59. Gustafsson P, Thernlund G, Ryding E, Rosén I, Cederblad M. Associations between cerebral blood-flow measured by single photon emission computed tomography (SPECT), electro-encephalogram (EEG), behaviour symptoms, cognition and neurological soft signs in children with attention-deficit hyperactivity disorder (ADHD). *Acta Paediatr.* (2000) 89:830–5. doi: 10.1111/j.1651-2227.2000.tb00391.x
60. Spalletta G, Pasini A, Pau F, Guido G, Menghini L, Caltagirone C. Prefrontal blood flow dysregulation in drug naive ADHD children without structural abnormalities. *J Neural Transm.* (2001) 108:1203–16. doi: 10.1007/s007020170010
61. Langleben DD, Austin G, Krikorian G, Ridlehuber HW, Goris ML, Strauss HW. Interhemispheric asymmetry of regional cerebral blood flow in prepubescent boys with attention deficit hyperactivity disorder. *Nucl Med Commun.* (2001) 22:1333–40. doi: 10.1097/00006231-200112000-00009
62. Ernst M, Liebenauer LL, King AC, Fitzgerald GA, Cohen RM, Zametkin AJ. Reduced brain metabolism in hyperactive girls. *J Am Acad Child Adolesc Psychiatry.* (1994) 33:858–68. doi: 10.1097/00004583-199407000-00012
63. Vaidya CJ, Austin G, Kirkorian G, Ridlehuber HW, Desmond JE, Glover GH, et al. Selective effects of methylphenidate in attention deficit hyperactivity disorder: a functional magnetic resonance study. *Proc Natl Acad Sci USA.* (1998) 95:14494–9. doi: 10.1073/pnas.95.24.14494
64. Akay AP, Kaya GÇ, Emiroglu NI, Aydin A, Monkul ES, Tasci C, et al. Effects of long-term methylphenidate treatment: A pilot follow-up clinical and SPECT study. *Prog Neuropsychopharmacol Biol Psychiatry.* (2006) 30:1219–24. doi: 10.1016/j.pnpbp.2006.02.014
65. Lee DO, Ousley OY. Attention-deficit hyperactivity disorder symptoms in a clinic sample of children and adolescents with pervasive developmental disorders. *J Child Adolesc Psychopharmacol.* (2006) 16:737–46. doi: 10.1089/cap.2006.16.737
66. Rubia K, Halari R, Christakou A, Taylor E. Impulsiveness as a timing disturbance: neurocognitive abnormalities in attention-deficit hyperactivity disorder during temporal processes and normalization with methylphenidate. *Philos Trans R Soc B Biol Sci.* (2009) 364:1919–31. doi: 10.1098/rstb.2009.0014
67. Durston S, Tottenham NT, Thomas KM, Davidson MC, Eigsti IM, Yank Y, et al. Differential patterns of striatal activation in young children with and without ADHD. *Biol Psychiatry.* (2003) 53:871–8. doi: 10.1016/S0006-3223(02)01904-2
68. Kim BN, Lee JS, Shin MS, Cho SC, Lee DS. Regional cerebral perfusion abnormalities in attention deficit/hyperactivity disorder. Statistical parametric mapping analysis. *Eur Arch Psychiatry Clin Neurosci.* (2002) 252:219–25.
69. Thornton JF, Schneider H, Cohen PF, DeBruin S, Uszler JM, Siow YH, et al. 3D thresholded SPECT brain scans as a biomarker of improvement in psychiatric disorders. *Front Psych*. (2021) 2.
70. Lorberboym M, Watemberg N, Nissenkorn A, Nir B, Lerman-Sagie T. Technetium 99m ethylcysteinate dimer single-photon emission computed tomography (SPECT) during intellectual stress test in children and adolescents with pure versus comorbid attention-deficit hyperactivity disorder (ADHD). *J Child Neurol.* (2004) 19:91–6. doi: 10.1177/088307380401900202O1
71. Ors M, Ryding E, Lindgren M, Gustafsson P, Blennow G, Rosén I. SPECT findings in children with specific language impairment. *Cortex.* (2005) 41:316–26. doi: 10.1016/S0010-9452(08)70269-7
72. Skalski S, Dobrakowski P. Vigilance, inhibitory control and regional cerebral blood oxygenation in the PFC – differences in ADHD types of presentations. *Adv Cogn Psychol.* (2020) 16:202–12. doi: 10.5709/acp-0297-5
73. Spencer T, Biederman J, Wilens T. Attention-deficit/hyperactivity disorder and comorbidity. *Pediatr Clin North Am*. (1999) 46:915–27, vii. doi: 10.1016/S0031-3955(05)70163-2
74. Newcorn JH, Halperin JM, Jensen PS, Abikoff HB, Arnold LE, Cantwell DP, et al. Symptom profiles in children with ADHD: effects of comorbidity and gender. *J Am Acad Child Adolesc Psychiatry.* (2001) 40:137–46. doi: 10.1097/00004583-200102000-00008
75. Biederman J, Milberger S, Faraone SV, Kiely K, Guite J, Mick E, et al. Family-environment risk factors for attention-deficit hyperactivity disorder. A test of Rutter's indicators of adversity. *Arch Gen Psychiatry*. (1995) 52:464–70. doi: 10.1001/archpsyc.1995.03950180050007
76. Gnanavel S, Sharma P, Kaushal P, Hussain S. Attention deficit hyperactivity disorder and comorbidity: a review of literature. *World J Clin Cases.* (2019) 7:2420–6. doi: 10.12998/wjcc.v7.i17.2420
77. Busch B, Biederman J, Cohen LG, Sayer JM, Monuteaux MC, Mick E, et al. Correlates of ADHD among children in pediatric and psychiatric clinics. *Psychiatr Serv.* (2002) 53:1103–11. doi: 10.1176/appi.ps.53.9.1103
78. Jensen PS, Hinshaw SP, Swanson JM, Greenhill LL, Conners CK, Arnold LE, et al. Findings from the NIMH Multimodal Treatment Study of ADHD (MTA): implications and applications for primary care providers. *J Dev Behav Pediatr.* (2001) 22:60–73. doi: 10.1097/00004703-200102000-00008
79. Angold A, Costello EJ, Erkanli A. Comorbidity. *J Child Psychol Psychiatry.* (1999) 40:57–87. doi: 10.1111/1469-7610.00424
80. Biederman J, Newcorn J, Sprich S. Comorbidity of attention deficit hyperactivity disorder with conduct, depressive, anxiety, and other disorders. *Am J Psychiatry.* (1991) 148:564–77. doi: 10.1176/ajp.148.5.564
81. August GJ, Stewart MA, Holmes CS. A four-year follow-up of hyperactive boys with and without conduct disorder. *Br J Psychiatry.* (1983) 143:192–8. doi: 10.1192/bjp.143.2.192
82. Wilens TE, Biederman J, Spencer TJ. Attention deficit/hyperactivity disorder across the lifespan. *Annu Rev Med.* (2002) 53:113–31. doi: 10.1146/annurev.med.53.082901.103945
83. Pary R, Lewis S, Matuschka PR, Rudzinskiy P, Safi M, Lippmann S. Attention deficit disorder in adults. *Ann Clin Psychiatry.* (2002) 14:105–11. doi: 10.3109/10401230209149097
84. Sobanski E. Psychiatric comorbidity in adults with attention-deficit/hyperactivity disorder (ADHD). *Eur Arch Psychiatry Clin Neurosci.* (2006) 256 (Suppl. 1):i26–31. doi: 10.1007/s00406-006-1004-4
85. Katzman MA, Bilkey TS, Chokka PR, Fallu A, Klassen LJ. Adult ADHD and comorbid disorders: clinical implications of a dimensional approach. *BMC Psychiatry*. (2017) 17:302. doi: 10.1186/s12888-017-1463-3
86. Kessler RC, Adler L, Barkley R, Biederman J, Conners CK, Demler O, et al. The prevalence and correlates of adult ADHD in the United States: results from the National Comorbidity Survey Replication. *Am J Psychiatry.* (2006) 163:716–23. doi: 10.1176/ajp.2006.163.4.716
87. Brus MJ, Solanto MV, Goldberg JF. Adult ADHD vs. bipolar disorder in the DSM-5 era: a challenging differentiation for clinicians. *J Psychiatr Pract*. (2014) 20:428–37. doi: 10.1097/01.pra.0000456591.20622.9e
88. Wingo AP, Ghaemi SN. A systematic review of rates and diagnostic validity of comorbid adult attention-deficit/hyperactivity disorder and bipolar disorder. *J Clin Psychiatry.* (2007) 68:1776–84. doi: 10.4088/JCP.v68n1118
89. van Emmerik-van Oortmerssen K, van de Glind G, van den Brink W, Smit F, Crunelle CL, Swets M, et al. Prevalence of attention-deficit hyperactivity disorder in substance use disorder patients: a meta-analysis and meta-regression analysis. *Drug Alcohol Depend.* (2012) 122:11–19. doi: 10.1016/j.drugalcdep.2011.12.007
90. Liou YJ, Wei HT, Chen MH, Hsu JW, Huang KL, Bai YM, et al. Risk of traumatic brain injury among children, adolescents, and young adults with attention-deficit hyperactivity disorder in Taiwan. *J Adolesc Health.* (2018) 63:233–8. doi: 10.1016/j.jadohealth.2018.02.012

Conflict of Interest: TH is the president and principal owner of the Synaptic Space, a neuroimaging consulting firm. He is also CEO and Chairman of the Board of Neuro-Luminance Corporation, a medical service company. He is also president and principal owner of Dr. Theodore Henderson, Inc., a medical service company. He is also Vice-President of the Neuro-Laser Foundation, a non-profit organization. He is a member of and a former officer of the Brain Imaging Council Board of the Society of Nuclear Medicine and Molecular Imaging (SNMMI). Since 2017, he has served in the SNMMI Brain Imaging Outreach Working Group. Currently, he serves as president of the International Society of Applied Neuroimaging. TH has no ownership in, and receives no remuneration from, any neuroimaging company. No more than 5% of his income is derived

from neuroimaging. DA is the sole owner of Amen Clinics, a group of nine neuropsychiatric clinics that perform brain SPECT imaging.

The remaining author declares that the research was conducted in the absence of any commercial or financial relationships that could be construed as a potential conflict of interest.

Publisher's Note: All claims expressed in this article are solely those of the authors and do not necessarily represent those of their affiliated organizations, or those of the publisher, the editors and the reviewers. Any product that may be evaluated in this article, or claim that may be made by its manufacturer, is not guaranteed or endorsed by the publisher.

frontiers in Psychiatry

HYPOTHESIS AND THEORY
published: 10 December 2021
doi: 10.3389/fpsyt.2021.715315

A New Way Forward: How Brain SPECT Imaging Can Improve Outcomes and Transform Mental Health Care Into Brain Health Care

Daniel G. Amen[1]* *and Michael Easton*[2]

[1] Amen Clinics, Costa Mesa, CA, United States, [2] Department of Psychiatry, Rush University Medical Center, Chicago, IL, United States

In the past three decades, brain single-photon-emission-computed-tomography (SPECT) imaging has garnered a significant, evidence-based foundation for a wide array of indications relevant to the field of clinical psychiatry, including dementia, traumatic brain injuries, seizures, cerebrovascular disease, complex neuropsychiatric presentations, and treatment-resistant disorders. In clinical psychiatric practice, however, SPECT remains underutilized. Only a small percentage of psychiatric clinicians use brain imaging technology. In this article, the authors provide a rationale for shifting the paradigm to one that includes broader use of SPECT in the clinical psychiatric setting, primarily for patients with complex conditions. This paper will outline seven specific clinical applications. Adding neuroimaging tools like SPECT to day-to-day clinical practice can help move psychiatry forward by transforming mental health care, which can be stigmatizing and often shunned by the general public, to brain health care, which the authors argue will be more likely to be embraced by a larger group of people in need.

Keywords: brain SPECT, evidence-based, brain trauma, dementia, hypofrontality, hyperfrontality, complex cases, brain health

OPEN ACCESS

Edited by:
Joe Cardaci,
University of Notre Dame, Australia

Reviewed by:
John Dimitrios Papatriantafyllou,
Third Age Day-Care Center,
IASIS, Greece
Gianluca Serafini,
San Martino Hospital (IRCCS), Italy

***Correspondence:**
Daniel G. Amen
docamen@amenclinics.com

Specialty section:
This article was submitted to Neuroimaging and Stimulation, a section of the journal Frontiers in Psychiatry

Received: *26 May 2021*
Accepted: *25 October 2021*
Published: *10 December 2021*

Citation:
Amen DG and Easton M (2021) A New Way Forward: How Brain SPECT Imaging Can Improve Outcomes and Transform Mental Health Care Into Brain Health Care. Front. Psychiatry 12:715315. doi: 10.3389/fpsyt.2021.715315

INTRODUCTION

Despite the early enthusiasm in the late '80s and early '90s about the use of functional neuroimaging in psychiatric practice, if you were to ask the majority of psychiatrists today why they don't utilize it, their response would most likely be, "there are no adequate large-scale studies demonstrating the validity of this in helping with psychiatric diagnosis and treatment." Yet there are nearly 15,000 references on www.pubmed.gov about brain single-photon-emission-computed-tomography (SPECT) imaging encompassing a wide variety of neuropsychiatric indications (1). Is there another reason clinicians are not using brain SPECT?

In 1992, Holman and Devous authored an important article titled "Functional Brain SPECT: The Emergence of a Powerful Clinical Method," which articulated the promise of functional brain imaging: "*SPECT techniques provide a powerful window into the function of the brain and promise to become an important component of the routine clinical evaluation of patients with neurological and psychiatric diseases* (2)."

In 1992 and 1993, the American Psychiatric Association's (APA) Annual Meeting on SPECT imaging in psychiatry included day-long courses, symposia, and workshops covering the technology. After reading Holman and Devous' seminal paper and attending those APA meetings, author DA began utilizing brain SPECT imaging in clinical practice for a range of

neuropsychiatric indications. Subsequently, he has amassed a database of more than 194,000 brain SPECT scans on patients with a vast array of complex neuropsychiatric conditions. Since the publication of Holman and Devous' paper in 1992, a wealth of scientific research has been published that lends support to the use of brain SPECT in psychiatric clinical practice. For example, in a 1996 issue of the Harvard Review of Psychiatry, Vasile wrote, "*The clinical utility of SPECT in neuropsychiatry is well established, and research devoted to its use in primary psychiatric disorders has been gaining momentum* (3)." In 2001, Camargo asserted that, "*Brain SPECT . . . is rapidly becoming a clinical tool in many places. The importance of this technique in nuclear medicine today should not be overlooked, particularly in cerebrovascular diseases, dementias, epilepsy, head injury, malignant brain tumors, movement disorders, obsessive-compulsive disorder, Gilles de la Tourette's syndrome, schizophrenia, depression, panic disorder, and drug abuse* (4)."

Although this evidence-based tool that is relevant to diagnosing and treating a multitude of psychiatric conditions has been available for three decades, only a small segment of psychiatrists worldwide have adopted the use of SPECT in clinical practice. Thus, the field of psychiatry continues to be the sole medical specialty that typically does not look at the organ it treats. In no other field of medicine do physicians make diagnoses or treatment recommendations without biological information. Psychiatry's refusal to widely adopt SPECT and/or other functional brain imaging tools—such as quantitative electroencephalography (qEEG), positron emission tomography (PET), or arterial spin labeling (ASL)—not only compromises its credibility as a branch of medical practice, but it also harms patients who suffer due to diagnoses or treatments that are inaccurate, inadequate, and/or stigmatizing and discouraging.

WHY PSYCHIATRY FAILED TO ADOPT SPECT

One of the primary reasons why psychiatry has failed to adopt SPECT in clinical practice over the past three decades lies in the medical specialty's adherence to categorical diagnostic nomenclature in the Diagnostic and Statistical Manual of Mental Disorders (DSM). When SPECT began generating excitement in the field of psychiatry in the late 1980s and early 1990s, researchers made attempts to match brain patterns seen on SPECT with specific diagnoses found in the DSM. When the scientific investigators failed to pinpoint consistent DSM patterns for mental health conditions, they discarded neuroimaging for clinical practice, claiming it was not yet a useful tool (5, 6). In hindsight, the problem likely did not lie in the neuroimaging tools, including SPECT, PET, and qEEG. These sophisticated brain imaging technologies accurately assess brain function in patients. It is more likely that the problem arose from psychiatry's diagnostic methodology, which presumed that the patterns seen in neuroimaging would correlate directly to the diagnostic categories found in the DSM.

Thomas Insel, the former Director of the National Institutes of Mental Health, said in his 2005 keynote speech to the American Psychiatric Association, "*The DSM-IV has 100% reliability and 0% validity. . . We need to develop biomarkers, including brain imaging, to develop the validity of these disorders. . . Trial-and-error diagnosis will move to an era where we understand the underlying biology of mental disorders . . . We are going to have to use neuroimaging to begin to identify the systems pathology . . . to develop treatments that go after the core pathology, understood by imaging* (7)." Unfortunately, psychiatrists have not yet moved beyond looking only at symptom clusters which have failed to demonstrate clear separation of distinct illnesses but have high levels of comorbidity in epidemiological, clinical, and genetic studies (8, 9).

In 2005, Dr. Insel also noted in writing, ". . . *patterns of regional brain activity associated with normal and pathological mental experience can be visualized . . . and ultimately, biomarkers for mental disorders may not be proteins or neurotransmitters but may emerge from neuroimaging (functional magnetic resonance imaging* (fMRI), *single photon emission computed tomography* (SPECT)*, etc.). Logically, if these are disorders of brain systems, then the visualization of abnormal patterns of brain activity should detect the pathology of these illnesses* (10)."

A psychiatrist trying to identify a singular neuroimaging pattern for major depressive disorder is similar to a cardiologist searching for a sole imaging pattern for angina. Just as there are a wide variety of causes and imaging patterns seen in patients with angina, there are also a multitude of causes and neuroimaging patterns seen in psychiatric conditions, such as major depressive disorder, attention-deficit hyperactivity disorder (ADHD), bipolar disorder, schizophrenia, and autism spectrum disorder (ASD). We can see five individuals with the same DSM diagnosis yet see five very different SPECT scans. Why would we treat them all the same? These individuals should not be expected to respond to similar interventions. We would miss important information by looking only at symptoms. As an adjunct tool, SPECT can inform the direction of treatment more precisely than a one-size-fits-all DSM-V diagnosis can. It has been shown that by utilizing functional brain imaging we can improve treatment decisions and outcomes (11, 12). Yet, the use of neuroimaging is still disregarded by traditional medical specialties.

Consider these two case examples of how mainstream psychiatry fails in an effort to treat complex patients without the use of SPECT neuroimaging:

Mr. C suffered from crippling anxiety, extreme mood swings, recurring panic attacks, negative thinking patterns, anger issues, and difficulty sleeping. These issues negatively impacted his relationships, both at work and in his social life. He was shy and reported always being in a bad mood. In his family, there was a history of addictions and depression. Mr. C first saw a psychiatrist when he was a teenager and was diagnosed with multiple disorders, including bipolar disorder, ADHD, and intermittent explosive disorder (IED).

In the years following his diagnoses, Mr. C tried a variety of medications in an attempt to stabilize his moods. The various prescriptions came with a host of detrimental side effects that exacerbated things and led to an 80-pound weight gain. When coupled with his social anxiety, the added weight pushed him

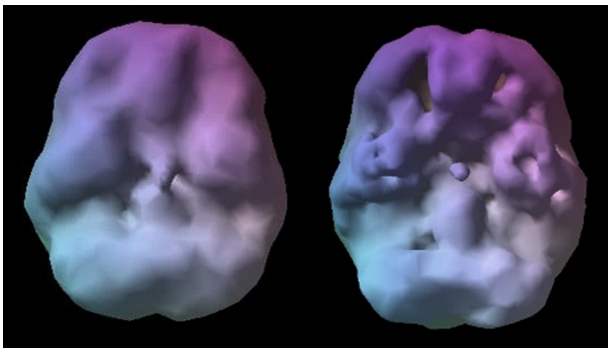

FIGURE 1 | Healthy SPECT image compared to C's pre-treatment SPECT image. A healthy SPECT image (L) shows full, even, symmetrical activity compared to C's pre-treatment SPECT image (R) with low activity, especially in the prefrontal cortex and temporal lobes. Photon emission was captured using a high-resolution Picker (Phillips) Prism 3,000 triple-headed gamma camera with fan beam collimator with data collected in 128 × 128 matrices, yielding 120 images per scan with each image separated by three degrees spanning 360 degrees. A low pass filter was applied with a high cutoff. A Chang attenuation correction was performed using linear methods. All images were processed using Odyssey software (Picker), with transaxial slices oriented horizontal to the AC-PC line. Coronal, sagittal, and transaxial slice images (6.6 mm apart, unsmoothed) were then rendered in the Odyssey step-20 scale. Image acquisition and processing methods apply to all images presented in this article.

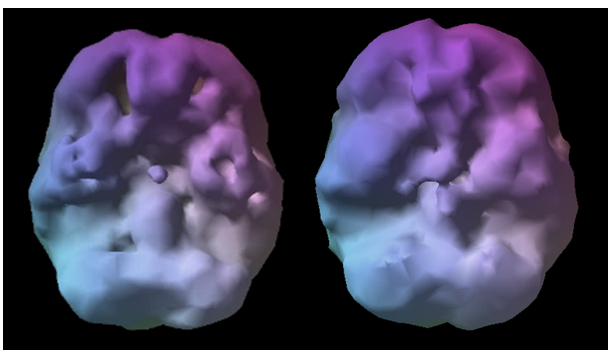

FIGURE 2 | C's SPECT surface underside view images before (L) and after (R) treatment. C's SPECT image before treatment (L) reveals low activity, especially in the prefrontal cortex and temporal lobes compared to post-treatment image (R) showing overall improvement.

further into isolation. He became unable to work and his family referred him to author DA for a comprehensive evaluation, including SPECT imaging. His SPECT scan (see **Figures 1**, **2**) showed significantly decreased overall cerebral blood flow, most pronounced in the prefrontal cortex (PFC) and temporal lobes. The blood flow and activity patterns seen on his scan were indicative of a past head injury and exposure to toxins. These findings led to additional questions to find the root causes for the abnormal blood flow and activity in his brain.

Mr. C eventually divulged that he grew up in a family that owned and operated a motor speedway. Since childhood, he had been racing cars and has spent substantial amounts of time around the speedway where he was exposed to toxic fumes from gasoline. In addition, he had experienced multiple concussions, one of which resulted from crashing into a wall while racing a car.

After reviewing his scans and learning more about his history, it was clear Mr. C was struggling with the lingering impacts from multiple head injuries as well as the exposure to toxic gasoline fumes and had previously been given psychiatric labels based on symptom clusters. His psychiatric medications were stopped, and he was given brain supportive supplements and placed on a program to rehabilitate his brain with diet, exercise, and hyperbaric oxygen therapy shown to help with traumatic brain injury (13). Mr. C came to see his problem as a brain health issue, rather than as a mental health issue, which shifted his mindset to being a more active participant in his own care. In just a few months, he lost 80 pounds, his mood was better, anxiety was decreased, and he had better control over his temper. Several months later, his brain also showed significant improvement on the follow-up SPECT scan. After seeing his brain SPECT scan and learning about why his brain looked so troubled, Mr. C made the decision to give up car racing.

This case demonstrates how functional neuroimaging can be a powerful tool helping to show that other factors are aggravating or are the primary cause of neuropsychiatric syndromes. As seen above, traumatic brain injury as well as toxic exposure are examples of causative factors that most psychiatrists would not generally look for. The most commonly unidentified contributor to psychiatric disorders is traumatic brain injury (TBI). Although there is substantial evidence indicating its role in neuropsychiatric conditions, TBI frequently goes unrecognized and untreated (14–17). SPECT gives us clues to help identify problems that were previously unseen and undiagnosed.

A common problem seen in clinical practice is that of patients who, after years of remission, become non-responders later in their lives. Functional imaging can help identify factors contributing to this.

Mr. O was a 77-year-old gentleman whose bipolar depression had been treated successfully for years but more recently had become progressively more difficult to treat. He no longer responded to various medications and had converted from being an excellent ECT responder to a non-responder. Upon looking at his SPECT scan, he presented with significant decreased perfusion in his temporal lobes, longitudinal fissure, and parietal regions (see **Figure 3**). It became clear that there was a potential history of brain injury as well as a possible neurodegenerative process contributing to his poor response. Instead of treating him with higher doses or more medications, he was continued on his current medication regiment, and was placed on brain supportive supplements and given a program to improve his brain health with diet and exercise, as well as a recommendation for hyperbaric oxygen therapy. With this treatment strategy, Mr. O converted back to being a treatment responder along with the family recognizing the need to become more involved in his care.

As with thousands of other patients who found relief of their symptoms because of the additional data provided by SPECT neuroimaging, had that not been incorporated, the underlying perfusion abnormalities in these patients would have

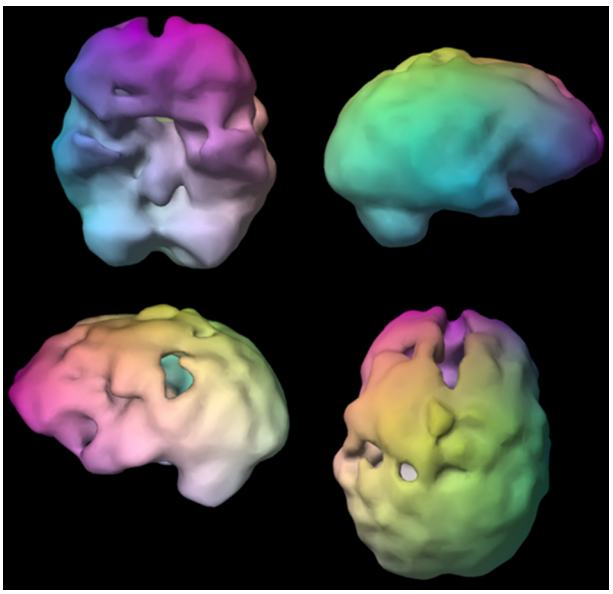

FIGURE 3 | Mr. O's surface view images. Note decrease perfusion in temporal lobes, longitudinal fissure, and parietal regions, as well as findings suggestive of ventricular dilation.

gone undetected, thus denying them the opportunity to reduce their symptoms.

THE CHALLENGES OF SHIFTING A PARADIGM

There is expanding knowledge about the influence various brain regions have on neuropsychiatric function and how changes in these areas can result in predictable symptoms. Yet little of this information has crossed over into clinical practice. Part of the problem is the neurobiology of psychiatric disorders do not typically line up with the Diagnostic Statistical Manuel (DSM), which defines illnesses as symptom clusters that should be distinguishable conditions with common underlying etiologies. In actuality, each DSM diagnosis represents a heterogenous group of illnesses with a variety of underly etiologies. Given the DSM has been the foundation of subject choice in most clinical research it is unlikely it will correlate with functional imaging. The authors believe this is the main reason neuroimaging has not been incorporated into clinical psychiatric practice (18).

Think about the many case conferences we've all attended. A group of psychiatrists looking at symptom clusters without looking at brain function, all of whom see the same patient and use their subjective impressions of an individual's symptoms (all too frequently influenced by psychodynamic interpretations) to come up with a variety of different diagnoses and treatment recommendations. To complicate matters further, these recommendations are all based on research evaluating a heterogeneous group as if they are a single illness. Clinical course and treatment response for a particular DSM diagnosis cannot be predictive using this methodology. It is not a surprise that the overall response and remission rates demonstrated in pharmacotherapeutic studies are low when <40% of the DSM-V diagnoses meet validity testing standards (19–21).

If psychiatry is to move forward, we must first challenge the use of the categorical DSM system as the only way to diagnose patients and learn how to incorporate the findings of evidence-based neuroimaging.

As is the case with any evolving clinical science, there is a need for more work to expand our knowledge of SPECT's benefits and limitations within the clinical setting. In this article, the authors detail the evidence-based rationale for more widespread use of SPECT in psychiatric clinical practice. It explores a number of the reasons why SPECT was derailed despite showing so much promise since the late 1980s and early 1990s, reviews the obstacles and limitations involved with utilizing SPECT, and presents numerous indications that clinical psychiatrists can use immediately. This article primarily looks at SPECT as opposed to other functional neuroimaging options for the following five reasons. First, the authors have extensive experience with SPECT, and as previously stated, have built a growing database of brain scans that currently totals over 194,000 scans. Second, all major hospitals throughout North America, South America, Asia, and Europe are equipped with SPECT cameras, which means it is already a neuroimaging tool that is widely available. Third, a growing body of scientific literature validates the usefulness of brain SPECT imaging for a variety of issues within the field of clinical psychiatry. Fourth, several expert review bodies have endorsed SPECT for numerous indications that are relevant to clinicians, including dementia and brain trauma. Fifth, compared with other neuroimaging tools, SPECT is typically a less expensive imaging modality and has been recognized by the health insurance industry in the United States with specific reimbursement codes for over three decades, although reimbursement is unpredictable, especially for purely psychiatric indications.

In 1962, scientific historian and philosopher, Thomas Kuhn, wrote that scientific revolutions typically occur in 5 stages (22).

Stage I: The Discrepancies Show

In the first stage, the revolution is started when the standard paradigm begins to fail. For example, when author DA would use DSM criteria to diagnose patients with major depression or ADHD and put them on standard treatments, such as fluoxetine or methylphenidate, some patients became suicidal or aggressive. This was a paradigm-based failure that occurred far too often and was traumatic for patients and caregivers.

Stage II: The Disagreements Start

Once the paradigm begins to fail, experts begin to look for ways to fix their theories, but they resist discarding their old models entirely and instead look for small fixes. Over time, the failing model splinters into many competing schools of thought. Kuhn wrote that no matter how wrong their models have become, the leaders maintain their beliefs and continue trying to tweak their ideas to preserve their power and influence. There are now six versions of the DSM, which has not been substantially overhauled since 1980's DSM-III.

Stage III: The Revolution

Over time, a new paradigm emerges that resolves many of the problems in the field. A new paradigm can be: "Most psychiatric illnesses are not mental health issues at all. Neuroimaging clearly shows they are brain health issues that steal the mind (23)." It reinterprets existing knowledge while retaining the best of the old thinking and integrating the latest knowledge into a fresh model, thereby creating a paradigm shift.

Stage IV: The Rejection

The new paradigm is then rejected and ridiculed by the leaders in the field. This is one of the most reliable stages of a scientific revolution. The old guard becomes frustrated that the new idea did not come from them, and because they hold tightly to their own theories, this period may last for decades until they retire or die. Max Planck, the noted Nobel Laureate in physics, once wrote, "*A new scientific truth does not triumph by convincing its opponents and making them see the light, but rather because its opponents eventually die, and a new generation grows up that is familiar with it*[1]*.*" Science advances through funerals.

Stage V: The Acceptance

The new theory is adopted gradually as younger, more open-minded scientists accept it early in their careers and later become the leaders of the field. Kuhn also noted that new paradigms are often championed by professionals who are outsiders and not wed to the status quo.

EVIDENCE-BASED MEDICINE: BRAIN SPECT IMAGING

Structural neuroimaging, such as MRI or CT scans, is routinely recommended for first-break psychoses. *"The use of anatomical scans of individuals with recent onset psychosis is justified in order to rule out neurological diagnoses that may mimic schizophrenia in their early stages. A scan also serves to reassure patient, family, and physician that diagnostic possibilities with visible cerebral insult have been considered* (24)*."* Despite this usage, research shows that such anatomical brain scans impact clinical decisions in only approximately one-half of 1% of all cases, which shows their clinical value is sorely limited (25). As evidenced in a 2-year review, when ordered appropriately in a hospital setting, SPECT provides significantly higher levels of information that is clinically relevant in complex mental health conditions (26).

Currently, the scientific literature on functional brain imaging related to conditions that are relevant to clinical psychiatry numbers in the tens of thousands and involves hundreds of thousands of patients[2]. The abundance of peer-reviewed research involving SPECT validates its reliability as a measure of brain function, and in particular, regional cerebral blood flow (rCBF). Well-respected medical organizations, including the American College of Radiology (ACR) (27), the Canadian Association of Nuclear Medicine (28), and the European Society of Nuclear Medicine (ESNM) (29), have reported evidence-based medicine (EBM) clinical indications for the use of brain SPECT imaging in the evaluation of patients. Generally accepted clinical indications for SPECT include, but are not limited to:

- Evaluation of patients with suspected dementia.
- Evaluation for differential diagnosis.
- Evaluation for early detection or pre-dementia, referred to as mild cognitive impairment (MCI), SPECT can detect a functional deficit and thus guide prognosis.
- Evaluation of patients for cerebrovascular disease.
- Preoperative localization of epileptic foci.
- Evaluation of traumatic brain injury (TBI), particularly if MRI and/or CT findings are unavailable. Blood flow abnormalities in TBI have been seen on SPECT even when anatomical scans appear normal, and SPECT findings are considered valuable for medical prognosis.
- Detecting and evaluating brain inflammation related to chronic inflammatory disorders such as HIV-encephalopathy, viral encephalitis, and vasculitis.
- Evaluating brain death.

Each of these indications—with the exception of brain death and the preoperative localization of epileptic foci—provide value to practicing psychiatrists who routinely evaluate and treat dementia, mental health symptoms related to brain trauma, and the consequences of cerebral vascular disease, infections, and inflammation.

In addition to the commonly accepted indications, the ESNM recommendations also report, "*SPECT can be useful in other indications such as movement disorders and psychiatric diseases (e.g., for follow-up of depression).*"

THE FUNDAMENTALS OF SPECT

SPECT is a nuclear imaging study that uses isotopes bound to ligands to measure rCBF and indirectly activity. Two common radiopharmaceuticals include HMPAO (Ceretec) and ECD (Neurolite); both provide images of rCBF, where each patient acts as their own control. The highest level of activity is typically seen in the cerebellum with HMPAO and the occipital lobes with ECD. Experienced clinicians look for symmetry and areas where perfusion is either increased and/or decreased. A SPECT scan of a healthy brain reveals full, even, symmetrical blood flow (30). See **Figures 4**, **5** for examples of healthy scans.

It is important to know a patient's age when evaluating their SPECT study, because rCBF changes as humans grow older. As a result of reduced myelinization and efficiency, children tend to have higher levels of activity in the brain compared to older adults who typically have decreased levels of perfusion.

In clinical practice, one problem that has been noted with SPECT is the variability of the imaging gamma cameras and resulting variability in image quality. Image quality can be significantly improved with multi-headed cameras and fan beam collimators. Multiple organizations, including the ACR, ESNM and the Society of Nuclear Medicine and Molecular Imaging (31), have each published similar procedure guidelines for SPECT.

[1]https://en.wikiquote.org/wiki/Max_Planck

[2]http://www.amenclinics.com/brain-science/spect-research/spect-abstracts/

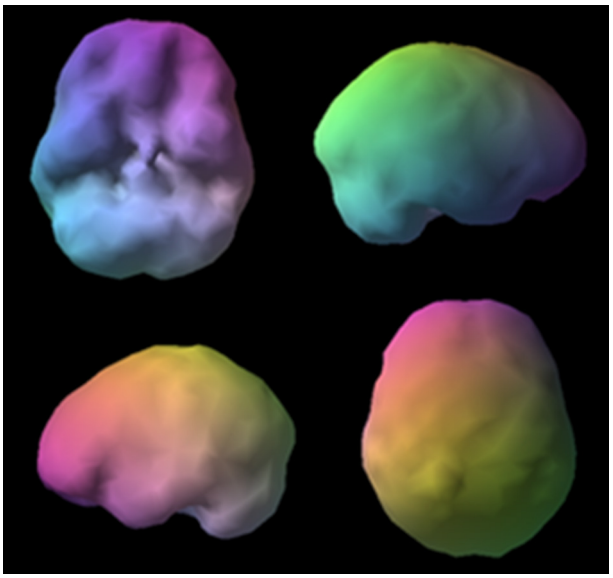

FIGURE 4 | Normal surface rendering. A healthy 3D surface rendering of SPECT information, looking at the top 45% of brain perfusion. A healthy scan shows full, even, symmetrical perfusion.

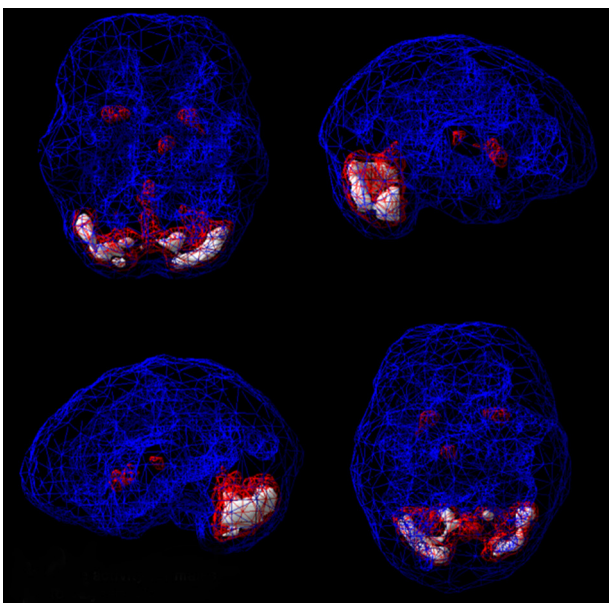

FIGURE 5 | Normal active rendering. A healthy 3D active rendering of SPECT information, looking at areas of increased perfusion. Blue equals average perfusion, red equals the top 15% of perfusion, and white is the top 8%. A healthy active scan with HMPAO shows increased perfusion in the cerebellum.

SPECT HAS AN IMAGE PROBLEM

One of the most commonly believed misconceptions about the clinical use of SPECT is that limited resolution restricts its value. In the early years of SPECT practice, single-headed cameras were utilized, producing low-resolution images, particularly in deep regions of the brain. For the past two decades however, sophisticated multi-headed gamma detectors with fan beam collimators have been available. According to George, multi-head SPECT camera resolution is comparable to PET at a much lower expense (32).

Another issue lies in the type of images provided by most nuclear medicine departments, namely they generate minute gray-scale coronal, sagittal, and horizontal SPECT slices (see **Figure 6**). These minuscule images are challenging to evaluate, including for nuclear clinicians who have years of experience. If radiologists or nuclear medicine departments provide images that clinicians find too difficult to interpret, those clinicians will consider the technology to be unhelpful. These challenges can be overcome with more advanced imaging options. For example, several manufacturers now provide software that produces three-dimensional image renderings—such as the images used in this article—that significantly enhance the images and make them far easier to interpret.

Another area of criticism surrounding SPECT lies in the potential for radiation exposure, particularly in children. For one single brain SPECT scan, the average radiation exposure is ∼0.68 rem, which is less than a head CT (0.90 rem), which is ordered tens of millions of times each year in the U.S., and similar to a bone scan (33). Head CTs and bone scans are commonly ordered for a number of medical conditions, such as head injuries or bone fractures, indicating that such exposure to radiation is considered acceptable in medical practice. The American Academy of Neurology guidelines for SPECT report it is a safe procedure (34). To put the level of radiation from SPECT into perspective, in the U.S, natural background radiation exposure is 0.293 rem on the coast, while in the mountains of Colorado it is 0.387 rem. A single SPECT study is about twice the radiation from that of the natural environment along with other incidental radiation exposure that comes from traveling by plane, as well as from computers, televisions, and other devices (35).

OVERVIEW OF COMMON BRAIN SPECT IMAGING PATTERNS RELEVANT TO CLINICAL USE

Based on the extensive volume of scientific literature on brain SPECT imaging, several key patterns have been detected that can be applied to clinical practice. Following, are seven of the most important examples:

Overall Decreased Perfusion, or "Scalloping"

A pattern of overall decreased perfusion that has a scalloped or wavy appearance on scans is associated with exposure to toxins, certain forms of illness, or insult to the brain. This pattern is often associated with substance abuse (36, 37); the use of

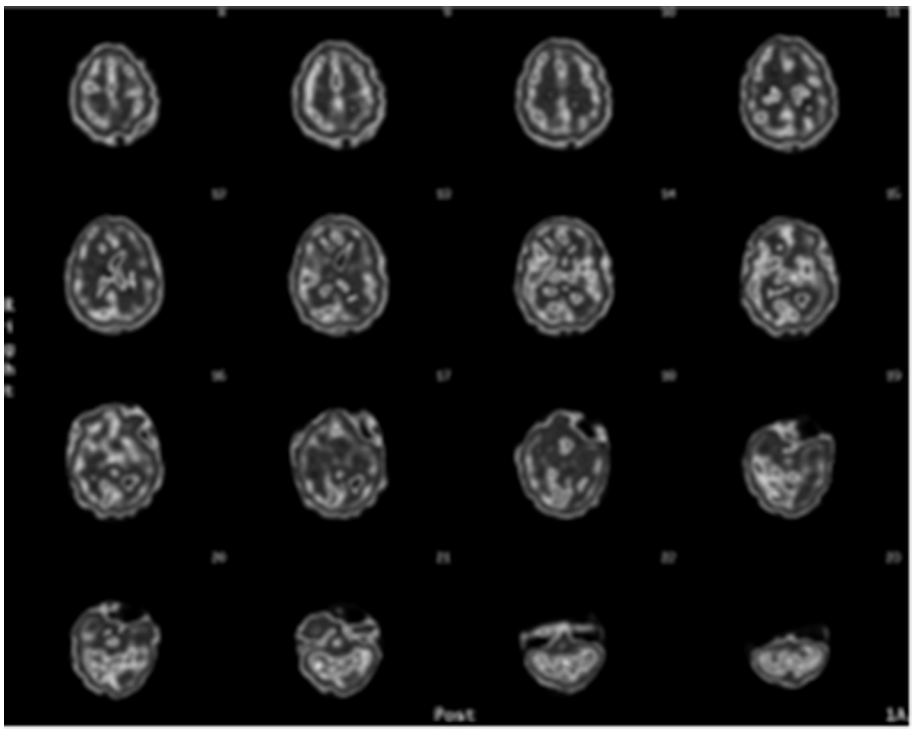

FIGURE 6 | Typical gray scale SPECT rendered transaxial sliced images.

certain prescription medications, such as benzodiazepines[3] (38); exposure to environmental toxins, such as carbon monoxide poisoning (39); infectious diseases, such as Lyme disease (40) or meningitis (41); severe hypothyroidism (42); anemia (43); anoxic states (44); hepatic encephalopathy (45); and exposure to general anesthesia (46, 47). The scalloping pattern does not indicate the etiology, rather it acts as an alert for clinicians to investigate further. Dr. Harold Bursztjan, who co-founded Harvard's Psychiatry and Law program, has said that SPECT scans do not provide answers, but rather they prompt clinicians to ask more pointed questions (48).

Consider this example:

A married couple came to Amen Clinics for evaluations after being told by their relationship counselor that they should end their marriage. This was after they had spent 3 years and thousands of dollars on therapy that wasn't effective. The problem appeared to be the husband who was diagnosed with mixed personality disorder including antisocial and narcissistic traits. The couple were upset by their therapist's suggestion to divorce and chose to seek a more thorough evaluation that included brain SPECT imaging. The husband's SPECT scan revealed overall reduced blood flow (**Figure 7**), which is often seen in substance abusers. However, the husband claimed that he didn't drink alcoholic beverages and had never engaged in the use of drugs. His wife confirmed that he didn't use alcohol or drugs. The scalloping pattern on his scan prompted his physician to question the man's personality disorder diagnosis. Upon further investigation, it was discovered that the husband was employed in a furniture factory, where he spent his days finishing cabinetry with toxic products. On scans, the use of inhalants is often associated with a toxic pattern (49). No amount of marital counseling would have helped this couple unless the husband's brain function improved. Removing him from the toxic environment at the furniture factory was an important step. The information about his brain dysfunction provided by the SPECT scans significantly altered his treatment plan and played a critical role in saving the couple's marriage.

Imaging Patterns Seen in Traumatic Brain Injury (TBI)

TBI, a major cause of disability and death, has often been called a silent epidemic because of the devastating effects it can have on a person's life. Among the many issues TBI sufferers may face are a number of psychiatric disorders involving mood, functional status, and cognitive performance (50). It is clear that lingering symptoms do not occur in every person who has experienced a head injury. However, how could a psychiatric clinician know if a past brain injury may be contributing to mental health issues without looking at the brain using functional neuroimaging? A patient's clinical history doesn't tell the whole story. For example, many patients don't remember suffering a head injury. Other patients may recall past head trauma, but they are unaware that

[3]https://www.psychiatrictimes.com/view/anti-youth-pill-alprazolam-toxicity-can-add-years-brain-age-and-appearance

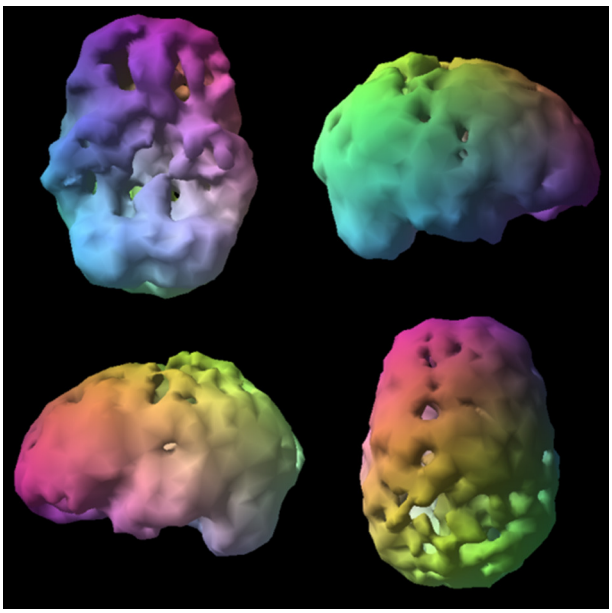

FIGURE 7 | Toxic surface scan. Notice the scalloped, "Swiss cheese," shriveled appearance indicating overall decreased perfusion. These are surface renderings of the SPECT information, looking at the top 45% of brain perfusion; anything below that level shows up as a hole or a dent. The holes do not mean no perfusion, they mean low perfusion, compared to a healthy dataset.

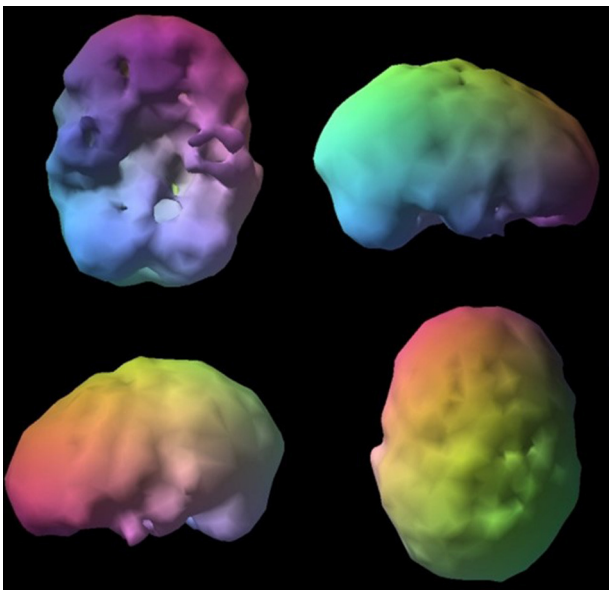

FIGURE 8 | Brain trauma. Asymmetrical decreased perfusion in left frontal and temporal lobes.

it can be linked to lasting mental health issues, so they don't mention it when discussing their clinical psychiatric history.

As an example, one severely depressed and impulsive patient with addiction issues was asked 10 times if he has suffered a head injury. Each time, the 26-year-old male responded that he had not experienced any form of head trauma. In evaluating his SPECT scan (**Figure 8**), abnormal perfusion in the left frontal-temporal region indicated brain trauma. After seeing his own scan, the young man remembered being involved in an accident while riding a motorcycle that resulted in breaking his jaw on the left side of his face. The physical injury he sustained was near the site of the abnormal activity seen on his SPECT scan.

SPECT is helpful in the evaluation of brain trauma and in identifying the affected brain regions and systems. SPECT provides additional information that is useful to clinicians to improve their understanding of a patient's symptomatology as well as in recommending more targeted treatment plans (51). For example, on SPECT, abnormally low perfusion in the prefrontal cortex is often seen in patients with executive dysfunction, which may be improved with prescription psychostimulants or with additional strategies intended to increase PFC activity. As another example, seeing low levels of blood flow in the temporal lobe is commonly seen in patients struggling with mood instability and irritability and may see improvement with the use of anticonvulsant medication. Scientific research also points to SPECT's ability to measure abnormal perfusion levels in cases of mild head injuries, such as whiplash or post-concussion syndrome (52). Patients who have experienced head trauma but whose MRI, CT, and/or EEG scans are normal, frequently complain of headaches, forgetfulness and memory problems, difficulty concentrating, emotional lability, dizziness, and perceptual sensitivities. These patients are often called malingerers when, in fact, they are experiencing the lasting impacts of head trauma-related brain dysfunction that can be seen on SPECT. Researchers in the nuclear medicine field have analyzed the sensitivity of both structural and functional imaging tools in patients with mild to severe head injuries and have concluded that SPECT has greater sensitivity (53).

Comparing and contrasting the benefits and limitations of both structural imaging techniques and functional imaging tools as they relate to prognosis and clinical outcome of head trauma has been the subject of scientific research. Jacobs et al. used brain SPECT imaging in a prospective evaluation of 67 patients with mild, moderate, or acute brain injuries. All of the patients participated in an initial clinical evaluation and SPECT imaging within the first month of the head trauma and were re-evaluated and had a follow-up scan 3 months after their initial scan. On the initial SPECT scans, significant abnormalities were noted in 34 of the patients. Of these patients, 59% continued to report clinical symptoms 3 months later upon follow-up. Among the 33 patients whose initial SPECT scans showed no significant abnormalities, 97% reported during re-evaluation that their clinical symptoms had resolved within the 3-month period. The positive predictive value (PPV) of an initial SPECT scan with abnormalities was 59%, however if the repeat SPECT 3 months later also revealed abnormalities the sensitivity for the follow-up scan was 95%. According to these authors, negative initial SPECT scans can be "a reliable predictor of a favorable clinical outcome (54)."

Similarly, a 2014 systematic review of 52 cross-sectional and 19 longitudinal studies showed PPV increases from initial brain SPECT imaging performed soon after a head injury incident

(PPV of 59%) to repeat scans after 12 months (PPV of 95%) (14). These results were replicated in subsequent studies involving a larger cohort. In cross-sectional and longitudinal studies, SPECT showed localization of lesions that were not detected on MRI or CT scans. In cross-sectional studies, the abnormalities seen on SPECT were most frequently seen in two brain regions: the frontal lobes (94%) and the temporal lobes (77%).

These findings show that SPECT can be useful in many areas of the clinical process in patients who have experienced varying degrees of head trauma. The functional brain imaging tool aids in making a diagnosis, determining a patient's prognosis, and developing an effective treatment plan in brain trauma survivors. In complex psychiatric cases, SPECT may also detect abnormalities associated with brain injuries even when the patient has no recollection of suffering a head trauma.

SPECT does have a limitation in its detection of brain trauma. In many cases, patients do not have a prior, or baseline, SPECT imaging study for comparison purposes. Thus, clinicians are unable to rely on neuroimaging to reveal the date when a trauma occurred. On functional imaging scans, brain trauma that occurred decades earlier or in childhood may look similar to trauma that happened more recently.

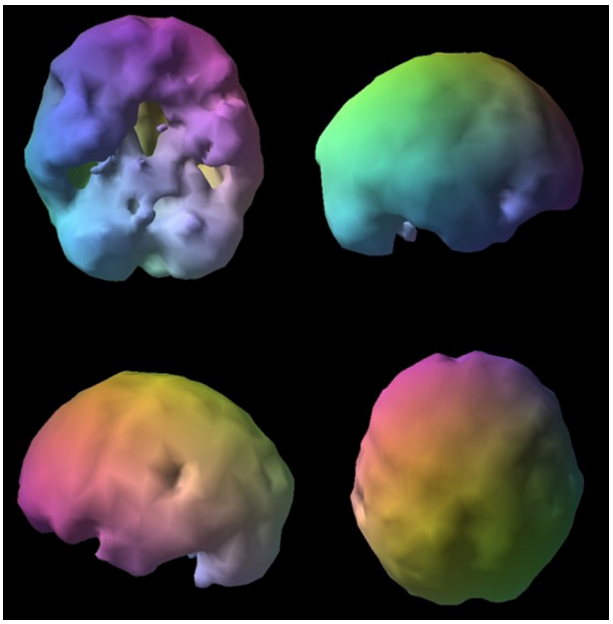

FIGURE 9 | Surface SPECT images. Decreases in medial undersurface (see top left view).

Functional Neuroimaging Patterns Associated With Cognitive Decline

In the diagnosis of Alzheimer's disease (AD), autopsy reports that include an analysis of brain tissue remain the "gold standard" in the medical field. A growing body of scientific evidence, however, suggests that when evaluating patients who are presenting with cognitive decline, it may be helpful to use brain SPECT imaging in addition to diagnostic testing and clinical history (55). A number of common functional neuroimaging patterns have been noted in dementia patients: decreased perfusion in the parietal lobes, posterior cingulate gyrus, and medial temporal lobes are associated with AD; perfusion deficits in the frontal lobes and temporal lobes are seen in frontal lobe dementia; abnormalities in the occipital lobes are seen in Lewy body dementia (56); decreased vascular activity in several areas of the brain is associated with multi-infarct dementia; and decreased activity in the left prefrontal cortex combined with overactivity in the limbic system—a pattern typically associated with depression—is seen in pseudodementia (57). Clinicians are aware that patients with similar symptomatology (i.e., isolation and behavioral disinhibition) can have different dementia diagnoses. Considering that treatment protocols differ depending on the specific dementia disorder, differential diagnosis is vitally important. It is even more critical when patients presenting with dementia symptoms may actually be experiencing issues such as depression or normal pressure hydrocephalus that when treated appropriately resolve dementia-like symptoms. However, the wrong treatment can be devastating. For example, the use of antipsychotics for patients with hallucinations who actually have Lewy body dementia, can cause severe and sometimes irreversible deterioration.

For example:

L, a 73-year-old male with declining memory visited a neurologist for an evaluation that did not include functional brain imaging and was given a diagnosis of Alzheimer's disease. The commonly used medications, memantine and donepezil, however, did not improve his symptoms. Concerned about his deteriorating memory, his family brought him to Amen Clinics for a more complete evaluation including brain SPECT imaging. What the 73-year-old's SPECT scan revealed—significantly enlarged ventricles—was only a fraction of the story (see **Figures 9**, **10**). What was *not* seen on the SPECT scan was even more telling. There was no hypoperfusion in the posterior cingulate and no bilateral decreased perfusion in the temporal and parietal lobes, which are commonly seen in AD. Based on the patterns seen on SPECT and on subsequent MRI neuroimaging, the man's diagnosis was changed from AD to normal pressure hydrocephalus. When treated appropriately for that diagnosis with the insertion of a shunt, he experienced marked improvements in his memory.

The results of SPECT studies in patients with suspected dementia to an elderly control group of healthy subjects were correlated with the histopathology of 54 subjects (biopsy in 3 and autopsy in 54) by Bonte et al. (58). The study revealed that the SPECT diagnoses were false-positive in 3 patients, false-negative in 6, true-positive in 37, and true-negative in 8 patients. Furthermore, the PPV was 92%, the sensitivity was 86%, and the specificity was 73%. These findings suggested that brain SPECT can be useful in both the early and late diagnosis of AD, as well as providing important differential-diagnosis information when the clinical presentation of demented patients is unclear or complicated.

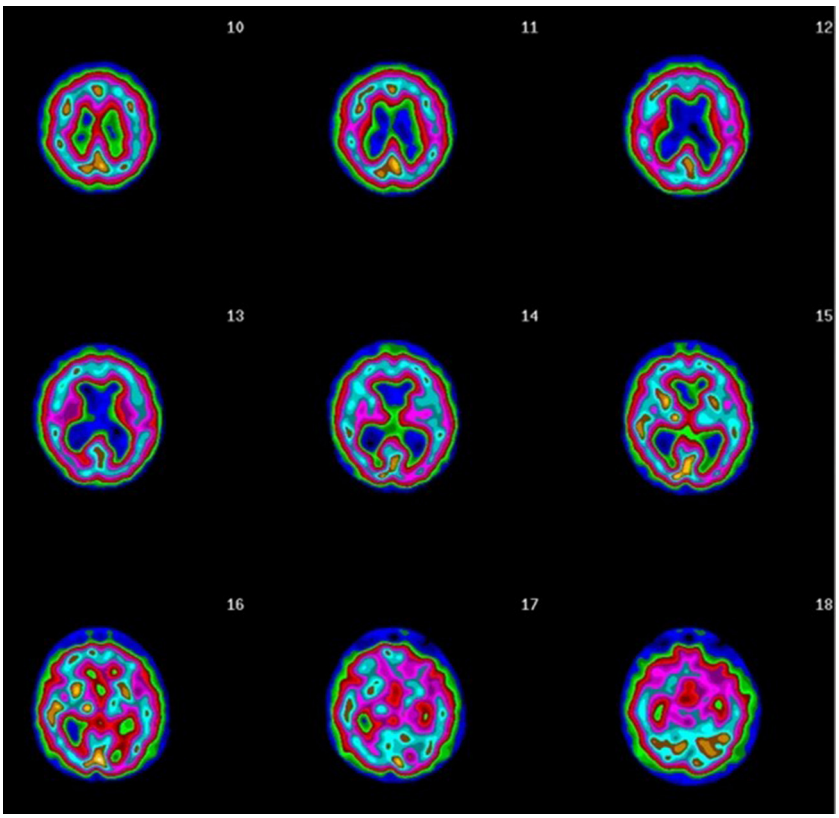

FIGURE 10 | Transaxial slices. Slices 12 and 13 show inverted "lobster pattern" associated with ventricular enlargement.

Jobst et al. (59) evaluated functional (SPECT) and structural (CT) neuroimaging procedures for the utility of differential diagnosis in cases of dementia in comparison to clinical diagnoses of the cases. With 119 control subjects and 200 subjects with dementia, the study participants underwent annual medial temporal lobe CT scans and annual HMPAO SPECT studies The authors were able to conclude that the use of CT and SPECT together was more diagnostically accurate than standard clinical diagnosis. The study also found that common neuroimaging findings show parietotemporal hypoperfusion together with medial temporal lobe atrophy are common in AD but considerably less common in other types of dementia, and usually not found in normal controls.

DaTscan, another SPECT technology, has also been shown to help separate Alzheimer's disease from Lewy body dementia (60), and may have predictive value in longevity (61).

How does SPECT compare to PET in the diagnosis of dementia? Published studies of SPECT accuracy show that it is a useful tool for differential diagnosis, with sensitivities of 65–85% for diagnosing Alzheimer's disease and specificities (for other neurodegenerative dementias) of 72–87%. PET studies generally report slightly higher accuracies. However, there have been few direct head-to-head comparisons, with some indicating SPECT and PET to be equally useful in dementia. Although some studies suggest superiority of PET over SPECT, the evidence base for this is actually quite limited. Many of these studies have small numbers and methodically with poorly matched control groups (62). One must also take into consideration that SPECT scanning is more widely available and cheaper than PET. A new multi-headed SPECT gamma camera costs $300,000–800,000, while a PET scanner costs significantly more. Additionally, SPECT radio tracers are less expensive and have half-lives of up to 6 h, allowing a longer imaging time.

Hyperfrontality

On SPECT, hyperperfusion or patterns of overactivity in the frontal lobes (anterior cingulate gyrus and prefrontal cortex) is called hyperfrontality. This functional neuroimaging finding is associated with a variety of psychiatric disorders involving cognitive inflexibility, which is seen in patients with a tendency to get stuck on negative or worrisome thoughts or unwanted or unhealthy behaviors. Hyperfrontality can cross several different diagnostic categories and can be seen in a variety of mental health conditions such as obsessive-compulsive disorder (OCD) (63), posttraumatic stress disorder (PTSD), autism spectrum disorder (ASD), some types of mood disorders, and certain types of anxiety disorders (64). Hyperfrontality is commonly noted in scans of patients who report being rigid, fixed, inflexible, argumentative, or oppositional and who have trouble adapting to new situations.

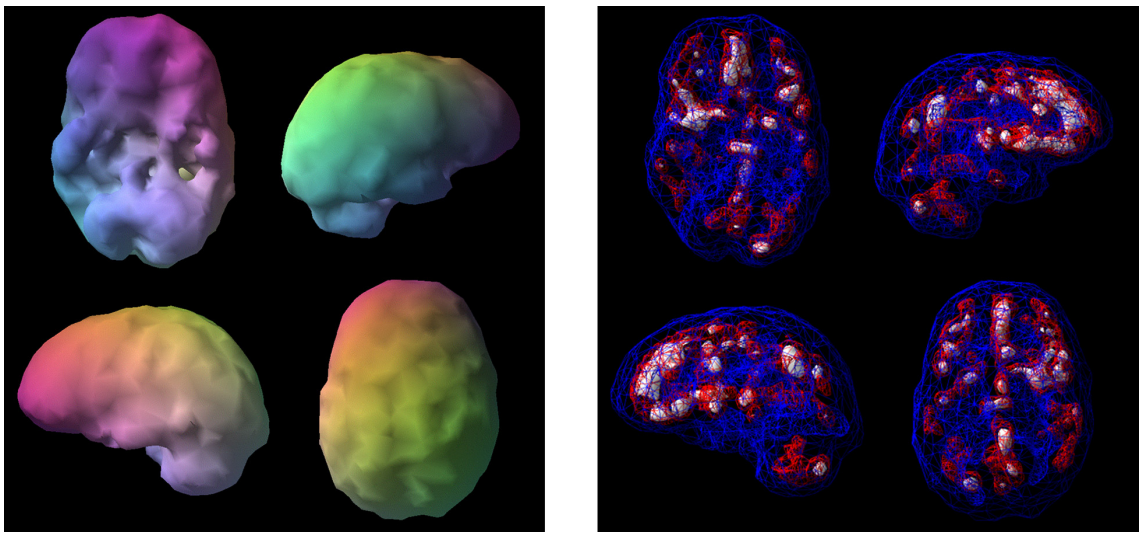

FIGURE 11 | Surface views (L) and active views (R). Surface views (L) show severe temporal lobe hypoperfusion and active views (R) show severe hyperfrontality. The image on the left shows the outside surface of the brain, looking at the top 45% of brain activity. The image on the right shows the active rendering, where blue equals average perfusion, red is the top 15% of perfusion, and white is the top 8%. A healthy scan shows a symmetrical pattern with the most intense uptake in the cerebellum.

Brain imaging research shows that hyperfrontality on SPECT has been predictive of a positive treatment response to serotonergic medication in depression (65) and OCD (66), to sleep deprivation (67), and repetitive transcranial magnetic stimulation (68) for depression, and to a cingulotomy in OCD (69). Seeing hyperfrontality on SPECT scans also aids in differentiating ADHD from OCD (70).

It is important for clinicians to understand that hyperfrontality is not considered a diagnosis. However, seeing the biological underpinnings associated with the clinical symptomology helps provide necessary information that informs treatment.

For example:

V, a 17-year-old male, presented with severe temporal lobe epilepsy, which developed following childhood meningitis. In addition, V displayed extreme aggression that had not responded to various behavioral interventions. His brain SPECT images showed severely reduced blood flow in his left temporal lobe (**Figure 11** image on left), which is a common finding in epilepsy, and it also revealed extremely heightened perfusion in the anterior cingulate gyrus and lateral frontal lobes (**Figure 11** image on right), which is often seen in obsessive-compulsive spectrum disorder. V's clinical history did not show symptomology typically associated with OCD; however, he did report being inflexible and rigid, and he had trouble coping when things did not go as planned. Amending his treatment plan by adding an antidepressant medication (escitalopram) that has been found to reduce overactivity in the frontal lobes significantly improved his behavior. Without the benefit of functional neuroimaging, it would have been more challenging to develop the most effective treatment protocol.

Hypofrontality

Another common functional brain imaging pattern is hypofrontality, in which there is decreased blood flow or activity in the prefrontal cortex (PFC). This important finding can help clinicians better understand patient symptomology and more effectively target treatment to individuals. In scientific literature, hypofrontality is associated with improved response to stimulant medication in patients with ADHD (71) and improved response to acetylcholine-esterase inhibitors in Alzheimer's disease (72). In patients with depression, decreased perfusion in the PFC is predictive of a negative response to serotonergic antidepressants (73). In addition, decreased PFC perfusion is predictive of relapse in alcohol abusers (74) and is associated with impulsivity, antisocial behaviors, and homicide (75).

As research shows, hypofrontality is associated with a wide array of mental health issues, but it is not in and of itself a psychiatric diagnosis. Even so, it provides clinicians with critical information about abnormalities in brain function that can be beneficial in understanding and treating cognitive, emotional, or behavioral issues.

For example:

J, a 62-year-old female, had struggled with a lifetime of issues such as being inattentive, easily distracted, disorganized, and unable to maintain relationships. In her clinical history, she admitted that she had been fired multiple times for turning in work that wasn't always up to her potential and for being unreliable. Despite these troubles, she was resistant to seeking help even after a family member said she might have ADHD that could be treated. J said she was "too old to change." With some prodding from her family, J eventually turned to Amen Clinics for an evaluation that included brain SPECT imaging. Her SPECT study showed significantly decreased PFC perfusion

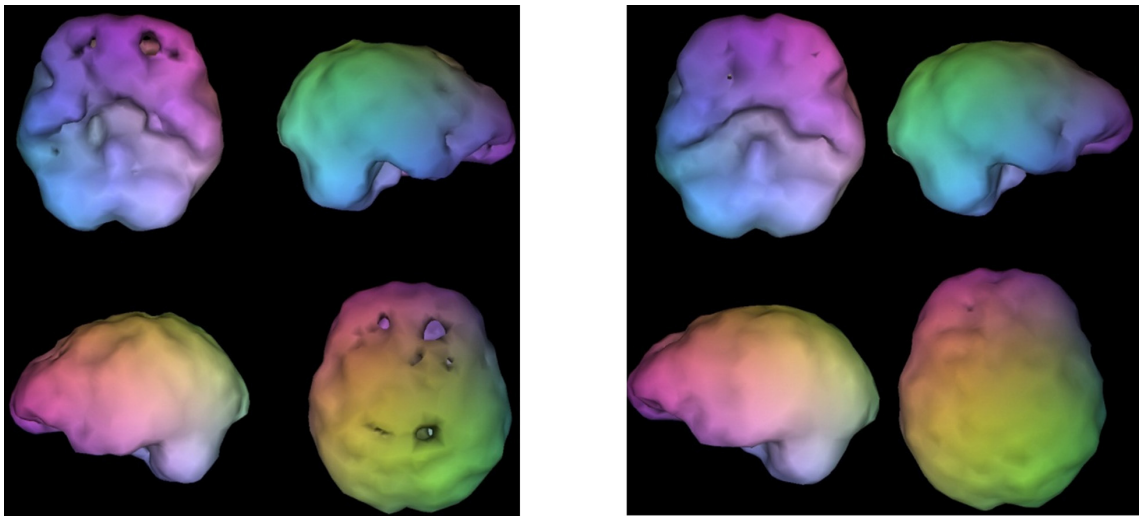

FIGURE 12 | SPECT surface images without medication (L) and on mixed amphetamine salts (R). Without medication, SPECT images (L) reveal overall decreased prefrontal perfusion and post-treatment images (R) show improved prefrontal perfusion.

during a concentration task, which is a hallmark finding with ADHD. For her second SPECT scan, she took 10 mg of mixed amphetamine salts, which is a common ADHD treatment. The second scan showed a marked increase in perfusion to the PFC (see **Figure 12**). On treatment for ADHD, J experienced improvements in her cognitive function, as well as in her relationships and career. The neuroimaging scans not only aided the clinician but also helped the patient to understand that her symptoms had a biological basis that was treatable, which increased her compliance.

Temporal Lobe Abnormalities

Abnormalities in temporal lobe perfusion are commonly seen in brain injuries and often relate to mood instability, temper problems, aggressive behavior, memory loss, and problems with language (76). This is why evaluating temporal lobe perfusion with a reliable neuroimaging tool such as SPECT is so critical in psychiatry. According to Devous et al. (77) *"Both SPECT and PET have localizing power approaching that of combined scalp and depth EEG."* In psychiatry, it is important to localize potential seizure activity in patients who have epilepsy because they tend to have a high rate of co-existing mental health conditions (78). In addition, in the psychiatric field, anticonvulsants have become more commonly prescribed to stabilize moods. These medications have been found to improve overall perfusion and activity in the brain with particular improvement in the temporal lobes (79).

Temporal lobe epilepsy (TLE), a common chronic epileptic disorder, is associated with a broad range of psychiatric symptoms, such as depressed or euphoric mood, anxiety, fear, anergia, atypical pain, irritability, and insomnia (80). EEG is routinely used in the evaluation of epilepsy, however, this technology has difficulty evaluating certain key areas that are frequently involved in TLE, namely the medial aspects of the temporal lobes. By contrast, SPECT can show abnormalities that are undetected by EEG. The most common SPECT findings in epilepsy include focal reduced perfusion in the interictal phase and focal elevated perfusion in the ictal phase of a seizure. In a meta-analysis of 30 studies, Devous et al. found that sensitivities for SPECT localization in patients with temporal lobe seizures were 0.44 (interictal), 0.75 (postictal) and 0.97 (ictal). False-positive rates were low (81). These findings show that SPECT may be beneficial to clinicians in evaluating temporal lobe function in several ways, including the identification of abnormalities in any areas, finding deficits that go undetected by EEG, and potential insight into how and why anticonvulsants may be useful for a variety of neuropsychiatric indications.

Based on our three decades of brain SPECT imaging experience and clinical practice, we recommend anticonvulsants as a first-line treatment in patients who present with mood instability or anger and aggression problems and whose brain scans show either high or low perfusion in the temporal lobes. For patients with memory problems or difficulties learning whose brain scans reveal decreased perfusion in the temporal lobes, we consider acetylcholine-esterase inhibitors, provided it is deemed appropriate when the full clinical picture is considered.

Here is an example of how SPECT can be helpful in evaluating temporal lobe dysfunction:

J, a 17-year-old male, presented with severe mood swings, extreme temper problems, homicidal and suicidal thoughts, and a history of addiction. Despite evaluations by several psychiatric professionals, an 18-month stint in a residential treatment facility, and multiple medications, he wasn't improving. An addiction counselor suggested he might benefit from getting a SPECT scan.

His SPECT scan showed a major abnormality (**Figure 13**) in the form of a large defect cyst that took up nearly 25% of the left prefrontal and temporal regions of his brain. A subsequent MRI

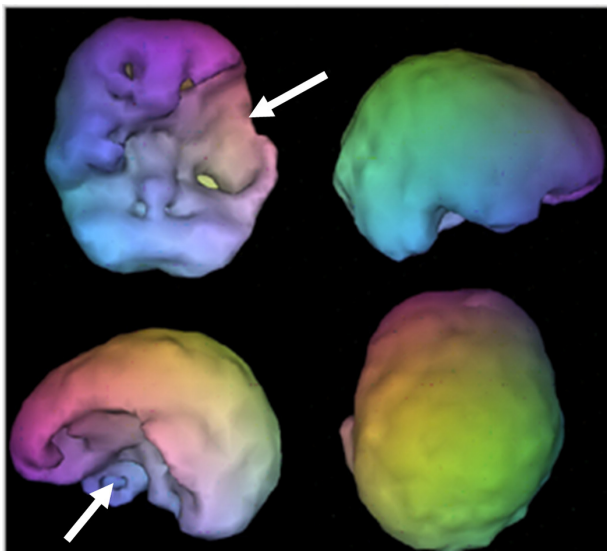

FIGURE 13 | Tennis ball sized cyst occupying the left prefrontal and temporal regions. Images show large defect in left hemisphere.

showed that inside his brain was a cyst the size of a tennis ball, which was causing compression of ventricles from a hemispheric shift. It is important to note that the results of J's neurological exam had been normal, but the SPECT scan clearly indicated that his brain was not normal.

Without the added information from the functional neuroimaging, most psychiatric professionals would give J multiple diagnoses, such as bipolar disorder and conduct disorder, which often leads to a subsequent diagnosis of antisocial personality disorder. J would then be placed on medications intended to treat those diagnoses and when those medications failed, psychiatrists might turn their attention to family therapy or other therapeutic strategies. But this is the wrong approach. It is clear that even the best family therapist wouldn't be able to help this teenager, nor would psychiatric medications. Unless the pressure in his brain was relieved, he would not get well.

Many psychiatric clinicians might argue that brain imaging with MRI would have sufficed in J's instance, and ultimately that proved to be the case. However, because the abnormality was clearly seen on SPECT, it is our opinion that SPECT is the preferred evaluation tool because it also provides valuable information on both increased and decreased perfusion, which MRI does not.

Using Functional Neuroimaging to Subtype Dimensional Behavior

Using functional brain imaging in psychiatric clinical practice is in line with the efforts of the Research Domain Criteria (RDoC) initiative from NIMH, which aims to develop more effective ways to categorize psychopathology based on both observable behavior and objective neurobiological measures. Subtyping mental health conditions, such as ADHD, depression, and OCD based on brain dysfunction will be a critical component in finding the most effective and targeted treatment plans for individual patients.

Consider aggression, which the NIMH has identified as one of five key areas of interest in terms of brain function and is an area where SPECT can deliver immediate benefits to the clinician. Based on our brain imaging work on 75 murderers, as well as on hundreds of patients with a history of violent crimes such as bombings, rape, and kidnapping, we have seen that aggression is not associated with one single pattern in the brain, but rather clusters in three or more regions of the brain. One subtype is impulsive aggressive, which is associated with decreased perfusion in the frontal lobes (hypofrontality) and has been noted in the literature in antisocial personality disorder (82, 83). Patients with decreased perfusion in the PFC are often unable to control aggressive impulses, putting them at increased risk for violent behavior. Another subtype we have observed is compulsive aggressive, which is seen with increased perfusion in the frontal lobes (hyperfrontality). These patients have a tendency to explode because of inflexibility or negative thoughts get stuck in their mind. A third subtype of aggression we have seen in our brain imaging work is associated with abnormalities in the temporal lobes. In a retrospective analysis of SPECT and MRI scans from 21 individuals convicted of impulsive violent crimes, Soderstrom et al. (84) found that 16 of the offenders had varying levels of decreased perfusion in the temporal lobes and/or frontal lobes. The MRI scans of the violent criminals, however, did not reveal any anatomical problems or other abnormalities.

Since there is variability in the underlying cause of brain dysfunction in violent offenders, using SPECT to identify and understand any brain abnormalities can prompt the psychiatric clinician to ask additional questions that can lead to a more individualized and effective treatment protocol for managing symptoms and behavior problems.

SUMMARY

By identifying a patient's specific brain system dysfunction, SPECT can provide important diagnostic information that helps to individualize treatment protocols to each patient's unique needs. The standard practice of relying solely on traditional diagnostic procedures and therapeutic interventions without imaging data in complex cases has been found to be less accurate and with diminished remission rates. We have described 7 clinical areas in this paper that illustrate the complexity of symptoms relative to brain function. The authors' experiences have found that a secondary benefit of using brain SPECT imaging is that by seeing images of their brains, the patients and their families are less burdened by the stigma of mental illness and the guilt and shame that accompany it. As such, they can see that their psychiatric illnesses have medical underpinnings and are not moral shortcomings. This in turn has led to greater compliance with treatment. Plus, after seeing their own scans, patients develop a personal relationship with their own brains and often desire to treat it better, including the avoidance of toxins, like recreational drugs and alcohol. After seeing his scan, one patient said, "I felt the same after seeing one of my children

for the first time; I knew I would never do anything again to hurt it."

As with all neuroimaging modalities, the findings from brain SPECT studies are not a stand-alone diagnosis but should always be incorporated into the overall clinical assessment. There have been many discussions over the course of the last 30 years with regard to the "Future of Psychiatry" (85) as medicine begins to adopt a more biologically-based paradigm. Within this new framework, some are concerned about being able to maintain a subjective focus on patients. Reynolds, Lewis, et al. (86) opined that it is vital to ensure resident trainees have ongoing exposure to translational neuroscience early on in their residencies, and that neuroimaging is included in the curriculum. A recent report (87) demonstrated the integration of a neuroimaging module within a residency program had wide approval by residents. Certain programs have included neuroimaging to some extent during the preliminary year of the internal medicine neurology rotation. The further development of this field will need to be taken on by the Resident Review Committee for the psychiatry branch of the Accreditation Council for Graduate Medical Education (88).

The field of psychiatry is likely to continue evolving over the course of the next three decades as it increasingly incorporates functional neuroimaging in clinical practice. Quantitative EEG, arterial spin labeling, PET, and other modalities are bolstering the arsenal of neuroimaging for the future.

In the early 1990s, the APA spent several years providing courses on SPECT, but ultimately dismissed the use of neuroimaging, because it threatened the perceived integrity of the DSM which they own and from which they make money (6). Sadly, the limitations of the APA's position completely overlooked the benefits that neuroimaging tools have for physicians and their patients. Because psychiatry is the only medical specialty that does not use objective visual data for the organ they treat, they are relegated to diagnosing complex patients by looking for symptom clusters deduced from talking to and looking at them. In 1840, that was the methodology Dr. Anson Henry used to diagnose Abraham Lincoln with melancholia.

The original DSM was created prior to the development of functional assessment tools, such as SPECT and qEEG, thus the DSM was not—and is not—based on underlying neuroscience. Because of this, physicians who include functional brain imaging in clinical practice understand that scans will never match up with the siloed categories of the DSM. Experienced clinicians can often tell, in simple cases, if some individuals are likely to have ADHD, OCD, or bipolar disorder without the benefit of these tools. Given the high overlap of symptoms in more difficult cases the appropriate diagnosis is frequently missed by looking only at symptom clusters. When misdiagnosed, the treatment implications in these clinical cases can be devastating. It has been our experience that looking at brain systems using functional neuroimaging such as SPECT is extremely helpful in aiding us in these more complicated presentations.

Without the use of functional brain imaging, it is impossible to identify any brain pathophysiology of the patients they treat. Without imaging the brain, psychiatrists would not even consider if a patient's inattention, depression, or aggression could be from:

- Toxic exposure
- Head trauma
- Early dementia process
- Hyperfrontality
- Hypofrontality
- Temporal lobe abnormalities
- Other potential causes

If we don't look at the brain, we are unnecessarily flying blind ***and will*** miss important diagnoses, and be led to the wrong treatment plan, potentially resulting in years of patients' suffering, disability, and potential suicide. This is a disservice to our patients and these errors can be minimized so we don't hurt the people and families we are entrusted to help.

The authors believe clinicians should consider ordering SPECT scans in complex cases, where traditional approaches prove to be ineffective. This will help clinicians move away from treating symptoms to looking at and treating dysregulation of various brain systems. Additionally it will help psychiatrists expand their recognition, understanding, and treatment of other comorbid factors affecting treatment efficacy such as TBI, infection, inflammation, and toxicities. In a large outcome study we performed at Amen Clinics on over 500 patients, before coming to us they failed 3.3 providers and 6 psychiatric medications (89). We suggest a SPECT scan should be considered after two treatment failures.

Be careful if you wish to change a paradigm, as it invites cruel and bitter criticism[4], which has been our experience. In the fifteenth century, the Italian politician, Niccolo Machiavelli, explained: *"It must be remembered there is nothing more difficult to plan, more doubtful of success, nor more dangerous to manage than a new system. For the initiator has the enmity of all who would profit by the preservation of the old institutions…"* (90).

DATA AVAILABILITY STATEMENT

The original contributions presented in the study are included in the article/supplementary material, further inquiries can be directed to the corresponding author/s.

ETHICS STATEMENT

For all case studies presented herein, written informed consent was obtained from the individual adult patients as well as from the minors' legal guardians for the publication of any potentially identifiable images or data included in this article.

AUTHOR CONTRIBUTIONS

All authors listed have made a substantial, direct, and intellectual contribution to the work and approved it for publication.

[4]https://www.washingtonpost.com/lifestyle/magazine/daniel-amen-is-the-most-popular-psychiatrist-in-america-to-most-researchers-and-scientists-thats-a-very-bad-thing/2012/08/07/467ed52c-c540-11e1-8c16-5080b717c13e_story.html

REFERENCES

1. National Library of Medicine. *Brain SPECT—Search Results—PubMed* (nih.gov) (2021). Available online at: https://pubmed.ncbi.nlm.nih.gov/ (accessed June 1, 2021).
2. Holman BL. and Devous MD Sr. *Functional brain SPECT: the emergence of a powerful clinical method J Nucl Med.* (1992) 33:1888–904.
3. Vasile RG. Single photon emission computed tomography in psychiatry: current perspectives. *Harv Rev Psychiatry.* (1996) 4:27–38. doi: 10.3109/10673229609030519
4. Camargo EE. Brain SPECT in neurology and psychiatry. *J Nucl Med.* (2001) 42:611–23.
5. APA Council on Children. *Adolescents and Families: Brain Imaging and Child and Adolescent PsychiatryWith Special Emphasis on Single Photon Emission Computed Tomography (SPECT), Resource Document.* (2005). Available online at: http://psych.org/Departments/EDU/Library/APAOfficialDocumentsandRelated/ResourceDocuments/200501.aspx
6. First MB, Drevets WC, Carter C, Dickstein DP, Kasoff L, Kim KL, et al. Clinical Applications of Neuroimaging in Psychiatric Disorders. *Am J Psychiatry.* (2018) 175:915–6. doi: 10.1176/appi.ajp.2018.17 50701
7. Insel, TR. *Judd Marmor Award Lecture: American Psychiatric Association Annual Meeting.* (2005). Atlanta, GA.
8. Boyd JH, Burke JD, Gruenberg E, Holzer CE, Rae DS, George LK, et al. Exclusion criteria of DSM-III: a study of co-occurrence of hierarchy-free syndromes. *Arch Gen Psychiatr.* (1984) 41:983–9. doi: 10.1001/archpsyc.1984.01790210065008
9. Regier DA, Farmer ME, Rae DS, Locke BZ, Keith SJ, Judd LL, et al. Comorbidity of mental disorders with alcohol and other drug abuse: results from the Epidemiologic Catchment Area (ECA) study. *JAMA.* (1990) 264:2511–8. doi: 10.1001/jama.1990.03450190043026
10. Insel TR, Quirion R. Psychiatry as a clinical neuroscience discipline. *JAMA.* (2005) 294:2221–4. doi: 10.1001/jama.294.17.2221
11. Thornton JF, Schneider H, McLean MK, van Lierop MJ, Tarzwell R. Improved outcomes using brain SPECT-guided treatment versus treatment-as-usual in community psychiatric outpatients: a retrospective case-control study. *J Neuropsychiatry Clin Neurosci.* (2014) 26:51–6. doi: 10.1176/appi.neuropsych.12100238
12. Amen DG, Jourdain M, Taylor DV, Pigott HE, Willeumier K. Multi-site six-month outcome study of complex psychiatric patients evaluated with addition of brain SPECT imaging. *Adv Mind Body Med.* (2013) 27:6–16.
13. Harch PG, Andrews SR, Fogarty EF, Amen D, Pezzullo JC, Lucarini J, et al. A phase I study of low-pressure hyperbaric oxygen therapy for blast-induced post-concussion syndrome and post-traumatic stress disorder. *J Neurotrauma.* (2012) 29:168–85. doi: 10.1089/neu.2011.1895
14. Raji CA, Tarzwell R, Pavel D, Schneider H, Uszler M, Thornton J, et al. Clinical utility of SPECT neuroimaging in the diagnosis and treatment of traumatic brain injury: a systematic review. *PLoS ONE.* (2014) 9:e91088. doi: 10.1371/journal.pone.0091088
15. Pavel D, Jobe T, Devore-Best S, Davis G, Epstein P, Sinha S, et al. Viewing the functional consequences of traumatic brain injury by using brain SPECT. *Brain Cogn.* (2006) 60:211–3.
16. Jorge RE, Robinson RG, Moser D, Tateno A, Crespo-Facorro B, Arndt S. Major depression following traumatic brain injury. *Arch Gen Psychiatry.* (2004) 61:42–50. doi: 10.1001/archpsyc.61.1.42
17. Fann JR, Burington B, Leonetti A, Jaffe K, Katon WJ, Thompson RS. Psychiatric illness following traumatic brain injury in an adult health maintenance organization population. *Arch Gen Psychiatry.* (2004) 61:53–61. doi: 10.1001/archpsyc.61.1.53
18. Henderson TA. Brain SPECT imaging in neuropsychiatric diagnosis and monitoring. *EPatient.* (2018) 1:40–7. Available online at: http://nmpangea.com/2018/10/09/738/
19. Regier DA, Narrow WE, Clarke DE, Kraemer HC, Kuramoto SJ, Kuhl EA, et al. DSM-5 field trials in the United States and Canada, Part II: test-retest reliability of selected categorical diagnoses. *Am J Psychiatry.* (2013) 170:59–70. doi: 10.1176/appi.ajp.2012.12070999
20. Insel T. *Judd Marmor Award Lecture: American Psychiatric Association Annual Meeting.* Atlanta GA. (2005).
21. Insel T. *Transforming Diagnosis, NIMH Director Post.* (2013). Available online at: https://www.nimh.nih.gov/about/directors/thomas-insel/blog/2013/transforming-diagnosis.shtml (accessed September 26, 2019).
22. Kuhn TS. *The Structure of Scientific Revolution.* Chicago, IL: University of Chicago Press. (1962).
23. Amen DG. *The End of Mental Illness: How Neuroscience Is Transforming Psychiatry and Helping Prevent or Reverse Mood and Anxiety Disorders, ADHD, Addictions, PTSD, Psychosis, Personality Disorders, and More.* Carol Stream, IL: Tyndale Momentum. (2020).
24. Ehmann, T, Hanson, L. *Early Psychosis, A Care Guide.* (2002). Available online at: http://www.health.gov.bc.ca/library/publications/year/2002/EarlyPsychosis_guide.pdf
25. Albon E, Tsourapas A, Frew E, Davenport C, Oyebode F, Bayliss S, et al. Structural neuroimaging in psychosis: a systematic review and economic evaluation. *Health Technol Assess.* (2008) 12:iii–iv. doi: 10.3310/hta12180
26. Sheehan W, Thurber S. Review of two years of experiences with SPECT among psychiatric patients in a rural hospital setting. *J Psychiatr Pract.* (2008) 14:318–23. doi: 10.1097/01.pra.0000336760.88178.e5
27. American College of Radiology. *ACR-ACNM-SNMMI-SPR Practice Parameter for the Performance of Single-Photon Emission Brain Perfusion Imaging (Including SPECT and SPECT/CT)* (2021). Available online at: https://www.acr.org/-/media/ACR/Files/Practice-Parameters/BrainPerf-SPECT.pdf
28. *Canadian Association of Nuclear Medicine—Guidelines* (canm-acmn.ca). (2021). (accessed June 1, 2021).
29. Kapucu OL, Nobili F, Varrone A, Booij J, Vander Borght T, Någren K, et al. EANM procedure guideline for brain perfusion SPECT using (99m)Tc-labelled radiopharmaceuticals, version 2. *Eur J Nucl Med Mol Imaging.* (2009) 36:2093–102. doi: 10.1007/s00259-009-1266-y
30. Datz FL, Patch GG, Arias JM, Morton KA. *Nuclear Medicine: A Teaching Profile*. St Louis, MO, Moseby-Yearbook. (1992).
31. Juni JE, Waxman AD, Devous Sr MD, Tikofsky RS, Ichise M, Van Heertum RL, et al. Society for Nuclear Medicine. Procedure guideline for brain perfusion SPECT using ^{99m}Tc radiopharmaceuticals 3.0. *J Nucl Med Technol.* (2009) 37:191–5. doi: 10.2967/jnmt.109.067850
32. George MS. *Neuroactivation and Neuroimaging with SPET*. New York, NY: Springer-Verlag (1991).
33. Power SP, Moloney F, Twomey M, James K, O'Connor OJ, Maher MM. Computed tomography and patient risk: Facts, perceptions and uncertainties. *World J Radiol.* (2016) 8:902–15. doi: 10.4329/wjr.v8.i12.902
34. Report of the Therapeutics and Technology. Assessment subcommittee of the american academy of neurology: assesment of brain. *SPECT.* (1996) 46:278–85. doi: 10.1212/WNL.46.1.278
35. Raji CA, Henderson TA, PET. and single-photon emission computed tomography in brain concussion. *Neuroimaging Clin N Am.* (2018) 28:67–82. doi: 10.1016/j.nic.2017.09.003
36. Demir B, Ulug B, Lay Ergün E, Erbaş B. Regional cerebral blood flow and neuropsychological functioning in early and late onset alcoholism. *Psychiatry Res.* (2002) 115:115–25. doi: 10.1016/S0925-4927(02)00071-9
37. Amen DG, Darmal B, Raji CA, Bao W, Jorandby L, Meysami S, et al. Discriminative properties of hippocampal hypoperfusion in marijuana users compared to healthy controls: Implications for marijuana administration in Alzheimer's dementia. *J Alzheimer's Dis.* (2017) 56:261–73. doi: 10.3233/JAD-160833
38. Shih WJ, Hyatt M. Volume and surface three-dimensional displays of Tc-99m HMPAO brain SPECT imaging in a chronic hypnosedative abuser. *Clin Nucl Med.* (1993) 18:506–9. doi: 10.1097/00003072-199306000-00010
39. Lu YY, Tsai SC, Kao CH, Lin WY. Regional cerebral blood flow in patients with carbon monoxide intoxication. *Ann Nucl Med.* (2012) 26:771–6. doi: 10.1007/s12149-012-0638-8
40. Donta ST, Noto RB, Vento JA, SPECT. brain imaging in chronic Lyme disease. *Clin Nucl Med.* (2012) 37:e219–22. doi: 10.1097/RLU.0b013e318262ad9b
41. Møller K, Høgh P, Larsen FS, Strauss GI, Skinhøj P, Sperling BK, et al. Regional cerebral blood flow during hyperventilation in patients with acute bacterial meningitis. *Clin Physiol.* (2000) 20:399–410. doi: 10.1046/j.1365-2281.2000.00276.x
42. Schnedl WJ, Mirzaei S, Wallner-Liebmann SJ, Tafeit E, Mangge H, Krause R, et al. Improvement of cerebral hypoperfusion with levothyroxine therapy in

Hashimoto's encephalopathy demonstrated by ^{99m}Tc-HMPAO-SPECT. *Eur Thyroid J.* (2013) 2:116–9. doi: 10.1159/000348523
43. Al-Kandari FA, Owunwanne A, Syed GM, Ar Marouf R, Elgazzar AH, Shiekh M, et al. Regional cerebral blood flow in patients with sickle cell disease: study with single photon emission computed tomography. *Ann Nucl Med.* (2007) 21:439–45. doi: 10.1007/s12149-007-0050-y
44. Rupright J, Woods EA, Singh A. Hypoxic brain injury: evaluation by single photon emission computed tomography. *Arch Phys Med Rehabil.* (1996) 77:1205–8. doi: 10.1016/S0003-9993(96)90150-1
45. Mouratidis B, Lomas F. Brain SPECT imaging with Tc-99m HMPAO in hepatic encephalopathy. *Clin Nucl Med.* (1995) 20:842. doi: 10.1097/00003072-199509000-00021
46. Quirce R, Carril J, Vallina N, Montero A, Uriarte I. Efecto sobre la perfusión cerebral del tratamiento con OKT3 en paciente con trasplante cardíaco mediante SPET con HMPAO-99mTc [Effects of treatment with OKT3 on brain perfusion in a heart transplant patient with SPET with 99mTc-HMPAO]. *Rev Esp Med Nucl.* (1999) 18:363–6.
47. Zhou ZB, Meng L, Gelb AW, Lee R, Huang WQ. Cerebral ischemia during surgery: an overview. *J Biomed Res.* (2016) 30:83–7. doi: 10.7555/JBR.30.20150126
48. Amen D, Bursztjan H. Oral conversation. Personal communication. (2005).
49. Küçük NO, Kiliç EO, Ibis E, Aysev A, Gençoglu EA, Aras G, et al. Brain SPECT findings in long-term inhalant abuse. *Nucl Med Commun.* (2000) 21:769–73. doi: 10.1097/00006231-200008000-00011
50. Jean-Bay E. The biobehavioral correlates of post-traumatic brain injury depression. *J Neurosci Nurs.* (2000) 32:169–76. doi: 10.1097/01376517-200006000-00009
51. Baulieu F, Fournier P, Baulieu JL, Dalonneau M, Chiaroni P, Eder V, et al. Technetium-99m ECD single photon emission computed tomography in brain trauma: comparison of early scintigraphic findings with long-term neuropsychological outcome. *J Neuroimaging.* (2001) 11:112–20. doi: 10.1111/j.1552-6569.2001.tb00020.x
52. Kant R, Smith-Seemiller L, Isaac G, Duffy J. Tc-HMPAO SPECT in persistent post-concussion syndrome after mild head injury: comparison with MRI/CT. *Brain Inj.* (1997) 11:115–24. doi: 10.1080/026990597123700
53. Goshen E, Zwas ST, Shahar E, Tadmor R. The role of 99Tcm-HMPAO brain SPET in paediatric traumatic brain injury. *Nucl Med Commun.* (1996) 17:418–22. doi: 10.1097/00006231-199605000-00011
54. Jacobs A, Put E, Ingels M, Bossuyt A. Prospective evaluation of technetium-99m-HMPAO SPECT in mild and moderate traumatic brain injury. *J Nucl Med.* (1994) 35:942–7.
55. Newberg AB, Alavi A, Payer F. Single photon emission computed tomography in Alzheimer's disease and related disorders. *Neuroimaging Clin N Am.* (1995) 5:103–23.
56. Goto H, Ishii K, Uemura T, Miyamoto N, Yoshikawa T, Shimada K, et al. Differential diagnosis of dementia with Lewy bodies and Alzheimer disease using combined MR imaging and brain perfusion single-photon emission tomography. *AJNR Am J Neuroradiol.* (2010) 31:720–5. doi: 10.3174/ajnr.A1926
57. Alexander GE, Prohovnik I, Sackeim HA, Stern Y, Mayeux R. Cortical perfusion and gray matter weight in frontal lobe dementia. *J Neuropsychiatry Clin Neurosci.* (1995) 7:188–96. doi: 10.1176/jnp.7.2.188
58. Bonte FJ, Weiner MF, Bigio EH, White CL. Brain blood flow in the dementias: SPECT with histopathologic correlation in 54 patients. *Radiology.* (1997) 202:793–7. doi: 10.1148/radiology.202.3.9051035
59. Jobst KA, Barnetson LP, Shepstone BJ. Accurate prediction of histologically confirmed Alzheimer's disease and the differential diagnosis of dementia: the use of NINCDS-ADRDA and DSM-III-R criteria, SPECT, X-ray CT, and APO E4 medial temporal lobe dementias. The Oxford Project to Investigate Memory and Aging. *Int Psychogeriatr.* (1997) 9:191–222. doi: 10.1017/S1041610297004912
60. Vaamonde-Gamo J, Flores-Barragán JM, Ibáñez R, Gudín M, Hernández A. DaT-SCAN SPECT en el diagnóstico diferencial entre demencia con cuerpos de Lewy y enfermedad de Alzheimer [DaT-SCAN SPECT in the differential diagnosis of dementia with Lewy bodies and Alzheimer's disease]. *Rev Neurol.* (2005) 15: 276-9. Spanish. Erratum in: *Rev Neurol.* (2005) 41:704. doi: 10.33588/rn.4105.2004561
61. Frings L, Henninger F, Treppner M, Köber G, Boeker M, Meyer PT, et al. DAT SPECT predicts survival in patients assessed for differential diagnosis of dementia. *J Alzheimer's Dis.* (2021) 82:215–20. doi: 10.3233/JAD-210062
62. Davison CM, O'Brien JT: A comparison of FDG-PET and blood flow SPECT in the diagnosis of neurodegenerative dementias: a systematic review *Int J Geriatr Psychiatry.* (2014) 29:551–61. doi: 10.1002/gps.4036
63. Lacerda AL, Dalgalarrondo P, Caetano D, Camargo EE, Etchebehere EC, Soares JC. Elevated thalamic and prefrontal regional cerebral blood flow in obsessive-compulsive disorder: a SPECT study. *Psychiatry Res.* (2003) 30:125–34. doi: 10.1016/S0925-4927(03)00061-1
64. Hollander E. Obsessive-compulsive disorder-related disorders: the role of selective serotonergic reuptake inhibitors. *Int Clin Psychopharmacol.* (1996) 11 Suppl 5:75–87. doi: 10.1097/00004850-199612005-00007
65. Mayberg HS, Brannan SK, Mahurin RK, Jerabek PA, Brickman JS, Tekell JL, et al. Cingulate function in depression: a potential predictor of treatment response. *Neuroreport.* (1997) 8:1057–61. doi: 10.1097/00001756-199703030-00048
66. Diler RS, Kibar M, Avci A. Pharmacotherapy and regional cerebral blood flow in children with obsessive compulsive disorder. *Yonsei Med J.* (2004) 45:90–9. doi: 10.3349/ymj.2004.45.1.90
67. Wu J, Buchsbaum MS, Gillin JC, Tang C, Cadwell S, Wiegand M, et al. Prediction of antidepressant effects of sleep deprivation by metabolic rates in the ventral anterior cingulate and medial prefrontal cortex. *Am J Psychiatry.* (1999) 156:1149–58.
68. Langguth B, Wiegand R, Kharraz A, Landgrebe M, Marienhagen J, Frick U, et al. Pre-treatment anterior cingulate activity as a predictor of antidepressant response to repetitive transcranial magnetic stimulation (rTMS). *Neuro Endocrinol Lett.* (2007) 28:633–8.
69. Dougherty, DD, Cosgrove GR, Weiss, AP, Alpert, NM, Cassem, EH, Niereneberg, A, et al. Cerebral metabolic correlates as potential predictors of response to anterior cingulotomy for major depressive disorder. *J Neurosurg.* (2003) 99:1010–7. doi: 10.3171/jns.2003.99.6.1010
70. Oner P, Oner O, Aysev A, Küçük O, Ibiş E. Comparison of cerebral blood flow in children with obsessive compulsive disorder and attention deficit hyperactivity disorder. *Turk Psikiyatri Derg.* (2008) 19:13–8.
71. Amen DG, Hanks C, Prunella J. Predicting positive and negative treatment responses to stimulants with brain SPECT imaging. *J Psychoactive Drugs.* (2008) 40:131–8. doi: 10.1080/02791072.2008.10400622
72. Mega MS, Dinov ID, Lee L, O'Connor SM, Masterman DM, Wilen B, et al. Orbital and dorsolateral frontal perfusion defect associated with behavioral response to cholinesterase inhibitor therapy in Alzheimer's disease. *J Neuropsychiatry Clin Neurosci.* (2000) 12:209–18. doi: 10.1176/jnp.12.2.209
73. Brockmann H, Zobel A, Joe A, Biermann K, Scheef L, Schuhmacher A, et al. The value of HMPAO SPECT in predicting treatment response to citalopram in patients with major depression. *Psychiatry Res.* (2009) 173:107–12. doi: 10.1016/j.pscychresns.2008.10.006
74. Noel X, Sferrazza R, Van Der Linden M, Paternot J, Verhas M, Hanak C, et al. Contribution of frontal cerebral blood flow measured by (99m)Tc-Bicisate SPECT and executive function deficits to predicting treatment outcome in alcohol-dependent patients. *Alcohol.* (2002) 37:347–54. doi: 10.1093/alcalc/37.4.347
75. Goethals I, Audenaert K, Jacobs F, Van den Eynde F, Bernagie K, Kolindou A, et al. Brain perfusion SPECT in impulsivity-related personality disorders. *Behav Brain Res.* (2005) 157:187–92. doi: 10.1016/j.bbr.2004.06.022
76. Hales, RE, Yudofsky, SC. *Textbook of Neuropsychiatry and Behavioral Neurosciences, Fifth Edition*, American Psychiatric Publishing, Inc. (2007).
77. Devous MD Sr, Leroy, RF, Homan, RW. Single photon emission computed tomography in epilepsy. *Seminars in Nuclear Medicine.* (1990) 10:325–41. doi: 10.1016/S0001-2998(05)80237-5
78. Titlic M, Basic S, Hajnsek S, Lusic I. Comorbidity psychiatric disorders in epilepsy: a review of literature. *Bratisl Lek Listy.* (2009) 110:105–9.
79. Leiderman DB, Balish M, Bromfield EB, Theodore WH. Effect of valproate on human cerebral glucose metabolism. *Epilepsia.* (1991) 32:417–22. doi: 10.1111/j.1528-1157.1991.tb04671.x
80. Blumer D. "Personality disorders in epilepsy," In: *Neuropsychiatry of Personality Disorders Edited by Ratey J* (Cambridge, MA: Blackwell Science). (1995).

81. Devous MD, Thisted RA, Morgan GF, Leroy RF, Rowe CC, SPECT. brain imaging in epilepsy: a meta-analysis. *J Nucl Med.* (1998) 39:285–93.
82. Kuruoglu AC, Arikan Z, Vural G, Karataş M, Araç M, Işik E. Single photon emission computerised tomography in chronic alcoholism. antisocial personality disorder may be associated with decreased frontal perfusion. *Br J Psychiatry.* (1996) 169:348–54. doi: 10.1192/bjp.169.3.348
83. Raine A, Lencz T, Bihrle S, LaCasse L, Colletti P. Reduced prefrontal gray matter volume and reduced autonomic activity in antisocial personality disorder. *Arch Gen Psychiatry.* (2000) 57:119–27. doi: 10.1001/archpsyc.57.2.119
84. Soderstrom H, Tullberg M, Wikkelso C, Ekholm S, Forsman A. Reduced regional cerebral blood flow in non-psychiatric violent offenders. *Psychiatry Res.* (2000) 98:29–41. doi: 10.1016/S0925-4927(99)00049-9
85. Reynolds CF. 3rd, Lewis DA, Detre T, Schatzberg AF, Kupfer DJ. The future of psychiatry as clinical neuroscience. *Acad Med.* (2009) 84:446–50. doi: 10.1097/ACM.0b013e31819a8052
86. Downar J, Krizova A, Ghaffar O, Zaretsky A. Neuroimaging week: a novel, engaging, and effective curriculum for teaching neuroimaging to junior psychiatric residents. *Acad Psychiatry.* (2010) 34:119–24. doi: 10.1176/appi.ap.34.2.119
87. Medina M, Lee D, Garza DM, Goldwaser EL, Truong TT, Apraku A, et al. Neuroimaging education in psychiatry residency training: needs assessment. *Acad Psychiatry.* (2020) 44:311–5. doi: 10.1007/s40596-019-01156-1
88. Amen DG, Trujillo M, Newberg A, Willeumier K, Tarzwell R, Wu JC, et al. Brain SPECT imaging in complex psychiatric cases: an evidence-based, underutilized tool. *Open Neuroimag J.* (2011) 5:40–8. doi: 10.2174/1874440001105010040
89. Amen DG, Jourdain M, Taylor DV, Pigott HE, Willeumier K. Multi-site six-month outcome study of complex psychiatric patients evaluated with addition of brain SPECT imaging. *Adv Mind Body Med.* (2013) 27:6–16.
90. *Famous Philosophers on Politics, Political Science, Globalisation, Oligarchy, Democracy* Available online at: https://www.spaceandmotion.com/Philosophy-Politics-Globalisation.htm (accessed June 1, 2021).

Conflict of Interest: DA is founder and owner of Amen Clinics, Inc.

The remaining author declares that the research was conducted in the absence of any commercial or financial relationships that could be construed as a potential conflict of interest.

frontiers in Psychiatry

MINI REVIEW
published: 15 December 2021
doi: 10.3389/fpsyt.2021.716600

The Emerging Role of SPECT Functional Neuroimaging in Schizophrenia and Depression

Anil Kalyoncu and Ali Saffet Gonul*

Department of Psychiatry, Ege University School of Medicine, Izmir, Turkey

Over the last three decades, the brain's functional and structural imaging has become more prevalent in psychiatric research and clinical application. A substantial amount of psychiatric research is based on neuroimaging studies that aim to illuminate neural mechanisms underlying psychiatric disorders. Single-photon emission computed tomography (SPECT) is one of those developing brain imaging techniques among various neuroimaging technologies. Compared to PET, SPECT imaging is easy, less expensive, and practical for radioligand use. Current technologies increased the spatial accuracy of SPECT findings by combining the functional SPECT images with CT images. The radioligands bind to receptors such as 5-hydroxytryptamine 2A, and dopamine transporters can help us comprehend neural mechanisms of psychiatric disorders based on neurochemicals. This mini-review focuses on the SPECT-based neuroimaging approach to psychiatric disorders such as schizophrenia and major depressive disorder (MDD). Research-based SPECT findings of psychiatric disorders indicate that there are notable changes in biochemical components in certain disorders. Even though many studies support that SPECT can be used in psychiatric clinical practice, we still only use subjective diagnostic criteria such as the Diagnostic Statistical Manual of Mental Disorders (DSM-5). Glimpsing into the brain's biochemical world via SPECT in psychiatric disorders provides more information about the pathophysiology and future implication of neuroimaging techniques.

Keywords: depression, SPECT, dopamine, schizophrenia, molecular imaging

OPEN ACCESS

Edited by:
Theodore A. Henderson, The Synaptic Space, Inc., United States; Neuro-Luminance, Inc., United States

Reviewed by:
Roberta Assante, University of Naples Federico II, Italy
Drozdstoy Stoyanov Stoyanov, Plovdiv Medical University, Bulgaria

****Correspondence:***
Anil Kalyoncu
anilkalyoncu@gmail.com

Specialty section:
This article was submitted to Neuroimaging and Stimulation, a section of the journal Frontiers in Psychiatry

Received: *28 May 2021*
Accepted: *15 November 2021*
Published: *15 December 2021*

Citation:
Kalyoncu A and Gonul AS (2021) The Emerging Role of SPECT Functional Neuroimaging in Schizophrenia and Depression. Front. Psychiatry 12:716600. doi: 10.3389/fpsyt.2021.716600

INTRODUCTION

Diagnosis of psychiatric disorders has always been debated, yet there is still no objective diagnostic tool. Throughout the diagnostic revision process of psychiatric diseases, schizophrenia, and depression are two of the most valid and stable psychiatric disorders regarding diagnostic criteria. However, even though diagnostic criteria have evolved to diagnose these diseases better, we still lack the insight to comprehend the biological aspects of these disorders. Thus, there is a huge gap in diagnosis and providing biological information for these disorders via neuroimaging methods.

Functional and structural imaging methods have contributed to a better understanding beyond the molecular process of psychiatric disorders (1). Magnetic resonance imaging (MRI), functional magnetic resonance imaging (fMRI), SPECT, and positron emission tomography (PET) have evolved to enlighten complex psychiatric disorders. Among these imaging methods, SPECT and PET have similar properties in terms of methods they use. Basically, both methods give information

based on the spatial concentration of injected radiopharmaceuticals. The fundamental difference between PET and SPECT stems from the radiotracers they utilize. While SPECT uses heavy isotopes like ^{99m}Tc and ^{123}I that emit gamma-ray, PET uses lighter isotopes such as ^{11}C, ^{13}N, and ^{18}F that emit positrons. The half-life of the pharmaceutical used in SPECT is longer than PET, which makes it possible to perform more longitudinal scans. The cost of SPECT is lower than PET which makes it much easier to use in clinical practice and more accessible. Despite the many advantages of SPECT imaging, PET offers more spatial resolution than SPECT (2).

Radiotracers used in brain imaging should have some features for obtaining high-quality images. These are high affinity, specificity for the desired target, low non-specific binding, low plasma protein binding, ability to pass through the blood-brain barrier, and high plasma clearance (3). The most used radiotracer in Brain SPECT is Tc-99m-hexamethylpropylene amine oxime (HMPAO) which shows perfusion. Perfusion SPECT can be used to diagnose and assess neuropsychiatric pathologies such as dementia, traumatic brain injury (TBI), toxin exposure, and inflammatory disorders by detecting hypoperfusion in the brain (4, 5). Moreover, perfusion SPECT gives us essential clues in many psychiatric disorders. Perfusion SPECT can help estimate typical stimulant medication response in children with attention deficiency and hyperactivity disorder (ADHD) (6). It can show blood perfusion alteration in treatment resistant MDD (7). Many SPECT studies regarding psychiatric disorders are based on perfusion, but neurochemical SPECT studies provide more specific information about the pathophysiology. That target-specific feature makes SPECT a valuable tool for psychiatric research.

In this mini-review, we summarized and discussed SPECT findings of schizophrenia and depression. To investigate SPECT studies in patients with schizophrenia and depression, we performed a systematic literature search on PubMed database using the keywords "SPECT," "Schizophrenia," and "Depression" and any of following words: "GABA," "Serotonin," "Glutamate," and "Dopamine." Most relevant and recent studies on the subject are included in this mini-review in consideration of the balance between developments and limitations in this area.

SPECT in Schizophrenia

Schizophrenia is a heterogenous and chronic psychiatric disorder that manifests with positive and negative symptoms. These symptoms arise from complex molecular alterations in the brain. The molecular aspect of schizophrenia has been investigated for many years to understand the nature of the disease better. One of the most studied molecular components of schizophrenia is dopamine (8). Dopaminergic pathways consist of presynaptic and post-synaptic compartments. The presynaptic compartment comprises dopamine synthesis, dopamine storage into vesicle by vesicular monoamine transporter 2 (VMAT), dopamine degradation by monoamine oxidase (MAO), dopamine release, and dopamine reuptake by dopamine transporter (DAT). The post-synaptic compartment includes dopamine receptors and post-receptor signaling [(9); **Figure 1**].

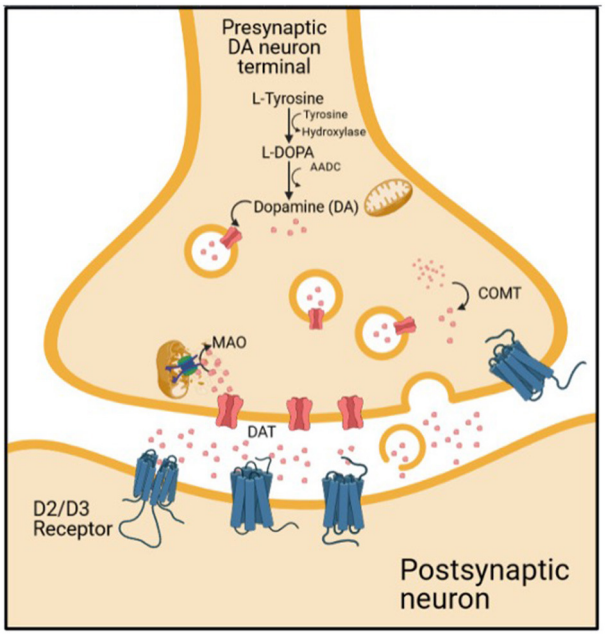

FIGURE 1 | The dopaminergic transmission on synaptic cleft.

Imaging of Dopaminergic System

It has been previously known that dopaminergic pathway alteration takes part in schizophrenia pathophysiology. Many studies with imaging methods indicate that increased subcortical dopamine activity and decreased cortical dopamine are part of the disease process (10). Of those imaging tools that are targeting the molecular mechanism of schizophrenia, SPECT has a significant contribution. The first SPECT study on schizophrenia was published in 1986 (11). ^{77}Br-bromospiperone, which is not popular today due to poor imaging characteristics, was used in that study to show D2 receptor density.

With the advancement of dopamine studies in schizophrenia, new molecules have emerged to assess post-synaptic dopaminergic activity, such as [^{123}I] iodobenzamide (IBZM) and [^{123}I] epidepride [(12); **Table 1**]. These radiotracers act by binding to the post-synaptic receptors and allow us to assess post-synaptic dopamine activity. However, antipsychotics used for the treatment of schizophrenia also bind to the same receptor and display the radiotracer. Thus, patients taking antipsychotic medications may test at lower levels of dopamine receptor availability than is actually the case (28). In studies on the effects of antipsychotics on dopamine receptors, the basal ganglia/frontal cortex ratio, which shows striatal dopaminergic activity, was found to be negatively correlated with extrapyramidal side effects (13, 14). In addition, the BG/FC ratio of IBZM was lower in inadequate treatment response to antipsychotics (14). In general, in meta-analysis studies, we see that the post-synaptic D2/D3 receptor activity of patients with schizophrenia is slightly elevated, but this effect is not significant in patients who do not receive treatment (16, 29).

TABLE 1 | Binding sites and summary of studies of available SPECT radiotracers for dopamine, serotonin, GABA, and glutamate.

Radiotracers	Neurotransmitters	Binding sites	Additional findings
[^{123}I] iodobenzamide	Dopamine	Striatal post-synaptic D_2/D_3 receptor	BG/FC binding ratio was found to be negatively correlated with EPS and lower in patients with schizophrenia on antipsychotic treatment (13, 14).
[^{123}I] epidepride	Dopamine	Extrastriatal frontal D_2/D_3 receptors	Frontal D_2/D_3 binding was found to be positively correlated with positive symptom reduction (15).
[^{123}I]-FP-CIT	Dopamine, serotonin	DAT, SERT	No significant difference was found between schizophrenia and HC in a meta-analysis study (16).
[^{123}I]-β-CIT	Dopamine, serotonin	DAT, SERT, NET	No significant difference was found between schizophrenia and HC in a meta-analysis study (16).
[^{123}I] nor-β-CIT	Dopamine, serotonin	DAT, SERT, NET	No significant difference was found between schizophrenia and HC in a meta-analysis study (16).
[^{99m}Tc]-TRODAT	Dopamine	DAT	No significant difference was found between schizophrenia and HC in a meta-analysis study (16).
[^{123}I] iomazenil	GABA	$GABA_A$ receptors (α1, α2, α3, and α6 subunits)	Inconsistent results have been reported in patients with schizophrenia (17).
[^{123}I] CNS-1261	Glutamate	NMDA receptor	Global binding was found to be reduced in schizophrenia on clozapine treatment. No significant difference was found between HC and treatment naïve schizophrenia (18).
[^{123}I] ADAM	Serotonin	SERT	Results are controversial. Some studies found no significant difference between HC and depression (19–21). Other studies found lower SERT bioavailability in depression (22–24).
[^{123}I] R91150	Serotonin	5HT2A	Compared to equivalent PET tracers, it has a lower signal-to-noise ratio. Harm avoidance was found correlated with high DLPFC 5HT2A binding (25–27).

Another process of the dopaminergic pathway, which is dopamine release into the synaptic cleft, could also be probed *in vivo* by IBZM (30). Dopamine release into the synaptic cleft could be assessed by the combination of dopamine release induction by amphetamine or methylphenidate and SPECT technique. When the dopamine receptors are occupied by dopamine, it results in decreased radiotracer binding. There is a negative linear relationship between dopamine release and radiotracer availability. Imaging studies assessing dopamine release in patients with schizophrenia indicate an increased amphetamine-induced dopamine release (31–33).

[^{123}I] epidepride is another radiotracer to identify extrastriatal frontal D_2/D_3 receptors, which involve cognitive functions like planning, attention, and task switching (34–36). Inhibition of these extrastriatal receptors by antipsychotics results in decreased attentional focus, as shown in a previous study (15). Moreover, positive symptom reduction was positively correlated with the binding potential of frontal D_2/D_3 receptors in the three mounts of zuclopenthixol and risperidone treatment study (15).

The dopamine transporter is another part of the dopaminergic system. SPECT studies comparing schizophrenia with healthy controls (HC) that assess dopamine transporter by [^{123}I]-FP-CIT (N-omega-fluoropropyl-2beta-carboxymethoxy-3beta-{4-iodophenyl} tropane), [^{123}I]-β-CIT (Iodine-123-beta-carbomethoxy-3 beta-(4-iodophenyltropane)), and [^{99m}Tc]-TRODAT show no difference (16). Besides the dopamine transport and post-synaptic dopamine receptor, dopamine synthesis is one of the important processes of the dopamine pathway in schizophrenia. Even though SPECT studies cannot address it, PET meta-analysis shows elevated dopamine synthesis capacity in schizophrenia (16).

It could be inferred from these findings that the synaptic space of the dopaminergic system might be affected by the treatment process rather than by the disease itself (29). Studies related to the presynaptic dopaminergic system, mainly investigated by PET rather than SPECT due to lack of suitable radiotracers, point out that increased dopamine release and dopamine synthesis capacity result in presynaptic dopaminergic neurotransmission activity (37). This presynaptic dopaminergic activity is regulated primarily by other neurotransmitter pathways such as glutamate and GABA (28).

Imaging of GABAergic System

GABA has an essential role in the molecular aspects of schizophrenia pathogenesis by regulating presynaptic dopaminergic activity (28, 38). *In vivo* imaging and post-mortem studies evaluating the role of GABA in schizophrenia show important results. SPECT studies can visualize α1, α2, α3, and α6 subunits of $GABA_A$ receptors by utilizing [^{123}I] iomazenil (39). Inconsistent results were reported in different studies evaluating GABA bioavailability and symptom severity in schizophrenia. While no correlation was found in two of the studies investigating the relationship between symptom severity and GABA receptor availability in patients with schizophrenia (40, 41), a correlation was found in one study evaluating this relationship based on negative and positive symptoms (42).

Negative symptoms were found to be negatively correlated with the GABA binding in medial frontal region, whereas positive symptoms were found to be negatively correlated with GABA binding in the medial temporal lobe (42). Three voxel-wise studies to evaluate regional differences in the brain show that GABA binding is generally low despite regional inconsistencies (40, 43, 44).

Even though there are inconsistent results in GABA studies in schizophrenia, the most replicated findings are reduced glutamic acid decarboxylase 67 (GAD67) mRNA, which plays a role in cytosolic GABA-synthesis, in post-mortem studies (45–47). Subtypes of alpha unit findings in post-mortem studies show that there is a decrease in alpha 1 (47–49) subunit and an increase in alpha 2 subunit (49, 50), and inconsistent results for alpha 5 subunit (50–52).

A systematic review comparing HC and schizophrenia regarding $GABA_A$/BZ receptor binding availability reported no significant group differences (17). Consequently, even consistent results have been replicated in post-mortem studies and *in vivo* neuroimaging studies have not shown promising results for GABA alteration in patients with schizophrenia.

Imaging of Glutamatergic System

Dysfunction in GABA results in disinhibition of the glutamatergic pathway and asynchronous cortical activity (17). Glutamate acts as a regulatory neurotransmitter in the presynaptic dopaminergic pathway as well as GABA. Glutamate has both G-coupled metabotropic and ligand-gated ionotropic receptors. It has been demonstrated that NMDA, which is an ion-gated glutamate receptor, is involved in schizophrenia pathogenesis (53). However, SPECT studies that investigate NMDA levels are insufficient despite the importance of glutamatergic transmission in schizophrenia. In literature, the glutamatergic pathway has been assessed by [^{123}I] CNS-1261. [^{123}I] CNS-1261 acts as an NMDA receptor ligand. One SPECT study indicates that the total volume binding distribution of [^{123}I] CNS-1261 does not show any difference between healthy control and drug-free schizophrenia patients (18). In the same study, global binding of [^{123}I] CNS-1261 was reduced in patients on clozapine treatment compared with drug-free patients (18). This result could be related to downregulation due to clozapine treatment, disease-related pathology, or competition of clozapine and radiotracer at the binding site. Further study revealed a significant negative correlation between [^{123}I] CNS-1261 binding and residual symptom severity in patients under treatment of typical antipsychotics (18). Otherwise, the symptom duration of the medication-free group was positively correlated with [^{123}I] CNS-1261 binding in the middle inferior frontal cortex (54). These two studies may underpin the probable importance of the glutamatergic system in schizophrenia.

SPECT in Depression

Depression is a widespread disabling mental disorder that lifetime prevalence is around 20%, with a high risk of recurrence (55). Various molecular pathologic processes lie behind depression, which have not been fully comprehended. Molecular imaging of depression has been a widely investigated field to establish molecular aspects of depression. One of the most prominent suggestions to elucidate this brain disorder is the monoamine hypothesis which proclaims that depressive patients have lower serotonin, noradrenaline, and dopamine (56). This argument has been studied for the last decades, and the research put forward some evidence on that subject. However, the monoamine hypothesis is still debated, and there is still insufficient evidence of this subject (57). Molecular imaging methods may help with this controversial topic via advanced radiotracers to assess dopamine, noradrenalin, and serotonin levels, and, lately, the degrading enzyme of these monoamines called monoamine oxidase (MAO). Unfortunately, MAO cannot be assessed by SPECT imaging due to lack of radiotracer.

Studies of Blood Perfusion

Although neuroimaging studies focus on brain function and cerebral blood flow, in this review, we will largely discourse the molecular imaging of neurotransmitters and receptors in major depressive disorder. Briefly, the articles have reported hypoactivity in dorsolateral prefrontal cortex, pregenual anterior cingulate cortex, posterior anterior cingulate cortex, left superior temporal gyrus, insula, and cerebellum (58). In contrast, the subcortical structures (caudate, thalamus) and limbic structures (amygdala, anterior hippocampus) show hyperactivity (58).

One of the other significant regional activity findings related to depression is subgenual anterior cingulate cortex (sgACC) hyperactivity, which has been shown in studies that hyperactivity of sgACC is related to treatment-resistant depression (59, 60). The relationship between sgACC activity and treatment response has been studied many times, and this finding could be beneficial for assessing treatment response in clinical practice in the future.

Imaging of Serotoninergic System

In addition to cerebral blood flow imaging studies, neurochemical imaging of depression provides information on molecular alteration. The most known neurotransmitter in depression is serotonin. The serotoninergic system is responsible for regulating sleep, stress responses, pain, motor activity, cognition, emotional behavior, appetite, aggression, and impulsivity which are prominently altered in depression (61). However, it is still not well-known how the serotoninergic system is impaired in depression.

Serotonin is synthesized from tryptophan which is transported by large amino acid transporter over the blood-brain barrier. First, tryptophan is hydroxylated by tryptophan hydroxylase to 5-hydroxy-tryptophan, and then 5-hydroxy-tryptophan is decarboxylated into 5-hydroxy-tryptamine (5-HT), which is known as serotonin (62). Then, the produced serotonin is stored into synaptic vesicles by a vesicular monoamine transporter. Vesicles fuse with the synaptic membrane, and serotonin is secreted into the synaptic cleft. After serotonin is released into the synaptic cleft, it binds to its specific receptor, crucial for post-synaptic transmission. The effect of synaptic transmission is resolved by serotonin reuptake via serotonin transporter (SERT) (62).

Another essential structure related to the serotonergic system in depression is the serotonin receptors, which have various

subtypes, including 5HT1A, 5HT1B, and 5HT2A. 5HT1A receptors are located in the presynaptic compartment of serotoninergic cell bodies of raphe nucleus and post-synaptic side of terminal area. The 5HT1A receptors are Gi-coupled receptors that hinder neuronal transmission (63). [^{123}I] p-MPPI (4-(2′-methoxy-) phenyl-1-[2′-(N-2′′-pyridinyl)-p-iodobenzamido-]ethyl-piperazine) is a SPECT radiotracer that binds 5HT1A receptors *in vivo* which is available for rat and non-human primate but not for human. 5HT1A imaging via SPECT radioligands is restricted due to possible brain excretion by efflux transporter (25). 5HT1B is the other receptor on serotoninergic neuron terminal, an autoreceptor that regulates 5-HT levels by downregulating the serotoninergic system (63). To investigate this molecular process, SPECT provides an opportunity to assess the serotoninergic system. However, evaluation of serotonin synthesis by SPECT is currently limited with SERT and 5HT2A receptors in humans due to the lack of suitable radiotracers.

Imaging of SERT

The SERT bioavailability is assessed by [^{123}I] β-CIT and its analog [^{123}I] nor-β-CIT, which has a 10-fold higher affinity to SERT than [^{123}I] β-CIT (62, 64, 65). These two radiotracers are not specifically binding to SERT but also bind to noradrenaline transporter (NET) and dopamine transporter (DAT) (66). [^{123}I] ADAM is a recently developed radiotracer for SPECT, and it is more specific to SERT than [^{123}I] β-CIT and [^{123}I] nor-β-CIT (67). However, it is still controversial what SERT availability represents. The increased availability of SERT might indicate enhanced serotonin clearance in the synaptic cleft and vice versa (68). On the other hand, the low level of endogenous serotonin might also impact SERT availability by downregulating it (69, 70). In consequence of unclear alteration of SERT bioavailability in depression, SPECT studies assessing SERT bioavailability in depression have inconsistent results.

The serotonin transporter enriched regions are midbrain, thalamus/diencephalon, and medial prefrontal cortex (mPFC) (71). Some SPECT studies comparing SERT availability in the midbrain between healthy controls and depressive patients show no difference (19–21). However, some studies also indicate that SERT binding is decreased in the midbrain (22–24). The SERT density in the midbrain might be negatively correlated with depression severity (24). Perceived adverse life events, which is considered a trigger of depression, impact SERT by reducing it even in healthy subjects (72). Moreover, one study asserts that higher midbrain SERT is related to antidepressant treatment efficiency (73). During treatment with selective serotonin reuptake inhibitors (SSRI), higher occupancy of SERT by SSRI is correlated with a lower Hamilton Depression Rating Scale Score (74). A recent study with drug-naïve first episode major depressive disorder (MDD) patients found no SERT bioavailability difference between HC and MDD, but found a positive correlation between SERT bioavailability and kynurenine/tryptophan ratio, which indicates tryptophan metabolism (75). A meta-analysis of *in vivo* SERT imaging studies found significantly reduced SERT availability in striatum, amygdala, and brainstem but no significant change in thalamus and hippocampus in *in vivo* studies. In addition, a meta-analysis of post-mortem studies did not find any SERT alteration in brainstem, frontal cortex, and hippocampus but found a significant reduction in amygdala and striatum (76). These inconsistent findings could be caused by different imaging methods, possible brain atrophy that influences the SERT quantification, and the strength of the studies (75).

Imaging of 5HT2A

Although there are few SPECT studies associated with 5HT2A receptors in depressed patients, [^{123}I] R91150, which better evaluates 5HT2A receptors than their PET equivalents because of their lower signal-to-noise ratio, provides essential information about depression (25–27). [^{123}I] R91150 studies are concerned with behavioral patterns in depression rather than directly reflecting the depressive scores. For example, one study evaluating the correlation between harm avoidance and 5HT2A receptors reported that high harm avoidance scores related to shyness, fearfulness, and fatigue are positively correlated with left DLPFC 5HT2A receptor binding (26). Another study of six mounts drug-free patients with suicide attempt reports reduced 5HT2A binding in the frontal cortex (27).

Conclusion

Many tools have provided advances in the knowledge of molecular aspects of psychiatric disorders. Significant contributors to this progress are molecular imaging methods, including SPECT and PET. Among those imaging methods, SPECT is remarkable for its feasibility and cheapness, which makes it useful in clinical practice (2). However, even though studies support SPECT usage in psychiatric disorders such as evaluating dementia, inflammation, toxic exposure, and TBI, there is still a lack of proper objective diagnostic tools besides the Diagnostic Statistical Manual of Mental Disorders (DSM-5), which is based on subjective criteria (5, 6, 77).

In addition, these subjective criteria address neither the pathophysiology nor the treatment of psychiatric disorders (77). As a result, the pathogenesis, correlation to neurological function, and treatment options of psychiatric disorders with profound morbidity, such as schizophrenia and depression, remain hotly debated. The fact that 60% of DSM-5 diagnoses lose their validity when tested in clinical studies supports this mismatch between DSM-5 diagnostic constructs and the neurobiology of patients (78). In view of the above, we can conclude that new diagnostic methodological approaches, including molecular imaging, are essential to elucidate the molecular pathophysiology underlying these complex psychiatric disorders.

Most of these SPECT studies have a small number of participants. Hence, significant but slight alterations could not be detected. Multi-centered and meta-analytic studies could reveal undetected pathophysiological changes. Available SPECT radiotracers to investigate the neurotransmission process in human is still insufficient. Novel radiotracers may help us obtain detailed information about neurochemical aspects of neurotransmission in psychiatric disorders. Furthermore, schizophrenia and depression have different subtypes and heterogeneity. Combined studies of structural and functional

MRI with SPECT might clarify this complexity derived by heterogeneity. Additionally, the machine-learning approach in molecular imaging could help the diagnostic process (79). Further studies using novel radiotracers, combined imaging techniques, and machine-learning algorithms are needed to understand psychiatric disorders better and support the clinical utility of SPECT in the future.

AUTHOR CONTRIBUTIONS

AK took the lead in writing the manuscript. AG provided critical feedback, supervision, and helped shape the manuscript. Both authors contributed to the article and approved the submitted version.

REFERENCES

1. Masdeu JC. Neuroimaging in psychiatric disorders. *Neurotherapeutics*. (2011) 8:93–102. doi: 10.1007/s13311-010-0006-0
2. Rahmim A, Zaidi H. PET versus SPECT: strengths, limitations and challenges. *Nucl Med Commun.* (2008) 29:193–207. doi: 10.1097/MNM.0b013e3282f3a515
3. Pimlott SL. Radiotracer development in psychiatry. *Nucl Med Commun.* (2005) 26:183–8. doi: 10.1097/00006231-200503000-00002
4. Pavel D, Jobe T, Devore-Best S, Davis G, Epstein P, Sinha S, et al. Viewing the functional consequences of traumatic brain injury by using brain SPECT. *Brain Cogn.* (2006) 60:211–3.
5. *CANM Guidelines for Brain Perfusion Single Photon Emission Computed Tomography (SPECT).* (2020). Available online at: https://www.canm-acmn.ca/guidelines (accessed October 4 2021).
6. Henderson TA, van Lierop MJ, McLean M, Uszler JM, Thornton JF, Siow YH, et al. Functional neuroimaging in psychiatry-aiding in diagnosis and guiding treatment. What the American psychiatric association does not know. *Front Psychiatry.* (2020) 11:276. doi: 10.3389/fpsyt.2020.00276
7. Tastevin M, Boyer L, Korchia T, Fond G, Lançon C, Richieri R, et al. Brain SPECT perfusion and PET metabolism as discordant biomarkers in major depressive disorder. *EJNMMI Res.* (2020) 10:121. doi: 10.1186/s13550-020-00713-2
8. Cumming P, Abi-Dargham A, Gründer G. Molecular imaging of schizophrenia: neurochemical findings in a heterogeneous and evolving disorder. *Behav Brain Res.* (2021) 398:113004. doi: 10.1016/j.bbr.2020.113004
9. Weinstein JJ, Chohan MO, Slifstein M, Kegeles LS, Moore H, Abi-Dargham A. Pathway-specific dopamine abnormalities in schizophrenia. *Biol Psychiatry.* (2017) 81:31–42. doi: 10.1016/j.biopsych.2016.03.2104
10. Conn KA, Burne THJ, Kesby JP. Subcortical dopamine and cognition in schizophrenia: looking beyond psychosis in preclinical models. *Front Neurosci.* (2020) 14:542. doi: 10.3389/fnins.2020.00542
11. Crawley JC, Crow TJ, Johnstone EC, Oldland SR, Owen F, Owens DG, et al. Uptake of 77Br-spiperone in the striata of schizophrenic patients and controls. *Nucl Med Commun.* (1986) 7:599–607. doi: 10.1097/00006231-198608000-00006
12. Barnas C, Quiner S, Tauscher J, Hilger E, Willeit M, Küfferle B, et al. *In vivo* (123)I IBZM SPECT imaging of striatal dopamine 2 receptor occupancy in schizophrenic patients. *Psychopharmacology.* (2001) 157:236–42. doi: 10.1007/s002130100813
13. Broich K, Grünwald F, Kasper S, Klemm E, Biersack HJ, Möller HJ. D2-dopamine receptor occupancy measured by IBZM-SPECT in relation to extrapyramidal side effects. *Pharmacopsychiatry.* (1998) 31:159–62. doi: 10.1055/s-2007-979321
14. Schröder J, Silvestri S, Bubeck B, Karr M, Demisch S, Scherrer S, et al. D2 dopamine receptor up-regulation, treatment response, neurological soft signs, and extrapyramidal side effects in schizophrenia: a follow-up study with 123I-iodobenzamide single photon emission computed tomography in the drug-naive state and after neuroleptic treatment. *Biol Psychiatry.* (1998) 43:660–5. doi: 10.1016/s0006-3223(97)00442-3
15. Nørbak-Emig H, Ebdrup BH, Fagerlund B, Svarer C, Rasmussen H, Friberg L, et al. Frontal D2/3 receptor availability in schizophrenia patients before and after their first antipsychotic treatment: relation to cognitive functions and psychopathology. *Int J Neuropsychopharmacol.* (2016) 19:pyw006. doi: 10.1093/ijnp/pyw006
16. Howes OD, Kambeitz J, Kim E, Stahl D, Slifstein M, Abi-Dargham A, et al. The nature of dopamine dysfunction in schizophrenia and what this means for treatment: meta-analysis of imaging studies. *Arch Gen Psychiatry*. (2012) 69:776–86. doi: 10.1001/archgenpsychiatry.2012.169
17. Lee JS, Lee JD, Park H, Oh M, Chun JW, Kim S, et al. Is the GABA system related to the social competence improvement effect of aripiprazole? An18F-fluoroflumazenil PET study. *Psychiatry Investig.* (2013) 10:75. doi: 10.4306/pi.2013.10.1.75
18. Bressan RA, Erlandsson K, Stone JM, Mulligan RS, Krystal JH, Ell PJ, et al. Impact of schizophrenia and chronic antipsychotic treatment on [123I]CNS-1261 binding to N-methyl-D-aspartate receptors *in vivo*. *Biol Psychiatry.* (2005) 58:41–6. doi: 10.1016/j.biopsych.2005.03.016
19. Ahonen A, Heikman P, Kauppinen T, Koskela A, Bergstrom K. Serotonin transporter availability in drug free depression patients using a novel SERT ligand. *Eur J Nuclear Med Mol Imaging*. (2004) 31:S227–8.
20. Catafau AM, Perez V, Plaza P, Pascual JC, Bullich S, Suarez M, et al. Serotonin transporter occupancy induced by paroxetine in patients with major depression disorder: a 123I-ADAM SPECT study. *Psychopharmacology.* (2006) 189:145–53. doi: 10.1007/s00213-006-0540-y
21. Dahlström M, Ahonen A, Ebeling H, Torniainen P, Heikkilä J, Moilanen I. Elevated hypothalamic/midbrain serotonin (monoamine) transporter availability in depressive drug-naive children and adolescents. *Mol Psychiatry.* (2000) 5:514–22. doi: 10.1038/sj.mp.4000766
22. Lehto S, Tolmunen T, Joensuu M, Saarinen PI, Vanninen R, Ahola P, et al. Midbrain binding of [123I]nor-β-CIT in atypical depression. *Progr Neuro Psychopharmacol Biol Psychiatry.* (2006) 30:1251–5. doi: 10.1016/j.pnpbp.2006.03.019
23. Tsai HC, Lin SH, Chen PS, Chang HH, Lee IH, Yeh TL, et al. Quantifying midbrain serotonin transporter in depression: a preliminary study of diagnosis and naturalistic treatment outcome. *Pharmacopsychiatry.* (2015) 48:58–64. doi: 10.1055/s-0034-1396800
24. Newberg AB, Amsterdam JD, Wintering N, Ploessl K, Swanson RL, Shults J, et al. 123I-ADAM binding to serotonin transporters in patients with major depression and healthy controls: a preliminary study. *J Nucl Med.* (2005) 46:973–7.
25. Paterson LM, Kornum BR, Nutt DJ, Pike VW, Knudsen GM. 5-HT radioligands for human brain imaging with PET SPECT. *Med Res Rev.* (2013) 33:54–111. doi: 10.1002/med.20245
26. Baeken C, Bossuyt A, De Raedt R. Dorsal prefrontal cortical serotonin 2A receptor binding indices are differentially related to individual scores on harm avoidance. *Psychiatry Res.* (2014) 221:162–8. doi: 10.1016/j.pscychresns.2013.12.005
27. Audenaert K, Van Laere K, Dumont F, Slegers G, Mertens J, van Heeringen C, et al. Decreased frontal serotonin 5-HT 2a receptor binding index in deliberate self-harm patients. *Eur J Nucl Med.* (2001) 28:175–82. doi: 10.1007/s002590000392
28. Dierckx RAJO, Otte A, de Vries EFJ, van Waarde A, den Boer JA. *PET and SPECT in Psychiatry*. Heidelberg: Springer. (2014) 35:57–67.doi: 10.1007/978-3-642-40384-2
29. Chen KC, Yang YK, Howes OD, Lee IH, Yeh TL, Chiu NT, et al. Striatal dopamine $D_{2/3}$ receptors in medication-naïve schizophrenia: an [^{123}I] IBZM SPECT study. *Psychol Med.* (2021) 8:1–9. doi: 10.1017/S0033291720005413
30. Laruelle M. Imaging dopamine transmission in schizophrenia. A review and meta-analysis. *Q J Nucl Med.* (1998) 42:211–21.
31. Abi-Dargham A, Gil R, Krystal J, Baldwin RM, Seibyl JP, Bowers M, et al. Increased striatal dopamine transmission in schizophrenia: confirmation in a second cohort. *Am J Psychiatry.* (1998) 155:761–7. doi: 10.1176/ajp.155.6.761
32. Breier A, Su TP, Saunders R, Carson RE, Kolachana BS, de Bartolomeis A, et al. Schizophrenia is associated with elevated amphetamine-induced

synaptic dopamine concentrations: evidence from a novel positron emission tomography method. *Proc Natl Acad Sci USA*. (1997) 94:2569–74. doi: 10.1073/pnas.94.6.2569
33. Laruelle M, Abi-Dargham A, van Dyck CH, Gil R, D'Souza CD, Erdos J, et al. Single photon emission computerized tomography imaging of amphetamine-induced dopamine release in drug-free schizophrenic subjects. *Proc Natl Acad Sci USA*. (1996) 93:9235–40. doi: 10.1073/pnas.93.17.9235
34. Kessler RM, Mason NS, Votaw JR, De Paulis T, Clanton JA, Ansari MS, et al. Visualization of extrastriatal dopamine D2 receptors in the human brain. *Eur J Pharmacol*. (1992) 223:105–7. doi: 10.1016/0014-2999(92)90825-o
35. Tsartsalis S, Tournier BB, Millet P. *In vivo* absolute quantification of striatal and extrastriatal $D_{2/3}$receptors with [^{123}I] epidepride SPECT. *EJNMMI Res*. (2020) 10:66. doi: 10.1186/s13550-020-00650-0
36. Fagerlund B, Pinborg LH, Mortensen EL, Friberg L, Baaré WF, Gade A, et al. Relationship of frontal D(2/3) binding potentials to cognition: a study of antipsychotic-naive schizophrenia patients. *Int J Neuropsychopharmacol*. (2013) 16:23–36. doi: 10.1017/S146114571200003X
37. Abi-Dargham A, van de Giessen E, Slifstein M, Kegeles LS, Laruelle M. Baseline and amphetamine-stimulated dopamine activity are related in drug-naïve schizophrenic subjects. *Biol Psychiatry*. (2009) 65:1091–3. doi: 10.1016/j.biopsych.2008.12.007
38. Taylor SF, Tso IF. GABA abnormalities in schizophrenia: a methodological review of *in vivo* studies. *Schizophr Res*. (2015) 167:84–90. doi: 10.1016/j.schres.2014.10.011
39. Lewis DA, Curley AA, Glausier JR, Volk DW. Cortical parvalbumin interneurons and cognitive dysfunction in schizophrenia. *Trends Neurosci*. (2012) 35:57–67. doi: 10.1016/j.tins.2011.10.004
40. Verhoeff NP, Soares JC, D'Souza CD, Gil R, Degen K, Abi-Dargham A, et al. [123I]Iomazenil SPECT benzodiazepine receptor imaging in schizophrenia. *Psychiatry Res Neuroimaging*. (1999) 91:163–73.
41. Abi-Dargham A. No evidence of altered *in vivo* benzodiazepine receptor binding in schizophrenia. *Neuropsychopharmacology*. (1999) 20:650–61.
42. Busatto GF, Pilowsky LS, Costa DC, Ell PJ, David AS, Lucey JV, et al. Correlation between reduced *in vivo* benzodiazepine receptor binding and severity of psychotic symptoms in schizophrenia. *Am J Psychiatry*. (1997) 154:56–63. doi: 10.1176/ajp.154.1.56
43. Hashimoto T, Volk DW, Eggan SM, Mirnics K, Pierri JN, Sun Z, et al. Gene expression deficits in a subclass of GABA neurons in the prefrontal cortex of subjects with schizophrenia. *J Neurosci*. (2003) 23:6315–26. doi: 10.1523/JNEUROSCI.23-15-06315.2003
44. Volk DW, Austin MC, Pierri JN, Sampson AR, Lewis DA. Decreased glutamic acid decarboxylase67 messenger RNA expression in a subset of prefrontal cortical gamma-aminobutyric acid neurons in subjects with schizophrenia. *Arch Gen Psychiatry*. (2000) 57:237–45. doi: 10.1001/archpsyc.57.3.237
45. Akbarian S, Kim JJ, Potkin SG, Hagman JO, Tafazzoli A, Bunney WE Jr., et al. Gene expression for glutamic acid decarboxylase is reduced without loss of neurons in prefrontal cortex of schizophrenics. *Arch Gen Psychiatry*. (1995) 52:258–66. doi: 10.1001/archpsyc.1995.03950160008002
46. Glausier JR, Lewis DA. Selective pyramidal cell reduction of GABA(A) receptor α1 subunit messenger RNA expression in schizophrenia. *Neuropsychopharmacology*. (2011) 36:2103–10. doi: 10.1038/npp.2011.102
47. Beneyto M, Abbott A, Hashimoto T, Lewis DA. Lamina-specific alterations in cortical GABA(A) receptor subunit expression in schizophrenia. *Cereb Cortex*. (2011) 21:999–1011. doi: 10.1093/cercor/bhq169
48. Volk DW, Pierri JN, Fritschy JM, Auh S, Sampson AR, Lewis DA. Reciprocal alterations in pre- and postsynaptic inhibitory markers at chandelier cell inputs to pyramidal neurons in schizophrenia. *Cereb Cortex*. (2002) 12:1063–70. doi: 10.1093/cercor/12.10.1063
49. Impagnatiello F, Guidotti AR, Pesold C, Dwivedi Y, Caruncho H, Pisu MG, et al. A decrease of reelin expression as a putative vulnerability factor in schizophrenia. *Proc Natl Acad Sci USA*. (1998) 95:15718–23.
50. Akbarian S, Huntsman MM, Kim JJ, Tafazzoli A, Potkin SG, Bunney WE, et al. GABAA receptor subunit gene expression in human prefrontal cortex: comparison of schizophrenics and controls. *Cereb Cortex*. (1995) 5:550–60. doi: 10.1093/cercor/5.6.550
51. Egerton A, Modinos G, Ferrera D, McGuire P. Neuroimaging studies of GABA in schizophrenia: a systematic review with meta-analysis. *Transl Psychiatry*. (2017) 7:e1147. doi: 10.1038/tp.2017.124
52. Kang JI, Park H, Kim SJ, Kim KR, Lee SY, Lee E, et al. Reduced binding potential of GABA-A/benzodiazepine receptors in individuals at ultra-high risk for psychosis: an [18F]-fluoroflumazenil positron emission tomography study. *Schizophr Bull*. (2014) 40:548–57. doi: 10.1093/schbul/sbt052
53. Balu DT. The NMDA receptor and schizophrenia: from pathophysiology to treatment. *Adv Pharmacol*. (2016) 76:351–82. doi: 10.1016/bs.apha.2016.01.006
54. Pilowsky LS, Bressan RA, Stone JM, Erlandsson K, Mulligan RS, Krystal JH, et al. First *in vivo* evidence of an NMDA receptor deficit in medication-free schizophrenic patients. *Mol Psychiatry*. (2006) 11:118–9. doi: 10.1038/sj.mp.4001751
55. Rush AJ, Trivedi MH, Wisniewski SR, Nierenberg AA, Stewart JW, Warden D, et al. Acute and longer-term outcomes in depressed outpatients requiring one or several treatment steps: a STAR*D report. *AJP*. (2006) 163:1905–17.doi: 10.1176/ajp.2006.163.11.1905
56. Ruhé HG, Mason NS, Schene AH. Mood is indirectly related to serotonin, norepinephrine and dopamine levels in humans: a meta-analysis of monoamine depletion studies. *Mol Psychiatry*. (2007) 12:331–59. doi: 10.1038/sj.mp.4001949
57. Lacasse JR, Leo J. Serotonin and depression: a disconnect between the advertisements and the scientific literature. *PLoS Med*. (2005) 2:e392. doi: 10.1371/journal.pmed.0020392
58. Fitzgerald PB, Laird AR, Maller J, Daskalakis ZJ. A meta-analytic study of changes in brain activation in depression. *Hum Brain Mapp*. (2008) 29:683–95. doi: 10.1002/hbm.20426
59. Drevets WC, Savitz J, Trimble M. The subgenual anterior cingulate cortex in mood disorders. *CNS Spectr*. (2008) 13:663–81. doi: 10.1017/s1092852900013754
60. Greicius MD, Flores BH, Menon V, Glover GH, Solvason HB, Kenna H, et al. Resting-state functional connectivity in major depression: abnormally increased contributions from subgenual cingulate cortex and thalamus. *Biol Psychiatry*. (2007) 62:429–37. doi: 10.1016/j.biopsych.2006.09.020
61. Olivier B. Serotonin: a never-ending story. *Eur J Pharmacol*. (2015) 753:2–18. doi: 10.1016/j.ejphar.2014.10.031
62. Best J, Nijhout HF, Reed M. Serotonin synthesis, release and reuptake in terminals: a mathematical model. *Theor Biol Med Model*. (2010) 7:34. doi: 10.1186/1742-4682-7-34
63. Barnes NM, Sharp T. A review of central 5-HT receptors and their function. *Neuropharmacology*. (1999) 38:1083–152. doi: 10.1016/s0028-3908(99)00010-6
64. Innis R, Baldwin R, Sybirska E, Zea Y, Laruelle M, Al-Tikriti M, et al. Single photon emission computed tomography imaging of monoamine reuptake sites in primate brain with [123I]CIT. *Eur J Pharmacol*. (1991) 200:369–70. doi: 10.1016/0014-2999(91)90599-l
65. Bergström KA, Halldin C, Hall H, Lundkvist C, Ginovart N, Swahn CG, et al. *In vitro* and *in vivo* characterisation of nor-beta-CIT: a potential radioligand for visualisation of the serotonin transporter in the brain. *Eur J Nucl Med*. (1997) 24:596–601. doi: 10.1007/BF00841395
66. Laruelle M, Baldwin RM, Malison RT, Zea-Ponce Y, Zoghbi SS, Al-Tikeriti MS, et al. SPECT imaging of dopamine and serotonin transporters with [123I]beta-CIT: pharmacological characterization of brain uptake in nonhuman primates. *Synapse*. (1993) 13:295–309. doi: 10.1002/syn.890130402
67. Frokjaer VG, Pinborg LH, Madsen J, de Nijs R, Svarer C, Wagner A, et al. Evaluation of the serotonin transporter ligand 123I-ADAM for SPECT studies on humans. *J Nucl Med*. (2008) 49:247–54. doi: 10.2967/jnumed.107.046102
68. Meyer JH. Neuroimaging markers of cellular function in major depressive disorder: implications for therapeutics, personalized medicine, and prevention. *Clin Pharmacol Ther*. (2012) 91:201–14. doi: 10.1038/clpt.2011.285
69. Meyer JH. Imaging the serotonin transporter during major depressive disorder and antidepressant treatment. *J Psychiatry Neurosci*. (2007) 32:86–102.
70. Rattray M, Baldessari S, Gobbi M, Mennini T, Samanin R, Bendotti C. p-Chlorphenylalanine changes serotonin transporter mRNA levels and expression of the gene product. *J Neurochem*. (1996) 67:463–72. doi: 10.1046/j.1471-4159.1996.67020463.x
71. Joensuu M, Lehto SM, Tolmunen T, Saarinen PI, Valkonen-Korhonen M, Vanninen R, et al. Serotonin-transporter-linked promoter

region polymorphism and serotonin transporter binding in drug-naïve patients with major depression. *Psychiatry Clin Neurosci.* (2010) 64:387–93.doi: 10.1111/j.1440-1819.2010.02111.x
72. Yeh TL, Lee IH, Chen KC, Chen PS, Yao WJ, Yang YK, et al. The relationships between daily life events and the availabilities of serotonin transporters and dopamine transporters in healthy volunteers–a dual-isotope SPECT study. *Neuroimage.* (2009) 45:275–9. doi: 10.1016/j.neuroimage.2008.12.004
73. Kugaya A, Sanacora G, Staley JK, Malison RT, Bozkurt A, Khan S, et al. Brain serotonin transporter availability predicts treatment response to selective serotonin reuptake inhibitors. *Biol Psychiatry.* (2004) 56:497–502. doi: 10.1016/j.biopsych.2004.07.001
74. Ruhé HG, Ooteman W, Booij J, Michel MC, Moeton M, Baas F, et al. Serotonin transporter gene promoter polymorphisms modify the association between paroxetine serotonin transporter occupancy and clinical response in major depressive disorder. *Pharmacogenet Genomics.* (2009) 19:67–76. doi: 10.1097/FPC.0b013e32831a6a3a
75. Chiu YC, Yang BH, Yang KC, Liu MN, Hu LY, Liou YJ, et al. A study of tryptophan, kynurenine and serotonin transporter in first-episode drug-naïve major depressive disorder. *Psychiatry Res Neuroimaging.* (2021) 312:111296. doi: 10.1016/j.pscychresns.2021.111296
76. Kambeitz JP, Howes OD. The serotonin transporter in depression: meta-analysis of *in vivo* and post mortem findings and implications for understanding and treating depression. *J Affect Disord.* (2015) 186:358–66. doi: 10.1016/j.jad.2015.07.034
77. Ghaemi SN. After the failure of DSM: clinical research on psychiatric diagnosis. *World Psychiatry.* (2018) 17:301–2. doi: 10.1002/wps.20563
78. Regier DA, Narrow WE, Clarke DE, Kraemer HC, Kuramoto SJ, Kuhl EA, et al. DSM-5 field trials in the United States and Canada, part II: test-retest reliability of selected categorical diagnoses. *Am J Psychiatry.* (2013) 170:59–70. doi: 10.1176/appi.ajp.2012.12070999
79. Veronese M, Santangelo B, Jauhar S, D'Ambrosio E, Demjaha A, Salimbeni H, et al. A potential biomarker for treatment stratification in psychosis: evaluation of an [^{18}F] FDOPA PET imaging approach. *Neuropsychopharmacology.* (2021) 46:1122–32. doi: 10.1038/s41386-020-00866-7

Conflict of Interest: The authors declare that the research was conducted in the absence of any commercial or financial relationships that could be construed as a potential conflict of interest.

Publisher's Note: All claims expressed in this article are solely those of the authors and do not necessarily represent those of their affiliated organizations, or those of the publisher, the editors and the reviewers. Any product that may be evaluated in this article, or claim that may be made by its manufacturer, is not guaranteed or endorsed by the publisher.

frontiers in Psychiatry

ORIGINAL RESEARCH
published: 13 January 2022
doi: 10.3389/fpsyt.2021.713141

Brain SPECT as an Imaging Biomarker for Evaluating Effects of Novel Treatments in Psychiatry–A Case Series

Steven R. D. Best[1]*, *Natalie Haustrup*[2†] and *Dan G. Pavel*[3‡]

[1] The Neuroscience Center, Deerfield, IL, United States, [2] Haustrup Scientific Consulting, Cork, Ireland, [3] PathFinder Brain SPECT, Deerfield, IL, United States

The difficulties of evaluating patients with complex neuropsychiatric conditions and prescribing appropriate treatments are well known. Imaging complements clinical assessments and allows a clinician to narrow the differential diagnosis by facilitating accurate and efficient evaluation. This is particularly relevant to neuropsychiatric conditions that are often diagnosed using a trial-and error process of exclusion. Single Photon Emission Computed Tomography (SPECT) is a functional brain imaging procedure that allows practitioners to measure the functional changes of gray matter structures based on regional cerebral blood flow (rCBF). The accurate diagnosis and treatment selection in psychiatry is challenging due to complex cases and frequent comorbidities. However, such complex neuropsychiatric conditions are increasingly benefitting from new treatment approaches, in addition to established medications. Among these are combination transcranial magnetic stimulation with ketamine infusions (CTK), hyperbaric oxygen therapy (HBOT) and perispinal administration of etanercept (PSE). This article provides readers with six case study examples that demonstrate how brain SPECT imaging can be used, both as a diagnostic tool, and as a potential biomarker for monitoring and evaluating novel treatments for patients with complex neuropsychiatric conditions. Six patients were assessed in our clinic and baseline brain SPECT imagesTourettes and a long history of alcohol were visually compared with SPECT images collected after periods of treatment with CTK or HBOT followed by PSE. This retrospective review demonstrates the clinical utility of these novel treatments and describes how SPECT imaging can complement standard diagnostic assessments. A novel display technique for SPECT images is described and we argue that SPECT imaging can be used for monitoring biomarker for clinical change.

Keywords: SPECT, biomarker, CTK, HBOT, depression, psychiatry, brain, treatment

OPEN ACCESS

Edited by:
Theodore A. Henderson, The Synaptic Space, Inc. and Neuro-Luminance, Inc., United States

Reviewed by:
Daniel Keeser, Ludwig Maximilian University of Munich, Germany
Richard Bruce Bolster, University of Winnipeg, Canada

***Correspondence:**
Steven R. D. Best
srdbest@neuroscience.md

†Present address:
Natalie Haustrup, Eli Lilly and Company, Cork, Ireland

‡*Posthumously (1934–2021)*

Specialty section:
This article was submitted to Neuroimaging and Stimulation, a section of the journal Frontiers in Psychiatry

Received: *21 May 2021*
Accepted: *13 December 2021*
Published: *13 January 2022*

Citation:
Best SRD, Haustrup N and Pavel DG (2022) Brain SPECT as an Imaging Biomarker for Evaluating Effects of Novel Treatments in Psychiatry–A Case Series. Front. Psychiatry 12:713141. doi: 10.3389/fpsyt.2021.713141

INTRODUCTION

While experienced psychiatrists may be able to diagnose patients with neuropsychiatric conditions based on behavioral criteria, functional brain imaging tools can inform the clinician of their underlying neurobiology. Functional brain imaging can therefore provide clinicians with insightful information that enables them to narrow the differential diagnosis and to monitor and to evaluate any therapeutic benefit of the treatment (1). Single Photon Emission

Computed Tomography (SPECT) is a functional brain imaging procedure that displays the functional status in the whole gray matter volume. A radiotracer is administered to the patient and is transported *via* the bloodstream and is quickly removed through normal kidney excretion. During circulation, some radiotracer is taken up by the brain tissue with the uptake of radiotracer dependent on the regional cerebral blood flow (rCBF). The detection of the radiotracer uptake across the brain allows the clinician to identify areas of both underperfusion (hypofunctioning) and of hyperperfusion (hyperfunctioning). Brain SPECT also has the functionality to detect the presence of comorbidity that can occur due to a variety of causes, including neurodevelopmental problems, traumatic brain injury, neuro-inflammation, non-convulsive epilepsy, neurotoxic exposure and nutritional deficiencies all of which contribute to altering the blood flow levels in various gray matter structures.

SPECT generates a three-dimensional (3-D) mapped representation of the brain that can be presented with color-coded intensities proportional to rCBF and correlating with the function in that region. Accurate and reliable visual interpretation of brain SPECT relies on optimizing the presentation of images using effective display tools and techniques, which are demonstrated herein. Diagnosis can also benefit from the complementary information exhibited by SPECT images displayed in a variety of formats including slices, surfaces and volumes. The optimal approach to accomplish accurate and efficient interpretation of brain imaging modalities is debated by researchers and clinicians in the literature (2–7), with discussions primarily centered on either conventional visual analysis by an experienced investigator and/or quantification techniques including voxel-wise analysis or region of interest (ROI) approaches (8–12). SPECT image quantification within clinical research typically identifies statistically significant differences based on mean group values, which do not always equate to individual differences, which is typically the focus in clinical practice (8). Therefore, the visual interpretation of individual SPECT images remains a foundational skill within clinical practice and quantification is considered favorable for larger studies for identifying trends (8, 13).

However, SPECT imaging is underutilized in clinical practice despite a growing, evidence-based foundation for its application in numerous indications relevant to psychiatric practice (14–23). This underutilization is particularly unfortunate as SPECT is an easy-to-perform, non-invasive procedure and remains among the least expensive neuroimaging tools available (24, 25). The historic underutilization of neuroimaging techniques in psychiatry has also led to the consequential inadequate biological understanding of neuropsychiatric conditions (26). Without such biological understanding it is also difficult to identify meaningful biomarkers for diagnosis, prognosis or risk, which is particularly relevant as psychiatric treatments can lead to biological changes (24, 26, 27). In addition, neuropsychiatric conditions are often diagnosed using a process of exclusion and additional information from brain SPECT imaging can complement the information gathered from clinical assessments. Given the current underutilization of SPECT, additional work is required to integrate the brain SPECT information in a more precise clinical context, given the extent of comorbidities present in many neuropsychiatric conditions.

Previous studies have demonstrated how SPECT can be utilized to diagnose psychiatric disorders (3, 28, 29) and to evaluate established treatments (4, 30–32). The accurate diagnosis and treatment selection is complicated in psychiatry by complex cases and frequent comorbidities (2). However, these conditions are increasingly benefitting from new treatment approaches, including Transcranial Magnetic Stimulation (TMS), combinations of TMS with ketamine infusion (CTK) and Hyperbaric Oxygen Therapy (HBOT) with perispinal administration of etanercept (PSE) (33–36)]. TMS is a non-invasive technique for stimulation of the brain that can induce antidepressant and anti-manic effects, however treatment response can be slow (37–39). Ketamine is effective in reducing depressive symptoms (40) *via* multiple mechanisms of action, including modulating signaling that stimulates neurogenesis and neuroplasticity, as well as acting as a tumor necrosis factor (TNF)-alpha inhibitor resulting in an anti-inflammatory effect (41–43). CTK is a patented procedure and studies have indicated that CTK is an effective, long-term therapy for patients with various neuropsychiatric conditions, whereby the coincident administration of ketamine allowed for higher TMS intensities than otherwise would be tolerated by patients (33, 44–46). Treatment with HBOT followed by PSE has also been identified as a possible treatment for cognitive impairment (35, 36, 47, 48). HBOT is believed to have anti-inflammatory effects by reducing excess pro-inflammatory cytokine activation, such as TNF-alpha, and facilitates improvement by provocation of stem cell activity, which can lessen the neurological impact of brain injuries (49–51). PSE injections modulate TNF-alpha directly to the central nervous system and act to normalize the inflammatory response in stroke, traumatic brain injury, and encephalopathic conditions (52). Despite supportive evidence of the clinical utility of novel treatments, such as CTK and HBOT with PSE, further investigation of these combination treatments is required.

This article builds on the current literature and presents a retrospective review of a case series including six patients with complex neuropsychiatric presentations. Baseline brain SPECT images were visually compared with SPECT images collected after periods of treatment with three novel treatments of CTK or HBOT followed by PSE during routine clinical practice. In this article we also describe a novel SPECT imaging display technique, present evidence of the clinical utility of CTK and HBOT with PSE and we propose that SPECT can be used as an imaging biomarker for monitoring and evaluating clinical change.

MATERIALS AND METHODS

Study Cases

Six patients presented to our clinic with disabling neuropsychiatric conditions of various causes following extensive unsuccessful periods of treatments. The conditions and comorbidities differed for each patient (I-VI). Treatments were selected for each patient following the clinical assessment of the patient. The six cases presented herein were purposefully

selected as they demonstrate the usefulness of brain SPECT imaging in evaluating patients with neuropsychiatric conditions and to monitor their response to treatment. An overview of the patients, their diagnosis and treatment are presented in **Table 1** with more thorough details of patient histories, selected treatments and outcomes presented in the Results section. All subjects consented to the use of their data and information for the research purposes described herein.

Novel Treatment Options

SPECT imaging was used to identify the extent and severity of hypoperfused areas, which complemented the standard clinical assessment data collected. Treatment decisions were based on the full baseline assessment and patients were either treated with CTK or HBOT followed by PSE. The CTK procedure has been described in detail previously (9). Patients who present at our clinic with TRD are treated with CTK before, or instead of, electroconvulsive therapy (ECT) or TMS or ketamine administered independently, based on evidence that CTK offers benefits over these established treatments for patients with TRD (33, 46). In brief, four patients treated with CTK received TMS (30 min) and 5 min after the commencement of TMS, intravenous infusions of the NMDA-receptor inhibitor, ketamine, began (20 min). The TMS (1 Hz) was applied continuously for 30 min at a power output setting equivalent to 130% of motor threshold (MT). A biomarker-dependent dosing strategy was applied, whereby ketamine was gradually titrated in small increments until the patient entered a mildly cataleptic state. Catalepsy refers to the neuromuscular condition characterized by muscular rigidity and fixity of posture regardless of external stimuli, as well as markedly decreased sensitivity to pain. Titrations began at 20 mg, with an average dosage range of 0.4–2.3 mg/kg (full range from 0.2 to 4.7 mg/kg). Once the patient began to stiffen or posture, the ketamine infusions could be discontinued. Following the completion of the ketamine infusion, the TMS would continue for a further 5 min, after which the CTK procedure was complete. Frequency of treatment is dependent on patient responsiveness (typically 10–30 sessions).

Two patients who presented to this clinic with treatment refractory illness in the context of traumatic brain injury (TBI) or mild TBI (mTBI) were treated with HBOT followed by PSE. Previous experiences of treating patients have indicated that the benefits of HBOT and PSE injection may be cumulative (53). HBOT treatments were administered daily in a multi-place chamber for 60 min at a depth of 1.75 atmosphere absolute (ATA). After the first ten HBOT treatments, one 25 mg PSE injection was administered approximately once weekly and the number of further HBOT sessions and PSE injections was tailored to the patient. The method of perispinal administration of etanercept was used under license from the patent holder, TACT IP, LLC[1].

[1]The method of perispinal administration of etanercept utilized was used under license from the patent holder, TACT IP, LLC, Boca Raton, FL, USA. TACT IP LLC claim methods of use of etanercept for the treatment of neurological disorders, including, but not limited to, US patents 6419944, 6537549, 6982089, 7214658, 7629311, 8119127, 8236306, and 8349323.

SPECT Imaging and Visual Analysis

Brain SPECT was carried out before (baseline) and after treatment for each patient. A triple head gamma SPECT camera (Picker Prism 3000XP), equipped with low-energy, ultra-high resolution (LEUHR) fan beam collimators was used to detect the uptake levels of the radiotracer, 99mTc-D, L-hexamethylene-propylene amine oxime (HMPAO), which is correlated with rCBF and metabolic activity. Reconstructions of multiparametric display were performed on the Picker Odyssey computer using filtered back projection and Chang attenuation correction (54). Once the final distribution is established post-injection and without significant change for 2–3 h, the visualization of the whole gray matter volume can be completed *via* a 3-D mapping of perfusion levels. Visual analysis was performed by an expert nuclear medicine physician with over 30 years of experience in SPECT.

In the absence of a qualified biomarker (27, 55), this study evaluates SPECT as an imaging biomarker based on the US Food and Drug Administration (FDA) monitoring biomarker definition (56). Monitoring biomarkers are analyzed at different time points to monitor the status of a disease or medical condition, and as a marker of the response to an intervention (56). In this review, the monitoring biomarker corresponds to the increase in brain perfusion detected with optimized displays of SPECT images before and after treatment. For each patient, the baseline SPECT images were compared with the post-treatment SPECT images to assess the functional improvements across different areas of the brain.

The increased perfusion was detected using a purposefully designed, discrete color scale (DGP40%) as a semi-quantitative tool that assessed relative perfusion across different displays. The distribution of the radiotracer within the brain was visualized in several ways during this study: Firstly, slicing, whereby processing was based on reconstruction, filtering, reorientation and attenuation correction and led to three orthogonal cuts (sagittal, coronal and transaxial) supplemented by a fourth axial display obtained along the temporal axis. Secondly, 3-D stereotactic surface projections were obtained with the Neurostat software (57). Stereotactic surface projection is a technique used for the analysis of SPECT images to extract functional areas projected onto the brain surface for the visual representation of brain perfusion. The discrete DGP40% color scale was applied to the orthogonal slice displays and the surface projection images to facilitate visualization of the level of perfusion. The maximum perfusion in the image was scaled to 100%, with each color band corresponding to a different level of perfusion, as measured in steps of approximately 3%. The threshold is set at 40% to suppress background noise.

Finally, thresholded volumetric displays were used to create a surface that represents voxels of a constant value and are therefore also termed iso-surface images. The region of the brain with the highest uptake of radiotracer was used as the reference value (the cerebellum in the majority of cases) and a 67% threshold value (relative to the reference value) was applied to generate 3-D iso-surface images with "holes" in

TABLE 1 | Characteristics of patients with complex neuropsychiatric conditions ($n = 6$) with selected treatment.

Patient	Age	Sex	Diagnosis	Treatment
I	62	F	Treatment-resistant depression (TRD) as well as grief and the effects of prolonged polypharmacy	CTK
II	34	F	Regulatory disorder of childhood, post-head injury epilepsy, reflex sympathetic dystrophy (RSD)	HBOT and PSE
III	54	M	Childhood-onset Tourettes, long history of alcohol abuse, severe depression, fatigue and sleep apnea	CTK
IV	55	F	Major depressive disorder (MDD), panic/agoraphobia, chronic back pain, frequent headaches	CTK
V	77	M	Dementia with major cognitive deficits and aphasia	HBOT and PSE
VI	43	M	Bipolar II, lifelong symptoms of depression, anxiety, impulsive behavior and family stressors	CTK

the image corresponding to areas of the cortex with lower perfusion. Since the images are continuous, the threshold value of 67% was selected as it accentuated corresponding areas in the color images, focused attention on hypoperfused areas and allowed for a better estimation of extent and severity. A threshold of 67% was applied to the iso-surface images shown herein. In addition to the 67% threshold, which depicts areas of hypoperfusion, thresholds of 85 and 90% were also used to create iso-surface images that visualized the size and location of areas of hyperperfusion. The application of multiple thresholds allowed the visualization of hypo- and hyper-perfusion areas across the brain. The clarity, complementarity and user-friendliness of these displays enabled a reliable visual evaluation before and after treatment.

RESULTS

Patient I: CTK Treatment

A 62-year-old female presented at the clinic on the verge of suicide. The patient had worked as a nurse prior and following episodes of alcohol abuse. The patient had a history of multiple medication trials and polypharmacy, physical pain and prolonged family stressors (sickness and eventual death of husband) and intense grief. The patient was classified as treatment-non-responsive following multiple treatment failures, which were intended to address her suffering. The patient's formal diagnoses were treatment-resistant depression (TRD) as well as grief and the effects of prolonged polypharmacy.

Baseline brain SPECT images for Patient I, shown in the top line of **Figure 1**, indicated a marked and very extensive bilateral hypoperfusion involving all lobes at baseline, and most accentuated on the right side. The more extensive hypoperfusion were located in the lateral frontal, frontoparietal and superior parietal areas. There was marked hypoperfusion in the dorsal aspect of the anterior cingulate. In the subcortical area, there was slight bilateral striatum hyperperfusion and robust perfusion of the thalamus. The patient was then treated with a total of 30 CTK sessions. SPECT images were subsequently taken following 5 months of CTK treatment (58 sessions) and are displayed in the bottom line of **Figure 1**. These images indicated a markedly improved perfusion across all cortical and subcortical structures. These improvements corresponded with dramatic clinical improvement leading to major changes in her daily life: enthusiastic, rational, planning for future, taking charge of her financial and family situation and a renewed religious sentiment.

Patient II: HBOT and PSE Treatments

A 34-year-old female presented with lifelong symptoms of regulatory disorder of childhood, two concussions, post-head injury epilepsy, and reflex sympathetic dystrophy (RSD). These ultimately led to marked suffering and extreme disability in activities of daily living. For almost 2 years the patient spent each day in a basement with dark glasses and protective hearing equipment due to intense photophobia and misophonia. Prior to visiting our clinic, the patient's medication history included over 30 types.

Baseline brain SPECT images for Patient II, shown in the top line of **Figure 2**, indicated extensive, diffuse bilateral hypoperfusion of the frontal (more accentuated on the left), temporal and orbitofrontal lobes and extended into the frontoparietal and parietal vertex areas. Additionally, there was bilateral hypoperfusion of the occipital lobes and hypoperfusion of the anterior cingulate in the dorsal aspect. The patient had robust perfusion of the thalamus and basal ganglia. There was also marked hyperperfusion in the cerebellar vermis.

HBOT was selected for patient II on account of multiple head injuries and a developmental history of a regulatory disorder. Following 40 HBOT treatments, brain SPECT images (**Figure 2** middle line) indicated increased perfusion in most areas of the cortex and in some subcortical structures.

At a later stage, PSE injections were started as another line of intervention. PSE clinical injections were given at weekly intervals. Following 4 PSE injections, SPECT was performed and images shown in the bottom line of **Figure 2** indicated major improvements (increased perfusion) in all lobes and subcortical areas. Specifically, the images showed increased perfusion in the orbito-frontal and apico-mesial temporal areas, bilaterally, and in the putamen bilaterally and in the mid thalamus. In addition, there was marked hyperperfusion in the mid posterior/inferior occipital area and, several areas of moderate cortical hyperperfusion in the lateral posterior aspect of both temporal lobes, as well as in the posterior cingulate/precuneus area. Significantly, these improvements were mirrored in the patient's cognition and ability to engage in daily acts of living.

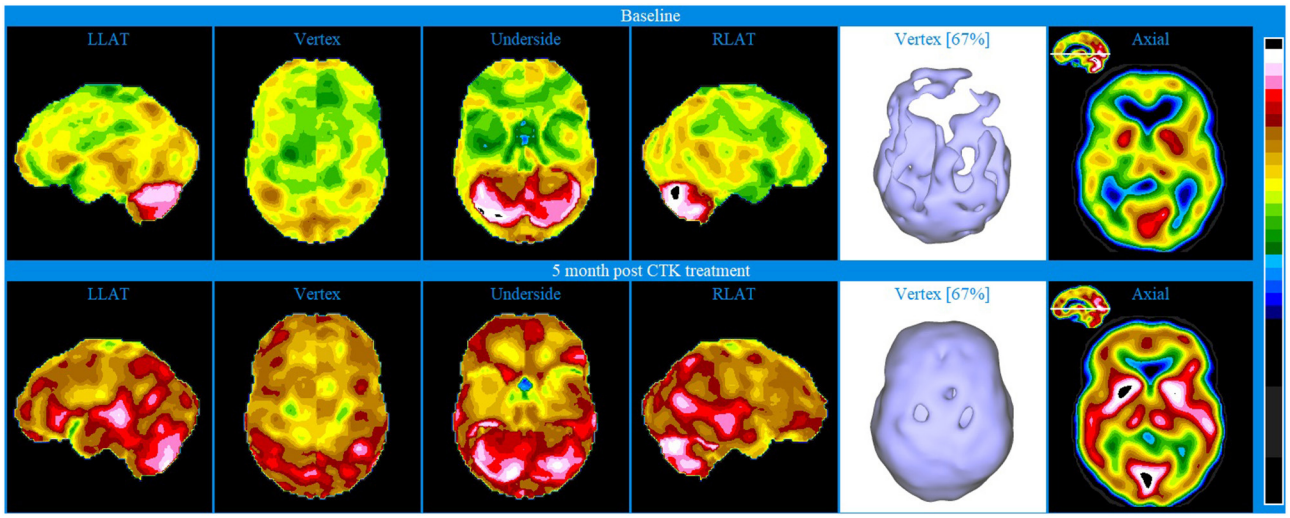

FIGURE 1 | Brain SPECT images from Patient I. Top line images relate to brain SPECT images at baseline. Bottom line images are taken following 5 months of CTK treatment. The six images on each row (from left to right) include four stereotactic surface projections of the left lateral (LLAT), vertex, underside and right lateral (RLAT), one iso-surface image of the vertex and one axial slice. Color-coded intensity indicates hyperfunctioning areas (blue hues) and hypofunctioning areas (white and black surrounded by white). Images are presented as described in the Methods.

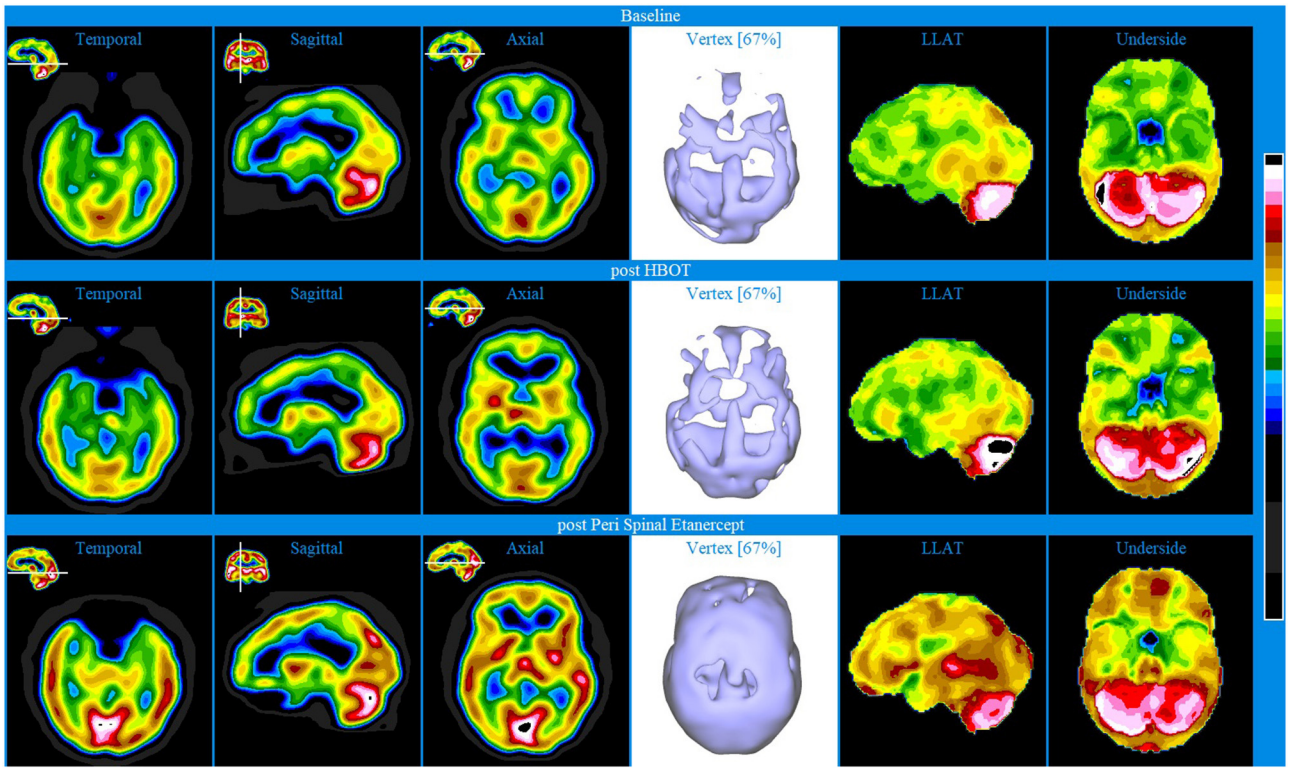

FIGURE 2 | Brain SPECT images for Patient II. Top line relates to brain SPECT images at baseline, indicating extensive areas of hypofunctioning in all lobes. Middle line shows SPECT images post-HBOT treatment. Bottom line of SPECT images collected post-PSE treatment. In each row (from left to right) one temporal axial image, two orthogonal slices (sagittal and axial), one iso-surface image of the vertex and two stereotactic surface projections of the left lateral (LLAT) and underside.

Patient III: CTK Treatment

A 54-year-old male emergency-room (ER) nurse presented with childhood-onset Tourettes and a long history of alcohol abuse, severe depression, fatigue and sleep apnea.

Baseline brain SPECT images for Patient III, shown in the top line of **Figures 3** and **4**, indicated extensive bilateral hypoperfusion with this most accentuated in the left frontal lobe. Additionally, there was localized hypoperfusion in the occipital and frontal poles. On the right side, there were multiple localized and confluent areas of hypoperfusion that were more accentuated in part of the frontal lobe extending to the superior aspect of the parietal lobe including the vertex. Marked hypoperfusion was also evidenced in the right striatum and right ventral striatum, and the thalamus had an asymmetric appearance with localized areas of marked hypoperfusion in the posterior aspect. There was moderate hyperperfusion in the anterior and posterior cingulate.

CTK treatment was selected and SPECT imaging was completed 5 months after the first CTK treatment (middle line of **Figures 3** and **4**). SPECT indicated several improvements, including in the area of severe frontal hypoperfusion at baseline. Subsequently the patient continued with medication, accepted continuous positive airway pressure (CPAP) treatment, and changed his lifestyle. Nonetheless, he was still unable to change his lifestyle completely at this stage. SPECT imaging completed 14 months later, as shown in the bottom line of **Figures 3** and **4**, indicated further significant improvements. There were extensive areas of relative increase in blood flow in the lateral aspect of the left hemisphere and bilateral vertex area, along with significantly improved perfusion in the orbitofrontal and apico-mesial temporal areas. Additionally, there was increased perfusion in the left striatum and in the cerebellum. These apparently minor improvements correlated with significant clinical improvements with the patient having resumed working (part-time job), had significantly changed lifestyle with a stable marriage.

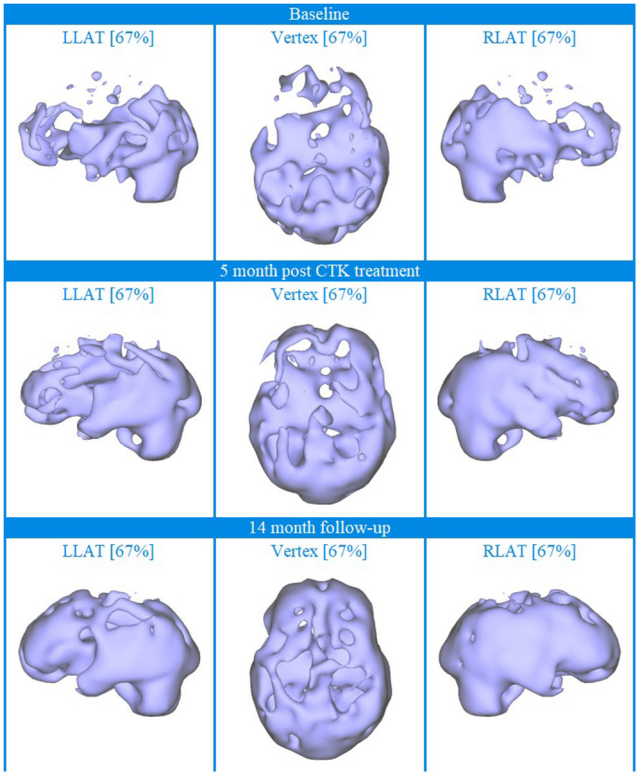

FIGURE 3 | Brain SPECT iso-surface images for Patient III. Top line relates to brain SPECT images at baseline. Middle line shows SPECT images 5 months after the first CTK treatment. Bottom line shows SPECT images 14 months following CTK treatment. In each row (from left to right) three iso-surface images of the left lateral (LLAT), vertex and right lateral (RLAT).

Patient IV: CTK Treatment

A 55-year-old female presented with major depressive disorder (MDD), panic/agoraphobia, chronic back pain and frequent headaches. The neurological exam did not indicate focal neurological dysfunction of the central nervous system. Intermittently, she had been treated with varied pharmacologic interventions and psychotherapy for 24 years, before presenting to this clinic. During that time, the patient's symptoms did not respond to Wellbutrin, Lexapro, Abilify, Viibryd, Paxil, Nardil, Vicodin, nor conventional psychotherapy.

Baseline brain SPECT images of Patient IV, shown in the top line of **Figure 5**, indicated extensive bilateral hypoperfusion in the frontal lobes (most accentuated on the left side), including the dorsolateral prefrontal regions and in the parietal vertex bilaterally. Not discernible in the images provided is the hypoperfusion in both orbitofrontal areas and in the mesial aspect of the right temporal lobe. There was moderate hyperperfusion of the thalamus and marked hyperperfusion in the mid posterior, inferior aspect of the occipital lobes.

The patient was treated with 30 CTK sessions and SPECT images shown in the bottom line of **Figure 5** were taken 14 months thereafter. Patient IV also received small amounts of anti-panic medicine that was used judiciously. The SPECT images indicated major bilateral perfusion improvement in the frontal conexities, fronto-parietal and anterior cingulate areas as well as bilateral increase in the basal ganglia. Not discernible in the images provided is the significant improvement of the orbitofrontal areas. There was also significantly increased perfusion in the thalamus and bilaterally in the striatum. Following treatment, the patient reported markedly improved symptoms: major decrease of depression, anxiety and back pain and greatly increased levels of life satisfaction. At the two-year follow-up, the patient had been practically free of suffering.

Patient V: HBOT and PSE Treatment

A 77-year-old male presented with onset of dementia induced by general anesthesia with major cognitive, physical and emotional impairments. Immediately post knee-replacement surgery the patient began to show dramatic cognitive, physical, and emotional impairment as compared with his pre-surgical state; these symptoms were still present when the patient arrived at our clinic 4 years post-surgery. Diagnoses of dementia with major cognitive deficits and aphasia was established.

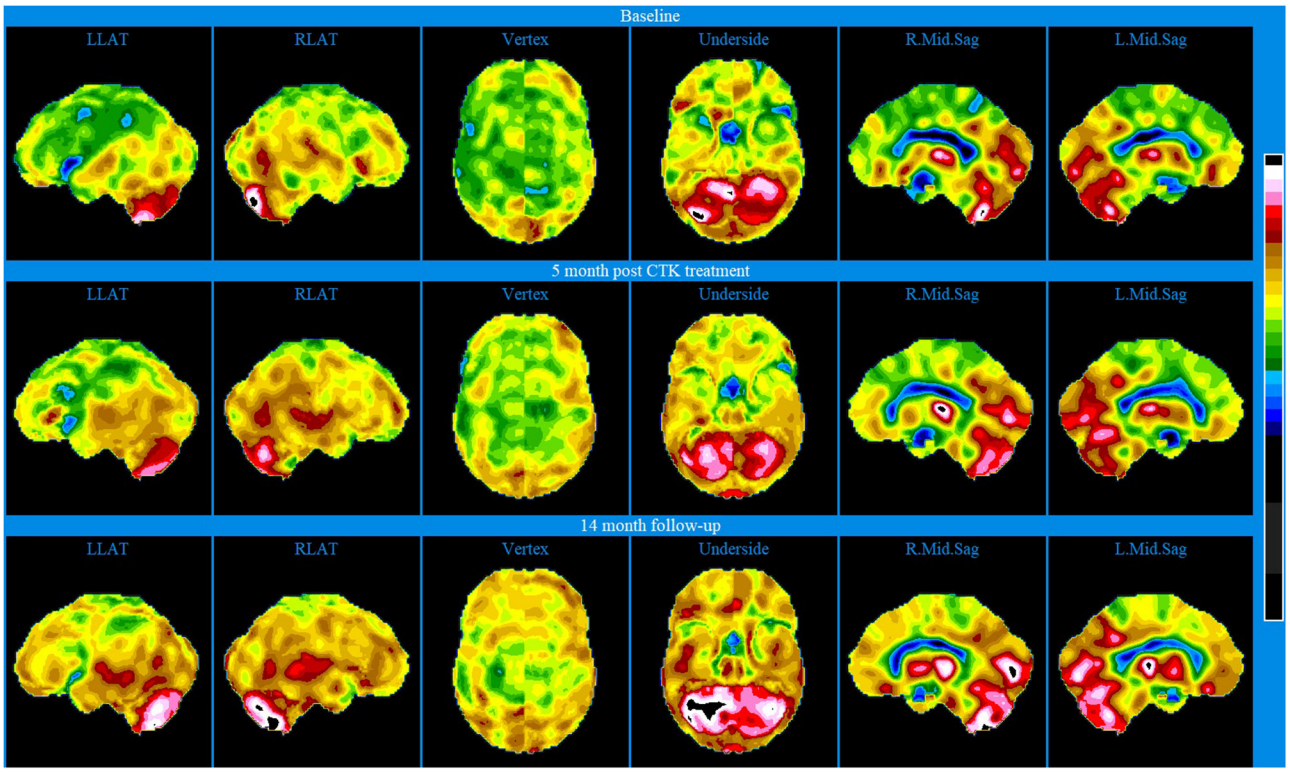

FIGURE 4 | Brain SPECT stereotactic surface projections for Patient III. Top line relates to brain SPECT images at baseline. Middle line shows SPECT images 5 months after the first CTK treatment. Bottom line shows SPECT images 14 months following CTK treatment. In each row (from left to right) six stereotactic surface projections of LLAT, RLAT, Vertex, Underside, right mod sagittal, and left mid sagittal.

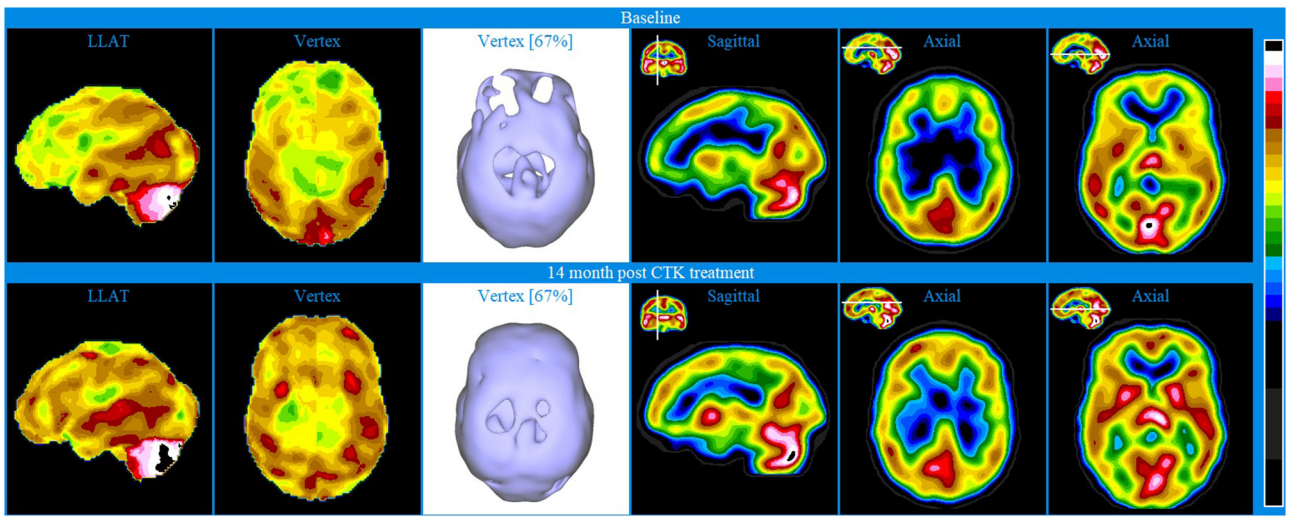

FIGURE 5 | Brain SPECT images for Patient IV. Top line relates to brain SPECT images at baseline. Bottom line shows SPECT images 14 months following 30 sessions of CTK treatment. In each row (from left to right) two stereotactic surface projections of the left lateral (LLAT) and vertex, one iso-surface image of the vertex, one sagittal slice and two axial slices.

Baseline brain SPECT images of Patient V, shown in the top line of **Figure 6**, indicated extensive hemispheric hypoperfusion and multiple localized hypoperfusion in the left hemisphere. Involvement extended to parts of the dorsolateral prefrontal (DLPF) cortex. There was also significant hypo-perfusion in the temporal lobes (more pronounced on the left) and to a lesser

extent in the orbitofrontal areas. To address these cognitive, physical, and emotional impairments, a treatment plan was prepared including a 40-session course of HBOT and PSE injections. After the first 10 HBOT treatments, the patient was administered 25 mg PSE injections approximately once weekly for 5 months.

At 5 months post-treatment with HBOT and PSE, SPECT images shown in the bottom line of **Figure 6** showed an overall similar appearance to baseline. However, there were localized increases in perfusion, as marked by the green arrows, in parts of the anterior aspect of the prefrontal cortex (including in the ventro-mesial aspect), right superior parietal, right lateral occipital, superior aspect of the left fronto-parietal area, posterior cingulate-precuneus and apico-mesial aspect of the right temporal. In addition, there was a significant increase in the striatum bilaterally.

Despite the follow-up SPECT remaining abnormal, the improved perfusion in small areas, specifically the mesial temporal lobe, prefrontal cortex, ventro-mesial frontal, posterior cingulate, precuneus and dorsal parietal are known to be key in contributing to memory, cognition and behavior. Indeed, initiating after the first PSE injection, the patient began showing progressive clinical improvements in cognitive and physical function. A follow-up visit 16 months after the end of treatment showed that the same level of clinical improvement had been maintained.

Patient VI: CTK Treatment

A 43-year-old male presented with bipolar II, lifelong symptoms of depression, anxiety, impulsive behavior and family stressors. Specifically, the patient reported struggling with intense depressed mood, substantial life stress, including a divorce in progress, and the inability to hold a job due to the impairment and distress associated with his symptoms. He had received psychopharmacological and psychotherapeutic treatment for the previous 6 years, but without improvement.

Baseline brain SPECT images of Patient VI, shown in the top line of **Figure 7**, indicated hypoperfusion in multiple hemispheric areas, most pronounced in the frontal lobes, anterior cingulate, orbitofrontal and apico-mesial areas of the temporal lobes. Hyperperfusion was indicated in the right putamen and in parts of the posterior cingulate and right cerebellum and vermis. This combination of hypoperfused areas is commonly associated with dysfunctions related to memory, executive function, social interaction and impulse control and the hyperperfused areas are often associated with anxiety and depression (58, 59). Based on the initial assessment, CTK treatment was selected, and the patient received a total of 24 sessions over 5 months.

SPECT was performed 5½ months after the first CTK treatment and images are displayed in the bottom line of **Figure 6**. Images indicated significantly improved relative perfusion in almost all previously under-perfused areas. Previously hyperperfused areas were either unchanged or increasingly hyperperfused. The patient also reported substantial improvements in symptoms related to functioning and psychometric assessments showed substantial decreases in symptoms related to both depression and mania.

To further display the utility of SPECT as an evaluative biomarker, **Figure 8** displays iso-surface images clearly indicating the increased perfusion following CTK treatment in almost all previously hypoperfused areas.

DISCUSSION

This article describes a novel display technique for SPECT images and provides readers with six case study examples that demonstrate how brain SPECT imaging can be used, both as a complementary diagnostic tool, and as a potential biomarker for monitoring and evaluating novel treatments for patients with complex neuropsychiatric conditions. Developing and applying clinical tools, such as SPECT imaging, can provide the clinician with complementary insights into the underlying neurobiology to standard clinical assessments. However, as SPECT imaging continues to be underutilized in clinical practice, more practical evidence, guidance and studies such as this one are required to demonstrate how SPECT can be utilized to evaluate the patient and to inform the clinician.

In this retrospective review, six patients presented with complex neuropsychiatric conditions and comorbidities following extensive unsuccessful periods of different treatments. While experienced psychiatrists may be able to diagnose patients with neuropsychiatric conditions based on behavioral criteria, functional brain imaging tools can inform the clinician of their underlying neurobiology. Additionally, the examination of different functional areas of the brain using SPECT imaging may provide insights into the patients' status that may not identifiable during clinical assessment. Particularly, in cases of diagnostic dilemma, such as those presented herein, SPECT images were used to identify areas of hypo- and hyper-perfusion to complement the initial clinical assessment. In the cases presented herein, the improved perfusion identified in the post-treatment SPECT images, whether extensive or localized, were mirrored by particular clinical improvements. Therefore, it is fundamental for the clinician to understand how clinical improvements manifest in the patients' underlying neurobiology. This case series effectively demonstrates the importance for the clinician to combine clinical assessments evaluating presenting behaviors and symptoms, with the underlying neurobiology attainable using SPECT imaging. Furthermore, building a database that correlates SPECT images with clinical assessments has the potential to develop more targeted treatments and to establish effective biomarkers.

In these complex cases, high-quality SPECT images provided valuable insights into the underlying neurobiological status of patients allowing the clinician to narrow the differential diagnosis. A high-quality brain SPECT will provide detailed information about the location, magnitude, and extent of areas of hyper- and/or hypoperfusion(s). The clinical efficacy of brain SPECT for the monitoring of patients with multiple co-morbidities and treatment-resistant conditions, is greatly enhanced by a standardized, comprehensive display of the results. This includes a user-friendly, color, multi-parametric set of 2D and 3D images. Consistency is also critically important, not

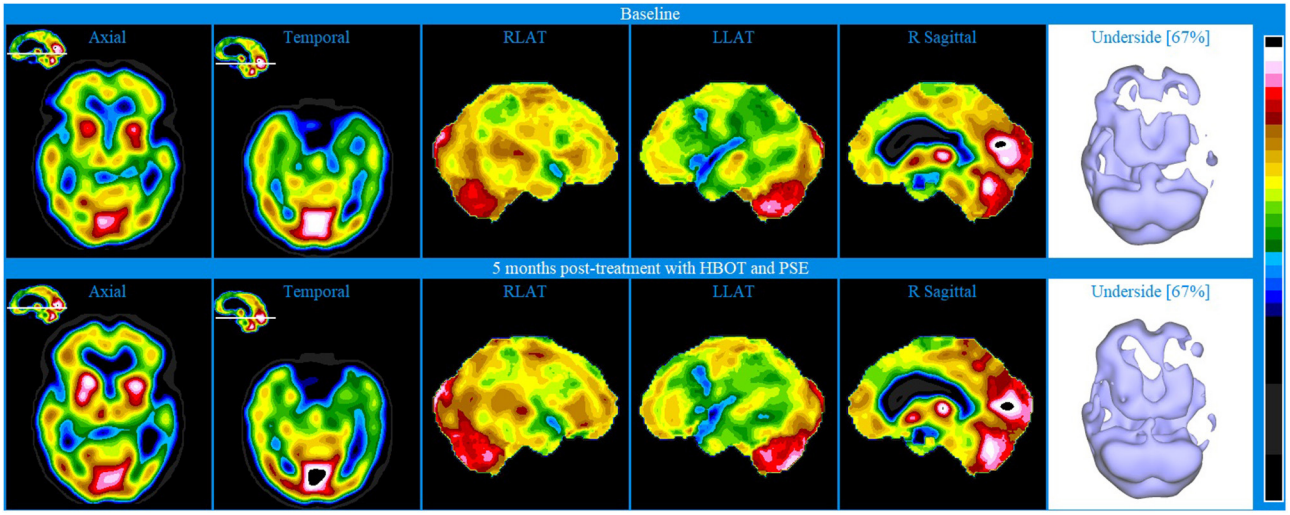

FIGURE 6 | Brain SPECT images for Patient V. Top line relates to brain SPECT images at baseline. Bottom line shows SPECT images 5 months post-treatment with HBOT and PSE. Green arrows indicate areas of increased perfusion. In each row (from left to right) one axial slice and one temporal slice, three stereotactic surface projections of the right lateral (RLAT), left lateral (LLAT) and right sagittal and one iso-surface image of the underside.

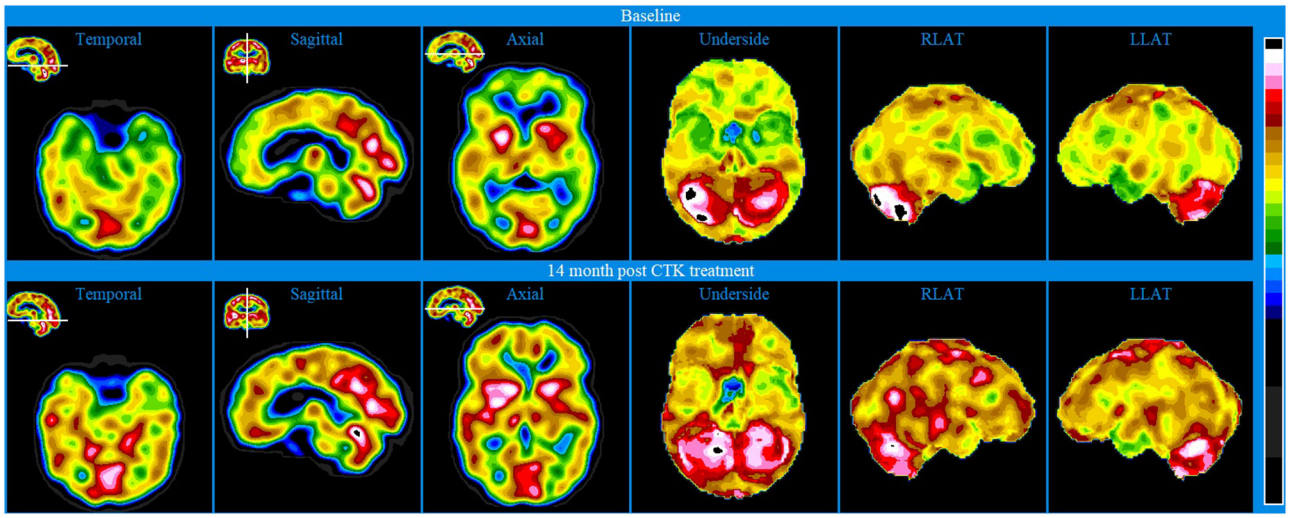

FIGURE 7 | Brain SPECT images for Patient VI. Top line relates to brain SPECT images at baseline. Bottom line shows SPECT images 5.5 months following 24 sessions of CTK treatment. In each row (from left to right) one temporal slice, one sagittal slice and one axial slice and three stereotactic surface projections of the underside, right lateral (RLAT) and left lateral (LLAT).

only in the execution of the procedure itself but also in the processing and display of the images. Whilst quantification of SPECT images may facilitate readers with limited experience to interpret SPECT scans and aid in the identification of trends (60, 61), it is imperative to also recognize any limitations of such quantitative analysis of imaging techniques, particularly within clinical practice and during the assessment of individual cases (8). The visual assessment of SPECT images pertaining to individual cases remains a foundational skill within clinical practice, the accuracy and reliability of which relies on the optimization of the presentation of images using effective display tools and techniques. In the clinical cases presented, we have demonstrated that the optimization of images using a novel set of display tools facilitated the visual interpretation of SPECT imaging data by expert clinicians, without the need for quantification or statistical analysis. A more detailed description of this display will be published shortly (62).

In the absence of a qualified biomarker (27, 55), this study evaluates SPECT as an imaging biomarker based on the US Food and Drug Administration (FDA) monitoring biomarker

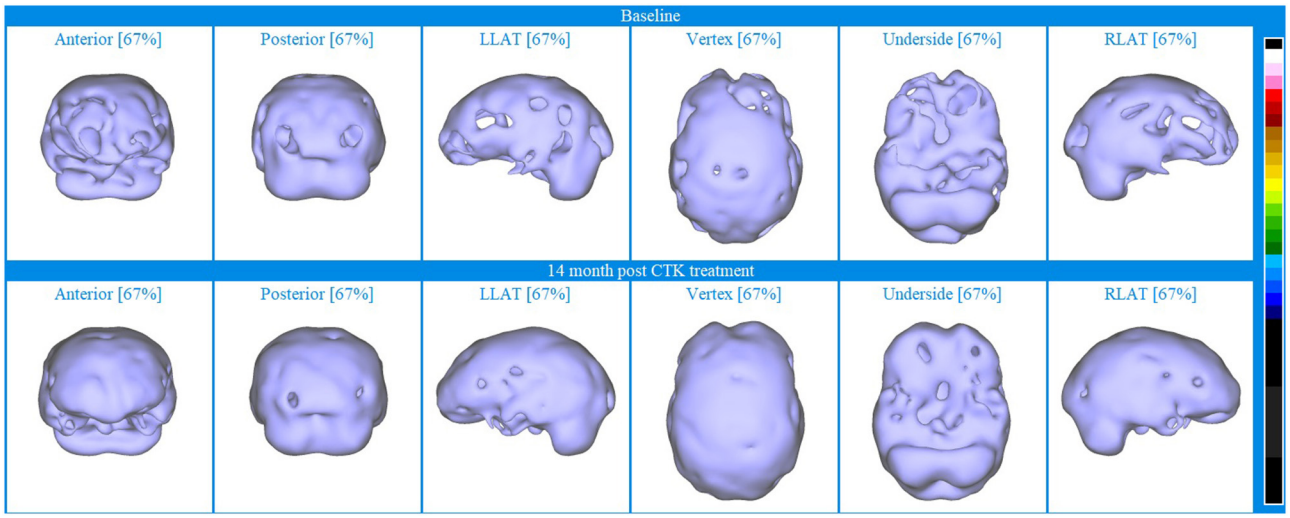

FIGURE 8 | Iso-surface SPECT images for Patient VI. Top line relates to brain SPECT images at baseline and bottom line are brain SPECT images 14 months after CTK treatment began. In each row (from left to right) are iso-surface images of the anterior, posterior left lateral (LLAT), vertex, underside and right lateral (RLAT).

definition (56). A monitoring biomarker is defined as "a biomarker measured repeatedly for assessing status of a disease or medical condition or for evidence of exposure to (or effect of) a medical product or an environmental agent" (56). In this review, the monitoring biomarker corresponds to the increase in brain perfusion detected with optimized displays of SPECT images before and after treatment. Following treatment, all patients demonstrated improvements measured *via* periodic clinical evaluations and in some cases neuropsychological testing and detailed observations from family members. These clinical improvements were also apparent from the increased perfusion evident in the brain SPECT images collected post-treatment compared with those collected at baseline. Whilst clinical improvements following treatment may be discernible during standard clinical assessment, SPECT was used as a monitoring biomarker to indicate the underlying neurobiological response of each individual to the treatment intervention. In this case series, SPECT images indicated the specific areas of improved brain perfusion that resulted following treatment and provided additional context to the clinical improvements identified. Therefore, the SPECT images provided insights into the functioning status of the patient in addition to monitoring symptoms during clinical assessment. These follow-up scans thereby informed how these novel treatments affected the underlying neurobiology of each individual and how perfusion improvements in specific areas correlated to clinical improvements.

The application of SPECT imaging as a monitoring biomarker also further contributes to the understanding and the growing literature that describes the clinical utility of these novel treatments for patients with neuropsychiatric conditions. In this case series, intervention with novel treatments of CTK or HBOT and PSE resulted in marked improvements in relative perfusion in previously hypoperfused areas, which correlated to the clinical improvements noted for each patient. These cases thereby provide further evidence of the clinical utility of these novel treatments for patients with complex neuropsychiatric conditions.

Despite the growing, evidence-based foundation for the application of SPECT in numerous indications relevant to psychiatric practice, there is a need for clinicians to utilize this powerful tool and contribute to our understanding of the neurobiology relating to different neuropsychiatric conditions and comorbidities. Greater biological understanding will result in the identification of meaningful biomarkers for diagnosis, prognosis or risk and can further aid the clinician in their evaluation of a patient before and after treatments. There is a particular value in sharing methodologies and results regarding the implementation of SPECT in routine practice in clinical settings. This retrospective review demonstrated that brain SPECT imaging could represent a potential imaging biomarker since syndrome status was correlated with changes in the perfusion pattern detected. Given the display modalities used, the relative perfusion assessment with SPECT imaging before and after treatment has acted as a monitoring biomarker that indicated the therapeutic benefit of the novel types of treatments used in this case-series. Furthermore, SPECT images have provided additional information that explains the functional changes that gave rise to the observed clinical improvements. This understanding of the topographic functional status is important if we are to further progress to personalized targeted treatments and the development of effective biomarkers.

This article has some limitations. First, these cases represent assessments carried out during routine clinical practice and not as part of a pre-planned study, therefore there is a small number of cases presented without a normalized reference cohort and

physicians were not blinded to the clinical context, however this does reflect a practical clinical routine.

Overall, this collection of these case studies further substantiates the clinical relevance of brain SPECT imaging in psychiatry and neuropsychiatry. This review demonstrates that SPECT imaging can be a valuable tool in cases of diagnostic dilemma and can complement standard assessment techniques and diagnostic tools. In our study, six patients with complex neuropsychiatric conditions and comorbidities were successfully treated, which contributes to the growing literature indicating the clinical utility of the novel therapies of CTK and HBOT with PSE (33, 47). The positive outcomes for these patients were facilitated by the detailed initial evaluation of patients that included baseline SPECT imaging that complemented the standard clinical assessment. The repetitious clinical approach, the novel display technique and positive treatment outcomes in these six cases has also demonstrated how image optimization and visual analysis of SPECT images can be utilized during clinical assessments of individual cases. Finally, we demonstrated how SPECT images recorded before and after treatment provided valuable insights into the improved neurobiological status of these patients in response to intervention. Therefore, we argue that perfusion assessed with SPECT images before and after treatment can be used as an imaging biomarker for monitoring, evaluating and explaining clinical change.

AUTHOR'S NOTE

Proper execution of a brain SPECT scan is an art and requires great attention to detail in order to obtain high quality images, such as the ones presented here. For specific information regarding imaging and processing protocols, please contact the authors directly.

DATA AVAILABILITY STATEMENT

The datasets presented in this article are not readily available because HIPAA-protected data. Requests to access the datasets should be directed to srdbest@neuroscience.md.

ETHICS STATEMENT

Ethical review and approval was not required for the study on human participants in accordance with the local legislation and institutional requirements. The patients/participants provided their written informed consent to participate in this study. Written informed consent was obtained from the individual(s) for the publication of any potentially identifiable images or data included in this article.

AUTHOR CONTRIBUTIONS

SB provided the CTK, HBOT and PSE treatments, as well as integrated the psychiatric and SPECT data. NH co-wrote the article and contributed to the discussion of the results. DP performed the SPECT imaging, as well as analyzed and interpreted the SPECT data. Please note that DP sadly passed away during the finalization of this manuscript, however all other authors read and approved the final manuscript.

ACKNOWLEDGMENTS

This article would not have been possible without the pioneering work of DP, who sadly passed away during the finalization of this manuscript. This paper is dedicated to his memory. The authors would also like to acknowledge Simon DeBruin of Good Lion Imaging for the image processing that resulted in the impressive and clear images displayed herein.

REFERENCES

1. Henderson T, van Lierop M, McLean M, Uszler JM, Thornton J, Siow Y, Functional neuroimaging in psychiatry-aiding in diagnosis and guiding treatment. what the american psychiatric association does not know. *Front Psychiatry*. (2020) 11:276. doi: 10.3389/fpsyt.2020.0027
2. Taber KH, Hurley RA, Yudofsky SC. Diagnosis and treatment of neuropsychiatric disorders. *Annu Rev Med.* (2010) 61:121–33. doi: 10.1146/annurev.med.051408.105018
3. Richieri R, Boyer L, Faget-Agius C, Farisse J, Mundler O, Lançon C, et al. (2015). Determinants of brain SPECT perfusion and connectivity in treatment-resistant depression. *Psychiatry Res.* (2014) 231:134–40. doi: 10.1016/j.pscychresns.2014.11.013
4. Escobar R, Rios A, Montoya ID, Lopera F, Ramos D, Carvajal C, et al. Clinical and cerebral blood flow changes in catatonic patients treated with ECT. *J Psychosom Res.* (2000) 49:423–9. doi: 10.1016/S0022-3999(00)00190-2
5. Ito H, Kawashima R, Awata S, Ono S, Sato K, Goto R, et al. Hypoperfusion in the limbic system and prefrontal cortex in depression: SPECT with anatomic standardization technique. *J Nucl Med.* (1996) 37:410–4
6. Dougherty DD, Rauch SL. Brain correlates of antidepressant treatment outcome from neuroimaging studies in depression. *Psychiatr Clin North Am.* (2006) 30:91–103. doi: 10.1016/j.psc.2006.12.007
7. Nishimiya M, Matsuda H, Imabayashi E, Kuji I, Sato N. Comparison of SPM and NEUROSTAT in voxelwise statistical analysis of brain SPECT and MRI at the early stage of Alzheimer's disease. *Ann Nucl Med*. (2008) 22:921–7. doi: 10.1007/s12149-008-0211-7
8. Catafau AM. Brain SPECT in Clinical Practice. Part I: Perfusion. *J Nucl Med.* (2001) 42:259–71.
9. Coburn KL, Lauterbach EC, Boutros NN, Black KJ, Arciniegas DB, Coffey CE. (2006). The value of quantitative electroencephalography in clinical psychiatry: a report by the committee on research of the American neuropsychiatric association. *J Neuropsychiatry Clin Neurosci.* (2006) 18:460–500. doi: 10.1176/jnp.2006.18.4.460
10. Evans JR, Budzynski TH, Budzynski HK, Abarbanel A. *Introduction to Quantitative EEG and Neurofeedback: Advanced Theory and Applications*. USA: Academic Press (2009).
11. Hoffman DA, Lubar JF, Thatcher RW, Sterman MB, Rosenfeld PJ, Striefel S, et al. Limitations of the American Academy of Neurology and American Clinical Neurophysiology Society Paper on QEEG. *J Neuropsychiatry Clin Neurosci.* (1999) 11:401–7. doi: 10.1176/jnp.11.3.401
12. Hughes JR, John ER. Conventional and Quantitative Electroencephalography in Psychiatry. *J Neuropsychiatry Clin Neurosci.* (1999) 11:190–208. doi: 10.1176/jnp.11.2.190
13. Huang C, Eidelberg D, Habeck C, Moeller J, Svensson L, Tarabula T, et al. (2007). Imaging markers of mild cognitive impairment:

Multivariate analysis of CBF SPECT. *Neurobiol Aging.* (2006) 28:1062–9. doi: 10.1016/j.neurobiolaging.2006.05.017
14. Amen DG, Trujillo M, Newberg A, Willeumier K, Tarzwell R, Wu JC, et al. Brain SPECT imaging in complex psychiatric cases: an evidence-based, underutilized tool. *Open Neuroimaging J.* (2011) 5:40–8. doi: 10.2174/1874440001105010040
15. Amen DG, Raji CA, Willeumier K, Taylor D, Tarzwell R, Newberg A, et al. Functional neuroimaging distinguishes posttraumatic stress disorder from traumatic brain injury in focused and large community datasets. *PLoS ONE.* (2015) 10:e0129659. doi: 10.1371/journal.pone.0129659
16. Cohen PF, Tarzwell R, Numerow L, Siow, Y-H, Uszler JM, et al. *CANM Guidelines For Brain Perfusion Single Photon Emission Computed Tomography (SPECT)*. Canadian Association of Nuclear Medicine (2021). Available online at: https://canm-acmn.ca/guidelines (accessed October 22, 2021)
17. Estudillo-Guerra MA, Pacheco-Barrios K, Cardenas-Rojas A, Adame-Ocampo G, Camprodon JA, Morales-Quezada L. Brain perfusion during manic episode and at 6-month follow-up period in bipolar disorder patients: Correlation with cognitive functions. *Brain Behav.* (2020) 10:e01615. doi: 10.1002/brb3.1615
18. Henderson T, Cohen P, van Lierop M, Thornton J, McClean M, Uszler J, et al. A reckoning to keep doing what we are already doing with PET and SPECT functional neuroimaging. *Am J Psychiatry.* (2020) 177:637–8. doi: 10.1176/appi.ajp.2020.19080801
19. Henderson T, van Lierop M, McLean M, Uszler JM, Thornton J, Siow Y, et al. Functional Neuroimaging in Psychiatry—Aiding in diagnosis and guiding treatment. What the American Psychiatric Association does not know. *Front Psychiatry.* (2020) 11:276. doi: 10.3389/fpsyt.2020.00276
20. Raji CA, Willeumier K, Taylor DT. Functional neuroimaging with default mode network regions distinguishes PTSD from TBI in a military veteran population. *Brain Imaging Behav.* (2015) 9:527–34. doi: 10.1007/s11682-015-9385-5
21. Pavel DG, Best SRD. Brain SPECT as Imaging Biomarker for Evaluating Effects of Novel Treatments in Psychiatry. *J Nucl Med.* (2017) 58(supplement 1):1298.
22. Walker Z, Moreno E, Thomas A, Inglis F, Tabet N, Rainer M, et al. Clinical usefulness of dopamine transporter SPECT imaging with 123I-FP-CIT in patients with possible dementia with Lewy bodies: Randomised study. *Br J Psychiatry.* (2018) 206:145–52. doi: 10.1192/bjp.bp.114.148643
23. Yeo JM, Lim X, Khan ZP. Systematic review of the diagnostic utility of SPECT imaging in dementia. *Eur Arch Psychiatry Clin Neurosci.* (2013) 263:539–52. doi: 10.1007/s00406-013-0426-z
24. Guinane J, Ng BL. Clinical utility of MRI and SPECT in the diagnosis of cognitive impairment referred to memory clinic. *Int Psychogeriatr.* (2018) 30:611–7. doi: 10.1017/S1041610217001624
25. Henderson TA. The diagnosis and evaluation of dementia and mild cognitive impairment with emphasis on SPECT perfusion neuroimaging. *CNS Spectr.* (2012) 17:176–206. doi: 10.1017/S1092852912000636
26. Milham MP, Craddock RC, Klein A. Clinically useful brain imaging for neuropsychiatry: How can we get there? *Depress Anxiety.* (2017) 34:578–87. doi: 10.1002/da.22627
27. Abi-Dargham A, Horga G. The search for imaging biomarkers in psychiatric disorders. *Nat Med.* (2016) 22:1248–55. doi: 10.1038/nm.4190
28. Camargo EE. Brain SPECT in neurology and psychiatry. *J Nucl Med.* (2001) 42:611–23.
29. Li J, Yang Y, Zhu Y, Zhou L, Han Y, Yin T, et al. Towards characterizing the regional cerebral perfusion in evaluating the severity of major depression disorder with SPECT/CT. *BMC Psychiatry.* (2018) 18:70. doi: 10.1186/s12888-018-1654-6
30. Karada,g F, Kalkan Oguzhanoglu N, Yüksel D, Kiraç S,Cura Ç, Özdel O, et al. The comparison of pre- and post-treatment 99mTc HMPAO brain SPECT images in patients with obsessive-compulsive disorder. *Psychiatry Res.* (2013) 213:169–177. doi: 10.1016/j.pscychresns.2012.07.005
31. Mottaghy FM, Keller CE, Gangitano M, Ly J, Thall M, Parker JA, et al. Correlation of cerebral blood flow and treatment effects of repetitive transcranial magnetic stimulation in depressed patients. *Psychiatry Res.* (2002) 115:1–14. doi: 10.1016/S0925-4927(02)00032-X
32. Raji CA, Tarzwell R, Pavel D, Schneider H, Uszler M, Thornton, et al. Clinical utility of SPECT neuroimaging in the diagnosis and treatment of traumatic brain injury: a systematic review. *PLoS ONE.* (2014) 9:e91088. doi: 10.1371/journal.pone.0091088
33. Best SRD, Pavel DG, Haustrup N. Combination therapy with transcranial magnetic stimulation and ketamine for treatment-resistant depression: a long-term retrospective review of clinical use. *Heliyon.* (2019) 5:e02187. doi: 10.1016/j.heliyon.2019.e02187
34. Griffiths C, O'Neill-Kerr A, de Vai R, Sore T, da Silva K. Ketamine infusion (KI) in treatment resistant depression (TRD): retrospective clinical data analysis. *Open J* Depress. (2019) 8:59–70. doi: 10.4236/ojd.2019.83007
35. Marcinkowska AB, Mankowska ND, Kot J, Winklewski PJ. Impact of hyperbaric oxygen therapy on cognitive functions: a systematic review. *Neuropsychol Rev.* (2021). doi: 10.1007/s11065-021-09500-9. [Epub ahead of print].
36. Tobinick E. Perispinal etanercept: a new therapeutic paradigm in neurology. *Expert Rev Neurother.* (2010) 10:985–1002. doi: 10.1586/ern.10.52
37. Fitzgerald PB, Hoy KE, Elliot D, McQueen SRN, Wambeek LE, Daskalakis ZJ. Accelerated repetitive transcranial magnetic stimulation in the treatment of depression. *Neuropsychopharmacology.* (2018) 43:1565–72. doi: 10.1038/s41386-018-0009-9
38. O'Reardon JP, Solvason HB, Janicak PG, Sampson S, Isenberg KE, Nahas Z, et al. Efficacy and safety of transcranial magnetic stimulation in the acute treatment of major depression: a multisite randomized controlled trial. *Biol Psychiatry.* (2007) 1:1208–16. doi: 10.1016/j.biopsych.2007.01.018
39. Perera T, George MS, Grammer G, Janicak PG, Pascual-Leone A, Wirecki TS. The clinical TMS society consensus review and treatment recommendations for TMS therapy for major depressive disorder. *Brain Stimul.* (2016) 9:336–46. doi: 10.1016/j.brs.2016.03.010
40. Singh JB, Fedgchin M, Daly E, Xi L, Melman C, Bruecker D, et al. Intravenous esketamine in adult treatment-resistant depression: a double-blind, double-randomization, placebo-controlled study. *Biol Psychiatry.* (2016) 80:424–31. doi: 10.1016/j.biopsych.2015.10.018
41. Xie Z- M, Wang X-M, Xu N, Wang J, Pan W, Tang XH, et al. Alterations in the inflammatory cytokines and brain-derived neurotrophic factor contribute to depression-like phenotype after spared nerve injury: improvement by ketamine. *Sci Rep.* (2017) 7:3124. doi: 10.1038/s41598-017-03590-3
42. Martin JL, Finsterwald C. Cooperation between BDNF and glutamate in the regulation of synaptic transmission and neuronal development. *Commun Integr Biol.* (2011) 4:14–6. doi: 10.4161/cib.13761
43. Zanos P. Mechanisms of ketamine action as an antidepressant. *Mol Psychiatry.* (2018) 23:801–11. doi: 10.1038/mp.2017.255
44. Best SRD. *Treatment of Thalamocortical Dysrhythmia*. World Intellectual Property Organization Patent No. WO2014081948A1. International Bureau, Virginia: Commission for patents (2014).
45. Best SRD. Treatment of thalamocortical dysrhythmia U.S. Patent No. US8974365B2. Washington DC: Patent US, and Trademark Office (2015).
46. Best SRD. Combined ketamine and transcranial magnetic stimulation for treatment resistant depression in the context of chronic OCD: a case report. *Neuropsychiatric Electrophysiology.* (2015) 1:2. doi: 10.1186/s40810-015-0003-y
47. Best SRD. Treatment of post-anesthesia dementia with perispinal etanercept injection and hyperbaric oxygen therapy: a case report. *J Med Case Rep.* (2017) 11. doi: 10.1186/s13256-017-1259-6
48. Tobinick E, Rodriguez-Romanacce H, Levine A, Ignatowski TA. Immediate neurological recovery following perispinal etanercept years after brain injury. *Clin Drug Investig.* (2014) 34:361–6. doi: 10.1007/s40261-014-0186-1
49. Gonzales-Portillo B, Lippert T, Nguyen H, Lee JY. Hyperbaric oxygen therapy: A new look on treating stroke and traumatic brain injury. *Brain circulation.* (2019) 5:101–5. doi: 10.4103/bc.bc_31_19
50. Golden Z, Golden CJ, Neubauer RA. Improving neuropsychological function after chronic brain injury with hyperbaric oxygen. *Disabil Rehabil.* (2006) 28:1379–86. doi: 10.1080/09638280600638364
51. Huang L, Obenaus A. Hyperbaric oxygen therapy for traumatic brain injury. *Med Gas Res.* (2011) 1:21. doi: 10.1186/2045-9912-1-21
52. Tobinick, E. Perispinal etanercept advances as a neurotherapeutic. *Expert Rev Neurother.* 18:453–455. doi: 10.1080/14737175.2018.1468253

53. Tobinick EL. Use and methods of use of etanercept and other TNF binding biologics to improve human cognitive function. United States Patent No. US20060009450A1. Washington, DC: Patent US, and Trademark Office (2006).
54. Chang LT. A method for attenuation correction in radionuclide computed tomography. *IEEE Transactions on Nuclear Science*. (1978) 25:638–43. doi: 10.1109/TNS.1978.4329385
55. Botteron K, Carter C, Castellanos FX, Dickstein DP, Drevets W, Kim KL, et al. *Consensus Report of the APA Work Group on Neuroimaging Markers of Psychiatric Disorders*. Am. Psychiatr Assoc (Ed.), Arlington, VA, USA (2012).
56. FDA-NIH Biomarker Working Group. BEST (Biomarkers, EndpointS, other Tools). Monitoring Biomarker. Food and Drug Administration (US) and National Institutes of Health (US) (2016). Availabble online at: https://www.ncbi.nlm.nih.gov/books/NBK402282 (accessed January 25, 2021).
57. Minoshima S, Koeppe RA, Frey KA, K.ã DE. Anatomic standardization: linear scaling and nonlinear warping of functional brain images. *J Nucl Med*. (1994) 35:1528–37
58. Pliszka SR, Glahn DC, Semrud-Clikeman M, Franklin C, Perez III, Xiong R, et al. Neuroimaging of inhibitory control areas in children with attention deficit hyperactivity disorder who were treatment naive or in long-term treatment. *Am J Psychiatry*. (2006) 163:1052–1060. doi: 10.1176/ajp.2006.163.6.1052
59. Sheehan W, Thurber S. Review of two years of experiences with SPECT among psychiatric patients in a rural hospital setting. *J Psychiatr Pract*. (2008) 14:318–23. doi: 10.1097/01.pra.0000336760.88178.e5
60. Booij J, Dubroff J, Pryma D, Yu J, Agarwal R, Lakhani P, et al. Diagnostic performance of the visual reading of 123 I-Ioflupane SPECT images with or without quantification in patients with movement disorders or dementia. *J Nucl Med*. (2017) 58:1821–6. doi: 10.2967/jnumed.116.189266
61. Mäkinen E, Joutsa J, Johansson J, Mäki M, Seppänen M, Kaasinen V. Visual versus automated analysis of [I-123] FP-CIT SPECT scans in parkinsonism. *J Neural Transm Suppl*. (2016) 123:1309–18. doi: 10.1007/s00702-016-1586-6
62. McLean M, Henderson TA, Pavel DG, Cohen P. Increase asymmetric perfusion of the cerebral cortices and thalamus indicates individuals at risk for bipolar disorder: a family Cohort SPECT neuroimaging study. *Front Psychiatry*. (2021).

Conflict of Interest: NH has since become an employee of Eli Lilly and Company. SB holds multiple patents claiming methods of use of CTK for treatment of neurological disorders.

The remaining author declares that the research was conducted in the absence of any commercial or financial relationships that could be construed as a potential conflict of interest.

The handling editor TH declared a past co-authorship/collaboration with one of the authors DP.

Publisher's Note: All claims expressed in this article are solely those of the authors and do not necessarily represent those of their affiliated organizations, or those of the publisher, the editors and the reviewers. Any product that may be evaluated in this article, or claim that may be made by its manufacturer, is not guaranteed or endorsed by the publisher.

frontiers in Psychiatry

ORIGINAL RESEARCH
published: 25 March 2022
doi: 10.3389/fpsyt.2022.787186

Longitudinal Single Photon Emission Computed Tomography Neuroimaging as an Indication of Improvement in Psychiatric Disorders in a Community Psychiatric Practice

John F. Thornton[1,2†], Howard Schneider[2,3†], Philip F. Cohen[2,4,5], Simon DeBruin[6], John Michael Uszler[2,7,8], Yin-Hui Siow[2,9], Mary K. McLean[2,10], Muriel J. van Lierop[2,10], Dan G. Pavel[2,11‡] and Theodore A. Henderson[2,12,13,14]*

[1] Rossiter-Thornton Associates, Toronto, ON, Canada, [2] International Society of Applied Neuroimaging, Denver, CO, United States, [3] Sheppard Clinic North, Vaughan, ON, Canada, [4] Nuclear Medicine, Lions Gate Hospital, Vancouver, BC, Canada, [5] Department of Radiology, University of British Columbia, Vancouver, BC, Canada, [6] Good Lion Imaging LLC, Columbia, MD, United States, [7] DrSPECTscan Inc., Lake Elsinore, CA, United States, [8] Department of Molecular and Medical Pharmacology, University of California, Los Angeles, Los Angeles, CA, United States, [9] Nuclear Medicine, Southlake Regional Health Centre, Newmarket, ON, Canada, [10] Private Practice, Toronto, ON, Canada, [11] PathFinder Brain SPECT LLC, Deerfield, IL, United States, [12] Dr. Theodore Henderson, Inc., Denver, CO, United States, [13] The Synaptic Space, Inc., Denver, CO, United States, [14] Neuro-Luminance, Inc., Denver, CO, United States

OPEN ACCESS

Edited by:
Ali Saffet Gonul, Ege University, Turkey

Reviewed by:
Anil Kalyoncu, Ege University School of Medicine, Turkey
Gianluca Serafini, San Martino Hospital (IRCCS), Italy

***Correspondence:**
Howard Schneider
hschneidermd@alum.mit.edu

†These authors share first authorship

‡Deceased

Specialty section:
This article was submitted to Neuroimaging and Stimulation, a section of the journal Frontiers in Psychiatry

Received: *30 September 2021*
Accepted: *21 February 2022*
Published: *25 March 2022*

Citation:
Thornton JF, Schneider H, Cohen PF, DeBruin S, Uszler JM, Siow Y-H, McLean MK, van Lierop MJ, Pavel DG and Henderson TA (2022) Longitudinal Single Photon Emission Computed Tomography Neuroimaging as an Indication of Improvement in Psychiatric Disorders in a Community Psychiatric Practice. Front. Psychiatry 13:787186. doi: 10.3389/fpsyt.2022.787186

In the community, there is a need to more objectively evaluate the response of common chronic psychiatric disorders to treatment. Brain single photon emission computed tomography (SPECT) indirectly measures cerebral functional activity by uptake of a radiotracer, which follows regional cerebral blood flow. Brain 3D Thresholded SPECT scans are thresholded three dimensional images derived from brain SPECT data. A retrospective community study of longitudinal (before and after treatment) brain 3D Thresholded SPECT scans of 73 patients with all-cause psychiatric disorders (most frequent diagnostic clusters: attention-deficit hyperactivity disorder, post-mild traumatic brain injury, affective disorders, psychotic disorders, post-viral chronic syndromes), shows these baseline SPECT scans predict improvement (non-worsening to large improvement) in clinical functioning with a sensitivity of 94% (95% confidence interval 86–98%) and a specificity of 67% (95% confidence interval 21–94%). In contrast, contemporaneous analysis by the same radiologist of conventional 2D reading of the same before and after treatment brain SPECT scan data of the same 73 patients, predicted improvement (non-worsening to large improvement) in clinical functioning with a sensitivity of only 26% (95% confidence interval 17–37%) although with a specificity of 100% (95% confidence interval 44–100%). These data suggest 3D Thresholded SPECT scans can provide the clinician with a more objective measure for verifying improvement in psychiatric disorders seen in the community, consistent with prior

studies of SPECT as a measure of neurobiological change. Furthermore, these data suggest 3D Thresholded SPECT scans may have clinical application in guiding treatment and potentially improving outcomes.

Keywords: neuroimaging, SPECT, biomarker, traumatic brain injury, attention-deficit hyperactivity disorder, post-viral syndrome, community psychiatry

INTRODUCTION

There is a need in community-based psychiatric practice to more accurately evaluate the response of common chronic psychiatric disorders to treatment. While the clinical exam, as well as various functional questionnaires, can and should continue to be used in the evaluation of a patient's progress, more objective tests are needed to directly evaluate the patient in an objective manner. At the time of this writing, there is still a paucity of clinically available and useful biomarkers in the field of psychiatry (1). Regardless of diagnosis and independent of the Diagnostic and Statistical Manual (DSM)-IV, DSM-IV-TR, or DSM-V criteria, symptoms such as pain, apprehension, distress, inflexibility, and/or cognitive clarity are important markers of treatment progress which remain largely subjective. The lack of psychiatric biomarkers impedes the clinician's ability to deliver the best personalized care.

Perfusion single photon emission computed tomography (SPECT) brain scans can measure aspects of brain function. The amount of radiotracer uptake in a brain region is proportional to the blood flow within gray matter over the physiological range. Since local cerebral blood flow is proportional to neurophysiological function, perfusion SPECT provides a one-off measure of brain function (2–4). Further computer processing of the SPECT data can result in a three-dimensional looking image of the brain (termed a brain 3D Thresholded SPECT scan) which provides more clinically relevant information than a two-dimensional tomogram (5).

Brain SPECT perfusion scans are emerging as potential biomarkers for identifying and separating comorbid conditions. For example, perfusion SPECT scans were able to differentiate traumatic brain injury (TBI) and post-traumatic stress disorder (PTSD) with a sensitivity of 92% and a specificity of 85% in a study of 196 veterans (6). Furthermore, these results were replicated in a civilian sample of over 24,000 individuals (7). In a recent study (8) SPECT perfusion scans could differentiate adults with attention-deficit hyperactivity disorder (ADHD) from normal controls with a sensitivity of 100% and a specificity of 97% in a study of over 1,000 individuals using regions of interest analysis of 3D Thresholded scan data. We (HS, JT, MM, and MvL) previously showed that 3D Thresholded SPECT scan analysis yielded greater sensitivity in detecting ADHD compared to conventional 2-D tomographic interpretation in a large retrospective analysis of 427 patients (5). Recently published procedure guidelines by Cohen et al. (9) reviews indications and applications for brain SPECT scans in a range of neuropsychiatric and psychiatric disorders. Pavel et al. (10) recently published an encyclopedic review of the SPECT findings associated with TBI, stroke, PTSD, dementia, and several neuropsychiatric conditions.

Perfusion SPECT has shown promise as a biomarker of previously subjective symptoms. SPECT was recently shown to provide an objective measure of pain in burn patients (11). SPECT also demonstrated specific findings in PTSD distinct from a trauma-exposed cohort (12). Perfusion SPECT has also been shown to provide objective evidence of neurophysiological changes in response to specific treatments, such as multi-watt infrared laser therapy for TBI (13), stem cell therapy for Lyme disease (14), and combined ketamine-transcranial magnetic stimulation (15). Studies have suggested SPECT scan data may improve clinical outcome by guiding treatment choices more quickly to successful strategies (4, 16–18). However, there has not been a study of perfusion SPECT scans as an objective measure of change in the broad spectrum of psychiatric disorders encountered in a community psychiatry practice.

Given the potential of brain SPECT perfusion scans to reveal comorbidities and to objectively indicate improvement in neuropsychiatric functioning, we have implemented the use of such scans in a community psychiatric practice from 2005 to 2019 to provide an additional measure of patients' clinical improvement, predominately in complex or treatment-unresponsive cases. In this paper we present a naturalistic retrospective study in which we compare the changes in the patients' 3D Thresholded SPECT scans with the improvements as assessed by conventional clinical observation and interview.

MATERIALS AND METHODS

3D Thresholded SPECT brain scans were offered to patients in the community psychiatric practice of one of the authors (JT) when a patient had refractory symptoms that had not responded to conventional treatments at least 6 months after the development of the mental health disorder. Otherwise, no other selection criteria were used. Where 3D Thresholded SPECT scans were initially offered, almost all patients (greater than 95%) accepted them. Risks, such as radiation exposure and the complex nature of the results, were explained to all patients offered scans and informed consent was obtained. All scans of these patients were processed to provide both 3D Thresholded SPECT scan displays and conventional SPECT scan tomographic images from the same raw SPECT data.

A total of 436 patients accepted 3D Thresholded SPECT scans before treatment. These patients were all offered a second scan after a period of treatment, again with informed consent, this time concerning a second scan. 73 of these patients accepted and underwent valid 3D Thresholded SPECT scans on average 450 days after (or during) a treatment. We herein present these

73 patients who received 3D Thresholded SPECT scans before and after (or during) a period of treatment.

Perfusion SPECT scans were performed at one of two tertiary care hospitals in Toronto, Ontario. The scanning procedures followed the guidelines of the Society of Nuclear Medicine (19). An intravenous dosage of 10–20 millicuries of Tc99m-hexamethylpropylene-amine oxime (HMPAO) (n = 53) or Tc99m-ethyl cysteinate dimer (ECD) (n = 19) was given. The patient then waited 30–60 min, and then the patient's head was imaged by gamma photon cameras. Both Tc99m-HMPAO and Tc99m-ECD radiotracers are taken up similarly by the brain, although they have small differences in retention and imaging activity (20). Whether a patient received Tc99m-HMPAO or Tc99m-ECD was independent of clinical diagnosis or other patient factors and depended on supply issues. In all cases except for one, a patient received the same type of radiotracer for the first and second SPECT scans.

All patients were scanned with a Picker Prism 3000 three-headed camera with continuous acquisition of a 128 × 128 pixel image via 120 steps (3 degrees/step) using fan beam collimation. A cloud of data pixels was obtained which represented the photons registered from the patient's brain. The cloud of data pixels was corrected for attenuation and filtered. The cloud of processed pixels was then sliced into orthogonal tomographic planes to produce what Schneider et al. (5) define as the "conventional SPECT" scan. As well, the cloud of pixels was also thresholded at various levels, i.e., only areas of activity exceeding a particular level of activity of the most active area of the patient's brain were displayed. For example, for surface views of the brain in the 3D Thresholded SPECT scans the pixels were thresholded at 55%, i.e., only pixels representing activity exceeding 55% of the most active areas of the brain were displayed. Within the interior of the brain, pixels were thresholded at levels representing activity exceeding 55, 85, and 92% of the most active areas of the brain. These thresholds reflect the work of Mena et al. (21), Darcourt et al. (22), and Payne et al. (23), and have been used by Amen (24) in tens of thousands of SPECT scans. Additional details concerning the scanning and thresholding process is given by Thornton et al. (25). These thresholded pixels are then rendered into a 3D form to produce what Schneider et al. (5) define as the "3D Thresholded SPECT" scan. **Figure 1** shows a conventional set of SPECT tomograms, along with an inferior view and a wire-frame view of the interior of the 3D Thresholded SPECT scan of a patient before and after treatment. **Figure 2** shows before and after treatment 3D Thresholded SPECT scans of additional patients.

The 3D Thresholded SPECT scans and the conventional SPECT scans from each patient were interpreted by a nuclear medicine radiologist with limited clinical information provided. To reduce confounding, all the radiologists agreed to read the scan based on what was seen in the image, rather than extrapolating from any clinical diagnoses. Some clinical information is required in all requests for imaging services in the community. Typically, the requisition form stated the patient's age, sex, occupation, the working diagnosis, and in some cases the patient's clinical progress. However, to reduce confounding and get the most objective comparison of before and after SPECT scans, the patient's progress was not emphasized. Again, as noted above, the radiologists reading the SPECT scans attempted to do so based on the imaging findings. The same radiologist would read a patient's 3D Thresholded SPECT images, and then read the Conventional SPECT images. There were four different radiologists who read different patients' images, but only one radiologist read any one particular patient's images, (i.e., there is no comparison possible between two different radiologists for one patient's images).

The radiologists systematically commented on the 3D Thresholded SPECT scans (i.e., providing their opinion about whether the patient's scan was worsening or improving). In reading the conventional SPECT scans, the radiologists provided a conventional report focused on any abnormalities in different neuroanatomical areas. The brain SPECT atlas compiled by Amen (24) was used as the reference source for normal versus abnormal SPECT images.

The one treating clinician independently considered whether each patient's clinical condition was worsening or improving as specified by the clinical notes prepared based on conventional clinical observation and patient interview. From this information, we then compared the direction of the patient's clinical condition, with the results of both the conventional and the 3D Thresholded SPECT scans to determine if the scan results represented a True Positive, False Negative, False Positive, or True Negative, for that patient. An improved or stable (i.e., non-worsening) clinical state with an improved or stable post-treatment SPECT scan compared to pre-treatment SPECT scan, would be a True positive. A worsened clinical state with a worsening in post-treatment SPECT scan compared to pre-treatment SPECT scan, would be a True Negative. An improved or stable (i.e., non-worsening) clinical state with a worsening in post-treatment SPECT scan compared to pre-treatment SPECT scan, would be a False Negative. A worsened clinical state with an improved or stable post-treatment SPECT scan compared to pre-treatment SPECT scan, would be a False Positive.

The True Positive, False Negative, False Positive, and True Negative values for the 73 patients' 3D Thresholded SPECT scans and the 73 patients' conventional SPECT scans were then used, by standard statistical methods, to calculate the sensitivity and the specificity for the 3D Thresholded SPECT scans and for the conventional SPECT scans. Software obtained from the Knowledge Translation Program (26) was used for statistical calculations.

RESULTS

Study Patient Population

As noted above, 73 patients received 3D Thresholded brain SPECT scans and conventional brain SPECT scans (both created from the same raw scanning data) before and after (or during) a period of treatment. The average age of patients was 49.6 years old with a standard deviation of 11.8 years. 60.3% of the patients were female. All patients were being treated by the same clinician (JT) at the time of both SPECT scans.

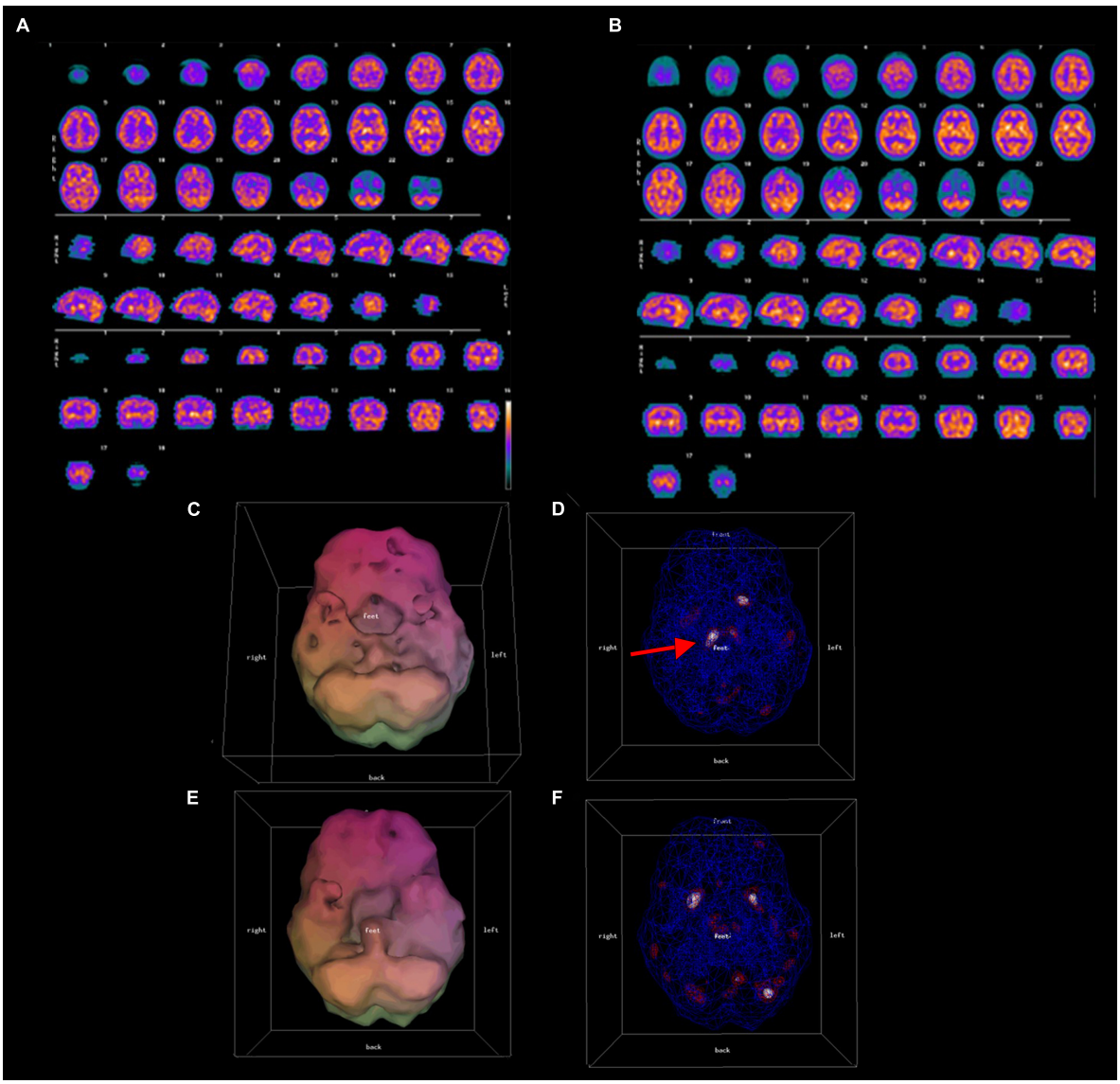

FIGURE 1 | Conventional **(A,B)** and 3D thresholded **(C–F)** displays of pre-treatment **(A,C,D)**, and post-treatment **(B,E,F)** SPECT scan results for one representative patient. A 49 year old male with symptoms of ADHD and mood dysregulation underwent a SPECT scan. Both conventional **(A)** and 3-D thresholded SPECT displays **(C,D)** prior to treatment show diffuse cortical hypoperfusion most severe in the bilateral temporal lobes and the orbitofrontal cortices, as well as over-activity of the thalamus [red arrow in panel **(D)**]. Post-treatment scans **(B,E,F)** show improved temporal, dorsal frontal, and parietal lobe perfusion, normalization of thalamic perfusion, and a reduction of hypoperfusion in the orbitofrontal cortices.

The average duration before and after scans, was 450 days. The DSM-5 diagnoses (27) or DSM-5-related diagnostic clusters of the patients are listed in **Table 1**. Many patients from early in the time period examined had DSM-IV or DSM-IV-TR diagnoses which were converted to equivalent DSM-5 or DSM-5-related diagnoses in **Table 1**.

Sensitivities and Specificities of 3D Thresholded SPECT Neuroimaging

Both pieces of data, i.e., the change in the 3D Thresholded SPECT scans and the change in the clinical functioning of the patient, are qualitative clinical interpretations, and thus at risk from bias for various reasons. However, a strong attempt was made by the radiologists to be consistent in 3D Thresholded SPECT reporting to a large extent independent of other factors. As noted above, the radiologists systematically commented on the 3D Thresholded SPECT scans, i.e., providing their opinion about whether the patient's scan was worsening or improving, following the interpretations according to the brain SPECT atlas compiled by Amen (24).

The sensitivity, specificity, and positive predictive value for 3D Thresholded SPECT and conventional SPECT results are shown in **Table 2**. Analysis of before and after treatment brain

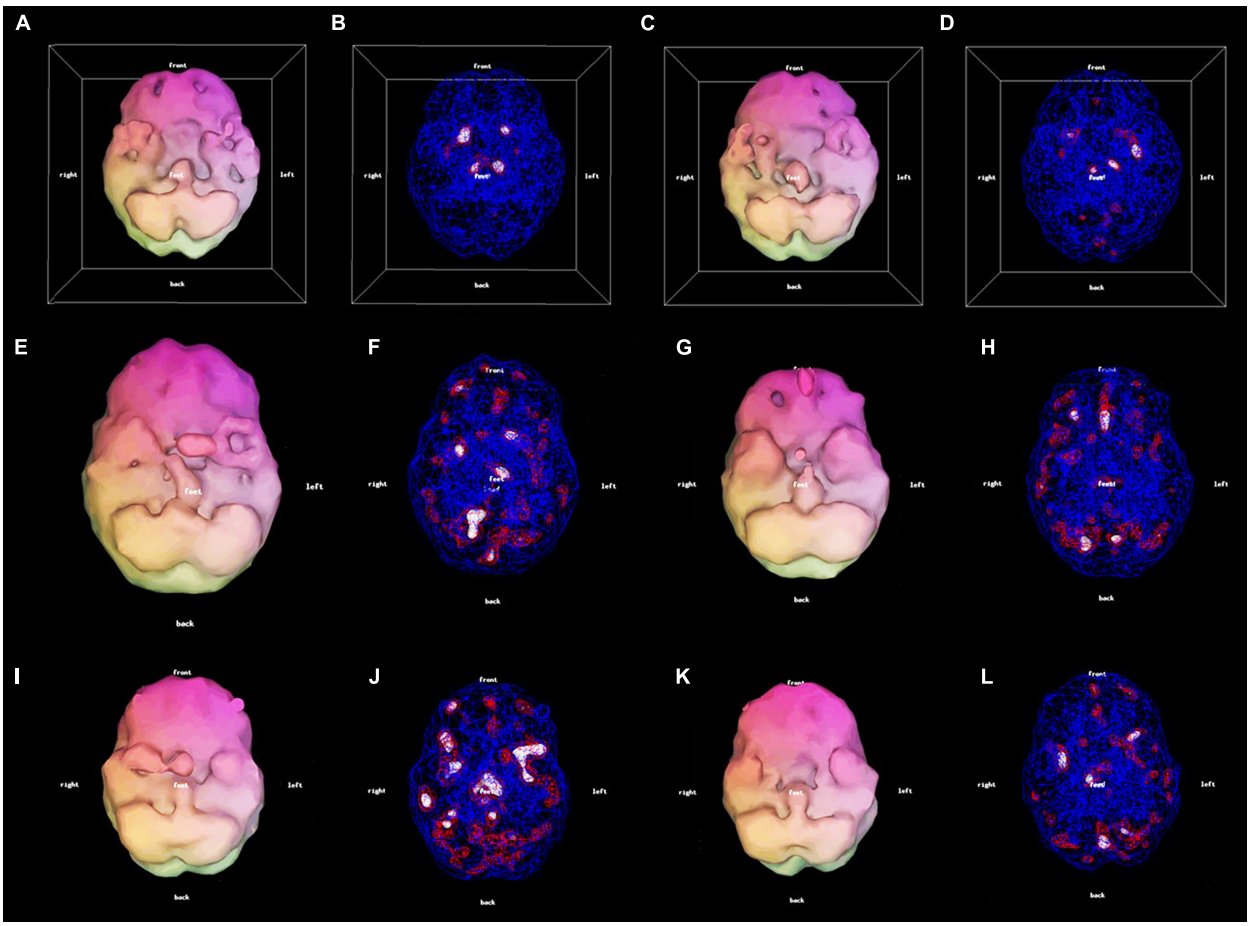

FIGURE 2 | 3D thresholded displays: 56-year-old female with Lyme disease pre-treatment **(A,B)** and post-treatment **(C,D)** clinically improved. 33-year-old male with mood dysregulation and ADHD pre-treatment **(E,F)** and post-treatment **(G,H)**. There was clinical improvement with a mood stabilizer. However, due to the prefrontal hypoperfusion **(G)** a stimulant was added resulting in further improvement. 26-year-old female with mTBI pre-treatment **(I,J)** and post-treatment **(K,L)** clinically improved.

3D Thresholded SPECT scans of 73 patients with all-cause psychiatric disorders, shows that they predict improvement (i.e., non-worsening to large improvement) in clinical functioning with a sensitivity of 94.3% (95% confidence interval 86-98%) and a specificity of 66.7% (95% confidence interval 21–94%).

Table 2 also shows the sensitivities, specificities, and positive predictive values for 3D Thresholded SPECT scans (and as well for the conventional ("2D") SPECT scans) in predicting improvement in the groups of patients with psychiatric disorders that occurred more commonly in this study. This is discussed in more detail below.

As noted above, due to supply issues out of the control of the clinician, 27% of the patients received Tc99m-ethyl cysteinate dimer (ECD) as the radiotracer, while the other 73% received Tc99m-HMPAO. Both Tc99m-HMPAO and Tc99m-ECD radiotracers are taken up similarly by the brain, although they have small differences in retention and imaging activity (20). For patients receiving ECD (n = 19), the before and after 3D Thresholded SPECT scans predicted improvements with a sensitivity of 88% (95% confidence interval 64–97%) and a specificity of 67% (95% confidence interval 21–94%). For patients receiving HMPAO (n = 53), the before and after 3D Thresholded SPECT scans predicted improvements with a sensitivity of 96% (95% confidence interval 87–99%). The specificity in this latter group is not computable as there are no false positives or true negatives in this sample.

Sensitivities and Specificities of Conventional SPECT Neuroimaging

As mentioned above, for each patient the raw brain SPECT data were used to generate conventional SPECT images as well as the 3D Thresholded SPECT images. A retrospective analysis of the before and the after treatment, conventional ("2D") brain SPECT images of the same 73 patients with all-cause psychiatric disorders, shows that they predict improvement in clinical functioning with a sensitivity of 25.7% (95% confidence interval 17–37%) and a specificity of 100% (albeit with a 95% confidence interval 44–100%). As noted above, due to the lack of full reporting by the nuclear radiologists on the conventional SPECT

TABLE 1 | Patient diagnoses.

Diagnostic cluster (DSM-5 diagnosis or chapter)	Number of patients	%	Mean age (standard deviation) (years)	Mean duration between scans (standard deviation)(days)
Attention-deficit/hyperactivity disorder	24	33%	47.5 (9.1)	347 (248)
Post-mTBI (mild traumatic brain injury) (DSM-5 chapter: Neurocognitive Disorders, those disorders "due to traumatic brain injury")	19	26%	45.4 (12.9)	405 (414)
Affective disorders (DSM-5 chapters: Bipolar and Related Disorders, Depressive Disorders)	11	15%	54.4 (16.9)	702 (1,043)
Psychotic disorders (DSM-5 chapter: Schizophrenia Spectrum and Other Psychotic Disorders)	4	5%	55.5 (7.0)	373 (305)
Post-viral chronic ("Long Haul") syndrome (DSM-5 chapter: Neurocognitive disorders, those disorders due to post-viral sequalae "due to another medical condition")	4	5%	51.8 (9.6)	263 (159)
Other neurological (DSM-5 chapter: Neurocognitive Disorders, due to neurological conditions)	4	5%	52.0 (11.2)	503 (396)
Chronic fatigue, fibromyalgia (DSM-5 diagnosis: Somatic Symptom Disorder)	3	4%	55.3 (10.0)	653 (479)
Anxiety disorders (DSM-5 chapter: Anxiety Disorders)	2	3%	51.0 (12.7)	896 (1118)
Chronic pain (DSM-5 diagnosis: Somatic Symptom Disorder, persistent, with predominant pain)	1	1%	42	105
Dementia (DSM-5 chapter: Neurocognitive Disorders, due to Alzheimer's disease or other medical conditions causing dementia)	1	1%	60	322
Total Patients	73			

TABLE 2 | Sensitivities, specificities and positive predictive values for conventional ("2D") brain SPECT and 3D thresholded brain SPECT images in predicting improvement in psychiatric disorders.

	Sensitivity (95% confidence interval)	Specificity (95% confidence interval)	Positive predictive value (PPV) (95% confidence interval)
All Conventional ("2D") SPECT Scans	25.7% (17-37%)	100% (44-100%)	100% (82%-100%)
All 3D Thresholded SPECT Scans	94.3% (86-98%)	66.7% (21%-94%)	98.5% (92-100%)
Scans by diagnosis			
Attention-Deficit Hyperactivity Disorder (ADHD)	3D:95.7% (79–99%)	3D:100% (21%–100%)	3D:100% (85–100%)
	2D:26.1% (13–47%)	2D:100% (21–100%)	2D:100% (61–100%)
Post-Mild Traumatic Brain Injury (mTBI)	3D: 89.5% (69–97%)	3D: not computable	3D: 100% (82–100%)
	2D:21% (9–43%)	2D: not computable	2D: 100% (51–100%)
Affective Disorders	3D: 100% (74–100%)	3D: not computable	3D: 100% (74–100%)
	2D:27.3% (10–57%)	2D: not computable	2D:100% (44–100%)
Psychotic Disorders	3D: 75% (30–95%)	3D: not computable	3D: 100% (44–100%)
	2D:0% (0–49%)	2D: not computable	2D: not computable
Post-Viral Chronic Syndromes	3D: 100% (44–100%)	3D: 100% (21–100%)	3D: 100% (44–100%)
	2D: 33.3% (6–79%)	2D: 100% (21–100%)	2D: 100% (21–100%)
Other Neurological	3D: 100% (44–100%)	3D: 0% (0–80%)	3D: 75% (30–95%)
	2D: 33.3% (6–79%)	2D:100% (21–100%)	2D: 100% (21–100%)

scans, the results are not directly comparable, although the magnitude of the values give a qualitative idea of the differences in the results of the methodologies. These values are in keeping with the low sensitivity rates found in the conventional brain SPECT scans by Schneider et al. (5) compared to the 3D Thresholded brain SPECT scans.

Inter-Rater Reliability of Radiologists

As noted above, there were four different nuclear medicine radiologists who read different patients' images, but only one radiologist read one patient's images, i.e., there is no comparison possible between two different radiologists for any one particular patient's images. However, as a rough estimate, if the patients with the largest common diagnosis in the study, which was ADHD, are examined, it is possible to see the sensitivities and specificities arrived at with different radiologists. There were three different radiologists who read the scans for patients with a diagnosis of ADHD. In **Table 3** it can be seen for the two radiologists who read the vast majority of the SPECT scans of patients in this sample with ADHD, both radiologists' scans were associated with similar sensitivities for the 3D Thresholded SPECT brain scan. Some

TABLE 3 | Sensitivities and specificities for conventional ("2D") brain SPECT and 3D thresholded brain SPECT scans in predicting improvement in patients with a diagnosis of ADHD associated with different nuclear medicine radiologists reading the scans.

Radiologist	3D thresholded SPECT sensitivity (95% confidence limits)	3D thresholded SPECT specificity (95% confidence limits)	2D conventional SPECT sensitivity (95% confidence limits)	2D conventional SPECT specificity (95% confidence limits)
A (*n* = 7)	100% (61–100%)	100% (21–100%)	0% (0–39%)	100% (21–100%)
B (*n* = 14)	100% (79–100%)	Not computable	43% (21–67%)	Not computable
C (*n* = 3)	67% (21–94%)	Not computable	0% (0–56%)	Not computable

of the specificities were not computable in **Table 3** due to the true negatives and false positives both being zero in these small sample sizes.

Applicability of the 3D Thresholded SPECT Scan Results to All-Cause Psychiatric Disorders

As can be seen from **Table 1**, the most frequent diagnoses or diagnostic clusters in this study were patients with ADHD, post-mild TBI (post-mTBI), affective disorders, psychotic disorders, post-viral chronic syndromes, and a group with "other neurological" diagnoses. **Table 2** shows the sensitivities, specificities, and positive predictive values for both conventional ("2D") brain SPECT images and 3D Thresholded SPECT images in predicting improvement in the groups of patients with these psychiatric disorders. Note that these do not necessarily represent the most common diagnoses in this clinician's practice; rather, these diagnoses were found among the complex or treatment-unresponsive cases.

DISCUSSION

The need exists in the community for psychiatric practitioners to be able to more objectively evaluate the response to treatment of patients with chronic psychiatric disorders. The implementation of longitudinal brain SPECT imaging in a community psychiatric practice is shown here to assist with such clinical evaluations. In considering 73 patients who received before and after treatment brain SPECT with 3D images, the SPECT scans predicted clinical improvement (non-worsening to large improvement) with a sensitivity of 94% (95% confidence interval 86–98%) and a specificity of 67% (95% confidence interval 21–94%). Thus, 3D thresholded brain SPECT imaging can assist the community psychiatric practitioner in the management of patients.

The more conventional 2D brain SPECT images from the same patients unfortunately predicted clinical improvement (non-worsening to large improvement) with a sensitivity of only 26% (95% confidence interval 17–37%). Thus, the data from this community study would indicate that the more conventional 2D brain SPECT imaging is less useful in assisting the community psychiatric practitioner in the management of patients. Other types of neuroimaging would also be expected to be less useful to the community psychiatric practitioner. For example, Raji et al. (28) review the literature to compare SPECT neuroimaging with other forms of neuroimaging in the setting of TBI. In this setting, conventional brain SPECT, as poor as it performed in our study above, was found to have significant advantages compared to computerized tomography (CT) or MRI in the detection of acute and chronic TBI, especially in mild TBI.

Although the sensitivity of the conventional 2D brain SPECT is poor at 26% (95% confidence interval 17–37%) its specificity was 100% (albeit with a 95% confidence interval 44–100%). If the confidence limits of the specificity are disregarded for a moment, the higher specificity of the conventional 2D brain SPECT is expected as changes in the brain images are more apparent on 3D images rather than on 2D images, and so, there will be fewer false positives read in the 2D conventional group (i.e., small changes will not appear significant as they may in a 3D thresholded image and will almost always be read as negative in the 2D image). In fact, in the 73 patients considered in this study, there were no false positives at all in the 2D brain SPECT results. Indeed, the specificity of the 3D thresholded brain SPECT was found to be lower at 67% (95% confidence interval 21–94%). On the other hand, the sensitivity of the 3D thresholded brain SPECT was found to be much higher at 94% (95% confidence interval 86–98%) again reflecting the ability to detect changes easier in the 3D thresholded brain SPECT scan.

From the perspective of the community psychiatric practitioner there is the question of whether a potential objective test such as brain SPECT imaging is applicable to only one particular diagnosis, [e.g. TBI, see (28)], or whether it can be useful in a community practice consisting of patients with a variety of psychiatric disorders. Even with regard to applying SPECT scanning to a particular diagnosis, Henderson and colleagues (29, 30), note that psychiatric diagnoses as defined by the Diagnostic and Statistical Manual 5 (DSM-5) of the American Psychiatric Association (APA) lack distinct boundaries from other diagnoses, as well as covering multiple combinations of disparate symptoms within the confines of a single diagnosis. Thus, it becomes difficult to identify a pure cohort of subjects with a common set of symptoms fitting a single distinct DSM-5 diagnosis in order to test a potential biomarker for sensitivity and specificity. As is shown in **Table 1**, the 73 patients studied in the community practice represented a variety of psychiatric diagnoses or diagnostic clusters. The most frequent diagnoses or diagnostic clusters in this study were patients with ADHD, post-mild TBI (post-mTBI), affective disorders, psychotic disorders, post-viral chronic syndromes and a group with "other neurological" diagnoses that were referred to psychiatry. **Table 2** shows the sensitivities, specificities, and positive predictive values for 3D Thresholded SPECT scans in

predicting improvement in the groups of patients with these psychiatric disorders. Additional research is required in order to evaluate the utility of 3D Thresholded SPECT scans in the large variety of patients the community psychiatric practitioner can encounter, but the results in **Table 2** indicate that it would seem by logical induction reasonable to consider that 3D Thresholded SPECT scans would yield useful results in the real-world diverse cases that present to the community psychiatric practice.

DATA AVAILABILITY STATEMENT

The datasets presented in this article are not readily available because they are derived from clinical patient data. Prefer to keep as confidential as possible. Requests to access the datasets should be directed to JT, jfthor@hotmail.com.

ETHICS STATEMENT

Ethical review and approval was not required for the study on human participants in accordance with the local legislation and institutional requirements. Written informed consent for participation was not required for this study in accordance with the national legislation and the institutional requirements.

AUTHOR CONTRIBUTIONS

JT was involved in the clinical care and imaging of patients, organizing, drafting, writing, and editing the manuscript. HS and TH were involved in organizing, drafting, writing, and editing the manuscript, and discussions concerning patient care and imaging. PC, MM, ML, SD, Y-HS, and JU were involved in organizing and editing the manuscript, and discussions concerning patient care and imaging. DP deceased at time of submission, was involved in discussions concerning patient care and imaging. All authors contributed to the article and approved the submitted version.

ACKNOWLEDGMENTS

Knowledge Translation Program, St. Michael's Hospital, Toronto, Canada for use of their statistical software. https://knowledgetranslation.net/.

REFERENCES

1. Mahmood T. Biomarkers in psychiatry: a clinician's viewpoint. *Br Med Bull.* (2020) 135:23–7. doi: 10.1093/bmb/ldaa019
2. Jueptner M, Weiller C. Review: does measurement of regional cerebral blood flow reflect synaptic activity? Implications for PET and fMRI. *Neuroimage.* (1995) 2:148–56. doi: 10.1006/nimg.1995.1017
3. Zerarka S, Pellerin L, Slosman D, Magistretti PJ. Astrocytes as a predominant cellular site of (99m)Tc-HMPAO retention. *J Cereb Blood Flow Metab.* (2001) 21:456–68. doi: 10.1097/00004647-200104000-00014
4. Henderson TA. Brain SPECT imaging in neuropsychiatric diagnosis and monitoring. *EPatient.* (2018) 1:40–7.
5. Schneider H, Thornton JF, Freeman MA, McLean MK, van Lierop MJ, Schneider J. Conventional SPECT versus 3D thresholded SPECT imaging in the diagnosis of ADHD: a retrospective study. *J Neuropsychiatry Clin Neurosci.* (2014) 26:335–43. doi: 10.1176/appi.neuropsych.12110280
6. Raji CA, Willeumier K, Taylor D, Tarzwell R, Newberg A, Henderson TA, et al. Functional neuroimaging with default mode network regions distinguishes PTSD from TBI in a military veteran population. *Brain Imaging Behav.* (2015) 9:527–34. doi: 10.1007/s11682-015-9385-5
7. Amen DG, Raji CA, Willeumier K, Taylor D, Tarzwell R, Newberg A, et al. Functional neuroimaging distinguishes posttraumatic stress disorder from traumatic brain injury in focused and large community datasets. *PLoS One.* (2015) 10:e0129659. doi: 10.1371/journal.pone.0129659
8. Amen DG, Henderson TA, Newberg A. SPECT functional neuroimaging distinguishes adult attention deficit hyperactivity disorder from healthy controls in big data imaging cohorts. *Front Psychiatry.* (2021) 12:725788. doi: 10.3389/fpsyt.2021.725788
9. Cohen PF, Tarzwell R, Numerow L, Siow Y-H, Uszler JM, Pavel DG, et al. *Canadian Association of Nuclear Medicine (CANM) Guidelines for Brain Perfusion Single Photon Emission Computed Tomography (SPECT).* (2021). Available online at: https://www.canm-acmn.ca/guidelines (accessed March 2, 2022).
10. Pavel DG, Henderson TA, DeBruin S. The legacy of the TTASAAN report – premature conclusions and forgotten promises: a review of policy and practice part I. *Front Neurol.* (2022) (in press).
11. Bermo M, Saqr M, Hoffman H, Patterson D, Sharar S, Minoshima S, et al. Utility of SPECT functional neuroimaging of pain. *Front Psychiatry.* (2021) 12:705242. doi: 10.3389/fpsyt.2021.705242
12. Lindauer RJ, Booij J, Habraken JB, Uylings HB, Olff M, Carlier IV, et al. Cerebral blood flow changes during script-driven imagery in police officers with posttraumatic stress disorder. *Biol Psychiatry.* (2004) 56:853–61. doi: 10.1016/j.biopsych.2004.08.003
13. Henderson TA, Morries LD. SPECT perfusion imaging demonstrates improvement of traumatic brain injury with transcranial near-infrared laser phototherapy. *Adv Mind Body Med.* (2015) 29: 27–33.
14. Shroff G. Single-photon emission tomography imaging in patients with Lyme disease treated with human embryonic stem cells. *Neuroradiol J.* (2018) 31:157–67. doi: 10.1177/1971400917742470
15. Haustrup N, Best S, Pavel D. Brain SPECT as an imaging biomarker for evaluating effects of novel treatments in psychiatry – a case series. *Front Psychiatry.* (2022) 12:713141. doi: 10.3389/fpsyt.2021.713141
16. Amen DG, Highum D, Licata R, Annibali JA, Somner L, Pigott HE, et al. Specific ways brain SPECT imaging enhances clinical psychiatric practice. *J Psychoactive Drugs.* (2012) 44:96–106. doi: 10.1080/02791072.2012.684615
17. Amen DG, Jourdain M, Taylor DV, Pigott HE, Willeumier K. Multi-site six-month outcome study of complex psychiatric patients evaluated with addition of brain SPECT imaging. *Adv Mind Body Med.* (2013) 27:6–16.
18. Amen DG, Easton M. A new way forward: how brain SPECT imaging can improve outcomes and transform mental health care into brain health care. *Front Psychiatry.* (2021) 12:715315. doi: 10.3389/fpsyt.2021.715315
19. Juni JE, Waxman AD, Devous MD Sr, Tikofsky RS, Ichise M, Van Heertum RL, et al. Procedure guideline for brain perfusion SPECT using (99m)Tc radiopharmaceuticals 3.0. *J Nucl Med Technol.* (2009) 37:191–5. doi: 10.2967/jnmt.109.067850
20. Léveillé J, Demonceau G, Walovitch RC. Intrasubject comparison between technetium-99m-ECD and technetium-99m-HMPAO in healthy human subjects. *J Nucl Med.* (1992) 33:480–4.
21. Mena FJ, Mena I, Alamos BA, Solé C, Neubauer S, de la Barra F. SPECT Tc99m-HMPAO brain uptake in normal children: a comparison to normal elderly subjects. *Alasbimn J.* (1998) 1:AJ01-3.
22. Darcourt J, Mena I, Cauvin J-C, Miller BL. Absolute calibration of HMPAO SPECT using 133-Xe rCBF values. *Alasbimn J.* (1999) 2.

23. Payne JK, Trivedi MH, Devous MD Sr. Comparison of technetium-99m-HMPAO and xenon-133 measurements of regional cerebral blood flow by SPECT. *J Nucl Med.* (1996) 37:1735–40.
24. Amen DG. *Images of Human Behavior: A Brain SPECT Atlas*. Newport Beach, CA: Mindworks Press (2004).
25. Thornton JF, Schneider H, McLean MK, van Lierop MJ, Tarzwell R. Improved outcomes using brain SPECT-guided treatment versus treatment-as-usual in community psychiatric outpatients: a retrospective case-control study. *J Neuropsychiatry Clin Neurosci.* (2014) 26:51–6. doi: 10.1176/appi.neuropsych.12100238
26. Knowledge Translation Program. *Evidence-Based Medicine Toolbox*. (2021). Available online at: https://knowledgetranslation.net/ (accessed March 2, 2022).
27. APA. *American Psychiatric Association: Diagnostic and Statistical Manual of Mental Disorders*. 5th ed. Arlington, VA: American Psychiatric Publishing (2013).
28. Raji CA, Tarzwell R, Pavel D, Schneider H, Uszler M, Thornton J, et al. Clinical utility of SPECT neuroimaging in the diagnosis and treatment of traumatic brain injury: a systematic review. *PLoS One.* (2014) 9:e91088. doi: 10.1371/journal.pone.0091088
29. Henderson TA, Uszler JM, Rossiter-Thornton JF, Siow Y-H, Pavel DG, McLean M, et al. The American psychiatric association fails to recognize the value of neuroimaging in psychiatry. *Interv Med Clin Imaging.* (2019) 1:1–8.
30. Henderson TA, van Lierop MJ, McLean M, Uszler JM, Thornton JF, Siow YH, et al. Functional neuroimaging in psychiatry-aiding in diagnosis and guiding treatment. what the American psychiatric association does not know. *Front Psychiatry.* (2020) 11:276. doi: 10.3389/fpsyt.2020.00276

Conflict of Interest: SD is President at Good Lion Imaging LLC, a neuroimaging-related company. JU is the Medical Director of DrSpectScan.org, a clinical service corporation and derives 25% of his income from neuroimaging. Y-HS derives 10% of his income from neuroimaging. DP is deceased. TH is the president and principal owner of The Synaptic Space, a neuroimaging consulting firm. He is also CEO and Chairman of the Board of Neuro-Luminance Corporation, a medical service company. He is also president and principal owner of Dr. Theodore Henderson, Inc, a medical service company. TH has no ownership in, and receives no remuneration from, any neuroimaging company. No more than 5% of his income is derived from neuroimaging.

The remaining authors declare that the research was conducted in the absence of any commercial or financial relationships that could be construed as a potential conflict of interest.

frontiers in Neurology

POLICY AND PRACTICE REVIEWS
published: 28 March 2022
doi: 10.3389/fneur.2021.749579

The Legacy of the TTASAAN Report—Premature Conclusions and Forgotten Promises: A Review of Policy and Practice Part I

Dan G. Pavel[1,2†], *Theodore A. Henderson*[2,3,4,5*] *and Simon DeBruin*[2,6]

[1] *Pathfinder Brain SPECT Imaging, Deerfield, IL, United States,* [2] *The International Society of Applied Neuroimaging (ISAN), Denver, CO, United States,* [3] *The Synaptic Space, Inc., Denver, CO, United States,* [4] *Neuro-Luminance, Inc., Denver, CO, United States,* [5] *Dr. Theodore Henderson, Inc., Denver, CO, United States,* [6] *Good Lion Imaging, Columbia, SC, United States*

Brain perfusion single photon emission computed tomography (SPECT) scans were initially developed in 1970's. A key radiopharmaceutical, hexamethylpropyleneamine oxime (HMPAO), was originally approved in 1988, but was unstable. As a result, the quality of SPECT images varied greatly based on technique until 1993, when a method of stabilizing HMPAO was developed. In addition, most SPECT perfusion studies pre-1996 were performed on single-head gamma cameras. In 1996, the Therapeutics and Technology Assessment Subcommittee of the American Academy of Neurology (TTASAAN) issued a report regarding the use of SPECT in the evaluation of neurological disorders. Although the TTASAAN report was published in January 1996, it was approved for publication in October 1994. Consequently, the reported brain SPECT studies relied upon to derive the conclusions of the TTASAAN report largely pre-date the introduction of stabilized HMPAO. While only 12% of the studies on traumatic brain injury (TBI) in the TTASAAN report utilized stable tracers and multi-head cameras, 69 subsequent studies with more than 23,000 subjects describe the utility of perfusion SPECT scans in the evaluation of TBI. Similarly, dementia SPECT imaging has improved. Modern SPECT utilizing multi-headed gamma cameras and quantitative analysis has a sensitivity of 86% and a specificity of 89% for the diagnosis of mild to moderate Alzheimer's disease—comparable to fluorodeoxyglucose positron emission tomography. Advances also have occurred in seizure neuroimaging. Lastly, developments in SPECT imaging of neurotoxicity and neuropsychiatric disorders have been striking. At the 25-year anniversary of the publication of the TTASAAN report, it is time to re-examine the utility of perfusion SPECT brain imaging. Herein, we review studies cited by the TTASAAN report vs. current brain SPECT imaging research literature for the major indications addressed in the report, as well as for emerging indications. In Part II, we elaborate technical aspects of SPECT neuroimaging and discuss scan interpretation for the clinician.

Keywords: dementia, traumatic brain injury, seizure, neurotoxicity, depression, bipolar disorder, ADHD, PTSD-posttraumatic stress disorder

OPEN ACCESS

Edited by:
Kristen Willeumier, Independent Researcher, Beverly Hills, United States

Reviewed by:
Daniel Gregory Amen, Amen Clinics, Inc., United States
Rodolfo Gabriel Gatto, University of Illinois at Chicago, United States

***Correspondence:**
Theodore A. Henderson
thesynapticspace7@gmail.com

[†]*Deceased*

Specialty section:
This article was submitted to Applied Neuroimaging, a section of the journal Frontiers in Neurology

Received: *29 July 2021*
Accepted: *14 December 2021*
Published: *28 March 2022*

Citation:
Pavel DG, Henderson TA and DeBruin S (2022) The Legacy of the TTASAAN Report—Premature Conclusions and Forgotten Promises: A Review of Policy and Practice Part I. Front. Neurol. 12:749579. doi: 10.3389/fneur.2021.749579

INTRODUCTION

In 1996, the Therapeutics and Technology Assessment Subcommittee of the American Academy of Neurology (TTASAAN) issued a report regarding the use of single photon emission computed tomography (SPECT) in functional brain imaging (1). Although the TTASAAN report was published in January 1996, it was completed and approved for publication in October of 1994. Consequently, the referenced brain SPECT studies relied upon to derive the conclusions of the TTASAAN report predominately pre-dated the introduction of stabilized radiopharmaceuticals in 1993. In fact, of the 97 references in the TTASAAN report, only 12 are from 1993 or later. Furthermore, the early gamma cameras used for SPECT neuroimaging were single-headed cameras with limited resolution. Thus, the conclusions provided in the TTASAAN report were premature.

In the 25 years since the TTASAAN report, the American Academy of Neurology (AAN) has never deemed to re-examine their premature position on the use of brain perfusion SPECT in the evaluation of traumatic brain injury (TBI), stroke, seizure disorders, dementia, and neuropsychiatric conditions. Despite extensive advances in technology, software, and technique, as well as, for example, the publication of over 120 research studies and articles and published data from over 23,000 subjects on the use of SPECT just in the evaluation of TBI, the AAN has largely taken an overcautious, and sometimes dismissive, position toward the use of SPECT scans. In contrast, the European Association of Nuclear Medicine (EANM) (2) has deemed that brain perfusion SPECT scans are appropriate for the evaluation of TBI and that SPECT scans have predictive value in the clinical outcome of TBI (2). Moreover, the Canadian Association of Nuclear Medicine recently has issued guidelines on the use of SPECT imaging in the evaluation of TBI, stroke, dementia, neurotoxicity, and psychiatric conditions (3).

Curiously, the authors of the TTASAAN report made it clear that this report was neither a position paper nor a solidified assessment of SPECT. The authors unambiguously articulated that the assessment was to be revised as the field advanced. Quoting from the opening paragraph of the TTASAAN report (1):

> *"This paper, provided to the Academy membership as an educational tool, will be subjected to periodic revision as new information becomes available."*

The periodic revision has never occurred. In many ways, this is the equivalent of assessing Xray computed tomography (CT) in its infancy and then never re-assessing its merit thereafter. The first CT scanner became commercially available in 1972. CT neuroimaging was met with skepticism among neurologists (4). CT neuroimaging was deemed, "a passing fancy." The American Neurological Association published a report in 1975 stating the new method of imaging the nervous system would greatly reduce the need for neurologists. Numerous articles in the late 1970's criticized CT neuroimaging for its failure to accurately detect brain pathology (5–8) during the early years of its clinical use. In 1975, a commission of the AAN reported,

> *"A CT scan can give a more accurate localization in far less time than a neurologist. Ultrasound of the carotid arteries can localize and indicate the degree of stenosis more accurately than a clinician with a stethoscope. The portent for the future is that neurologists who rely exclusively on their wits and their pins and hammers, unaware the machine age has finally come to neurology, may become obsolete"* (9).

Despite the initial skepticism and concern that CT neuroimaging would replace the need for neurologists, the use of CT scanning expanded exponentially. CT neuroimaging is now a cornerstone of neurological evaluations, particularly in the acute setting. Nonetheless, as will be elaborated below, CT is very limited in what it can reveal about brain function.

In the same 25-year period, functional magnetic resonance imaging (fMRI) has undergone explosive growth. Hundreds of millions of dollars in research funding in the United States have been poured into fMRI studies. According to PubMed, over 40,000 research articles have been published. Despite the massive investment of time and effort, fMRI has yet to provide a clinically useful diagnostic tool for assessing brain function in individual cases. Indeed, the American Psychiatric Association recently issued a position paper (10) stating,

> *"(fMRI) neuroimaging has yet to have a significant impact on the diagnosis or treatment of individual patients in clinical settings."*

Moreover, a recent analysis of post-processing statistical validity revealed that a potentially staggering 70% of fMRI studies had false positive results (11), which could mean much of the fMRI research findings are invalid. The AAN has seemingly scrupulously ignored this serious caveat to the application of fMRI in research or clinical practice (12).

Similarly, extensive funding and effort has been invested in diffusion tensor imaging. However, it has been plagued by inconsistencies across centers due to technical elements arising from different hardware, competing software, varying sequences, dissimilar reconstruction algorithms, and technique. For example, eddy current distortion is often found to be larger than the acquisition voxel size (13). While a thorough analysis of diffusion tensor imaging is beyond the scope of this review, it will suffice to say that anisotropy can be either elevated or depressed following TBI. There have been numerous studies with contradictory findings (14, 15). Variations in technique or the unreliability of diffusion tensor imaging in TBI has been suggested as the cause for the conflicting data (14, 15).

Thus, while the AAN, and neurologists in general, have distanced themselves from SPECT neuroimaging based, in part, on the now outdated TTASAAN report and embraced other technologies, they have been left with technically flawed methods of visualizing brain function (11, 14, 15). Meanwhile, extensive advancements have been made in the practice and technology of perfusion SPECT neuroimaging and massive databases have been accumulated. Together, these factors lead to the need to re-examine the policy and practice set forth by the AAN in 1996.

Defining SPECT

SPECT is a type of nuclear medicine scan to create 2-dimensional (2-D) and 3-dimensional (3-D) pictures of functional processes within the patient's body. A radiopharmaceutical is administered to detect specific activities within the body. A gamma camera measures the radiation emitted by the radiopharmaceutical and rotates around the patient to acquire a set of 2-D planar images. Using a reconstruction technique, these planar images are reconstructed into a 3-D volume from which slices at various angles can be extracted to visualize the distribution of activity within the patient's body. In the case of perfusion SPECT neuroimaging, the radiopharmaceutical is transported via the bloodstream and is quickly taken up by neurons (16) (see below), such that the uptake of radiotracer is dependent upon, and therefore reflective of, the regional cerebral blood flow (rCBF). Cerebral blood flow at the level of cortical columns or functional subregions is regulated by neuronal activity. Increased activity induces increased local blood flow, while decreased activity results in reduced blood flow. The detection of the radiotracer uptake throughout the brain allows the clinician to identify both areas of hypoperfusion (hypo-functioning) and of increased perfusion (hyper-functioning). SPECT post-processing generates tomograms and a 3-D mapped representation of the brain, *ideally* with color-coded intensities proportional to rCBF which correlate with the brain function in that region.

ASSESSMENT OF GUIDELINES AND IMPLICATIONS

The Technical Aspects of Early SPECT Neuroimaging

Brain perfusion SPECT scans were initially developed in the 1970's. After the development of the Anger scintillation detector in 1950 (17) and the invention of the Anger circuitry in 1969 (17), several groups developed scintillation cameras. Paul Harper et al. with the University of Chicago first explored transaxial tomography using the Anger camera (18). The first whole body SPECT cameras were developed by 1976 (17). Brill et al. at Vanderbilt University and Jaszczak et al. at Searle Radiographics independently developed brain-specific gamma cameras.

While the technology of the scintillation camera was ongoing, the development of brain specific tracers was advancing rapidly. The early SPECT cerebral blood flow studies utilized ^{133}Xenon which can provide a quantitative measure of cerebral blood flow. However, ^{133}Xenon has relatively low energy and required a special breathing apparatus which was cumbersome and uncomfortable for the patient. Tracers with high energy gamma radiation were sought and ^{123}Iodine (^{123}I) or ^{99m}Technetium (^{99m}Tc) became the primary candidate radiolabels. An ^{123}I tracer, ^{123}I-N-isopropyl-iodo-amphetamine (^{123}I-IMP), was developed in 1980 for cerebral perfusion using iodinated amphetamine. It could be tagged with either ^{123}I or ^{125}I. This tracer showed high brain extraction and linear uptake over a wide range of blood flow rates (19). It remains in use today; however, there were some distinct disadvantages to this tracer. The first is the use of ^{123}I requires pretreatment to protect the thyroid. The second is that the tracer is redistributed from the lungs to the brain over the first 20 min after injection leading to a smearing of activity over time. Brain areas demonstrating high cerebral blood flow at the time of injection may not maintain that level of blood flow during the 20-min interval when ^{123}I-IMP is cleared from the lungs and accumulates in the brain (16).

The more lipophilic agent propylene amine oxime, which could be labeled with ^{99m}Tc, was explored as a brain perfusion tracer during the late 1970's and early 1980's. Initial agents had rapid clearing and so required fast imaging. In 1985, a methylated version of the agent was developed, which had almost ideal properties—^{99m}Tc- hexamethylpropyleneamine oxime (HMPAO) (20). First, ^{99m}Tc has a long half-life of 6 h and can be made independent of a cyclotron. Second, neither ^{99m}Tc nor HMPAO interfere with any biological processes in the body, unlike ^{123}I or the amphetamine tracer. Third, HMPAO is retained in the cell due to conversion to a less lipophilic form, which reduces washout and prolongs the window for scanning to several hours (16, 20–22). Fourth, the accumulation of HMPAO in the brain is very rapid, being virtually complete in 40 s and it maintains a fixed distribution after 5 min (16, 22). Thus, the scan measures the cerebral blood flow at the time of injection, not at the time the scan is actually performed. In essence, a SPECT scan captures a frozen image of brain function at the time of injection (16, 22). This makes ^{99m}Tc-HMPAO ideal for capturing brain activity during transient conditions (e.g., seizures, transient ischaemic attacks) or psychological challenges (e.g., concentration tasks). At very high perfusion rates, ^{99m}Tc-HMPAO accumulation and back diffusion becomes disproportional; thus, ^{99m}Tc-HMPAO uptake is non-linear compared to ^{133}Xenon (16, 23). Lassen et al. (23) proposed a correction algorithm which has been shown to closely approximate rCBF in comparison to $^{15}CO_2$ PET (24). Nevertheless, accumulation is linear within the normal physiological range in the human brain (16, 23).

Limited Stability of HMPAO Pre-1996

At the time that ^{99m}Tc-HMPAO was originally approved by the FDA in 1988, a key technical flaw still remained. The agent was unstable and would decompose rapidly after reconstitution. Realistically, it was only viable for 30 min after reconstitution (16). The work of quality checking, measuring the radioactivity, calculating and drawing up the dose, and patient preparation had to be accomplished very hastily prior to injecting the patient. As a result, the quality of the SPECT images varied greatly based on the deftness and technique of the technologist handling the tracer. In 1993, the addition of methylene blue proved effective in stabilizing HMPAO for several hours after reconstitution. This contributed to improved scan quality.

HMPAO was not truly stabilized for clinical application until 1993. In addition, most of the brain SPECT perfusion studies pre-1994 were performed on single-head gamma cameras. Since, then the quality of SPECT neuroimaging has greatly improved with the use of multi-head gamma cameras (See **Figure 1**). In addition, refinements in post-processing, as well as the introduction of statistical comparison to normative databases, have greatly enhanced the quality and diagnostic capacity of SPECT scans.

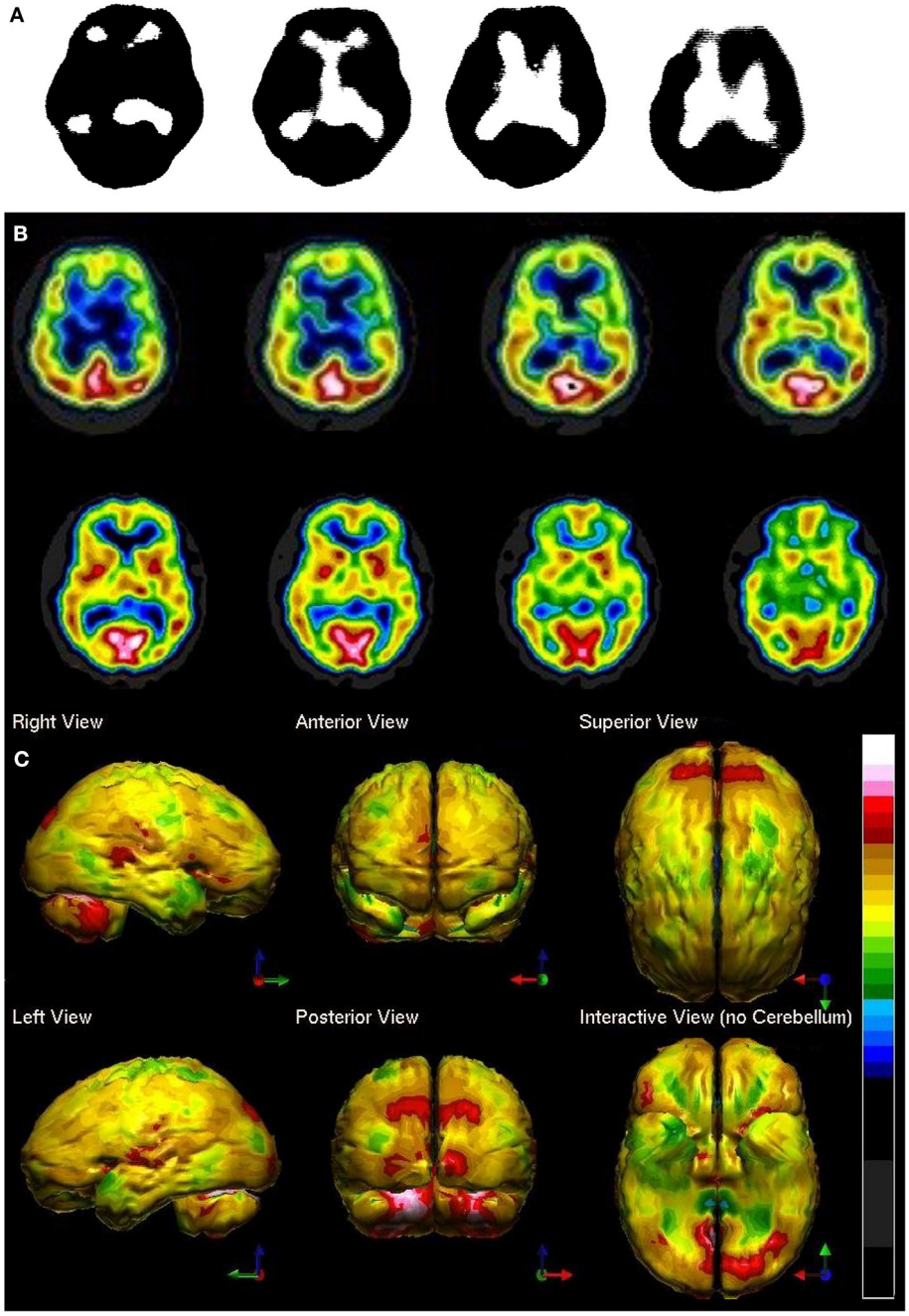

FIGURE 1 | Perfusion SPECT scan of normal control. **(A)** Four horizontal tomograms from a ^{99m}Tc-ECD perfusion SPECT scan performed on a single-headed gamma camera in 1989 [The figure was originally published in JNM. © SNMMI (25)]. **(B)** Eight horizontal tomograms from a modern ^{99m}Tc-HMPAO perfusion SPECT scan obtained from a dual-headed gamma camera. The color scale is scaled relative to the patient's mean cerebral perfusion. Mean blood flow (72%) is in yellow. Color shifts occur at approximately every 0.5 SD (3%) relative to the patient's mean. Details of the brain can be appreciated, including the thalamus, head of the caudate nuclei, lentiform nuclei, anterior cingulate gyri, and distinct cortical regions. **(C)** The modern SPECT scan displayed in 3-dimensional reconstruction. Increased perfusion in the visual cortex and the slightly lower average perfusion level in the temporal lobes bilaterally can be appreciated. The color scale is the same as **(B)**.

Display Limitations

Early SPECT studies were compromised by limitations of post-processing and display. Methods for correcting energy attenuation were imprecise. Displays were often essentially binomial—-above a certain threshold (1) the display showed black and below that threshold (0) the display showed an absence of black, as illustrated in **Figures 1A**, **3C**. Some effort at a gray scale was introduced by Ismael Mena and his group at Harbor

UCLA as illustrated in **Figure 3B**. The challenge with SPECT scans is that they are detecting changes in *degree* of function, which is displayed as changes in the *intensity* of the signal. Greyscale permits finer details to be seen, making it ideal for anatomical MRI; however, when discerning changes in intensity over large areas, color displays improve detection. For example, Stapleton et al. (29) examined this issue using SPECT scan data. The study involved the use of scan data from one-half of a brain, which was then inverted to create a symmetrical template of a brain. Then an artificial defect was created in the cerebellum by decreasing pixel values in the designated area by 1–12.5%. This construct was displayed in greyscale, a red color scale similar to "heated object," and blue/green/red where low counts were blue, mid counts were green and high counts were red. Despite the expressed bias toward greyscale among the radiologists tested, subject readers detected the artificial lesion much better in either of the color scales. In fact, the more subtle the lesion (pixel value decreases < 10%), the better color aided in detecting the lesion.

Humans, like all primates, have superior discrimination of color vision (30). One need only look at a Monet painting in greyscale to see the importance of color is discerning complex visual information. While greyscale allows superior detail discrimination, it does not foster the detection of changes in intensity. This was more recently demonstrated in fluid-attenuated inversion recovery (FLAIR) anatomical MRI in stroke (31). A large retrospective sample of FLAIR images were displayed in greyscale and a color scale. The addition of color increased detection of stroke and inter-rater agreement by 23%. The positive predictive value similarly increased from 85.3 to 95.7% (31).

Ismael Mena et al. at Harbor UCLA did extensive studies with normal subjects with ^{133}Xenon to determine quantitative data on the normal range of cerebral blood flow in humans (32). In a brief summary of an extensive body of work, mean cerebral blood flow was determined to be 70.3% of the maximum cerebral blood flow. The standard deviation (SD) was 8.35%. This work has been corroborated by several others and summarized by Devous et al. (33). **Figure 2** illustrates the mean ± 1 and ± 2 SD set against various color scales and greyscale. One can quickly see that in greyscale neither an increase in 2 SD nor a decrease in 2 SD can be detected. In contrast, in the Heated Object color scale a decrease of 2 SD can be easily discerned.

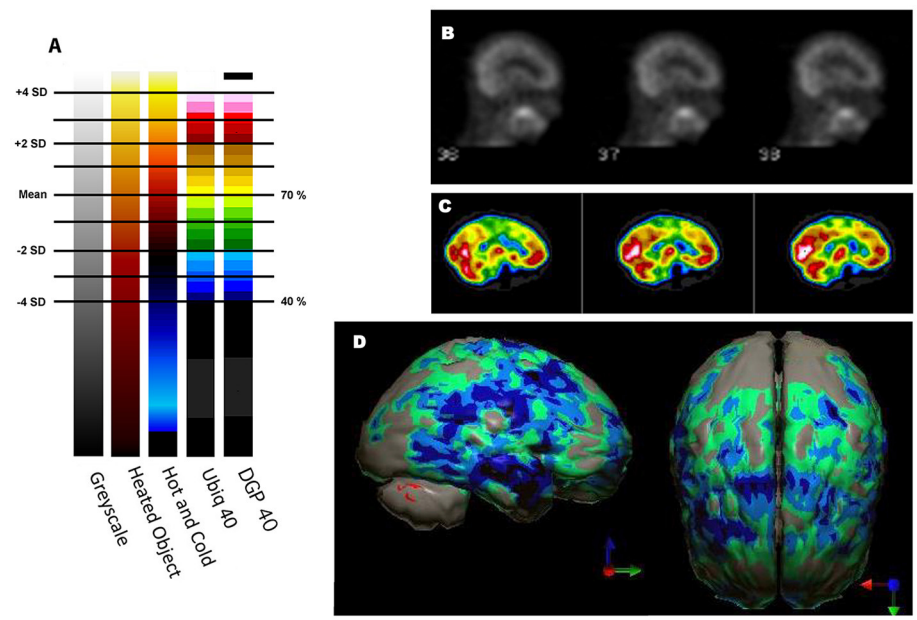

FIGURE 2 | Humans, like all primates, have superior discrimination of color vision. While greyscale allows superior detail discrimination, it does not foster the detection of changes in intensity. Since functional neuroimaging is about changes in the intensity of the signal, it is important that the observer can readily detect small changes. **(A)** Various commonly used color scales and a greyscale are displayed. The mean cerebral perfusion in the human brain is 70.3% of the maximal flow with a standard deviation (SD) of 8.35%. The mean and ± 1, 2 SD, 3 SD, and 4 SD are indicated. A change of ± 2 SD is unlikely to be appreciated in greyscale but can be readily distinguished in Heated Object, Ubiq40, and DGP40 color scales. An increase of 2 SD can be distinguished in Hot and Cold color scale, but a decrease of 2 SD or less would not be discernable. A 1 SD increase or decrease would be difficult to discern in greyscale, Heated Object and Hot and Cold color scale, but are readily detected in Ubiq40 and DGP40. **(B)** A representative low quality ^{99m}Tc-HMPAO perfusion SPECT scan demonstrates poor technique with the inclusion of extracranial structures. The scan was read in greyscale and interpreted as a normal scan. **(C)** The same patient was rescanned with proper technique. Decreased perfusion in the posterior frontal and temporal cortices can be appreciated when viewed using the Ubiq40 color scale. **(D)** The patient's data is compared to a normative database ($N = 68$). A map of statistically significant differences can be generated using the Oasis software by Segami, Inc. Here, the color scale indicates gray for areas that do not differ significantly from the normative database. In contrast, areas of green, light blue, and dark blue represent areas of more than 2, 3, and 4 SD below the mean perfusion of the normative database, respectively. Statistically significant increases in perfusion are illustrated in the red color scale. Decreased perfusion in the bilateral temporal cortex and bilateral posterior frontal cortex, but with sparing of the anterior cingulate gyri, can be appreciated. The findings are consistent with mild cognitive impairment of the frontal-temporal variant and the patient showed consistent findings on neuropsychological assessment.

It is less clear that a decrease of 1 SD or an increase of 1 or 2 SD could be detected in Heated Object scale. In the Hot and Cold color scale, both increases and decreases of 2 SD could be easily detected, but changes of 1 SD might be more challenging. Lastly, the Ubiq 40 color scale, developed by Ismael Mena based on his quantitative data, and the DGP40, developed by one of the authors - DGP, has incremental color changes at approximately 2.7%. Changes in perfusion as small as 0.3 SD can be detected in either direction. The distinction between the DGP40 and the Ubiq40 is that the top 2% of the DGP40 is black, which allow easy identification of the most active or highly perfused part of the brain. An illustrative case is provided in **Figure 2**—a patient with signs of mild cognitive impairment and decreased performance on neurocognitive testing. The scan in greyscale is read as normal (**Figure 2B**). The tomograms in Ubiq40 show subtle decreases in perfusion in the frontal and parietal cortices (**Figure 2C**). However, when the scan is compared to a normal database of age-matched controls, statistical analysis reveals a pattern of hypoperfusion consistent with mild cognitive impairment of the frontal-temporal variant. This case illustrates the value of using color scale for SPECT scans wherein changes in intensity are more important than anatomical detail.

Throughout this article, early SPECT scans in greyscale will be contrasted with modern SPECT scans using color display and statistical comparison to a normal database. The wealth of information that becomes visible in color scale is self-evident. Nonetheless, despite extensive research supporting the value of color display, many radiologists and nuclear medicine physicians persist in using greyscale to read SPECT scans.

ASSESSMENT OF THE STATE OF THE ART—SPECT IN BRAIN DISORDERS

Herein, we will provide technical background on the studies cited by the TTASAAN report and then provide technical details from state-of-the-art studies in modern brain perfusion SPECT imaging. We will begin with and illustrate most extensively the state of the art in the evaluation of head trauma and traumatic brain injury (TBI), because this indication has been quite controversial and has raised the most strident criticisms.

Head Trauma

The definition of TBI has evolved since the publication of the TTASAAN report. At that time, "concussion" was considered a transient state. Now concussion is recognized as a form of TBI, despite an absence of a loss of consciousness (LOC). Because of this shift and the recognition that: 1) concussions can have persistent effects on the brain (34, 35), 2) repeated concussions can have cumulative damage (36), and 3) persistent pathological changes can occur following even a single concussive event (37, 38), we refer to the Centers for Disease Control (36) for a basic definition of the levels of severity of TBI.

The World Health Organization defines post-concussion syndrome (PCS) as "persistence of a constellation of physical, cognitive, emotional and sleep symptoms beyond the usual recovery period after a concussion" (39), including 3 or more of the following after head injury: headache, dizziness, fatigue, irritability, insomnia, reduced tolerance of stress, concentration difficulty, or memory difficulty.

The TTASAAN report (1) included seven early studies of TBI with a total of 253 subjects. All studies were conducted on single-head gamma cameras. Two studies utilized ^{125}I-IMP and five studies utilized ^{99m}Tc-HMPAO with three of those studies conducted prior to the stabilization of HMPAO. All scans were assessed visually only. Jacobs et al. (40) will be discussed in detail below. Abdel-Dayem et al. (41) examined a series of 14 acute moderate-to-severe TBI cases with HMPAO SPECT scans performed within 72 h. Seven of the 14 cases did not survive. The number and extent of lesions observed by SPECT were compared to the number and extent of lesions seen by CT scan. Ducours et al. (42) examined 10 comatose TBI patients and 10 patients with TBI, but no LOC. All had a negative CT scan and a ^{125}I-IMP perfusion SPECT scan. Patients without LOC had a normal ^{125}I-IMP scan, while 9 out of 10 of the comatose patients had functional deficits on SPECT scan. Roper et al. (27) examined CT and HMPAO perfusion SPECT scans in 15 patients with mild, moderate or severe head injury (**Figure 3B**). SPECT revealed more focal lesions than CT. Gray et al. (28) examined 53 chronic (>6 months) TBI patients (20 mild, 33 severe TBI) compared to 14 normal controls using HMPAO SPECT (**Figure 3C**) and comparison to CT. Over 90% of the chronic severe TBI cases had areas of decreased perfusion on SPECT, but only 72% showed abnormalities on CT scan. Conversely, 100% of the patients with a normal SPECT scan had a normal CT scan. Ichise et al. (26) examined 29 chronic (> 6 months) TBI patients (15 mild, 14 severe TBI) and compared the HMPAO perfusion SPECT scans and neuropsychological testing results to those of 17 normal controls (**Figure 3A**). Trail Making A and B, Digit Symbol, and Wisconsin Card Sorting stood out as tests which strongly differentiated brain injured patients from controls ($p < 0.001$). Most lesions were in the frontal and temporal lobes and correlated with decreased neuropsychological scores on memory, attention, and executive function (26). Masdeu et al. (43) attempted to utilize negative controls (normal control) and positive controls (human immunodeficiency virus encephalopathy {HIV}) to examine mild TBI. Fourteen patients with mild TBI underwent CT scan and IMP or HMPAO perfusion SPECT scans within 48 h of head trauma. The results were compared to 15 normal controls and 12 patients with HIV encephalopathy. None of the normal controls were read as TBI; however, 40–50% of the TBI cases were read as HIV encephalopathy and 14–28% of the TBI cases were read as normal. The latter study highlights the jeopardy involved in visually interpreting SPECT scans, particularly in greyscale. As detailed above, the human eye is unable to separate 2 standard deviations in greyscale, because it is designed for color vision. Areas of hypoperfusion of <2 SD will be missed by visual read. Moreover, the absence of statistical comparison to a normative database or a matched set of normal also risks false negatives. This is strikingly demonstrated in **Figures 3–5**.

We (TAH, DGP), along with our colleagues, published a systematic review in 2014 which examined the entire extant literature on SPECT scans in the evaluation of TBI (44). The

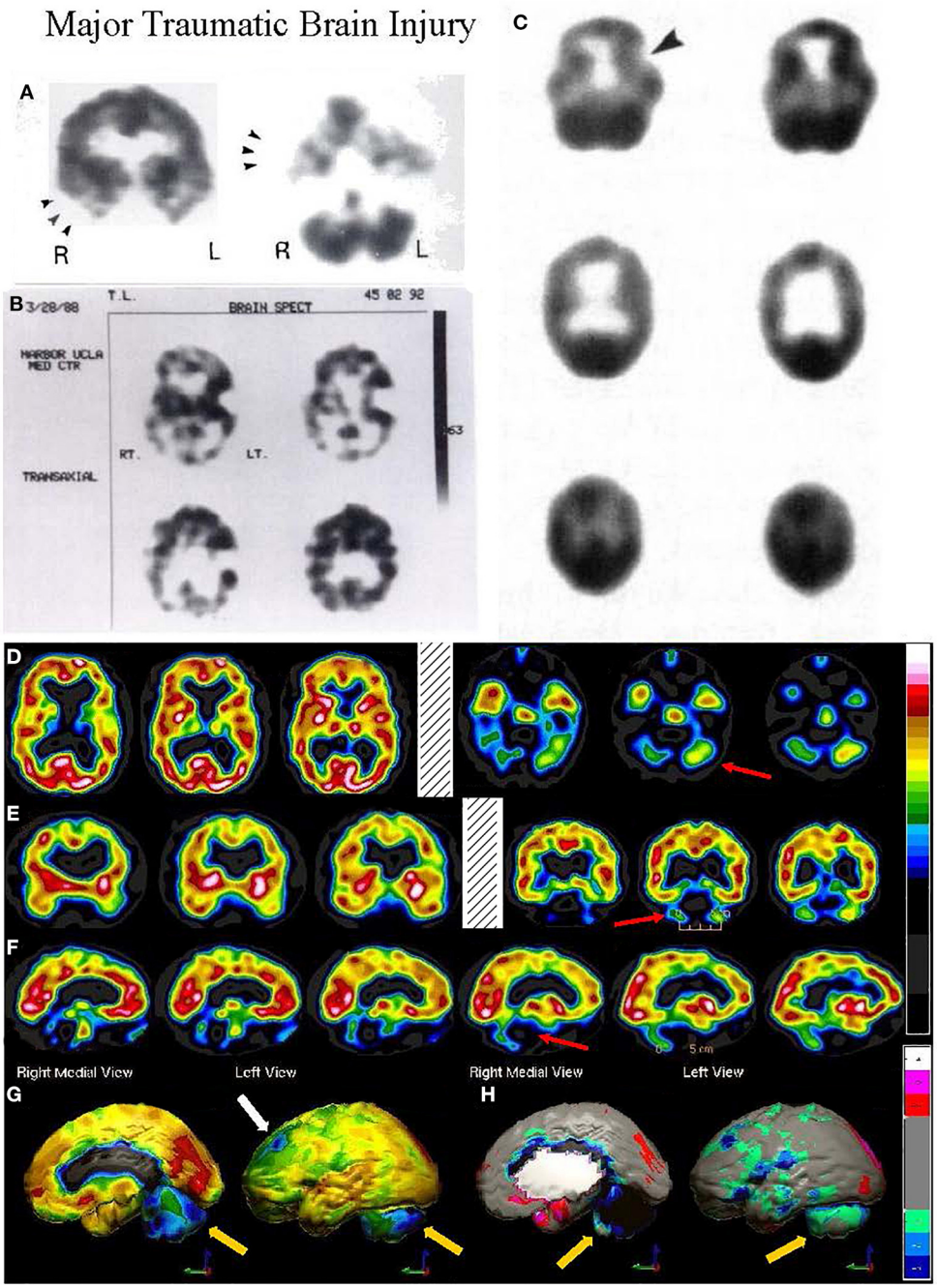

FIGURE 3 | (A–C) Examples of SPECT scans cited in TTASAAN report. Anatomical details are lacking. **(A)** 40-year-old female with major head trauma showed decreased perfusion of the right temporal lobe, whilst CT and MRI scans were normal [The figure was originally published in JNM. © SNMMI (26)], **(B)** 45-year-old male thrown from a horse showed decreased bilateral occipital perfusion [The figure was originally published in JNM. © SNMMI (27)]; **(C)** 37-year-old female with major head trauma from a motor vehicle accident (MVA). Perfusion is decreased in the bilateral frontal and temporal lobes [The figure was originally published in JNM. © SNMMI (28)]. **(D–F)** A 19-year-old woman was involved in a head-on collision MVA as a passenger. She suffered severe trauma to the back of her head. A modern ^{99m}mTc-HMPAO perfusion SPECT scan was performed with a dual-head camera. **(D)** Horizontal tomograms (non-sequential, break in sequence shown by cross-hatched bar) illustrate intact cortical function but marked hypoperfusion in the cerebellum bilaterally (red arrows). **(E)** Coronal tomograms (non-sequential). **(F)** Sagittal tomograms (sequential). **(G)** 3-D representation of SPECT scan data illustrating a small area of marked hypoperfusion in the left frontal cortex (white arrow) and profound hypoperfusion in the cerebellum (yellow arrows) which is more pronounced in the medial aspects. **(H)** The patient's data is compared to a normative database using Segami Inc. Oasis software. The color scale is the same as in **Figure 2D**. The injury to the left frontal cortex and lateral aspects of the frontal cortex can more clearly be visualized. Area of white in the right medial view is an area where there is no statistical comparison data.

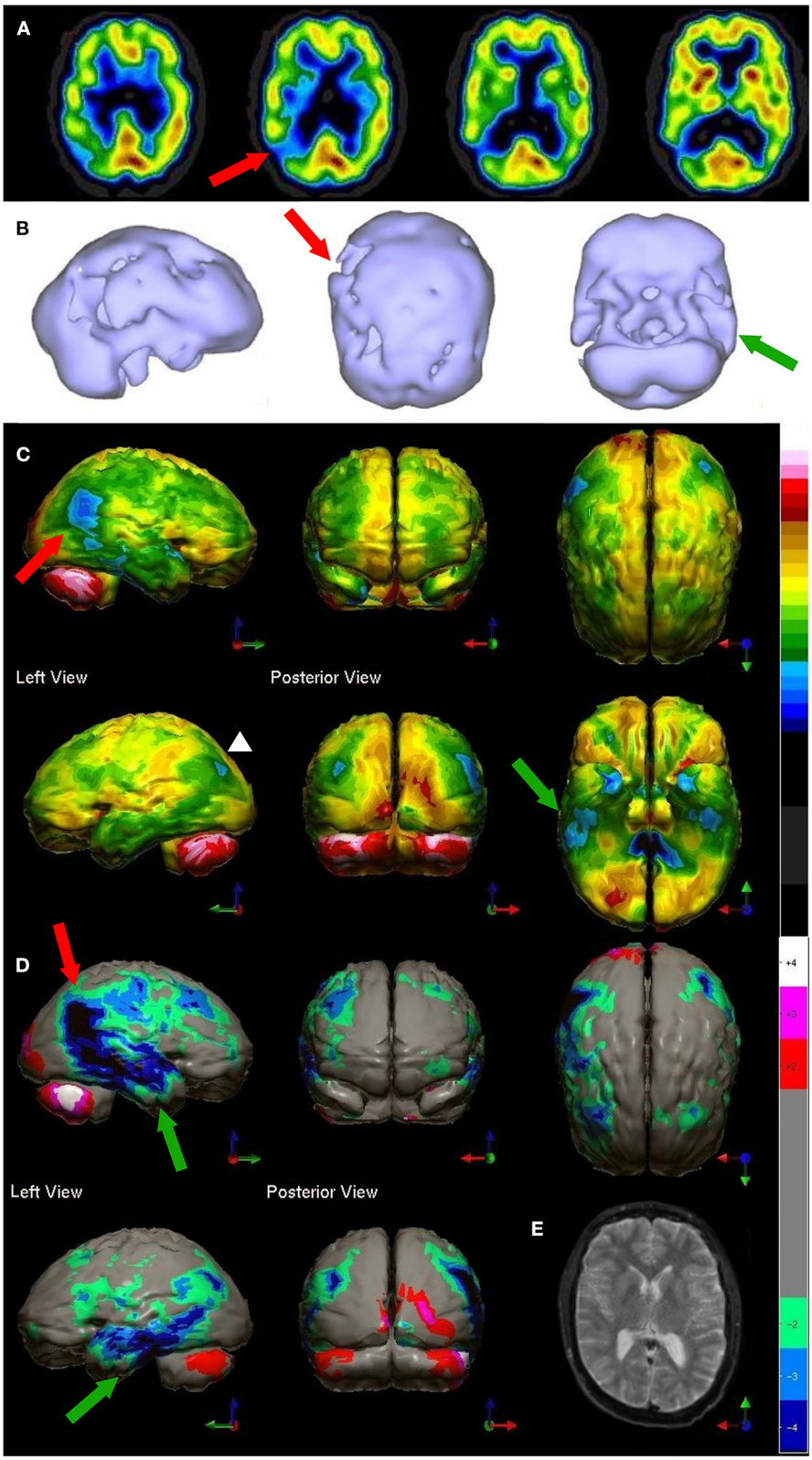

FIGURE 4 | Tomographic and multiple 3-D representations of major TBI. A 58-yr-old female was struck on the right parietal region by a heavy object with loss of consciousness of approximately 2 hours. Perfusion SPECT scan was performed seven years after the injury with ^{99m}mTc-HMPAO and a dual-head gamma camera. **(A)** 4mm horizontal sections illustrate decreased perfusion in the right parietal region (red arrow). The color scale is the same as **Figure 1B**.

(Continued)

FIGURE 4 | (B) SPECT data can be displayed in 3-D representations that facilitate the identification of large, diffuse, or subtle lesions. Here, data is presented as an isocontour display wherein cortical areas which fall below 60% of the maximal cerebral blood flow are displayed as a depression or hole. The large parietal defect is apparent on the right (red arrow), as well as bilateral temporal lobe hypoperfusion (green arrow). **(C)** Another 3-D representation utilizes the same color scale as **(A)**. The right parietal defect appears as an area of blue and green (red arrow). A contra-coup injury can be visualized in this representation (white arrowhead). Temporal lobe hypoperfusion is again evident bilaterally (green arrow). **(D)** The patient's data is compared to a normative database using Segami Inc. Oasis software. The color scale is the same as in **Figure 2D**. The parietal lobe injury (red arrow) and the contra-coup injury are easily visualized, along with more diffuse penumbra injury and bilateral lateral temporal lobe hypoperfusion (green arrows). **(E)** Anatomical MRI completed at the time of the SPECT scan showed no abnormalities. Section at same level as far right horizontal tomogram in **(A)**.

systematic review showed Level IIA evidence (at least one randomized controlled trial) for the utility of brain SPECT in TBI. The review identified 52 cross-sectional studies and 19 longitudinal studies including a total of 2,634 individuals over 30 years of literature. In addition, seven studies which were not included in the systematic review contain 223 subjects (45–51). Subsequently, two large retrospective studies comparing SPECT neuroimaging in TBI, post-traumatic stress disorder (PTSD), and normals containing over 21,399 subjects have been published (52, 53). Thus, besides the studies included in the TTASAAN report (1), there are an additional 69 studies containing 23,944 subjects on the utility of perfusion SPECT neuroimaging in the evaluation of TBI.

In addition, there have been numerous editorials and opinion pieces criticizing the use of SPECT to evaluate TBI (54–56). Central to the criticism is there is no gold-standard SPECT finding for TBI, particularly mild TBI. Another criticism is that many of the studies of TBI have a small number of subjects and lack a control group (54–56). A third criticism is SPECT may not provide additional benefit over CT or MRI (55, 56). A fourth criticism is that SPECT findings do not correlate with neuropsychological testing (54–56). A fifth criticism is that it has been unclear that SPECT scans can predict clinical outcome (54–56). Each of these criticisms will be addressed in turn.

Lack of Gold-Standard Finding

This position reflects an almost foolish belief that such a gold-standard could or should exist. By its very nature, TBI is highly variable. The mechanism of injury (impact, rotational, etc.), point of impact, presence or absence of contra coup injury, handedness, presence of prior injury, and other factors all contribute to the manifestation of TBI in each patient (34, 38, 57). The neuropsychological sequalae of injury will also depend upon what areas of the brain are affected, the inter-connectedness of affected areas, handedness, nutrition, toxic exposures, premorbid intelligence, and history of prior injury (58). This confound is not limited to SPECT, but also plagues other forms of neuroimaging, such as diffusion tensor imaging, when applied to the evaluation of TBI.

Small N Studies or Lack of a Control Group

By the very nature of TBI, it is not possible to have a randomized study of neuroimaging applied to TBI. How does one recruit a sample of subjects with normal baseline SPECT scans and then subject them randomly to a head injury followed by a repeat SPECT scan? As a result, there can never be true Class I evidence (well-designed, randomized, controlled clinical trial), as defined in the TTASAAN report (1), for the diagnostic and/or prognostic effectiveness of SPECT in the situation of TBI. This same limitation applies to studies of fMRI, CT, anatomical MRI, MEG, and diffusion tensor imaging. An early approach to this barrier was to randomly present cases of TBI with positive and negative controls to reading physicians (43). The study was technically flawed as described above.

Of the 54 published cross-sectional studies of perfusion SPECT neuroimaging in the evaluation of TBI, 26 had 20 subjects or less. Seven studies had 100 subjects or more (52, 53, 59–63). One study had over 7,600 subjects with TBI (53). Of the 19 longitudinal studies, nine had 20 subjects or less. Four longitudinal studies had 100 subjects or more (64–67). For example, Gowda et al. (66) prospectively performed CT and perfusion SPECT scans on 92 patients with acute TBI. Both scans were performed within 72 h of injury. Abnormal SPECT scans were found in 63% of cases—-half of these cases had normal CT scans. Two patients showed CT abnormalities without corresponding SPECT findings. A subarachnoid hemorrhage was the finding in both cases. The Newcastle-Ottawa Scale (NOS) was developed to assess the quality of non-randomized studies (68). The scale was applied to all the longitudinal SPECT studies by Raji et al. (44). The mean score for the 19 studies was 6 ± 1.4, which is considered to be high quality (NOS range 0–9).

Among the 71 studies included in the aforementioned systematic review (44), 15 included a control group. In addition, Stamatakis et al. examined SPECT scans and MRI from 51 subjects with TBI using statistical parametric mapping in comparison to 32 subjects in a control group (47). Atighechi et al. examined 21 subjects with TBI and anosmia compared to positive and negative control groups (50). Amen et al. conducted a retrospective comparison of TBI and PTSD (52). All patients underwent extensive psychiatric interview and completion of a battery of questionnaires. The diagnosis was made by Board-certified psychiatrists based on DSM-IV or V criteria. Baseline perfusion SPECT scans differentiated TBI from PTSD with a sensitivity of 92% and a specificity of 85% (52). Amen et al. replicated these findings in a separate retrospective evaluation of SPECT scans from distinct and closely matched groups of patients with TBI ($N = 104$), PTSD ($N = 104$), both TBI and PTSD ($N = 73$) and 116 healthy controls (53). All patients were diagnosed by a similar extensive battery of questionnaires and psychiatric interview. Controls were found to be free of psychiatric conditions, TBI, or substance abuse by extensive psychiatric interview and completion of a battery of questionnaires using DSM-IV or V criteria. The baseline perfusion SPECT scans were compared

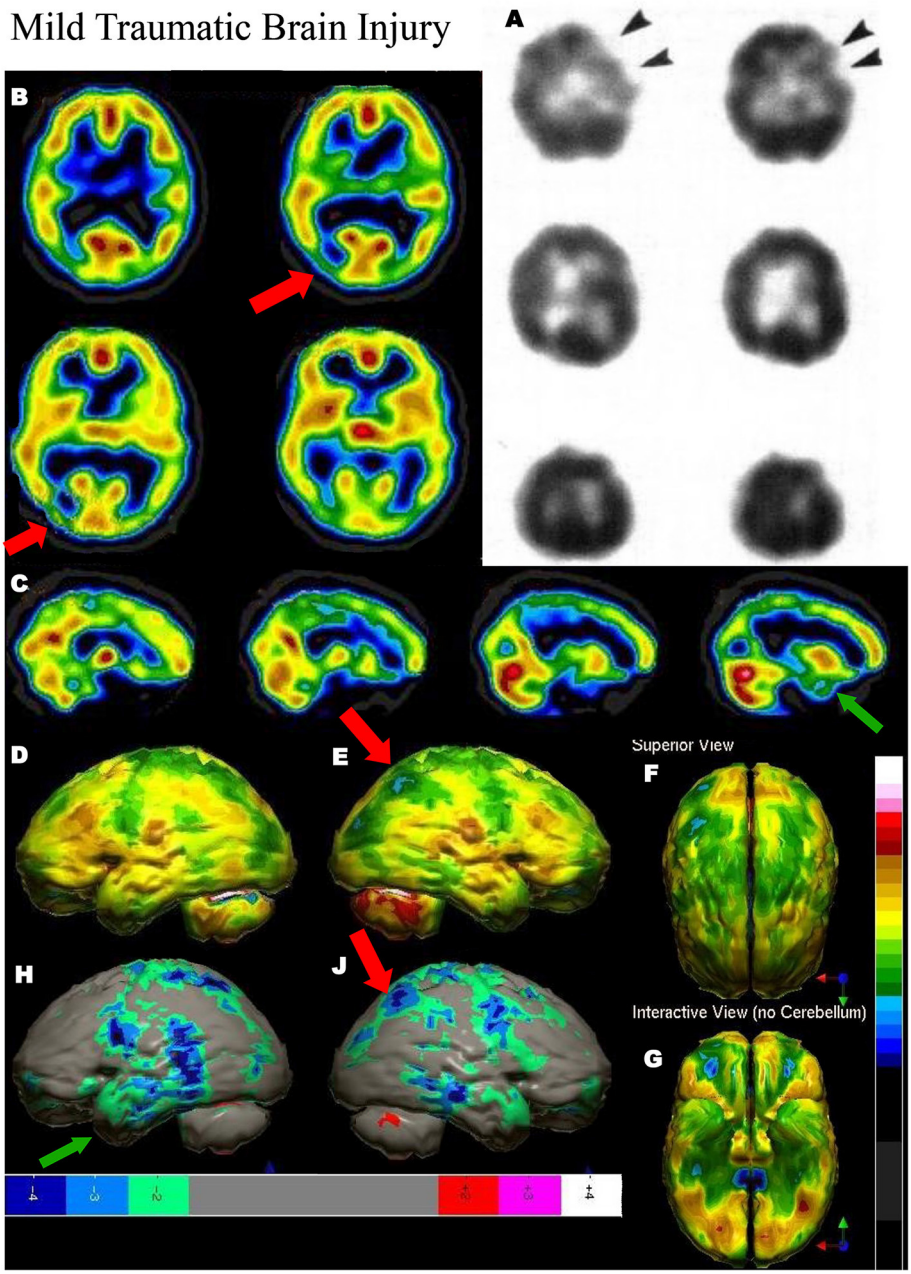

FIGURE 5 | Mild TBI. **(A)** Example of SPECT scans cited in TTASAAN report. Anatomical details are lacking. 50-year-old male with minor head trauma after a motor vehicle accident showed decreased perfusion of the left inferior frontal and left anterior temporal lobe, whilst MRI scan was normal [The figure was originally published in JNM. © SNMMI (28)]. **(B–G)** A 2019 SPECT scan using a dual-headed gamma camera of an 18-year-old male who struck a tree while mountain biking and briefly lost consciousness. A modern ^{99m}mTc-HMPAO perfusion SPECT scan was performed with a dual-head gamma camera. **(B)** Horizontal tomograms show detail of thalamus, anterior cingulate, caudate, and lentiform nuclei. A focal area of hypoperfusion can be seen in the right parietal cortex (red arrow). Color scale is the same as in **Figure 1B**. **(C)** Sagittal tomograms reveal decreased inferior frontal perfusion and decreased medial temporal perfusion bilaterally (green arrow). **(D–G)** 3-D representation of SPECT scan data showing left lateral **(D)**, right lateral showing the area of hypoperfusion in the right parietal cortex (red arrow) **(E)**, superior **(F)**, and inferior views **(G)**. **(H–J)** The patient's data is compared to a normative database using Segami Inc. Oasis software. The color scale is the same as in **Figure 2D**. Areas of relatively decreased perfusion are more evident, such as the area of hypoperfusion in the right parietal cortex (red arrow).

visually and by quantitative region of interest analysis. TBI could be distinguished from controls with a sensitivity of 100% and a specificity of 100% in both visual reads and quantitative analysis. In distinguishing TBI from PTSD, the sensitivity was 100% and the specificity was 100% for quantitative analysis and a sensitivity of 86% and specificity of 81% for visual reads. In addition, they

conducted a larger comparison of 7,505 patients with TBI and other psychiatric comorbidities compared to 11,147 psychiatric patients without TBI who served as controls (53). With this more diverse group, sensitivity was 70% and specificity was 54% for both visual reads and quantitative analysis. The comparison of TBI and PTSD yielded somewhat higher accuracy with a sensitivity of 80% and a specificity of 60–62% (53).

In summary, there are numerous large-N cross-sectional, longitudinal and retrospective studies of the utility of SPECT in the evaluation of TBI. Indeed, thousands of subjects have been compared to hundreds of controls across 18 studies.

Does SPECT Provide Additional Information Over CT or Anatomical MRI?

Since perfusion in the gray matter is regulated by neuronal activity, as described above, perfusion SPECT provides a method of detecting neuronal dysfunction in the absence of anatomical change. Areas of the brain which are stunned, surviving, but not functioning (as in the ischemic, or otherwise functionally compromised) show no anatomical changes. However, the decreased function can lead to decreased perfusion. We (TAH) have demonstrated this in a case of chronic TBI wherein cerebral perfusion surrounding the injury and even in the contralateral hemisphere was decreased, despite normal appearance of the involved areas on MRI (69). These affected areas responded to treatment and showed improved perfusion upon repeat SPECT imaging. Acute TBI (within 72 h) represents a unique situation wherein perfusion can increase or decrease depending upon a number of factors, such as neuronal dysfunction and shutdown, inflammation, changes in blood-brain barrier permeability, excitotoxicity, and more. For example, Obrist et al. (70) performed serial quantitative perfusion SPECT (^{133}Xenon) scans and found that rCBF was initially reduced (12 h) and then increased to hyperemic levels at 57 h after injury. Hyperemia was associated with increased intracranial pressure. The changes in perfusion may be due to loss of autoregulation (71) and/or transient disruption of the blood-brain barrier (72).

The collective literature (44) indicates that perfusion SPECT scans are superior to CT scans for detecting functional injury following head trauma in subacute and chronic TBI, and potentially acute TBI, as well. Over 96% of the studies which compared SPECT to CT found SPECT identified lesions which were not evident on CT. For example, Abdel-Dayem et al., evaluated 228 subjects with mild-to-moderate TBI and found abnormally low perfusion in the frontal, temporal, and parietal lobes (60). A follow up study by Abu-Judeh et al. (61) in the same population found that abnormalities that were identified on SPECT were often not seen or were underestimated in magnitude on CT scan in those receiving both SPECT and CT (61). Ichise et al. (26) found similar discordance with 79% of SPECT abnormalities lacking a matching abnormality of CT and concordant lesions were larger on perfusion SPECT scan than on CT scan (26). Emanuelson et al. (73) showed that SPECT lesions were concordant in severe TBI, but SPECT was more sensitive than CT in mild TBI. In another study, SPECT scans in the acute setting detected abnormalities in 75% of patients who had amnesia symptoms, while the CT scans were read as normal (74). Given that CT scans have become the cornerstone of evaluating concussion and TBI in the acute setting wherein they readily reveal hemorrhage and fractures, it becomes important to recognize that CT scans fail to show functional deficits seen on SPECT for which there may be no structural correlates. Thus, CT scans for head trauma in the emergency department may be negative, but do not rule out future functional deficits. To this point, all subjects in the longitudinal study by Jacobs had negative CT scans in the acute setting (40, 64); however, a positive baseline SPECT scan had high sensitivity and specificity for persistent neurological symptoms (see below).

Similarly, SPECT is more sensitive for TBI than anatomical MRI across multiple studies. In a series of 13 patients with moderate TBI, Shin et al. (75) found that MRI was negative in 50% of the cases, while the SPECT scans analyzed with statistical parametric analysis were positive for brain injury in 100% of cases. Abu-Judeh et al. examined 228 patients with mild to moderate TBI in a retrospective review (61). Both CT and MRI within 2 weeks of injury were negative, while SPECT scans revealed frontal lobe injury in 24% of cases and temporal lobe injury in 13% of the cases. Likewise, Stamatakis et al. (47) examined 62 patients with TBI using MRI and SPECT, which were performed within 2 weeks of injury. Using statistical parametric analysis, they found SPECT detected more lesions and more lesion volume than anatomical MRI. Ichise et al. (26) found SPECT scans more sensitive than MRI as well, with 79% of SPECT abnormalities lacking a concordant MRI lesion. Conversely, MRI detected white matter hyperintensities which did not show a matching lesion on SPECT (26). Kinuya et al. (48) found SPECT detected hypoperfusion in 94% of cases wherein MRI scans were normal; however, cases of subdural hematoma did not show abnormal SPECT findings. SPECT findings correlated strongly with symptoms, such as personality change or amnesia.

Does SPECT Correlate With Neuropsychological Findings?

The current trend in neuropsychological assessment is toward the profiling of functional performance to detect TBI. The field is still hampered using many tests that are antiquated, excessively long, or of dubious psychometric quality (76). A neuropsychological assessment can consist of a multitude of tests; there are over 100 separate neuropsychological assessment tests that are frequently utilized in TBI cases (77). Because no single neuropsychological test is particularly sensitive for TBI (78, 79), they are generally used in batteries. However, a lack of consensus exists about which tests are appropriate to include in a battery (79). Accordingly, the choice of tests to include is subjective. In addition, variances between how individual neuropsychologists administer the tests, interpret the results, apply failure criteria and decide whether to test for effort are additional subjective variables (80). Moreover, comorbid conditions, such as pain, anxiety, depression, sleep disturbance, medications, and alcohol use can interfere with cognitive performance obscuring the effects associated with mild or even much more significant brain injury (77, 80). Lastly, the validity of a neuropsychological assessment battery is based on the norms, decision rules, false positives, false negatives, hit rates,

and the compounding of these variables when multiple tests are combined in a battery (77). Hence, neuropsychological testing is not considered diagnostic for TBI (81).

Brain SPECT imaging provides neuropsychologists an objective way to address these problems. SPECT has, in fact, been correlated with several individual neuropsychological assessment tests such as the Wisconsin Card Sort (82–85), the Stroop Colored Word Test (86, 87), the Tower of London Test (88, 89), the Clock Drawing test (90, 91), the Test of Verbal Fluency (92) and the Auditory Verbal Learning test (93). SPECT perfusion patterns have also been found to correlate with the predicted localization of neurological damage, based on neuropsychological battery testing, in a number of conditions including Lyme's disease (94), Sjorgren's syndrome (95), Klein-Levin syndrome (96), obsessive compulsive disorder (97), migraine headaches (98), paraneoplastic encephalitis (99), cerebral microvascular disease (100), chronic alcoholism (101), Alzheimer's disease and dementia (102), and neurological impairment following coronary artery bypass grafting (103).

Additionally, 18 out of 21 cross-sectional studies (81%) included in a systematic review showed correlation between abnormal SPECT findings and neuropsychological deficits (44). This suggests that abnormalities found with brain SPECT can correlate with and therefore can be predictive of functional outcomes and/or neuropsychological test performance. Davalos and Bennett (54) examined this question based on three studies (26, 104, 105); however, two of the studies lacked a control group and one included only four patients. Nevertheless, they concluded that this correlation warranted further study and that the confound of depression, possibly secondary to the TBI, must be carefully considered. We do not disagree with these conclusions, given the extensive literature presented above.

Do SPECT Scans Predict Clinical Outcome?

Neuroimaging for head trauma serves multiple purposes. Establishing the presence/absence of TBI is first and foremost. Predicting clinical outcome is an important additional benefit which may or may not be realistic. For example, diffusion tensor imaging has not shown clear predictive utility for clinical outcome (106). Nevertheless, critics are quick to hold SPECT in rebuke for failing to absolutely predict clinical outcome. For example, a critical opinion piece on the use of SPECT to evaluate mild TBI by Wortzel et al. (55), which was poorly referenced, cites an unnamed study in which an abnormal scan was predictive of persistent clinical symptoms in 59% of cases. Presumably, this unnamed study is Jacobs et al. (40) based on the reference in Davalos and Bennett (54), which Wortzel et al. (55) were discussing when describing this unnamed study. However, this reference is flawed on several levels. First, Jacobs et al. (40) included subjects with both mild and moderate TBI. Second, this study was examining SPECT findings in the subacute setting (within 1 week) as predictors of persisting symptoms. Recovery was an expected outcome for a significant proportion of subjects. Thirdly, Wortzel et al. (55) ignore the further longitudinal data from Jacobs et al. (64). Therefore, these results will be detailed here.

TABLE 1 | Outcome data from Jacobs et al. (40, 64).

Number of months post-TBI	0	3	6	12
Sensitivity	78%	91%	100%	100%
Specificity	61%	61%	53%	85%
Negative Predictive Value (NPV)	92% (3 mth) 100% (12 mth)	–	100%	100%
Positive Predictive Value (PPV)	44%	64%	52%	83%

Patients who had a positive SPECT scan and clinical symptoms based on neurological examination, neuropsychological testing, and concussion questionnaires, had repeat SPECT scans at 3 months. If they had a positive SPECT scan at 3 months, then they had a repeat SPECT scan at 6 months, etc. The sensitivity and specificity of the baseline SPECT for clinical symptoms at 3 months was 78 and 61%, respectively. A persistently positive SPECT scan was predictive of persisting neuropsychological symptoms. A positive scan at 3 months had a sensitivity and specificity for persisting symptoms of 91 and 61%, respectively. If a scan was still positive at 12 months, the sensitivity and specificity of persisting symptoms was 100 and 85%, respectively. The PPV of the baseline SPECT scan was relatively low (44%) largely reflecting the degree of recovery seen in this population. Among patients with a negative SPECT scan at baseline, 92% were free of clinical symptoms by 3 months and 100% were free of symptoms at 12 months (NPV).

Jacobs et al. (40) published the first part of a two-part longitudinal study of the correlation between acute SPECT scan findings and persistent neuropsychological symptoms in 1994. It is one of a number of studies which have documented the positive predictive value (PPV) and negative predictive value (NPV) of SPECT in the prediction of lasting neuropsychological effects of TBI. It was included in the TTASAAN report and is also likely the study referenced by Wortzel et al. (55) above. Jacobs et al. (40) conducted a scrupulous study of 67 subjects with acute TBI (42 moderate TBI, 25 mild TBI) who were then followed over the subsequent year (64). Furthermore, Jacobs et al. added an additional 69 subjects with mild TBI to the longitudinal sample. All subjects had baseline perfusion SPECT scans and CT scans obtained within 4 weeks (83% within 1 week) of the head injury event. All subjects had *baseline neuropsychological testing*.

Subjects with a positive finding on SPECT had a repeat SPECT scan at 3 months, 6 months, and at 1 year, while all subjects underwent repeat neuropsychological testing at 3 months, 6 months, and 1 year (64). These studies captured three key concepts in the evolution of mild TBI. First, a substantial proportion of patients with mild TBI recover over the course of the year, regardless of whether they have positive SPECT findings at baseline. The second, not every patient with mild TBI will have a positive SPECT scan. The third, the sensitivity and specificity of baseline SPECT for predicting persistent neuropsychological symptoms and findings can be calculated. In addition, the PPV and the NPV of a baseline SPECT scan in acute TBI was determined (**Table 1**).

Based on this large sample of 136 subjects, a negative baseline SPECT scan was highly predictive of normal neuropsychological testing in the future. In other words, a negative SPECT scan shortly after initial injury predicts the absence of long-term functional deficits. This predictive value cannot be matched by other imaging modalities such as conventional CT or MRI. The positive predictive value of baseline SPECT scans was also quite high. An abnormal baseline SPECT scan that remained positive

at 12 months predicted persistent neuropsychological deficits with a sensitivity of 100% and a specificity of 85% (64). This gives a strong argument for serial SPECT scans in cases with both positive baseline scan and neuropsychological symptoms. Similarly, a second prospective study by an independent group (107) found an abnormal baseline SPECT correlated strongly with abnormal neuropsychological testing in patients participating in a cognitive rehabilitation program.

Lastly, the lack of a randomized, placebo-controlled clinical trial of SPECT in the diagnosis of TBI is a deficit cited by *both critics* (54–56) *and proponents* (54, 108–110). The improbability of a gold-standard and randomizing patients to experience TBI make this critically needed study impossible. However, an additional, more nefarious, barrier has prevented such a study from occurring. One of us (TH) collaborated with Drs. Davalos and Bennett to implement a study to evaluate mild TBI with perfusion SPECT which addressed the concerns they raised in their review. Essentially, this study would have replicated Jacobs et al.' work (64) with better SPECT imaging, larger sample size, more extensive neuropsychological testing, and comparison to a carefully vetted normative dataset. Unfortunately, repeated funding attempts failed due to wholesale rejection of SPECT neuroimaging by grant reviewers. Comments such as, "The use of SPECT, a technique with poor spatial resolution, poses a concern." and "use outdated techniques" peppered the peer review panel summary statements. Again, it seems odd that perfusion SPECT imaging is held to an unrealistic standard that fMRI, diffusion tensor imaging, FDG-PET, amyloid PET and other forms of neuroimaging do not meet. For example, numerous diffusion tensor imaging studies of mild TBI lack the rigorous criteria established by Davalos and Bennett (54) but these studies were still funded and published after these criteria were set (106, 111–118). For example, several diffusion tensor imaging studies lack control groups (115, 118), several have small sample sizes (111–115), several examined limited neuropsychological testing (112, 113, 115–119), and all lacked randomization.

Experts in the field are calling for greater collaboration between neurologists and nuclear medicine physicians to conduct the needed studies required to convince Neurology of the value of SPECT neuroimaging in the assessment of TBI (67, 108–110). Critics continue to claim that SPECT is not useful in the evaluation of TBI. Conversely, *according to the criteria set forth in the TTASAAN report* (1), the current literature supports the use of perfusion SPECT neuroimaging to evaluate TBI as a Type A Recommendation (strong positive recommendation) based on Class II evidence derived from multiple clinical studies with large N and control comparison groups (40, 47, 52, 53, 63, 64, 86) as presented above.

Stroke

Stroke remains a leading cause of death and disability throughout the world. In 1996, the rate of new stroke cases was ∼269 per 100,000 (120) and the prevalence was 988 per 100,000. In 2017, the rate of new stroke cases declined 11% to 150 per 100,000 (121), while the prevalence increased by 37% to 1363.5 per 100,000 (121). As a result, ∼104.2 million people worldwide have experienced a stroke (122). Neuroimaging has a pivotal role in the assessment and clinical management of stroke.

The TTASAAN report (1) included 12 research studies on stroke, in which 10 were performed using single-head gamma cameras (25, 123–127). Since the publication of the TTASAAN report, significant advancements have occurred in imaging techniques to assess vascular anatomy and integrity. Magnetic resonance angiography (MRA), computed tomography angiography (CTA) and diffusion weight MR (DWI) have proven effective, safe, and rapid in modern hospital settings (128). However, much of the world does not enjoy the technical riches of hospitals in the United States. Thus, many of the MRI and CT techniques employed in stroke assessment are not available elsewhere. Perfusion SPECT remains a valuable tool for assessing acute strokes prior to administering intravenous tissue plasminogen activator (IV tPA) (129, 130), assessing subacute strokes for viability and size of the penumbra (131, 132), and assessing persistent stroke-related symptoms (133). Perfusion SPECT may also contribute to stroke risk assessment (134, 135).

Nevertheless, the first step in assessing a patient with symptoms of stroke or transient ischaemic attack (TIA) is a non-contrast CT scan. CT remains a rapid, safe, and effective means of determining if a stroke is hemorrhagic or not. The introduction of IV tPA as a treatment for dissolving and clearing clots, as well as clot retrieval techniques, has increased the need for *rapid* determination that a stroke is not hemorrhagic. Candidates for IV tPA need to be treated within 4.5 h of stroke onset. Thus, MR techniques, which are more rapid, have largely replaced perfusion SPECT scans in the assessment of acute stroke/TIA patients.

CT and diffusion/perfusion-weighted MRI have largely replaced perfusion SPECT in the assessment of subacute or chronic cerebrovascular disease. However, in certain conditions in which the variability of clinical presentation can be high (e.g., transient ischemic attacks, Moyamoya disease), SPECT may still offer value as part of the overall assessment plan. Perfusion SPECT neuroimaging is useful in delineating the extent of ischemic infarction and correlates well with severity of neurologic deficits and clinical outcomes. It may be useful in demonstrating the ischaemic penumbra at the margins of an ischaemic infarct, which may be salvaged with neuro-interventional procedures (132). This is due to the fact that perfusion SPECT imaging does not simply demonstrate the presence or absence of vascular occlusion. Rather, localized cerebral blood flow is regulated by the brain region itself. As the activity of a particular brain region increases, so does its need for oxygen and glucose. By a signaling mechanism involving neurons, glial cells, and the arterioles, the brain region calls for increase localized blood flow to meet its needs. Thus, perfusion SPECT neuroimaging shows active brain tissue, inactive brain tissue, and compromised brain tissue. Similarly, perfusion SPECT can be useful in assessing response to treatment or interventions (136, 137). A smaller volume of penumbra (138) and the absence of crossed cerebellar diaschisis (139) can be predictive of better clinical response. The technical improvements in gamma cameras and in post-processing software have markedly improved the resolution, anatomical detail, and information density of perfusion SPECT scans (**Figure 6**). 3-dimensional reconstruction allows more

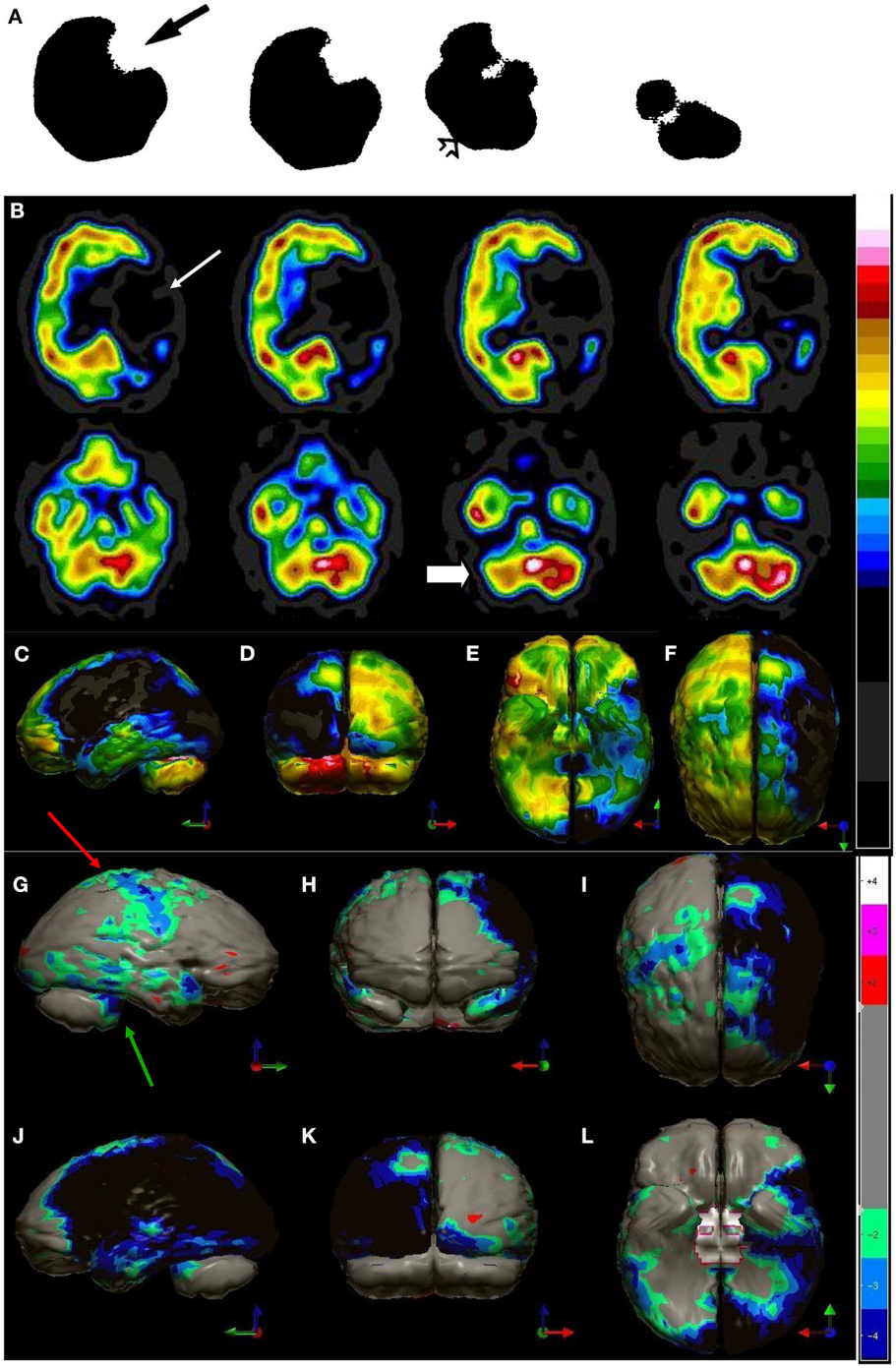

FIGURE 6 | (A) Example of SPECT scan studies cited in TTASAAN report. Anatomical details are lacking. A ^{99m}Tc-ECD perfusion SPECT scan from 1989 illustrating a left middle cerebral artery stroke (black arrow) with crossed cerebellar diaschisis (open arrow). This scan was performed on a single-head gamma camera [The figure was originally published in JNM. © SNMMI (25)]. **(B)** Modern 99mTc-HMPAO SPECT scan using a dual-head gamma camera illustrating a left middle and posterior cerebral artery stroke (white arrow) involving the left posterior frontal, temporal, parietal, and occipital cortices. Color scale is the same as in **Figure 1B**. Crossed cerebellar diaschisis is apparent (white block arrow), as well as involvement of the left thalamus and left basal ganglia. **(C–F)** left lateral, posterior, inferior (cerebellum removed) and superior 3-dimensional views, respectively. **(G–L)** Right lateral, frontal, superior, left lateral, posterior, and inferior (cerebellum removed) views of scan compared to normative database. Color scale is the same as in **Figure 2D**. Involvement of the contralateral cortex (red arrow) and the crossed cerebellar diaschisis (green arrow) are evident.

complete understanding of the stroke and penumbra volume. Statistical parametric analysis, particularly with comparison to a normative database, reveal details which might otherwise not be discernible (**Figures 6G–L**).

Cerebrovascular reserve capacity (CVRC) is an important parameter which guides treatment decisions in chronic cerebrovascular diseases. The cerebral circulation is complex with multiple arterial inputs to the Circle of Willis, with altered hemodynamics resulting from gradual occlusion of one of more vessels over time. In additional, there is highly responsive intracerebral autoregulation to maintain blood flow, particularly when cerebral perfusion pressure is reduced. Determining reserve capacity can be critical in assessing a patient for carotid endarterectomy or carotid stenting. Perfusion SPECT neuroimaging allows a global assessment of the integrated effects of hemodynamic factors, as it measures cerebral cortical and subcortical gray matter blood flow (140). Furthermore, dynamic assessment using intravenous acetazolamide or inhaled CO_2 followed by perfusion SPECT provides an accurate measure of cerebrovascular reserve. Both acetazolamide and inhaled CO_2 cause vasodilation of cerebral microvasculature (141). By challenging the vascular system with additional flow demands, these techniques reveal if the smaller arteries fed by the carotid arteries can support the flow demand (141). This is illustrated in **Figure 7**. This technique can be useful in decision making for patients with Moyamoya disease, as well.

Epilepsy

The incidence of seizure disorders in the United States is 39 per 100,000, representing about 3.4 million cases (142). Approximately, one-third of all cases prove intractable or treatment-resistant—virtually unchanged from the time of the TTASAAN report, despite 25 years of new anticonvulsant medications. Surgical or laser ablation of the seizure focus/foci remains the most effective treatment in these cases. Ictal and inter-ictal perfusion SPECT scans remain an integral part of the pre-surgical evaluation of such cases (143–145).

The TTASAAN report (1) included 17 papers and reviews on the use of perfusion SPECT scans in the evaluation of epilepsy with a total of 182 patients (146–151). Based on this very preliminary data, the conclusion was that perfusion SPECT performed during the seizure event (ictal) could localize the seizure focus in 71–93% of cases with a positive predictive value of 95% (1).

In the last decade alone (2012–2021), there have been over 181 research articles and reviews containing a total of 8,516 patients on the topic of the utility of perfusion SPECT scans in the evaluation of epilepsy. The predominate topic was pre-surgical planning; however, diagnosis of pseudoseizures and seizures due to other medical conditions were also topics. In addition, over 85 cases studies of 1–3 patients each covered the utility of perfusion SPECT imaging in the *differential diagnosis* of a wide variety of medical causes of seizures, including TBI (152), tuberous sclerosis (153), vascular disease (154), neoplasms (155), systemic lupus (156), rare autoimmune disorders [e.g., anti-NMDA receptor autoimmune encephalitis (157, 158), hyperglycemia (159), and Lewy Body dementia (160)].

Two significant advancements in perfusion SPECT imaging, beyond the stabilization of HMPAO and the improvements in both gamma camera technology and post-processing software, have impacted the utility of SPECT imaging in the localization of seizure foci. The first is subtraction ictal SPECT co-registered to MRI (SISCOM). In essence, the interictal data is subtracted from the ictal data to reveal a focus or foci of increased perfusion during the ictus. The focus/foci are then mapped onto the patient's anatomical MRI (161–164). A retrospective study of 90 patients undergoing surgical resection of seizure foci between 1995 and 2013 revealed SISCOM predicted patients being seizure-free up to 5 years after ablative surgery (69.2%), comparable to FDG-PET localization (162). Smaller studies have found similar positive predictive value [76.9% - (165)]. The ability of SISCOM to accurately localize a seizure focus ranged from 73 to 85% (mean 77.3%) across multiple studies (164–172). A meta-analysis of 11 studies found SISCOM accurately localized

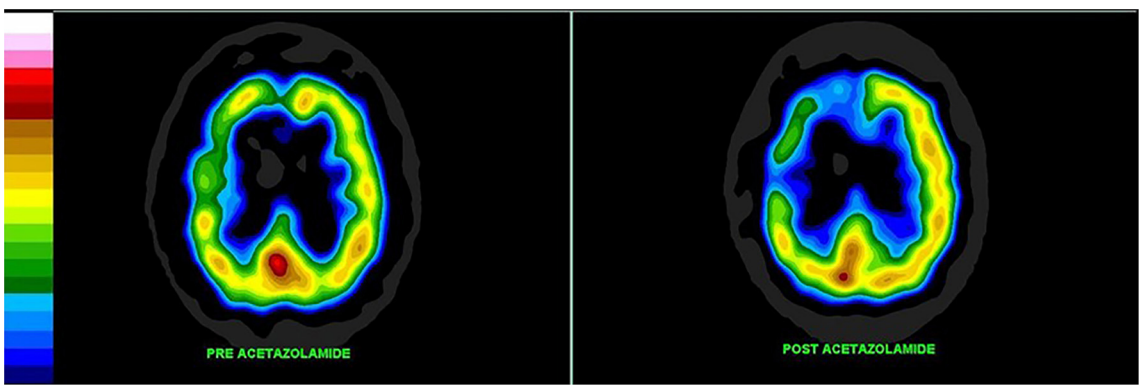

FIGURE 7 | Patient with high grade carotid stenosis and multiple co-morbidities. The left hemisphere (on the right of the image) is able to augment its blood flow with acetazolamide, but there is restriction of flow to the right side leading to relative deterioration in right perfusion after acetazolamide administration, compared to the left. Color scale is the same as **Figure 1B**. Courtesy of J. Cardaci, MBBS, FAANMS, FRACP - Diagnostic Nuclear Imaging, Perth, West Australia; University of Notre Dame, Fremantle, Australia.

seizure focus in 85.9% of cases and was concordant with EEG data in 65.3% of cases (166). SISCOM had an odds ratio of the patient being seizure-free post-operatively of 1.90 in non-concordant cases and of 6.23 in concordant cases (166). Recently, the diagnostic accuracy and predictive value of ictal perfusion SPECT was compared to magnetoencephalography (MEG) in a group of 158 surgical candidates. The accuracy of ictal SPECT was 78.57% in localizing the seizure focus, while the accuracy of MEG was 74.26% (1, 171). The odds ratio for a patient being seizure-free after surgery was 5.0 and 2.43 for ictal SPECT and MEG, respectively (171). **Figure 8** illustrates the advances in perfusion SPECT imaging, including the SISCOM technique for localizing seizure foci.

The second advancement has been the use of automated injectors to reduce the lag time between the onset of seizure activity and the injection of the tracer (173, 174). Automated injectors can reduce lag time from 60 s with hand administration to 18.5 s using an automated method (175). Since seizure activity is initially limited to the focus/foci, but then spreads to adjacent or even contralateral brain areas, capturing the perfusion pattern early increases the accuracy of the localization by perfusion SPECT (176, 177). For example, using automated injectors increased localization of seizure foci from 62.9 to 81.8% (175).

Perfusion SPECT also has proven useful in cases of non-convulsive status epilepticus (NSE) among medically complicated patients (178). NSE can prove to be a challenging diagnosis and is more likely in critically ill patients with multiple overlapping diagnoses. In a group of 55 patients, initial EEG had a sensitivity of 61.1% and a specificity of 89%. In contrast, a perfusion SPECT had a sensitivity of 80.5% and a specificity of 89.5% in diagnosing NSE (178).

Dementia and Alzheimer's Disease

The TTASAAN report (1) included 25 research articles and reviews on dementia (179–185). All of the studies were conducted using single-head gamma cameras, except one which used an annular crystal. Since the TTASAAN publication, over 600 research studies have been published on the subject of perfusion SPECT in the evaluation of dementia.

Currently, the most reliable neuroimaging findings for Alzheimer's disease (AD) are the observed decreased metabolic activity and associated decreased perfusion of the posterior parietal and temporal lobes bilaterally and the posterior cingulate gyri bilaterally with relative sparing of the basal ganglia, thalamus, and primary sensory-motor cortex (186–191). The early SPECT perfusion studies of AD relied on single-headed or low-resolution gamma cameras (192–194). Nevertheless, a meta-analysis of these early studies concluded perfusion SPECT has a sensitivity of 74% and a specificity of 81% for the differentiation of AD from elderly controls (195).

Since 2009, there have been three meta-analyses (196–198), a comprehensive review with meta-analysis (191), and a systematic review (199) addressing the clinical utility of perfusion SPECT neuroimaging in AD. Yuan et al. (196) found SPECT had a sensitivity of 84% and a specificity of 70%, while Bloudek et al. (197), performing a meta-analysis on selected research from 1990 to 2010, concluded that perfusion SPECT had a sensitivity of 79% and a specificity of 84%. Subsequently, Frisoni et al. examined 32 studies and found SPECT had a sensitivity of 76% and a specificity of 84% (198). In contrast, the sensitivity of FDG-PET ranged from 76 to 89% and the specificity ranged from 74 to 85% (191). The meta-analyses described above all co-mingled SPECT studies using single-headed gamma cameras with studies using multi-headed gamma cameras. Moreover, the summary sensitivity/specificity figures result from combined comparisons of AD cases vs. mild cognitive impairment (MCI), fronto-temporal dementia (FTD), vascular dementia (VaD), dementia with Lewy Bodies (DLB), and healthy elderly controls. As a result, these meta-analyses are not consistent with the conclusions of others (200, 201). For example, Bonte et al. (201) found that based on correlation to autopsy data, decreased posterior cingulate perfusion alone has a positive predictive value of 93% and a negative predictive value of 81%.

A more recent meta-analysis was conducted which grouped data based on camera type and comparator group (FTD, VaD, DLB, MCI, healthy elderly control) (191). When differentiating AD from healthy elderly controls, studies using relatively low-resolution, single-headed gamma cameras yielded an overall sensitivity of 84% and an overall specificity of 83% (187, 200, 202–211). Studies utilizing multi-headed gamma cameras and often quantitative analysis (91, 186, 212–231) yielded a modest, but clinically significant, increase in overall sensitivity to 89% and overall specificity to 89%. **Figure 9** illustrates the advancements in the images produced by perfusion SPECT imaging including statistical parametric analysis to an age-matched normative database as depicted for AD.

Longitudinal clinical studies have corroborated that perfusion SPECT scans can predict the advancement of SPECT-identified AD to autopsy-proven AD, as well as the progression of MCI to AD. Jobst et al. (210) followed 200 patients with dementia and 119 controls over 7 years. Seventy patients were autopsied, and baseline clinical evaluation alone yielded a sensitivity of 93% and a specificity of 46% in predicting histopathology consistent with AD, while baseline SPECT scans combined with clinical diagnosis did not change the sensitivity, but increased the specificity to 84%. Hanyu et al. (200) examined a group of 219 patients and were able to distinguish 56 cases that would progress to AD based on decreased perfusion of the temporal and parietal lobes (sensitivity 82%, specificity 89%). Matsuda et al. (232) utilized Z-score analysis to demonstrate that decreased posterior cingulate/precuneus perfusion could distinguish 40 patients with MCI suspected of being the AD-type from 40 controls with an accuracy of 86%. Taken together, studies of perfusion SPECT in the diagnosis of AD with comparison to a longitudinal clinical course and/or histopathology demonstrate sensitivity in the range of 82–96% and specificity in the range of 83–89% (191).

SPECT neuroimaging can be extremely helpful in the evaluation of dementia of a vascular origin (VaD). VaD can show widely varying regional blood flow patterns, reflecting its variable vascular source (233). As such, there is not a single characteristic pattern of perfusion or metabolic activity

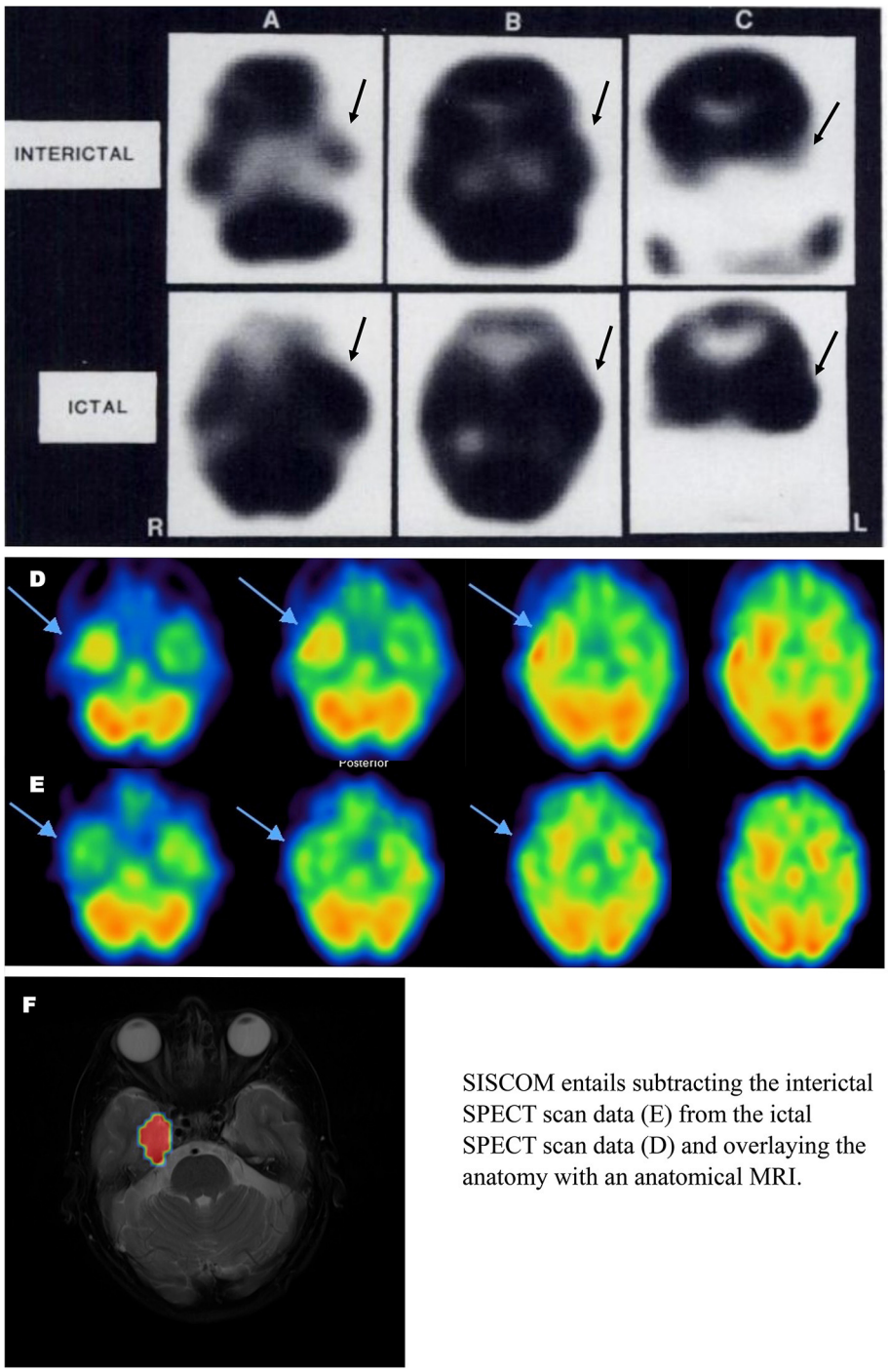

FIGURE 8 | Ictal and Interictal SPECT **(A–C)** Example of SPECT scan studies cited in TTASAAN report. Perfusion tracer is iodinated N,N,N'-trimethyl-N'-(2-hydroxy-3– methyl-5-iodobenzyl)-1,3-propane-diamine (HIPDM). Anatomical details are lacking [The figure was originally published in JNM. © SNMMI (149)]. **(D,E)** Modern 2021 HMPAO SPECT perfusion scans for seizure localization. **(D)** Ictal scan. **(E)** Interictal scan. **(F)** SISCOM image wherein interictal scan data is subtracted from ictal scan data and the resulting data is overlayed on an anatomical MRI. Images courtesy of– Leonard Numerow MD FRCP(C), Radiology and Nuclear Medicine, Cumming School of Medicine, University of Calgary, Calgary, Alberta, Canada.

that identifies VaD dementia (191, 233, 234). However, certain features are highly suggestive of vascular dementia (235), such as hypoperfusion of the anterior cingulate gyrus (which mitigates relatively against AD) or reduced perfusion of the pulvinar of the thalamus as seen in subcortical VaD (191). Rather, it is often the varied, bilaterally disparate, and irregular

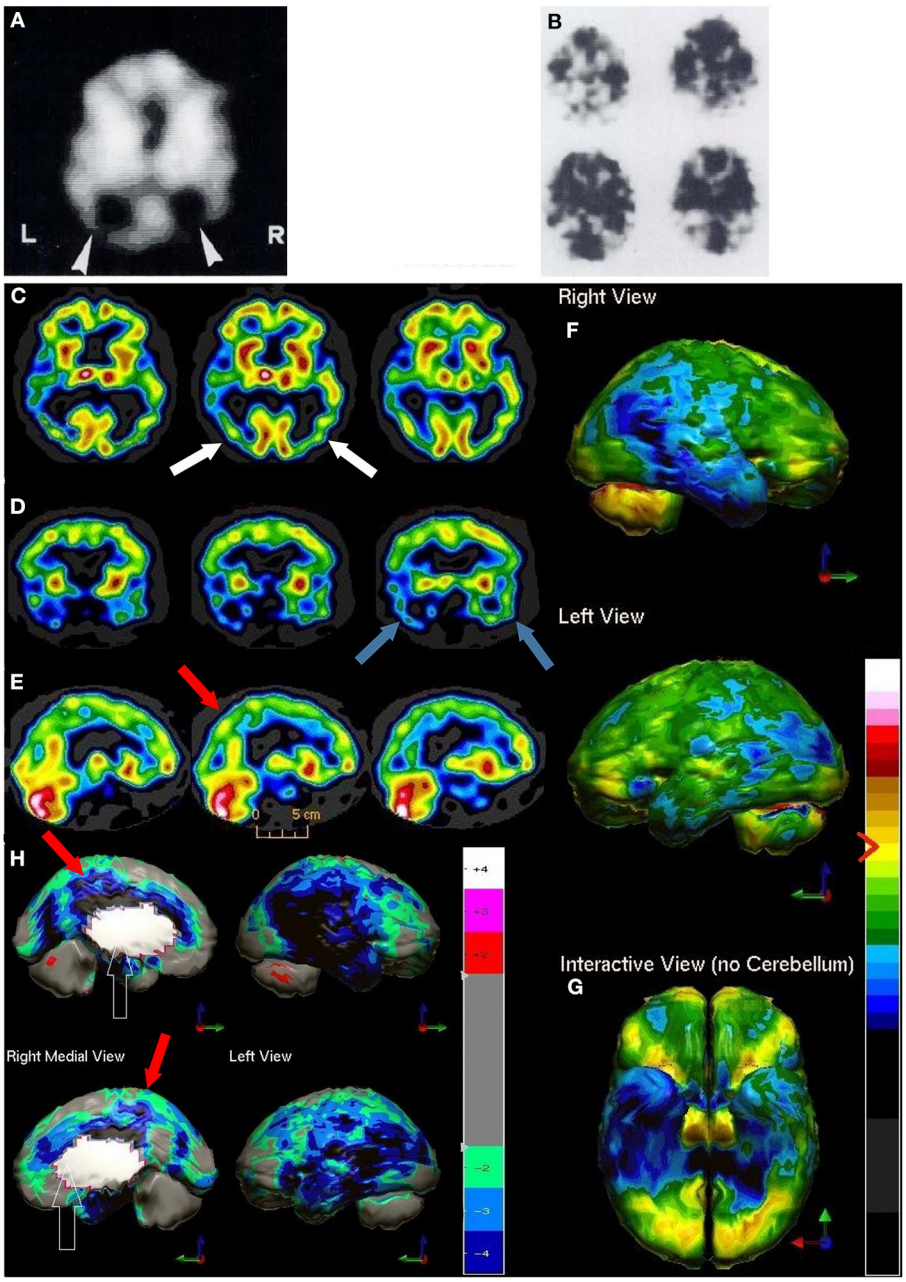

FIGURE 9 | (A,B) Examples of SPECT scan studies cited in TTASAAN report. Anatomical details are lacking. **(A)** An ^{99m}Tc-HMPAO perfusion SPECT performed in 1988 using a single head gamma camera illustrated a 75-year-old male with severe dementia and showed decreased perfusion of the bilateral parietal cortices [The figure was originally published in JNM. © SNMMI (202)]. **(B)** Example of ^{133}Xenon perfusion SPECT scan obtained with a ring-type tomogram circa 1988 [The figure was originally published in JNM. © SNMMI (180)]. C-H) Modern ^{99m}Tc-HMPAO SPECT scan performed on a dual-head camera illustrating Alzheimer's disease. **(C–E)** Horizontal, coronal, and sagittal tomograms, respectively, show decreased perfusion of the bilateral parietal cortices (white arrows), bilateral temporal cortices (blue arrows) and the posterior cingulate gyri (red arrow). Color scale is the same as in **Figure 1B**. **(F,G)** 3-D representation of SPECT scan data showing right lateral, left lateral **(F)**, and inferior views **(G)**. In the 3-D representations the asymmetry is much better seen with greater involvement of the right parietal and temporal lobes. **(H)** The patient's data is compared to a normative database using Segami Inc. Oasis software. The color scale is the same as in **Figure 2D**. Areas of relatively decreased perfusion are much more evident. The hypoperfusion of the posterior cingulate gyri (red arrows) is much better demonstrated.

pattern that aids in the diagnosis of vascular dementia. A meta-analysis of perfusion SPECT studies utilizing single-headed gamma cameras with only visual interpretation to distinguish AD from VaD found sensitivity to be 70% and specificity to be 76.6% (191, 236–240). In contrast, the use of multi-headed gamma cameras and quantitative analysis improved

sensitivity to 90%, while specificity remained slightly better than 76% (191, 218, 230, 241, 242). Neuroimaging data suggest that different types of VaD can be distinguished by SPECT; indeed, some authors feel that SPECT is more helpful in the diagnosis of different forms of vascular disease than PET (191, 233).

Frontal temporal dementia (FTD) can be characterized on functional brain imaging by decreased function and associated hypo- perfusion in the frontal lobes, caudate nuclei, and anterior temporal lobes (243–247). Hypoperfusion also can be found in the anterior cingulate gyrus. In FTD, perfusion is generally spared in the posterior cingulate gyrus/precuneus (91, 201, 248, 249). For example, Bonte et al. (186) followed 54 patients to autopsy, and a SPECT scan up to 1 year prior to death predicted the histopathology with a 96% sensitivity and an 84% specificity. The meta-analysis of all studies utilizing single-headed gamma cameras yielded a sensitivity of 71.5% and a specificity of 78.2% in the differentiation of AD from FTD (191, 244, 250–252). In contrast, a meta-analysis of studies utilizing multi-headed gamma cameras and quantitative analysis found the sensitivity was 96% and the specificity was 80% in differentiating AD from FTD (91, 191, 246, 249, 253). For example, in a careful study with quantitative analysis of SPECT data from a multi-headed gamma camera compared to autopsy findings, the temporal-parietal and posterior cingulate gyrus hypoperfusion had high sensitivity and specificity for distinguishing AD from FTD (91).

Similarly, the differentiation of AD from Lewy Body dementia (DLB) by perfusion SPECT imaging has benefited from improved hardware and analysis techniques. Shimizu et al. (254) examined the differentiation of DLB and AD using statistical parametric analysis to evaluate cortical, as well as deep nuclei, perfusion. They found that while hypoperfusion in the occipital lobe was predictive of DLB, the additional findings of increased perfusion in the thalamus and bilateral striatum strengthened the accuracy of the diagnosis of DLB. Sato et al. similarly found increased perfusion of the thalamus and striatum differentiated DLB from AD (255). Goto et al. (256) also found striatal parameters useful in differentiating early mild DLB from early mild AD. They found striatal volume to be reduced in early DLB, along with reduced occipital perfusion. The sensitivity of these parameters was 89%, while the specificity was 84%.

The accurate and early identification of Mild Cognitive Impairment (MCI) with perfusion SPECT has been examined extensively in several longitudinal studies. A total of 495 patients with MCI have been followed over 2–3 years [one study to 5 years (257)] in 10 longitudinal studies that included a baseline SPECT scan. All the studies used multi-headed gamma cameras and quantitative analysis (191, 257–266). Overall, 43% of MCI patients showing decreased perfusion in the: 1) posterior cingulate gyri, 2) posterior parietal cortices, and/or 3) temporal cortices converted to AD with an average conversion rate of 20% per annum. The remaining patients showed no change in cognition (stable MCI). Thus, the key SPECT findings found in AD were already present 2–3 years before the onset of the clinical symptoms of AD (191, 228, 229, 266). With quantitative analysis, the predictive value of perfusion SPECT in MCI can be increased considerably. Quantitative analysis yielded a sensitivity of 97%, a specificity of 100%, and an accuracy of 99% in one study (228). SPECT outperforms clinical assessment for MCI, which is generally 49–63% sensitive and 89–94% specific (267). Using older, single-headed gamma cameras and visual inspection, several studies found that SPECT can differentiate MCI with a sensitivity of ∼84% and a specificity of 83% (191). In contrast, multi-headed gamma cameras and quantitative analysis yields sensitivity and specificity exceeding 97% depending on the study (191, 228, 268).

Given that gamma cameras are much more readily available than PET scanners in much of the world and perfusion SPECT scans can be performed at a much lower cost than FDG-PET scans (191, 269–271), it is important to assess the value-added benefit of choosing PET or SPECT imaging (See **Table 2**). A relatively small number of studies have examined the distinction between SPECT and PET imaging in the evaluation of AD in the same patients. For example, a pivotal study by Herholz et al. (269) compared FDG-PET and perfusion SPECT in the same 26 patients with probable AD. In the key areas of the temporal, parietal, and posterior cingulate cortices, FDG-PET and SPECT yielded corresponding findings ($r = 0.90$) using statistical parametric analysis. Silverman (188) summarized the comparison of PET and SPECT well, noting that the sensitivity and specificity of PET and SPECT have considerable overlap. Similarly, a systematic review of studies comparing perfusion SPECT and FDG_PET in the diagnosis of AD and other dementias (199) found the two techniques quite comparable in terms of accuracy of diagnosis. The application of quantitative analysis greatly enhances both PET and SPECT. With appropriate quantitative analysis, both neuroimaging modalities can achieve high sensitivity and specificity in the diagnostic evaluation of AD and MCI, and in the differentiation of AD from LBD. Specifically, FDG-PET was found to predict the conversion from MCI to AD with a sensitivity of 70–90% and a specificity of 82.4–90% depending on the study (191, 196, 272, 273), while perfusion SPECT scans predict the conversion

TABLE 2 | Sensitivity and specificity of perfusion SPECT neuroimaging for differentiating Alzheimer's disease (AD) from controls, vascular dementia (VaD), and fronto-temporal dementia (FTD).

	SINGLE-HEAD		MULTI-HEAD	
	Sensitivity	**Specificity**	**Sensitivity**	**Specificity**
AD vs. Control	84%	83%	89%	88%
AD vs. VaD	70%	76.6%	90%	76.4%
AD vs. FTD	71.5%	78.2%	96%	80%
MCI → AD	84%	83%	89–97%	89–100%
FDG MCI → AD	–	–	89%	84%
Amyloid PET MCI → AD	–	–	67–87%	51–71%

Also shown are the sensitivity and specificity for predicting the progression of mild cognitive impairment (MCI) to AD. Results for perfusion SPECT imaging are separated based on data derived from studies utilizing single-headed vs. dual-headed cameras. Also shown are sensitivity and specificity of predicting the progression from MCI to AD for fluoro-deoxyglucose positron emission tomography (FDG-PET) and for amyloid tracer PET.

from MCI to AD with a sensitivity ranging from 89 to 97% and a specificity of 89–100% depending on the study (191, 196, 221, 225, 263, 274). Amyloid PET scans also should be included in this discussion given the growing number of amyloid tracers available. PET scans using amyloid-specific markers, such as florbetaben or florbetapir, yield very high sensitivity. A widely held belief is that a positive amyloid scan is 100% predictive of a progression to AD. However, specificity varies with age. A caveat for amyloid markers, regardless of the marker, is non-specific binding does occur and increases with age. Such non-specific binding occurs in ∼20% of 60-year-old controls, but this increases with age to ∼40% of 80-year-olds (275, 276). A recent Cochrane Review (277) found that amyloid markers predicted the progression from MCI to AD over a 4-year period with a sensitivity of 67% and a specificity of 71%. Shorter follow-up time courses yielded different metrics with a sensitivity of 89% and a specificity of 58% at 2 years (277).

Neuropsychiatric Conditions

Neurotoxicity

While not addressed in the TTASAAN report (1), perfusion SPECT neuroimaging has proven valuable in the evaluation of encephalopathy and of psychiatric cases wherein toxic encephalopathy may be a contributing factor to symptomatology. Solvent-induced encephalopathy has been investigated with perfusion SPECT (109, 278–280). Perfusion SPECT revealed diffuse hypoperfusion in 94% of cases in one study (279), while CT and MRI identified abnormalities in only 7 and 29%, respectively. Perfusion SPECT reveals diffuse hypoperfusion in metal toxicity (281), mold toxicity (282), and other toxin exposure (109, 283, 284), including recreational toxins (284–290). SPECT is also beneficial in the identification and grading of severity of hepatic encephalopathy due to ammonia toxicity (291–295), even in mild cases (296), as well as for tracking progress (295). Carbon monoxide poisoning is characterized by decreased perfusion of the bilateral frontal cortex, bilateral temporal cortex, and the globus pallidus (297–301) and perfusion SPECT has been used to document these findings. To the extent that toxicity can induce symptoms which can be confused with psychiatric symptoms, perfusion SPECT can lead to clarification of the diagnosis and detoxification, rather than psychiatric pharmacology. For example, in a patient with signs of decreased frontal lobe function (e.g., ADHD, aggression, anti-social personality disorder) a perfusion SPECT finding of diffuse hypoperfusion increases the likelihood of toxicity as the true cause of the frontal lobe dysfunction (109, 110, 302).

Specifically concerning recreational drugs, perfusion SPECT imaging reveals diffuse hypoperfusion throughout the cerebral cortices, but predominately in the frontal and temporal cortices (303–307). Dopamine transporter SPECT scans (DaTscans) demonstrate the presence and availability of dopamine transporter sites (DAT). A recent meta-analysis demonstrated reduced DAT density in the striatum, as well as all areas of cortex, among abusers of cocaine, methamphetamine, and amphetamine, consistent with down-regulation of the dopamine system among stimulant abusers (308, 309). In contrast, nicotine abusers did not show decreased DAT availability (309). Similar decreases in DAT density have been reported in opiate abusers (310). Similar findings have been reported with PET tracers for the DAT (311).

Carbon monoxide (CO) poisoning warrants a separate description because of its distinct findings on perfusion neuroimaging. In addition to the acute toxic effects of CO, victims can experience delayed neurological symptoms. Often significant recovery from the acute neurological insult can occur followed by a dramatic decline in neurological function, including loss of cognitive function, behavioral changes, gait disturbances, Parkinsonian symptoms, incontinence, and aphasia (301, 312–315). In acute CO toxicity, perfusion SPECT neuroimaging can reveal decreased perfusion in the basal ganglia (300, 316–318), along with decreased perfusion of the bilateral frontal, temporal, and (to a lesser extent) parietal cortices (300, 301, 316, 318). The degree of cortical hypoperfusion can be correlated with the degree of neuropsychological impairment (300, 317, 319, 320). Often CT scans are normal, with 0% sensitivity vs. 70% sensitivity for SPECT scan in one study (309). Perfusion SPECT scans were also more sensitive (66%) than EEG (25%) in the acute setting (321).

Similarly, perfusion SPECT neuroimaging has proven useful in the evaluation of delayed neuropsychiatric sequalae of CO poisoning, as well in assessing response to treatments (301, 314, 315, 322–325). Hypoperfusion of the basal ganglia have been correlated with the well-established finding of T2 hyperintensities in the globus pallidus by MRI (314, 320, 324). Similarly, hypoperfusion in bilateral frontal and temporal cortices has been correlated with reduced anisotropy by diffusion tensor imaging (325). The degree of cerebral hypoperfusion has been correlated with cognitive impairment (299, 301, 320) and with symptomatic improvement following treatments, such as hyperbaric oxygen therapy (314, 315, 322, 325). While bilateral globus pallidus injury, edema, and necrosis are considered a hallmark MRI finding in chronic CO toxicity, not every patient manifests these severe findings. For example, in a series of 21 patients with chronic CO toxicity, 38% had abnormal MRI findings, while 67% had abnormal perfusion SPECT scans (319). This question was again examined with a group of 30 patients with chronic CO toxicity (320). MRI demonstrated greater sensitivity, while perfusion SPECT had higher specificity, positive predictive value, and negative predictive value for persistent neuropsychiatric symptoms (320).

Psychiatric Indications

The use of perfusion SPECT neuroimaging for psychiatric indications has increased significantly over the past two decades. Unfortunately, it has not been widely adopted in either nuclear medicine or psychiatry for several reasons. First unlike neurological diagnoses, which are ultimately verifiable by biopsy, there are no recognized histopathological markers for psychiatric diagnoses, which is the case with Alzheimer's disease, stroke, or other dementias. Rather, psychiatric disorders are defined by the Diagnostic and Statistical Manual of Mental Disorders Version 5 (DSM-5). Psychiatric diagnoses are based not on pathology but upon a constellation of symptoms. However, there

is often tremendous range in how patient's symptoms present. For example, using the DSM-5 (326) diagnostic criteria for Major Depressive Disorder (110, 327), there are over 20 possible distinct phenotypes of this single diagnosis. The failure of clinical trials to effectively treat depression has led experts to state,

> *"…that major depressive disorder is biologically heterogeneous, such that different treatments differ in the likelihood of achieving remission in different patients" (328).*

Since psychiatry has difficulty establishing correct diagnoses and therapies, it is not surprising that perfusion SPECT has not established pathognomonic perfusion patterns.

Second, comorbidity is the rule rather than the exception in psychiatric conditions. It is difficult to identify a patient with pure bipolar disorder, for example, when the comorbidity of attention-deficit-hyperactivity-disorder (ADHD) occurs in ∼57% of adult bipolar patients (329) and up to 98% of pediatric bipolar cases (330). Similarly, in depression, in addition to having a multiplicity of presentations, many depressed patients also are comorbid for anxiety in up to 60% of cases (327, 331, 332). Patients with ADHD frequently have coexisting mood disorders (59%), anxiety, oppositional disorders, or learning disorders (327, 333–336). For all these reasons, it is highly unlikely that a pathognomonic finding or a "neuroimaging fingerprint" will be found for depression, anxiety, bipolar disorder, obsessive compulsive disorder (OCD), or ADHD. Indeed, these complexities result in widespread failure of the diagnostic criteria in field testing (337).

Despite these limitations, a substantial body of research literature exists for brain perfusion SPECT in the evaluation of psychiatric disorders. In addition, hundreds of thousands of perfusion SPECT scans have been performed worldwide since the development of the technology in the 1990's. Certain patterns or highly consistent findings have been replicated in the research literature. Findings with extensive clinical correlation will be noted here.

Attention Deficit Hyperactivity Disorder

Decreased frontal lobe perfusion is a consistent finding in ADHD across multiple SPECT studies (327, 338–345) and confirmed by multiple functional MRI studies (346, 347) and infrared spectroscopy (348). For example, SPECT scans of medication-naïve children with ADHD ($N = 40$) were compared to normal controls using statistical parametric analysis (338). Decreased perfusion was found in the prefrontal cortex, orbitofrontal cortex, and middle temporal gyri, while increased perfusion was found in the somatosensory cortex and anterior cingulate gyri (338). With stimulant treatment, perfusion increased in the prefrontal cortex (338, 343) corresponding with clinical improvement of ADHD symptoms. Clinical experience has heavily supported these findings (109, 302, 349).

Perfusion SPECT neuroimaging also is beneficial in the differential diagnosis of ADHD. Since inattention, impulsivity, and hyperactivity are non-specific signs of frontal lobe dysfunction, it is not surprising that toxicity, concussive brain injury, incipient bipolar disorder, infection, and inflammation can produce similar symptom constellations as ADHD. SPECT can reveal these alternative causes (109, 110, 302, 349). For example, infection or toxicity likely will appear as diffuse hypoperfusion as elaborated in the section on Neurotoxicity above. Brain injury will likely appear as an asymmetrical area of hypoperfusion. In contrast, bipolar disorder will present as described in the next section.

Bipolar Disorder

In contrast, bipolar mania, which can present symptomatically like ADHD, often demonstrates increased perfusion in the frontal cortex, particularly the dorsolateral prefrontal cortex and possibly greater on the left (350, 351). Patients with bipolar mania also typically do not show the decrease in prefrontal perfusion unless they have comorbid ADHD as described above (109). While the total number of subjects studied in ADHD and bipolar disorder number <200, the clinical experience across hundreds of thousands of scans supports the correlation of these disease processes with these perfusion patterns.

Increased and asymmetric perfusion of the thalamus may serve as a possible endophenotypic pattern of bipolar disorder in the manic or euthymic states (352–354). Bipolar depression may be similar to unipolar depression in terms of decreased frontal cortex perfusion (355), but it is possible the two can be distinguished by differences in the perfusion of the thalamus and basal ganglia in the depressed state. Perfusion, whether measured by SPECT or fMRI, is increased in the thalamus in bipolar disorder (350, 353–357). It must be emphasized that these types of endophenotypic patterns may not be evident upon visual inspection of tomographic data for an individual SPECT scan. Rather, these findings may only be manifest in the statistical comparison of perfusion data to normative databases.

Depression

Over 150 studies of perfusion SPECT imaging in depression containing more than 12,100 subjects have been completed. A consistent finding in early SPECT (Xenon or HMPAO) studies of depression was decreased perfusion in the frontal, and often temporal, cortices, as well as the superior anterior cingulate gyri (358–361). Later, two distinct patterns of perfusion were recognized – decreased perfusion in typical and melancholic depression and increased frontal lobe perfusion in atypical depression (362–365). Increased perfusion in the subgenual anterior cingulate gyrus in treatment-resistant depression was first described by Goodwin et al. (366) and has been recognized as a hallmark sign of treatment resistant depression, subsequently (365, 367, 368). Remission or response to treatment is characteristically followed by increased perfusion in the affected areas (366, 369, 370). Response could be predicted by the degree of frontal hypoperfusion and of subgenual hyperperfusion. Notably, response to serotonin reuptake inhibitors was predicted by higher frontal and cingulate perfusion (368, 371, 372), while response to electroconvulsive therapy (ECT) or transcranial magnetic stimulation (TMS) was predicted by lower frontal and

cingulate perfusion. Increased metabolic activity and perfusion in the thalamus (373, 374) is also a frequently reported finding in unipolar depression. Increased symmetrical perfusion of the thalamus has been consistently seen by clinicians on tens of thousands of perfusion SPECT scans.

Obsessive Compulsive Disorder

OCD is considered to result from an abnormal overactivity of a circuit involving the frontal cortices, anterior cingulate gyri, caudate nuclei and the thalami (375). Increased perfusion of the caudate nuclei and the anterior cingulate gyri have been reliable perfusion SPECT findings across 10 studies involving 196 subjects with OCD vs. 117 controls (376–385). Similar increased metabolism in these same areas has been found in studies utilizing FDG-PET (386, 387) and fMRI (388, 389). These findings were recently reviewed by Hazari et al. (390). Moreover, these findings have been consistently seen by clinicians on tens of thousands of perfusion SPECT scans.

Post-traumatic Stress Disorder

The symptom overlap between post-traumatic stress disorder (PTSD) and traumatic brain injury has complicated the correct diagnosis, particularly among military personnel (391, 392). Perfusion SPECT studies and FDG-PET studies have made similar findings in PTSD. Increased perfusion of the caudate nuclei is often found in PTSD (52, 53, 393). Another SPECT study showed that compared to controls, PTSD patients had increased cerebral blood flow in the limbic regions along with decreased perfusion in the superior frontal, parietal, and temporal regions (394). Systematic analyses of multiple regions of the default mode network involving 10,076 patients with TBI, PTSD, or both compared to 11,263 controls, revealed that PTSD resulted in increased perfusion in the basal ganglia, cingulate gyri, thalami, prefrontal cortices, and medial temporal cortices in both military (52) and civilian (53) populations. Provocation studies using perfusion SPECT, perfusion PET, and fMRI have shown increased perfusion in the amygdala, hippocampus, insula, but decreased perfusion in the medial prefrontal cortex (395–398).

DISCUSSION AND ACTIONABLE RECOMMENDATIONS

Given the major advances in our understanding of the SPECT functional neuroimaging findings for both neurological and psychiatric conditions as iterated above, the position assumed in the wake of the TTASAAN report by both the fields of Neurology and Psychiatry do not appear tenable. As a result, the following recommendations are made for the revisions of the current policies and practices as they relate to perfusion SPECT functional neuroimaging:

1) Increase awareness of the actual current state of the art as iterated above.
2) Replace assumptions about the inferiority of SPECT neuroimaging compared to PET, fMRI, diffusion tensor imaging, and MEG neuroimaging, particularly in the areas of dementia, TBI, seizure disorders, and neuropsychiatric indications with updated comparisons as elaborated herein.
3) Foster collaboration and communication between Nuclear Medicine physicians knowledgeable about perfusion SPECT neuroimaging and neurologists, psychiatrists, and other prescribers.
4) Improve knowledge of the technical aspects of perfusion SPECT neuroimaging to improve understanding of the limitations and strengths of the procedure. This will be addressed in Part II of this two-part series (399).
5) Revise Nuclear Medicine procedure guidelines to match the current state of the art as elaborated herein. This process has already begun with the publication of the new Canadian Association of Nuclear Medicine Guidelines for Brain Perfusion Single Photon Emission Computed Tomography (SPECT) (3).
6) Revise Neurology practice guidelines to include the use of perfusion SPECT neuroimaging in the areas for which it has been shown to be most effective or on par with FDG-PET neuroimaging (e.g., seizure disorders, dementia, stroke). The case is made herein that SPECT is a potent tool in the evaluation of TBI and warrants inclusion in Neurology practice guidelines based on Level IIa evidence meeting the criteria for a Type A recommendation by the standards set forth in the TTASAAN report (1) and the moral impossibility of achieving Class I evidence.
7) Revise Neurology and Psychiatry practice guidelines to recognize the advances in the state of the art of SPECT neuroimaging in the *evaluation of* neuropsychiatric indications. As the Canadian Association of Nuclear Medicine Guidelines for Brain Perfusion Single Photon Emission Computed Tomography (SPECT) (3) describes, the diagnostic picture for all of neuroimaging is clouded due to the subjective and non-physiological bases of psychiatric diagnoses. This remains an unresolved issue.
8) Understand the basics of reading and interpreting a perfusion brain SPECT scan based on the findings summarized herein. This will be addressed in Part II of this two-part series (399).

Perfusion SPECT scans require rigorous technique and correct adjustment of the equipment. An enormous variability in SPECT images results from technical inconsistency. The number of brain SPECT procedures performed annually is relatively small, largely due to the small number of scans ordered by treating physicians. One of the reasons why brain SPECT imaging is not prescribed more often is that prior encounters with sub-optimal images resulting from poor technique and lack of experience, have produced unhelpful findings. These negative experiences deter further use of SPECT scans and leads to fewer referrals. In part because of this dynamic and the parallel academic pressure to move to PET-based procedures, the attention, experience, and interest of nuclear medicine physicians has shifted away from SPECT imaging. In addition, the wholesale bias against perfusion SPECT scans discussed heretofore has stymied the clinical growth of this inexpensive, useful, and readily available procedure. The technical aspects of correctly performing and

reading these scans will be detailed in part II of this two-part series (399).

Although the focus within the nuclear medicine community has shifted toward brain PET imaging, there currently is a growing interest in brain SPECT from the field of psychiatry as it becomes more evident that these scans can be immensely helpful in developing treatment plans for certain conditions. Moreover, with the recent introduction of new camera technologies detailed in part II of this two-part series (399), it is possible to produce images that rival FDG-PET quality with lower radiation exposure and less cost.

CONCLUSIONS

Simply put—this is not your father's Oldsmobile. The SPECT scans of the early 1990's were limited due to single-headed gamma cameras, unstable or rapidly decaying tracers, limited post-processing techniques, and absence of quantitative analysis. Twenty-five years later, SPECT scans have much greater resolution, multiple normative databases, numerous studies often with quite large sample sizes, and sophisticated post-processing software. Moreover, the introduction of a new solid-state detector system utilizing cadmium-zinc-telluride (CZT) diodes will greatly increase the resolution of SPECT and reduce the radiation dose required. These improvements will address two limitations often cited concerning SPECT. These technical aspects are detailed in Part II of this series.

The path into the future will be paved with collaborations between nuclear medicine physicians, neurologists, and psychiatrists. Hopefully, enlightened clinicians in these fields will join together to deepen their clinical experience; hence, advancing and expand our understanding of the perfusion SPECT neuroimaging correlates in neurology and neuropsychiatry yielding improved treatment outcomes as has been demonstrated in several pilot studies (109, 110, 302, 349, 400).

AUTHOR CONTRIBUTIONS

DP and TH conceived the manuscript. DP, TH, and SD wrote initial drafts. TH and SD prepared revisions and prepared the figures. All authors contributed to the article and approved the submitted version.

ACKNOWLEDGMENTS

We would like to acknowledge the following individuals, as well as the entire International Society of Applied Neuroimaging, for their contributions to the discussions of these matters reviewed herein: Phil Cohen, MD, FRCPC; Muriel J. van Lierop, MBBS, MDPAC(M); Mary McLean, MB, ChB, FRCP; John Michael Uszler, MD, MS; John F. Rossiter-Thornton, MB, FRCPC; J. Cardaci, MBBS, FAANMS, FRACP; Leonard Numerow MD FRCP(C); Yin-Hui Siow, MD, FRCPC. We also acknowledge Jenny Faherty for technical assistance and copy-editing. We acknowledge Alaina M. Henderson for assistance with the preparation of the figures.

REFERENCES

1. Report of the Therapeutics Technology Assessment Subcommittee of the American Academy of Neurology. Assessment of brain SPECT. *Neurology*. (1996) 46:278–85. doi: 10.1212/WNL.46.1.278
2. Kapucu OL, Nobili F, Varrone A, Booij J, Vander Borght T, Någren K, et al. EANM procedure guideline for brain perfusion SPECT using 99mTc-labelled radiopharmaceuticals, version 2. *Eur J Nucl Med Mol Imaging*. (2009) 36:2093–102. doi: 10.1007/s00259-009-1266-y
3. Canadian Association of Nuclear Medicine. *CANM Guidelines for Brain Perfusion Single Photon Emission Computed Tomography (SPECT)*. (2021). Available online at: https://canm-acmn.ca/guidelines/ (accessed July 14, 2021).
4. Mazziotta JC, Collins RC. William H. Oldendorf, M.D. (1925-1992). *J Comput Assist Tomogr*. (1993) 17:169–71. doi: 10.1097/00004728-199303000-00001
5. van Dellen JR, Danziger A. Failure of computerized tomography to differentiate between radiation necrosis and cerebral tumour. *S Afr Med J*. (1978) 53:171–2.
6. Phillips DF. The efficacy of CT: what the studies show. *Hosp Med Staff*. (1978) 4:12–9.
7. French BN. Limitations and pitfalls of computed tomography in the evaluation of craniocerebral injury. *Surg Neurol*. (1978) 10:395–401.
8. Stockburger WT. CT imaging, then and now: a 30-year review of the economics of computed tomography. *Radiol Manage*. (2004) 26: 24–7.
9. McKinney W. *History of Neuroimaging. The American Society of Neuroimaging*. (2021). Available online at: https://www.asnweb.org/i4a/pages/index.cfm?pageID=3334&activateFull=true (accessed June 6, 2021).
10. First MB, Drevets WC, Carter C, Dickstein DP, Kasoff L, Kim KL. Clinical applications of neuroimaging in psychiatric disorders. *Am J Psychiatry*. (2018) 175:915–16. doi: 10.1176/appi.ajp.2018.1750701
11. Eklund A, Nichols TE, Knutsson H. Cluster failure: why fMRI inferences for spatial extent have inflated false-positive rates. *Proc Natl Acad Sci USA*. (2016) 113:7900–5. doi: 10.1073/pnas.1602413113
12. Szaflarski JP, Gloss D, Binder JR, Gaillard WD, Golby AJ, Holland SK, et al. Practice guideline summary: Use of fMRI in the presurgical evaluation of patients with epilepsy: Report of the Guideline Development, Dissemination, and Implementation Subcommittee of the American Academy of Neurology. *Neurology*. (2017) 88:395–402. doi: 10.1212/WNL.0000000000003532
13. Wang ZJ, Seo Y, Babcock E, Huang H, Bluml S, Wisnowski J, et al. Assessment of diffusion tensor image quality across sites and vendors using the American College of Radiology head phantom. *J Appl Clin Med Phys*. (2016) 17:442–51. doi: 10.1120/jacmp.v17i3.5972
14. Eierud C, Craddock RC, Fletcher S, Aulakh M, King-Casas B, Kuehl D, et al. Neuroimaging after mild traumatic brain injury: review and meta-analysis. *Neuroimage Clin*. (2014) 4:283–94. doi: 10.1016/j.nicl.2013.12.009
15. Asken BM, DeKosky ST, Clugston JR, Jaffee MS, Bauer RM. Diffusion tensor imaging (DTI) findings in adult civilian, military, and sport-related mild traumatic brain injury (mTBI): a systematic critical review. *Brain Imaging Behav*. (2018) 2:585–612. doi: 10.1007/s11682-017-9708-9
16. Patterson J Wyper DJ. Basics of SPECT. In: Duncan R, editors. *SPECT Imaging of the Brain*. Lancaster: Kluwer Academic Publishers (1997). doi: 10.1007/978-94-011-5398-0_1
17. Jaszczak RJ. The early years of single photon emission computed tomography (SPECT): an anthology of selected reminiscences. *Phys Med Biol*. (2006) 51:R99–115. doi: 10.1088/0031-9155/51/13/R07

18. Harper PV, Beck RM, Charleston DE, Brunsten B, Lathrop KA. Three-dimensional mapping and display of radioisotope distributions. *J Nucl Med.* (1965) 6:332.
19. Winchell HS, Horst WD, Braun L, Oldendorf WH, Hattner R, Parker H. N-isopropyl-[123I] p-iodoamphetamine: single-pass brain uptake and washout; binding to brain synaptosomes; and localization in dog and monkey brain. *J Nucl Med.* (1980) 21:947–52.
20. Ell PJ, Hocknell JM, Jarritt PH, Cullum I, Lui D, Campos-Costa D, et al. A 99Tcm-labelled radiotracer for the investigation of cerebral vascular disease. *Nucl Med Commun.* (1985) 6:437–41. doi: 10.1097/00006231-198508000-00002
21. Neirinckx RD, Burke JF, Harrison RC, Forster AM, Andersen AR, Lassen NA. The retention mechanism of technetium-99m-HM-PAO: intracellular reaction with glutathione. *J Cereb Blood Flow Metab.* (1988) 8:S4–12. doi: 10.1038/jcbfm.1988.27
22. Sharp PF, Smith FW, Gemmell HG, Lyall D, Evans NT, Gvozdanovic D, et al. Technetium-99m HM-PAO stereoisomers as potential agents for imaging regional cerebral blood flow: human volunteer studies. *J Nucl Med.* (1986) 27:171–7.
23. Lassen NA, Andersen AR, Friberg L, Paulson OB. The retention of [99mTc]-d,l-HM-PAO in the human brain after intracarotid bolus injection: a kinetic analysis. *J Cereb Blood Flow Metab.* (1988) 8:S13–22. doi: 10.1038/jcbfm.1988.28
24. Inugami A, Kanno I, Uemura K, Shishido F, Murakami M, Tomura N, et al. Linearization correction of 99mTc-labeled hexamethyl-propylene amine oxime (HM-PAO) image in terms of regional CBF distribution: comparison to C15O2 inhalation steady-state method measured by positron emission tomography. *J Cereb Blood Flow Metab.* (1988) 8:S52–60. doi: 10.1038/jcbfm.1988.33
25. Holman BL, Hellman RS, Goldsmith SJ, Mena IG, Leveille J, Gherardi PG, et al. Biodistribution, dosimetry, and clinical evaluation of technetium-99m ethyl cysteinate dimer in normal subjects and in patients with chronic cerebral infarction. *J Nucl Med.* (1989) 30:1018–24.
26. Ichise M, Chung DG, Wang P, Wortzman G, Gray BG, Franks W. Technetium-99m-HMPAO SPECT, CT and MRI in the evaluation of patients with chronic traumatic brain injury: a correlation with neuropsychological performance. *J Nucl Med.* (1994) 35:217–26.
27. Roper SN, Mena I, King WA, Schweitzer J, Garrett K, Mehringer CM, et al. An analysis of cerebral blood flow in acute closed-head injury using technetium-99m-HMPAO SPECT and computed tomography. *J Nucl Med.* (1991) 32:1684–7.
28. Gray BG, Ichise M, Chung DG, Kirsh JC, Franks W. Technetium-99m-HMPAO SPECT in the evaluation of patients with a remote history of traumatic brain injury: a comparison with x-ray computed tomography. *J Nucl Med.* (1992) 33:52–8.
29. Stapleton SJ, Caldwell CB, Leonhardt CL, Ehrlich LE, Black SE, Yaffe MJ. Determination of thresholds for detection of cerebellar blood flow deficits in brain SPECT images. *J Nucl Med.* (1994) 35:1547–55.
30. Krupinski EA. The role of perception in imaging: past and future. *Semin Nucl Med.* (2011) 41:392–400. doi: 10.1053/j.semnuclmed.2011.05.002
31. Kim BJ, Kim YH, Kim YJ, Ahn SH, Lee DH, Kwon SU, et al. Color-coded fluid-attenuated inversion recovery images improve inter-rater reliability of fluid-attenuated inversion recovery signal changes within acute diffusion-weighted image lesions. *Stroke.* (2014) 45:2801-4. doi: 10.1161/STROKEAHA.114.006515
32. Mena FJ, Mena I, Alamos F, Solé C, Neurbauer S, et al. SPECT Tc99m-HMPAO brain uptake in normal children: a comparison to normal elderly subjects. *ALASBINM J.* (1998) 1:4055.
33. Devous MD Sr, Stokely EM, Chehabi HH, Bonte FJ. Normal distribution of regional cerebral blood flow measured by dynamic single-photon emission tomography. *J Cereb Blood Flow Metab.* (1986) 6:95–104. doi: 10.1038/jcbfm.1986.12
34. Bigler ED. Neurobiology and neuropathology underlie the neuropsychological deficits associated with traumatic brain injury. *Arch Clin Neuropsychol.* (2003) 18:595–621. doi: 10.1016/S0887-6177(02)00156-7
35. Bigler ED, Maxwell WL. Neuropathology of mild traumatic brain injury: relationship to neuroimaging findings. *Brain Imaging Behav.* (2012) 6:108–36. doi: 10.1007/s11682-011-9145-0
36. Centers for Disease Control and Prevention, National Center for Injury Prevention and Control. *Report to Congress on Traumatic Brain Injury in the United States: Epidemiology and Rehabilitation*. Atlanta, GA: Centers for Disease Control and Prevention (2015).
37. Mountney A, Boutté AM, Cartagena CM, Flerlage WF, Johnson WD, Rho C, et al. Functional and molecular correlates after single and repeated rat closed-head concussion: indices of vulnerability after brain injury. *J Neurotrauma.* (2017) 34:2768–89. doi: 10.1089/neu.2016.4679
38. Barkhoudarian G, Hovda DA, Giza CC. The molecular pathophysiology of concussive brain injury - an update. *Phys Med Rehabil Clin N Am.* (2016) 27:373–93. doi: 10.1016/j.pmr.2016.01.003
39. WHO (World Health Organization). *International Statistical Classification of Diseases and Related Health Problems.* (2010). Available online at: http://apps.who.int/classifications/icd10/browse/2010/en (accessed May 24, 2018).
40. Jacobs A, Put E, Ingels M, Bossuyt A. Prospective evaluation of technetium-99m-HMPAO SPECT in mild and moderate traumatic brain injury. *J Nucl Med.* (1994) 35:942–7.
41. Abdel-Dayem HM, Sadek SA, Kouris K, Bahar RH, Higazi I, Eriksson S, et al. Changes in cerebral perfusion after acute head injury: comparison of CT with Tc-99m HM-PAO SPECT. *Radiology.* (1987) 165:221–6. doi: 10.1148/radiology.165.1.3498184
42. Ducours JL, Role C, Guillet J, San Galli F, Caix P, Wynchank S. Cranio-facial trauma and cerebral SPECT studies using N-isopropyl-iodo-amphetamine (123I). *Nucl Med Commun.* (1990) 11:361–7. doi: 10.1097/00006231-199005000-00003
43. Masdeu JC, Van Heertum RL, Kleiman A, Anselmi G, Kissane K, Horng J, et al. Early single-photon emission computed tomography in mild head trauma. A controlled study. *J Neuroimaging.* (1994) 4:177–81. doi: 10.1111/jon199444177
44. Raji CA, Tarzwell R, Pavel D, Schneider H, Uszler M, Thornton J, et al. Clinical utility of SPECT neuroimaging in the diagnosis and treatment of traumatic brain injury: a systematic review. *PLoS ONE.* (2014) 9:e91088. doi: 10.1371/journal.pone.0091088
45. Nedd K, Sfakianakis G, Ganz W, Uricchio B, Vernberg D, Villanueva P, et al. 99mTc-HMPAO SPECT of the brain in mild to moderate traumatic brain injury patients: compared with CT-a prospective study. *Brain Inj.* (1993) 7:469–79. doi: 10.3109/02699059309008174
46. Kesler SR, Adams HF, Bigler ED. SPECT, MR and quantitative MR imaging: correlates with neuropsychological and psychological outcome in traumatic brain injury. *Brain Inj.* (2000) 14:851–7. doi: 10.1080/026990500445682
47. Stamatakis EA, Wilson JT, Hadley DM, Wyper DJ. SPECT imaging in head injury interpreted with statistical parametric mapping. *J Nucl Med.* (2002) 43:476–83.
48. Kinuya K, Kakuda K, Nobata K, Sakai S, Yamamoto K, Itoh S, et al. Role of brain perfusion single-photon emission tomography in traumatic head injury. *Nucl Med Commun.* (2004) 25:333–7. doi: 10.1097/00006231-200404000-00004
49. Pavel D, Jobe T, Devore-Best S, Davis G, Epstein P, Sinha S, et al. Viewing the functional consequences of traumatic brain injury by using brain SPECT. *Brain Cogn.* (2006) 60:211–3.
50. Atighechi S, Salari H, Baradarantar MH, Jafari R, Karimi G, Mirjali M. A comparative study of brain perfusion single-photon emission computed tomography and magnetic resonance imaging in patients with post-traumatic anosmia. *Am J Rhinol Allergy.* (2009) 23:409–12. doi: 10.2500/ajra.2009.23.3345
51. Joglekar SS, Bell JR, Caroline M, Chase PJ, Domesek J, Patel PS, et al. Evaluating the role of single-photon emission computed tomography in the assessment of neurotologic complaints. *Ear Nose Throat J.* (2014) 93:168–73. doi: 10.1177/0145561314093004-512
52. Raji CA, Willeumier K, Taylor D, Tarzwell R, Newberg A, Henderson TA, et al. Functional neuroimaging with default mode network regions distinguishes PTSD from TBI in a military veteran population. *Brain Imaging Behav.* (2015) 9:527–34. doi: 10.1007/s11682-015-9385-5
53. Amen DG, Raji CA, Willeumier K, Taylor D, Tarzwell R, Newberg A, et al. Functional neuroimaging distinguishes posttraumatic stress disorder from traumatic brain injury in focused and large community datasets. *PLoS ONE.* (2015) 10:e0129659. doi: 10.1371/journal.pone.0129659

54. Davalos DB, Bennett TL. A review of the use of single-photon emission computerized tomography as a diagnostic tool in mild traumatic brain injury. *Appl Neuropsychol.* (2002) 9:92–105. doi: 10.1207/S15324826AN0902_4
55. Wortzel HS, Filley CM, Anderson CA, Oster T, Arciniegas DB. Forensic applications of cerebral single photon emission computed tomography in mild traumatic brain injury. *J Am Acad Psychiatry Law*. (2008) 36:310–22.
56. Amyot F, Arciniegas DB, Brazaitis MP, Curley KC, Diaz-Arrastia R, Gandjbakhche A, et al. A review of the effectiveness of neuroimaging modalities for the detection of traumatic brain injury. *J Neurotrauma.* (2015) 32:1693–721. doi: 10.1089/neu.2013.3306
57. Bigler ED. Systems biology, neuroimaging, neuropsychology, neuroconnectivity and traumatic brain injury. *Front Syst Neurosci.* (2016) 10:55. doi: 10.3389/fnsys.2016.00055
58. Yeates KO, Levin HS, Ponsford J. The neuropsychology of traumatic brain injury: looking back, peering ahead. *J Int Neuropsychol Soc.* (2017) 23:806–17. doi: 10.1017/S1355617717000686
59. Sataloff RT, Mandel S, Muscal E, Park CH, Rosen DC, Kim SM, et al. Single-photon-emission computed tomography (SPECT) in neurotologic assessment: a preliminary report. *Am J Otol.* (1996)17:909–16.
60. Abdel-Dayem HM, Abu-Judeh H, Kumar M, Atay S, Naddaf S, El-Zeftawy H, et al. SPECT brain perfusion abnormalities in mild or moderate traumatic brain injury. *Clin Nucl Med.* (1998) 23:309–17. doi: 10.1097/00003072-199805000-00009
61. Abu-Judeh HH, Parker R, Aleksic S, Singh ML, Naddaf S, Atay S. SPECT brain perfusion findings in mild or moderate traumatic brain injury. *Nucl Med Rev Cent East Eur*. (2000) 3:5–11.
62. Mazzini L, Cossa FM, Angelino E, Campini R, Pastore I, Monaco F. Posttraumatic epilepsy: neuroradiologic and neuropsychological assessment of long-term outcome. *Epilepsia.* (2003) 44:569–74. doi: 10.1046/j.1528-1157.2003.34902.x
63. Amen DG, Newberg A, Thatcher R, Jin Y, Wu J, Keator D, et al. Impact of playing American professional football on long-term brain function. *J Neuropsychiatry Clin Neurosci.* (2011) 23:98–106. doi: 10.1176/appi.neuropsych.23.1.98
64. Jacobs A, Put E, Ingels M, Put T, Bossuyt A. One-year follow-up of technetium-99m-HMPAO SPECT in mild head injury. *J Nucl Med.* (1996) 37:1605–9.
65. Mazzini L, Campini R, Angelino E, Rognone F, Pastore I, Oliveri G. Posttraumatic hydrocephalus: a clinical, neuroradiologic, and neuropsychologic assessment of long-term outcome. *Arch Phys Med Rehabil.* (2003) 84:1637–41. doi: 10.1053/S0003-9993(03)00314-9
66. Gowda NK, Agrawal D, Bal C, Chandrashekar N, Tripati M, Bandopadhyaya GP, et al. Technetium Tc-99m ethyl cysteinate dimer brain single-photon emission CT in mild traumatic brain injury: a prospective study. *Am J Neuroradiol.* (2006) 27:447–51.
67. Amen DG, Wu JC, Taylor D, Willeumier K. Reversing brain damage in former NFL players: implications for traumatic brain injury and substance abuse rehabilitation. *J Psychoactive Drugs.* (2011) 43:1–5. doi: 10.1080/02791072.2011.566489
68. Wells GA, Shea B, O'Connell D, Peterson J, Welch V, Losos M, et al. *The Newcastle-Ottawa Scale (NOS) for Assessing the Quality of Nonrandomized Studies in Meta-Analyses. The Ottawa Hospital Research Institute.* (2021). Available online at: http://www.ohri.ca/programs/clinical_epidemiology/oxford.asp (accessed June 20, 2021).
69. Henderson TA, Morries LD. SPECT perfusion imaging demonstrates improvement of traumatic brain injury with transcranial near-infrared laser phototherapy. *Adv Mind Body Med*. (2015) 29:27–33. doi: 10.2147/NDT.S65809
70. Obrist WD, Gennarelli TA, Segawa H, Dolinskas CA, Langfitt TW. Relation of cerebral blood flow to neurological status and outcome in head-injured patients. *J Neurosurg*. (1979) 51:292–300. doi: 10.3171/jns.1979.51.3.0292
71. Vavilala MS, Farr CK, Watanitanon A, Clark-Bell BC, Chandee T, Moore A, et al. Early changes in cerebral autoregulation among youth hospitalized after sports-related traumatic brain injury. *Brain Inj.* (2018) 32:269–75. doi: 10.1080/02699052.2017.1408145
72. Mathew P, Bullock R, Teasdale G, McCulloch J. Changes in local microvascular permeability and in the effect of intervention with 21-aminosteroid (Tirilazad) in a new experimental model of focal cortical injury in the rat. *J Neurotrauma*. (1996) 13:465–72. doi: 10.1089/neu.1996.13.465
73. Emanuelson IM, von Wendt L, Bjure J, Wiklund LM, Uvebrant P. Computed tomography and single-photon emission computed tomography as diagnostic tools in acquired brain injury among children and adolescents. *Dev Med Child Neurol.* (1997) 39:502–7. doi: 10.1111/j.1469-8749.1997.tb07477.x
74. Lorberboym M, Lampl Y, Gerzon I, Sadeh M. Brain SPECT evaluation of amnestic ED patients after mild head trauma. *Am J Emerg Med.* (2002) 20:310–3. doi: 10.1053/ajem.2002.34201
75. Shin YB, Kim SJ, Kim IJ, Kim YK, Kim DS, Park JH, et al. Voxel-based statistical analysis of cerebral blood flow using Tc-99m ECD brain SPECT in patients with traumatic brain injury: group and individual analyses. *Brain Inj.* (2006) 20:661–7. doi: 10.1080/02699050600677071
76. Randolph C. Neuropsychological testing: evolution and emerging trends. *CNS Spectr.* (2002) 7:307–12. doi: 10.1017/S1092852900017727
77. Sherman E, Brooks B, Iverson G, Slick D, Strauss E. Reliability and Validity in Neuropsychology. In: Schoenberg MR, Scott JG, editors. *The Little Black Book of Neuropsychology: A Syndrome-Based Approach*. New York, NY: Springer Science+Business Media, LLC (2011). doi: 10.1007/978-0-387-76978-3_30
78. Oestreicher JM, O'Donnell JP. Validation of the general neuropsychological deficit scale with nondisabled, learning-abled and head-injured young adults. *Arch Clin Neuropsychol.* (1995) 10:185–91. doi: 10.1016/0887-6177(94)E0039-R
79. Reitan RM, Wolfson D. The two faces of mild head injury. *Arch Clin Neuropsychol.* (1999) 14:191–202. doi: 10.1093/arclin/14.2.191
80. Green P. Why clinicians often disagree about the validity of test results. *NeuroRehabilitation.* (2001) 16:231–6. doi: 10.3233/NRE-2001-16407
81. Wade JB, DeMatteo D, Hart RP. Neuropsychologists diagnose traumatic brain injury. *Brain Inj.* (2004) 18:629–43. doi: 10.1080/02699050310001646198
82. Marenco S, Coppola R, Daniel DG, Zigun JR, Weinberger DR. Regional cerebral blood flow during the Wisconsin Card Sorting Test in normal subjects studied by xenon-133 dynamic SPECT: comparison of absolute values, percent distribution values, and covariance analysis. *Psychiatry Res.* (1993) 50:177–92. doi: 10.1016/0925-4927(93)90029-H
83. Kawasaki Y, Maeda Y, Suzuki M, Urata K, Higashima M, Kiba K, et al. SPECT analysis of regional cerebral blood flow changes in patients with schizophrenia during the Wisconsin Card Sorting Test. *Schizophr Res.* (1993) 10:109–16. doi: 10.1016/0920-9964(93)90045-K
84. Catafau AM, Parellada E, Lomena F, Bernardo M, Setoain J, Catarineu S, et al. Role of the cingulate gyrus during the Wisconsin Card Sorting Test: a single photon emission computed tomography study in normal volunteers. *Psychiatry Res.* (1998) 83:67–74. doi: 10.1016/S0925-4927(98)00031-6
85. Yang YK, Chen CC, Lee IH, Chou YH, Chiu NT, Jeffries KJ, et al. Association between regional cerebral blood flow and eye-tracking performance and the Wisconsin Sorting Test in schizophrenics: a single photon emission computed tomography study. *Psychiatry Res.* (2003) 123:37–48. doi: 10.1016/S0925-4927(03)00021-0
86. Goethals I, Audennaert K, Jacobs F, Lannoo E, Van de White C, Ham H, et al. Cognitive neuroactiviation using SPECT and the Stroop Colored Word Test in patients with diffuse brain injury. *J Neurotrauma*. (2004) 21:1059–69. doi: 10.1089/0897715041651051
87. Audenaert K, Lahorte P, Brans B, van Laere K, Goethals I, van Heeringen K, et al. The classical stroop interference task as a prefrontal activation probe: a validation study using 99T cm-ECD brain SPECT. *Nucl Med Commun.* (2001) 22:135–43. doi: 10.1097/00006231-200102000-00004
88. Goethals I, Audenaert K, Jacobs F, Van de Wiele C, Pyck H, Ham H, et al. Application of neuropsychological activation probe with SPECT: the "Tower of London" task in healthy volunteers. *Nucl Med Commun*. (2004) 25:177–82. doi: 10.1097/00006231-200402000-00015
89. Morris RG, Ahmed S, Syed GM, Toone BK. Neural correlates of planning ability: frontal lobe activation during the Tower of London test. *Neuropsychologia.* (1993) 31:1367–78. doi: 10.1016/0028-3932(93)90104-8

90. Ueda H, Kitabayashi Y, Narumoto J, Nakamura K, Kita H, Kishikawa Y, et al. Relationship between clock drawing test performance and regional cerebral blood flow in Alzheimer's disease: a single photon emission computed tomography study. *Psychiatry Clin Neurosci.* (2002) 56:25–9. doi: 10.1046/j.1440-1819.2002.00940.x
91. Bonte FJ, Harris TS, Roney CA, Hynan LS. Differential diagnosis between Alzheimer's disease and frontotemporal disease by the posterior cingulate sign. *J Nucl Med.* (2004) 45:771–74.
92. Audenaert K, Goethals I, Van Laere K, Lahorte P, Brans B, Versijpt J, et al. SPECT neuropsychological activation procedure with the Verbal Fluency Test in attempted suicide patients. *Nucl Med Commun.* (2002) 23:907–16. doi: 10.1097/00006231-200209000-00015
93. Wszolek ZK, Herkes GK, Lagerlund TD, Kokmen E. Comparison of EEG background frequency analysis, psychologic test scores, short test of mental status, and quantitative SPECT in dementia. *J Geratr Psychiatry Neurol.* (1992) 5:22–30. doi: 10.1177/002383099200500104
94. Fallon BA, Das S, Plutchok JJ, Tager F, Liegner K, Van Heertum R. Functional brain imaging and neuropsychological resting in Lyme disease. *Clin Infect Dis.* (1997) 25:S57–63. doi: 10.1086/516175
95. Belin C, Moroni C, Caillat-Vigneron N, Debray M, Baudin M, Dumas JL, et al. Central nervous system development in Sjogren's syndrome: evidence from neuropsychological testing and HMPAO-SPECT. *Ann Med Interne.* (1999) 150:598–604.
96. Landtblom AM, Dige N, Schwerdt K, Safstrom P, Granerus G. A case of Kleine-Levin Syndrome examined with SPECT and neuropsychological testing. *Acta Neurol Scand.* (2002) 105:318–21. doi: 10.1034/j.1600-0404.2002.1c162.x
97. Lacerda AL, Dalgalarrondo P, Caetano D, Haas GL, Camargo EE, Keshavan MS. Neuropsychological performance and regional cerebral blood flow in obsessive-compulsive disorder. *Prog Neuropsychopharmacol Biol Psychiatry.* (2003) 27:657–65. doi: 10.1016/S0278-5846(03)00076-9
98. Calandre EP, Bembibre J, Arnedo ML, Becerra D. Cognitive disturbances and regional cerebral blood flow abnormalities in migraine patients: their relationship with the clinical manifestations of the illness. *Cephalalgia.* (2002) 22:291–302. doi: 10.1046/j.1468-2982.2002.00370.x
99. Bak TH, Antoun N, Balan KK, Hodges JR. Memory lost, memory regained: neuropsychological findings and neuroimaging in two cases of paraneoplastic limbic encephalitis with radically different outcomes. *J Neurol Neurosurg Psychiatry*. (2001) 71:40–7. doi: 10.1136/jnnp.71.1.40
100. Sabri O, Ringelstein EB, Hellwig D, Schneider R, Schreckenberger M, Kaiser HJ, et al. Neuropsychological impairment correlates with hypoperfusion and hypometabolism but not with severity of white matter lesions on MRI in patients with cerebral microangiopathy. *Stroke.* (1999) 30:556–66. doi: 10.1161/01.STR.30.3.556
101. Nicolas JM, Catafau AM, Estruch R, Lomena FJ, Salamero M, Herranz R et al. Regional cerebral blood flow-SPECT in chronic alcoholism: relation to neuropsychological testing. *J Nucl Med.* (1993) 34:1452–9.
102. Arbizu J, Larumbe R, Gamez C, Marti J, Martinez-Lage J, Richter J. Correlations between brain SPECT and neuropsychology in assessments in mild and moderate stages of Alzheimer's disease. *Rev Esp Med Nucl.* (1999) 18:252–60.
103. Hall RA, Fordyce DJ, Lee ME, Eisenberg B, Lee RF, Holmes JH, et al. Brain SPECT imaging and neuropsychological testing in coronary artery bypass patients: single photon emission computed tomography. *Ann Thorac Surg.* (1999) 68:2082–8. doi: 10.1016/S0003-4975(99)01213-8
104. Kant R, Smith-Seemiller L, Isaac G, Duffy J. Tc-HMPAO SPECT in persistent post-concussion syndrome after mild head injury: comparison with MRI/CT. *Brain Inj.* (1997) 11:115–24. doi: 10.1080/026990597123700
105. Umile EM, Plotkin RC, Sandel ME. Functional assessment of mild traumatic brain injury using SPECT and neuropsychological testing. *Brain Inj.* (1998) 12:577–94. doi: 10.1080/026990598122340
106. Matsushita M, Hosoda K, Naitoh Y, Yamashita H, Kohmura E. Utility of diffusion tensor imaging in the acute stage of mild to moderate traumatic brain injury for detecting white matter lesions and predicting long-term cognitive function in adults. *J Neurosurg.* (2011) 115:130–9. doi: 10.3171/2011.2.JNS101547
107. Laatsch L, Pavel D, Jobe T, Lin Q, Quintana JC. Incorporation of SPECT imaging in a longitudinal cognitive rehabilitation therapy programme. *Brain Inj.* (1999) 13:555–70. doi: 10.1080/026990599121304
108. Mez J, Stern RA, McKee AC. Chronic traumatic encephalopathy: where are we and where are we going? *Curr Neurol Neurosci Rep.* (2013) 13:407. doi: 10.1007/s11910-013-0407-7
109. Henderson TA, Uszler JM, Rossiter-Thornton JF, Siow Y-H, Pavel DG, McLean M, et al. The American Psychiatric Association fails to recognize the value of neuroimaging in psychiatry. *Interv Med Clin Imaging.* (2019) 1:1–8. Available online at: https://researchopenworld.com/the-american-psychiatric-association-fails-to-recognize-the-value-of-neuroimaging-in-psychiatry/
110. Henderson TA, van Lierop MJ, McLean M, Uszler JM, Thornton JF, Siow YH. Functional neuroimaging in psychiatry-aiding in diagnosis and guiding treatment. What the American Psychiatric Association does not know. *Front Psychiatry.* (2020) 11:276. doi: 10.3389/fpsyt.2020.00276
111. Wozniak JR, Krach L, Ward E, Mueller BA, Muetzel R, Schnoebelen S, et al. Neurocognitive and neuroimaging correlates of pediatric traumatic brain injury: a diffusion tensor imaging (DTI) study. *Arch Clin Neuropsychol.* (2007) 22:555–68. doi: 10.1016/j.acn.2007.03.004
112. Newcombe VF, Williams GB, Nortje J, Bradley PG, Harding SG, Smielewski P, et al. Analysis of acute traumatic axonal injury using diffusion tensor imaging. *Br J Neurosurg.* (2007) 21:340–8. doi: 10.1080/02688690701400882
113. Avants B, Duda JT, Kim J, Zhang H, Pluta J, Gee JC, et al. Multivariate analysis of structural and diffusion imaging in traumatic brain injury. *Acad Radiol.* (2008) 15:1360–75. doi: 10.1016/j.acra.2008.07.007
114. Mayer AR, Ling J, Mannell MV, Gasparovic C, Phillips JP, Doezema D, et al. A prospective diffusion tensor imaging study in mild traumatic brain injury. *Neurology.* (2010) 74:643–50. doi: 10.1212/WNL.0b013e3181d0ccdd
115. Matthews SC, Strigo IA, Simmons AN, O'Connell RM, Reinhardt LE, Moseley SA. A multimodal imaging study in U.S. veterans of Operations Iraqi and Enduring Freedom with and without major depression after blast-related concussion. *Neuroimage.* (2011) 54:S69–75. doi: 10.1016/j.neuroimage.2010.04.269
116. Lange RT, Iverson GL, Brubacher JR, Mädler B, Heran MK. Diffusion tensor imaging findings are not strongly associated with postconcussional disorder 2 months following mild traumatic brain injury. *J Head Trauma Rehabil.* (2012) 27:188–98. doi: 10.1097/HTR.0b013e318217f0ad
117. Yuh EL, Cooper SR, Mukherjee P, Yue JK, Lingsma HF, Gordon WA, et al. Diffusion tensor imaging for outcome prediction in mild traumatic brain injury: a TRACK-TBI study. *J Neurotrauma.* (2014) 31:1457–77. doi: 10.1089/neu.2013.3171
118. Gonzalez AC, Kim M, Keser Z, Ibrahim L, Singh SK, Ahmad MJ, et al. Diffusion tensor imaging correlates of concussion related cognitive impairment. *Front Neurol.* (2021) 12:639179. doi: 10.3389/fneur.2021.639179
119. Jones DK, Dardis R, Ervine M, Horsfield MA, Jeffree M, Simmons A, et al. Cluster analysis of diffusion tensor magnetic resonance images in human head injury. *Neurosurgery.* (2000) 47:306–13. doi: 10.1097/00006123-200008000-00008
120. Williams GR. Incidence and characteristics of total stroke in the United States. *BMC Neurol.* (2001) 1:2. doi: 10.1186/1471-2377-1-2
121. Avan A, Digaleh H, Di Napoli M, Stranges S, Behrouz R, Shojaeianbabaei G, et al. Socioeconomic status and stroke incidence, prevalence, mortality, and worldwide burden: an ecological analysis from the Global Burden of Disease Study 2017. *BMC Med.* (2019) 17:191. doi: 10.1186/s12916-019-1397-3
122. Kim J, Thayabaranathan T, Donnan GA, Howard G, Howard VJ, Rothwell PM, et al. Global stroke statistics 2019. *Int J Stroke.* (2020) 15:819–38. doi: 10.1177/1747493020909545
123. Yeh SH, Liu RS, Hu HH, Wong WJ, Lo YK, Lai ZY, et al. Brain SPECT imaging with 99Tcm-hexamethylpropyleneamine oxime in the early detection of cerebral infarction: comparison with transmission computed tomography. *Nucl Med Commun.* (1986) 7:873–8. doi: 10.1097/00006231-198612000-00004
124. Vallar G, Perani D, Cappa SF, Messa C, Lenzi GL, Fazio F. Recovery from aphasia and neglect after subcortical stroke: neuropsychological and cerebral perfusion study. *J Neurol Neurosurg Psychiatry.* (1988) 51:1269–76. doi: 10.1136/jnnp.51.10.1269

125. Rango M, Candelise L, Perani D, Messa C, Scarlato G, Canal N, Franceschi M, Fazio F. Cortical pathophysiology and clinical neurologic abnormalities in acute cerebral ischemia. A serial study with single photon emission computed tomography. *Arch Neurol.* (1989) 46:1318–22. doi: 10.1001/archneur.1989.00520480060021
126. De Roo M, Mortelmans L, Devos P, Verbruggen A, Wilms G, Carton H, et al. Clinical experience with Tc-99m HM-PAO high resolution SPECT of the brain in patients with cerebrovascular accidents. *Eur J Nucl Med.* (1989) 15:9–15. doi: 10.1007/BF00253592
127. Brass LM, Walovitch RC, Joseph JL, Léveillé J, Marchand L, Hellman RS, et al. The role of single photon emission computed tomography brain imaging with ^{99m}Tc-bicisate in the localization and definition of mechanism of ischemic stroke. *J Cereb Blood Flow Metab.* (1994) 1:S91–8.
128. Wintermark M, Sanelli PC, Albers GW, Bello JA, Derdeyn CP, Hetts SW, et al. Imaging recommendations for acute stroke and transient ischemic attack patients: A joint statement by the American Society of Neuroradiology, the American College of Radiology, and the Society of NeuroInterventional Surgery. *AJNR Am J Neuroradiol.* (2013) 34:E117–27. doi: 10.3174/ajnr.A3690
129. Alexandrov AV, Masdeu JC, Devous MD Sr, Black SE, Grotta JC. Brain single-photon emission CT with HMPAO and safety of thrombolytic therapy in acute ischemic stroke. Proceedings of the meeting of the SPECT Safe Thrombolysis Study Collaborators and the members of the Brain Imaging Council of the Society of Nuclear Medicine. *Stroke.* (1997) 28:1830–4. doi: 10.1161/01.STR.28.9.1830
130. Rizk H, Allam M, Hegazy A, Khalil H, Helmy H, Hashem HS, et al. Predictors of poor cerebral collaterals and cerebrovascular reserve in patients with chronic total carotid occlusion. *Int J Neurosci.* (2019) 129:455–60. doi: 10.1080/00207454.2018.1538990
131. Alexandrov AV, Ehrlich LE, Bladin CF, Black SE. Clinical significance of increased uptake of HMPAO on brain SPECT scans in acute stroke. *J Neuroimaging.* (1996) 6:150–5. doi: 10.1111/jon199663150
132. Thakkar MD, Qavi A, Singh AK, Maurya PK, Kulshreshtha D, Thacker AK, et al. Clinical value of perilesional perfusion deficit measured by Technetium-99m-ECD single-photon emission computed tomography in hypertensive intracerebral hemorrhage. *World J Nucl Med.* (2020) 19:246–54. doi: 10.4103/wjnm.WJNM_76_19
133. Okamoto K, Shiga H, Nakamura H, Matsui M, Miwa T. Relationship between olfactory disturbance after acute ischemic stroke and latent thalamic hypoperfusion. *Chem Senses.* (2020) 45:111–8. doi: 10.1093/chemse/bjz077
134. Sato K, Shimizu H, Inoue T, Fujimura M, Endo H, Tominaga T. Temporal and spatial changes in cerebral blood flow during management for preventing delayed cerebral ischemia after aneurysmal subarachnoid hemorrhage: serial semiquantitative analysis. *J Stroke Cerebrovasc Dis.* (2017) 26:2027–37. doi: 10.1016/j.jstrokecerebrovasdis.2017.06.006
135. Hashimoto H, Nakanishi R, Mizumura S, Hashimoto Y, Okamura Y, Yamanaka K, et al. Prognostic value of (99m)Tc-ECD brain perfusion SPECT in patients with atrial fibrillation and dementia. *EJNMMI Res.* (2020) 10:3. doi: 10.1186/s13550-019-0589-3
136. Hara T, Abo M, Kobayashi K, Watanabe M, Kakuda W, Senoo A. Effects of low-frequency repetitive transcranial magnetic stimulation combined with intensive speech therapy on cerebral blood flow in post-stroke aphasia. *Transl Stroke Res.* (2015) 6:365–74. doi: 10.1007/s12975-015-0417-7
137. Ward A, Carrico C, Powell E, Westgate PM, Nichols L, Fleischer A, et al. Safety and improvement of movement function after stroke with atomoxetine: A pilot randomized trial. *Restor Neurol Neurosci.* (2017) 35:1–10. doi: 10.3233/RNN-160673
138. Golan H, Makogon B, Volkov O, Smolyakov Y, Hadanny A, Efrati S. Imaging-based predictors for hyperbaric oxygen therapy outcome in post-stroke patients. Report 1. *Med Hypotheses.* (2020) 136:109510. doi: 10.1016/j.mehy.2019.109510
139. Kim Y, Lim SH, Park GY. Crossed cerebellar diaschisis has an adverse effect on functional outcome in the subacute rehabilitation phase of stroke: a case-control study. *Arch Phys Med Rehabil.* (2019) 100:1308–16. doi: 10.1016/j.apmr.2019.01.026
140. Wong TH, Shagera QA, Ryoo HG, Ha S, Lee DS. Basal and acetazolamide brain perfusion SPECT in internal carotid artery stenosis. *Nucl Med Mol Imaging.* (2020) 54:9–27. doi: 10.1007/s13139-019-00633-7
141. Matsuda H, Higashi S, Kinuya K, Tsuji S, Nozaki J, Sumiya H, et al. SPECT evaluation of brain perfusion reserve by the acetazolamide test using Tc-99m HMPAO. *J Clin Nucl Med.* (1991) 16:572–9. doi: 10.1097/00003072-199108000-00008
142. CDC. (2021). Available online at: https://www.cdc.gov/epilepsy/data/index.html. (accessed May 30, 2021).
143. Reddy SD, Younus I, Sridhar V, Reddy DS. Neuroimaging biomarkers of experimental epileptogenesis and refractory epilepsy. *Int J Mol Sci.* (2019) 20:220. doi: 10.3390/ijms20010220
144. Moreau JT, Saint-Martin C, Baillet S, Dudley RWR. MNI SISCOM: an open-source tool for computing subtraction ictal single-photon emission CT coregistered to MRI. *J Digit Imaging.* (2021) 34:357–61. doi: 10.1007/s10278-021-00422-9
145. Goffin K, van Laere K. Single-photon emission tomography. *Handb Clin Neurol.* (2016) 135:241–50. doi: 10.1016/B978-0-444-53485-9.00013-1
146. Lee BI, Markand ON, Wellman HN, Siddiqui AR, Park HM, Mock B, et al. HIPDM-SPECT in patients with medically intractable complex partial seizures. *Ictal study Arch Neurol.* (1988) 45:397–402. doi: 10.1001/archneur.1988.00520280043014
147. Rowe CC, Berkovic SF, Sia ST, Austin M, McKay WJ, Kalnins RM, et al. Localization of epileptic foci with postictal single photon emission computed tomography. *Ann Neurol.* (1989) 26:660–8. doi: 10.1002/ana.410260512
148. Stefan H, Bauer J, Feistel H, Schulemann H, Neubauer U, Wenzel B, et al. Regional cerebral blood flow during focal seizures of temporal and frontocentral onset. *Ann Neurol.* (1990) 27:162–6. doi: 10.1002/ana.410270211
149. Shen W, Lee BI, Park HM, Siddiqui AR, Wellman HH, Worth RM, et al. HIPDM-SPECT brain imaging in the presurgical evaluation of patients with intractable seizures. *J Nucl Med.* (1990) 31:1280–4.
150. Rowe CC, Berkovic SF, Austin MC, Saling M, Kalnins RM, McKay WJ, et al. Visual and quantitative analysis of interictal SPECT with technetium-99m-HMPAO in temporal lobe epilepsy. *J Nucl Med.* (1991) 32:1688–94.
151. Marks DA, Katz A, Hoffer P, Spencer SS. Localization of extratemporal epileptic foci during ictal single photon emission computed tomography. *Ann Neurol.* (1992) 31:250–5. doi: 10.1002/ana.410310304
152. Takeda T, Osawa M, Toi S, Mizuno S, Shimizu Y, Uchiyama S. Adversive seizures associated with periodic lateralised epileptiform discharges (PLEDs) after left orbital contusion. *Epileptic Disord.* (2012) 14:422–5. doi: 10.1684/epd.2012.0537
153. Tovar-Spinoza Z, Ziechmann R, Zyck S. Single and staged laser interstitial thermal therapy ablation for cortical tubers causing refractory epilepsy in pediatric patients. *Neurosurg Focus.* (2018) 45:E9. doi: 10.3171/2018.6.FOCUS18228
154. Volkan-Salanci B, Lay Ergün E, Genc Sel Ç, Yalnizoglu D, Turanli G. The role of brain perfusion SPECT in Moyamoya disease. *Rev Esp Med Nucl Imagen Mol.* (2012) 31:216–8. doi: 10.1016/j.remn.2012.02.006
155. Siasios I, Valotassiou V, Kapsalaki E, Tsougos I, Georgoulias P, Fotiadou A, et al. Magnetic resonance spectroscopy and single-photon emission computed tomography in the evaluation of cerebral tumors: a case report. *J Clin Med Res.* (2017) 9:74–8. doi: 10.14740/jocmr2775w
156. Tsuchiya H, Iwasaki Y, Shoda H, Takahashi Y, Fujio K. Limbic encephalitis in a patient with systemic lupus erythematosus successfully treated with high-dose glucocorticoids and intravenous cyclophosphamide therapy: the potential pathogenicity of anti-glutamate receptor antibodies. *Mod Rheumatol Case Rep.* (2021) 9:1–6. doi: 10.1080/24725625.2021.1876340
157. Barros P, Brito H, Ferreira PC, Ramalheira J, Lopes J, Rangel R, et al. Resective surgery in the treatment of super-refractory partial status epilepticus secondary to NMDAR antibody encephalitis. *Eur J Paediatr Neurol.* (2014) 18:449–52. doi: 10.1016/j.ejpn.2014.01.013
158. Kasahara H, Sato M, Nagamine S, Makioka K, Tanaka K, Ikeda Y. Temporal changes on (123)I-Iomazenil and cerebral blood flow single-photon emission computed tomography in a patient with anti-N-methyl-D-aspartate receptor encephalitis. *Intern Med.* (2019) 58:1501–5. doi: 10.2169/internalmedicine.0987-18
159. Kang KW, Kim SH, Kim JM, Nam TS, Choi KH, Kim MK. Ictal SPECT in diagnosis of non-ketotic hyperglycemia-related seizure manifesting as speech arrest. *J Clin Neurol.* (2019) 15:253–5. doi: 10.3988/jcn.2019.15.2.253

160. Tun MZ, Soo WK, Wu K, Kane R. Dementia with Lewy bodies presenting as probable epileptic seizure. *BMJ Case Rep.* (2017) 2017:bcr2017221454. doi: 10.1136/bcr-2017-221454
161. Chiron C. SPECT (single photon emission computed tomography) in pediatrics. *Handb Clin Neurol.* (2013) 111:759–65. doi: 10.1016/B978-0-444-52891-9.00078-6
162. Cho EB, Joo EY, Seo DW, Hong SC, Hong SB. Prognostic role of functional neuroimaging after multilobar resection in patients with localization-related epilepsy. *PLoS ONE.* (2015) 10:e0136565. doi: 10.1371/journal.pone.0136565
163. Jin P, Wu D, Li X, Ren L, Wang Y. Towards precision medicine in epilepsy surgery. *Ann Transl Med.* (2016) 4:24. doi: 10.3978/j.issn.2305-5839.2015.12.65
164. Jalota A, Rossi MA, Pylypyuk V, Stein M, Stoub T, Balabanov A, et al. Resecting critical nodes from an epileptogenic circuit in refractory focal-onset epilepsy patients using subtraction ictal SPECT coregistered to MRI. *J Neurosurg.* (2016) 125:1565–76. doi: 10.3171/2015.6.JNS141719
165. Tepmongkol S, Tangtrairattanakul K, Lerdlum S, Desudchit T. Comparison of brain perfusion SPECT parameters accuracy for seizure localization in extratemporal lobe epilepsy with discordant pre-surgical data. *Ann Nucl Med.* (2015) 29:21–8. doi: 10.1007/s12149-014-0905-y
166. Chen T, Guo L. The role of SISCOM in preoperative evaluation for patients with epilepsy surgery: a meta-analysis. *Seizure.* (2016) 41:43–50. doi: 10.1016/j.seizure.2016.06.024
167. Perissinotti A, Niñerola-Baizán A, Rubí S, Carreño M, Marti-Fuster B, Aparicio J, et al. PISCOM: a new procedure for epilepsy combining ictal SPECT and interictal PET. *Eur J Nucl Med Mol Imaging.* (2018) 45:2358–67. doi: 10.1007/s00259-018-4080-6
168. Jayalakshmi S, Nanda SK, Vooturi S, Vadapalli R, Sudhakar P, Madigubba S, et al. Focal cortical dysplasia and refractory epilepsy: role of multimodality imaging and outcome of surgery. *AJNR Am J Neuroradiol.* (2019) 40:892–8. doi: 10.3174/ajnr.A6041
169. Pawar SU, Ravat SH, Muzumdar DP, Sankhe SS, Chheda AH, Manglunia AS. Does Tc-99m ECD ictal brain SPECT have incremental value in localization of epileptogenic zone and predicting postoperative seizure freedom in cases with discordant video electroencephalogram and MRI findings? *Nucl Med Commun.* (2020) 41:858–70. doi: 10.1097/MNM.0000000000001240
170. Oliveira Young C, Etchbehere ECSC, Souza EM, Brunetto SQ, Santos AO, Lima MCL, et al. Clinical usefulness of SISCOM-SPM compared to visual analysis to locate the epileptogenic zone. *Front Neurol.* (2020) 11:467. doi: 10.3389/fneur.2020.00467
171. Kaur K, Garg A, Tripathi M, Chandra SP, Singh G, Viswanathan V, et al. Comparative contribution of magnetoencephalography (MEG) and single-photon emission computed tomography (SPECT) in pre-operative localization for epilepsy surgery: A prospective blinded study. *Seizure.* (2021) 86:181–8. doi: 10.1016/j.seizure.2021.02.005
172. Yassin A, El-Salem K, Al-Mistarehi AH, Momani A, Zein Alaabdin AM, Shah P, et al. Use of innovative SPECT techniques in the presurgical evaluation of patients with nonlesional extratemporal drug-resistant epilepsy. *Mol Imaging.* (2021) 2021:6614356. doi: 10.1155/2021/6614356
173. Lee JJ, Lee SK, Choi JW, Kim DW, Park KI, Kim BS, et al. Ictal SPECT using an attachable automated injector: clinical usefulness in the prediction of ictal onset zone. *Acta Radiol.* (2009) 50:1160–8. doi: 10.3109/02841850903215926
174. Kim S, Holder DL, Laymon CM, Tudorascu DL, Deeb EL, Panigrahy A, et al. Clinical value of the first dedicated, commercially available automatic injector for ictal brain SPECT in presurgical evaluation of pediatric epilepsy: comparison with manual injection. *J Nucl Med.* (2013) 54:732–8. doi: 10.2967/jnumed.112.105189
175. Yassin A, Al-Mistarehi AH, El-Salem K, Urban A, Plummer C, Mohammadi S, et al. Effect of automatic injectors on the injection latency, safety, and seizure onset zone localization of ictal single photon emission computed tomography studies in adult epilepsy monitoring unit. *Epilepsy Res.* (2021) 169:106522. doi: 10.1016/j.eplepsyres.2020.106522
176. Stamoulis C, Connolly J, Axeen E, Kaulas H, Bolton J, Dorfman K, et al. Non-invasive seizure localization with ictal single-photon emission computed tomography is impacted by preictal/early ictal network dynamics. *IEEE Trans Biomed Eng.* (2018) 66:1863–71. doi: 10.1109/TBME.2018.2880575
177. Foiadelli T, Lagae L, Goffin K, Theys T, De Amici M, Sacchi L, et al. Subtraction ictal SPECT coregistered to MRI (SISCOM) as a guide in localizing childhood epilepsy. *Epilepsia Open.* (2019) 5:61–72. doi: 10.1002/epi4.12373
178. Jaraba S, Reynés-Llompart G, Sala-Padró J, Veciana M, Miró J, Pedro J, et al. Usefulness of HMPAO-SPECT in the diagnosis of nonconvulsive status epilepticus. *Epilepsy Behav.* (2019) 101:106544. doi: 10.1016/j.yebeh.2019.106544
179. Bonte FJ, Ross ED, Chehabi HH, Devous MD Sr. SPECT study of regional cerebral blood flow in Alzheimer disease. *J Comput Assist Tomogr.* (1986) 10:579–83. doi: 10.1097/00004728-198607000-00005
180. Komatani A, Yamaguchi K, Sugai Y, Takanashi T, Kera M, Shinohara M, et al. Assessment of demented patients by dynamic SPECT of inhaled xenon-133. *J Nucl Med.* (1988) 29:1621–6.
181. Gemmell HG, Sharp PF, Smith FW, Besson JA, Ebmeier KP, Davidson J, et al. Cerebral blood flow measured by SPECT as a diagnostic tool in the study of dementia. *Psychiatry Res.* (1989) 29:327–9. doi: 10.1016/0165-1781(89)90079-6
182. Montaldi D, Brooks DN, McColl JH, Wyper D, Patterson J, Barron E, et al. Measurements of regional cerebral blood flow and cognitive performance in Alzheimer's disease. *J Neurol Neurosurg Psychiatry.* (1990) 53:33–8. doi: 10.1136/jnnp.53.1.33
183. Holman BL, Johnson KA, Gerada B, Carvalho PA, Satlin A. The scintigraphic appearance of Alzheimer's disease: a prospective study using technetium-99m-HMPAO SPECT. *J Nucl Med.* (1992) 33:181–5.
184. Jobst KA, Smith AD, Barker CS, Wear A, King EM, Smith A, et al. Association of atrophy of the medial temporal lobe with reduced blood flow in the posterior parietotemporal cortex in patients with a clinical and pathological diagnosis of Alzheimer's disease. *J Neurol Neurosurg Psychiatry.* (1992) 55:190–4. doi: 10.1136/jnnp.55.3.190
185. Bonte FJ, Tintner R, Weiner MF, Bigio EH, White CL 3rd. Brain blood flow in the dementias: SPECT with histopathologic correlation. *Radiol.* (1993) 186:361–5. doi: 10.1148/radiology.186.2.8421735
186. Bonte FJ, Weiner MF, Bigio EH, White CL. Brain blood flow in the dementias: SPECT with histopathologic correlation in 54 patients. *Radiology.* (1997) 202:793–7. doi: 10.1148/radiology.202.3.9051035
187. Jagust W, Thisted R, Devous MD, Sr., Van Heertum R, Mayberg H, et al. SPECT perfusion imaging in the diagnosis of Alzheimer's disease: a clinical-pathologic study. *Neurology.* (2001) 56:950–6. doi: 10.1212/WNL.56.7.950
188. Silverman DH. Brain 18F-FDG PET in the diagnosis of neurodegenerative dementias: comparison with perfusion SPECT and with clinical evaluations lacking nuclear imaging. *J Nucl Med.* (2004) 45:594–607.
189. Pavel D, Devore-Best S, Craita I. Routine use of high-resolution brain SPECT and multiple display modes for dementia differential and follow-up. In: *9th International Conference on Alzheimer's Disease and Related Disorders*. Philadelphia, PA (2004).
190. Mistur R, Mosconi L, Santi SD, Guzman M, Li Y, Tsui W, et al. Current challenges for the early detection of Alzheimer's disease: brain imaging and CSF studies. *J Clin Neurol.* (2009) 5:153–66. doi: 10.3988/jcn.2009.5.4.153
191. Henderson TA. The diagnosis and evaluation of dementia and mild cognitive impairment with emphasis on SPECT perfusion neuroimaging. *CNS Spectr.* (2012) 17:176–206. doi: 10.1017/S1092852912000636
192. Battistin L, Pizzolato G, Dam M, Ponza I, Borsato N, Zanco PL, et al. Regional cerebral blood flow study with 99mTc-hexamethyl-propyleneamine oxime single photon emission computed tomography in Alzheimer's and multi-infarct dementia. *Eur Neurol.* (1990) 30:296–301. doi: 10.1159/000117384
193. Knapp WH, Dannenberg C, Marschall B, Zedlick D, Löschmann K, Bettin S, et al. Changes in local cerebral blood flow by neuroactivation and vasoactivation in patients with impaired cognitive function. *Eur J Nucl Med.* (1996) 23:878–88. doi: 10.1007/BF01084360
194. Mattman A, Feldman H, Forster B, Li D, Szasz I, Beattie BL, et al. Regional HmPAO SPECT and CT measurements in the diagnosis of Alzheimer's disease. *Can J Neurol Sci.* (1997) 24:22–8. doi: 10.1017/S0317167100021041
195. Dougall NJ, Bruggink S, Ebmeier KP. Systematic review of the diagnostic accuracy of 99mTc-HMPAO-SPECT in dementia. *Am J Geriatr Psychiatry.* (2004) 12:554–70. doi: 10.1097/00019442-200411000-00002
196. Yuan Y, Gu ZX, Wei WS. Fluorodeoxyglucose-positron-emission tomography, single-photon emission tomography, and structural MR imaging for prediction of rapid conversion to Alzheimer disease in patients

with mild cognitive impairment: a meta-analysis. *AJNR Am J Neuroradiol.* (2009) 30:404–10. doi: 10.3174/ajnr.A1357
197. Bloudek LM, Spackman DE, Blankenburg M, Sullivan SD. Review and meta-analysis of biomarkers and diagnostic imaging in Alzheimer's disease. *J Alzheimer's Dis.* (2011) 26:627–45. doi: 10.3233/JAD-2011-110458
198. Frisoni GB, Bocchetta M, Chételat G, Rabinovici GD, de Leon MJ, Kaye J, et al. ISTAART's neuroimaging professional interest area. Imaging markers for Alzheimer disease: which vs how. *Neurology.* (2013) 81:487–500. doi: 10.1212/WNL.0b013e31829d86e8
199. Davison CM, O'Brien JT. A comparison of FDG-PET and blood flow SPECT in the diagnosis of neurodegenerative dementias: a systematic review. *Int J Geriatr Psychiatry.* (2014) 229:551–61. doi: 10.1002/gps.4036
200. Hanyu H, Abe S, Arai H, Asano T, Iwamoto T, Takasaki M. Diagnostic accuracy of single photon emission computed tomography in Alzheimer's disease. *Gerontology.* (1993) 39:260–6. doi: 10.1159/000213541
201. Bonte FJ, Harris TS, Hynan LS, Bigio EH, White CL. Tc-99m HMPAO SPECT in the differential diagnosis of the dementias with histopathologic confirmation. *Clin Nucl Med.* (2006) 31:376–8. doi: 10.1097/01.rlu.0000222736.81365.63
202. Perani D, Di Piero V, Vallar G, Cappa S, Messa C, Bottini G, et al. Technetium-99m HM-PAO-SPECT study of regional cerebral perfusion in early Alzheimer's disease. *J Nucl Med.* (1988) 29:1507–14.
203. Leys D, Steinling M, Petit H, Salomez JL, Gaudet Y, Ovelacq E, et al. [Alzheimer's disease: study by single photon emission tomography (Hm PAO Tc99m)]. *Rev Neurol.* (1989) 145:443–50.
204. Hurwitz TA, Ammann W, Chu D, Clark C, Holden J, Brownstone R. Single photon emission computed tomography using 99mTc-HM-PAO in the routine evaluation of Alzheimer's disease. *Can J Neurol Sci.* (1991) 18:59–62. doi: 10.1017/S0317167100031292
205. O'Brien JT, Eagger S, Syed GM, Sahakian BJ, Levy R. A study of regional cerebral blood flow and cognitive performance in Alzheimer's disease. *J Neurol Neurosurg Psychiatry.* (1992) 55:1182–7. doi: 10.1136/jnnp.55.12.1182
206. Claus JJ, van Harskamp F, Breteler MM, Krenning EP, van der Cammen TJ, Hofman A, et al. Assessment of cerebral perfusion with single-photon emission tomography in normal subjects and in patients with Alzheimer's disease: effects of region of interest selection. *Eur J Nucl Med.* (1994) 21:1044–51. doi: 10.1007/BF00181058
207. O'Mahony D, Coffey J, Murphy J, O'Hare N, Hamilton D, Freyne P, et al. The discriminant value of semiquantitative SPECT data in mild Alzheimer's disease. *J Nucl Med.* (1994) 35:1450–5.
208. Hellman RS, Tikofsky RS, Van Heertum R, Coade G, Carretta R, Hoffmann RG. A multi-institutional study of interobserver agreement in the evaluation of dementia with rCBF/SPET technetium-99m exametazime (HMPAO). *Eur J Nucl Med.* (1994) 21:306–13. doi: 10.1007/BF00947965
209. Sloan EP, Fenton GW, Kennedy NS, MacLennan JM. Electroencephalography and single photon emission computed tomography in dementia: a comparative study. *Psychol Med.* (1995) 25:631–8. doi: 10.1017/S0033291700033535
210. Jobst KA, Barnetson LP, Shepstone BJ. Accurate prediction of histologically confirmed Alzheimer's disease and the differential diagnosis of dementia: the use of NINCDS-ADRDA and DSM-III-R criteria, SPECT, X-ray CT, and Apo E4 in medial temporal lobe dementias. Oxford project to investigate memory and aging. *Int Psychogeriatr.* (1998) 10:271–302. doi: 10.1017/S1041610298005389
211. O'Brien JT, Ames D, Desmond P, Lichtenstein M, Binns D, Schweitzer I, et al. Combined magnetic resonance imaging and single-photon emission tomography scanning in the discrimination of Alzheimer's disease from age-matched controls. *Int Psychogeriatr.* (2001) 13:149–61. doi: 10.1017/S1041610201007554
212. Johnson KA, Kijewski MF, Becker JA, Garada B, Satlin A, Holman BL. Quantitative brain SPECT in Alzheimer's disease and normal aging. *J Nucl Med.* (1993) 34:2044–8.
213. Waldemar G, Bruhn P, Kristensen M, Johnsen A, Paulson OB, Lassen NA. Heterogeneity of neocortical cerebral blood flow deficits in dementia of the Alzheimer type: a [99mTc]-d,l-HMPAO SPECT study. *J Neurol Neurosurg Psychiatry.* (1994) 57:285–95. doi: 10.1136/jnnp.57.3.285
214. Karbe H, Kertesz A, Davis J, Kemp BJ, Prato FS, Nicholson RL. Quantification of functional deficit in Alzheimer's disease using a computer-assisted mapping program for 99mTc-HMPAO SPECT. *Neuroradiology.* (1994) 36:1–6. doi: 10.1007/BF00599183
215. Messa C, Perani D, Lucignani G, Zenorini A, Zito F, Rizzo G, et al. High-resolution technetium-99m-HMPAO SPECT in patients with probable Alzheimer's disease: comparison with fluorine-18-FDG PET. *J Nucl Med.* (1994) 35:210–6.
216. Ichise M, Crisp S, Ganguli N, Tsai S, Gray BG. A method of two-dimensional mapping of cortical perfusion by cylindrical transformation of HMPAO SPET data. *Nucl Med Commun.* (1995) 16:386–94. doi: 10.1097/00006231-199505000-00011
217. Hashikawa K, Matsumoto M, Moriwaki H, Oku N, Okazaki Y, Seike Y, et al. Three-dimensional display of surface cortical perfusion by SPECT: application in assessing Alzheimer's disease. *J Nucl Med.* (1995) 36:690–6.
218. deFigueiredo RJ, Shankle WR, Maccato A, Dick MB, Mundkur P, Mena I, et al. Neural-network-based classification of cognitively normal, demented, Alzheimer disease and vascular dementia from single photon emission with computed tomography image data from brain. *Proc Natl Acad Sci USA.* (1995) 92:5530–4. doi: 10.1073/pnas.92.12.5530
219. van Dyck CH, Lin CH, Smith EO, Wisniewski G, Cellar J, Robinson R, et al. Comparison of technetium-99m-HMPAO and technetium-99m-ECD cerebral SPECT images in Alzheimer's disease. *J Nucl Med.* (1996) 37:1749–55.
220. Bartenstein P, Minoshima S, Hirsch C, Buch K, Willoch F, Mösch D, et al. Quantitative assessment of cerebral blood flow in patients with Alzheimer's disease by SPECT. *J Nucl Med.* (1997) 38:1095–101.
221. Johnson KA, Jones K, Holman BL, Becker JA, Spiers PA, Satlin A, et al. Preclinical prediction of Alzheimer's disease using SPECT. *Neurology.* (1998) 50:1563–71. doi: 10.1212/WNL.50.6.1563
222. Honda N, Machida K, Hosono M, Matsumoto T, Matsuda H, Oshima M, et al. Interobserver variation in diagnosis of dementia by brain perfusion SPECT. *Radiat Med.* (2002) 20:281–9.
223. Soonawala D, Amin T, Ebmeier KP, Steele JD, Dougall NJ, Best J, et al. Statistical parametric mapping of (99m)Tc-HMPAO-SPECT images for the diagnosis of Alzheimer's disease: normalizing to cerebellar tracer uptake. *Neuroimage.* (2002) 17:1193–202. doi: 10.1006/nimg.2002.1259
224. Elgh E, Sundström T, Näsman B, Ahlström R, Nyberg L. Memory functions and rCBF (99m)Tc-HMPAO SPET: developing diagnostics in Alzheimer's disease. *Eur J Nucl Med Mol Imaging.* (2002) 29:1140–8. doi: 10.1007/s00259-002-0829-y
225. Honda N, Machida K, Matsumoto T, Matsuda H, Imabayashi E, Hashimoto J, et al. Three-dimensional stereotactic surface projection of brain perfusion SPECT improves diagnosis of Alzheimer's disease. *Ann Nucl Med.* (2003) 17:641–8. doi: 10.1007/BF02984969
226. Kubota T, Ushijima Y, Yamada K, Okuyama C, Kizu O, Nishimura T. Diagnosis of Alzheimer's disease using brain perfusion SPECT and MR imaging: which modality achieves better diagnostic accuracy? *Eur J Nucl Med Mol Imaging.* (2005) 32:414–21. doi: 10.1007/s00259-004-1704-9
227. Kemp PM, Hoffmann SA, Holmes C, Bolt L, Ward T, Holmes RB, et al. The contribution of statistical parametric mapping in the assessment of precuneal and medial temporal lobe perfusion by 99mTc-HMPAO SPECT in mild Alzheimer's and Lewy body dementia. *Nucl Med Commun.* (2005) 26:1099–106. doi: 10.1097/00006231-200512000-00009
228. Chaves R, Ramírez J, Górriz JM, López M, Salas-Gonzalez D, Alvarez I, et al. SVM-based computer-aided diagnosis of the Alzheimer's disease using t-test NMSE feature selection with feature correlation weighting. *Neurosci Lett.* (2009) 461:293–7. doi: 10.1016/j.neulet.2009.06.052
229. Pagani M, Salmaso D, Rodriguez G, Nardo D, Nobili F. Principal component analysis in mild and moderate Alzheimer's disease–a novel approach to clinical diagnosis. *Psychiatry Res.* (2009) 173:8–14. doi: 10.1016/j.pscychresns.2008.07.016
230. Ishii S, Shishido F, Miyajima M, Sakuma K, Shigihara T, Tameta T, et al. Comparison of Alzheimer's disease with vascular dementia and non-dementia using specific voxel-based Z score maps. *Ann Nucl Med.* (2009) 23:25–31. doi: 10.1007/s12149-008-0210-8
231. Rusina R, Kukal J, Belícek T, Buncová M, Matej R. Use of fuzzy edge single-photon emission computed tomography analysis in definite

Alzheimer's disease–a retrospective study. *BMC Med Imaging.* (2010) 10:20. doi: 10.1186/1471-2342-10-20
232. Matsuda H, Mizumura S, Nagao T, Ota T, Iizuka T, Nemoto K, et al. Automated discrimination between very early Alzheimer disease and controls using an easy Z-score imaging system for multicenter brain perfusion single-photon emission tomography. *AJNR Am J Neuroradiol.* (2007) 28:731–6. doi: 10.1097/MNM.0b013e328013eb8b
233. Wu CC, Mungas D, Eberling JL, Reed BR, Jagust WJ. Imaging interactions between Alzheimer's disease and cerebrovascular disease. *Ann N Y Acad Sci.* (2002) 977:403–10. doi: 10.1111/j.1749-6632.2002.tb04844.x
234. Ravona-Springer R, Davidson M, Noy S. The role of cardiovascular risk factors in Alzheimer's disease. *CNS Spectr.* (2003) 8:824–33. doi: 10.1017/S109285290001926X
235. Hanyu H, Shimuzu S, Tanaka Y, Takasaki M, Koizumi K, Abe K. Cerebral blood flow patterns in Binswanger's disease: a SPECT study using three-dimensional stereotactic surface projections. *J Neurol Sci.* (2004) 220:79–84. doi: 10.1016/j.jns.2004.02.011
236. Launes J, Sulkava R, Erkinjuntti T, Nikkinen P, Lindroth L, Liewendahl K, et al. 99Tcm-HMPAO SPECT in suspected dementia. *Nucl Med Commun.* (1991) 12:757–65. doi: 10.1097/00006231-199109000-00002
237. Houston AS, Kemp PM, Macleod MA. A method for assessing the significance of abnormalities in HMPO brain SPECT images. *J Nucl Med.* (1994) 35:239–44.
238. Mielke R, Pietrzyk U, Jacobs A, Fink GR, Ichimiya A, Kessler J, et al. HMPAO SPET and FDG PET in Alzheimer's disease and vascular dementia: comparison of perfusion and metabolic pattern. *Eur J Nucl Med.* (1994) 21:1052–60. doi: 10.1007/BF00181059
239. Bergman H, Chertkow H, Wolfson C, Stern J, Rush C, Whitehead V, et al. HM-PAO (CERETEC) SPECT brain scanning in the diagnosis of Alzheimer's disease. *J Am Geriatr Soc.* (1997) 45:15–20. doi: 10.1111/j.1532-5415.1997.tb00972.x
240. Pávics L, Grünwald F, Reichmann K, Horn R, Kitschenberg A, Hartmann A, et al. Regional cerebral blood flow single-photon emission tomography with 99mTc-HMPAO and the acetazolamide test in the evaluation of vascular and Alzheimer's dementia. *Eur J Nucl Med.* (1999) 26:239–45. doi: 10.1007/s002590050383
241. Butler RE, Costa DC, Greco A, Ell PJ, Katona CLE. Differentiation between Alzheimer's disease and multi-infarct dementia: SPECT vs MR imaging. *Int J Geriatr Psychiatry.* (1995) 10:121–8. doi: 10.1002/gps.930100207
242. Uchida Y, Minoshima S, Okada S, Kawata T, Ito H. Diagnosis of dementia using perfusion SPECT imaging at the patient's initial visit to a cognitive disorder clinic. *Clin Nucl Med.* (2006) 31:764–73. doi: 10.1097/01.rlu.0000246818.24566.54
243. Talbot PR, Goulding PJ, Lloyd JJ, Snowden JS, Neary D, Testa HJ. Inter-relation between "classic" motor neuron disease and frontotemporal dementia: neuropsychological and single photon emission computed tomography study. *J Neurol Neurosurg Psychiatry.* (1995) 58:541–7. doi: 10.1136/jnnp.58.5.541
244. Talbot PR, Lloyd JJ, Snowden JS, Neary D, Testa HJ. A clinical role for 99mTc-HMPAO SPECT in the investigation of dementia? *J Neurol Neurosurg Psychiatry.* (1998) 64:306–13. doi: 10.1136/jnnp.64.3.306
245. Small GW. What does imaging add to the management of Alzheimer's disease? *CNS Spectr.* (2004) 9:20–3. doi: 10.1017/S1092852900024779
246. Tranfaglia C, Palumbo B, Siepi D, Sinzinger H, Parnetti L. Semi-quantitative analysis of perfusion of Brodmann areas in the differential diagnosis of cognitive impairment in Alzheimer's disease, fronto-temporal dementia and mild cognitive impairment. *Hell J Nucl Med.* (2009) 12:110–4.
247. Van Heertum RL. Dementia: diagnosis of dementia. In: Van Heertum RL, Tikofsky RS, Ichise M, editors. *Functional Cerebral SPECT and PET Imaging, 4th ed*. Philadelphia, PA: Lippincott Williams & Wilkins. (2010) p. 81–95.
248. Devous MD. Functional brain imaging in the dementias: role in early detection, differential diagnosis, and longitudinal studies. *Eur J Nucl Med Mol Imaging.* (2002) 29:1685–96. doi: 10.1007/s00259-002-0967-2
249. Horn JF, Habert MO, Kas A, Malek Z, Maksud P, Lacomblez L, et al. Differential automatic diagnosis between Alzheimer's disease and frontotemporal dementia based on perfusion SPECT images. *Artif Intell Med.* (2009) 47:147–58. doi: 10.1016/j.artmed.2009.05.001
250. Neary D, Snowden JS, Shields RA, Burjan AW, Northen B, MacDermott N, et al. Single photon emission tomography using 99mTc-HM-PAO in the investigation of dementia. *J Neurol Neurosurg Psychiatry.* (1987) 50:1101–9. doi: 10.1136/jnnp.50.9.1101
251. Testa HJ, Snowden JS, Neary D, Shields RA, Burjan AW, Prescott MC, et al. The use of [99mTc]-HM-PAO in the diagnosis of primary degenerative dementia. *J Cereb Blood Flow Metab.* (1988) 8:S123–6. doi: 10.1038/jcbfm.1988.42
252. McNeill R, Sare GM, Manoharan M, Testa HJ, Mann DM, Neary D, et al. Accuracy of single-photon emission computed tomography in differentiating frontotemporal dementia from Alzheimer's disease. *J Neurol Neurosurg Psychiatry.* (2007) 78:350–5. doi: 10.1136/jnnp.2006.106054
253. Charpentier P, Lavenu I, Defebvre L, Duhamel A, Lecouffe P, Pasquier F, et al. Alzheimer's disease and frontotemporal dementia are differentiated by discriminant analysis applied to (99m)Tc HmPAO SPECT data. *J Neurol Neurosurg Psychiatry.* (2000) 69:661–3. doi: 10.1136/jnnp.69.5.661
254. Shimizu S, Hanyu H, Kanetaka H, Iwamoto T, Koizumi K, Abe K. Differentiation of dementia with Lewy bodies from Alzheimer's disease using brain SPECT. *Dement Geriatr Cogn Disord.* (2005) 20:25–30. doi: 10.1159/000085070
255. Sato T, Hanyu H, Hirao K, Shimizu S, Kanetaka H, Iwamoto T. Deep gray matter hyperperfusion with occipital hypoperfusion in dementia with Lewy bodies. *T Eur J Neurol.* (2007) 14:1299–301. doi: 10.1111/j.1468-1331.2007.01951.x
256. Goto H, Ishii K, Uemura T, Miyamoto N, Yoshikawa T, Shimada K, et al. Differential diagnosis of dementia with Lewy Bodies and Alzheimer Disease using combined MR imaging and brain perfusion single-photon emission tomography. *AJNR Am J Neuroradiol.* (2010) 31:720–5. doi: 10.3174/ajnr.A1926
257. Johnson KA, Moran EK, Becker JA, Blacker D, Fischman AJ, Albert MS. Single photon emission computed tomography perfusion differences in mild cognitive impairment. *J Neurol Neurosurg Psychiatry.* (2007) 78:240–7. doi: 10.1136/jnnp.2006.096800
258. Kogure D, Matsuda H, Ohnishi T, Asada T, Uno M, Kunihiro T, et al. Longitudinal evaluation of early Alzheimer's disease using brain perfusion SPECT. *J Nucl Med.* (2000) 41:1155–62.
259. Huang C, Wahlund LO, Svensson L, Winblad B, Julin P. Cingulate cortex hypoperfusion predicts Alzheimer's disease in mild cognitive impairment. *BMC Neurol.* (2002) 2:9. doi: 10.1186/1471-2377-2-9
260. Encinas M, De Juan R, Marcos A, Gil P, Barabash A, Fernández C, et al. Regional cerebral blood flow assessed with 99mTc-ECD SPET as a marker of progression of mild cognitive impairment to Alzheimer's disease. *Eur J Nucl Med Mol Imaging.* (2003) 30:1473–80. doi: 10.1007/s00259-003-1277-z
261. Borroni B, Anchisi D, Paghera B, Vicini B, Kerrouche N, Garibotto et al. Combined 99mTc-ECD SPECT and neuropsychological studies in MCI for the assessment of conversion to AD. *Neurobiol Aging.* (2006) 27:24–31. doi: 10.1016/j.neurobiolaging.2004.12.010
262. Ishiwata A, Sakayori O, Minoshima S, Mizumura S, Kitamura S, Katayama Y. Preclinical evidence of Alzheimer changes in progressive mild cognitive impairment: a qualitative and quantitative SPECT study. *Acta Neurol Scand.* (2006) 114:91–6. doi: 10.1111/j.1600-0404.2006.00661.x
263. Caroli A, Testa C, Geroldi C, Nobili F, Barnden LR, Guerra UP, et al. Cerebral perfusion correlates of conversion to Alzheimer's disease in amnestic mild cognitive impairment. *J Neurol.* (2007) 254:1698–707. doi: 10.1007/s00415-007-0631-7
264. Nobili F, De Carli F, Frisoni GB, Portet F, Verhey F, Rodriguez G, et al. SPECT predictors of cognitive decline and Alzheimer's disease in mild cognitive impairment. *J Alzheimer's Dis.* (2009) 17:761–72. doi: 10.3233/JAD-2009-1091
265. Edman A, Edenbrandt L, Fredén-Lindqvist J, Nilsson M, Wallin A. Asymmetric cerebral blood flow in patients with mild cognitive impairment: possible relationship to further cognitive deterioration. *Dement Geriatr Cogn Dis Extra.* (2011) 1:228–36. doi: 10.1159/000329447
266. Habert MO, Horn JF, Sarazin M, Lotterie JA, Puel M, Onen F, et al. Brain perfusion SPECT with an automated quantitative tool can identify prodromal Alzheimer's disease among patients with mild cognitive impairment. *Neurobiol Aging.* (2011) 32:15–23. doi: 10.1016/j.neurobiolaging.2009.01.013

267. Petersen RC, Stevens JC, Ganguli M, Tangalos EG, Cummings JL, DeKosky ST. Practice parameter: early detection of dementia: mild cognitive impairment (an evidence-based review). Report of the Quality Standards Subcommittee of the American Academy of Neurology. *Neurology.* (2001) 56:1133–42. doi: 10.1212/WNL.56.9.1133
268. Hirao K, Ohnishi T, Hirata Y, Yamashita F, Mori T, Moriguchi Y, et al. The prediction of rapid conversion to Alzheimer's disease in mild cognitive impairment using regional cerebral blood flow SPECT. *Neuroimage.* (2005) 28:1014–21. doi: 10.1016/j.neuroimage.2005.06.066
269. Herholz K, Schopphoff H, Schmidt M, Mielke R, Eschner W, Scheidhauer K, et al. Direct comparison of spatially normalized PET and SPECT scans in Alzheimer's disease. *J Nucl Med.* (2002) 43:21–6.
270. Pimlott SL, Ebmeier KP. SPECT imaging in dementia. *Br J Radiol.* (2007) 80:S153–9. doi: 10.1259/bjr/89285735
271. Weih M, Degirmenci U, Kreil S, Lewczuk P, Schmidt D, Kornhuber J, et al. Perfusion imaging with SPECT in the era of pathophysiology-based biomarkers for Alzheimer's disease. *Int J Alzheimer's Dis.* (2010) 2010:109618. doi: 10.4061/2010/109618
272. Ito K, Fukuyama H, Senda M, Ishii K, Maeda K, Yamamoto Y, et al. Prediction of Outcomes in Mild Cognitive Impairment by Using 18F-FDG-PET: A Multicenter Study. *J Alzheimers Dis.* (2015) 45:543–52. doi: 10.3233/JAD-141338
273. Inui Y, Ito K, Kato T. Longer-term investigation of the value of 18F-FDG-PET and magnetic resonance imaging for predicting the conversion of mild cognitive impairment to Alzheimer's disease: A multicenter study. *J Alzheimers Dis.* (2017) 60:877–87. doi: 10.3233/JAD-170395
274. Sanchez-Catasus CA, Stormezand GN, van Laar PJ, De Deyn PP, Sanchez MA, Dierckx RA. FDG-PET for prediction of AD dementia in mild cognitive impairment. A review of the state of the art with particular emphasis on the comparison with other neuroimaging modalities (MRI and Perfusion SPECT). *Curr Alzheimer Res.* (2017) 14:127–42. doi: 10.2174/1567205013666160629081956
275. Rowe CC, Ng S, Ackermann U, Gong SJ, Pike K, Savage G, et al. Imaging beta-amyloid burden in aging and dementia. *Neurology.* (2007) 68:1718–25. doi: 10.1212/01.wnl.0000261919.22630.ea
276. Rodrigue KM, Kennedy KM, Park DC. Beta-amyloid deposition and the aging brain. *Neuropsychol Rev.* (2009) 19:436–50. doi: 10.1007/s11065-009-9118-x
277. Martínez G, Vernooij RW, Fuentes Padilla P, Zamora J, Bonfill Cosp X, Flicker L. 18F PET with florbetapir for the early diagnosis of Alzheimer's disease dementia and other dementias in people with mild cognitive impairment (MCI). *Cochrane Database Syst Rev.* (2017) 11:CD012216. doi: 10.1002/14651858.CD012216.pub2
278. Hagstadius S, Orbaek P, Risberg J, Lindgren M. Regional cerebral blood flow at the time of diagnosis of chronic toxic encephalopathy induced by organic-solvent exposure and after the cessation of exposure. *Scand J Work Environ Health.* (1989) 15:130–5. doi: 10.5271/sjweh.1872
279. Callender TJ, Morrow L, Subramanian K, Duhon D, Ristovv M. Three-dimensional brain metabolic imaging in patients with toxic encephalopathy. *Environ Res.* (1993) 60:295–319. doi: 10.1006/enrs.1993.1039
280. Visser I, Lavini C, Booij J, Reneman L, Majoie C, de Boer AG, et al. Cerebral impairment in chronic solvent-induced encephalopathy. *Ann Neurol.* (2008) 63:572–80. doi: 10.1002/ana.21364
281. Geier DA, Pretorius HT, Richards NM, Geier MR. A quantitative evaluation of brain dysfunction and body-burden of toxic metals. *Med Sci Monit.* (2012) 18:CR425-431. doi: 10.12659/MSM.883210
282. Rea WJ, Didriksen N, Simon TR, Pan Y, Fenyves EJ, Griffiths B. Effects of toxic exposure to molds and mycotoxins in building-related illnesses. *Arch Environ Health.* (2003) 58:399–405. doi: 10.1080/00039896.2003.11879140
283. Véra P, Rohrlich P, Stiévenart JL, Elmaleh M, Duval M, Bonnin F, et al. Contribution of single-photon emission computed tomography in the diagnosis and follow-up of CNS toxicity of a cytarabine-containing regimen in pediatric leukemia. *J Clin Oncol.* (1999) 17:2804–10. doi: 10.1200/JCO.1999.17.9.2804
284. Küçük NO, Kiliç EO, Ibis E, Aysev A, Gençoglu EA, Aras G, et al. Brain SPECT findings in long-term inhalant abuse. *Nucl Med Commun.* (2000) 21:769–73. doi: 10.1097/00006231-200008000-00011
285. Holman BL, Carvalho PA, Mendelson J, Teoh SK, Nardin R, Hallgring E, et al. Brain perfusion is abnormal in cocaine-dependent polydrug users: a study using technetium-99m-HMPAO and ASPECT. *J Nucl Med.* (1991) 32:1206–10.
286. Devous MD. Comparison of SPECT applications in neurology and psychiatry. *J Clin Psychiatry.* (1992) 53:13–9.
287. Miller BL, Mena I, Giombetti R, Villanueva-Meyer J, Djenderedjian AH. Neuropsychiatric effects of cocaine: SPECT measurements. *J Addict Dis.* (1992) 11:47–58. doi: 10.1300/J069v11n04_04
288. Holman BL, Mendelson J, Garada B, Teoh SK, Hallgring E, Johnson KA, et al. Regional cerebral blood flow improves with treatment in chronic cocaine polydrug users. *J Nucl Med.* (1993) 34:723–7.
289. Kuruoglu AC, Arikan Z, Vural G, Karataş M, Araç M, Işik E. Single photon emission computerised tomography in chronic alcoholism. Antisocial personality disorder may be associated with decreased frontal perfusion. *Br J Psychiatry.* (1996) 169:348–54. doi: 10.1192/bjp.169.3.348
290. Noël X, Paternot J, Van der Linden M, Sferrazza R, Verhas M, Hanak C, et al. Correlation between inhibition, working memory and delimited frontal area blood flow measure by 99mTc-Bicisate SPECT in alcohol-dependent patients. *Alcohol Alcohol.* (2001) 36:556–63. doi: 10.1093/alcalc/36.6.556
291. Ohta H, Matsumoto R, Kato T, Tomono N, Shimizu T. Tc-99m HMPAO brain perfusion SPECT images in a patient with portal-systemic encephalopathy. *Clin Nucl Med.* (1998) 23:634–6. doi: 10.1097/00003072-199809000-00025
292. Catafau AM, Kulisevsky J, Bernà L, Pujol J, Martin JC, Otermin P, et al. Relationship between cerebral perfusion in frontal-limbic-basal ganglia circuits and neuropsychologic impairment in patients with subclinical hepatic encephalopathy. *J Nucl Med.* (2000) 41:405–10.
293. Iwasa M, Matsumura K, Kaito M, Ikoma J, Kobayashi Y, Nakagawa N, et al. Decrease of regional cerebral blood flow in liver cirrhosis. *Eur J Gastroenterol Hepatol.* (2000) 12:1001–6. doi: 10.1097/00042737-200012090-00006
294. Nakagawa Y, Matsumura K, Iwasa M, Kaito M, Adachi Y, Takeda K. Single photon emission computed tomography and statistical parametric mapping analysis in cirrhotic patients with and without minimal hepatic encephalopathy. *Ann Nucl Med.* (2004) 18:123–9. doi: 10.1007/BF02985102
295. Romeiro FG, Ietsugu MDV, Franzoni LC, Augusti L, Alvarez M, Santos LAA, et al. Which of the branched-chain amino acids increases cerebral blood flow in hepatic encephalopathy? A double-blind randomized trial. *Neuroimage Clin.* (2018) 19:302–10. doi: 10.1016/j.nicl.2018.03.028
296. Sunil HV, Mittal BR, Kurmi R, Chawla YK, Dhiman RK. Brain perfusion single photon emission computed tomography abnormalities in patients with minimal hepatic encephalopathy. *J Clin Exp Hepatol.* (2012) 2:116–21. doi: 10.1016/S0973-6883(12)60099-1
297. Choi IS, Lee MS. Early hypoperfusion of technetium-99m hexamethylprophylene amine oxime brain single photon emission computed tomography in a patient with carbon monoxide poisoning. *Eur Neurol.* (1993) 33:461–4. doi: 10.1159/000116994
298. Denays R, Tondeur M, Noël P, Ham HR. Bilateral cerebral mediofrontal hypoactivity in Tc-99m HMPAO SPECT imaging. *Clin Nucl Med.* (1994) 19:873–6. doi: 10.1097/00003072-199410000-00006
299. Chu K, Jung KH, Kim HJ, Jeong SW, Kang DW, Roh JK. Diffusion-weighted MRI and 99mTc-HMPAO SPECT in delayed relapsing type of carbon monoxide poisoning: evidence of delayed cytotoxic edema. *Eur Neurol.* (2004) 51:98–103. doi: 10.1159/000076536
300. Pach D, Hubalewska A, Huszno B, Pach J. Evaluation of regional cerebral perfusion using 99mTc-HmPAO single photon emission tomography (SPET) in carbon monoxide acutely poisoned patients. *Przegl Lek.* (2004) 61:217–21.
301. Tsai CF, Yip PK, Chen SY, Lin JC, Yeh ZT, Kung LY, et al. The impacts of acute carbon monoxide poisoning on the brain: Longitudinal clinical and 99mTc ethyl cysteinate brain SPECT characterization of patients with persistent and delayed neurological sequelae. *Clin Neurol Neurosurg.* (2014) 119:21–27. doi: 10.1016/j.clineuro.2014.01.005
302. Amen DG, Jourdain M, Taylor DV, Pigott HE, Willeumier K. Multi-site six month outcome study of complex psychiatric patients evaluated with addition of brain SPECT imaging. *Adv Mind Body Med.* (2013) 27:6–16.
303. Danos P, Kasper S, Grünwald F, Klemm E, Krappel C, Broich K, et al. Pathological regional cerebral blood flow in opiate-dependent patients

during withdrawal: a HMPAO-SPECT study. *Neuropsychobiology.* (1998) 37:194–9. doi: 10.1159/000026502
304. Gerra G, Calbiani B, Zaimovic A, Sartori R, Ugolotti G, Ippolito L et al. Regional cerebral blood flow and comorbid diagnosis in abstinent opioid addicts. *Psychiatry Res.* (1998) 83:117–26. doi: 10.1016/S0925-4927(98)00030-4
305. Amen DG, Waugh M. High resolution brain SPECT imaging of marijuana smokers with AD/HD. *J Psychoactive Drugs.* (1998) 2:209–14. doi: 10.1080/02791072.1998.10399692
306. Amen DG, Darmal B, Raji CA, Bao W, Jorandby L, Meysami S, et al. Discriminative properties of hippocampal hypoperfusion in marijuana users compared to healthy controls: implications for marijuana administration in Alzheimer's dementia. *J Alzheimer's Dis.* (2017) 56:261–73. doi: 10.3233/JAD-160833
307. Yang W, Yang R, Tang F, Luo J, Zhang J, Chen C, et al. Decreased relative cerebral blood flow in unmedicated heroin-dependent individuals. *Front Psychiatry.* (2020) 11:643. doi: 10.3389/fpsyt.2020.00643
308. Ashok AH, Mizuno Y, Volkow ND, Howes OD. Association of stimulant use with dopaminergic alterations in users of cocaine, amphetamine, or methamphetamine: a systematic review and meta-analysis. *JAMA Psychiatry.* (2017) 74:511–9. doi: 10.1001/jamapsychiatry.2017.0135
309. Proebstl L, Kamp F, Manz K, Krause D, Adorjan K, Pogarell O, et al. Effects of stimulant drug use on the dopaminergic system: A systematic review and meta-analysis of *in vivo* neuroimaging studies. *Eur Psychiatry.* (2019) 59:15–24. doi: 10.1016/j.eurpsy.2019.03.003
310. Liang CS, Ho PS, Yen CH, Yeh YW, Kuo SC, Huang CC, et al. Reduced striatal dopamine transporter density associated with working memory deficits in opioid-dependent male subjects: a SPECT study. *Addict Biol.* (2016) 21:196–204. doi: 10.1111/adb.12203
311. Fowler JS, Volkow ND, Wang GJ, Gatley SJ. Logan [(11)] Cocaine: PET studies of cocaine pharmacokinetics, dopamine transporter availability dopamine transporter occupancy. *J Nucl Med Biol.* (2001) 28:561–72. doi: 10.1016/S0969-8051(01)00211-6
312. Ernst A, Zibrak JD. Carbon monoxide poisoning. *N Engl J Med.* (1998) 339:1603–8. doi: 10.1056/NEJM199811263392206
313. Bhatia R, Chacko F, Lal V, Mittal BR. Reversible delayed neuropsychiatric syndrome following acute carbon monoxide exposure. *Indian J Occup Environ Med.* (2007) 11:80–2. doi: 10.4103/0019-5278.34534
314. Sung YF, Chen MH, Peng GS, Lee JT. Generalized chorea due to delayed encephalopathy after acute carbon monoxide intoxication. *Ann Indian Acad Neurol.* (2015) 18:108–10. doi: 10.4103/0972-2327.144288
315. Chen SY, Lin CC, Lin YT, Lo CP, Wang CH, Fan YM. Reversible changes of brain perfusion SPECT for carbon monoxide poisoning-induced severe akinetic mutism. *Clin Nucl Med.* (2016) 41:e221–7. doi: 10.1097/RLU.0000000000001121
316. Wu CI, Changlai SP, Huang WS, Tsai CH, Lee CC, Kao CH. Usefulness of 99mTc ethyl cysteinate dimer brain SPECT to detect abnormal regional cerebral blood flow in patients with acute carbon monoxide poisoning. *Nucl Med Commun.* (2003) 24:1185–8. doi: 10.1097/00006231-200311000-00009
317. Ozyurt G, Kaya FN, Kahveci F, Alper E. Comparison of SPECT findings and neuropsychological sequelae in carbon monoxide and organophosphate poisoning. *Clin Toxicol.* (2008) 46:218–21. doi: 10.1080/15563650701378704
318. Lu YY, Tsai SC, Kao CH, Lin WY. Regional cerebral blood flow in patients with carbon monoxide intoxication. *Ann Nucl Med.* (2012) 26:771–6. doi: 10.1007/s12149-012-0638-8
319. Gale SD, Hopkins RO, Weaver LK, Bigler ED, Booth EJ, Blatter DD. MRI, quantitative MRI, SPECT, and neuropsychological findings following carbon monoxide poisoning. *Brain Inj.* (1999) 13:229–43. doi: 10.1080/026990599121601
320. Chen NC, Chang WN, Lui CC, Huang SH, Lee CC, Huang CW, et al. Detection of gray matter damage using brain MRI and SPECT in carbon monoxide intoxication: a comparison study with neuropsychological correlation. *Clin Nucl Med.* (2013) 38:e53–9. doi: 10.1097/RLU.0b013e31827082a7
321. Denays R, Makhoul E, Dachy B, Tondeur M, Noel P, Ham HR, et al. Electroencephalographic mapping and 99mTc HMPAO single-photon emission computed tomography in carbon monoxide poisoning. *Ann Emerg Med.* (1994) 24:947–52. doi: 10.1016/S0196-0644(94)70212-8
322. Chang DC, Lee JT, Lo CP, Fan YM, Huang KL, Kang BH, et al. Hyperbaric oxygen ameliorates delayed neuropsychiatric syndrome of carbon monoxide poisoning. *Undersea Hyperb Med.* (2010) 37:23–33.
323. Chang CC, Chang WN, Lui CC, Huang SH, Lee CC, Chen C, et al. Clinical significance of the pallidoreticular pathway in patients with carbon monoxide intoxication. *Brain.* (2011) 134:3632–46. doi: 10.1093/brain/awr287
324. Iwamoto K, Ikeda K, Mizumura S, Tachiki K, Yanagihashi M, Iwasaki Y. Combined treatment of methylprednisolone pulse and memantine hydrochloride prompts recovery from neurological dysfunction and cerebral hypoperfusion in carbon monoxide poisoning: a case report. *J Stroke Cerebrovasc Dis.* (2014) 23:592–5. doi: 10.1016/j.jstrokecerebrovasdis.2013.05.014
325. Lin YT, Chen SY, Lo CP, Lee JT, Tsai CF, Yip PK, et al. Utilizing cerebral perfusion scan and diffusion-tensor MR imaging to evaluate the effect of hyperbaric oxygen therapy in carbon monoxide-induced delayed neuropsychiatric sequalae - a case report and literature review. *Acta Neurol Taiwan.* (2015) 24:57–62.
326. American Psychiatric Association. *Diagnostic and Statistical Manual of Mental Disorders*. Arlington, VA: American Psychiatric Association (2013). doi: 10.1176/appi.books.9780890425596
327. Henderson TA. Brain SPECT imaging in neuropsychiatric diagnosis and monitoring. *EPatient.* (2018) 1:40–7. Available online at: http://nmpangea.com/2018/10/09/738/
328. Rush AJ, Trivedi MH, Wisniewski SR, Nierenberg AA, Stewart JW, Warden D, et al. Acute and longer-term outcomes in depressed outpatients requiring one or several treatment steps: a STAR*D report. *Am J Psychiatry.* (2006) 163:1905–17. doi: 10.1176/ajp.2006.163.11.1905
329. West SA, McElroy SL, Strakowski SM, Keck PE Jr, McConville BJ. Attention deficit hyperactivity disorder in adolescent mania. *Am J Psychiatry.* (1995) 152:271–3. doi: 10.1176/ajp.152.2.271
330. Scheffer RE, Kowatch RA, Carmody T, Rush AJ. Randomized, placebo-controlled trial of mixed amphetamine salts for symptoms of comorbid ADHD in pediatric bipolar disorder after mood stabilization with divalproex sodium. *Am J Psychiatry.* (2005) 162:58–64. doi: 10.1176/appi.ajp.162.1.58
331. McElroy E, Fearon P, Belsky J, Fonagy P, Patalay, P. Networks of depression and anxiety symptoms across development. *J Am Acad Child Adolesc. Psychiatry.* (2018) 57:964–73. doi: 10.1016/j.jaac.2018.05.027
332. Kaufman J, Charney D. Comorbidity of mood and anxiety disorders. *Depress Anxiety.* (2000) 12:69–76. doi: 10.1002/1520-6394 (2000) 12:1+ <69::AID-DA9>3.0.CO;2-K
333. Dilsaver SC, Henderson-Fuller S, Akiskal HS. Occult mood disorders in 104 consecutively presenting children referred for the treatment of attention-deficit/hyperactivity disorder in a community mental health clinic. *J Clin Psychiatry.* (2003) 64:1170–6. doi: 10.4088/JCP.v64n1005
334. Spencer T, Biederman J, Wilens, T. Attention-deficit/hyperactivity disorder and comorbidity. *Pediatr Clin North Am.* (1999) 46:915–27. doi: 10.1016/S0031-3955(05)70163-2
335. Newcorn J, Halperin JM, Jensen PS, Abikoff HB, Arnold LE, Cantwell DP, et al. Symptom profiles in children with ADHD: effects of comorbidity and gender. *J Am Acad Child Adolesc Psychiatry.* (2001) 40:137–46. doi: 10.1097/00004583-200102000-00008
336. Pliszka SR. Psychiatric comorbidities in children with attention deficit hyperactivity disorder: implications for management. *Paediatr Drugs.* (2003) 5:741–50. doi: 10.2165/00148581-200305110-00003
337. Regier DA, Narrow WE, Clarke DE, Kraemer HC, Kuramoto, SJ, et al. DSM-5 field trials in the United States and Canada, Part II: test-retest reliability of selected categorical diagnoses. *Am J Psychiatry.* (2013) 170:59–70. doi: 10.1176/appi.ajp.2012.12070999
338. Lee JS, Kim BN, Kang E, Lee DS, Kim YK, Chung JK, et al. Regional cerebral blood flow in children with attention deficit hyperactivity disorder: comparison before and after methylphenidate treatment. *Hum Brain Mapp.* (2005) 24:157–64. doi: 10.1002/hbm.20067
339. Gustafsson P, Thernlund G, Ryding E, Rosen I, Cederblad M. Associations between cerebral blood-flow measured by single photon emission computed tomography (SPECT), electro-encephalogram (EEG), behaviour

symptoms, cognition and neurological soft signs in children with attention-deficit hyperactivity disorder (ADHD). *Acta Paediatr.* (2000) 89:830–5. doi: 10.1111/j.1651-2227.2000.tb00391.x

340. Spalletta G, Pasini A, Pau F, Guido G, Menghini L, Caltagirone C. Prefrontal blood flow dysregulation in drug naive ADHD children without structural abnormalities. *J Neural Transm.* (2001) 108:1203–16. doi: 10.1007/s007020170010
341. Langleben DD, Acton PD, Austin G, Elman I, Krikorian G, Monterosso JR, et al. Effects of methylphenidate discontinuation on cerebral blood flow in prepubescent boys with attention deficit hyperactivity disorder. *J Nucl Med.* (2002) 43:1624–9.
342. Kim BN, Lee JS, Shin MS, Cho SC, Lee DS. Regional cerebral perfusion abnormalities in attention deficit/hyperactivity disorder. Statistical parametric mapping analysis. *Eur Arch Psychiatry Clin Neurosci.* (2002) 252:219–25. doi: 10.1007/s00406-002-0384-3
343. Cho SC, Hwang JW, Kim BN, Lee HY, Kim HW, Lee JS, et al. The relationship between regional cerebral blood flow and response to methylphenidate in children with attention-deficit hyperactivity disorder: comparison between non-responders to methylphenidate and responders. *J Psychiatr Res.* (2007) 41:459–65. doi: 10.1016/j.jpsychires.2006.05.011
344. Cherkasova MV, Hechtman L. Neuroimaging in attention-deficit hyperactivity disorder: beyond the frontostriatal circuitry. *Can J Psychiatry.* (2009) 54:651–64. doi: 10.1177/070674370905401002
345. Kim BN, Kim JW, Kang H, Cho SC, Shin MS, Yoo HJ, et al. Regional differences in cerebral perfusion associated with the alpha-2A-adrenergic receptor genotypes in attention deficit hyperactivity disorder. *J Psychiatry Neurosci.* (2010) 35:330–6. doi: 10.1503/jpn.090168
346. Pliszka SR, Glahn DC, Semrud-Clikeman M, Franklin C, Perez R, Xiong J, et al. Neuroimaging of inhibitory control areas in children with attention deficit hyperactivity disorder who were treatment naive or in long-term treatment. *Am J Psychiatry.* (2006) 163:1052–60. doi: 10.1176/ajp.2006.163.6.1052
347. Smith AB, Taylor E, Brammer M, Toone B, Rubia K. Task-specific hypoactivation in prefrontal and temporoparietal brain regions during motor inhibition and task switching in medication-naive children and adolescents with attention deficit hyperactivity disorder. *Am J Psychiatry.* (2006) 163:1044–51. doi: 10.1176/ajp.2006.163.6.1044
348. Skalski S, Dobrakowski P. Vigilance, inhibitory control and regional cerebral blood oxygenation in the PFC - differences in ADHD types of presentations. *Adv Cogn Psychol.* (2020) 16:202–12. doi: 10.5709/acp-0297-5
349. Thornton JF, Schneider H, McLean MK, van Lierop MJ, Tarzwell R. Improved outcomes using brain SPECT-guided treatment versus treatment-as-usual in community psychiatric outpatients: a retrospective case-control study. *J Neuropsychiatry Clin Neurosci.* (2014) 26:51–6. doi: 10.1176/appi.neuropsych.12100238
350. Mena I, Correa R, Nader A, Boehme V. Bipolar affective disorders: assessment of functional brain changes by means of Tc99mHMPAO neuroSPECT. *ALASBIMN Journal.* (2004) 6:18.
351. Mena I, Correa R, Nader A. Bipolar disorder complicated by self-mutilation: neurofunctional changes demonstrated by Tc99mHMPAO neuroSPECT. *ALASBIMN J.* (2007) 10:15.
352. Lenox RH, Gould TD, Manji HK. Endophenotypes in bipolar disorder. *Am J Med Genet.* (2002) 114:391–406. doi: 10.1002/ajmg.10360
353. Mena I. Neurospect applications in Psychiatry. *ALASBIMN J.* (2009) 11:23.
354. McLean M, Henderson TA, Pavel DG, Cohen P. Increased asymmetric perfusion of the cerebral cortices and thalamus indicates individuals at risk for bipolar disorder: a family cohort single photon emission computed tomography neuroimaging study. *Front. Psychiatry.* (2022) 13:829561. doi: 10.3389/fpsyt.2022.829561
355. Price JL, Drevets WC. Neurocircuitry of mood disorders. *Neuropsychopharmacology.* (2010) 35:192–216. doi: 10.1038/npp.2009.104
356. Caligiuri MP, Brown GG, Meloy MJ, Eberson SC, Kindermann SS, Frank LR, et al. An fMRI study of affective state and medication on cortical and subcortical brain regions during motor performance in bipolar disorder. *Psychiatry Res.* (2003) 123:171–82. doi: 10.1016/S0925-4927(03)00075-1
357. Hasler G, Drevets WC, Manji HK, Charney DS. Discovering endophenotypes for major depression. *Neuropsychopharmacology.* (2004) 29:1765–81. doi: 10.1038/sj.npp.1300506
358. Lesser IM, Mena I, Boone KB, Miller BL, Mehringer CM, Wohl M. Reduction of cerebral blood flow in older depressed patients. *Arch Gen Psychiatry.* (1994) 51:677–86. doi: 10.1001/archpsyc.1994.03950090009002
359. Ito H, Kawashima R, Awata S, Ono S, Sato K, Goto R, et al. Hypoperfusion in the limbic system and prefrontal cortex in depression: SPECT with anatomic standardization technique. *J Nucl Med.* (1996) 37:410–4.
360. Ebmeier KP, Cavanagh JT, Moffoot AP, Glabus MF, O'Carroll RE, Goodwin GM. Cerebral perfusion correlates of depressed mood. *Br J Psychiatry.* (1997) 170:77–81. doi: 10.1192/bjp.170.1.77
361. Galynker II, Cai J, Ongseng F, Finestone H, Dutta E, Serseni D. Hypofrontality and negative symptoms in major depressive disorder. *J Nucl Med.* (1998) 39:608–12.
362. Fountoulakis KN, Iacovides A, Gerasimou G, Fotiou F, Ioannidou C, Bascialla F, et al. The relationship of regional cerebral blood flow with subtypes of major depression. *Prog Neuropsychopharmacol Biol Psychiatry.* (2004) 28:537–46. doi: 10.1016/j.pnpbp.2004.01.006
363. Pagani M, Salmaso D, Nardo D, Jonsson C, Jacobsson H, Larsson SA, et al. Imaging the neurobiological substrate of atypical depression by SPECT. *Eur J Nucl Med Mol Imaging.* (2007) 34:110–20. doi: 10.1007/s00259-006-0177-4
364. Nagafusa Y, Okamoto N, Sakamoto K, Yamashita F, Kawaguchi A, Higuchi T, et al. Assessment of cerebral blood flow findings using 99mTc-ECD single-photon emission computed tomography in patients diagnosed with major depressive disorder. *J Affect Disord.* (2012) 140:296–9. doi: 10.1016/j.jad.2012.03.026
365. Li J, Yang Y, Zhu Y, Zhou L, Han Y, Yin T, et al. Towards characterizing the regional cerebral perfusion in evaluating the severity of major depression disorder with SPECT/CT. *BMC Psychiatry.* (2018) 18:70. doi: 10.1186/s12888-018-1654-6
366. Goodwin GM, Austin MP, Dougall N, Ross M, Murray C, O'Carroll RE, et al. State changes in brain activity shown by the uptake of 99mTc-exametazime with single photon emission tomography in major depression before and after treatment. *J Affect Disord.* (1993) 29:243–53. doi: 10.1016/0165-0327(93)90014-B
367. Drevets WC, Savitz J, Trimble M. The subgenual anterior cingulate cortex in mood disorders. *CNS Spectr.* (2008) 13:663–81. doi: 10.1017/S1092852900013754
368. Brockmann H, Zobel A, Joe A, Biermann K, Scheef L, Schuhmacher A, et al. The value of HMPAO SPECT in predicting treatment response to citalopram in patients with major depression. *Psychiatry Res.* (2009) 173:107–12. doi: 10.1016/j.pscychresns.2008.10.006
369. Ogura A, Morinobu S, Kawakatsu S, Totsuka S, Komatani A. Changes in regional brain activity in major depression after successful treatment with antidepressant drugs. *Acta Psychiatr Scand.* (1998) 98:54–9. doi: 10.1111/j.1600-0447.1998.tb10042.x
370. Loo CK, Sachdev PS, Haindl W, Wen W, Mitchell PB, Croker VM, et al. High (15 Hz) and low (1 Hz) frequency transcranial magnetic stimulation have different acute effects on regional cerebral blood flow in depressed patients. *Psychol Med.* (2003) 33:997–1006. doi: 10.1017/S0033291703007955
371. Hanada H, Imanaga J, Yoshiiwa A, Yoshikawa T, Tanaka Y, Tsuru J, et al. The value of ethyl cysteinate dimer single photon emission computed tomography in predicting antidepressant treatment response in patients with major depression. *Int J Geriatr Psychiatry.* (2013) 28:756–65. doi: 10.1002/gps.3887
372. Amen DG, Taylor DV, Meysami S, Raji CA. Deficits in regional cerebral blood flow on brain SPECT predict treatment resistant depression. *J Alzheimer's Dis.* (2018) 63:529–38. doi: 10.3233/JAD-170855
373. Drevets WC. Functional neuroimaging studies of depression: the anatomy of melancholia. *Annu Rev Med.* (1998) 49:341–61. doi: 10.1146/annurev.med.49.1.341
374. Milak MS, Parsey RV, Keilp J, Oquendo MA, Malone KM, Mann JJ. Neuroanatomic correlates of psychopathologic components of major depressive disorder. *Arch Gen Psychiatry.* (2005) 62:397–408. doi: 10.1001/archpsyc.62.4.397
375. Saxena S, Brody AL, Schwartz JM, Baxter LR. Neuroimaging and frontal-subcortical circuitry in obsessive-compulsive disorder. *Br J Psychiatry Suppl.* (1998) 35:26–37 doi: 10.1192/S0007125000297870
376. Rubin RT, Villanueva-Meyer J, Ananth J, Trajmar PG, Mena I. Regional xenon 133 cerebral blood flow and cerebral technetium 99m HMPAO uptake

in unmedicated patients with obsessive-compulsive disorder and matched normal control subjects. Determination by high-resolution single-photon emission computed tomography. *Arch Gen Psychiatry.* (1992) 49:695–702. doi: 10.1001/archpsyc.1992.01820090023004
377. Harris GJ, Hoehn-Saric R, Lewis R, Pearlson GD, Streeter C. Mapping of SPECT regional cerebral perfusion abnormalities in obsessive-compulsive disorder. *Hum Brain Mapp.* (1994) 1:237–48. doi: 10.1002/hbm.460010403
378. Crespo-Facorro B, Cabranes JA, López-Ibor Alcocer MI, Payá B, Fernández Pérez C, Encinas M, et al. Regional cerebral blood flow in obsessive-compulsive patients with and without a chronic tic disorder. A SPECT study. *Eur Arch Psychiatry Clin Neurosci.* (1999) 249:156–61. doi: 10.1007/s004060050081
379. Busatto GF, Buchpiguel CA, Zamignani DR, Garrido GE, Glabus MF, Rosario-Campos MC, et al. Regional cerebral blood flow abnormalities in early-onset obsessive-compulsive disorder: an exploratory SPECT study. *J Am Acad Child Adolesc Psychiatry.* (2001) 40:347–54. doi: 10.1097/00004583-200103000-00015
380. Diler RS, Kibar M, Avci A. Pharmacotherapy and regional cerebral blood flow in children with obsessive compulsive disorder. *Yonsei Med J.* (2004) 45:90–9. doi: 10.3349/ymj.2004.45.1.90
381. Castillo AR, Buchpiguel CA, de Araújo LA, Castillo JC, Asbahr FR, Maia AK, et al. Brain SPECT imaging in children and adolescents with obsessive-compulsive disorder. *J Neural Transm.* (2005) 112:1115–29. doi: 10.1007/s00702-004-0240-x
382. Ho Pian KL, van Megen HJ, Ramsey NF, Mandl R, van Rijk PP, Wynne HJ, et al. Decreased thalamic blood flow in obsessive-compulsive disorder patients responding to fluvoxamine. *Psychiatry Res.* (2005) 138:89–97. doi: 10.1016/j.pscychresns.2004.12.003
383. Yamanishi T, Nakaaki S, Omori IM, Hashimoto N, Shinagawa Y, Hongo J, et al. Changes after behavior therapy among responsive and nonresponsive patients with obsessive-compulsive disorder. *Psychiatry Res.* (2009) 172:242–50. doi: 10.1016/j.pscychresns.2008.07.004
384. Karadag F, Kalkan Oguzhanoglu N, Yüksel D, Kiraç S, Cura C, Ozdel O, et al. The comparison of pre- and post-treatment (99m)Tc HMPAO brain SPECT images in patients with obsessive-compulsive disorder. *Psychiatry Res.* (2013) 213:169–77. doi: 10.1016/j.pscychresns.2012.07.005
385. Wen SL, Cheng MH, Cheng MF, Yue JH, Wang H. Pharmacotherapy response and regional cerebral blood flow characteristics in patients with obsessive-compulsive disorder. *Behav Brain Funct.* (2013) 9:31. doi: 10.1186/1744-9081-9-31
386. Perani D, Colombo C, Bressi S, Bonfanti A, Grassi F, Scarone S, et al. [18F]FDG PET study in obsessive-compulsive disorder. A clinical/metabolic correlation study after treatment. *Br J Psychiatry.* (1995) 166:244–50. doi: 10.1192/bjp.166.2.244
387. Brody AL, Saxena S, Schwartz JM, Stoessel PW, Maidment K, Phelps ME, et al. FDG-PET predictors of response to behavioral therapy and pharmacotherapy in obsessive compulsive disorder. *Psychiatry Res.* (1998) 84:1–6. doi: 10.1016/S0925-4927(98)00041-9
388. Hou JM, Zhao M, Zhang W, Song LH, Wu WJ, Wang J, et al. Resting-state functional connectivity abnormalities in patients with obsessive-compulsive disorder and their healthy first-degree relatives. *J Psychiatry Neurosci.* (2014) 39:304–11. doi: 10.1503/jpn.130220
389. Tomiyama H, Nakao T, Murayama K, Nemoto K, Ikari K, Yamada S, et al. Dysfunction between dorsal caudate and salience network associated with impaired cognitive flexibility in obsessive-compulsive disorder: A resting-state fMRI study. *Neuroimage Clin.* (2019) 24:102004. doi: 10.1016/j.nicl.2019.102004
390. Hazari N, Narayanaswamy JC, Venkatasubramanian G. Neuroimaging findings in obsessive-compulsive disorder: A narrative review to elucidate neurobiological underpinnings. *Indian J Psychiatry.* (2019) 61(Suppl 1):S9–29. doi: 10.4103/psychiatry.IndianJPsychiatry_525_18
391. Tanielan T, Jaycox LH. *Invisible Wounds of War: Psychological and Cognitive Injuries, Their Consequences, and Services to Assist Recovery.* Santa Monica, CA: RAND Corporation (2008). doi: 10.1037/e527612010-001
392. Rosenfeld JV, McFarlane AC, Bragge P, Armonda RA, Grimes JB, Ling GS. Blast-related traumatic brain injury. *Lancet Neurol.* (2013) 12:882–93. doi: 10.1016/S1474-4422(13)70161-3
393. Sachinvala N, Kling A, Suffin S, Lake R, Cohen M. Increased regional cerebral perfusion by 99mTc hexamethyl propylene amine oxime single photon emission computed tomography in post-traumatic stress disorder. *Mil Med.* (2000) 165:473–9. doi: 10.1093/milmed/165.6.473
394. Chung YA, Kim SH, Chung SK, Chae JH, Yang DW, Sohn HS, et al. Alterations in cerebral perfusion in posttraumatic stress disorder patients without re-exposure to accident-related stimuli. *Clin Neurophysiol.* (2006) 117:637–42. doi: 10.1016/j.clinph.2005.10.020
395. Rauch SL, van der Kolk BA, Fisler RE. A symptom provocation study of posttraumatic stress disorder using positron emission tomography and script-driven imagery. *Arch Gen Psychiatry.* (1996) 53:380–7. doi: 10.1001/archpsyc.1996.01830050014003
396. Liberzon I, Taylor SF, Amdur R, Jung TD, Chamberlain KR, Minoshima S, et al. Brain activation in PTSD in response to trauma-related stimuli. *Biol Psychiatry.* (1999) 45:817–26. doi: 10.1016/S0006-3223(98)00246-7
397. Lindauer RJ, Booij J, Habraken JB, van Meijel EP, Uylings HB, Olff M, et al. Effects of psychotherapy on regional cerebral blood flow during trauma imagery in patients with post-traumatic stress disorder: a randomized clinical trial. *Psychol Med.* (2008) 38:543–54. doi: 10.1017/S0033291707001432
398. Hughes KC, Shin LM. Functional neuroimaging studies of post-traumatic stress disorder. *Expert Rev Neurother.* (2011) 11:275–85. doi: 10.1586/ern.10.198
399. Pavel DG, Henderson TA, DeBruin S. The legacy of the TTASAAN report premature conclusions and forgotten promises: A review of policy and practice Part II. *Front Neuro.* (in press).
400. Amen DG, Trujillo M, Newberg A, Willeumier K, Tarzwell R, Wu JC, et al. Brain SPECT imaging in complex psychiatric cases: an evidence-based, underutilized tool. *Open Neuroimag J.* (2011) 5:40–8. doi: 10.2174/1874440001105010040

Conflict of Interest: DP is Director of PathFinder Brain SPECT which is a clinical service corporation providing SPECT functional neuroimaging and had no research funding. He is deceased. TH is the president and principal owner of The Synaptic Space, a neuroimaging consulting firm. He is also CEO and Chairman of the Board of Neuro-Luminance Corporation, a medical service company. He is also president and principal owner of Dr. Theodore Henderson, Inc., a medical service company. He is also Vice-President of the Neuro-Laser Foundation, a non-profit organization. He is a member of and a former officer of the Brain Imaging Council Board of the Society of Nuclear Medicine and Molecular Imaging (SNMMI). Since 2017, he has served in the SNMMI Brain Imaging Outreach Working Group. Currently, he serves as president of the International Society of Applied Neuroimaging. TH has no ownership in, and receives no remuneration from, any neuroimaging company. No more than 5% of his income is derived from neuroimaging. SD is President of Good Lion Imaging LLC involved in the post-processing and display of functional brain scan data.

The reviewer DA declared a past co-authorship with one of the authors TH to the handling editor.

Publisher's Note: All claims expressed in this article are solely those of the authors and do not necessarily represent those of their affiliated organizations, or those of the publisher, the editors and the reviewers. Any product that may be evaluated in this article, or claim that may be made by its manufacturer, is not guaranteed or endorsed by the publisher.

frontiers | Frontiers in Neurology

ORIGINAL RESEARCH
published: 11 April 2022
doi: 10.3389/fneur.2022.704844

Using Single-Photon Emission Computerized Tomography on Patients With Positive Quantitative Electroencephalogram to Evaluate Chronic Mild Traumatic Brain Injury With Persistent Symptoms

Alexi Gosset[1], Hayley Wagman[1], Dan Pavel[2], Philip Frank Cohen[3], Robert Tarzwell[3], Simon de Bruin[4], Yin Hui Siow[5], Leonard Numerow[6], John Uszler[7], John F. Rossiter-Thornton[8], Mary McLean[9,10], Muriel van Lierop[9], Zohar Waisman[1], Stephen Brown[1], Behzad Mansouri[11], Vincenzo Santo Basile[1], Navjot Chaudhary[2] and Manu Mehdiratta[1]

[1] Faculty of Medicine, University of Toronto, Toronto, ON, Canada, [2] University of Illinois Medical Center, Chicago, IL, United States, [3] Faculty of Medicine, University of British Columbia, Vancouver, BC, Canada, [4] Good Lion Imaging, Columbia, MD, United States, [5] Southlake Regional Health Centre, Newmarket, ON, Canada, [6] Faculty of Medicine, University of Calgary, Calgary, AB, Canada, [7] Faculty of Medicine, University of California, Los Angeles, Los Angeles, CA, United States, [8] Rossiter-Thornton Associates, Toronto, ON, Canada, [9] Private Practice, Toronto, ON, Canada, [10] The International Society of Applied Neuroimaging (ISAN), Toronto, ON, Canada, [11] Faculty of Medicine, University of Manitoba, Winnipeg, MB, Canada

OPEN ACCESS

Edited by:
Freimut Dankwart Juengling, University of Alberta, Canada

Reviewed by:
Catherine R. Jutzeler, ETH Zürich, Switzerland
Karen M. Barlow, The University of Queensland, Australia

***Correspondence:**
Manu Mehdiratta
manu.mehdiratta@trilliumhealthpartners.ca

Specialty section:
This article was submitted to Applied Neuroimaging, a section of the journal Frontiers in Neurology

Received: *04 May 2021*
Accepted: *24 February 2022*
Published: *11 April 2022*

Citation:
Gosset A, Wagman H, Pavel D, Cohen PF, Tarzwell R, Bruin Sd, Siow YH, Numerow L, Uszler J, Rossiter-Thornton JF, McLean M, Lierop Mv, Waisman Z, Brown S, Mansouri B, Basile VS, Chaudhary N and Mehdiratta M (2022) Using Single-Photon Emission Computerized Tomography on Patients With Positive Quantitative Electroencephalogram to Evaluate Chronic Mild Traumatic Brain Injury With Persistent Symptoms. Front. Neurol. 13:704844. doi: 10.3389/fneur.2022.704844

Background: Following mild traumatic brain injury (mTBI), also known as concussion, many patients with chronic symptoms (>3 months post injury) receive conventional imaging such as computed tomography (CT) or magnetic resonance imaging (MRI). However, these modalities often do not show changes after mTBI. We studied the benefit of triaging patients with ongoing symptoms >3 months post injury by quantitative electroencephalography (qEEG) and then completing a brain single positron emission computed tomography (SPECT) to aid in diagnosis and early detection of brain changes.

Methods: We conducted a retrospective case review of 30 outpatients with mTBI. The patients were assessed by a neurologist, consented, and received a qEEG, and if the qEEG was positive, they consented and received a brain SPECT scan. The cases and diagnostic tools were collectively reviewed by a multidisciplinary group of physicians in biweekly team meetings including neurology, nuclear medicine, psychiatry, neuropsychiatry, general practice psychotherapy, neuro-ophthalmology, and chiropractic providers. The team noted the cause of injury, post injury symptoms, relevant past medical history, physical examination findings, and diagnoses, and commented on patients' SPECT scans. We then analyzed the SPECT scans quantitatively using the 3D-SSP software.

Results: All the patients had cerebral perfusion abnormalities demonstrated by SPECT that were mostly undetectable by conventional imaging (CT/MRI). Perfusion changes were localized primarily in the cerebral cortex, basal ganglia, and cingulate cortex, and correlated with the patients' symptoms and examination findings. Qualitative and quantitative analyses yielded similar results. Most commonly, the patients experienced

persistent headache, memory loss, concentration difficulties, depression, and cognitive impairment post mTBI. Because of their symptoms, most of the patients were unable to return to their previous employment and activity level.

Conclusion: Our findings outline the physical basis of neurological and psychiatric symptoms experienced by patients with mTBI. Increased detection of mTBI can lead to development of improved targeted treatments for mTBI and its various sequelae.

Keywords: single photon emission computed tomography (SPECT), quantitative EEG (qEEG), traumatic brain injury (TBI), concussion, neuropsychiatric symptoms, post-concussion syndrome (PCS)

INTRODUCTION

There has been a lack of tools available for diagnosing mild traumatic brain injury (mTBI) objectively, therefore, the diagnosis has remained clinical using subjective signs and symptoms. mTBI is defined by the American Congress of Rehabilitation Medicine as a traumatic physiologic disruption of brain function that manifests as loss of consciousness (LOC), memory loss, altered mental state, or focal neurological deficits. Mild, by definition, means that the LOC is <30 min, Glasgow Coma Scale is 13–15 after the first 30 min, and posttraumatic amnesia resolves within the first day (1). There is also a subset of patients who have ongoing symptoms beyond the expected period. This has led to a significant amount of new research on the diagnosis, natural history, and treatment of concussion/mTBI (2, 3). We now know that mTBI and concussion affect the physical, cognitive, sleep, and emotional domains of a person's well-being and subsequent function (4). According to an ongoing study called transforming research and clinical knowledge in traumatic brain injury (TRACK-TBI) that compares the outcomes of patients with mTBI to those of orthopedic controls presenting to the ER, 52.8% of patients with mTBI suffer from ongoing functional limitations 1 year later (5).

Given the prevalence of ongoing symptoms causing functional limitations in patients with mTBI, validated and objective diagnostic and prognostic biomarkers for mTBI are needed to provide evidence-based diagnosis and treatment for patients. Previous studies on mTBI have shown that 90% of CT scans and 70% of patients receiving MRI have no findings of trauma such as subdural or subarachnoid injury (6, 7). Furthermore, these imaging techniques do not provide functional or prognostic indicators.

Research on mTBI reveals disruption in neuronal networks, which can be diffuse or focal and produces distinct clinical syndromes such as difficulty with memory, balance, and vestibular issues (8). There can also be evidence of traumatic axonal injury in mTBI, which is not usually seen on CT or MRI (9). There are helpful treatments for patients with mTBI that can improve symptoms and quality of life. Aiding in the clinical diagnosis of mTBI with qEEG and SPECT in patients with mTBI not seen on MRI or CT could improve early detection and treatment.

The literature states that quantitative electroencephalography (qEEG) and single photon emission computed tomography (SPECT) are evidence-based technologies clinically available to provide objective biomarkers for concussion (6, 10, 11).

BrainScope® One is a noninvasive class 2 medical device that measures brain electrical activity using electroencephalography (EEG), artificial intelligence ("AI"), and machine learning to assess the likelihood that a person undergoing a test experienced a traumatic brain injury. Electrical signals are received through 19 electrodes placed on different areas of the scalp. While qEEG has been used as a screening tool immediately following injury, it has also been validated as an effective screening tool for diagnosing brain injury beyond the first 72 h post-concussion in selected populations (11). qEEG was effective in showing significant changes in veterans with mTBI more than 3 months after injury (12). Conventional neuroimaging tests like CT and MRI detect structural damages by looking for presence of blood, lesions, and bone injury. EEG-based methods can detect changes in electrical patterns, giving information beyond structural injury. This information is further enhanced by a SPECT scan, which is a functional imaging technique. These technologies can provide information critical for adequately treating patients with mTBI (13).

Brain SPECT scan has been studied extensively in patients with mTBI, and investigators have noted certain patterns of hypometabolism in the posterior cingulate gyrus, parieto-occipital lobe, frontal lobe, temporal lobe, and cerebellum (14). Additionally, a prior study demonstrated the clinical utility of SPECT in predicting cognitive performance in mild traumatic brain injury, though only after blood flow quantification analysis (15).

OBJECTIVES

The primary objective of this study is to look for objective measures in the diagnosis of mTBI by analyzing case reports of patients with mTBI including clinical history, physical examination, and qEEG and SPECT imaging.

Hypothesis/Key Questions

We aimed to determine the objective basis for symptoms in subjects 18 years and older who experienced an mTBI and underwent a thorough history and physical examination, and had qEEG and SPECT neuroimaging scans. Our primary research question is: do patients diagnosed with mTBI using the Ontario Neurotrauma Foundation guidelines and with ongoing post-concussion symptoms and a positive qEEG show changes in SPECT scan that corroborate their symptoms and functional limitations?

We hypothesized that nearly all patients experiencing long-term symptoms after mTBI will have evidence of changes indicative of positive structural or functional injury, as evidenced by positive qEEG, and that these patients will have significant functional deviations from normal brain perfusion, as evidenced by an abnormal SPECT scan.

The weight of current evidence suggests that mTBI can produce lasting changes in neuro-axonal architecture and brain perfusion, which are commonly missed by routine imaging of CT and MRI but may be visible on qEEG and SPECT (10).

MATERIALS AND METHODS

Overview

We conducted a retrospective case review of 30 outpatients with mTBI who received technetium-99 m ethyl cysteinate dimer (ECD) cerebral SPECT scans in Vancouver, BC. The patients were assessed by a neurologist. If patients were diagnosed with mTBI, they would have a discussion with their neurologist about the risks and benefits of qEEG and SPECT. Participants signed a consent form at this appointment, which occurred between 2018–2020. Some patients also received an additional psychiatric assessment. We performed SPECT scans only on patients who were diagnosed with mTBI by a neurologist based on the Ontario Neurotrauma Foundation (ONF) guidelines and had qEEG that was positive for structural injury (16). qEEG was designed to evaluate signs of cerebral hemorrhage (i.e., structural injury), but we hypothesized that it could also determine signs of functional injury in mTBI, which would clinically present as persistent post-concussion syndrome (PPCS) (6). Patients who consented but had a negative qEEG were excluded from the study and did not receive a SPECT scan. Inclusion criteria for the study were (1) mTBI based on the ONF guidelines and (2) positive qEEG for structural injury. Exclusion criteria for the study were (1) artifact in qEEG or SPECT scan that renders it unable for interpretation and (2) patients who did not consent to get a SPECT scan after a positive qEEG.

Neurological and Psychiatric Examinations

The method of injury, post-injury symptoms, relevant past medical history, physical examination findings, and diagnoses were elicited from patient history during neurological and psychiatric appointments. This history was further discussed as context for SPECT images in the team meetings. The Brain Function Index (BFI) is an EEG-based quantitative tool that reflects brain electrical activity associated with TBI (17). It was scored relative to normative data using percentile. "Average or above" (A) refers to results equal to or above the 10th percentile. "Below average" (B) refers to results equal to or above the 2.5th percentile to the 10th percentile. "Clearly below average" (C) refers to results below the 2.5th percentile. Based on recent literature, patients with BFI at the 50th percentile or below were significantly more likely to experience concussive symptoms compared to those above the 50th percentile (6).

Cognitive function was further assessed at the neurological visit through the Montreal Cognitive Assessment (MoCA), as well as through Complex Reaction Time and Match to Sample neuro-cognitive assessments, both of which were built into the qEEG device. In the Complex Reaction Time test, the patients were given a tablet and asked to press the left side of the screen if a number 2 or 3 appeared, and the right side of the screen if a number 4 or 5 appeared. In the Match to Sample test, the patients were briefly shown a pattern of colors on a grid, and after the pattern disappeared, they were asked to match that pattern to one of two options. Performance on the two neuro-cognitive tests was scored relative to normative data by percentile. "Average or above" (A) refers to results at or above the 10th percentile. "Below average" (B) refers to results between the 3rd and 9th percentile. "Clearly below average" (C) refers to results in the 2nd percentile or below.

Analysis Meetings

During biweekly focus group virtual meetings, SPECT images for each case were reviewed by 5-10 clinicians specializing in one of the following: neurology, nuclear medicine, psychiatry, general practice psychotherapy, neuropsychiatry, neuro-ophthalmology, and chiropractic. Each clinician had extensive experience reviewing SPECT scans for TBI and over 10 years of clinical experience. The team discussed the method of injury, post-injury neurological and psychiatric symptoms, relevant past medical history, physical examination findings, and diagnoses, and commented on the patients' SPECT scans. Two research assistants recorded the reported findings and SPECT scan commentaries (**Supplementary Table 1**). We then made a note of the qEEG BFI percentile score for each patient and calculated the overall average for the group. We, the authors, represent the multidisciplinary team in the writing of our findings.

Post-meeting Analysis

For our qualitative analysis, the following terms used to describe cortical blood flow in brain surface SPECT imaging denote regions of hypoperfusion: "hypoperfused", "cold", "down", "injury", "damage", "dinge", "divot", "notch", "scalloping", "flattening", "lesion", and "hole". The following terms used to describe blood flow in the deep brain imaging denote regions of hyperperfusion: "hyperperfused", "warm", and "hot". "Scalloping" was commonly used to describe patches of hypoperfusion over the cortex (**Supplementary Table 1**). Additionally, we interpreted the images in the context of extensive clinical experience, as well as knowledge of previous studies examining normal ECD-SPECT brain perfusion patterns and the 3D-SSP (Minoshima) database of healthy controls (18, 19).

For our quantitative analysis, we compared the perfusion patterns of subjects in our study to the 3D-SSP database of healthy controls. The reconstructed and attenuation-corrected SPECT data are spatially normalized with the 3D-SSP application, transforming the slices into Talairach space. Comparison against the included age-matched ECD database produces positive and negative Z-score images that provide localization and severity information for hyper- and hypoperfused areas, respectively. We applied a threshold of $+/-2$ standard deviations to show the localization and extent of the abnormalities.

TABLE 1 | Summary of findings and visual single positron emission computed tomography (SPECT) interpretation.

Injury method	Symptom types	Return to activities	Conventional imaging	Neuro-cognitive assessment	Regions of hypoperfusion	Regions of hyperperfusion
MVA-driver/passenger (21) MVA-pedestrian (4) MVA-cyclist (3) MVA-motorcyclist (1) Other-falling objects (1)	Headache (29) Neck pain (22) Low back pain (20) Memory loss (29) Concentration (29) Dizziness (23) Tinnitus (8) Depression (26) Anxiety (22) Irritability (22) Sleep issues (22) Numbness/tingling (9) Fatigue (6) Smell (10) Taste (8) Speech (2)	Work: Full (0) Limited (12) No (17) N/A (1) Social: Full (5) Limited (11) No (11) N/A (3) Recreational: Full (3) Limited (8) No (17) N/A (2) Household chores: Full (8) Limited (15) No (7) N/A (0)	CT: Negative (14) Positive (4) N/A (12) MRI: Negative (8) Positive (3) N/A (19)	MoCA: Abnormal (10) Normal (5) N/A (15) BFI: A (25) B (5) C (0) Complex Reaction Time: A (8) B (4) C (15) N/A (3) Match to Sample: A (9) B (3) C (15) N/A (3)	Cerebellum (18) Temporal lobes (29) Frontal lobes (28) Parietal lobes (14) Occipital lobes (9) Global (7) Specifics: Visual cortex (4) Broca's area (4) Thalamus (2) Basal ganglia (1) Hippocampus (1)	Deep: Thalamus (10) Basal ganglia (19) Anterior cingulate gyrus (14) Posterior cingulate gyrus (6) Caudate (2) Putamen (2) Insula (3) Retrosplenial cortex (4) Cortical: Medial temporal lobes (1) Frontal lobes (1) Parietal lobes (1) Occipital lobes (1) Global: (3)

Ethics

Ethical approval for the study was obtained in November 2020 *via* Veritas Independent Review Board (IRB tracking number: 2020-2451-3468-3).

RESULTS

Patient Characteristics

The mean age at the time of assessment of the 30 patients (21 males and nine females) was 46 years old. All the patients suffered a traumatic brain injury and were diagnosed with mTBI. The patients were given SPECT scans an average of 547 days (∼1.5 years) after their accident. We classified the mechanism of injury into motor vehicle accident (MVA) as driver/passenger ($n = 21$), MVA as pedestrian ($n = 4$), MVA as cyclist ($n = 4$), MVA as motorcyclist ($n = 1$), or other/injury from falling object ($n = 2$) (**Table 1**).

Symptom Types

During the neurological assessment, the patients described persistent post-injury symptoms.

The most common symptoms included headaches in 29/30 patients (97% of total patients), memory loss in 29/30 (97%), difficulty with concentration in 29/30 (97%), depression/low mood in 26/30 (87%), dizziness in 23/30 (77%), neck pain in 22/30 (73%), anxiety in 22/30 (73%), irritability in 22/30 (73%), and sleep difficulty in 22/30 (73%).

Effect on Employment, Recreational and Social Activities, and Household Chores

We determined whether the patients returned to employment, social activities, recreational activities, or household chores and in what capacity. At the time of injury, 29/30 (97%) patients were fully employed or on short-term leave. None (0%) of the patients fully returned to their employment. Twelve (40%) of the patients returned to work with a limited or modified capacity. Seventeen (57%) of the patients did not return to work in any capacity. Five (17%) of the patients made a full return to social activities. Eleven (37%) of the patients returned to social activities with a limited capacity. Eleven (37%) of the patients were not able to return to any social activities. Three (10%) of the patients had an undetermined return to social activity status.

Three (10%) of the patients fully returned to recreational activities. Eight (27%) of the patients returned to their recreational activities with a limited capacity. Seventeen (57%) of the patients did not return to any recreational activities. Two (7%) of the patients had an undetermined return to recreational activity status.

All the patients at the time of injury were able to complete household chores with no limitations. Eight (27%) of the patients were able to fully return to household chores. Fifteen (50%) of the patients were able to perform household chores with a limited capacity at the time of assessment. Seven (23%) of the patients were no longer able to complete household chores in any capacity.

MRI and CT

Among the 30 cases, 24 received either CT or MRI, or both after their injury. Fourteen (78%) of the patients who received a CT scan had a negative or entirely normal scan. Eight (73%) of the patients who received an MRI scan had a negative or entirely normal scan. On review of CT and MRI reports interpreted by board-certified radiologists, scans that were reported as "positive" were within the realm of normal and had only minor changes, but with the exception of two. The first was a subdural hemorrhage. The second was a finding of swelling that promptly resolved with

treatment before the SPECT scan was completed. While these patients had normal results on conventional imaging, 100% of the patients had an abnormal SPECT scan and qEEG, largely showing evidence of perfusion abnormalities related to mTBI. Additionally, there was no evidence of potentially confounding, significant cerebral atrophy in these patients; they were too young and did not have a prior diagnosis consistent with atrophy (i.e., Alzheimer's disease).

Cognitive Testing

After injury, the neurologist determined whether a formal cognitive assessment was indicated. Fifteen of the 30 patients received a Montreal Cognitive Assessment (MoCA). The average MoCA score in the case series was 21.8/30. Of the 15 patients who received a MoCA, 10 (67%) had an abnormal result, indicating some form of cognitive impairment (i.e., score below 26/30). Twenty-seven of the 30 patients received further neuro-cognitive testing. On the Complex Reaction Time assessment, eight patients scored "average or above", four patients scored "below average", and 15 patients scored "clearly below average". On the Match to Sample assessment, nine patients scored "average or above", three patients scored "below average", and 15 patients scored "clearly below average". Therefore, on both neuro-cognitive assessments, 15/27 (56%) of the patients scored in the 2nd percentile or below compared to a normative sample. These scores are evidence of severe neuro-cognitive impairment post mTBI. Premorbid cognitive ability was not determined. We used the patients' employment status as a proxy for premorbid level of cognitive functioning.

qEEG and SPECT Analysis

Among the 30 cases, the mean Brain Functional Index, as found by qEEG, was in the 38.8th percentile. This result falls within the "average or above" category based on the test and comparison to normative data. Twenty-six patients (90%) were in the "average or above" BFI category, 4 (13%) in the "below average" category, and 0 (0%) in the "clearly below average" category. Additionally, all the patients tested positive for structural injury on qEEG.

We categorized the SPECT findings into regions of cerebral hypoperfusion or hyperperfusion. The following cortical brain regions were most commonly hypoperfused: temporal lobe (29/30, 97%), frontal lobe (28/30, 93%), cerebellum (18/30, 60%), and parietal lobe (15/30, 50%). The following deep brain structure regions were most commonly hyperperfused: basal ganglia (20/30, 67%), anterior cingulate gyrus (15/30, 50%) thalamus (11/30, 37%), and posterior cingulate gyrus (6/30, 20%). In a systematic review of SPECT perfusion patterns after mTBI, the frontal lobe (94%), temporal lobe (77%), parietal lobe (74%), occipital lobe (52%), and cerebellum (25%) were the most common regions with abnormality. The frequency of hypoperfused areas in our study are similar (10). The areas of hyperperfusion in our study may be related to subsequent psychiatric sequelae. The patients were found to have various neurologic and psychiatric diagnoses only after a complete neurologic and/or psychiatric evaluation. Although SPECT scan findings may suggest the possibility of additional diagnoses, this would require further clinical assessment.

TABLE 2 | Comparison of visual and quantitative SPECT interpretations of hypoperfused brain regions.

Brain region	Visual	Quantitative
Frontal lobe	28	30
Temporal lobe	29	30
Parietal lobe	14	21
Occipital lobe	9	9
Cerebellum	18	7

The second column titled "visual" displays the number of patients with evidence of hypoperfusion for each major brain region based on qualitative or visual analysis conducted during group meetings. The third column displays the number of patients with evidence of hypoperfusion based on quantitative analysis using the 3D-SSP software. A hypoperfused region is defined as one containing clusters of pixels with perfusion greater than 2 SD below the normal control perfusion level.

Quantitative SPECT Analysis

We analyzed the brain SPECT scans using the 3D-SSP software and quantitative methods described. Remaining clinically relevant to mTBI patterns of injury, we evaluated 5 major brain regions for presence of hypoperfusion. Hypoperfusion is defined as a cluster of pixels on brain SPECT scan that falls below 2 standard deviations from the perfusion value of the normal 3D-SSP database. We found similar numbers of patients with patterns of hypoperfusion for each brain region in both visual and quantitative analyses (**Table 2**). Our quantitative analysis demonstrated the following number of patients out of the sample of 30 with patterns of hypoperfusion in each of the five major brain regions: frontal lobe (30), temporal lobe (30), parietal lobe (21), occipital lobe (9), cerebellum (7).

Sample Case of 3D-SSP Analysis

This patient was a 58 year old male pedestrian involved in a motor vehicle accident (MVA) in November 2018. After his MVA in 2018, he had constant headache, neck pain, numbness in the 4th and 5th digits of his hands bilaterally and all of his toes, tinnitus, dizziness, trouble sleeping, decreased sense of taste, depression (23 on PHQ9), and exacerbation of his rheumatoid arthritis. He was unable to return to work, household chores, or recreational activities, and had trouble singing as he could not remember song lyrics. On neurological examination, he had decreased sense of smell, positive Romberg, bilateral convergence insufficiency, and essential tremor.

Using 3D-SSP analysis of the above patient (**Figure 1**), we found significant hypoperfusion (greater than two standard deviations below the level of perfusion in the normal comparison) in the frontal, temporal, and occipital lobes.

DISCUSSION

In this study, we demonstrate the usefulness of qEEG and SPECT scans in patients diagnosed with mTBI. qEEG and SPECT were more sensitive than conventional imaging (CT/MRI) in detecting cerebral changes in our case series of patients diagnosed with mTBI: SPECT identified changes in cerebral perfusion in 100% of the patients who had negative CT and/or MRI but had a

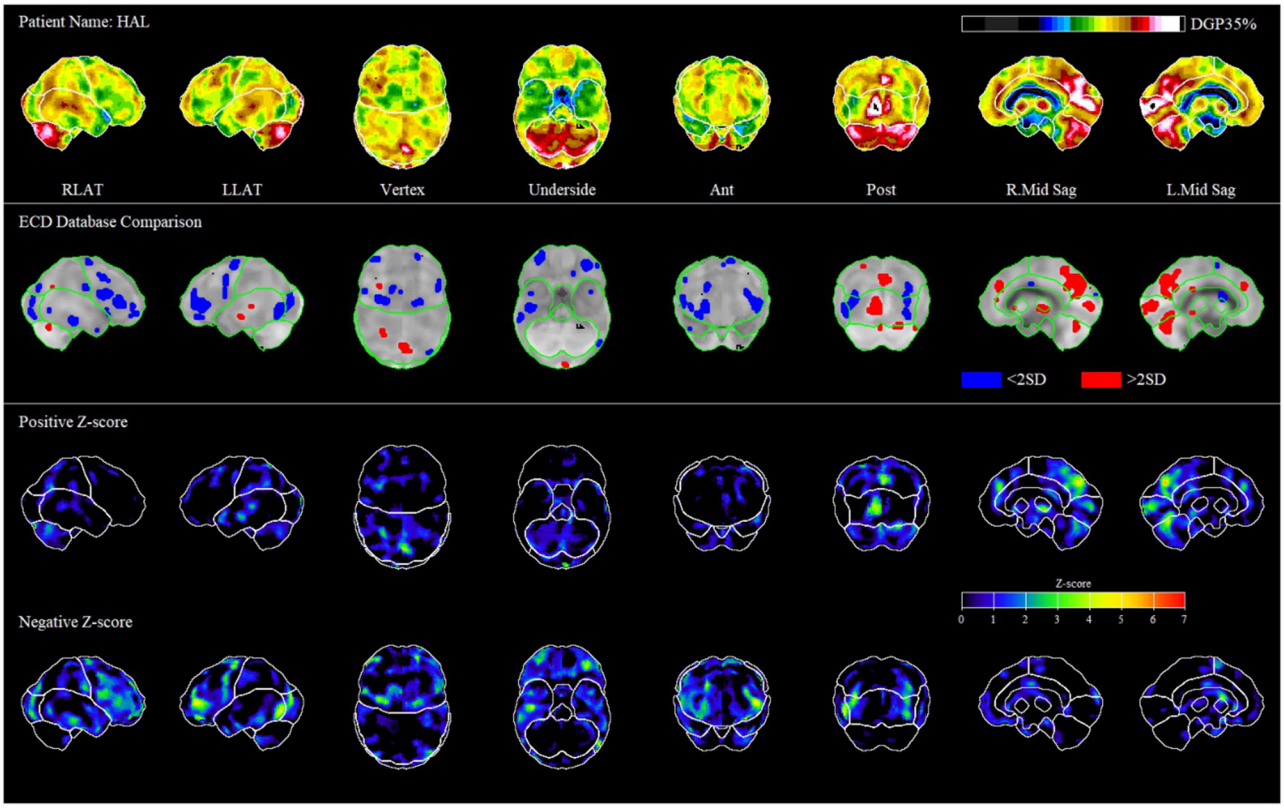

FIGURE 1 | Representative patient case. The first row of images shows different levels of perfusion relative to the maximum perfusion level in the brain (occipital lobe in ethyl cysteinate dimer, ECD). In the second row of images, we compare the patient to the average of normal scans in the database. Hypoperfusion is in blue, and hyperperfusion is in red; only pixels >2 standard deviations from normal are shown. In the third and 4th rows of images, we represent the positive and negative Z-scores, which outline the regions of heightened and diminished perfusion relative to control.

positive qEEG for structural injury. Our quantitative analysis conducted using the 3D-SSP software yielded similar results to our visual interpretation, and all the 30 subjects demonstrated areas of significant hypoperfusion in the frontal and temporal lobes, a finding consistent with mTBI (10). Therefore, we can conclude that in our case series, qEEG and SPECT were superior to the gold standard of CT and MRI in detecting brain changes after mTBI. We did not find any instance where CT or MRI was more informative than qEEG and SPECT in our case series. Additionally, in the cases where CT/MRI and SPECT were abnormal, SPECT provided different information. It highlighted very specific brain areas linked to functional and behavioral changes. This allowed for the clinicians to better understand these manifestations and subsequently propose a potential treatment targeted to the specific brain perfusion abnormality.

Access to SPECT scan is limited in Canada, and these scans use radioactive tracers. Because of these limitations, we cannot send every patient with mTBI for a SPECT scan. Therefore, qEEG can help determine which patients should be sent for SPECT imaging for further characterization of the injury and treatment implications.

By corroborating the symptoms and functional limitations reported by patients with mTBI using the qEEG and SPECT scan qualitative and quantitative analysis techniques, we outline the physical basis of neurological and psychiatric symptoms experienced by these patients. This has important implications, as we outlined that undetected mTBI can lead to severe consequences in productivity and functional ability. The fact that none of the patients were able to make full return to employment and very few to social, recreational, and household activities outlines the severity of consequences of "mild" traumatic brain injury. The SPECT and qEEG evidence shows that these patients have abnormal brain perfusion patterns consistent with mTBI, which can lead to many neurological and psychiatric symptoms. Our findings are in line with the weight of current evidence, which suggests that mTBI can lead to lasting changes in neuro-axonal architecture and brain perfusion, which are commonly missed by the routine imaging of CT and MRI but may be visible on qEEG and SPECT (6, 7, 9, 10, 14).

The findings in our case series may have implications in patient treatment. SPECT outlined the areas in the brain of our patients with most significant disturbance. This aids both in diagnosis and prioritizing issues, so patients can be followed by the most appropriate specialist. This was also the case in a previous study where SPECT was used to differentiate PTSD from TBI based on different cerebral blood flow pattern; thus, it can be used to evaluate and differentiate between neurological and psychiatric conditions (20). There are established cerebral

perfusion patterns consistent with a history of TBI, as well as other psychiatric conditions. In our case series, all the patients had a pattern consistent with mTBI. Given that most patients have other comorbidities, SPECT can be useful to differentiate which conditions are present in a patient (20–22). While many patients had SPECT findings that were expected based on their history and physical examinations, not all scans were correlated with all symptoms. For example, some patients had symptoms of depression or anxiety but no evidence of depression and anxiety on SPECT, as compared to previously established SPECT findings in patients with psychiatric conditions, as well as the Canadian Association of Nuclear Medicine (CANM) SPECT guidelines (22, 23). This suggests an alternate explanation for the symptoms rather than a primary mood disorder, such as inability to function. If patients are experiencing mood dysregulation because of functional decline, medications that can dampen the activity in the frontal lobe may be less effective. With further study, SPECT has the potential to inform decisions for improved targeted treatments for neurological and psychiatric sequelae of mTBI.

The similarity between the visual and quantitative analyses determined using the 3D-SSP program supports our proposed systematic approach of brain SPECT analysis. The discrepancies could be partially explained by the inclusion of "global" hypoperfusion to reflect the author's overall visual impression of the image, as we do not have a quantitative equivalent. Our selected patient case (**Figure 1**) illustrates a picture of mTBI both clinically through his symptoms post MVA, and through imaging by analysis using 3D-SSP when comparing to normal controls. The rest of our sample showed similar patterns of hypoperfusion in the frontal and temporal lobes consistent with mTBI.

Our study has some limitations. Although symptom severity and type were correlated with the SPECT findings, further studies and larger sample sizes are still required. We also did not have access to any previous scans that the patients had before injury occurrence. Our case series only studied patients with positive qEEG, and we did not have controls with negative qEEG, which would be a valuable comparator to see SPECT changes in this population. Additionally, confounding factors for patient SPECT scans include injury mechanisms like acceleration-deceleration traumas and comorbidities like depression, chronic alcohol use, certain medications, chronic pain, and other factors that can alter SPECT scans. Moreover, SPECT findings could be altered by injury mechanisms and comorbidities like psychiatric illnesses.

We suggest further studies using a systematic approach of interpreting brain SPECT imaging based on clinical context: conducting an in-depth neurological and psychiatric clinical history evaluation and examination, and imaging only those with a positive qEEG screening result for brain injury. The qEEG used as a screening tool, akin to an electrocardiogram (ECG) used in patients with chest pain when deciding who to take for an angiogram, enhanced the clinical utility of SPECT and limits unnecessary radiation exposure.

DATA AVAILABILITY STATEMENT

The original contributions presented in the study are included in the article/**Supplementary Material**, further inquiries can be directed to the corresponding author.

ETHICS STATEMENT

The studies involving human participants were reviewed and approved by Veritas Independent Review Board. Written informed consent for participation was not required for this study in accordance with the national legislation and the institutional requirements. Written informed consent was not obtained from the individual(s) for the publication of any potentially identifiable images or data included in this article.

AUTHOR CONTRIBUTIONS

AG, HW, and SB analyzed the data. All authors contributed to the preparation and revision of the manuscript.

SUPPLEMENTARY MATERIAL

The Supplementary Material for this article can be found online at: https://www.frontiersin.org/articles/10.3389/fneur.2022.704844/full#supplementary-material

REFERENCES

1. Kay T, Harrington DE, Adams R, Anderson T, Berrol S, Cicerone K, et al. Definition of mild traumatic brain injury. *J Head Trauma Rehabil.* (1993) 8:86–7. doi: 10.1097/00001199-199309000-00010
2. Rathbone M, Mehdiratta M, Finlayson H. Mild head injury. *Can J Cardiol.* (2000) 15:76–93
3. Bigler ED, Maxwell Neuropathology of mild traumatic brain injury: relationship to neuroimaging findings. *Brain Imaging Behav.* (2012) 6:108–36. doi: 10.1007/s11682-011-9145-0
4. Marshall S, Bayley M, McCullagh S, Velikonja D, Berrigan L, Ouchterlony D, et al. Updated clinical practice guidelines for concussion/mild traumatic brain injury and persistent symptoms. *Brain Inj.* (2015) 29:688–700. doi: 10.3109/02699052.2015.1004755
5. Nelson L, Temkin N. Recovery after mild traumatic brain injury in patients presenting to US level i trauma centers: a transforming research and clinical knowledge in traumatic brain injury (TRACK-TBI) study. *JAMA Neurol.* 76:1049–59. doi: 10.1001/jamaneurol.2019.1313
6. Naunheim R, Covassin T, Jacquin A, Hanley D, Michelson E. Using a brain electrical activity biomarker could aid in the objective identification of mild Traumatic Brain Injury Patients. *Am J Emerg Med.* (2018) 36:1. doi: 10.1016/j.ajem.2017.07.007
7. Borg J, Holm L, Peloso PM, Cassidy JD, Carroll LJ, von Holst H, et al. Non-surgical intervention and cost for mild traumatic brain injury: Results of the WHO Collaborating Centre Task Force on Mild Traumatic Brain Injury. *J Rehabil Med.* (2004) 76–83. doi: 10.1080/16501960410023840
8. Mittl RL, Grossman RI, Hiehle JF, Hurst RW, Kauder DR, Gennarelli TA, et al. Prevalence of MR evidence of diffuse axonal injury in patients with mild head injury and normal head CT findings. *AJNR Am J Neuroradiol.* (1994) 15:1583–9.
9. Kuthcer J, Giza C. Sports Concussion Diagnosis and Management. *Sports Neurology.* (2014) 20:1552–69. doi: 10.1212/01.CON.0000458974.78766.58

10. Shenton M.E. et al. A review of magnetic resonance imaging and diffusion tensor imaging findings in mild traumatic brain injury. *Brain Imaging Behav*. (2012) 6:137–92. doi: 10.1007/s11682-012-9156-5
11. Raji C, Tarzwell R, Pavel D, Schneider H, Uszler M, Thornton J, et al. Clinical utility of SPECT neuroimaging in the diagnosis and treatment of traumatic brain injury: a systematic review. *PLoS ONE*. (2014). doi: 10.1371/journal.pone.0091088
12. Bazarian JJ, Elbin RJ, Casa DJ, et al. Validation of a Machine Learning Brain Electrical Activity–Based Index to Aid in Diagnosing Concussion Among Athletes. *JAMA Netw Open*. (2021). 4(2):e2037349. doi: 10.1001/jamanetworkopen.2020.37349
13. Lewine JD, Plis S, Ulloa A, Williams C, Spitz M, Foley J, et al. Quantitative EEG biomarkers for mild traumatic brain injury. *Clin Neurophysiol Pract*. (2019) 36:298–305. doi: 10.1097/WNP.0000000000000588
14. Boshra R, Dhindsa K, Boursalie O, Ruiter KI, Sonnadara R, Samavi R, et al. From group-level statistics to single-subject prediction: machine learning detection of concussion in retired athletes. *IEEE Trans Neural Syst Rehabilitation Eng*. (2019) 27:1492–501. doi: 10.1109/TNSRE.2019.2922553
15. Romero K, Lobaugh NJ, Black SE, Ehrlich L, Feinstein A. Old wine in new bottles: validating the clinical utility of SPECT in predicting cognitive performance in mild traumatic brain injury. *Psychiatry Res*. (2015) 231:15–24. doi: 10.1016/j.pscychresns.2014.11.003
16. Koerte IK, Hufschmidt J, Muehlmann M, Lin AP, Shenton ME. Advanced neuroimaging of mild traumatic brain injury. In: Laskowitz D, Grant G, editors. *Translational Research in Traumatic Brain Injury*. Boca Raton, FL: CRC Press/Taylor and Francis Group. (2016) p. 13.
17. Guideline for concussion/mild traumatic brain injury & prolonged symptoms. Available online at: https://braininjuryguidelines.org/concussion/
18. Alison Brooks M, Bazarian JJ, Prichep LS, Ghosh-Dastidar S, Talavage TM, Barr W. The use of an electrophysiological brain function index in the evaluation of concussed athletes? *J Head Trauma Rehabil*. (2018) 33:1–6. doi: 10.1097/HTR.0000000000000328
19. Tanaka F, Vines D, Tsuchida T, Freedman M, Ichise M. Normal patterns on ^{99m}Tc-ECD brain SPECT scans in adults. *J Nucl Med*. (2000) 41:1456–64.
20. Minoshima S, Koeppe RA, Frey KA, Kuhl DE. Anatomical standardization: linear scaling and nonlinear warping of functional brain images. *J Nucl Med*. (1994) 35:1528–37.
21. Amen D, Raji C, Willeumier K, Taylor D, Tarzwell R, Newberg A, Henderson T. Functional neuroimaging distinguishes posttraumatic stress disorder from traumatic brain injury in focused and large community datasets. *PLoS ONE*. (2015). doi: 10.1371/journal.pone.0129659
22. Santra, A & Kumar, R. Brain perfusion single photon emission computed tomography in major psychiatric disorders: From basics to clinical practice. *IJNM*. (2014) 29:210–21. doi: 10.4103/0972-3919.142622
23. Cohen P, Tarzwell R, Numerow L, Siow Y, Mehdiratta M, et al. CANM guidelines for brain perfusion single photon emission computed tomography (SPECT). *Can Assoc*. (2021). Available online at: https://canm-acmn.ca/resources/Documents/Guidelines%20Brain_SPECT%20(1).pdf

Conflict of Interest: MM has an interest in iScope Concussion and Pain Clinics, which uses qEEG and SPECT as part of the clinic.

The remaining authors declare that the research was conducted in the absence of any commercial or financial relationships that could be construed as a potential conflict of interest.

Publisher's Note: All claims expressed in this article are solely those of the authors and do not necessarily represent those of their affiliated organizations, or those of the publisher, the editors and the reviewers. Any product that may be evaluated in this article, or claim that may be made by its manufacturer, is not guaranteed or endorsed by the publisher.

frontiers | Frontiers in Psychiatry

ORIGINAL RESEARCH
published: 10 May 2022
doi: 10.3389/fpsyt.2022.829561

Increased Asymmetric Perfusion of the Cerebral Cortices and Thalamus Indicates Individuals at Risk for Bipolar Disorder: A Family Cohort Single Photon Emission Computed Tomography Neuroimaging Study

Mary McLean[1,2], Theodore A. Henderson[2,3,4,5,6], Dan G. Pavel[2,7†] and Phil Cohen[2,8,9]*

[1] Private Practice, Toronto, ON, Canada, [2] The International Society of Applied Neuroimaging (ISAN), Denver, CO, United States, [3] The Synaptic Space, Inc., Denver, CO, United States, [4] Neuro-Luminance, Inc., Denver, CO, United States, [5] Dr. Theodore Henderson, Inc., Denver, CO, United States, [6] The Neuro-Laser Foundation, Denver, CO, United States, [7] PathFinder Brain SPECT, Deerfield, IL, United States, [8] Lions Gate Hospital, Vancouver, BC, Canada, [9] Department of Radiology, University of British Columbia, Vancouver, BC, Canada

OPEN ACCESS

Edited by:
Alessandra Maria Passarotti, University of Illinois at Chicago, United States

Reviewed by:
Sandipan Pati, University of Texas Health Science Center at Houston, United States
Gianluca Serafini, Department of Neuroscience, San Martino Hospital (IRCCS), Italy

***Correspondence:**
Theodore A. Henderson
thesynapticspace7@gmail.com

†Deceased

Specialty section:
This article was submitted to Neuroimaging and Stimulation, a section of the journal Frontiers in Psychiatry

Received: 06 December 2021
Accepted: 23 February 2022
Published: 10 May 2022

Citation:
McLean M, Henderson TA, Pavel DG and Cohen P (2022) Increased Asymmetric Perfusion of the Cerebral Cortices and Thalamus Indicates Individuals at Risk for Bipolar Disorder: A Family Cohort Single Photon Emission Computed Tomography Neuroimaging Study. Front. Psychiatry 13:829561. doi: 10.3389/fpsyt.2022.829561

Bipolar disorder is a significant mental illness affecting over 4 million people in North America and approximately 46 million worldwide. While the onset of bipolar disorder is typically in late adolescence and early adulthood, the correct diagnosis can be delayed for several years. This delay can result in inappropriate pharmaceutical interventions, loss of career or productivity, suicide, family hardship, and unnecessary expense. Moreover, prolonged untreated or inappropriately treated bipolar disorder may cause damage to the brain. Early diagnosis is a critical need to circumvent the damage, suffering, and expense caused by the current delay. Brain perfusion single photon emission computed tomography (SPECT) neuroimaging reveals visual correlates of brain function. Herein, a family cohort all with bipolar disorder is described and their symptoms correlated with findings on the individual SPECT brain scans. The family consisted of two parents and three children (one female). The scans were interpreted by a panel of experts. Then a *post hoc* region-of-interest (ROI) analysis was conducted on SPECT data normalized to the cerebellum maximum with comparison to similarly normalized data from a normative sample. These findings support two distinct patterns of SPECT perfusion scan changes that can be found in individuals with bipolar disorder. In addition, these findings indicate that SPECT scan findings may be predictive of individual risk for progressing to symptomatic bipolar disorder. While preliminary, the findings in this cohort support the need for larger, diverse cohort studies of bipolar and control subjects to assess the predictive value of these particular SPECT perfusion findings in bipolar disorder.

Keywords: biomarker, thalamus, psychiatry, perfusion, prodromal, seizure, single photon emission computed tomography, ADHD

INTRODUCTION

Bipolar disorder is a spectrum of mood disorders with significant morbidity. Bipolar I disorder, previously known as manic depressive disorder, is characterized by one or more manic episodes, alternating with episodes of depression or euthymia. Bipolar II disorder is characterized by cyclic episodes of hypomania alternating with episodes of depression or euthymia. A third presentation, referred to as a "Mixed State," features negative feelings of depression along with agitation, restlessness, or a "wired" state of mania. Besides these three defined entities, the spectrum of mood disorders with a cyclic component is broad and diverse. Bipolar disorder has a prevalence of 1%, which equates to approximately 46 million patients worldwide (1). In North America, the prevalence is approximately 1–1.5% (2) or approximately 4 million people.

While the onset of bipolar disorder is typically in late adolescence and early adulthood, the correct diagnosis can be delayed for several years. Retrospective studies in multiple nations have shown delays of greater than 5 years between the onset of symptoms and the correct diagnosis (3–6). However, some studies have shown delays of greater than 10 years (6–8). In addition, patients are often initially treated with antidepressants or stimulants (5, 9–11), which can lead to exacerbation of symptoms, manic episodes, and a worsening of the course of the illness. For example, antidepressant monotherapy is associated with increased incidence of manic episodes and suicide (12, 13). This diagnostic delay can take on more serious consequences in the case of early-onset bipolar disorder among children. Treatment with stimulant medications for presumptive attention-deficit/hyperactivity disorder (ADHD) can lead to mania, hypomania, or accelerated cycling (12, 14–18). Alternative treatments for ADHD, such as atomoxetine, have also been shown to precipitate mania in children (19, 20). Early diagnosis and differentiating bipolar disorder from ADHD are key steps in reducing later morbidity.

Bipolar disorder is the 12th leading cause of disability worldwide (21). Untreated bipolar disorder leads to impaired ability to work, difficulty maintaining relationships, and academic failure (7, 22). Being untreated or incorrectly treated (due to misdiagnosis with unipolar depression) amplifies the already heavy burdens associated with bipolar disorder. Despite treatment, patients with bipolar disorder have higher healthcare costs, more frequent emergency room visits, more frequent hospitalizations, and more frequent psychiatric appointments (23, 24). Despite treatment, patients with bipolar disorder also experience higher rates of unemployment (25) lower levels of work productivity (26), and higher rates of short-term disability (24). Patients with bipolar disorder are more likely to have comorbid medical problems and a shorter lifespan (27, 28). Furthermore, patients with bipolar disorder are more likely to fail to adhere or comply with a medication regimen long-term. Multiple factors underlie this tendency toward non-adherence, including impulsivity, personality traits, anxiety, substance use, beliefs, and impaired insight (29). Adherence issues created added costs for both patients and providers/systems (29). The individual medical expenses associated with bipolar disorder are estimated to range from $11,000–$46,800 (USD) annually (24). The direct and indirect costs of bipolar disorder have been estimated at between $194–$219 billion (USD) annually in the United States (23, 27).

Altogether, the diagnostic delay can result in inappropriate pharmaceutical interventions, loss of career or productivity, family hardship, suicide, and unnecessary expense. Moreover, prolonged untreated or inappropriately treated bipolar disorder may cause damage to the brain (30). Early diagnosis is a critical need to circumvent the damage, suffering, and expense caused by the current delay in diagnosis and treatment.

Can Neuroimaging Provide a Biomarker?

Given the substantial overlap of symptoms between bipolar disorder, unipolar depression, ADHD, and oppositional defiant disorder (ODD), a biomarker for bipolar disorder would be invaluable. Short of a definitive molecular biomarker, neuroimaging findings which are consistent and predictive would aid the diagnostic process. It is important to understand that the predictive value of a neuroimaging finding need not be perfect. A marker with reasonably high sensitivity and specificity (>75%) would be sufficient to warrant pharmacological interventions targeting a bipolar phenotype. Since the medications to treat bipolar disorder include several with very low risks and side effects, the danger of making an incorrect pharmacological choice also is low. On the other hand, in the case of localizing a seizure focus for surgical ablation, high sensitivity and specificity would be paramount. Nevertheless, positron emission tomography (PET) for localizing seizure foci has a sensitivity of 65–95% and a specificity of 90–95% (31, 32). Hence, it is *not unreasonable* to explore neuroimaging markers for bipolar disorder that would expedite reaching the correct diagnosis and treatment even if they lack perfect 100% sensitivity and specificity. Certain findings that we have consistently observed in our clinical practices utilizing single photon emission computed tomography (SPECT) neuroimaging in the evaluation of literally thousands of patients with bipolar disorder also have been described in the research literature.

Perfusion SPECT Findings in Bipolar Disorder

SPECT neuroimaging has demonstrated moderate consistency across multiple studies in both depressed and manic states. Early perfusion SPECT studies utilizing ^{133}Xenon gas focused only on cerebral cortex (33–37) and found decreased frontal lobe perfusion during bipolar and unipolar depression. With the advent of stabilized tracers, such as ^{99m}Tc-ethyl cysteinate dimer (ECD) and ^{99m}Tc-hexamethylpropyleneamine oxime (HMPAO), additional observations became evident. Decreased frontal lobe perfusion is widely reported in bipolar depression (38–43). In contrast, mania can present with more profound hypoperfusion in the orbitofrontal cortex and the anterior temporal lobes (42, 44). Moreover, a left-right asymmetry has been reported by some (36, 45, 46). This asymmetry also can be found in the thalami (42, 47–49). For example, Juckel et al. (50) described a case of bipolar disorder with ultrarapid cycling that received a SPECT

scan during a manic phase and again during a depressive phase (within 48 hours). During the manic phase, thalamic perfusion was markedly elevated and asymmetrical. On the following day, when the patient was in a depressed phase, thalamic perfusion was less asymmetrical (50).

Lithium withdrawal frequently precipitates mania and was used to elucidate mood and perfusion changes in a sample of 7 patients converted from a euthymic state (on lithium for over one year) to a manic state. Perfusion increased in the posterior temporal and parietal cortices (51). Recently, perfusion SPECT scans were examined in a group of patients with bipolar I during a manic episode and 6 months later (52). A sample of 10 patients with bipolar mania (diagnosed based on DSM-IV criteria and an elevated Young Mania Rating Scale score) underwent perfusion SPECT with statistical comparison to a normative database. Overall, perfusion was increased more in the right hemisphere than in the left hemisphere. Compared to the normative database, perfusion was elevated throughout the cerebral cortices, including the frontal lobes. The perfusion in the temporal poles bilaterally stood out as markedly elevated. At 6-month follow-up, the patients were all euthymic. Perfusion was still elevated in the bilateral temporal and parietal cortices, but the bilateral frontal cortices showed lower perfusion than the normative database. Notably, the asymmetry still was present (52). Our extensive clinical experience spanning decades and tens of thousands of SPECT scans support the consistent finding of asymmetry in the cortex and, prominently, in the thalamus (48).

Other Neuroimaging Modality Findings in Bipolar Disorder

Other neuroimaging modalities provide supporting evidence. PET neuroimaging using ^{18}F-fluorodeoxyglucose (FDG) to visualize regional glucose uptake as a measure of regional brain activity have shown the thalamus to be involved in mood disorders. Milak et al. (53) examined FDG PET scans of 298 medication-free patients with depression. They performed factor analysis to correlate brain activity with various factors of the Hamilton Depression Rating Scale. Increased metabolism in the thalamus, as well as the subgenual anterior cingulate, subgenual basal forebrain, posterior cingulate, and ventral striatum correlated positively with the emotional metrics of depressed mood, guilt, suicidal ideation, helplessness and hopelessness. In contrast, psychotic symptoms endorsed on the Hamilton Scale did not correlate positively or negatively with any brain region, while the symptoms of low motivation correlated with the dorsolateral prefrontal cortex, but not with the thalamus. Brody et al. examined metabolism changes in 24 patients at baseline and after treatment for depression (54). When compared to a control cohort of 16 subjects, patients with depression showed higher metabolism in the bilateral thalamus, as well as the prefrontal cortex and striatum. They also noted that decreases in the Hamilton Depression Scale score were correlated with decreases in thalamic metabolism. Ketter et al. (55) examined treatment-resistant, rapid-cycling bipolar disorder patients compared to age-matched healthy controls using FDG-PET. They found that bipolar disorder was characterized by increased metabolism in the thalamus, striatum, and right amygdala, but decreased metabolism in the frontal cortex (55). Also, they noted an increase in cerebellar metabolism, which appeared to be independent of mood state.

PET perfusion studies of bipolar mania using ^{15}O-H_2O also found hypoperfusion of the orbitofrontal cortex (56) but increased anterior cingulate perfusion (57). Similarly, fMRI studies show increased perfusion in multiple cortical areas and the thalamus, in combination with decreased ventral frontal cortex perfusion (most often more severe on the right), has been reported in unmedicated bipolar disorder patients while performing a motor task (58). Similar fMRI findings have been reported in a number of studies, as well as phase-dependent changes, such as increased thalamic perfusion (greater on the left) during mania and decreased asymmetric perfusion of the ventral frontal cortex (59). Altogether, these findings are consistent with an asymmetrical dysfunction within prefrontal-striatal-thalamic and amygdala-thalamic-cortical circuits, as well as the ventral striatum-limbic-thalamic circuit, which are believed to underlie the pathophysiology of bipolar disorder (59, 60).

A Clinical Pearl

In the present study, a diverse group with extensive experience reading and interpreting SPECT scans focused attention on a retrospective review of a single family in which every member manifested mood disorder symptoms. The SPECT neuroimaging findings in each member of this family demonstrated findings we have typically seen and associated with bipolar disorder in our diverse and international practices – namely, increased asymmetrical perfusion of the thalamus and increased asymmetrical perfusion of the cerebral cortices. This unique nuclear family – all with the diagnosis of bipolar disorder and providing perfusion SPECT scan data – is a first inroad into defining a working hypothesis about potential neuroimaging biomarkers for bipolar disorder.

In addition, these findings are presented herein using a novel display methodology and subjected to quantitative analysis using a novel method, both of which are described in detail in the methods, due to their innovation.

MATERIALS AND METHODS

The method of analysis of the SPECT scans for interpretation and the search for similarities was by expert consensus panel. The scans were presented to a group of clinicians from diverse backgrounds that all had extensive experience with the interpretation of SPECT scans. The group included four nuclear medicine physicians, one general psychiatrist, one child/adult psychiatrist, one psychiatrist cross-trained in nuclear medicine, and one general practitioner with advanced training in psychiatry. The physicians practice in either the United States, Australia, or Canada. Collectively the committee has read/interpreted/analyzed over 61,700 perfusion SPECT scans. Specifically, they are: Dan Pavel, MD (over 20,000 scans); John Michael Uszler, MD, MS (over 10,000 scans); Theodore Henderson, MD, PhD (over 20,000 scans – over 14,000 scans in

published articles); Phil Cohen, MD, FRCPC (over 3,000 scans); J. Cardaci, MBBS, FAANMS, FRACP (over 4,000 scans); Yin-Hui Siow, MD, FRCPC (over 3,000 scans); John F. Rossiter-Thornton, MB, FRCPC (over 800 scans); Mary McLean, MB, ChB, FRCP (over 600 scans); Muriel J. van Lierop, MBBS, MDPAC(M) (over 300 scans) (61–65).

The patients were all members of a single family in the clinical practice of one of the authors (MML). The SPECT scans were performed as part of the ongoing assessment and treatment of these patients, each of whom was diagnosed with bipolar disorder. As such, the symptom data collected on these patients was not quantitative, nor systematic. Rather, it was clinical records of the assessment and management of these patients. The study is retrospective and naturalistic in that regard. However, the analysis of the scans utilized modern displays and interpretation by a group of clinicians with the experience of collectively interpreting thousands of SPECT scans. A subsequent *post hoc* regions of interest (ROI) analysis was performed comparing the results of the family cohort to a group of non-aged-matched patients who did not have the diagnosis of bipolar disorder.

Each family member's case was presented to the group *via* monthly electronic conferences. A detailed history of the patient was provided verbally without identifying information. Then the de-identified SPECT scan results of that patient were shown and discussed by the group. The SPECT images were presented first in tomograms (horizontal, coronal, and sagittal) displayed in a polychromic color scale based on normal physiological cerebral perfusion. Then the scan results were shown in 3-dimensional displays wherein cortical perfusion falling below 60% of cerebral maximal perfusion presents as holes or depressions. Lastly, the results were displayed as a 3-dimensional model using the polychromic color scale. During the discussion, all displays were accessed and deliberated upon until a consensus opinion was reached.

Scanning Protocol

The scans themselves were performed at Mt. Sinai Hospital, Toronto, ON. The nuclear medicine department followed standard imaging procedures. The patient was positioned under dimmed lights lying supine. An intravenous line was started. The HMPAO was administered after allowing the patient to rest quietly for at least 5 minutes. After a 30-minute washout period, the patient was placed in a Picker Prism 3000 three-head gamma camera equipped with a low-energy, ultra-high resolution fan beam collimator. A step and shoot method of acquisition was used with 120 steps, 3 degrees per step, using 128 × 128 matrix and continuous acquisition. Approximately 22–30 seconds per stop yielded 3–4 million counts for each scan. The data was then passed through a ramp backprojection filter and a 3D Butterworth filter (order 5.0, cutoff frequency 0.2–0.3 cycle per pixel). Non-neural structures were masked. Attenuation correction was applied by the method of Chang (66, 67).

Analysis and Display Protocols

The data was then processed using a proprietary method (Good Lion Imaging, Columbia, MD, United States). Briefly, this methodology visualizes the reconstructed data of a brain SPECT scan in three distinct but complementary displays. Extra-cerebral activity is masked from the volumetric data and the data is scaled to the maximum value in the brain. Each display is designed to assist the reader in easily extracting the key perfusion information necessary to arrive at a consistent and meaningful interpretation. The display has the following features: (1) The standard set of 2-D orthogonal slices (horizontal, coronal, sagittal) are displayed in a unique color scale with 21 discrete, equal width, color steps in a geographic progression which allows for a semi-quantitative evaluation. The color scale includes a threshold setting at 40% of maximal perfusion within the brain (usually cerebellum) to suppress background activity which otherwise would distract from the usable information. This threshold setting is the floor of the first color step. A 4th slice orientation along the temporal lobe axis is provided to visualize the distribution within this lobe in a more natural way. (2) The so-called multi-volume threshold display is a 3-D presentation of the volumetric data in 6 orientations using four different iso-contour thresholds. The lower two thresholds of 55% and 65% of maximal brain perfusion, respectively, help in identifying areas of hypo-perfusion as well as their extent. The upper two thresholds of 85% and 90% of maximal brain perfusion, respectively, help to identify possible areas of hyper-perfusion. (3) A set of 3-D surface projections mapping the maximum cortical activity on a surface rendering of the brain. This display is somewhat analogous to the polar plot in cardiac imaging, providing an overview of brain activity distribution in a single view. These 3-D displays have the advantage of illustrating both subtle widespread cortical abnormalities, as well as illustrating general patterns of both hypoperfusion, but, in particular, increased perfusion, in a manner more easily appreciated compared to tomograms. The latter two displays, while presented in a static form, can also be made available in a dynamic, rotating cine format, to enhance the 3-D impression which are extremely useful in communicating the imaging results to the referring clinicians. See **Figure 1** for illustrative example.

Post hoc Regions of Interest Analysis

A *post hoc* ROI analysis was conducted to provide a secondary confirmation of the expert consensus visual interpretations. A total of 67 ROIs were uniquely developed based on atlas normalized SPECT and MRI datasets. This set of region templates was then applied to each scan after Talairach transformation using the Neurostat software (68) and normalization to the cerebellar maximum. Median and maximum counts for each region were determined. The data were presented in bar graph form to visualize the regional activity on a scale wherein the cerebellar maximum equaled 100% for each patient for each scan. Then, the median count value of a normative sample for each ROI was indicated by a white horizontal line on the bar. Similarly, the maximal count value of a normative sample for each ROI was indicated by a red horizontal line on the bar. This allowed the simultaneous comparison of the counts in each ROI relative to the

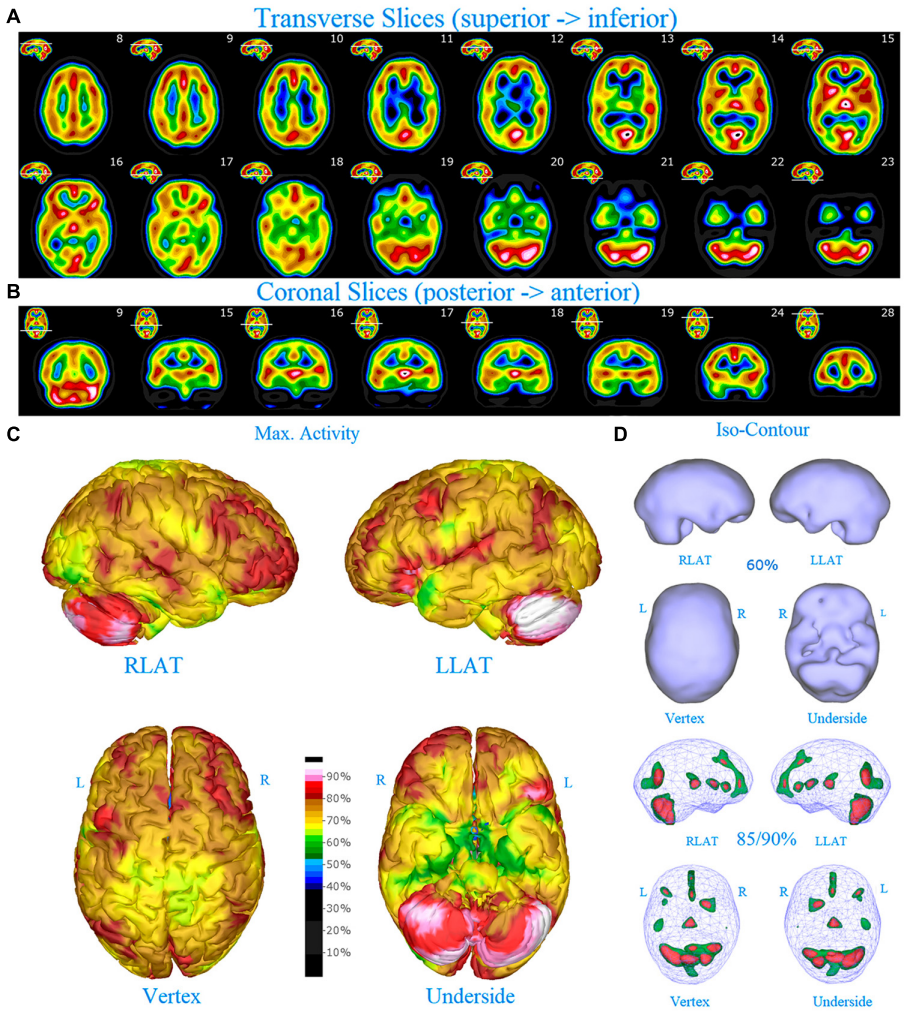

FIGURE 1 | Perfusion SPECT scan of normal control. **(A)** Horizontal tomograms from a ^{99m}Tc-HMPAO perfusion SPECT scan spanning much of the brain from near superior surface to lower cerebellum (see locator images). **(B)** Coronal tomograms spanning from anterior margin of cerebellum to anterior cingulate (see locator images). The color scale is scaled relative to the patient's mean cerebral perfusion. Mean blood flow (72%) is in yellow. Color shifts occur at approximately every 0.5 SD (3%) relative to the patient's mean. Details of the brain can be appreciated, including the thalamus, head of the caudate nuclei, lentiform nuclei, anterior cingulate gyri, and distinct cortical regions. The perfusion of the thalamus (white with black central dot), right caudate (on the left side of the tomogram), visual cortex and cerebellum are highest in this example. **(C)** The modern SPECT scan displayed in 3-dimensional reconstruction. Right lateral (RLAT), left lateral (LLAT), Vertex, and underside views are provided. The color scale is the same as panel **(B)**. **(D)** Isocontour representations of the SPECT data in 3 dimensions. Surface isocontour representations allow visualization of areas of decreased cortical perfusion. Areas in which perfusion falls below 60% of the maximal cerebral blood flow appear as depressions or holes depending on how far below 60% the perfusion falls. Wireframe representations allow visualization of areas of increased perfusion. Areas with perfusion at 85% of the maximal cerebral blood flow appear in green, while areas at 90% of maximal cerebral blood flow appear in red. It is evident that the thalamus, right caudate, cerebellum, and visual cortex are perfused at 90% of maximal cerebral blood flow. This corresponds to what is seen in the tomograms.

patient's own cerebellar maximum counts and to the median and maximum of the normative sample. The intent of this counts-based ROI analysis was to perform a semi-quantitative *post hoc* recheck of the committee's findings which were derived from visual reading of the scans, not as a stand-alone analysis.

An abbreviated history and key scan findings will be presented here for each patient in the family case series, followed by extrapolated results on the SPECT neuroimaging findings in bipolar disorder.

RESULTS

The family consisted of five members. The father (Patient A) was scanned in 2009 at age 47. The mother (Patient B) was scanned in 2012 at age 48. The oldest daughter (Patient C) was scanned in 2009 at age 10 and again at age 15 (2014). The older son (Patient D) was scanned in 2012 at age 10 and again at age 13. The younger son (Patient E) was scanned (in 2012) at age 6 and again at age 9. Each patient's case history and scan analysis will be presented in turn. A SPECT scan from a patient without

psychiatric conditions is shown in **Figure 1** for comparison purposes.

Patient A

Patient A (the father) grew up in rural Ontario with a mother who was housebound and a father with alcoholism. He displayed numerous signs of mania and hypomania as a child. He leaped off a cliff when he was 12 years old, engaged in heavy drinking and glue-sniffing, and arrived drunk at a school function and danced about the gymnasium with a teacher's wife at age 14. He left home upon high school graduation and was estranged from his father. He struggled with depression and suicidal ideation in college.

When he first presented for treatment, Patient A was 38 years old. He had participated in psychotherapy for several years and had started Paroxetine one year prior. His mood had worsened on Paroxetine and it was discontinued. Nevertheless, depression and anxiety escalated, and notably, he developed verbal aggression, which was out of character. The patient had an inconsistent work history, characterized by periods of intense activity alternating with periods of listlessness, procrastination and anxiety. The patient commented, "I groove on adrenaline and anger." Suspecting a bipolar mixed state, the clinician started Moclobemide (reversible MAO-I). The patient experienced a significant reduction in aggression and irritability, as well as reduced alcohol use and risky behavior. After one year, Moclobemide was discontinued. The patient experienced a renewed depression, as well as increased anxiety. He was restarted on Moclobemide. He was stable for two years and then the medication lost efficacy. The patient was switched to Bupropion. Later, Adderall was added due to difficulties with concentration.

After some years of stability on Buproprion and Adderall, Patient A's mood crashed, accompanied by overwhelming panic. He was described by his wife as "a 3-year-old in a 47-year-old body." His symptoms included depression, agitation, severe anxiety, panic attacks, and irritability. A SPECT Scan was obtained (**Figure 2**) and, based on the results of the scan, psychiatric stability was achieved by adding Gabapentin to his regimen. In sessions, for the first time in many years, the couple was able to comfort each other.

At various times, Patient A had brief trials of Oxcarbazepine and Lurasidone, while in a mixed state. Neither was successful. Overall, the patient did best on the regimen of Adderall, Bupropion, and Gabapentin, which were determined based on the SPECT scan results.

Single photon emission computed tomography scan findings for Patient A (**Figure 2**) included: multiple cortical areas of increased perfusion ("hot spots"), increased frontal lobe perfusion (right > left), dramatically increased perfusion of the posterior cingulate gyrus, and increased perfusion of the basal ganglia (left > right). Notably, the perfusion of the thalamus was asymmetrical in its perfusion.

Patient B

Patient B (the mother) was initially seen in psychotherapy following the breakup of her first marriage at age 30. She is described as "a caregiver to all" and is called on by members of her family in any moment of crisis. She is a peacemaker. She has always worked excessively and in the not-for-profit sector, in areas of community development. She is described as being very organized, busy, and a tower of strength.

The Patient B began taking Adderall at age 36, when she identified similar struggles with concentration as described by Patient A. She initially became depressed during her third pregnancy coinciding with a period of financial crisis. She stayed in bed for 2 weeks after the birth. Two years later, she again expressed concerns about her ability to concentrate and Adderall was again started. She continued to work prodigious hours and attended graduate school (on a full scholarship) when the youngest child was 6 years old. During this time, she would be in her office 10–12 hours per day, 7 days per week. Patient B described herself as "Putting a quart into a pint pot" and "I'm too busy to see the whole picture."

Despite her productivity, Patient B struggled with persistent anxiety, periodic outbursts of rageful anger, and low-grade depressive symptoms of low mood and guilt. The diagnostic picture was clouded. A SPECT Scan was ordered in 2012 (**Figure 3**). Based on the results of the SPECT scan, she was diagnosed with bipolar disorder and ADHD. Gabapentin was started and the dose of Adderall was increased. Patient B stabilized.

Unfortunately, the ongoing family psychiatric difficulties added to her stress. Gradually, all three of her children were put onto medication. Her daughter developed Bipolar Mixed State and ran away from home. However, her husband's condition stabilized, and the family financial situation improved.

Because of depressive symptoms, Patient B started on Bupropion in 2014, without any benefit. At that point and based on the SPECT scan findings, Lamotrigine was added. After the dose was titrated to 100 mg per day, Lamotrigine provided relief. However, Patient B stopped both medications when she felt "back to her normal self." She recently restarted Lamotrigine after discussion about ongoing potential benefits. She felt that a medication, in addition to Lisdexamfetamine, was necessary as she struggles with the stress of multiple family members who have physical and psychiatric illnesses.

SPECT scan findings for Patient B included: multiple cortical areas of increased perfusion ("hot spots"), increased perfusion of the posterior cingulate gyrus (right > left), increased perfusion in the cerebellum (right > left), and increased perfusion of the caudate head (left > right). Perfusion of the thalamus was also asymmetrical (right > left).

Patient C

Patient C (the eldest child, a daughter) was stubborn and oppositional from a very young age. Nonetheless, she was able to follow a routine: at age 3 using an alarm clock, getting up, getting dressed, and eating breakfast, if left to do so independently. She was bright, a loner, and a voracious reader in the early years of school.

At age 9, Patient C was initially assessed psychiatrically for daydreaming and socially isolating, yet she was oppositional with adults at school. She noted "I don't like school. I like reading. That is the only thing I like at school." She was able to sit

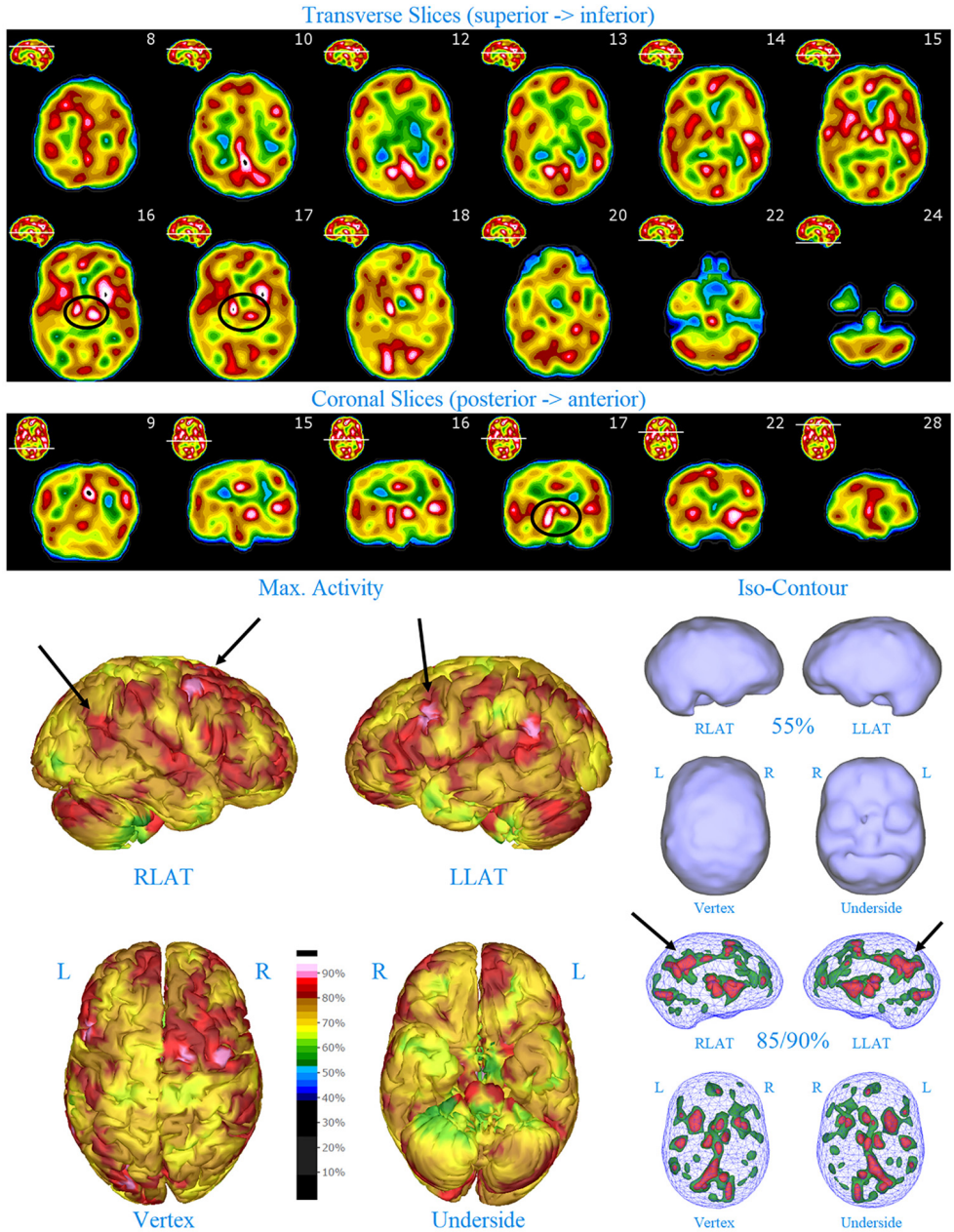

FIGURE 2 | Perfusion SPECT scan of Patient A. Arrangement, color scales, and views are identical to **Figure 1**. Perfusion of the thalamus is increased and asymmetrical (circled in horizontal and coronal tomograms). Perfusion also is increased in the basal ganglia, particularly on the left (above and to the right of the encircled thalamus). Multiple areas of increased perfusion are seen throughout the cerebral cortices in both the 3-dimensional reconstruction and the wireframe isocontour representations (arrows). The frontal lobe on the right show more substantial increases in cerebral perfusion.

for a long time, but squirmed and wriggled. Often, she found school boring and did not like to listen. She noted that she didn't like going to bed or getting up. Her creative play was very complex, and her self-organization a challenge. She met criteria for ADHD and ODD.

When started on Adderall, Patient C blossomed. Her parents found her pleasurable, rather than a drain on precious emotional resources. Unfortunately, early the next year, Patient C threatened to kill a child at after school daycare. The School Board reached out for an assessment. Notably, in total, she had three aggressive outbursts during her first year on stimulants.

A SPECT scan was obtained at age 10 (2009) due to her extreme behaviors (**Figure 4**). Based on the SPECT scan results, a low dose of Gabapentin was added to Patient C's regimen of Adderall to calm her aggression. Overall, Gabapentin proved helpful.

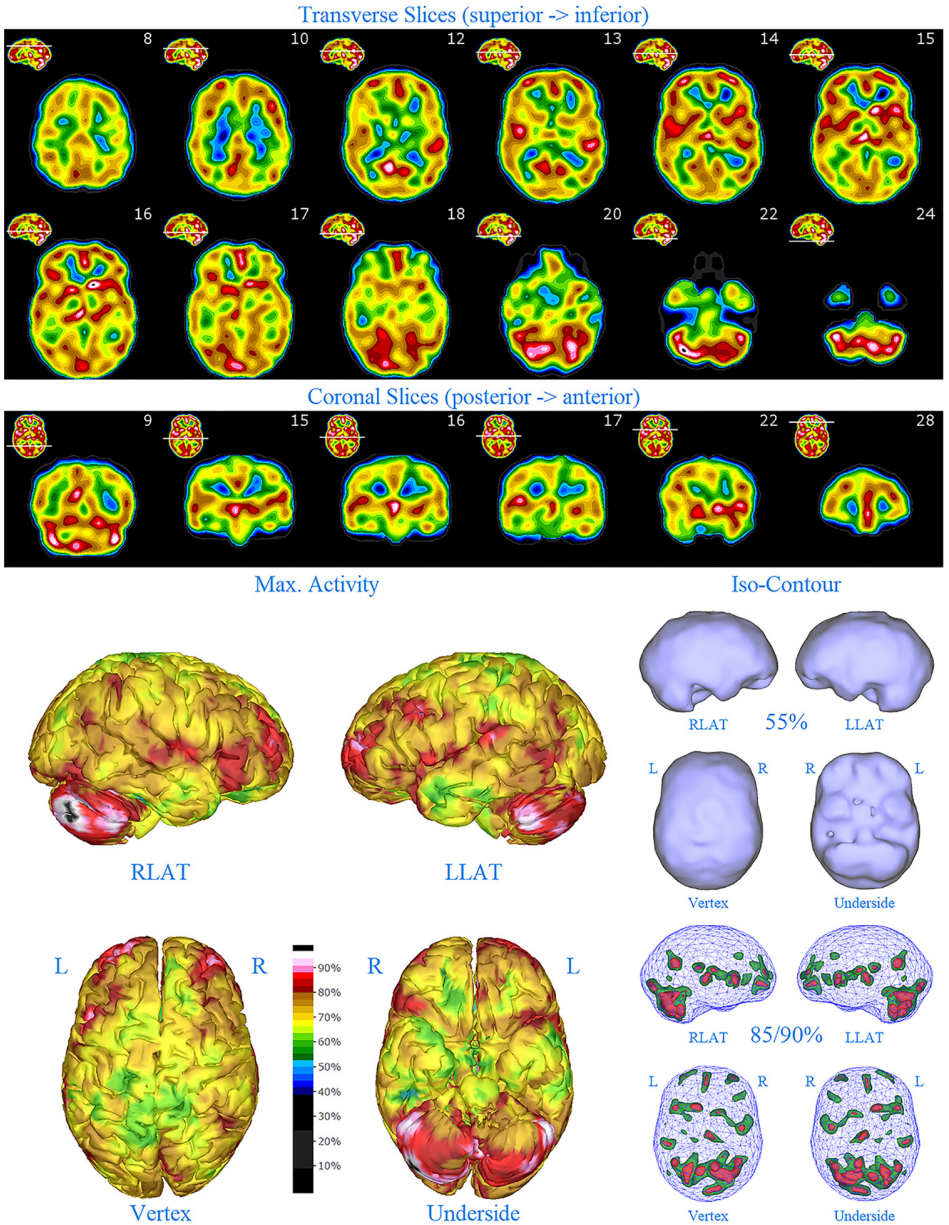

FIGURE 3 | Perfusion SPECT scan of Patient B. Arrangement, color scales, and views are identical to **Figure 1**. Anatomical structures such as the thalamus are positioned similarly to the scan shown in **Figure 2**. Labeling was eliminated to avoid obscuring the scan details. Perfusion of the thalamus is increased and asymmetrical. Perfusion is markedly increased in the left caudate. Multiple cortical areas of increased perfusion are evident, predominately in the frontal cortices.

The following year, Patient C reported her parents to the Children's Aid Society. It was unfounded and the investigator commented on how well the parents coped in a very difficult set of circumstances. A teacher commented at the time, that Patient C "is doing very well. She is a gifted writer and, as her parents point out, can embellish facts in her writing, and in her real life."

Patient C, with her unusual and uncanny awareness of the family, commented "Mum is the hyper one, you're (Father) the depressed one." She commented to her youngest brother on their similarities "Although I explode 'in' you explode 'out.'"

At the end of Grade 8, Patient C represented her age group on the Ontario School Council, a huge honor. She had a very positive summer working in a market stall and planting a large vegetable garden. She matured enormously and presented as a delightful young woman. She noted, "I could see I'm prone to Bipolar."

Parents noted Patient C developed depressive symptoms in Grade 11. It was a challenging time in the family, with her father diagnosed with advanced cancer. Quite suddenly, as her final year of high school began Patient C became increasingly

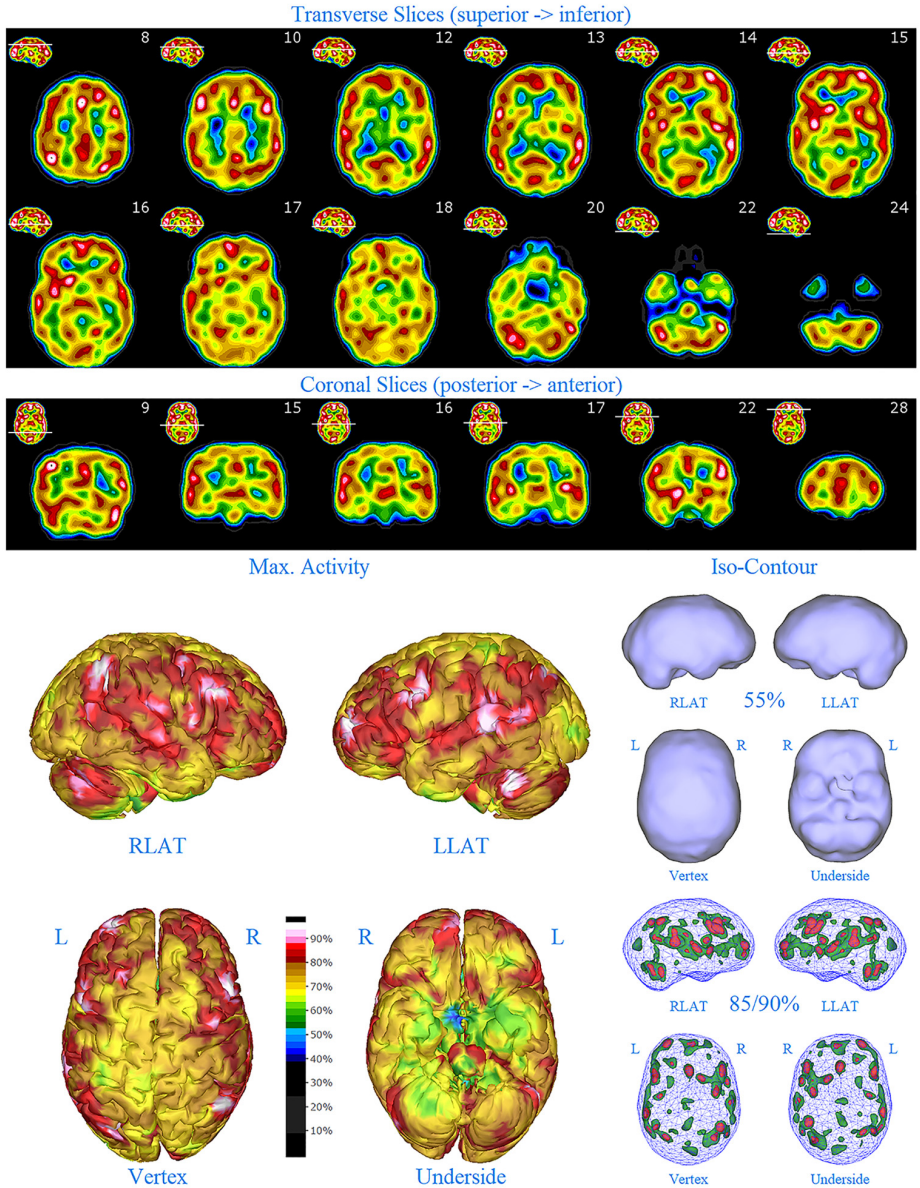

FIGURE 4 | First perfusion SPECT scan of Patient C. Arrangement, color scales, and views are identical to **Figure 1**. Anatomical structures such as the thalamus are positioned similarly to the scan shown in **Figure 2**. Labeling was eliminated to avoid obscuring the scan details. Perfusion of the thalamus is essentially symmetrical. Perfusion is markedly increased in the right caudate. Multiple cortical areas of markedly increased perfusion are evident. For example, the highest signal is found in the right posterior parietal cortex (white area with black central dot in horizontal tomograms).

angry, irritable, anxious, and depressed. She also developed panic attacks. Her parents also were concerned about her increasing use of marijuana. A second SPECT scan (see **Figure 5**) was performed (2014).

Based on the findings in the second SPECT scan, Lurasidone and Clonazepam were begun, and Patient C expressed gratitude that she could be effectively treated. Her response to Lurasidone was initially favorable. Unfortunately, facts are difficult to ascertain as to the events of the subsequent 4 months. Patient C purportedly stopped taking Lurasidone and resumed taking Gabapentin and Lisdexamfetamine. Her mood worsened dramatically on a Christmas trip to see her grandparents. She became agitated and suicidal. In hindsight, marijuana withdrawal was a major factor.

A month later, when forbidden to smoke in bed, Patient C ran away from home. She completed her high school while living in a shelter for teenagers and working at a McDonald's restaurant. She was estranged from her parents but had contact with her brother. He noted that she looked very anxious and could not make eye contact. Nevertheless, she then supported herself and saved for university.

Currently, Patient C is thriving academically at university, generally appreciative of family, but largely independent. She has moved from an interest in English and music to the sciences and hopes to pursue a pharmacy degree.

SPECT scan findings (**Figure 4**) for Patient C at age 10 (2009) included: multiple cortical areas of increased perfusion ("hot spots"), increased perfusion of the anterior cingulate gyrus (right > left), increased perfusion in the cerebellum (right > left), and increased perfusion of the basal ganglia (right > left). Notably, the perfusion of the thalamus was essentially symmetrical. The diffuse pattern of increased perfusion has been referred to as the "ring of fire," indicative of pervasive over-activity in the cerebral cortex.

The second SPECT scan (see **Figure 5**) at age 16 again showed pervasive over-activity. In this scan, the perfusion of the thalamus is asymmetrical. Scattered areas of the parietal cortex showed significant hypoperfusion (appearing green on the 3-D image). This likely was due to extensive use of marijuana at that time.

Patient D

Patient D (the second child, a son) is 2 years younger than his sister. He is, and was, the most easygoing of the three siblings. As a small child he was always very active physically. At home he was more oppositional, and easily slipped into a rage when roughhousing with friends. However, in school he was focused and productive. Reading was delayed.

Patient D met criteria for ADHD and Lisdexamfetamine was begun at age 9, with many benefits. Nonetheless, the parents saw many similarities between Patient D and Patient C in terms of oppositional behavior and sudden aggressive outbursts with peers. They requested a scan.

The first SPECT scan for Patient D (**Figure 6**) was obtained at age 10 (2012). Based on the results of the scan, Gabapentin was added. Patient D responded favorably with reduced agitation, reduced oppositional behavior, fewer tantrums, and improved academic performance.

SPECT scan findings for Patient D included: multiple cortical areas of markedly increased perfusion ("hot spots") in the right frontal and right parietal cortices, increased perfusion of the anterior cingulate gyrus, increased and asymmetrical perfusion of the thalamus, and normal perfusion of the basal ganglia (**Figure 6**). The diffuse pattern of increased perfusion has been referred to as the "ring of fire," indicative of pervasive over-activity in the cerebral cortex.

Patient D had several stable years. However, at age 13 he began to struggle with mood swings and other symptoms. He noted that he dreaded big assignments and did not tell anyone. "I fall off the horse and cannot get back on." At times he had tons of energy and work was easy. At other times, he was lethargic, unmotivated, and overwhelmed. Regardless of whether he was "high" or "low," he was more irritable, angry and non-compliant. A second SPECT scan (2015) was done due to the cyclical mood symptoms (**Figure 7**). The scan results revealed considerably less cortical overactivity (areas of increased perfusion), but the thalamus remained intensely perfused and asymmetrical. A plan was made to add a mood stabilizer, but it did not happen at the time because the family struggled with bigger issues.

In his first year of university during the COVID19 pandemic, Patient D became aware that he was struggling again and reached out for help. He remained on Lisdexamfetamine. He reported feeling he had been depressed most of his life but recalled the occasional high. He felt that working for a welder one day a week helped him through starting university in the COVID19 era. Patient D agreed to starting Lurasidone and demonstrated mood stabilization and improved academic success.

Patient E

Patient E (the third child and younger son) was conceived at a time of challenges and financial instability within the family. By 2 years of age, he was called the "little emperor" due to the violent tantrums he would throw if he did not get his own way. For example, he vomited if his parents were upset with him. This terrorized his older brother, but his sister did not tolerate it. His family described him as an experiential learner. For example, at age 5, he dove from a tree house to see what it felt like to land face-first on the rocks 4 m below. Such impulsive behaviors – despite knowing that such behaviors were strictly forbidden led to many frightening episodes followed by deep remorse characterized by inconsolable crying and vomiting.

Patient E was first assessed psychiatrically at age 6 because of his odd behaviors, including hyperactivity, oppositionality, making frequent clicking sounds, screaming loudly, screeching, aggression with family members, and insomnia. He was diagnosed with ADHD and started on Lisdexamfetamine.

On his first day on Lisdexamfetamine, Patient E reported "lots of love inside." He was less angry. The temper tantrums remained but were shorter and seemingly more intense (e.g., "I will kill you!"). However, he also experienced decreased appetite and bedtime became extended and more difficult with worsening insomnia. He also continued to demonstrate striking impulsivity, as described above. A low dose of Gabapentin was added and seemed to be somewhat helpful, but his insomnia remained.

A SPECT scan was obtained on Patient E at age 6 (2012) to parse out if incipient bipolar disorder might be responsible for the partial response to Lisdexamfetamine and the continued mood symptoms (**Figure 8**). Based on the results of the scan, Risperidone 0.5 mg was started. The Risperidone provided immense relief. Patient E became happier, less anxious and more independent. He remained stable for several years.

SPECT scan findings (**Figure 8**) for Patient E included: multiple cortical areas of increased perfusion ("hot spots") diffusely throughout the cortices, mildly increased perfusion of the anterior cingulate gyrus, increased and highly asymmetrical perfusion of the thalamus, and increased perfusion of the left basal ganglia. The diffuse pattern of increased perfusion has been referred to as the "ring of fire," indicative of pervasive over-activity in the cerebral cortex.

At age 9, Patient E began having multiple violent episodes of screaming, yelling, and physical violence toward his father. He also began endorsing impulsive suicidal thoughts. He endorsed racing thoughts and insomnia. Because of these rapidly escalating symptoms, a second SPECT scan was ordered on Patient E (2015). There was little change in the appearance

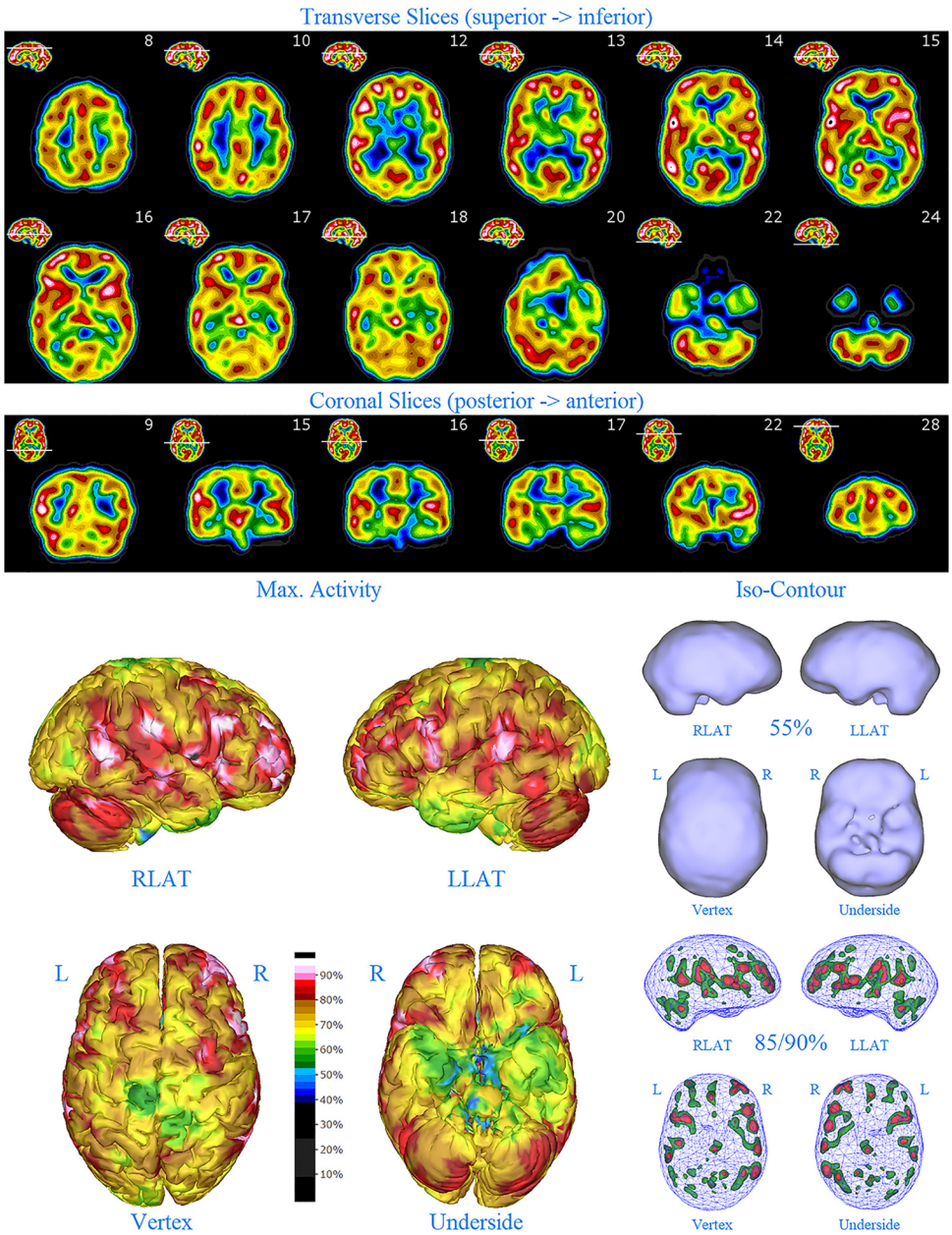

FIGURE 5 | Second perfusion SPECT scan of Patient C. Arrangement, color scales, and views are identical to **Figure 1**. Anatomical structures such as the thalamus are positioned similarly to the scan shown in **Figure 2**. Labeling was eliminated to avoid obscuring the scan details. Perfusion of the thalamus is increased and asymmetrical. Multiple areas of markedly increased perfusion are found throughout the cerebral cortices. Also, areas of cortical hypoperfusion can be seen in the parietal cortices bilaterally (green on the 3-dimensional reconstruction).

of his two SPECT scans. Both showed asymmetric thalamic perfusion (more pronounced in the first scan) and diffuse increased cerebral perfusion, which had become even more pronounced at the time of the second scan. Based on the second SPECT scan findings (**Figure 9**), his dosage of Risperidone was increased, and Gabapentin was added. The patient responded favorably with significant modulation of his disruptive and unpleasant symptoms.

Post-hoc Analysis

The *post hoc* semi-quantitative analysis of the SPECT scans independently supported and validated the findings of the consensus opinion of the expert committee. Asymmetric perfusion was evident in multiple regions of the cerebral cortex, particularly the frontal and temporal lobes. Perfusion of the thalamus was asymmetrical in every case with the right thalamus showing higher counts in 3 out of the five cases. In addition,

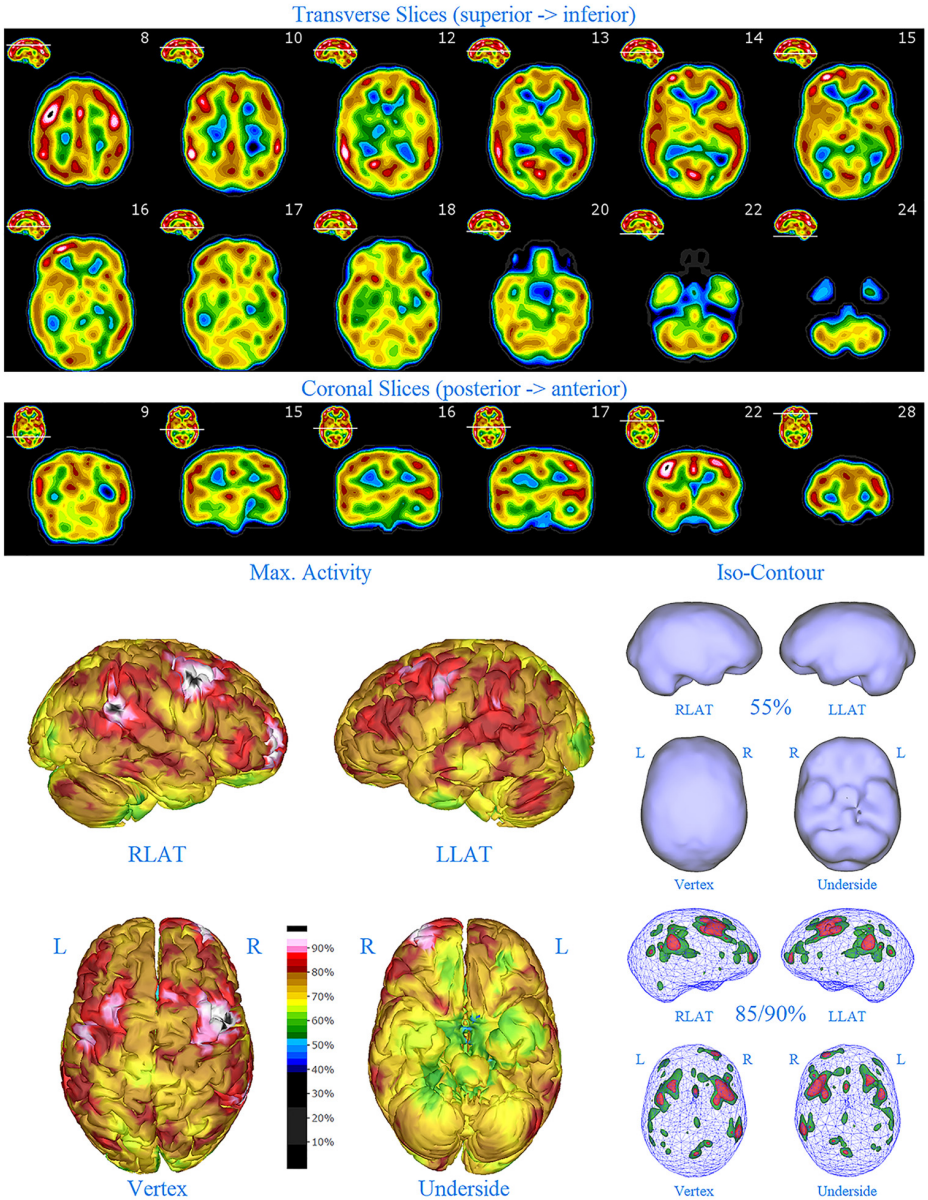

FIGURE 6 | First perfusion SPECT scan of Patient D. Arrangement, color scales, and views are identical to **Figure 1**. Anatomical structures such as the thalamus are positioned similarly to the scan shown in **Figure 2**. Labeling was eliminated to avoid obscuring the scan details. Perfusion of the thalamus is increased and asymmetrical. Multiple cortical areas of markedly increased perfusion are evident in the right frontal and right parietal cortices.

semi-quantitative analysis revealed that the right putamen had elevated perfusion frequently. **Figures 10–14** show a bar graph representation for each patient. For each patient, the scan data was normalized to the cerebellum. Data for each ROI is represented as a bar graph. Most areas have two bars representing the left and right ROI. Some midline ROI are represented by a single bar graph, because the two areas are too close together to separate accurately. The orange bar graph represents maximal counts (perfusion) in the specific ROI and the purple bar represents mean count in the specific ROI relative to the specific patient in the specific scan. The median count of each ROI from the normative sample is represented by a white line. The red line illustrates the cerebellar maximal value for each ROI from the normative sample. Notably, in all cases cortical perfusion in at least one area exceeded the maximal perfusion in the cerebellum, which is usually the most highly perfused portion of the human brain. The findings illustrated in the semi-quantitative analysis match the description of findings in each case. For example, the scan of Patient B, the mildest of the cases clinically, showed frontal cortical areas approaching but not exceeding the cerebellar maximum (**Figure 11**). The thalamus is slightly asymmetrical and approaches the cerebellar

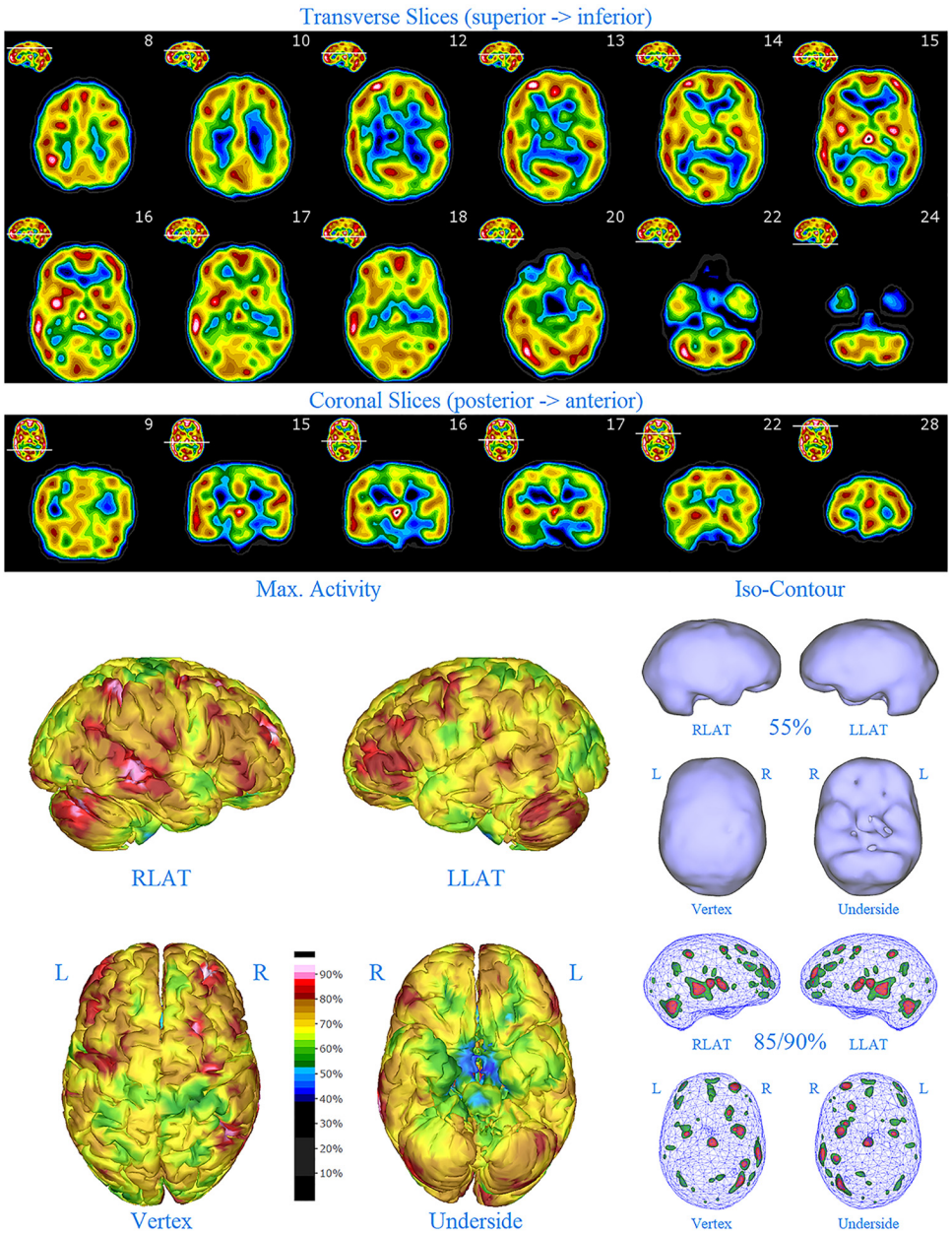

FIGURE 7 | Second perfusion SPECT scan of Patient D. Arrangement, color scales, and views are identical to **Figure 1**. Anatomical structures such as the thalamus are positioned similarly to the scan shown in **Figure 2**. Labeling was eliminated to avoid obscuring the scan details. Perfusion of the thalamus is intensely increased and asymmetrical. Areas of increased perfusion in the cerebral cortices are considerably less prominent.

maximum, but the left caudate is as highly perfused as the cerebellar maximum. Meanwhile, the second scan of Patient E showed multiple cortical areas of increased perfusion ("hot spots") diffusely throughout the cortices, increased and highly asymmetrical perfusion of the thalamus, and increased perfusion of the left basal ganglia. The corresponding bar graph (**Figure 14**) shows multiple areas of asymmetric perfusion in the frontal, temporal and parietal (not shown) cortices, as well as increased perfusion of the right thalamus and increased perfusion of the left caudate and putamen.

DISCUSSION

In this retrospective review of a family cohort collected under naturalistic circumstances in the routine clinical practice of one of the authors, we have found two distinct findings. The first is asymmetric increased perfusion of the thalamus, which replicates earlier neuroimaging findings, regardless of the modality (SPECT, PET, fMRI). The second is patchy and markedly increased perfusion throughout the cerebral cortices, which also was asymmetrical. Each of the family members

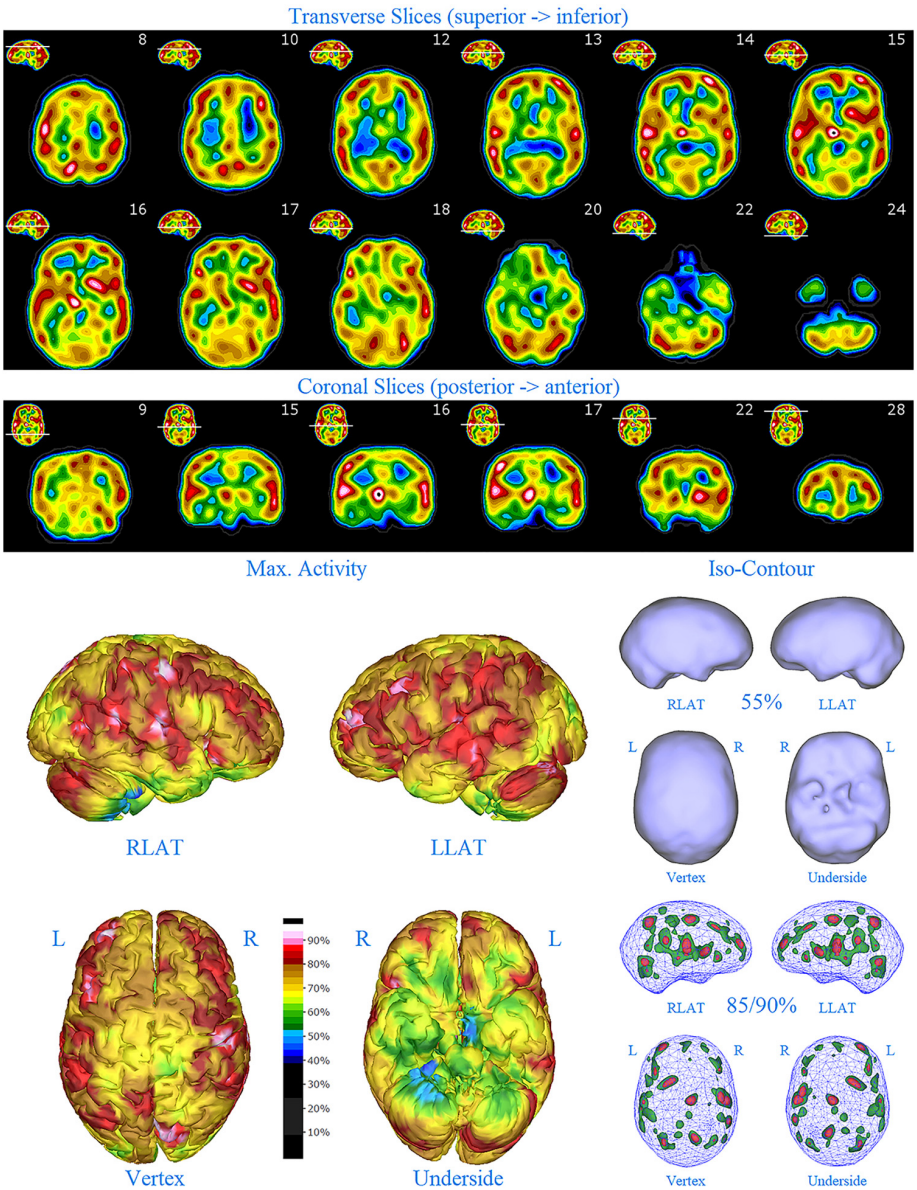

FIGURE 8 | First perfusion SPECT scan of Patient E. Arrangement, color scales, and views are identical to **Figure 1**. Anatomical structures such as the thalamus are positioned similarly to the scan shown in **Figure 2**. Labeling was eliminated to avoid obscuring the scan details. Perfusion of the thalamus is intensely increased and asymmetrical. Multiple cortical areas of increased perfusion are seen throughout the cerebral cortices.

displayed asymmetrical perfusion of the thalamus (Patient D to the least extent, while Patient E provided the most striking example). This finding was often accompanied by asymmetric cortical perfusion as shown in the vertex view of the 3-D reconstruction images (best seen in Patient A, C, and D). All family members demonstrated patchy increased perfusion of the cerebral cortices. Distinct focal areas of intense perfusion were indicated by red areas with white central regions. These can be referred to as "hotspots." The focal areas which were the most highly perfused point in the brain were marked by a black focus within the white central region (see Patient D 3-D reconstruction and tomograms – **Figures 6**, **7**, for example). These ***potential*** diagnostic markers, which the authors and expert panel members have observed clinically in hundreds – if not thousands – of patients are ***potential*** endophenotypic markers for bipolar disorder.

Increased Asymmetric Thalamic Perfusion

The finding of asymmetrical increased perfusion of the thalamus is supported by the observations of Juckel et al. (50), as well as others (47, 69, 70). Similarly, fMRI studies (58, 59, 71) reveal increased and often asymmetrical perfusion of the thalamus in

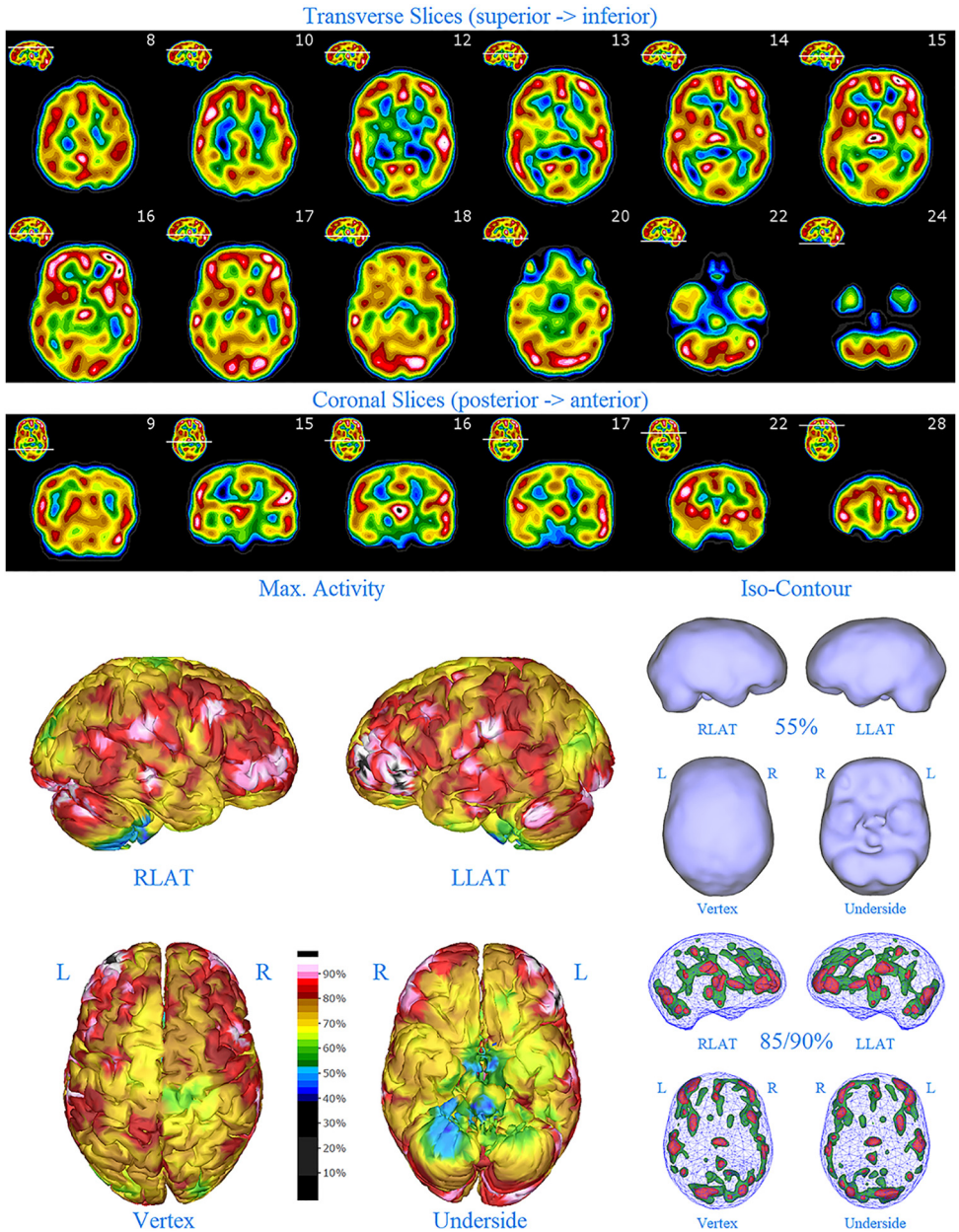

FIGURE 9 | Second perfusion SPECT scan of Patient E. Arrangement, color scales, and views are identical to **Figure 1**. Anatomical structures such as the thalamus are positioned similarly to the scan shown in **Figure 2**. Labeling was eliminated to avoid obscuring the scan details. Perfusion of the thalamus is increased and asymmetrical. Areas of increased perfusion are considerably more prominent compared to the first scan, particularly in the left frontal cortex.

patients with bipolar disorder. Again, our clinical observation across many patients with bipolar disorder support this finding.

Diffuse Increased Cortical Perfusion

Diffuse increased cortical perfusion is evidence of elevated cortical activity. Compared to a normal scan in which the visual cortex is the most active cortical area (see **Figure 1**), the scans in the present series are strikingly different. Areas throughout the cortex, including the frontal, temporal, and parietal cortices are extremely active, often exceeding the maximal activity in the cerebellum (see **Figures 2–9** and the same data presented in semi-quantitative graphic form in **Figures 10–14**). Notably, some areas are so active as to be "hotspots," resembling in many ways the appearance of seizure foci on SPECT scan. This correlation between bipolar disorder and seizure disorders may have a molecular root. The ankyrin 3 gene (*Ank3*) regulates neuronal circuit activity and abnormalities in the function of one of the products of *Ank3*, a voltage-gated sodium channel, leads to excessive firing in circuits which are involved in emotions, memory, and epilepsy (72). *Ank3* is

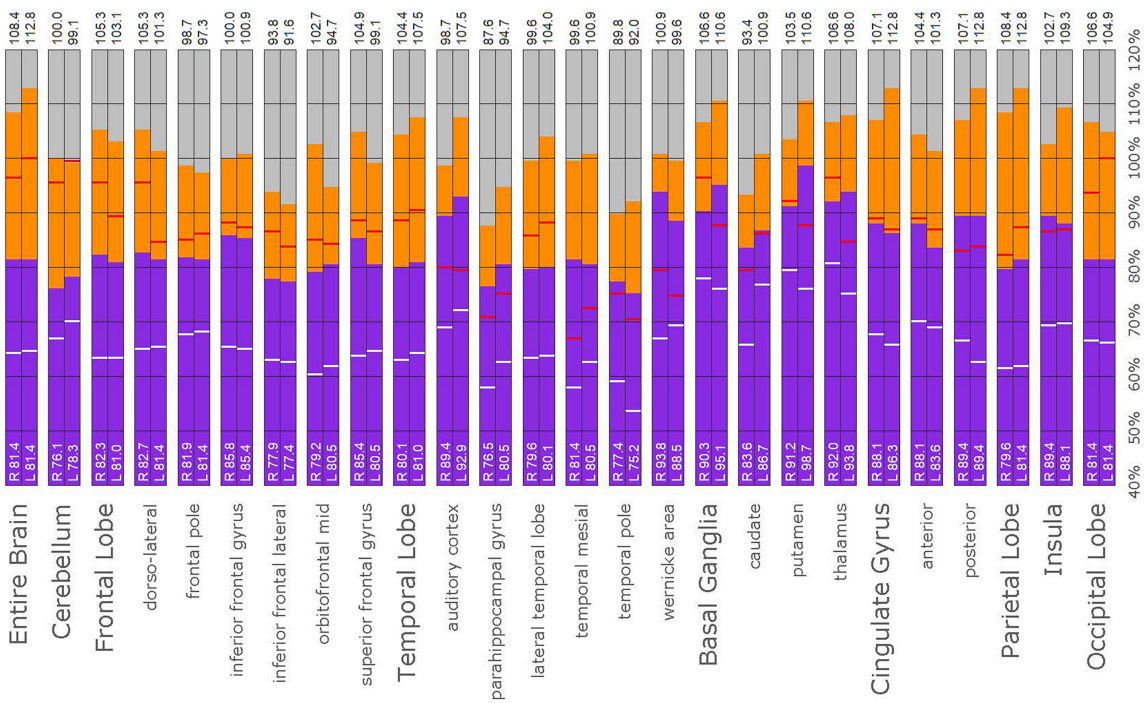

FIGURE 10 | Semi-quantitative region of interest analysis of the SPECT scan of Patient A in comparison to the normative sample. The scan data was normalized to the cerebellar maximal counts (cerebellar maximal for each patient equals 100% on bar graph). The median counts in each ROI is shown in purple and the maximal counts in each ROI is shown in orange. Right and left regions are illustrated as separate bar graphs with the median value printed in white lettering at the base of each bar. All 67 regions could not be illustrated in a single graph, so multiple ROI's from the frontal, temporal, and cingulate cortices are illustrated, while the parietal, occipital, and insular cortices are each illustrated by a single bar. The median counts of the normative sample for that particular ROI are illustrated as a white line on each bar of the graph. The maximum counts of the normative sample for that particular ROI are illustrated as a red line on each bar of the graph. Markedly increased perfusion is evident in the thalamus (exceeding the maximal value in the cerebellum and the comparable maximal value of the normative sample). Markedly increased perfusion is seen in the frontal, temporal, parietal, insular, and cingulate cortices, again exceeding the maximal perfusion of the cerebellum and the comparable maximal value of the normative sample. In all ROI, with the exception of the cerebellum, the patient's maximal counts exceed that of the normative sample (red line). In all ROIs, the patient's median counts exceed that of the normative sample (white line). The asymmetry evident in the thalamus upon inspection of the scan is less obvious with ROI analysis. Asymmetry is notable throughout the cortices.

a leading candidate gene in bipolar disorder. If, indeed, this SPECT perfusion finding is associated with excessive firing in circuits involved in emotions, then medications which block or modify voltage-gated sodium channels (e.g., Carbamazepine, Lamotrigine, Valproic acid) would be expected to be effective for the treatment of bipolar disorder. Similarly, medications which block or modify voltage-gated calcium channels (e.g., Gabapentin, Pregabalin) likely will modulate the symptoms of bipolar disorder.

All members of the family showed diffuse increased cortical perfusion. All members responded favorably to a greater or lesser degree to Gabapentin. In Patient D, the improvement of cortical increased perfusion can be seen by comparing **Figures 6** and **7**. While, he still had troublesome symptoms and showed asymmetric thalamic perfusion, the overactivity of the cerebral cortices was reduced. In contrast, **Figures 8** and **9** illustrate Patient E, who was on a low dose of Gabapentin at the time of both scans; yet, still had diffuse increased cerebral perfusion, along with disruptive behaviors, volcanic temper tantrums, racing thoughts, and insomnia – classic mania/hypomania symptomatology. Notably, after an increase in the dosage of both Gabapentin and Risperidone, his difficulties resolved.

The implication here is not that bipolar disorder is a form of seizure disorder. Rather, it is that the two phenomena share common features, both at the molecular level and at the whole-organ neurophysiological level as seen with SPECT scans and other forms of functional neuroimaging. Areas of increased cortical perfusion or "hotspots" should be taken into consideration when evaluating a SPECT scan for evidence consistent with the diagnosis of bipolar disorder.

Detecting Prodromal/Incipient Bipolar Disorder

The issue of detecting prodromal or incipient bipolar disorder remains a critically unmet need in psychiatry. The clinical presentation of a first depressive episode gives no clue or insight into whether the patient has unipolar depression or a first depressive episode of bipolar disorder. In this retrospective review of a single-family case series, the overactive cerebral cortices appeared to be a consistent warning sign of the potential

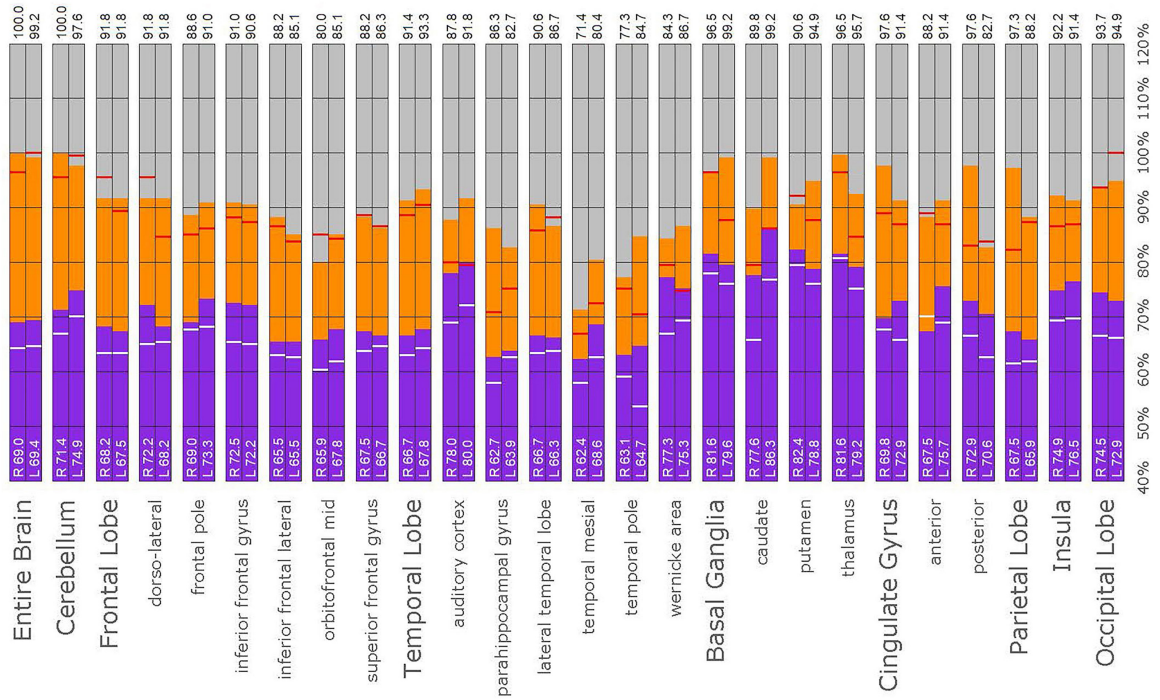

FIGURE 11 | Semi-quantitative region of interest analysis of the SPECT scan of Patient B. Data analysis and presentation is as described in **Figure 10**. Perfusion of the thalamus is increased and asymmetrical, although not as obviously as upon inspection of the scan. Perfusion is markedly increased in the left caudate, approaching the maximal count of the cerebellum. Multiple cortical areas of increased perfusion are evident, predominately in the frontal cortices. In many ROIs, the patient's maximal counts exceed that of the normative sample, though not to the degree seen in the other cases. Portions of the frontal cortex, the lateral temporal lobe, cingulate gyri, the putamen, and the occipital lobe, which show maximal counts less than that of the normative sample, are the exceptions. In all ROIs, the patient's maximal counts exceed that of the normative sample (red line). In all ROI, the patient's median counts exceed that of the normative sample, with the exception of the right anterior cingulate gyrus (white line).

risk for activation or frank mania/hypomania if any of these patients were given a traditional antidepressant. This conclusion is supported by the adverse reaction displayed by Patient A when administered paroxetine. Based on the results of the SPECT scans, the clinician elected to avoid using antidepressants in these five patients.

As exemplified by the first scans of Patients D and E (obtained at age 10 and 6, respectively), the aforementioned neuroimaging "markers" were already quite evident at a young age. Given the reality that the diagnosis of bipolar disorder is often delayed by 5–10 years, as described above, these perfusion SPECT markers could serve to expedite the diagnosis of bipolar disorder. To reiterate, the predictive value of a neuroimaging marker need not be perfect in the situation of bipolar disorder wherein the risks of using medications appropriate for that diagnosis are relatively small. In contrast, the risks of delaying the diagnosis and giving medications which exacerbate bipolar disorder are substantial. For example, Henderson and Hartman (19) showed that the ADHD medication, Atomoxetine, can precipitate mania. The use of stimulants can lead to rapid cycling and more severe course of illness (12, 14–18). Notably, as a young adult Patient C was assessed by a different psychiatrist, who dismissed the diagnosis of bipolar disorder due to the absence of a documented manic episode. Nevertheless, the mood state prior to her second SPECT scan was most likely a mixed state, she responded favorably to Lurasidone, and her scan results demonstrated both neuroimaging markers.

An additional observation can be made in this case series. Patient C demonstrated diffuse areas of hypoperfusion in her second scan, which is often associated with toxic brain injury. Later, it was learned that she was using marijuana heavily. Published clinical research (73, 74) and our extensive clinical experience has shown that the use of marijuana can lead to varying degrees of toxic encephalopathy. Indeed, decreased perfusion in the hippocampus can be closely correlated to reported frequency of marijuana use (74). On a related technical note, the relatively subtle hypoperfusion which signaled these neurotoxic changes were not appreciated on the decades-old processing software originally used to examine the scan of Patient C (**Figure 15**). Advances in SPECT scan camera technology and in post-processing software are yielding marked increases in the information which can be derived from perfusion SPECT scans (75).

While this case series is unique in that it consists of members of a single nuclear family, there are certain limitations. First, it represents a very small sample. Second, the data were interpreted without blinding to the clinical circumstances, as is typical for case series. Third, the patients were treated individually and in

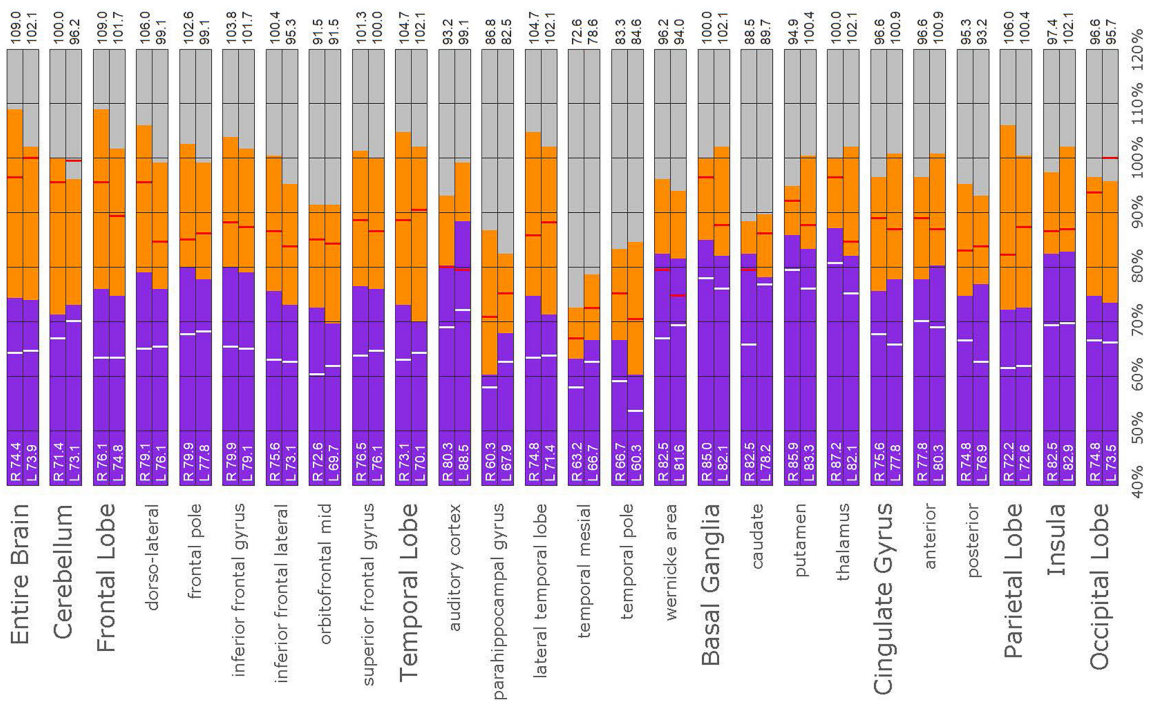

FIGURE 12 | Semi-quantitative region of interest analysis of the SPECT scan of Patient C. Data analysis and presentation is as described in **Figure 10**. Thalamic perfusion is asymmetrical and exceeds that of the cerebellar maximum. Multiple cortical areas show increased perfusion which exceeds the cerebellar maximum and the comparable maximal value of the normative sample. Asymmetric perfusion is seen in most cortical areas. In all ROI, with the exception of the cerebellum and left occipital lobe, the patient's maximal counts exceed that of the normative sample (red line). In all ROIs, the patient's median counts exceed that of the normative sample (white line).

a naturalistic setting. Treatment was not uniform. As such, the present data can not define a biomarker. However, these data suggest certain neuroimaging findings may be reliable, providing initial evidence for a marker with reasonable uniformity in at least this small population. These findings warrant further investigations into perfusion SPECT neuroimaging biomarkers for a bipolar phenotype. These limitations notwithstanding, the use of perfusion SPECT scans has a place in the psychiatric evaluation of patients, as evidenced by the incorporation of psychiatric indications into the Canadian Association of Nuclear Medicine Guidelines for Brain Perfusion Single Photon Emission Computed Tomography (SPECT) published in 2021 and the recent comprehensive review of perfusion SPECT neuroimaging (76).

Incorporating SPECT Scans Into Psychiatric Practice

SPECT Scans as a Tool

Perfusion SPECT scans have been vilified because they do not match up one-to-one with DSM-5 diagnoses (77). It is not surprising that SPECT scans do not yield a pathognomonic imaging result for each DSM condition. The diagnoses in the DSM-5 are replete with overlapping symptoms, comorbidity, and an absence of neurophysiological correlates (48, 78). Moreover, there is often tremendous range in how patients' symptoms present. For example, using the DSM-5 (77) diagnostic criteria for Major Depressive Disorder (79, 80), there are over 20 possible distinct phenotypes of this single diagnosis. After multiple clinical trials failed to treat major depression, one expert stated,

"that major depressive disorder is biologically heterogeneous, such that different treatments differ in the likelihood of achieving remission in different patients" (81).

On the other hand, a common neurophysiological process, such as abnormally functioning voltage-gated channels due to *Ank-3* genetic anomalies, might lead to symptoms consistent with ADHD, ODD, intermittent explosive disorder, or disruptive mood dysregulation disorder. Furthermore, perfusion SPECT neuroimaging can help rule out toxic injury or traumatic brain injury–both of which can also lead to impulsivity, inattention, and mood symptoms (80).

In other words, perfusion SPECT scans are a tool. They help the physician understand the functioning of the brain better. SPECT findings might lead to an alternate differential diagnosis list. For example, an oppositional and defiant child with markedly increased cortical perfusion most likely has a different diagnosis than a similar behaving child who has significantly decreased cortical perfusion. Alternatively, as described by Pavel et al. (75), a patient can present with symptoms suggestive of bipolar mania, but have a diffusely hypoperfused brain suggesting infection, toxicity, or autoimmune disease. Follow-up testing in that particular case described by Pavel et al.

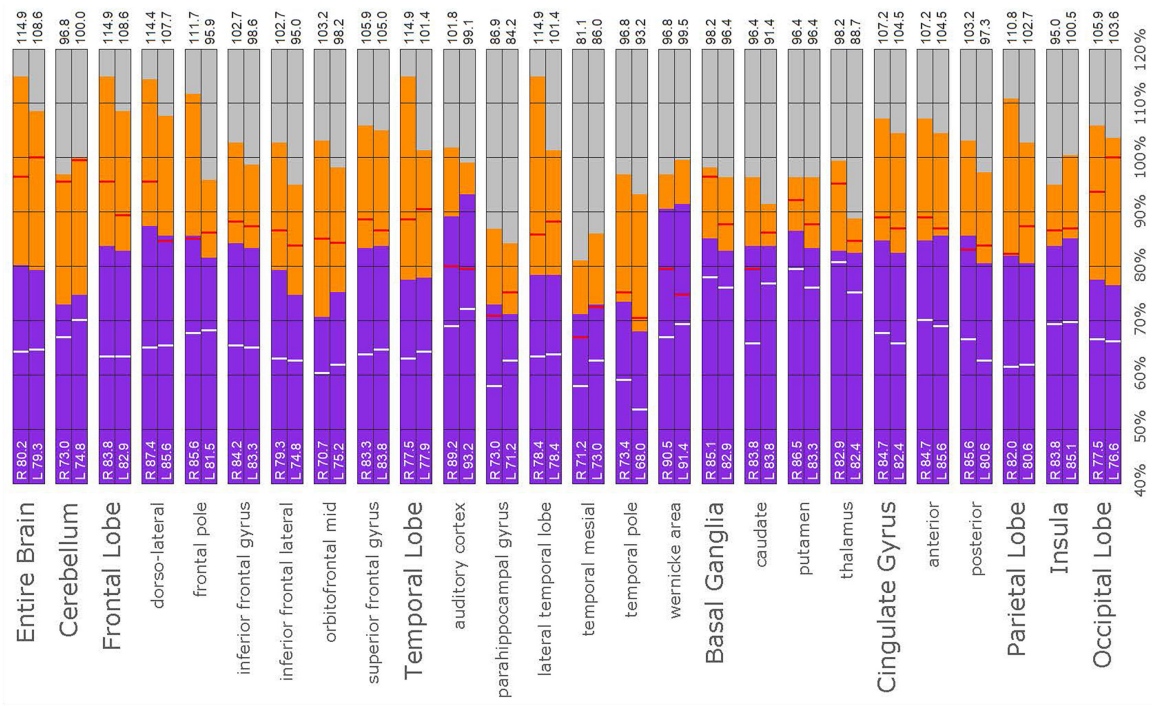

FIGURE 13 | Semi-quantitative region of interest analysis of the SPECT scan of Patient D. Data analysis and presentation is as described in **Figure 10**. Thalamic perfusion exceeds the maximum in the cerebellum and is highly asymmetrical. The median and maximal counts in the thalamus exceed those of the normative sample. Multiple cortical areas of markedly increased perfusion are noted with marked asymmetry. In all ROI, with the exception of the cerebellum, the patient's maximal counts exceed that of the normative sample (red line). In all ROIs, the patient's median counts exceed that of the normative sample (white line).

(75) demonstrated infection, rather than bipolar disorder. The patient was correctly treated with antibiotics and a lifetime of psychotropic medications was averted. SPECT scans can aid clinicians to unravel complex cases.

Patient Confidence and Compliance

One barrier to the diagnosis of bipolar disorder is stigma. Patients are loath to accept the diagnosis and psychiatrists are reluctant to make the diagnosis (6). A very large threshold of evidence must be surmounted before the diagnosis can be made. From the perspective of psychiatrists among the authors, this diagnostic hesitancy is almost unforgivable in the modern era. It seems to be a holdover from the days when we only had lithium and electroconvulsive shock therapy to treat bipolar disorder. However, modern pharmaceuticals, such as lurasidone, cariprazine, lamotrigine, and others carry far fewer risks and much more manageable side effects. Moreover, most of them have antidepressant qualities which, in some cases, are superior to the serotonin reuptake inhibiting antidepressants. Nevertheless, the hesitancy exists.

For patients, perfusion SPECT brain scans bring a certain degree of confidence in their diagnosis. This was clearly evident in the family reported herein. The first member of the family to undergo brain SPECT scanning was the daughter (Patient C) due to her aggressive behavior. After hearing the description of the benefits and risks of a SPECT scan, the father (Patient A) requested to undergo a scan, as well. He expressed the desire to understand how his brain was working. Similarly, when both sons were scanned, the mother (Patient B) requested that she also be scanned. All family members have independently expressed that the scans helped them understand why they had the symptoms they had and how the selected medications could be beneficial. Both parents were very concerned that medications were used sparingly and as effectively as possible. They found the SPECT scans guided this process well.

The SPECT scans gave the family confidence that their treatments would be helpful. The scans also strengthened the compliance of each patient. For example, the younger son (Patient E) has been extremely compliant with a mood stabilizer from a young age. He notes that his medication greatly helps his sleep and his anxiety. Similarly, the older son (Patient D), who was actually inadequately treated during his high school years, reached out to the psychiatrist during his university years and self-identified symptoms of anxiety and hypomania. He requested to start taking a mood stabilizer.

Lastly, the presence of bipolar disorder, in and of itself, has been shown to increase the risk of suicide, up to 14-fold (28), underscoring the importance of early and correct diagnosis. Children with bipolar disorder are at higher risk for suicide than children with unipolar depression (82, 83). Suicide attempts are considerably more likely to be lethal among those with bipolar disorder (84) and occur at a younger age (83, 84). Recently, Orsolini et al. (85) thoroughly reviewed suicide and depressive disorders, noting the interwoven

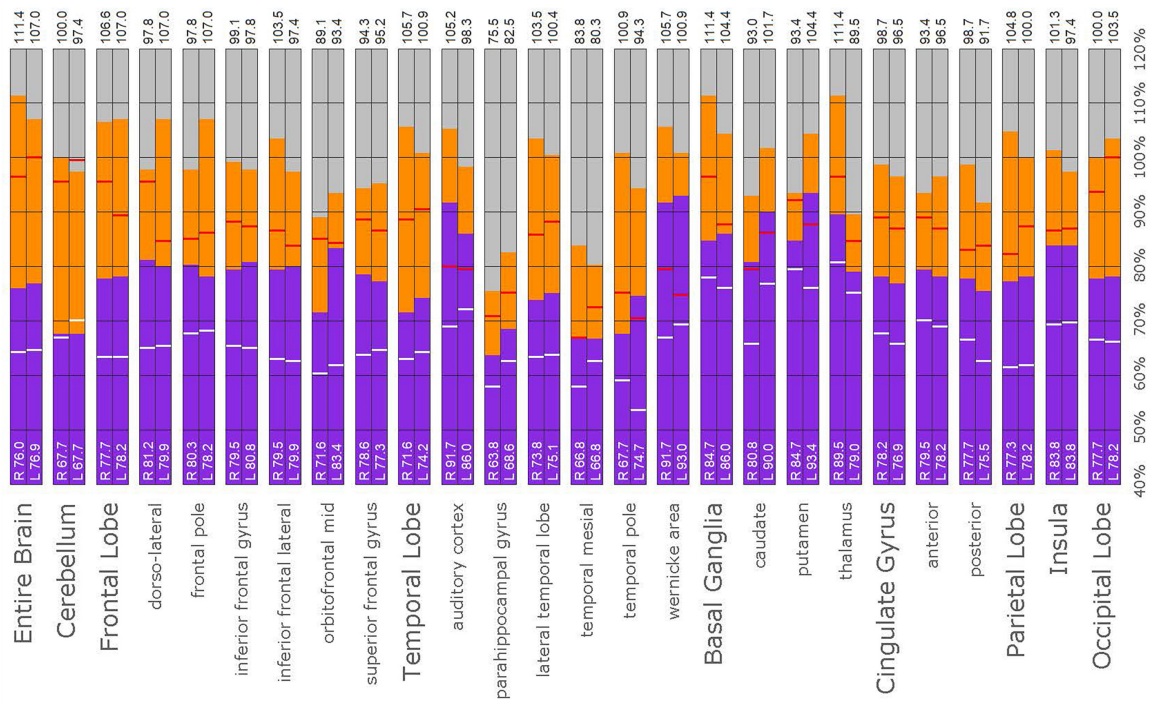

FIGURE 14 | Semi-quantitative region of interest analysis of the SPECT scan of Patient E. Data analysis and presentation is as described in **Figure 10**. Thalamic perfusion exceeds the cerebellar maximum with marked asymmetry. Multiple cortical areas show asymmetrical and highly elevated perfusion exceeding the maximum in the cerebellum. Perfusion in the caudates and putamina is also elevated. In all ROI, with the exception of the cerebellum, the patient's maximal counts exceed that of the normative sample (red line). In all ROIs, with the exception of the cerebellum, the patient's median counts exceed that of the normative sample (white line).

roles of neurobiological, neuroimmunological, and psychosocial factors. Recently, the COVID-19 pandemic has increased the factors that can contribute to suicidal ideation (86), as exemplified by Patient D. The multi-faceted etiological factors described elegantly by Orsolini et al. (85) underscore the value of a single-family study, such as this, wherein some of the variables can be controlled. Earlier diagnosis, patient belief and confidence in the diagnosis, increased insight, and enhanced therapeutic alliance, as exemplified in this case series, improve medication adherence (29) and reduce suicide risk (28, 84, 85).

Minding the "Hotspots"

Another important aspect of incorporating SPECT scans into psychiatric practice is that both areas of *underactivity* (as seen in depression, brain injury, stroke, ADHD, etc.) and areas of *overactivity* (as seen in bipolar disorder, obsessive-compulsive disorder, post-traumatic stress disorder, etc.) are important. The traditional training in Nuclear Medicine is to pay attention to the areas of decreased activity with decreased tracer uptake (hypoperfusion). This allows the nuclear medicine physician to identify brain injury, dementia, and strokes–the most common indications for which SPECT scans are ordered. In the psychiatric realm, clinicians must not only be mindful of these possible diagnoses, but also of the diagnoses that can lead to increased activity with increased tracer uptake (increased perfusion), such as illustrated in the present case series. Collaboration between the psychiatrist and the nuclear medicine physician become essential, along with displaying the scan data in such a manner, as illustrated herein, that "hotspots" can be identified. Notably, a color scale rather than a gray scale is needed to highlight areas of increased perfusion, as well as areas of diffuse hypoperfusion (in contrast to focal areas of hypoperfusion) which are much harder to appreciate in gray scale (75, 76). More importantly, a 3-D presentation of the data allows the focal areas of increased perfusion to be more prominent and more easily localized compared to just reading the scan in tomograms. In this case series, the "hotspots" in Patient B (**Figure 3**) and Patient C (**Figure 4**) were much harder to appreciate in tomograms.

These findings, along with recent publications (49, 76), point the way to future collaborations between nuclear medicine physicians and psychiatrists. Until recently, very few nuclear medicine physicians had experience with neuropsychiatric diagnoses, because nuclear medicine physicians receive few referrals for neuropsychiatric disorders and so have little clinical experience with patterns of increased perfusion. This situation is aggravated by the absence of referrals for neuropsychiatric evaluations, compounded recently by the American Psychiatric Association dismissing neuroimaging as a valuable adjunct in the evaluation of psychiatric patients (48, 78, 80, 87). Hopefully, enlightened clinicians in both fields will join together to deepen their clinical experience to advance and

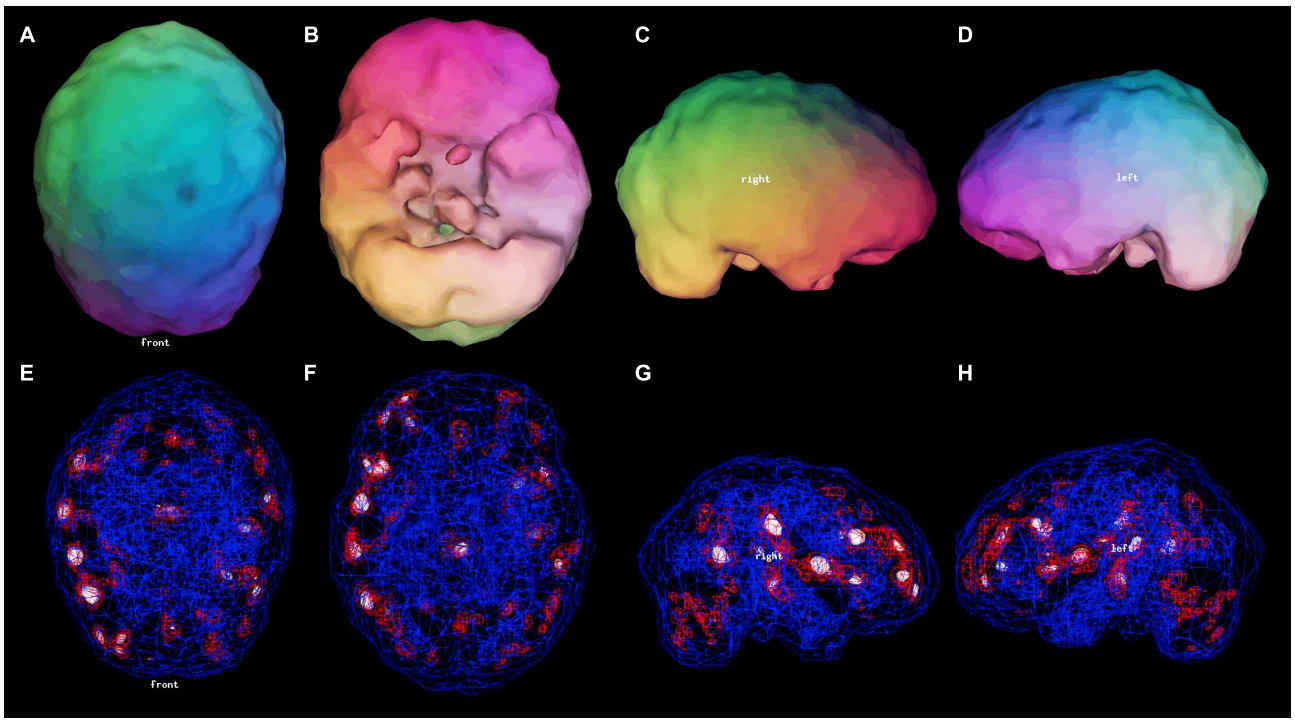

FIGURE 15 | The second SPECT scan of Patient C shown as it was originally viewed after processing with the Picker Odyssey software. **(A–D)** 3-D representation of the scan data is shown. The surface is set at 60% of brain maximum. Areas which fall below 55% are represented as indentations or holes depending on how far below 55% the activity falls. **(A)** Vertex view, **(B)** Underside view, **(C)** Right Lateral, **(D)** Left Lateral. **(E–H)** A wireframe brain representation is shown, wherein the areas of brain with activity at 85% of maximum or greater are shown in red and areas of 92% or greater are shown in white. **(E)** Vertex view, **(F)** Underside view, **(G)** Right Lateral, **(H)** Left Lateral. The details of the SPECT scan are much harder to appreciate without the tomograms. The extent of the diffuse cortical increased perfusion is much more difficult to appreciate with this post-processing software. The extent of the co-existing areas of hypoperfusion in the parietal cortices are not evident with this post-processing software.

expand our understanding of the neuroimaging correlates in neuropsychiatry. As psychiatric and nuclear medicine practitioners, the authors and the International Society of Applied Neuroimaging have developed working models of how neuroimaging can contribute to the evaluation of, and more rapid diagnosis and successful treatment of, neuropsychiatric patients.

CONCLUSION

We have presented a retrospective review of a family cohort including every member of a single family collected under naturalistic circumstances that illustrates clinical symptom development and parallel brain perfusion findings consistent with bipolar disorder. The advantage of this single-family study is that many socioeconomic, developmental, and social variables were controlled. As a result, and consistent with our extensive experience in interpreting SPECT scans, these perfusion findings have substantive correlation to bipolar disorder. These correlations *suggest potential* perfusion SPECT biomarkers for bipolar disorder. The potential biomarkers of: (1) asymmetric and increased perfusion of the thalamus and (2) diffusely increased cortical perfusion (that may be asymmetrical) proposed herein warrant further attention. The increased cortical perfusion or "hotspots" facilitates the differentiation of bipolar depression from unipolar depression, which tends to show symmetrical increased perfusion in the thalamus and basal ganglia, but hypoperfusion throughout the frontal and temporal cortices. Recognizing that bipolar disorder is increasingly seen as a spectrum of symptoms, rather than the simplistic bipolar I and II dichotomy, symptoms such as mania, hypomania, smoldering mixed mood episodes, impulsivity, irritability, and anxiety can all exist together or separately at various times in the life of a patient with bipolar disorder. Hence, a symptom-based diagnostic strategy would benefit greatly from neuroimaging correlates or biomarkers. These data encourage further study of larger populations with comparison to normative databases and/or control groups to test the robustness of these potential biomarkers for bipolar disorder.

More general and widespread awareness of the information provided by SPECT scans would likely improve: (1) the latency to diagnosis, (2) treatment, and (3) lifetime outcome of patients suffering from bipolar disorder. Patient confidence in their diagnoses would likely improve, leading to increased treatment compliance. Improved display parameters, as presented herein, facilitate the interpretation of SPECT scan data, allowing for

wider acceptance and adoption of SPECT scans as a tool to aid in the diagnostic process.

DATA AVAILABILITY STATEMENT

The raw data supporting the conclusions of this article will be made available by the authors, without undue reservation.

ETHICS STATEMENT

Ethical review and approval was not required for the study on human participants in accordance with the local legislation and institutional requirements. Written informed consent to participate in this study was provided by the participants' legal guardian/next of kin. Written informed consent was obtained from the individual(s), and minor(s)' legal guardian/next of kin, for the publication of any potentially identifiable images or data included in this article.

AUTHOR CONTRIBUTIONS

MM was responsible for care of patients, analysis, and writing of manuscript. TH involved in analysis, figure preparation, and writing of manuscript. DP involved in analysis of data and preparation of preliminary drafts of manuscript. PC involved in analysis of data and editing of manuscript. All authors contributed to the article and approved the submitted version.

ACKNOWLEDGMENTS

We would like to acknowledge the following individuals, as well as the entire International Society of Applied Neuroimaging, for their contributions to the discussions of these cases: Muriel J. van Lierop, John Michael Uszler, John F. Rossiter-Thornton, Yin-Hui Siow, and Joe Cardaci. We acknowledge Simon DeBruin of Good Lion Imaging for the processing of scan images. We also acknowledge James McLean and Jenny Faherty for technical assistance and copy-editing. We acknowledge Alaina M. Henderson for assistance with the preparation of the figures.

REFERENCES

1. Dattani S, Ritchie H, Roser M. *Mental Health. On Our World in Data Website*. (2018). Available online at: https://ourworldindata.org/mental-health (accessed August 2, 2021).
2. Government of Canada. *What Should I Know About Bipolar Disorder (Manic-Depression)?* Public Health Agency of Canada (2009). Available online at: https://www.canada.ca/en/public-health/services/chronic-diseases/mental-illness/what-should-know-about-bipolar-disorder-manic-depression.html (accessed August 2, 2021).
3. Hirschfeld RM, Lewis L, Vornik LA. Perceptions and impact of bipolar disorder: how far have we really come? Results of the national depressive and manic-depressive association 2000 survey of individuals with bipolar disorder. *J Clin Psychiatry.* (2003) 64:161–74.
4. Berk M, Dodd S, Callaly P, Berk L, Fitzgerald P, de Castella AR, et al. History of illness prior to a diagnosis of bipolar disorder or schizoaffective disorder. *J Affect Disord.* (2007) 103:181–6. doi: 10.1016/j.jad.2007.01.027
5. Marchand WR, Wirth L, Simon C. Delayed diagnosis of pediatric bipolar disorder in a community mental health setting. *J Psychiatr Pract.* (2006) 12:128–33. doi: 10.1097/00131746-200603000-00011
6. Lublóy Á, Keresztúri JL, Németh A, Mihalicza P. Exploring factors of diagnostic delay for patients with bipolar disorder: a population-based cohort study. *BMC Psychiatry.* (2020) 20:75. doi: 10.1186/s12888-020-2483-y
7. Hirschfeld RM. Bipolar spectrum disorder: improving its recognition and diagnosis. *J Clin Psychiatry.* (2001) 62(Suppl. 14):5–9.
8. Medici CR, Videbech P, Gustafsson LN, Munk-Jørgensen P. Mortality and secular trend in the incidence of bipolar disorder. *J Affect Disord.* (2015) 183:39–44. doi: 10.1016/j.jad.2015.04.032
9. Goldberg JF, Ernst CL. Features associated with the delayed initiation of mood stabilizers at illness onset in bipolar disorder. *J Clin Psychiatry.* (2002) 63:985–91. doi: 10.4088/jcp.v63n1105
10. Goldberg JF. When do antidepressants worsen the course of bipolar disorder? *J Psychiatr Pract.* (2003) 9:181–94. doi: 10.1097/00131746-200305000-00002
11. Post RM, Leverich GS, Kupka RW, Keck PE Jr, McElroy SL, Altshuler LL, et al. Early-onset bipolar disorder and treatment delay are risk factors for poor outcome in adulthood. *J Clin Psychiatry.* (2010) 71:864–72. doi: 10.4088/JCP.08m04994yel
12. Cicero D, El-Mallakh RS, Holman J, Robertson J. Antidepressant exposure in bipolar children. *Psychiatry.* (2003) 66:317–22. doi: 10.1521/psyc.66.4.317.25437
13. Simon GE, Hunkeler E, Fireman B, Lee JY, Savarino J. Risk of suicide attempt and suicide death in patients treated for bipolar disorder. *Bipolar Disord.* (2007) 9:526–30. doi: 10.1111/j.1399-5618.2007.00408.x
14. Koehler-Troy C, Strober M, Malenbaum R. Methylphenidate-induced mania in a prepubertal child. *J Clin Psychiatry.* (1986) 47:566–7.
15. DelBello MP, Soutullo CA, Hendricks W, Niemeier RT, McElroy SL, Strakowski SM. Prior stimulant treatment in adolescents with bipolar disorder: association with age at onset. *Bipolar Disord.* (2001) 3:53–7. doi: 10.1034/j.1399-5618.2001.030201.x
16. Faedda GL, Baldessarini RJ, Glovinsky IP, Austin NB. Treatment-emergent mania in pediatric bipolar disorder: a retrospective case review. *J Affect Disord.* (2004) 82:149–58. doi: 10.1016/j.jad.2003.12.011
17. Tillman R, Geller B. Controlled study of switching from attention-deficit/hyperactivity disorder to a prepubertal and early adolescent bipolar I disorder phenotype during 6-year prospective follow-up: rate, risk, and predictors. *Dev Psychopathol.* (2006) 18:1037–53. doi: 10.1017/S0954579406060512
18. Jerrell JM, McIntyre RS, Park YM. Correlates of incident bipolar disorder in children and adolescents diagnosed with attention-deficit/hyperactivity disorder. *J Clin Psychiatry.* (2014) 75:e1278–83. doi: 10.4088/JCP.14m09046
19. Henderson TA, Hartman K. Aggression, mania, and hypomania induction associated with atomoxetine. *Pediatrics.* (2004) 114:895–6. doi: 10.1542/peds.2004-1140
20. Henderson TA. Mania induction associated with atomoxetine. *J Clin Psychopharmacol.* (2004) 24:567–8. doi: 10.1097/01.jcp.0000139760.11458.aa
21. WHO. *The Global Burden of Disease: 2004 Update*. Geneva: WHO Press (2008).
22. Cotton SM, Berk M, Jackson H, Murray G, Filia K, Hasty M, et al. Improving functional outcomes in early-stage bipolar disorder: the protocol for the research into cognitive and behavioural versatility trial. *Early Interv Psychiatry.* (2019) 13:1470–9. doi: 10.1111/eip.12797
23. Dilsaver SC. An estimate of the minimum economic burden of bipolar I and II disorders in the United States: 2009. *J Affect Disord.* (2011) 129:79–83. doi: 10.1016/j.jad.2010.08.030
24. Bessonova L, Ogden K, Doane MJ, O'Sullivan AK, Tohen M. The economic burden of bipolar disorder in the United States: a systematic literature review. *Clinicoecon Outcomes Res.* (2020) 12:481–97. doi: 10.2147/CEOR.S259338
25. Cloutier M, Greene M, Guerin A, Touya M, Wu E. The economic burden of bipolar I disorder in the United States in 2015. *J Affect Disord.* (2018) 226:45–51. doi: 10.1016/j.jad.2017.09.011

26. McMorris BJ, Downs KE, Panish JM, Dirani R. Workplace productivity, employment issues, and resource utilization in patients with bipolar I disorder. *J Med Econ.* (2010) 13:23–32. doi: 10.3111/13696990903475833
27. Bagalman E, Muser E, Choi JC, Durden E, Macfadden W, Haskins JT, et al. Health care resource utilization and costs in a commercially insured population of patients with bipolar disorder type I and frequent psychiatric interventions. *Clin Ther.* (2011) 33:1381–90.e4. doi: 10.1016/j.clinthera.2011.09.005
28. Hayes JF, Miles J, Walters K, King M, Osborn DP. A systematic review and meta-analysis of premature mortality in bipolar affective disorder. *Acta Psychiatr Scand.* (2015) 131:417–425. doi: 10.1111/acps.12408
29. Pompili M, Venturini P, Palermo M, Stefani H, Seretti ME, Lamis DA, et al. Mood disorders medications: predictors of nonadherence – review of the current literature. *Expert Rev Neurother.* (2013) 13:809–25. doi: 10.1586/14737175.2013.811976
30. Serafini G, Pardini M, Monacelli F, Orso B, Girtler N, Brugnolo A, et al. Neuroprogression as an illness trajectory in bipolar disorder: a selective review of the current literature. *Brain Sci.* (2021) 11:276. doi: 10.3390/brainsci11020276
31. Tomás J, Pittau F, Hammers A, Bouvard S, Picard F, Vargas MI, et al. The predictive value of hypometabolism in focal epilepsy: a prospective study in surgical candidates. *Eur J Nucl Med Mol Imaging.* (2019) 46:1806–16. doi: 10.1007/s00259-019-04356-x
32. Widjaja E, Shammas A, Vali R, Otsubo H, Ochi A, Snead OC, et al. FDG-PET and magnetoencephalography in presurgical workup of children with localization-related nonlesional epilepsy. *Epilepsia.* (2013) 54:691–9. doi: 10.1111/epi.12114
33. Silfverskiöld P, Risberg J. Regional cerebral blood flow in depression and mania. *Arch Gen Psychiatry.* (1989) 46:253–9. doi: 10.1001/archpsyc.1989.01810030059008
34. Delvenne V, Delecluse F, Hubain PP, Schoutens A, De Maertelaer V, Mendlewicz J. Regional cerebral blood flow in patients with affective disorders. *Br J Psychiatry.* (1990) 157:359–65. doi: 10.1192/bjp.157.3.359
35. Rubin E, Sackeim HA, Prohovnik I, Moeller JR, Schnur DB, Mukherjee S. Regional cerebral blood flow in mood disorders: IV. Comparison of mania and depression. *Psychiatry Res.* (1995) 61:1–10. doi: 10.1016/0925-4927(95)02594-n
36. Migliorelli R, Starkstein SE, Tesón A, de Quirós G, Vázquez S, Leiguarda R, et al. SPECT findings in patients with primary mania. *J Neuropsychiatry Clin Neurosci.* (1993) 5:379–83. doi: 10.1176/jnp.5.4.379
37. Kawakatsu S, Komatani A. [Xe-133 inhalation single photon emission computerized tomography in manic-depressive illness]. *Nihon Rinsho.* (1994) 52:1180–4.
38. Fischler B, D'Haenen H, Cluydts R, Michiels V, Demets K, Bossuyt A, et al. Comparison of 99m Tc HMPAO SPECT scan between chronic fatigue syndrome, major depression and healthy controls: an exploratory study of clinical correlates of regional cerebral blood flow. *Neuropsychobiology.* (1996) 34:175–83. doi: 10.1159/000119307
39. Ito H, Kawashima R, Awata S, Ono S, Sato K, Goto R, et al. Hypoperfusion in the limbic system and prefrontal cortex in depression: SPECT with anatomic standardization technique. *J Nucl Med.* (1996) 37:410–4.
40. Milo TJ, Kaufman GE, Barnes WE, Konopka LM, Crayton JW, Ringelstein JG, et al. Changes in regional cerebral blood flow after electroconvulsive therapy for depression. *J ECT.* (2001) 17:15–21. doi: 10.1097/00124509-200103000-00004
41. Vangu MD, Esser JD, Boyd IH, Berk M. Effects of electroconvulsive therapy on regional cerebral blood flow measured by 99mtechnetium HMPAO SPECT. *Prog Neuropsychopharmacol Biol Psychiatry.* (2003) 27:15–9. doi: 10.1016/s0278-5846(02)00309-3
42. Benabarre A, Vieta E, Martínez-Arán A, Garcia-Garcia M, Martín F, Lomeña F, et al. Neuropsychological disturbances and cerebral blood flow in bipolar disorder. *Aust N Z J Psychiatry.* (2005) 39:227–34. doi: 10.1080/j.1440-1614.2004.01558.x
43. Kohn Y, Freedman N, Lester H, Krausz Y, Chisin R, Lerer B, et al. 99mTc-HMPAO SPECT study of cerebral perfusion after treatment with medication and electroconvulsive therapy in major depression. *J Nucl Med.* (2007) 48:1273–8. doi: 10.2967/jnumed.106.039354
44. O'Connell RA, Van Heertum RL, Luck D, Yudd AP, Cueva JE, Billick SB, et al. Single-photon emission computed tomography of the brain in acute mania and schizophrenia. *J Neuroimaging.* (1995) 5:101–4. doi: 10.1111/jon199552101
45. Bolwig TG. Regional cerebral blood flow in affective disorder. *Acta Psychiatr Scand Suppl.* (1993) 371:48–53. doi: 10.1111/j.1600-0447.1993.tb05374.x
46. Gyulai L, Alavi A, Broich K, Reilley J, Ball WB, Whybrow PC. I-123 iofetamine single-photon computed emission tomography in rapid cycling bipolar disorder: a clinical study. *Biol Psychiatry.* (1997) 41:152–61. doi: 10.1016/S0006-3223(96)00002-9
47. Bhardwaj R, Chakrabarti S, Mittal BR, Sharan P. A single photon emission computerized tomography (SPECT) study of regional cerebral blood flow in bipolar disorder. *World J Biol Psychiatry.* (2010) 11(2 Pt 2):334–43. doi: 10.3109/15622970802575977
48. Henderson TA, Uszler JM, Rossiter-Thornton JF, Siow Y-H, Pavel DG, McLean M, et al. The American psychiatric association fails to recognize the value of neuroimaging in psychiatry. *Interv Med Clin Imaging.* (2019) 1:1–8.
49. Cohen PF, Tarzwell R, Numerow L, Siow Y-H, Uszler JM, Pavel DG, et al. *CANM Guidelines for Brain Perfusion Single Photon Emission Computed Tomography (SPECT).* (2021). Available online at: https://www.canm-acmn.ca/guidelines (accessed October 3, 2021).
50. Juckel G, Hegerl U, Mavrogiorgou P, Gallinat J, Mager T, Tigges P, et al. Clinical and biological findings in a case with 48-hour bipolar ultrarapid cycling before and during valproate treatment. *J Clin Psychiatry.* (2000) 61:585–93. doi: 10.4088/jcp.v61n0808
51. Goodwin GM, Cavanagh JT, Glabus MF, Kehoe RF, O'Carroll RE, Ebmeier KP. Uptake of 99mTc-exametazime shown by single photon emission computed tomography before and after lithium withdrawal in bipolar patients: associations with mania. *Br J Psychiatry.* (1997) 170:426–30. doi: 10.1192/bjp.170.5.426
52. Estudillo-Guerra MA, Pacheco-Barrios K, Cardenas-Rojas A, Adame-Ocampo G, Camprodon JA, Morales-Quezada L, et al. Brain perfusion during manic episode and at 6-month follow-up period in bipolar disorder patients: correlation with cognitive functions. *Brain Behav.* (2020) 10:e01615. doi: 10.1002/brb3.1615
53. Milak MS, Parsey RV, Keilp J, Oquendo MA, Malone KM, Mann JJ. Neuroanatomic correlates of psychopathologic components of major depressive disorder. *Arch Gen Psychiatry.* (2005) 62:397–408. doi: 10.1001/archpsyc.62.4.397
54. Brody AL, Saxena S, Stoessel P, Gillies LA, Fairbanks LA, Alborzian S, et al. Regional brain metabolic changes in patients with major depression treated with either paroxetine or interpersonal therapy: preliminary findings. *Arch Gen Psychiatry.* (2001) 58:631–40. doi: 10.1001/archpsyc.58.7.631
55. Ketter TA, Kimbrell TA, George MS, Dunn RT, Speer AM, Benson BE, et al. Effects of mood and subtype on cerebral glucose metabolism in treatment-resistant bipolar disorder. *Biol Psychiatry.* (2001) 49:97–109. doi: 10.1016/s0006-3223(00)00975-6
56. Blumberg HP, Stern E, Ricketts S, Martinez D, de Asis J, White T, et al. Rostral and orbital prefrontal cortex dysfunction in the manic state of bipolar disorder. *Am J Psychiatry.* (1999) 156:1986–8. doi: 10.1176/ajp.156.12.1986
57. Blumberg HP, Stern E, Martinez D, Ricketts S, de Asis J, White T, et al. Increased anterior cingulate and caudate activity in bipolar mania. *Biol Psychiatry.* (2000) 48:1045–52. doi: 10.1016/s0006-3223(00)00962-8
58. Caligiuri MP, Brown GG, Meloy MJ, Eberson SC, Kindermann SS, Frank LR, et al. An fMRI study of affective state and medication on cortical and subcortical brain regions during motor performance in bipolar disorder. *Psychiatry Res.* (2003) 123:171–82. doi: 10.1016/s0925-4927(03)00075-1
59. Dell'Osso B, Dobrea C, Palazzo MC, Cremaschi L, Penzo B, Benatti B, et al. Neuroimaging procedures and related acquisitions in bipolar disorder: state of the art. *Riv Psichiatr.* (2014) 49:2–11. doi: 10.1708/1407.15619
60. Strakowski SM, Delbello MP, Adler CM. The functional neuroanatomy of bipolar disorder: a review of neuroimaging findings. *Mol Psychiatry.* (2005) 10:105–16. doi: 10.1038/sj.mp.4001585
61. Uszler JM. *Personal Communication.*
62. Cardaci J. *Personal Communication.*
63. Siow Y-H. *Personal Communication.*
64. Rossiter-Thornton JF. *Personal Communication.*

65. Van Lierop M. *Personal Communication.*
66. Chang LT. A method for attenuation correction in radionuclide computed tomography. *IEEE Trans Nucl Sci.* (1977) 25:638–43. doi: 10.1109/tns.1978.4329385
67. Jaszczak RJ, Chang LT, Stein NA, Moore FE. Whole-body single-photon emission computed tomography using dual, large-field-of-view scintillation cameras. *Phys Med Biol.* (1979) 24:1123–43. doi: 10.1088/0031-9155/24/6/003
68. Minoshima S, Koeppe RA, Frey KA, Kuhl DE. Anatomic standardization: linear scaling and nonlinear warping of functional brain images. *J Nucl Med.* (1994) 35:1528–37.
69. Lenox RH, Gould TD, Manji HK. Endophenotypes in bipolar disorder. *Am J Med Genet.* (2002) 114:391–406. doi: 10.1002/ajmg.10360
70. Mena I. Neurospect applications in psychiatry. *ALASBIMN J.* (2009) 11:23.
71. Hasler G, Drevets WC, Manji HK, Charney DS. Discovering endophenotypes for major depression. *Neuropsychopharmacology.* (2004) 29:1765–81. doi: 10.1038/sj.npp.1300506
72. Lopez AY, Wang X, Xu M, Maheshwari A, Curry D, Lam S, et al. Ankyrin-G isoform imbalance and interneuronopathy link epilepsy and bipolar disorder. *Mol Psychiatry.* (2017) 22:1464–72. doi: 10.1038/mp.2016.233
73. Amen DG, Waugh M. High resolution brain SPECT imaging of marijuana smokers with AD/HD. *J Psychoactive Drugs.* (1998) 30:209–14. doi: 10.1080/02791072.1998.10399692
74. Amen DG, Darmal B, Raji CA, Bao W, Jorandby L, Meysami S, et al. Discriminative properties of hippocampal hypoperfusion in marijuana users compared to healthy controls: implications for marijuana administration in Alzheimer's dementia. *J Alzheimers Dis.* (2017) 56:261–73. doi: 10.3233/JAD-160833
75. Pavel DG, Henderson TA, DeBruin S. The legacy of the TTASAAN report – premature conclusions and forgotten promises: a review of policy and practice. Part I. *Front Neurol.* (2022) 12:749579. doi: 10.3389/fneur.2021.749579
76. Pavel DG, Henderson TA, DeBruin S. The Legacy of the TTASAAN report – premature conclusions and forgotten promises: a review of policy and practice. Part II. *Front Neurol.* (in press).
77. APA. *Diagnostic and Statistical Manual of Mental Disorders*. 5th ed. Arlington VA: American Psychiatric Association (2013).
78. Henderson TA, Cohen P, van Lierop M, Thornton J, McLean MK, Uszler JM, et al. A reckoning to keep doing what we are already doing with PET and SPECT functional neuroimaging. *Am J Psychiatry.* (2020) 177:637–8. doi: 10.1176/appi.ajp.2020.19080801
79. Henderson TA. Brain SPECT imaging in neuropsychiatric diagnosis and monitoring. *EPatient.* (2018) 1:40–7.
80. Henderson TA, van Lierop MJ, McLean M, Uszler JM, Thornton JF, Siow YH, et al. Functional neuroimaging in psychiatry—aiding in diagnosis and guiding treatment. What the American psychiatric association does not know. *Front Psychiatry.* (2020) 11:276. doi: 10.3389/fpsyt.2020.00276
81. Rush AJ, Trivedi MH, Wisniewski SR, Nierenberg AA, Stewart JW, Warden D, et al. Acute and longer-term outcomes in depressed outpatients requiring one or several treatment steps: a STAR*D report. *Am J Psychiatry.* (2006) 163:1905–17. doi: 10.1176/ajp.2006.163.11.1905
82. Craney JL, Geller B. A prepubertal and early adolescent bipolar disorder-I phenotype: review of phenomenology and longitudinal course. *Bipolar Disord.* (2003) 5:243–56. doi: 10.1034/j.1399-5618.2003.00044.x
83. das Neves Peixoto FS, de Sousa DF, Luz DCRP, Vieira NB, Gonçalves Júnior J, Dos Santos GCA, et al. Bipolarity and suicidal ideation in children and adolescents: a systematic review with meta-analysis. *Ann Gen Psychiatry.* (2017) 16:22. doi: 10.1186/s12991-017-0143-5
84. Baldessarini RJ, Pompili M, Tondo L. Suicide in bipolar disorder: risks and management. *CNS Spectr.* (2006) 11:465–71. doi: 10.1017/s1092852900014681
85. Orsolini L, Latini R, Pompili M, Serafini G, Volpe U, Vellante F, et al. Understanding the complex of suicide in depression: from research to clinics. *Psychiatry Investig.* (2020) 17:207–21. doi: 10.30773/pi.2019.0171
86. Pompili M. Can we expect a rise in suicide rates after the covid-19 pandemic outbreak? *Eur Neuropsychopharmacol.* (2021) 52:1–2. doi: 10.1016/j.euroneuro.2021.05.011
87. First MB, Drevets WC, Carter C, Dickstein DP, Kasoff L, Kim KL, et al. Clinical applications of neuroimaging in psychiatric disorders. *Am J Psychiatry.* (2018) 175:915–6. doi: 10.1176/appi.ajp.2018.1750701

Conflict of Interest: TH is the president and principal owner of The Synaptic Space, a neuroimaging consulting firm. He is also CEO and Chairman of the Board of Neuro-Luminance Corporation, a medical service company. He is also president and principal owner of Dr. TH, Inc., a medical service company. He is also Vice-President of the Neuro-Laser Foundation, a non-profit organization. He is a member of and a former officer of the Brain Imaging Council Board of the Society of Nuclear Medicine and Molecular Imaging (SNMMI). Since 2017, he has served in the SNMMI Brain Imaging Outreach Working Group. Currently, he serves as president of the International Society of Applied Neuroimaging. TH has no ownership in, and receives no remuneration from, any neuroimaging company. No more than 5% of his income is derived from neuroimaging. DP was Director of PathFinder Brain SPECT which is a clinical service corporation providing SPECT functional neuroimaging and had no research funding.

The remaining author declares that the research was conducted in the absence of any commercial or financial relationships that could be construed as a potential conflict of interest.

Publisher's Note: All claims expressed in this article are solely those of the authors and do not necessarily represent those of their affiliated organizations, or those of the publisher, the editors and the reviewers. Any product that may be evaluated in this article, or claim that may be made by its manufacturer, is not guaranteed or endorsed by the publisher.

frontiers | Frontiers in Neurology

POLICY AND PRACTICE REVIEWS
published: 17 May 2022
doi: 10.3389/fneur.2022.851609

The Legacy of the TTASAAN Report – Premature Conclusions and Forgotten Promises About SPECT Neuroimaging: A Review of Policy and Practice Part II

Dan G. Pavel[1,2†], *Theodore A. Henderson*[2,3,4,5,6*], *Simon DeBruin*[2,7] *and Philip F. Cohen*[2,8,9]

[1] PathFinder Brain SPECT, Deerfield, IL, United States, [2] The International Society of Applied Neuroimaging (ISAN), Denver, CO, United States, [3] The Synaptic Space, Inc., Denver, CO, United States, [4] Neuro-Luminance, Inc., Denver, CO, United States, [5] Dr. Theodore Henderson, Inc., Denver, CO, United States, [6] Neuro-Laser Foundation, Denver, CO, United States, [7] Good Lion Imaging, Baltimore, MD, United States, [8] Nuclear Medicine, Lions Gate Hospital, Vancouver, BC, Canada, [9] Department of Radiology, University of British Columbia, Vancouver, BC, Canada

Brain perfusion single photon emission computed tomography (SPECT) scans were initially developed in 1970s. A key radiopharmaceutical, hexamethylpropyleneamine oxime (HMPAO), was not stabilized until 1993 and most early SPECT scans were performed on single-head gamma cameras. These early scans were of inferior quality. In 1996, the Therapeutics and Technology Assessment Subcommittee of the American Academy of Neurology (TTASAAN) issued a report regarding the use of SPECT in the evaluation of neurological disorders. This two-part series explores the policies and procedures related to perfusion SPECT functional neuroimaging. In Part I, the comparison between the quality of the SPECT scans and the depth of the data for key neurological and psychiatric indications at the time of the TTASAAN report vs. the intervening 25 years were presented. In Part II, the technical aspects of perfusion SPECT neuroimaging and image processing will be explored. The role of color scales will be reviewed and the process of interpreting a SPECT scan will be presented. Interpretation of a functional brain scans requires not only anatomical knowledge, but also technical understanding on correctly performing a scan, regardless of the scanning modality. Awareness of technical limitations allows the clinician to properly interpret a functional brain scan. With this foundation, four scenarios in which perfusion SPECT neuroimaging, together with other imaging modalities and testing, lead to a narrowing of the differential diagnoses and better treatment. Lastly, recommendations for the revision of current policies and practices are made.

Keywords: SPECT, procedure, Parkinsonian, traumatic brain injury, differential diagnosis, comorbidity

OPEN ACCESS

Edited by:
Jan Kassubek,
University of Ulm, Germany

Reviewed by:
Kiyotaka Nemoto,
University of Tsukuba, Japan
Joachim Strobel,
Universitätsklinikum Ulm, Germany

***Correspondence:**
Theodore A. Henderson
thesynapticspace7@gmail.com

[†]*Deceased*

Specialty section:
This article was submitted to Applied Neuroimaging, a section of the journal Frontiers in Neurology

Received: *10 January 2022*
Accepted: *28 February 2022*
Published: *17 May 2022*

Citation:
Pavel DG, Henderson TA, DeBruin S and Cohen PF (2022) The Legacy of the TTASAAN Report – Premature Conclusions and Forgotten Promises About SPECT Neuroimaging: A Review of Policy and Practice Part II. Front. Neurol. 13:851609. doi: 10.3389/fneur.2022.851609

INTRODUCTION

In 1996, the Therapeutics and Technology Assessment Subcommittee of the American Academy of Neurology (TTASAAN) issued a report regarding the use of perfusion single photon emission computed tomography (SPECT) in functional brain imaging (1). While the authors of the TTASAAN report did not intend this to be the definitive position of perfusion SPECT neuroimaging (in the text, they mandated periodic revision as the field advanced), this 1996 report,

nonetheless, has stood and remains to stand as the final word on perfusion SPECT neuroimaging in Neurology and Psychiatry since. As a result, neurologists and psychiatrists have distanced themselves or outright disparaged SPECT neuroimaging and its role in the evaluation of a patient. Allegorically, there were no smartphones in 1996. Rather there were brick-like mobile phones with external antenna. In 2000, the first touchscreen became available and integrated cameras became available in 2002. Finally, in 2007, the I-phone was unveiled ushering in the era of the smart phone. Relying on the TTASAAN report today is equivalent to relying on an assessment of modern cell phone technology and applications based on 1996 technology. Just as the smartphone computer in your hand bears little resemblance to the bulky, heavy, dialing devices of old, modern SPECT neuroimaging bears little resemblance to its 1996 predecessor. In 1996, there were only single-headed gamma cameras, unstable radiotracers, no quantitative software, no normative databases, no advanced image reconstruction software, no iterative reconstruction, no CT hybrid imagers, no solid-state detectors, and no artificial intelligence algorithms. All of these advances have radically changed and improved perfusion SPECT neuroimaging. Furthermore, the research literature encompassing over 60,000 patients across multiple neurological and neuropsychiatric disorders did not exist (as reviewed extensively in Part I of this two-part series).

This two-part series explores the policies and procedures related to perfusion SPECT functional neuroimaging and, ultimately, makes recommendations for revisions to the current policies and practices. In Part I, the comparison between the quality of the SPECT scans and the depth of the data for key neurological and psychiatric indications at the time of the TTASAAN report vs. the intervening 25 years were presented (2). We reviewed the research literature on traumatic brain injury (TBI) (encompassing over 24,000 subjects) and showed SPECT perfusion imaging is more sensitive that CT or MRI for detecting TBI. We rebutted many criticisms of detecting TBI with perfusion SPECT, and demonstrated that perfusion SPECT meets the criteria for a Type A recommendation based on the criteria set forth in the TTASAAN report. We reviewed the use of perfusion SPECT in epilepsy, including the findings that ictal-interictal SPECT has an accuracy of 85.9% in localizing seizure foci. The vast field of neuroimaging in dementia was reviewed and perfusion SPECT was shown to have 96% sensitivity and 80% specificity in differentiating Alzheimer's disease (AD) from fronto-temporal dementia (FTD), comparable to fluorodeoxyglucose-positron emission tomography (FDG-PET) (2, 3). Similarly, the conversion from mild cognitive impairment (MCI) to AD or FTD can be predicted with both perfusion SPECT and FDG-PET. FDG-PET was found to predict the conversion from MCI to AD with a sensitivity of 70–90% and a specificity of 82.4–90%, while perfusion SPECT scans predict the conversion from MCI to AD with a sensitivity ranging from 89 to 97% and a specificity of 89–100% (2). In addition, we reviewed the SPECT neuroimaging research findings in neurotoxicity, attention-deficit hyperactivity disorder, depression, bipolar disorder, obsessive compulsive disorder, and stroke.

In Part II, the technical aspects of perfusion SPECT neuroimaging and the process of interpreting a SPECT scan will be presented.

Limitations in Functional Neuroimaging

Interpretation of a functional brain scan requires not only anatomical knowledge, but also technical understanding on how to correctly perform a scan. This is no less true for positron emission tomography (PET) or functional magnetic resonance imaging (fMRI) than it is for SPECT scanning. Our intent here is not to paint a rosy picture of perfusion SPECT imaging at the expense of other modalities. Rather, we merely wish to remind the field that PET, diffusion tensor imaging (DTI), and fMRI have limitations, as well.

The usefulness of any imaging technique, as well as its widespread adoption into clinical practice and clinical research is ultimately dependent upon the consistency, rigor, and quality of the methodology used to create the images. An MRI from a 0.5 Tesla magnet is quite different from that of a 3 Tesla magnet. Moreover, the technique of obtaining the MRI image has significant effects upon the resulting image. If the sequences for T2 weighted imaging, proton-density weighted, or DTI are not programmed correctly and motion is not controlled, then the resulting images can be uninterpretable.

While technically not functional neuroimaging, DTI is being studied as a method of detecting TBI. DTI is a highly sophisticated sequence of MRI imaging. Yet, there is not an agreed upon protocol for obtaining DTI images. As a result, the quality, accuracy, and clinical significance of DTI imaging varies greatly across facilities. This has led to conflicting results for certain conditions and a lack of uniformity in the field (4, 5). According to some experts, while DTI may be a sensitive measure, currently it lacks the level of specificity necessary for application in clinical practice (5). Similarly, fMRI has suffered from a lack of unified protocols.

Functional neuroimaging is particularly vulnerable to technical errors or flaws. As discussed in Part I (2), an analysis of the validity of fMRI post-processing methods has revealed significant flaws which potentially invalidate many fMRI studies and the resulting conclusions about fMRI findings in certain conditions (6). The American Psychiatric Association has questioned the value of fMRI research into psychiatric disorders (7).

An important distinction often lost in the textbook or the lecture hall concerning neuroimaging modalities is the distinction between ***resolution*** and ***contrast***. While anatomical MRI and of CT (to a lesser extent) have superior resolution (1 mm), FDG-PET scans have a resolution of 5 mm and SPECT using standard sodium iodide crystals have a resolution close to 10 mm. On the other hand, contrast is the ability to discern an abnormal signal from background. The sensitivity of CT for detecting contrast agents is in the millimolar range, while that of MRI is in the micromolar range. The sensitivity of SPECT neuroimaging for detecting a radiopharmaceutical is in the nanomolar range, exceeding MRI by a thousand-fold and exceeding CT by a million-fold (8–10). This is perhaps best illustrated with seizure imaging, wherein CT and MRI show no

abnormality, while perfusion SPECT can reliably localize the seizure focus or foci. (11–19). Similarly, as reviewed extensively in Pavel and colleagues (2), CT and MRI often miss areas of cortical dysfunction following concussion or TBI [e.g., Figure 4 in (2)], while perfusion SPECT can readily detect TBI and differentiate TBI from control with a >95% accuracy (20, 21).

Modern fMRI has limited resolution and contrast (6) with pixel size generally 2–3 mm (22), as discussed in Part I. In PET imaging, it is important to recall that PET scanners visualize the annihilation of a positron, not the release of a positron from a tracer. In contrast to gamma radiation emitters (as used in SPECT) wherein the point of gamma photon release corresponds to the exact site at which the radiopharmaceutical is bound or retained; positron emitters have a degree of inaccuracy related to the physics of positrons and the range that they travel before annihilation (23–25). For example, the range of ^{18}F is up to 6 mm (26, 27) and the range of ^{18}O is up to 10 mm (27). In the case of ^{18}F, this can lead to a 3.5% degradation of resolution for soft tissue, such as brain (27).

On the other hand, resolution in many cases is a red herring that matters very little in the pragmatic clinical practice. For example, the resolution of amyloid PET imaging is immaterial. If amyloid is present in the grey matter, then the scan is considered positive for Alzheimer's disease. If it is negative, then Alzheimer's disease is unlikely (caveats discussed below). The scan can be read from across the room. Similarly, a ^{123}I-ioflupane scan (DaTscan) has relatively low resolution, but the pattern is distinctive. If the tracer is absent from the striatal "tail," then the scan reveals degeneration of the dopamine system in the striatum.

In the interpretation of perfusion SPECT scans compared to FDG PET scans, the resolution differences of modern versions of these modalities matters very little. As described in depth in Part I (2), both modalities can visualize the posterior cingulate gyrus, the parietal cortices, and the temporal cortices and render, for example, a diagnosis of Alzheimer's disease with similar accuracy (89 vs. 89%) (2, 3, 28, 29).

In part II of this Policy and Practice Review, we will address the technical aspects of perfusion SPECT functional neuroimaging which can gravely affect the quality of the scan. We will describe future changes which are now months to years away. We will also articulate best practices for obtaining, processing, and interpreting a perfusion SPECT scan. Lastly, we will discuss the integration of perfusion SPECT scans into coordinated and insightful utilization of multiple neuroimaging modalities. This integrative philosophy will be illustrated with four clinical examples. These technical aspects, together with the aforementioned extensive review of perfusion SPECT findings in a number of conditions (2), will guide recommendations for changes in policy and practice.

TECHNICAL ASPECTS OF SPECT NEUROIMAGING

Perfusion SPECT functional neuroimaging is no less vulnerable to degradation resulting from poor or flawed technique. As has been laid out in detail in Part I (2), the SPECT images of the early 1990s which were the basis of the TTASAAN committee's decisions and report, are technically far removed from the current high-quality perfusion SPECT images we consistently work with today. Nonetheless, technique still varies widely from facility to facility. Hence, the process of interpreting a perfusion SPECT scan necessitates an appreciation of neuroanatomy, the effects of altered anatomy, camera properties, acquisition methods, reconstruction and filtering algorithms, and attenuation correction. It is time to have a closer look at the technical considerations of SPECT instrumentation and processing that contribute to the execution of high-quality brain SPECT scans.

The Gamma Camera

Most commercial gamma cameras today are based on a scintillating sodium-iodide (Na-I) crystal, coupled to an array of photomultiplier tubes (PMTs). The field of view of the camera is given by the size of the crystal. A gamma photon released in the radioactive decay of the radiopharmaceutical that reaches the crystal, causes it to emit a brief flash of light which scatters in all directions, with a strength proportional to the energy of the gamma radiation (**Figure 1**). The light is detected, amplified, and converted into an electrical pulse by the PMTs. The amount of light measured by each PMT depends on its location in reference to the origin of the light flash. The PMT closest to the event location produces a greater electrical pulse compared to the surrounding PMTs. The exact location is determined by a center of mass calculation according to the methodology developed by Hal Anger. Even though the typical PMT has a diameter of 2 in. or 3 in, the Anger principle gives the gamma camera an intrinsic resolution on the order of 4 mm at 140 keV (the gamma energy of ^{99m}-Technetium, the most common radionuclide in SPECT imaging).

To obtain useful images, the incoming angles of incidence of gamma photons must be restricted. For this purpose, a collimator is positioned between the patient (the source of radiation) and the crystal (the detector). A collimator is made of a perforated slab of lead, absorbing most gamma photons except those which arrive parallel to the axis of the collimator holes (**Figure 1**). The design parameters of the collimator (e.g., hole diameter and length, septa thickness), determine the overall resolution of the imaging system. The commonly used collimator for ^{99m}-Technetium studies is the studies is the low energy/high resolution (LEHR) collimator with a resolution of ∼6.5 mm at 10 cm distance. Note: the resolution of the collimator is a function of distance; thus, to maximize image quality, the distance between the patient and the surface of the collimator must be minimized.

As the collimator rejects most of the incoming radiation, it shall be clear that it has a huge impact on the overall system sensitivity. Specialized collimator geometries have been developed over the years such as fan beam or cone beam but their prevalence in the field is small.

The size of the detector determines the efficiency with which a particular nuclear medicine procedure can be executed. For a general-purpose gamma camera, the most common detector size is 21 in. × 15 in. allowing a whole-body bone scan (one of the most frequently ordered SPECT scans) to be performed

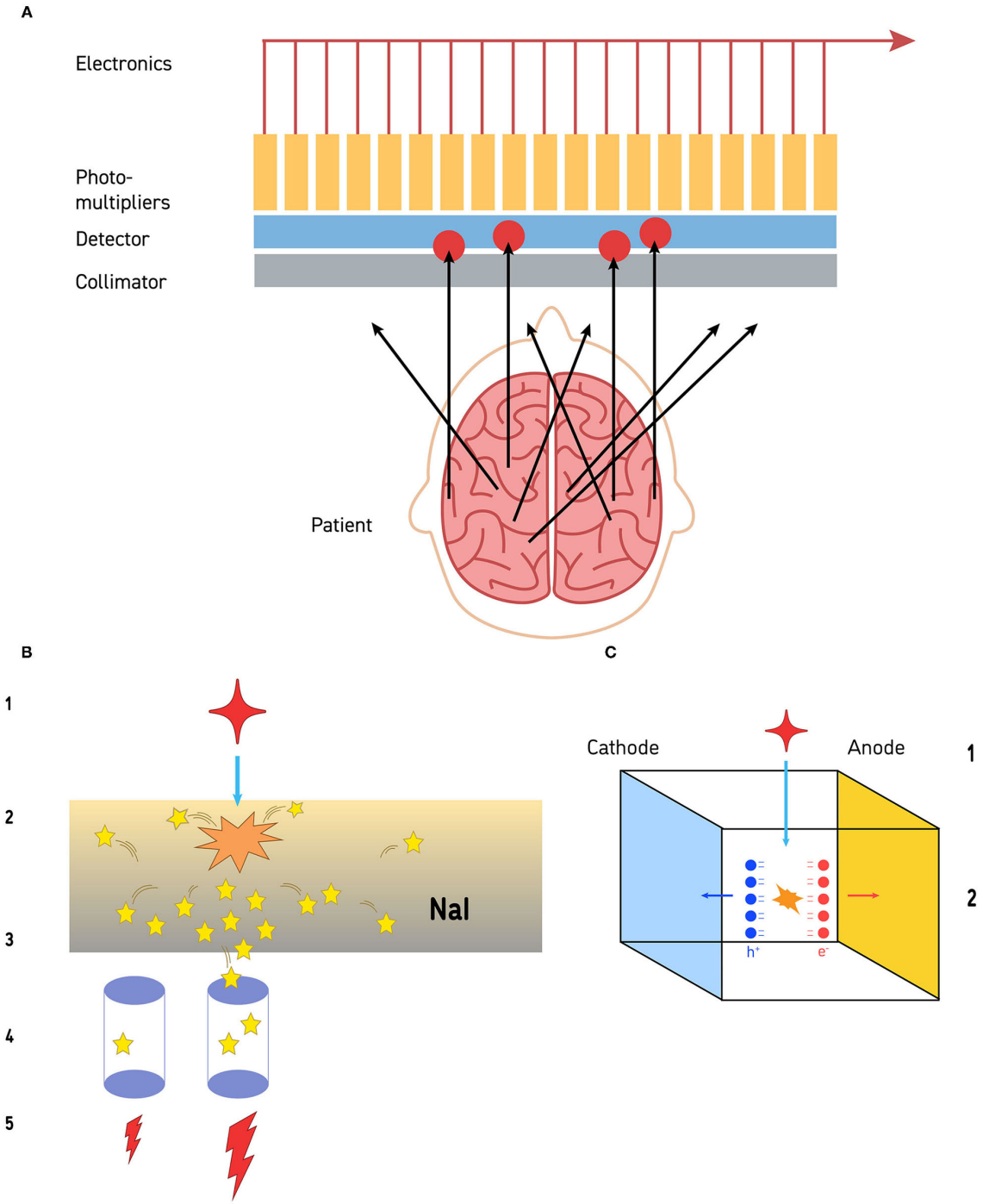

FIGURE 1 | (A) The collimation process is illustrated. Gamma photons released by the radiopharmaceutical travel away from the site of emission in all directions. Those that impact the collimator at an angle cannot pass through. Gamma photons that reach the collimator in alignment with the channels of the collimator can pass through and reach the detector (a sodium iodide crystal in this illustration). The limit to resolution is the ***size of the photomultipliers***, distance from the structure of interest, and the resolution of the collimator. **(B)** Detection of gamma photons by sodium iodide crystal detectors is a multi-step process. The gamma photon (red star −1) strikes the sodium iodide crystal (orange starburst) and a burst of visible light photons (yellow stars) is released (2). The light photons radiate in all directions (3). Some of those visible light photons will impact on photodetectors (purple cylinders −4). Photodetectors closer to the site of gamma photon impact will receive more visible light photons, while those further away from the site will receive less (4). Those photodetectors that receive more visible light photons will release a greater electrical current, while the detectors further away will release a small electrical current (5). This is the basis of the Anger circuitry for geometric localization. **(C)** Cadmium-zinc-telluride (CZT) detectors are solid-state and directly convert gamma photons into electrons at room temperature. When a gamma photon (1) strikes a CZT detector (2), pairs of electrons and holes are generated (red and blue balls, respectively). These create an electrical potential across the detector which is proportional to the energy of the impinging radiation. The resolution is limited by the size of the CZT detector—currently about 2.4 mm on a side.

in a single pass. Obviously, this size is much more than what is needed for a brain scan and complicates patient positioning as the large physical size of the detectors make it harder to get close to the patient's head without truncating parts of the brain. These pragmatic limitations result in the brain being a greater distance from the detector and therefore occupying a smaller percentage of the detector's field of view. Hence, fewer counts accumulate in each cell of the matrix (see Acquisition Matrix and Acquisition Zoom below) and many cells have no counts whatsoever.

One way to increase gamma camera sensitivity is by using more detectors. The most common gamma camera today has 2 detectors, cutting imaging time in half for most procedures (or doubling the statistics compared to a single detector camera). In many cameras, these heads can be positioned in opposition to each other or at a right angle to each other. In the past, triple detector cameras were manufactured specifically for brain imaging, but small production volumes meant that such products were not viable, and manufacture of these cameras has ceased. Nonetheless, surviving triple detector cameras are still widely used.

A fundamental advance in gamma camera technology has been underway over the past decade and new cameras with higher resolution and higher efficiency are now commercially available. Essentially, gamma photon detectors have changed little since the early days of research. The workhorse of the gamma camera has been the sodium iodide (NaI) crystal described above (**Figure 1B**).

In contrast, the recently developed Cadmium Zinc Telluride (CZT) detector is a semiconductor that directly converts x-ray or gamma-ray photons into electrons at room temperature. Typical CZT detectors are fabricated with a thin layer of metal deposited on both of surfaces of the detector to act as electrodes. These electrodes then allow the detectors to be electrically biased and, thus, creating an electrical potential across the detector. One surface acts as a cathode and one acts as an anode. As shown in **Figure 1C**, when a gamma photon collides with the biased CZT, a pair of electron/hole is generated, which are proportional to the energy of the absorbed radiation. Negatively charged electrons and positively charged holes migrate to their respective electrodes and are collected. This process is referred to as photoelectric absorption.

CZT detectors have led to the development of cameras with much higher resolution. The resolution is no longer limited by the spread of visible light photons in the NaI crystal or by the collimator. CZT detectors can be made very small (e.g., 2.4 mm square). There are 1,000 CZT detectors in each camera head. Each functions essentially as a pin-hole camera. As a result, the intrinsic spatial resolution (ISR) of a modern CZT gamma camera falls to 2.46 mm. This is considerably higher than the 7.0 mm ISR of current dual-head gamma cameras and exceeds the 4.0 mm ISR of currently available PET cameras.

Patient Preparation and Positioning

Equally critical in obtaining a quality SPECT scan is the proper preparation of the patient. This will be briefly explored here, but a detailed description is provided in the Canadian Association of Nuclear Medicine guidelines (30). Patient preparation begins long before the day of the scan and includes potentially stopping medications. The decision to stop current medications prior to a scan should never be made lightly. Some patients or referring clinicians may prefer to obtain a scan without medications; however, scans are still informative if patients do not stop their current medications—with a few exceptions. The decision should be made in consultation with the referring or treating physician. If the decision is made to stop medications, then a safe and comfortable taper should be planned.

There are a small number of medications which should always be stopped prior to a functional brain scan, because they either artificially increase or decrease brain perfusion. A number of commonly ingested substances increase cerebral blood flow. For example, all stimulant medications should be withheld for 72 h prior to a scan. Patients should avoid caffeine for 48 h prior to a scan. Similarly, over-the-counter medications or supplements containing pseudoephedrine, caffeine, ephedrine, guarana, or taurine, as well as energy drinks, should be avoided. Nicotine should be avoided for 48 h, but this is difficult for most individuals who use nicotine. Therefore, a modified restriction for 12 h prior to the scan is often acceptable. Acetazolamide (Diamox) is used to treat glaucoma and high altitude sickness. This medication robustly increases cerebral blood flow and should be stopped 48 h prior to a scan. Substances that artificially lower cerebral blood flow should be avoided as well. Benzodiazepines should be withheld for 48 h prior to a scan. If a patient is on a stable dose of a benzodiazepine, they may require a careful taper to discontinue the medication or it may be necessary to accept a low dose of benzodiazepine, if the risk of withdrawal or seizures is too great. Alcohol and marijuana, as well as any illicit drugs, should be avoided for 48 h before a functional brain scan. Caution should be exercised with patients who are heavy users of alcohol, caffeine, nicotine or illicit drugs to not precipitate a dangerous withdrawal situation.

Patients should be cautioned to avoid chewing gum or eating in the 2 h prior to injection of the radiopharmaceutical for a perfusion SPECT scan. This reduces extraneous uptake of tracer into salivary glands. Similarly, keeping patients calm and limiting situations that induce weeping will reduce uptake in lacrimal glands. Patients should be well hydrated prior to a SPECT scan.

At the time of radiopharmaceutical injection, the patient should be positioned in a comfortable reclining chair or exam table with raised head and an IV started. Ideally, lights should be dimmed and the room quiet. Sound-dampening headphones can be helpful. For a baseline scan, the patient should be asked to close their eyes at the time of injection of the radiopharmaceutical and keep them closed for 2 mins. Closing the eyes reduces visual cortex activity. Regardless of whether ^{99m}Tc- ethyl cysteinate dimer (ECD) or ^{99m}Tc- hexamethylpropyleneamine oxime (HMPAO) is utilized, the activity of the brain will be captured, essentially a frozen distribution of radiopharmaceutical, within 2 mins of injection.

Scrupulous technique must be utilized in quality control and preparation of the radiopharmaceutical. The details of this process extend beyond the scope of this article. Suffice to say, it is critical not to spill radiopharmaceutical on the patient or the patient's clothing near the head.

Following radiopharmaceutical injection, the patient should have ∼40 mins to allow for washout of non-specific binding. During this time, the patient should be encouraged to drink at least 16–24 ounces (500–750 ml) of water and to void urine at least once. This facilitates comfort during the scanning process, reduces motion, and eliminates excess unbound radiopharmaceutical (HMPAO and ECD are predominately cleared by the kidneys). Further discussion of radiation safety is beyond the scope of this article but are reviewed at length elsewhere (31–33).

Positioning the patient in the gamma camera is a critical step in the production of a quality SPECT scan (**Figure 3**). The camera heads should be as close to the patient as possible without actually hitting the head or shoulders during rotation. CTZ cameras will greatly alleviate the geometrical limitations posed by large sodium iodide detectors, as shown in **Figure 2**. The settings of distance from detector, acquisition zoom, and collection matrix determines the counts per pixel, as described below. Assuring that the correct matrix setting is utilized will maximize the statistics of the SPECT scan.

The patient's head should be positioned in the head holder in a comfortable manner. Soft padding and soft compression wrapping can be utilized to minimally restrain the head to assure the least motion. The patient should be instructed to avoid head movement and, in particular, avoid nodding the head. Rotational movement is exceedingly difficult to correct. Motion can be checked using the sinogram or linogram (see **Figure 3)** in the camera software. If motion is excessive, then the scan should be repeated. The consequences of poor technique and patient preparation are illustrated in **Figure 2**.

Data Acquisition

As in all nuclear medicine studies a trade-off must be made between counts (statistics) and scan time. For patient comfort, shorter scan times are preferred, and it is recommended to keep acquisition time within the clinical tolerable limit (30 min). For good image quality, more counts are better, and for a brain SPECT scan it is recommended to acquire 10M brain-specific counts minimum. This will necessitate acquiring more than 10M total counts due to extraneous counts from non-neural structures (e.g., scalp, facial structures).

There are several factors that have an impact on the acquired number of counts in a scan. The following factors increase the number of counts, and they are reviewed below:

1. utilizing a camera with multiple detectors.
2. using a collimator with higher sensitivity.
3. increasing acquisition time.
4. increasing radiopharmaceutical dose.

Number of Detectors

Brain SPECT scans require a full 360° rotation around the subject's head. The total number of acquired counts increases proportionally with the number of detectors. Single detector cameras should not be utilized [as shown in Part I (2)]. The new CZT detector-based cameras will greatly enhance scan resolution and quality.

Collimation

The reconstructed resolution of a gamma camera system is determined largely by the collimator resolution. Brain SPECT perfusion studies are acquired with ^{99m}Tc and require a "low energy" (LE) collimator. Collimator design is a trade-off between resolution, sensitivity, and septal penetration (rejection of unwanted photons). Because collimator terminology is not standardized between vendors, it is important to review the collimator specifications rather than relying on terms like high resolution (LEHR) or general purpose (LEAP).

Acquisition Time

The total number of counts in a SPECT scan is proportional to the acquisition time. Longer acquisition times will increase the susceptibility to patient motion which has a detrimental effect on image quality. Therefore, every effort should be made to maximize patient comfort during the scan. However, there is a limit to how far the acquisition time can be extended without risking patient motion. A practical limit is 30 min. For uncooperative patients, other measures may be necessary such as head restraints or sedation. Note that sedation can be used without interfering with the scan if it is administered after the injection of the radiopharmaceutical. Since the perfusion image is captured within ∼40 secs of radiopharmaceutical injection and remains largely unchanged thereafter, tranquilizers or full sedation can be administered without altering the scan image.

Injected Dose

The total number of counts is proportional to the injected dose. It is recommended to maximize the allowable dosage without exceeding radiation limits for best results. Details are provided in the Canadian Association of Nuclear Medicine guidelines (30).

Acquisition Matrix and Acquisition Zoom

The acquisition matrix determines the granularity of the acquired images. However, unlike in photography, a higher matrix in nuclear medicine does not necessarily produce a better image. The reason is that count statistics are low in nuclear medicine and pixel density drops by a factor of 4 for each doubling of matrix size. Lower pixel density means more noise which can be reduced by filtering, but filtering lowers the resolution of the image. Thus, there is a trade-off in choosing an optimum value for the matrix size in SPECT scans.

Typically, acquisition matrices are not arbitrary in size but limited to powers of 2. This reduces the useful choices for SPECT imaging to 3 values: 64, 128, and 256. The optimal choice is determined by the field of view of the detector and the expected/desired image resolution. It is the collimator, not the intrinsic resolution of the camera, that determines the overall resolution of the system. For a high-resolution collimator, the reconstructed resolution of a clinical SPECT scan using a sodium iodide crystal scintillation camera is on the order of 8 mm. The sampling theorem states that the sampling size (the pixel size) must be half, or less, of this value. This means the SPECT scan pixel size should be no larger than 4 mm. A general-purpose dual detector camera typically has a 20 in. field of view (FOV = 508 mm). Continuing with the example, to sample with 4.0 mm

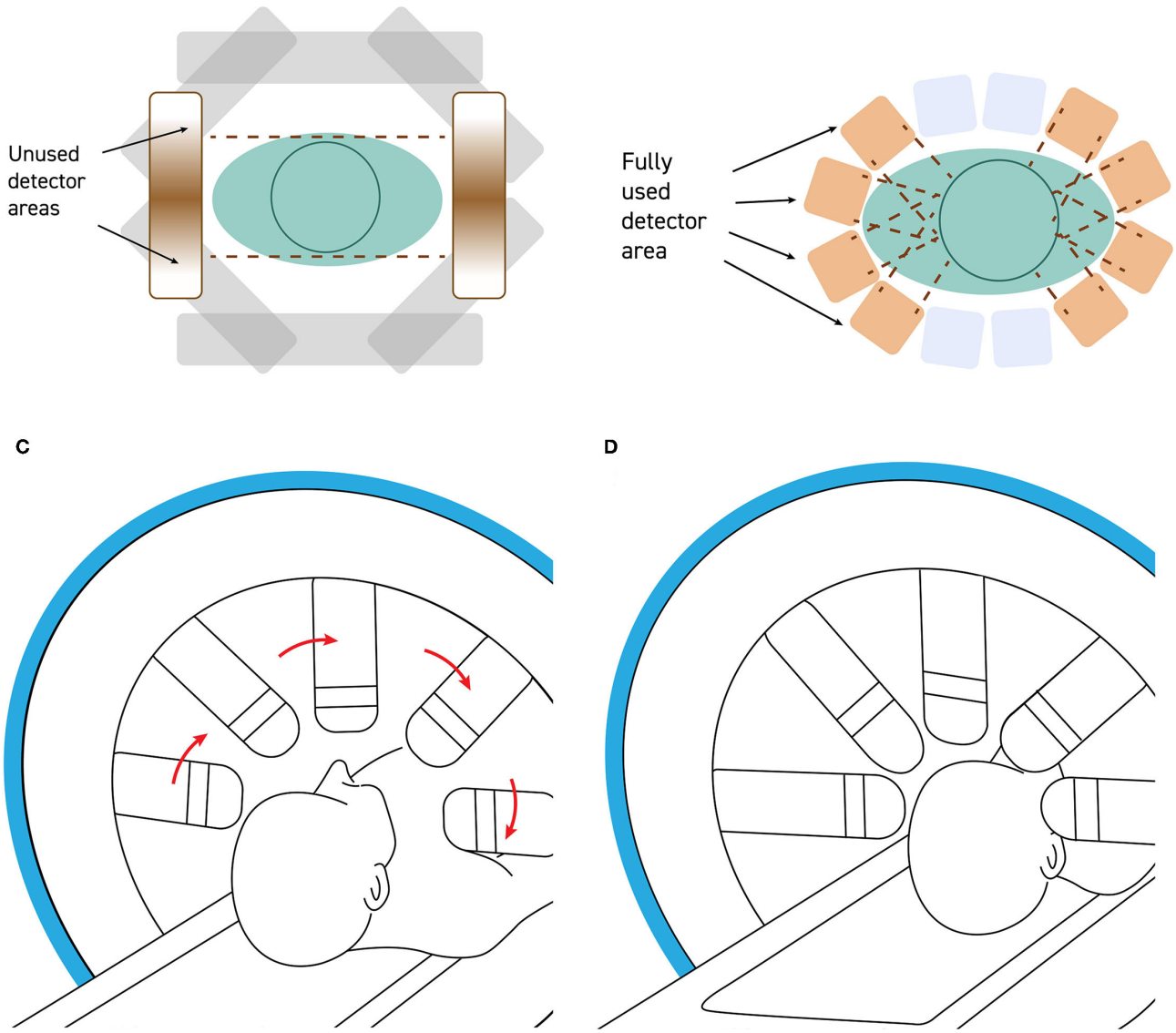

FIGURE 2 | (A) Standard dual-head gamma cameras are too large to get close to the patient's head without hitting the shoulders during rotation. As a result, the field of view of the detector is often poorly utilized with a significant portion of the detector collecting no signal from the brain. **(B)** CZT detectors are quite small and can be mounted such that the detectors can get very close to the patient's head, maximizing the portion of the field of view occupied by the patient's head. **(C)** Modern CZT gamma cameras can be configured to withdraw the detectors heads during rotation and then **(D)** extend the detectors to close proximity of the patient's head during the scanning portion of a step-and-shoot protocol.

pixels, the required minimum matrix size would be $508/4 = 127$. This means that in this example the 128 matrix is the best choice.

Thus far, it has been assumed the acquisition zoom is 1.0 (i.e., no zoom). Setting an acquisition zoom >1 means that the effective field of view of the detector is reduced by this factor. This is an option when the acquired object (the human brain in our case) is significantly smaller than the size of the detector. The zoom factor gives finer control over the pixel size as the increase/decrease of matrix size changes the pixel size by a factor of 2. For example, given a detector with a 15 in. field of view (381 mm), and the goal of a pixel size of 4.0 mm, the choice of matrix will affect the count density. The pixels size for a 128-matrix would be $381/128 = 2.98$ mm, which is a bit smaller than needed. Count density is computed as the number of counts accumulated per unit area; a smaller pixel size therefore reduces the count density as there are more pixels per unit area. Since the area of one pixel is the square of its size, a reduction in size from 4.0 mm to 2.98 mm lowers the count density by a factor of 2. A

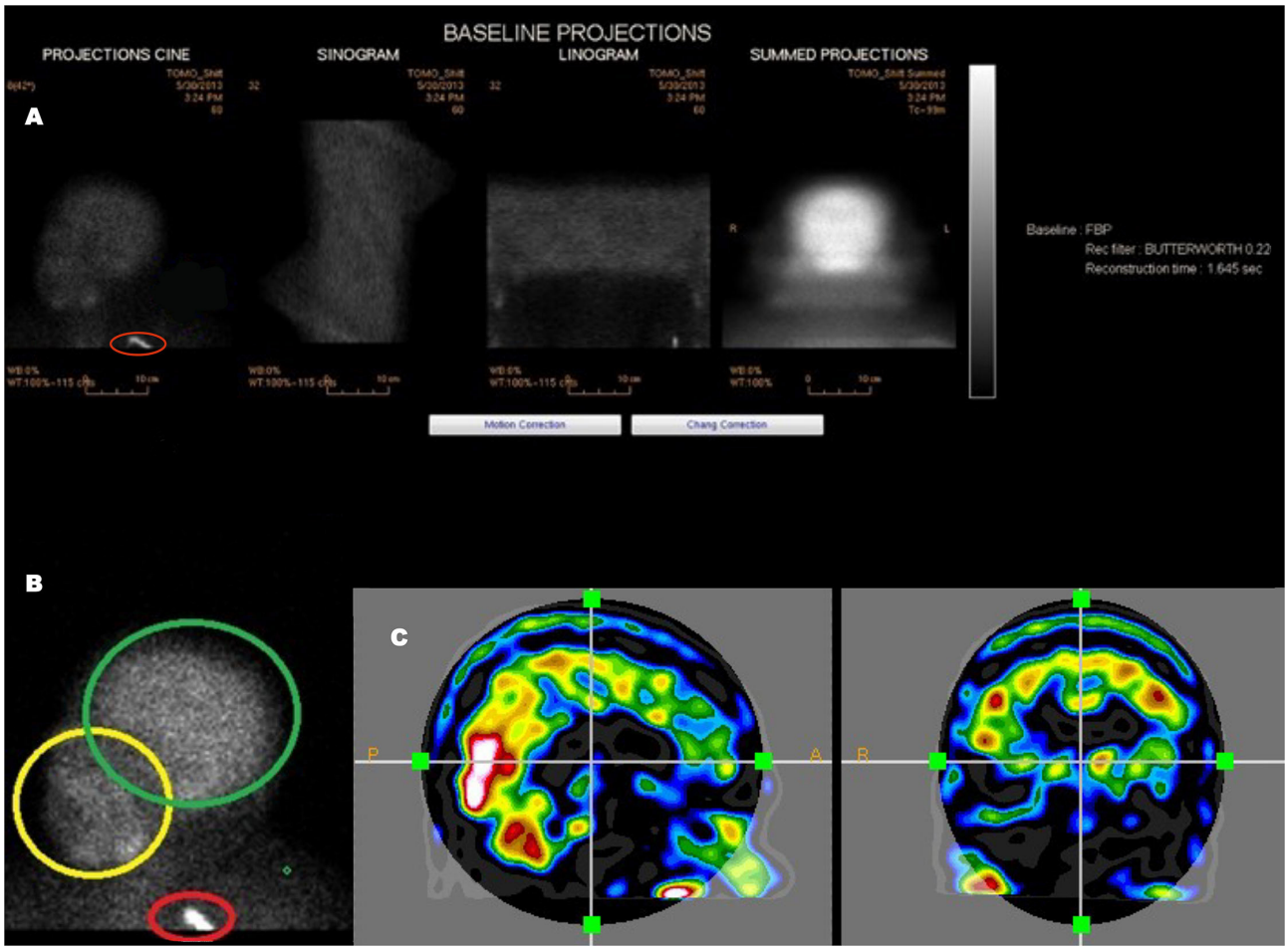

FIGURE 3 | An example of a poorly executed perfusion SPECT scan. **(A)** Projection cine, sinogram, linogram, and summed projections illustrate minimal motion artifact. However, multiple technical errors are evident. The detectors were positioned excessively far from the patient and the acquisition zoom was not correctly set which resulted in large areas of empty space above the head and inclusion down to at least the clavicle in the field of view. In addition, a spill artifact is seen at the level of the clavicle (red circle). The area occupied by the organ of interest—the brain—makes up a small part of the acquisition matrix, best demonstrated in the summed projections. **(B)** A close-up view of the projection cine illustrated relatively high uptake in the facial region (yellow circle) relative to the uptake in the brain (green circle) and the spill artifact (red circle) contributing significant number of counts which are unrelated to the brain. **(C)** Sagittal and coronal alignment images illustrating considerable uptake in the salivary glands and free technetium in the scalp. All of these extraneous counts will reduce the statistics available from the brain. Furthermore, the low spatial resolution of this poorly executed scan is clearly evident.

64-matrix size on the other hand gives a pixel size of 5.95 mm which is too large. However, the desired pixel size of 4.0 mm can be obtained by using an acquisition zoom of 5.95/4.0 = 1.49. This zoom will reduce the field of view by the same factor to 381/1.49 = 256 mm. If the patient's head is properly positioned this would just suffice to acquire a brain SPECT scan without truncation, while maximizing pixel count density and pixel size.

Image Reconstruction

A series of raw images (i.e., projection data) as acquired by a SPECT camera cannot be interpreted directly but must first be reconstructed. Reconstruction is a part of the image generation process and should therefore be considered an extension of the gamma camera. In other modalities, such as CT, the user is often removed from the reconstruction process but in SPECT imaging, the choice of reconstruction parameters is paramount to the attainable image quality and depends strongly on the imaging equipment, the local acquisition parameters, and quite often the patient itself.

In terms of image reconstruction, a general distinction is made between filtered back projection and iterative reconstructions. They differ considerably and are discussed in some detail below.

There are other image processing functions that can be considered part of image reconstruction, most notably: attenuation correction, which is an essential element of brain SPECT imaging. Other optional functions include scatter correction and resolution recovery which are also discussed below.

Filtered Back Projection (FBP)

Back projection (BP) has traditionally been used, because it is simple, fast and readily available. While reviewed briefly here,

a much more detailed description is provided in the Canadian Association of Nuclear Medicine guidelines (30). However, BP is not the best suited method for SPECT reconstruction. The prerequisites for BP to work correctly are that it is expected that the data has unlimited statistics and has perfect resolution (pencil beam reconstruction). For SPECT data these two requirements are not valid and represent an approximation. To deal with these limitations a filtering function is introduced to reduce the noise level in the reconstructed images to make them interpretable. The combination of filtering and back projection is commonly referred to as Filtered Back Projection (FBP). The filter is commonly implemented as a pre-filter, i.e., the raw projection images are filtered prior to back projection. The typical type of filter used in SPECT imaging is the Butterworth filter which is controlled by two parameters: cut-off and order. The order is usually fixed at 3 or 5, and the cut-off determines the final resolution and noise level (image texture). Please note that the cut-off is related to the sampling, i.e., the pixel size of the images. Higher sampling (i.e., smaller pixels) require a lower cut-off to achieve a similar smoothness compared to images acquired with larger pixels.

Iterative Reconstruction (IR)

Unlike FBP, iterative reconstruction is more of an umbrella term, which does not say much about the method or its performance. The Canadian Association of Nuclear Medicine guidelines (30) provides a more detailed discussion.

Two of the most common generic iterative reconstruction schemes are known as maximum likelihood estimation method (MLEM) and ordered subset expectation maximization (OSEM). The latter is more frequently used in SPECT imaging because it is a faster algorithm. For performance reasons, most OSEM implementations were initially in 2D (i.e., slice by slice) but nowadays most vendors have switched to a full 3D implementation. OSEM-3D is the preferred method in SPECT, because the limited resolution of the data results in considerable crosstalk between slices which is ignored in 2D implementations.

An iterative reconstruction engine goes through several iterations whereby the forward projection of the reconstructed slices is compared to the raw projection images. An error signal is added, or multiplied, to the synthetic projections and back projected again. This process repeats itself until the differences between the original projections and the computed projections are below a certain error threshold or until a set number of iterations is reached.

The most important advantage of iterative reconstruction in SPECT imaging is the fact that the imaging system (i.e., gamma camera and collimator) can be modeled in the algorithm, resulting in more accurate images. Iterative reconstruction methods tend to provide greater image contrast, i.e., the differences between areas of high and low uptake are enhanced and the overall dynamic range of useful information is extended. However, it also causes structures that appear singular and smooth in FBP to be visualized as clusters of hotspots. The images may appear sharper and of higher resolution, however the additional detail can appear noisy. A smoothing step is often utilized.

It should be noted that unconventional detection geometries such as line array detectors and multi-pinhole collimation, require specialized iterative reconstruction technique to produce images. However, the computational performance available today, allow such sophisticated algorithms to run in clinically acceptable time frames. In other words, these new technologies allow extraction of more information from scans performed under similar conditions.

Attenuation Correction (AC)

All SPECT imaging is affected by attenuation which must be corrected for in brain imaging. The effect of attenuation depends on the energy of the emitted gamma quants, the density of the medium, and the distance traveled by the quant through the patient's body. The loss of transmission due to attenuation is an exponential function of distance. For ^{99m}Tc (140 keV) the attenuation coefficient is 0.15 cm^{-1}, which translates to a transmission loss of 50% when photons travel 4.58 cm through water (density = 1.0). As a result, photons originating from the center of the brain (basal ganglia) are detected with an apparent lower count rate than photons originating from the surface of the brain (cortex). Since the objective of brain SPECT perfusion imaging is to measure and compare regional blood flow in different functional areas of the brain; this cannot be done without attenuation correction.

Note: the theoretical attenuation coefficient of 0.15 cm^{-1} for ^{99m}Tc in water must typically be reduced to 0.12 cm^{-1} to compensate for the presence of scatter. The exact value can be determined through a phantom measurement acquired under the same conditions as a brain SPECT scan.

The most common implementation of attenuation correction in brain SPECT imaging is a post-reconstruction technique based on the method developed by Chang (34). This method assumes that the attenuation within the patient's brain is uniform which is a first order approximation, because it does not consider the bony structures surrounding the brain. Given the overall resolution of SPECT imaging this simplification is acceptable because the differences compared to more accurate attenuation models are insignificant. Most modern cameras and software automate the attenuation process.

Hybrid SPECT/CT cameras have a CT scanner on board which can be used to obtain a real density map of the patient's head from which an attenuation map, a so-called μ-map, is computed. This μ-map is then used within the iterative reconstruction engine to correct for attenuation during the forward and backward projections, referred to as CT-guided attenuation correction (CTAC). Although the CT scan itself is of limited diagnostic use in brain SPECT perfusion imaging, and the CT scan adds to the total radiation exposure, it is still considered the most accurate implementation of attenuation correction.

Resolution Recovery

The resolution of a gamma camera equipped with a collimator changes with distance. A parallel hole collimator basically is a slab of lead of a certain thickness, with lots of small (circular) holes in it. The intent is to only pass gamma photons that

enter a hole perpendicular to the surface of the collimator. Photons arriving from different angles are attenuated by the lead walls between the holes and do not reach the detector. Due to the final length of the holes, they have an acceptance angle, i.e., photons arriving from angles that are slightly off perpendicular still make it to the detector. Looking back from the detector through the collimator holes, the circular area that is seen increases with distance which means the resolution of the imaging system decrease with distance. This is the reason why in nuclear medicine the imaging distance is so important to obtaining data of high quality (resolution).

The loss of resolution with distance is a pure geometrical effect and it is constant for a given collimator design. The collimator can be modeled in the iterative reconstruction engine with just a few parameters. During each forward and backward projection cycle the change in resolution is accounted for, and thereby resolves a higher resolution image. This method is also known as collimator deblurring which more accurately describes its function.

Today most iterative reconstruction implementations for SPECT imaging include this function. It is a good reason to switch from FBP to iterative as it brings a real advantage to the imaging chain.

Scatter Correction

All gamma camera systems can acquire multiple energy windows simultaneously. This feature was originally developed for dual-isotope imaging to capture photon events at multiple energy levels. However, it can also be used to capture scattered events which can provide information that can be used to our advantage.

Scatter correction typically requires the acquisition of two additional energy windows, surrounding the photopeak window, in separate image channels (triple energy window technique). Because the scatter windows contain scattered events only, and their energy is in close proximation to the photopeak events, their noise spectrum is considered like the noise spectrum of the scattered events recorded in the photopeak window. By means of a weighted subtraction technique, the noise content of the photopeak images may be reduced; however, it can never be completely removed.

In theory, scatter correction will increase the signal-to-noise ratio of the acquired images. Phantom measurements are typically used to show its effectiveness; however, its performance on clinical data is highly dependent on the correct adjustment of weighting and care must be taken not to overcorrect the images. We want to separate the good counts (wanted signal) from the bad counts (noise), by subtracting out an estimation of the noise. Because the noise estimation can never be exact, the process can easily subtract too much and degrade our signal.

Comparing Methods

Images produced by FBP and iterative reconstruction from the same projection data will be different (**Figure 4**). Most of the differences will be due to image texture (e.g., signal-to-noise ratio, resolution, etc). However, it cannot be excluded that a different image may lead to a different interpretation. This can be a complication, especially in a mixed environment. Because each brain is unique, it can take years of experience to become a fully-rounded reader. Therefore, it is so important to produce images in a consistent way. Despite their assumed superiority

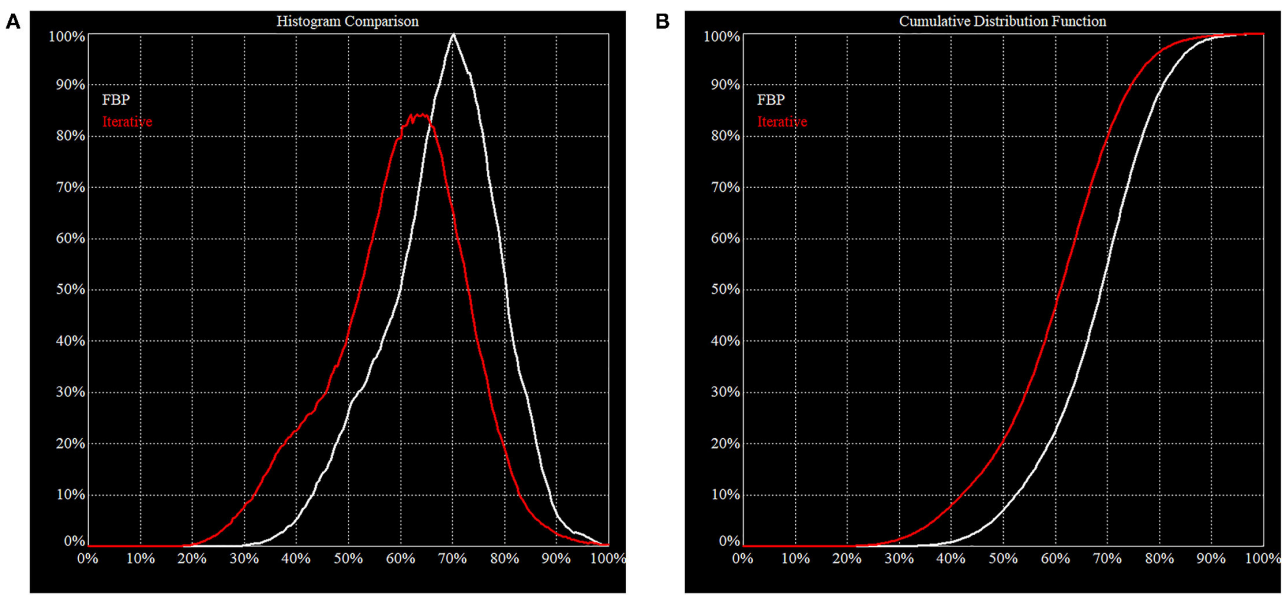

FIGURE 4 | Histogram of FBP (white line) vs. Iterative Reconstruction (red line). These figures illustrate the difference in behavior of FBP vs. IR on the same clinical projection data. **(A)** The area under the histogram curves is the same but the peak is shifted downwards for IR. This is consistent with our expectation that IR will increase image contrast, i.e., the noise is pushed down, and a higher maximum is resolved. **(B)** In a cumulative distribution curve, the median count of the reconstructed volume is lower which must be considered when making direct comparisons.

over FBP, the challenge for using iterative reconstruction is the lack of standardization. These issues are explored in greater detail in the Canadian Association of Nuclear Medicine guidelines (30).

Reading a Perfusion SPECT Scan

The evaluation and interpretation of a brain SPECT scan is a complex matter, and each person is certain to develop an individual approach. Although there currently is no universal recipe for reading a brain SPECT scan, there are several basics that must be covered. Indications or disease states, including psychiatric indications were explored in detail in Part I of this two-part series (2) and are codified in the Canadian Association of Nuclear Medicine guidelines (30).

Before reading a brain SPECT scan, the reader should verify that the technical quality of the scan is acceptable. If the scan quality does not meet expectations, the patient should be re-scanned. In marginal situations, the reader should at least be aware of the technical problems and take them into consideration when interpreting the scan. The following list of items should be checked against the raw projection data:

(1) patient motion: re-scan the patient if too much motion.
(2) sufficient counts: >10 M are desired, <5 M unacceptable.
(3) absence of truncation: the entire brain should be in the field of view.
(4) sufficient delay between injection and imaging: minimal scalp and facial structure uptake.
(5) correct pixel size: 2–4 mm desired range.

Ideally, these items should be checked immediately after the scan and before the patient is released. The patient can be re-imaged within 2–3 h after injection without the need for re-injection.

Once the raw data is accepted, it can now be reconstructed. The checklist for the reconstructed data should include the following items:

(1) free from artifacts.
(2) properly masked: remove any activity outside of the brain, like salivary glands, nasal cavity, lacrimal glands.
(3) properly re-oriented.
(4) image resolution and texture correctly set (i.e., not too noisy, not too smooth).

SPECT scan data can be displayed in a number of ways. Tomograms provide the most anatomical information, particularly about deep structures. The tomograms and reconstructed images should be displayed in a suitable color scale. Although grayscale images are commonly used in radiology to visualize anatomy, it should be note that perfusion SPECT neuroimaging is a functional imaging modality, and most studies are best displayed in color as reviewed at length in Part I (2). To briefly reiterate, SPECT functional brain scans are demonstrating differences in perfusion as a one-off metric of neural activity. The difference in perfusion in an area of impaired function can differ by 12% or less and still have clinical significance. Several studies have shown that color vision is superior for detecting low contrast differences (35–38). While gray scale provides superior resolution of spatial details, it is considerably less sensitive at differentiating low-contrast signals. The selection of color scale is often a matter of personal preference; however, certain color scales have embedded reference to the physiological parameters of interest. In the case of perfusion SPECT neuroimaging, the use of a color scale that provide convenient and practical reference to the physiological properties of perfusion is highly recommended.

The regional cortical counts of both ^{99m}TC-HMPAO (39, 40) and ^{99m}TC-ECD (41) have been compared to direct measurements of regional cerebral blood flow using ^{133}Xenon. Both neurological and psychiatrically normal subjects and subjects with known perfusion defects were scanned both with ^{133}Xenon and the respective radiopharmaceutical sequentially in the same scanner with no change in position. Regional cerebral blood flow (rCBF) was calculated by the method of Kanno and Lassen (42) from ^{133}Xenon data. Linear regression analysis was utilized to characterize the relationship between count densities for ECD or HMPAO and rCBF based on ^{133}Xenon. For ECD, the correlation was good ($r = 0.88$) with a slope of 0.83 (41). In the case of HMPAO, the correlation was also good (0.92) with a slope of 0.82 (40). Both ECD and HMPAO correlate well with ^{133}Xenon studies over physiological ranges but do underestimate blood flow at high velocities (40).

The same group (43) had earlier examined ^{133}Xenon CBF in 97 volunteers free of psychiatric or neurological conditions. They determined that the mean CBF was 71 ± 12 ml/min/100 g of grey matter. A number of groups have examined CBF in whole brain, gray matter and white matter using Xenon SPECT (43–47), Xenon CT (48, 49), ^{15}O-water PET 48, and arterial spin labeling MRI (50–52). Across the techniques and research groups, the estimated mean CBF in gray matter is 70.3 ± 8.35. **Figure 5** illustrates the color scales with the mean and standard deviations labeled. In addition, a case is illustrated using isocontour representation, two different, but similar color scales (described below) and a statistical comparison to a normative database. The figure is an adaptation of **Figure 4** from Part I of this series (2) and the case is more fully described therein.

For brain SPECT perfusion studies, we recommend the DGP40% scale for HMPAO (illustrated as the color scale on the right in **Figure 5**) and the DGP35% scale for ECD studies. A very similar, earlier, rendition of these color scales is the Ubiq40, also illustrated here. These color scales were specifically developed for brain SPECT imaging by one of the authors (DGP) and they have several design features that make them especially useful. These two scales are static and do not require any manual window leveling; in fact, the user should refrain from making any window level adjustments to allow for consistent and reproducible settings. The two scales have a lower threshold of 40 and 35% respectively, removing any background noise that would otherwise interfere with the images. These color scales are discrete and are made up of 21 color bands of a fixed width. The color progresses in a natural fashion from dark blue to white, based on the geographic model. The very top of the scale is black, which allow the reader to immediately locate the hottest area in the scan as it appears as a small black spot or area within a larger white area. The location of the maximum is an important clinical parameter. Typically, the maximum is located in the cerebellum (HMPAO) or visual cortex (ECD). A maximum located elsewhere (e.g., thalamus) is an important clinical finding.

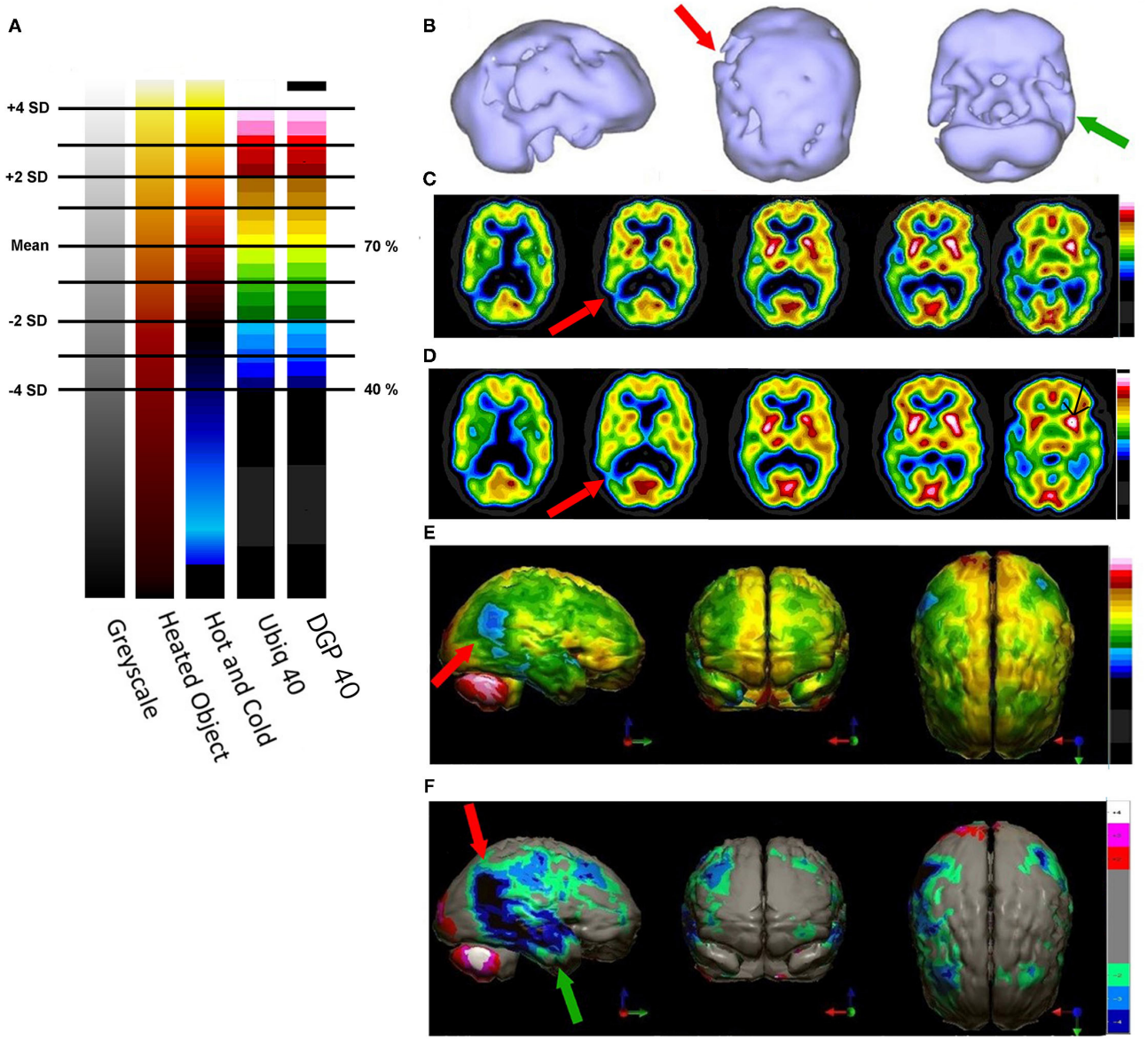

FIGURE 5 | (A) Various commonly used color scales and a greyscale are displayed. The mean cerebral perfusion in the human brain is 70% of the maximal flow with a standard deviation (SD) of 8.35%. The mean and ± 1 and 2 SD are indicated. A change of ± 2 SD is unlikely to be appreciated in greyscale but can be readily distinguished in Heated Object and Ubiq40 color scales. An increase of 2 SD can be distinguished in Hot and Cold color scale, but a decrease of 2SD or less would not be discernable. A 1 SD increase or decrease would be difficult to discern in greyscale, Heated Object and Hot and Cold color scale, but are readily detected in Ubiq40 and DPG40. **(B)** A 58-yr-old female was struck on the right parietal region by a heavy object with loss of consciousness of ∼2 h. Perfusion SPECT scan was performed 7 years after the injury with ^{99m}Tc-HMPAO and a dual-head gamma camera. SPECT data can be displayed in 3-D representations that facilitate the identification of large, diffuse, or subtle lesions. Here, data is presented as an isocontour display wherein cortical areas which fall below 60% of the maximal cerebral blood flow are displayed as a depression or hole. The large parietal defect is apparent on the right (red arrow), as well as bilateral temporal lobe hypoperfusion (green arrow). **(C)** 4 mm horizontal sections illustrate decreased perfusion in the right parietal region (red arrow). The color scale is the Ubiq40. **(D)** 4 mm horizontal sections illustrate decreased perfusion in the right parietal region (red arrow). The color scale is the DPG40. Note the black spot at the point of highest perfusion in the left thalamus (black arrow). **(E)** 3-D representation utilizes the Ubiq40 color scale. The right parietal defect appears as an area of blue and green (red arrow). **(F)** The patient's data is compared to a normative database ($N = 68$). A map of statistically significant differences can be generated using the Oasis software by Segami, Inc. Here, the color scale indicates gray for areas that do not differ significantly from the normative database. In contrast, areas of green, light blue, and dark blue represent areas of more than 2, 3, and 4 SD below the mean perfusion of the normative database, respectively. Statistically significant increases in perfusion are illustrated in the red color scale. The parietal lobe injury (red arrow) and the contra-coup injury are easily visualized, along with more diffuse penumbra injury and bilateral lateral temporal lobe hypoperfusion (green arrows).

The SPECT scan images should be read in a systematic fashion. In one approach, the 3-D reconstructions are examined to detect any large or subtle areas of hypoperfusion or increased perfusion which might be missed in the tomograms. Cortex wide patterns, such as diffuse scattered hypoperfusion will be evident. Alternatively, the tomograms are initially evaluated. Regardless, each area of the brain should be consciously visualized.

Often, it is useful to begin with the horizontal tomograms. Careful attention should be given to the subcortical structures, such as the thalami, basal ganglia, cinguli, and the brainstem (see **Figure 6**). Then attention should be turned to examine each area of the cerebral cortices, including the insula, bilaterally. The cerebellum should be examined with attention to the vermis and the hemispheres. Structures should be examined in all three planes (horizontal, coronal, sagittal) as abnormalities may be apparent in one plane but hidden in other planes. Areas of overactivity and areas of decreased activity should be noted. Asymmetry should be noted. The pattern of perfusion should be noted in the 3-D reconstructions.

Particular attention should be given to the posterior cingulate in cases of suspected dementia, given the high sensitivity and specificity of this structure in the diagnosis of Alzheimer's disease (2). The basal ganglia and anterior cingulate have particular relevance to OCD. The orbitofrontal cortex should be examined both in tomograms and in 3-D reconstructions if executive dysfunction (ADHD, TBI etc.) are being considered (30). Understand that multiple findings are the norm, rather than the exception, as comorbidity is common. If an area of hypoperfusion is detected, then the size and structures involved should be noted to facilitate clinical correlation. For example, if hypoperfusion is seen in the inferior occipital cortex and inferior parietal cortex on one side (suggestive of posterior cerebral artery infarct), then involvement of the thalamus and basal ganglia, as well as changes in the contralateral cerebellum, should be assessed. While it is important to look for a primary cause of the patient's symptoms, it is vital to remember that most patients have co-morbidities (see Part I), and these co-morbidities play a pivotal role in effective treatment planning. A full discussion of the reading of a SPECT scan is beyond the scope of this paper and will be addressed in the future.

Statistical Analysis

The Normal Database

Statistical comparison to a normative database is often cited as an important step in the characterization of a pathological SPECT scan. However, the definition and vetting of a normative database is complicated. The first issue is that each radiopharmaceutical has a different activity distribution and vulnerability to back diffusion as detailed in Part I of this two-part series (2). For example, ECD favors the temporal lobes, while HMPAO levels tend to be lower there. Technically, each radiopharmaceutical should have its own normal database. This is not surprising as we would not expect to use the same normal database for FDG-PET as we would for HMPAO. The second issue is how is a "normal" subject defined. Ideally, the subject should be free of psychiatric illness or symptoms, free of alcohol, tobacco, marijuana, or illicit drug use, without family history of first° relatives with psychiatric or neurological illness, and without history of concussion or TBI. Structured clinical interviews, extensive questionnaires, and drug screens can help to obtain a population free of exclusion criteria (53–55). To quote Dr. Mena's seminal work:

> *"The procedure for the selection of the normal pediatric subjects was as follows: the children were selected from two sources: a) those attending elective non cranial surgery at a public hospital and b) volunteer health personnel relatives. Neuropsychiatric screening included: a) semi-structured interview of the mother and child, b) mental status and neurologic examination performed by two child psychiatrists. Exclusion criteria included the following: positive pre-, peri- or post-natal history, developmental disorder or delay of any kind, learning disorder, psychiatric disorder or isolated emotional or behavioral symptoms, severe family psychopathology or neurologic disorder, abnormal neurologic examination, and school underachievement. Using these criteria more than 50% of potential subjects were rejected."* (53).

Dr. Amen has taken a similar transparent and rigorous approach to defining a normal database:

> *The Control group was recruited using local advertisements in newspapers and local colleges. Each subject met the clinical criteria for a healthy brain subject based on our criteria that included the absence of current medical illnesses, brain trauma, family history of psychiatric illness, drug/alcohol abuse and no current or past evidence of behavioral or psychiatric issues as measured by a detailed clinical history, Minnesota Multiphasic Personality Inventory (MMPI) and Structured Clinical Interview for Diagnosis (SCID) for DSM-IV* (55).

Both male and female subjects should be included as there are perfusion differences between the genders (56). Also, a wide age range should be included in the database. Perfusion changes with age (54, 57). Most statistical analysis programs separate the normal database into age groups. The index patient's data is compared to the appropriate age-specific subgroup.

Statistical Analysis of SPECT Scan Data

The statistical analysis of perfusion SPECT scan data can be conducted at a number of levels. The simplest approach is a regions of interest analysis. Early studies defined regions of interest visually and compared data within these regions to identify differences.

A more rigorous statistical analysis of brain SPECT data can be either voxel-based or region-based; however, in both cases it is necessary to spatially normalize the data first. Examples of such spatial normalization are the Tailarach atlas (58) and the Montreal Neurological Institute atlas (59). These methods are based on a registration of anatomical references which are extracted by the software algorithm from the image data. The registration is non-linear (i.e., requires warping), because human brain shapes differ substantially between subjects. As a result, the temporal pole of the index patient can be mapped precisely to the temporal pole of the comparator group or normal database. This process is certainly not unique to the analysis of perfusion SPECT scans and is widely used in both functional and anatomical neuroimaging. The advantage of analyzing individual voxels is

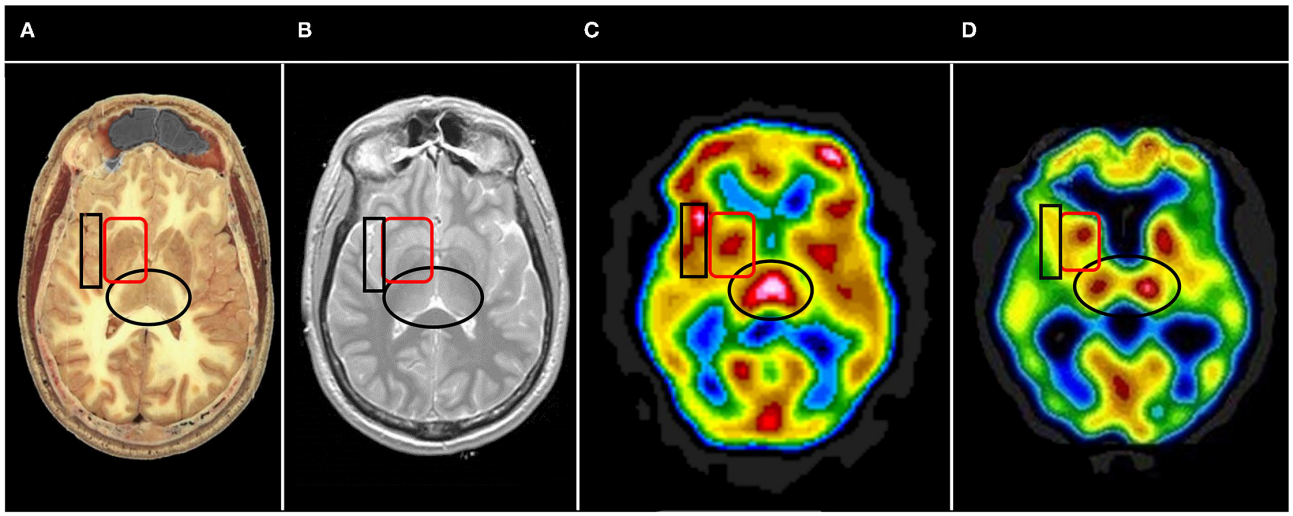

FIGURE 6 | Representative horizontal sections at the level of the thalamus and basal ganglia from **(A)** human cadaver, **(B)** MRI, **(C)** SPECT of healthy individual, and **(D)** SPECT of individual with advanced Alzheimer's disease. The thalami are indicated by the black oval in each frame. In healthy individuals the thalami are closely approximated with a narrow 3rd ventricle separating each side. Note the separation of the thalami in **(D)**, consistent with volume loss due to degenerative changes. The basal ganglia are indicated by the red rounded square. The insula is indicated by the black box. Note the close approximation of the insular cortex to the lateral aspect of the basal ganglia separated only by the thin external capsule.

that it tends to be more sensitive; however, the disadvantage is that the result may not be meaningful to the reader/clinician, because of the limited context. Regions on the other hand, are logical groups of voxels that are based on anatomical or functional areas (e.g., Brodmann areas) in the brain which are more relevant to the reader/clinician. For example, data within regions of interest can be compared statistically across conditions or against a control dataset (20, 21, 55).

In addition to a spatial normalization, the SPECT scan data also must be normalized in intensity because the measured blood flow by either ECD or HMPAO is relative. HMPAO and ECD trapping is not perfectly proportional to rCBF as measured by ^{133}Xenon studies (60, 61). While generally these pharmaceuticals are rapidly converted to a hydrophilic form and become trapped (as described in Part I), the trapping is not perfect, nor instantaneous (A more significant redistribution occurs with ^{123}I-IMP as described in Part I). As a result, there is not an exact linear proportionality between rCBF and retention of ECD or HMPAO. Nonetheless, the distribution and level of radiopharmaceutical closely approximates rCBF over physiological ranges (60).

Typically, the images are normalized to the maximum value in the subject's brain—this is most often the cerebellum or the visual cortex. Although the maximum value is a somewhat noisy parameter, it actually works quite well in SPECT imaging due to its somewhat limited spatial resolution and the smoothing of the data as part of the reconstruction process, as described above. Sometimes, the maximum value in the subject's brain is elsewhere, such as the thalamus. The biasing of the data that can result in this situation is avoided by using the cerebellum or visual cortex consistently; however, there is a caveat. In the situation in which the cerebellum is damaged or there is cross-cerebellar diaschisis, then a cerebellar normalization can falsely elevate the findings in the remainder of the brain. Hence, attention to each brain scan is necessary to avoid these errors.

At this point, a statistical analysis can be performed on the index patient's data. For each pixel, a comparison is made to the range of pixel values at the same spatial point within the reference dataset. The resulting data can be displayed as charts, graphs, or as 3-dimensional surface displays (62–65). A color-coded map of statistically significant differences can be generated as illustrated in **Figures 2**–**6**, **9** in Part I of this two-part series (2), as well as in **Figures 5**, **10**, **12** below using software from Segami Corp. (Columbia, MD). Statistical parametric mapping has been used to differentiate AD from controls with high accuracy (3, 66–69).

Artificial Intelligence and Machine Learning

Artificial Intelligence (AI) and machine learning are currently gaining interest in the research communities of almost all fields because it can be performed at low cost and with potentially high benefits. However, the application in clinical brain SPECT imaging has not been established. In general, these methods rely on huge quantities of data and are an attempt to automate the comparison process, but also allow artificial intelligence algorithms to explore the data in novel and/or complex ways. These methods attract considerable attention, but the reader and reviewer must be careful to distinguish research applications and clinical applications, as well as statistically significant differences which lack clinical meaning from those with substantial clinical significance. Nonetheless, as AI has become more sophisticated, it is possible for a program to parse the data in novel and unexpected ways as the program learns from the data.

Because AI can apply complex calculations to datasets iteratively and at high speed, it is possible to test the data against itself. The software can repeatedly select subsets of data to serve as a temporary reference or rule dataset and then

iteratively compare the remaining data against this rule dataset. By repeating this process over and over with different temporary rule datasets, a new feature can be identified, or an identified feature can be confirmed as valid. While unsupervised learning by AI algorithms may yield clinically irrelevant features, both supervised and unsupervised learning algorithms may produce or verify clinically recognized features, known from decades of visual reads of SPECT scan data. AI techniques have been applied to attenuation correction with promising results (70–72). Improved classification of ^{123}I-ioflupane (DatScan) findings for differentiating Parkinson's disease from other neurodegenerative disorders has been demonstrated (73, 74). Perhaps the most interesting recent development is the first steps in creating an AI driven SPECT image reconstruction algorithm (75).

Several groups have explored machine learning algorithms to differentiate Alzheimer's disease from controls. The process of developing a pattern-recognition algorithm for distinguishing a disease state from controls or another disease state begins with creating a training data set. Carefully selected cases of the disease state (e.g, AD) are collected. The size of this training data set must be large enough to allow a robust signal (e.g., decreased parietal and posterior cingulate perfusion) against the background noise of intersubject variability. Then algorithms can be applied to separate the data into different categories. Support vector analysis (76), which identifies multiple features that distinguish one group from another, is one form of analysis and it has been used to differentiate AD from controls yielded a sensitivity of 97%, a specificity of 100%, and an accuracy of 99% (77). Principal component analysis is another method which extracts features by representing the data in a covariance matrix (78, 79). The algorithm can then be trained on the training set by using a series of subsets to compare back to the training data set. The training data set is randomly divided into a number of subsets. Then N-1 subsets are then tested against the left-out subset. This process is repeated sequentially leaving out a different subset to be used as the test subset. After thousands of iterations of this process, the best classification rule can be determined. The method is often referred to as "leave one out cross-validation." Finally, the machine learned algorithm can be compared to a new set of data to validate the accuracy of the process in differentiating one group (disease state) from another (control or different disease state).

COMBINING PERFUSION SPECT SCANS WITH OTHER MODALITIES FOR IMPROVED DIAGNOSTICS

The authors realize that perfusion SPECT neuroimaging, while extremely sensitive, needs to be used in the context of complete patient clinical information - history, physical examination, other imaging and laboratory tests, and other neuropsychiatric evaluations to be of greatest value. Perfusion SPECT neuroimaging adds valuable neurobiological information to the subjective realm of symptomatology. Furthermore, perfusion SPECT can add additional dimensions to the results of other neuroimaging modalities resulting in better and more reliable differential diagnoses. We will illustrate this point with four situations commonly encountered in psychiatry and neurology.

Situation 1

The first scenario is a 72-year-old patient with a 2-year history of progressively worsening memory problems. She denies hallucinations, tremor, or difficulty with her gait. The long-time course makes delirium less of a consideration. The absence of Parkinsonian symptoms reduces the need to consider that group of disorders. The patient undergoes a Montreal Cognitive Assessment (MOCA) and scores 22/30 placing her in the mild cognitive impairment (MCI) range. However, is this early AD, early vascular dementia, early FTD, or early Lewy Body dementia (LBD) without tremor? An MRI might show widening of the sulci, but this might be no greater than is expected for age. The neurologist might, at this point, order an amyloid scan. If the amyloid scan is positive, then we can proceed on the assumption that the patient has MCI of the AD type; however, there is a false positive rate among aged normals which is due to increasing nonspecific binding with age. Approximately 20% of controls at age 60 years and 40% of controls at age 80 years had false-positive scans (80, 81). Thus, there is a >20–30% chance that the patient does not have AD, even with a positive amyloid scan. The situation is even more dire if the amyloid scan is negative. We can rule out AD as the cause of the patient's memory problems, but we cannot narrow the differential any further.

Unfortunately, the amyloid scan is a binomial test—the result is either positive for AD or negative. The amyloid scan can yield no further clues in the differential diagnosis. This is where perfusion SPECT or FDG-PET can be highly beneficial (3, 82). By following up with a perfusion SPECT scan, the diagnosis may be revealed. For example, if there is frontal and temporal lobe hypoperfusion with a negative amyloid scan, the likelihood of FTD is greatly increased. An example of fronto-temporal MCI is illustrated in Figure 2 of Part I of this two-part series (2). If there is hypoperfusion of the occipital lobes, then the risk of LBD increases substantially, even in the absence of tremor (83) (A follow-up DaTscan might be indicated at that point). If diffuse hypoperfusion is found, then a number of differential diagnoses need to be considered (82, 84), including toxic brain injury, diffuse post-concussive brain injury, vascular dementia, and infectious brain injury. The research literature supporting SPECT findings in neurotoxicity were extensively reviewed in Part I of this series (2). A case of infectious brain injury is illustrated below.

Recent work on PET markers for tau (e.g., AVI451, also known as ^{18}F-flortaucipir and the tradename Tauvid^{TM}) have been fruitful and extensive literature now exists on tau protein labeling in AD (85–88). In contrast, the tau imaging characteristics of chronic traumatic encephalopathy (CTE) remain poorly understood with a dearth of studies (89–91). Pathological studies have confirmed that CTE (92) is characterized by a distinctive accumulation of tau and neurofibrillary tangles in a perivascular distribution in an irregular pattern in the cortex favoring the depths of cortical sulci (93–95). Furthermore, the tau protein tends to predominate in cortical layers 2 and 3 (96). This is distinct from the pattern seen in AD (88, 96, 97) wherein tau

accumulates in cortical layers 3–5 involving both sulci and gyri and with a preferential accumulation in the precuneus, posterior cingulate gyrus, hippocampus and subiculum (88, 98–100). It also stands in contrast to the findings in progressive supranuclear palsy (PSP) wherein the accumulation of tau protein is distinctive in the cerebellum and cerebellar dentate nucleus (101, 102) or in corticobasal degeneration (CBD) wherein tau accumulation is found in the striatum and globus pallidus (although severe CTE can show subcortical accumulation of tau, but this tends to be in the mamillary bodies, thalamus, and other structures vs. the basal ganglia) (95, 103). A recent small study utilized ^{18}F-flortaucipir to predict amyloid status (regardless of diagnosis) vs. controls with a sensitivity of 94% and specificity of 83% (104). However, ^{18}F-flortaucipir binding in early AD (Braak stages I-IV) is much less reliable and likely will hamper its efficacy in predicting MCI type and progression (88). At least one longitudinal study has shown a small predictive value (risk ratio 1.40) for ^{18}F-flortaucipir scan in the progression mild cognitive impairment (105). The utility of tau neuroimaging as a predictor in preclinical and prodromal stages of AD remains uncertain (106). Moreover, the presence of tau binding in mild TBI (107), FTD, PSP, and several other degenerative disorders clouds the picture further.

As detailed in Part I of this two-part series (2), perfusion SPECT neuroimaging has high sensitivity (89%) and specificity (89%) for differentiating AD from controls. When paired with quantitative analysis, perfusion SPECT can predict the progression of MCI to AD with a sensitivity of 97% and a specificity 100%. FTD can be distinguished from AD with a sensitivity of 96% and a specificity of 80% (2, 3, 30). Perfusion SPECT scans can clarify the differential diagnosis in cases of cognitive impairment, MCI, and dementia.

Situation 2

The second scenario involves a 54-year-old patient early in the progression of Parkinsonian symptoms. Tremor, postural instability, and bradykinesia might predominate. But what is the diagnosis? Statistically speaking, there is a fair chance it is Idiopathic Parkinson's disease (IPD). However, multiple other Parkinsonian syndromes cannot be ruled out.

IPD is a progressive neurological disorder characterized by selective degeneration of dopaminergic neurons in the substantia nigra. While IPD may be the most prevalent form of parkinsonism, it shares, in part, symptoms with progressive supranuclear palsy (PSP), multiple system atrophy (MSA), corticobasal degeneration (CBD), vascular parkinsonism, and dementia with Lewy bodies (DLB). Symptoms of tremor, bradykinesia, postural instability, rigidity, and autonomic dysfunction can overlap, to a greater or lesser degree, in each of these disorders. When only tremor is present, differentiation from essential tremor also is relevant. Specific clinical symptoms, such as cerebellar signs in MSA, gaze palsy in PSP, atrophy of the mesencephalon seen with MRI in PSP, or overt dementia and visual hallucinations in DLB, may only manifest at a later stage of the disease. Given the multifarious presentation of IPD, the discrimination of these diseases ***early in the course of illness*** can be challenging. Yet, the correct diagnosis is critical, as each disease process has a different pathology, different progression, and different response to medication. No single test has emerged as capable of sufficient sensitivity and specificity to serve as a stand-alone diagnostic tool.

Dopamine transporter proteins (DAT) can be visualized in the striatum using ^{123}I-ioflupane or ^{123}I-FP-CIT, commercially marketed as DaTscan (108). ^{123}I-ioflupane demonstrates decreased DAT density in the striatum and caudate nucleus consistently in IPD. The challenge has been to differentiate IPD from other parkinsonian syndromes. For example, MSA cannot be reliably distinguished from IPD based on DAT labeling alone (109). However, the combination of decreased striatal DAT labeling and increased striatal perfusion (metabolism) appears to be highly sensitive and specific for IPD, differentiating IPD from MSA in up to 99% of cases (110). By way of contrast, the Unified Parkinsons' disease rating scale (UPDRS) can readily differentiate IPD or MSA from controls with a sensitivity of 91%, but the UPDRS cannot distinguish IPD and MSA (111, 112).

SPECT perfusion neuroimaging repeatedly has shown an increased perfusion of the striatum in IPD (112–116). In contrast, hypoperfusion (or hypometabolism) in the striatum is consistently reported in MSA using SPECT or FDG-PET (110, 115, 117–119). Similarly, perfusion tends to be increased in the cerebellum in IPD (112, 115, 116, 120–122), while cerebellar perfusion (or metabolism) is decreased in MSA (113, 123). For example, Van Laere and colleagues (110) utilized ^{99m}Tc-ECD and ^{125}I-FP-CIT to study perfusion and DaT binding in patients with IPD, MCA, PSP, and LBD. Patients with MSA showed a statistically significant decrease in perfusion in the bilateral posterior putamen and cerebellar vermis and hemispheres relative to patients with either IPD or essential tremor. Patients with PSP demonstrated decreased perfusion in multiple areas, including left frontal lobe, left caudate, anterior cingulate, and thalamus relative to IPD. Patients with DLB were distinguished by pronounced hypoperfusion of the posterior temporoparietal cortex bilaterally. Patients with IPD demonstrated significantly increased perfusion of the cerebellum relative to essential tremor, MSA, PSP, and DLB (124). Notably, DaT binding alone did not consistently distinguish among the different diseases with an accuracy of only 58%. However, the combination of the two techniques increased classification accuracy or differentiation of the degenerative diseases to 99% (110). See **Table 1** and **Figure 7** for a diagnostic flow diagram. These data support the increased use of perfusion SPECT, in combination with DaTscan, anatomical MRI, and other tools, in the differential diagnosis of Parkinsonian syndromes.

Situation 3

The third scenario involves a 29-year-old male who was involved in a motor vehicle accident. The patient was stunned at the scene but there was no evidence of loss of consciousness. He was taken to the emergency room and underwent a CT scan, which was read as normal (**Figure 8**). Within days of the accident, the patient was experiencing severe headaches, photophobia, and memory problems. Nine months later, the patient had persistent symptoms of frequent headaches, memory difficulties, cognitive slowing, and irritability. The patient underwent an anatomical MRI. This showed a slight high

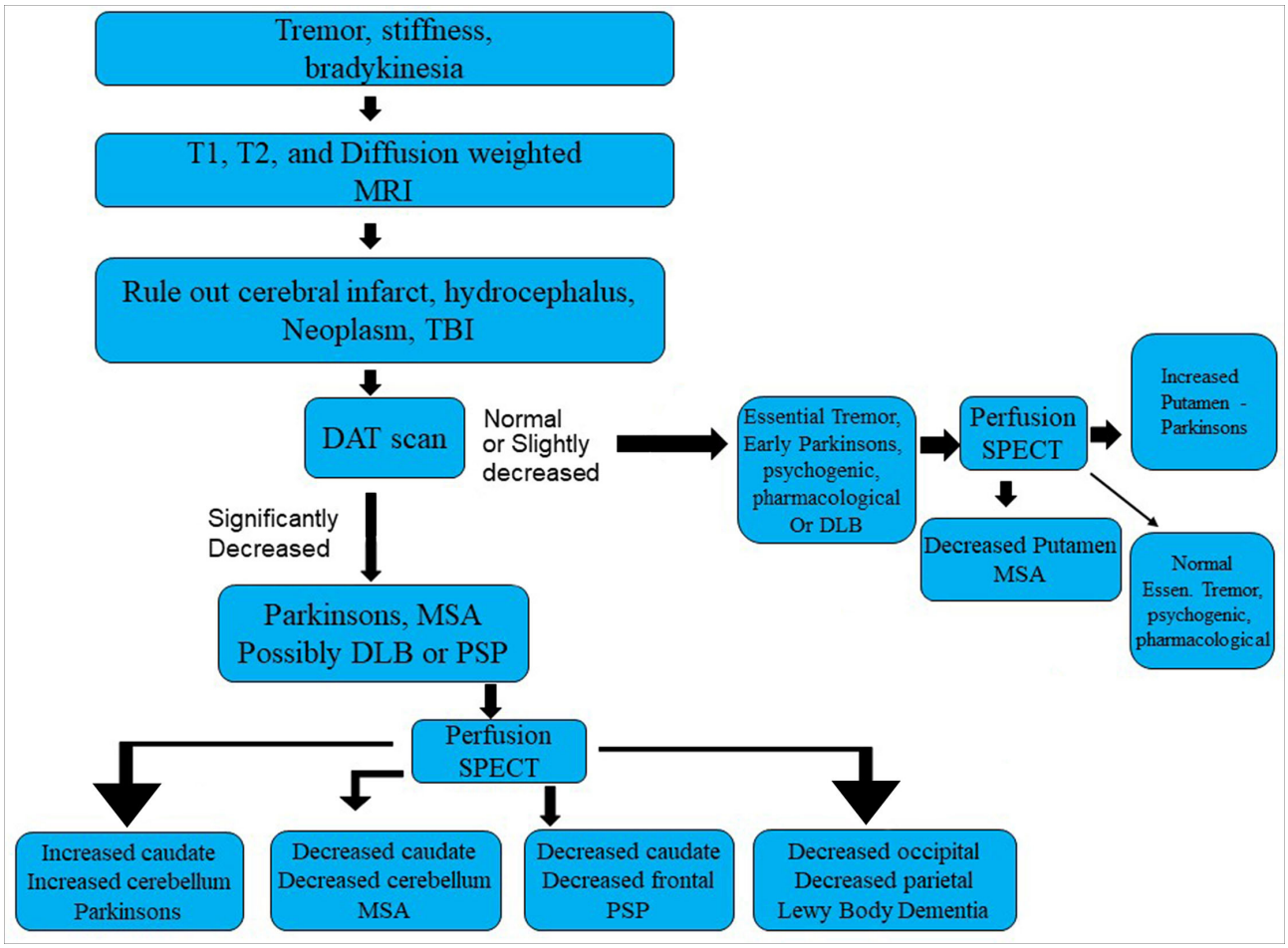

FIGURE 7 | Flowchart for evaluation of Parkinsonian syndromes.

TABLE 1 | The role of functional neuroimaging in the differential diagnosis of Parkinsonian syndromes.

	Essential tremor	Idiopathic Parkinson's disease	Multiple system atrophy	Progressive supranuclear palsy	Lewy body dementia
Symptoms	Tremor	Tremor Bradykinesia Rigidity Autonomic Instability	Tremor Bradykinesia Rigidity Autonomic Instability	Tremor Bradykinesia Rigidity Autonomic Instability	Tremor Bradykinesia Rigidity Autonomic Instability Late Visual Hall.
Course	Stable	Progressive	Progressive	Progressive	Progressive
DAT	DAT—normal	DAT—decreased Statistically Significant	DAT- decreased Statistically Significant	DAT—decreased variable	DAT—slightly decreased
Perfusion SPECT or FDG PET	Normal	Increased in putamen Increased in cerebellum Decreased parietal lobes	Decreased in putamen Decreased in cerebellum	Decreased left frontal Decreased left caudate Decreased thalamus Decreased ant. cingulate	Decreased in occipital Decreased in parietal
UPSIT	Normal	Impaired	Normal	Variably impaired	Impaired

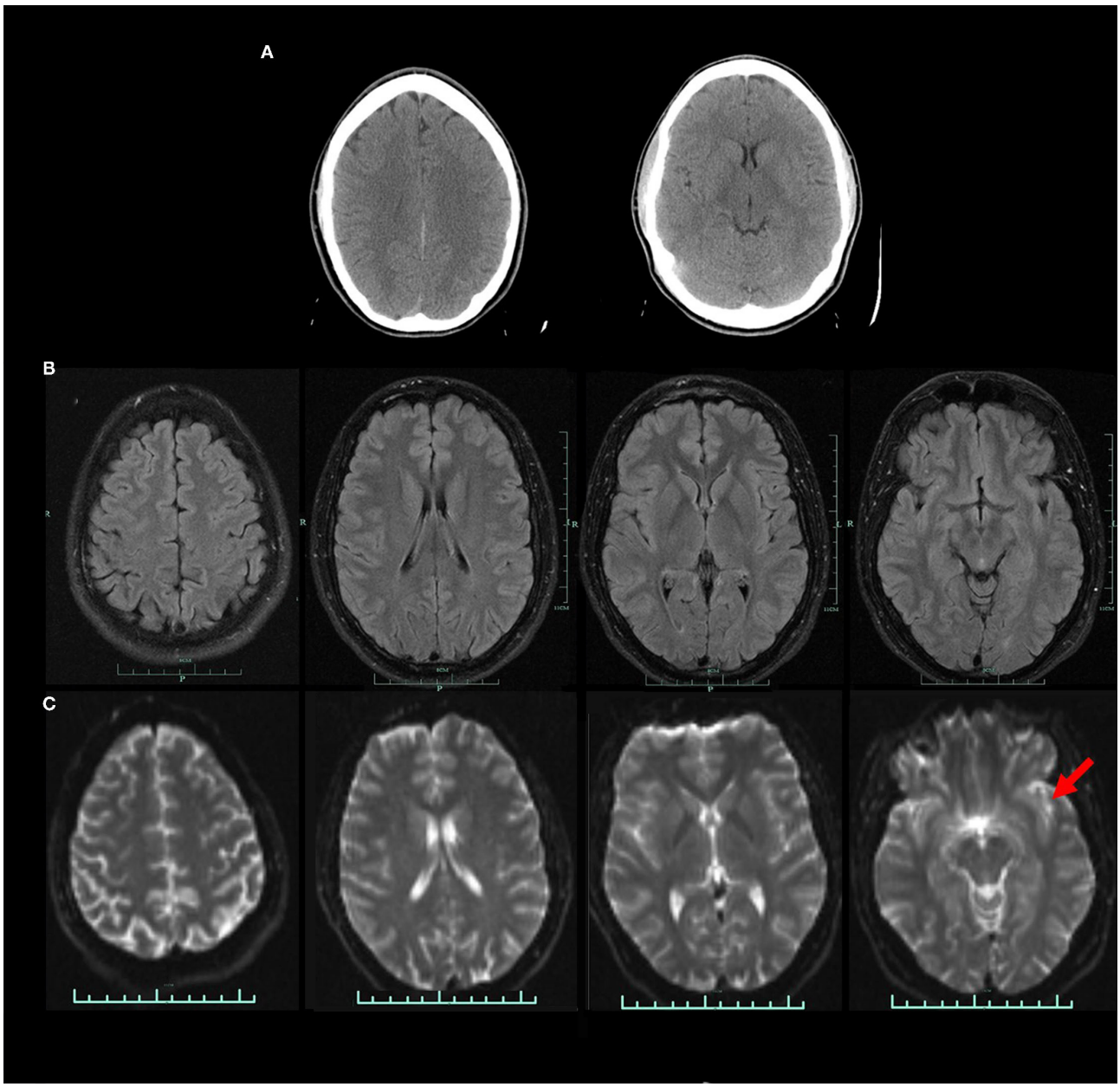

FIGURE 8 | (A) CT scan at two levels obtained in the acute setting. CT read as normal. **(B)** FLAIR protocol MRI at four levels. No abnormality visible. **(C)** DTI MRI at four levels. A small area of high signal is noted in the left temporal lobe (red arrow).

signal abnormality in the left temporal lobe visible only on T-2 weighted images (**Figure 8**). He then underwent a perfusion SPECT scan.

The perfusion SPECT scan revealed hypoperfusion in the bilateral temporal lobes (left worse than right), bilateral frontal cortex (right worse than left), and scattered hypoperfusion in the bilateral parietal cortices (**Figure 9**). The scan is illustrated as both tomograms and a 3-dimensional map in **Figure 9**. Lastly, the scan was compared statistically to a normal database (**Figure 10**).

As discussed at length in Part I of this two-part series (2), perfusion SPECT is more sensitive than either CT or anatomical MRI for detecting TBI, including mild TBI as in the illustrated case. In longitudinal studies of TBI, SPECT identified lesions not found in CT or MRI in 100% of these studies (30, 125). Even in the acute setting, SPECT scans revealed lesions in 75% of patients who presented with amnesia symptoms, while CT scans were negative (126). Likewise, Stamatakis and colleagues (127) examined 62 patients with TBI using MRI and SPECT, which were performed within

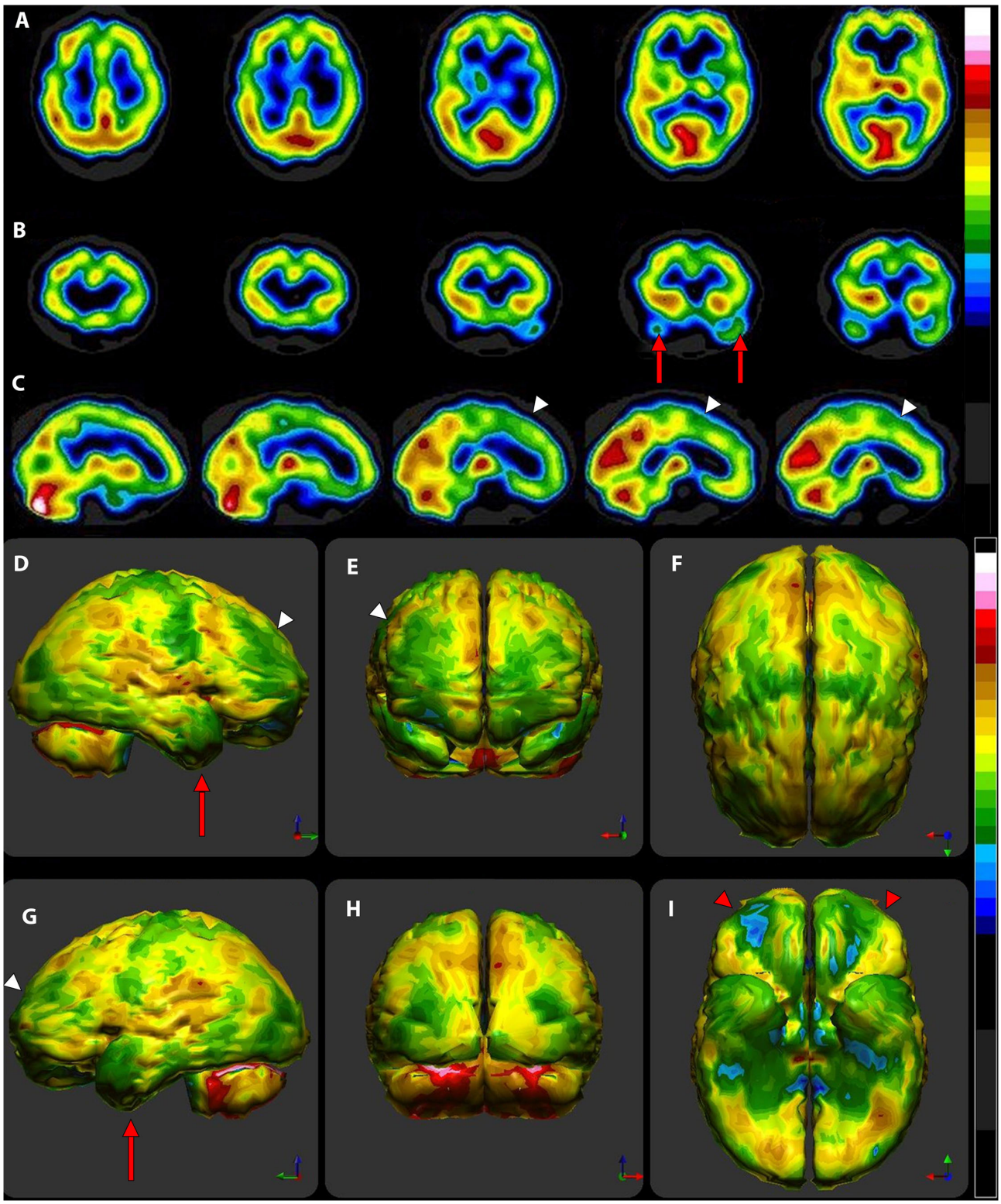

FIGURE 9 | Tomograms and 3-D surface projections of perfusion SPECT scan showing mild TBI. **(A)** Selected transverse sections. **(B)** Selected coronal sections. Decreased perfusion in the temporal lobes is evident (red arrows) **(C)** Selected sagittal sections. Hypoperfusion is seen in the bilateral frontal cortex with greater involvement of the left side (white arrowheads). **(D–I)** 3-D surface projection views show the more extensive injury to the temporal (red arrows) and frontal cortices (white arrowheads) and scattered involvement of the bilateral parietal cortices. Marked hypoperfusion is seen in the orbitofrontal cortex (red arrowheads). **(D)** Left lateral view. **(E)** Anterior view. **(F)** Superior view. **(G)** Right lateral view. **(H)** Posterior view. **(I)** Inferior view with cerebellum removed. Hypoperfusion is evident in the orbitofrontal cortices bilaterally (red arrowheads). Color scale is the Ubiq40 color scale as described in **Figure 5**.

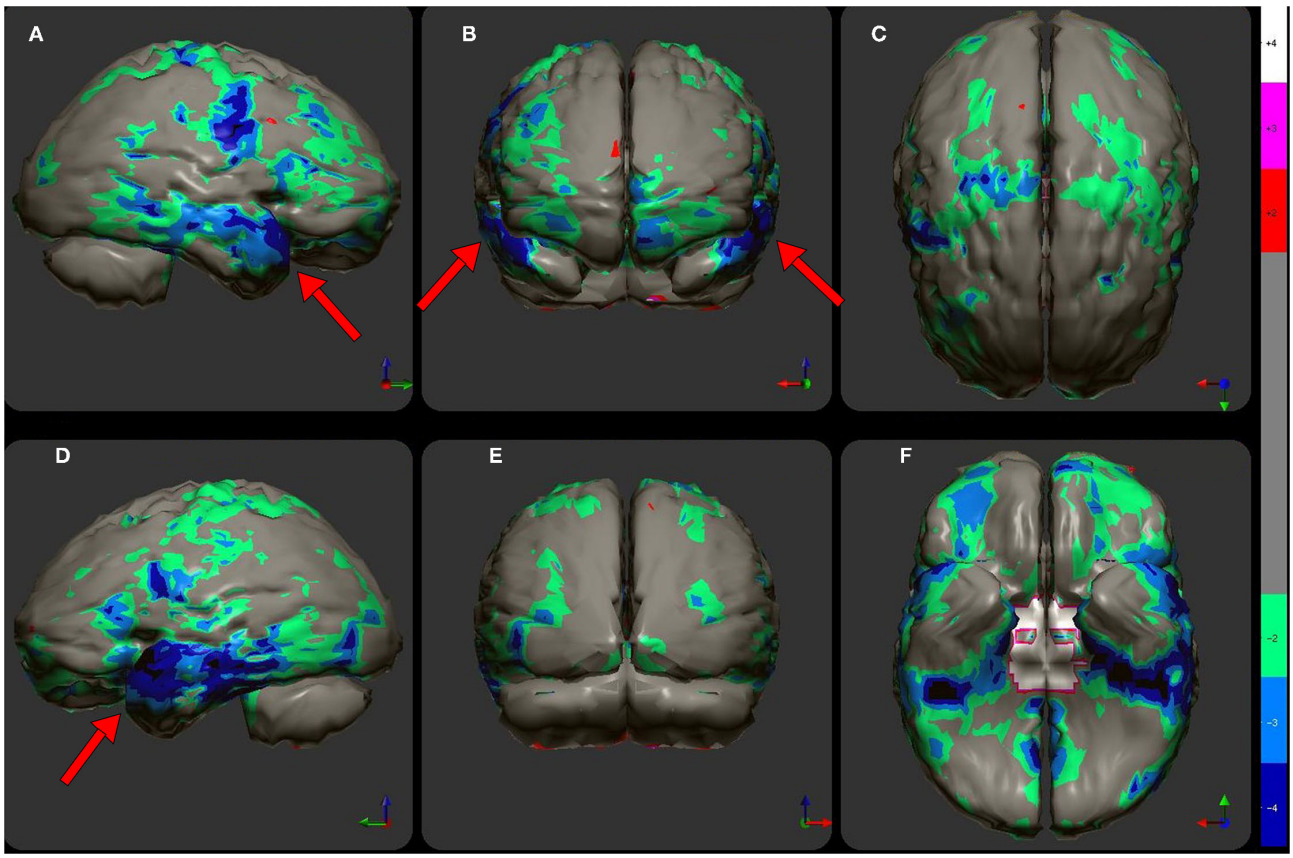

FIGURE 10 | The patient's data is compared to a normative database ($N = 68$). A map of statistically significant differences can be generated using the Oasis software by Segami, Inc. Here, the color scale indicates gray for areas that do not differ significantly from the normative database. In contrast, areas of green, light blue, and dark blue represent areas of more than 2, 3, and 4 SD below the mean perfusion of the normative database, respectively. Statistically significant increases in perfusion are illustrated in the red color scale. Decreased perfusion in the bilateral temporal cortex and bilateral orbitofrontal cortex can be appreciated. Map is displayed in the following views: **(A)** right lateral, **(B)** frontal, **(C)** superior, **(D)** left lateral, **(E)** posterior, and **(F)** inferior with cerebellum removed.

2 weeks of injury. Using statistical parametric analysis, they found SPECT detected more lesions and more lesion volume than anatomical MRI. Ichise and colleagues (128) found SPECT scans more sensitive than MRI as well, with 79% of SPECT abnormalities lacking a concordant MRI lesion. Kinuya and colleagues (129) found SPECT detected hypoperfusion in 94% of cases wherein MRI scans were read as normal. These data call into question the position of several groups, the American College of Radiology, the American Psychiatric Association, and the American Academy of Neurology, which embrace the use of CT and MRI in the evaluation of concussive or traumatic injuries to the brain which constitute ***functional dyscracias***. A brain perfusion SPECT scan can not only help confirm or disprove TBI, but could give considerable aid in evaluating alternate or comorbid diagnoses, help evaluate the degree of injury, and aid the patients, themselves, understand the severity of their injury. The utility of SPECT perfusion neuroimaging in the evaluation of concussion and TBI is more extensively discussed in Part I of this two-part series (2).

Situation 4

The fourth scenario involves a 23-year-old man with a prior history of social anxiety treated with sertraline, who suddenly developed an agitated state of motor restlessness and derealization. He described things seemed to be repeating themselves as though he was having recurrent déjà vu. The clocks seemed to be moving too slowly. He experienced difficulty understanding what others or television announcers were saying. His family described him as constantly moving—pacing and tapping on things. He repeatedly asked philosophical questions, such as "What is truth?," What is good? What is evil?" He became increasingly confused—unsure if he was wearing a shirt or not—and paranoid. However, he was sleeping normally (8–9 h per night). He was seen in an emergency room. A neurological examination was normal. He had a negative CT, negative MRI, and negative electroencephalogram. Toxicology screen and laboratories were normal. He was eventually diagnosed with a manic episode and bipolar 1 disorder. He was prescribed olanzapine. While olanzapine improved the psychotic symptoms of derealization and paranoia,

its efficacy did not answer the question of what caused the psychotic symptoms.

A perfusion SPECT scan was performed. The typical findings of bipolar disorder were not evident. Specifically, the perfusion of the thalamus was not increased and was not asymmetrically perfused (30, 84, 129–131). Similarly, there was no evidence of increased cortical perfusion (30, 84, 130–132). Rather, the perfusion SPECT scan showed diffuse hypoperfusion (see **Figures 11**, **12**). This finding is suggestive of a toxic brain injury or infection (2, 30, 82, 84). These perfusion SPECT findings prompted further questions (133).

Further history revealed no use of alcohol, marijuana, other substances of abuse, solvent sniffing, or other possible toxin exposures. The patient consumed city-provided water rather than well water, eliminating another possible source of toxins. History of travel revealed a trip to the Minnesota lakes region and multiple tick bites ∼10 months prior to the index episode. The extensive involvement of the temporal lobes was consistent with findings in Lyme disease in the research literature (134, 135).

Blood tests were obtained from specialty labs. The patient had positive immunoglobulins for *Bartonella quintana* and for *Bartonella henselae*. Polymerase chain reaction (PCR) tests were also positive for these two infections. Northern blots were positive for both IgM and IgG for *Borrelia burgdorferi* based on Centers for Disease Control (CDC) research criteria (136) (IgM immunoblot positive for bands 23 and 41 with a negative Epstein-Barr test; IgG immunoblot positive for bands 28,30,45,58,66). Labs were negative for *Babesia microti*. Both *B. burdorferi* and *B. henselae* has been associated with psychiatric symptoms, including psychosis (137–142). Antibiotic therapy over the subsequent months brought resolution of symptoms and a repeat PCR was negative for both infectious agents. The patient was spared a lifetime diagnosis of bipolar disorder with the attendant psychopharmacological treatment and its potential adverse side effects.

DISCUSSION AND ACTIONABLE RECOMMENDATIONS

Perfusion SPECT neuroimaging is a highly sensitive modality which has much higher contrast that CT or MRI, although it lacks the higher spatial resolution. This makes it ideal for looking at subtle (and not so subtle) changes in function over large areas using the one-off metric of local cerebral perfusion. SPECT scans now have much greater resolution, multiple normative databases, and sophisticated post-processing software. Moreover, the introduction of a new solid-state detector system utilizing CZT diodes will greatly increase the resolution of SPECT and reduce the radiation dose required. There are now numerous studies, often with quite large sample sizes, showing consistent and reproducible SPECT findings for a number of disorders. Given the major advances in our understanding of the SPECT functional neuroimaging findings for both neurological and psychiatric conditions as extensively reviewed in Part I of this two-part series, the position assumed in the wake of the TTASAAN report by both the fields of Neurology and Psychiatry is no longer tenable. As a result, the following recommendations are made for the revisions of the current policies and practices as they relate to perfusion SPECT functional neuroimaging:

1) Increase awareness of the actual current state of the art as iterated in Part I (2).
2) Replace assumptions about the inferior sensitivity and specificity of SPECT neuroimaging compared to PET, fMRI, diffusion tensor imaging, and MEG neuroimaging, particularly in the areas of dementia, TBI, seizure disorders, and neuropsychiatric indications with updated comparisons as elaborated in Part I (2) and as demonstrated in the clinical examples herein. This includes appreciating that SPECT neuroimaging does not need to be ***diagnostic*** as a freestanding technique. The clinical examples herein emphasized the role that SPECT neuroimaging plays in distinguishing among overlapping diagnoses, recognizing comorbidities, and prompting the "asking of better questions."
3) Foster collaboration and communication between Nuclear Medicine physicians knowledgeable about perfusion SPECT neuroimaging and neurologists, psychiatrists, and other prescribers.
4) Enhance knowledge of the technical aspects of perfusion SPECT neuroimaging to improve understanding of the limitations and strengths of the procedure as elaborated herein.
5) Explore revision of Nuclear Medicine procedure guidelines to match the current state of the art as elaborated in Part I and Part II of this two-part series. This process has already begun with the publication of the new Canadian Association of Nuclear Medicine Guidelines for Brain Perfusion Single Photon Emission Computed Tomography (SPECT) (30).
6) Explore revision of Neurology practice guidelines to include the use of perfusion SPECT neuroimaging in the areas for which it has been shown to be most effective or on par with FDG-PET neuroimaging (e.g., seizure disorders, dementia, stroke). The case is made herein that SPECT is a potent tool in the evaluation of TBI and warrants inclusion in Neurology practice guidelines based on Level IIa evidence meeting the criteria for a Type A recommendation by the standards set forth in the TTASAAN report (1) and the moral impossibility of achieving Class I evidence.
    a. Additional guideline modifications to include the use of perfusion SPECT neuroimaging, when appropriate, in the differential diagnosis of dementia cases among amyloid-positive cases in the elderly (wherein false positives can occur) and in amyloid-negative cases of any age (as set forth in the clinical example herein).
    b. Additional guideline modifications to include the use of perfusion SPECT neuroimaging, when appropriate, in the differential diagnosis of Parkinsonian syndromes (as set forth in **Table 1** and **Figure 7** herein).
    c. Additional guideline modifications to include the use of perfusion SPECT neuroimaging, when appropriate, in the evaluation of toxic, infectious,

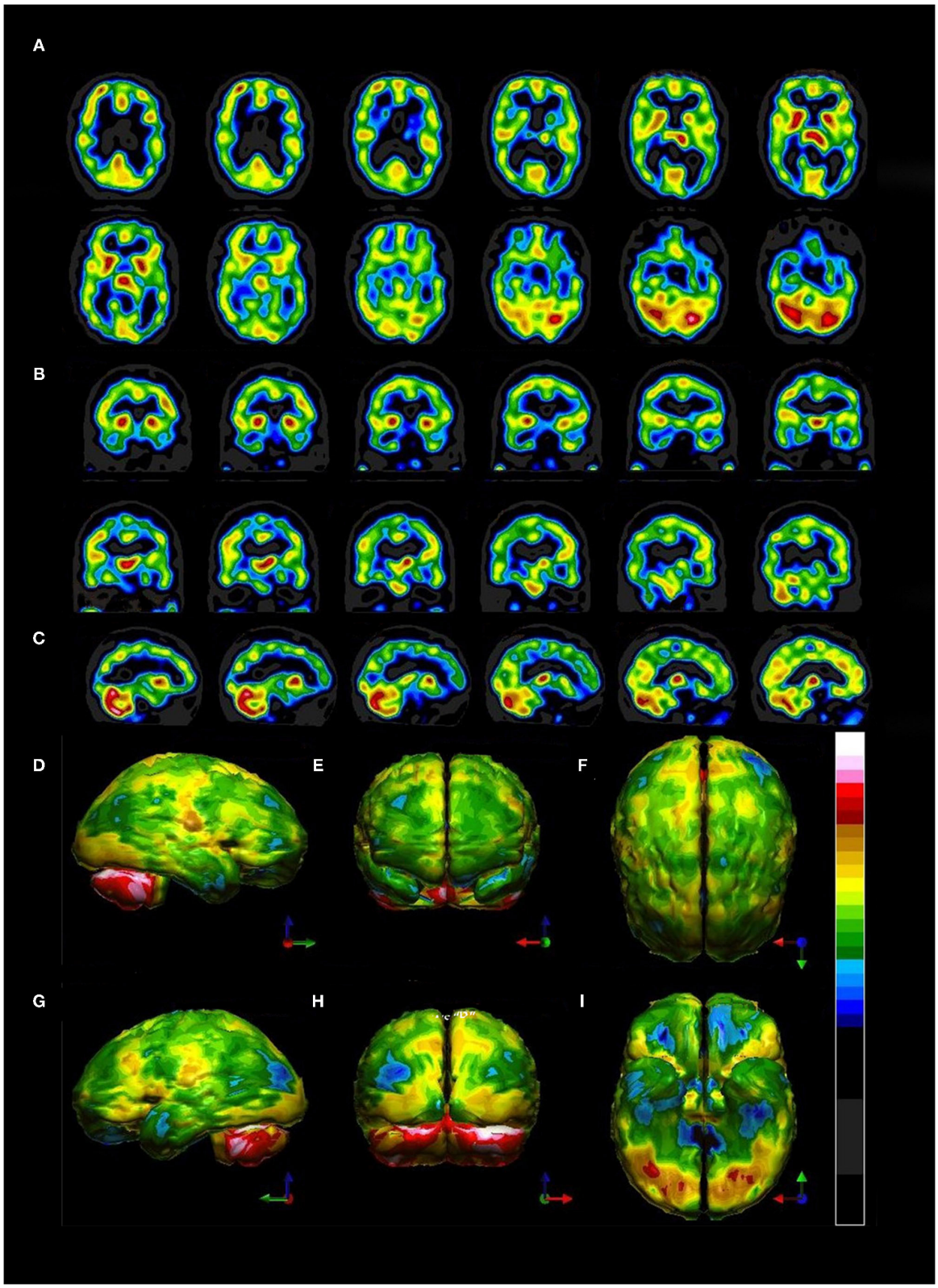

FIGURE 11 | Tomograms and 3-D surface projections of perfusion SPECT scan showing diffuse hypoperfusion. **(A)** Selected transverse sections. Of note, the thalamus is neither hyper-perfused nor asymmetrical as is typically seen in bipolar disorder. **(B)** Selected coronal sections. The thalamus can be seen in a different orientation and is neither hyper-perfused nor asymmetrical. **(C)** Selected sagittal sections. **(D–I)** 3-D surface projection views show the highly difuse nature of the hypoperfusion involving frontal, temporal, parietal, and even occipital cortices. **(D)** Left lateral view. **(E)** Anterior view. **(F)** Superior view. **(G)** Right lateral view. **(H)** Posterior view. **(I)** Inferior view with cerebellum removed. Color scale is the Ubiq40 color scale as described in **Figure 5**.

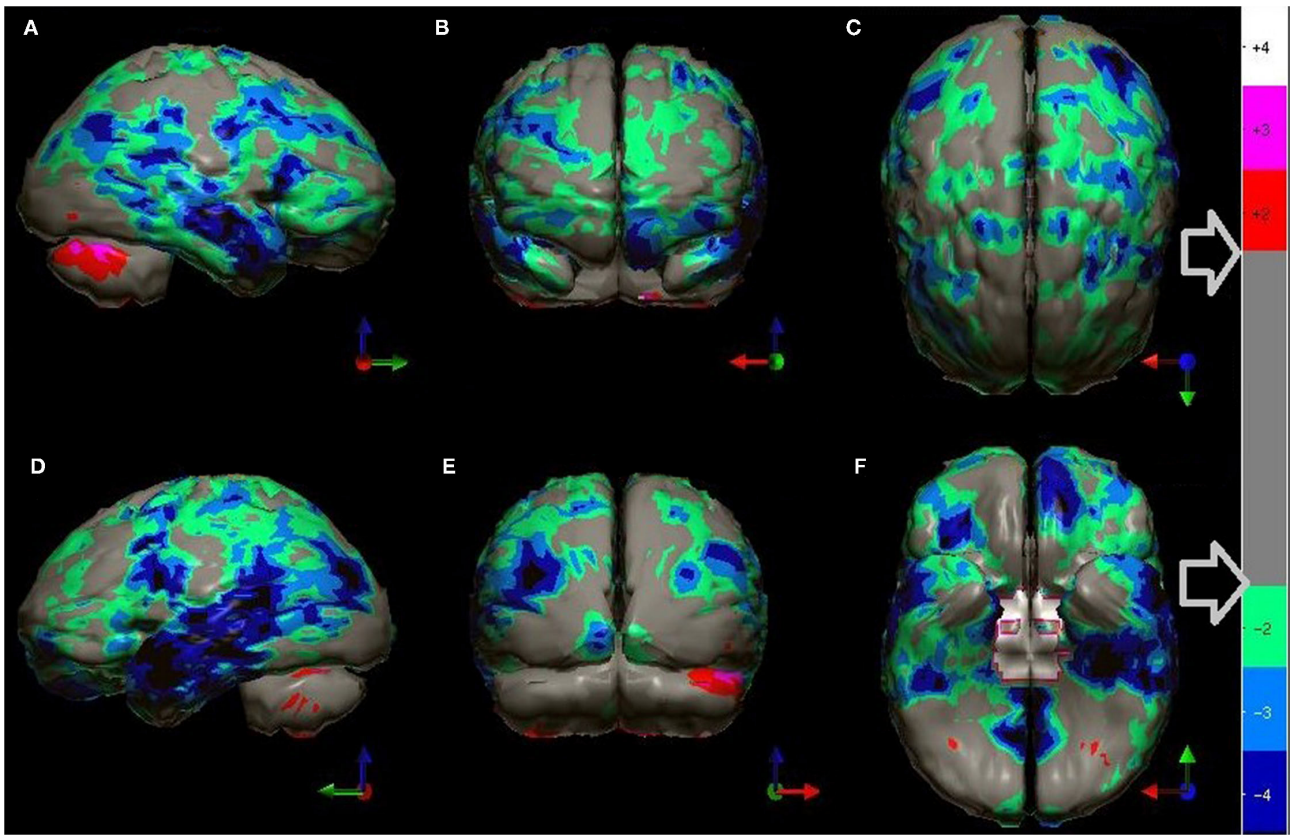

FIGURE 12 | The patient's data is compared to a normative database ($N = 68$). A map of statistically significant differences can be generated using the Oasis software by Segami, Inc. The color scale is the same as in **Figure 10**. Diffuse decreased perfusion in all cortical areas can be appreciated. More extensive involvement of the bilateral temporal lobes is more clearly demonstrated with this map of statistical differences. Map is displayed in the following views: **(A)** right lateral, **(B)** frontal, **(C)** superior, **(D)** left lateral, **(E)** posterior, and **(F)** inferior with cerebellum removed.

or autoimmune encephalopathy. This may become particularly important in the growing population of patients with post-COVID fatigue or persistent encephalopathy (143).

7) Explore revision of Neurology and Psychiatry practice guidelines to recognize the advances in the state of the art of SPECT neuroimaging in the ***evaluation of neuropsychiatric indications***. As the Canadian Association of Nuclear Medicine Guidelines for Brain Perfusion Single Photon Emission Computed Tomography (SPECT) (30) describes, the diagnostic picture for all of neuroimaging is clouded due to the subjective and non-physiological bases of psychiatric diagnoses. This remains an unresolved issue.
   a. Include perfusion SPECT neuroimaging in the evaluation of encephalopathy, dementia, and toxic exposures (30).
   b. Recognize the value of SPECT in the monitoring or tracking of changes in brain function as a consequence of treatment (e.g., a biomarker) (130, 144, 145).
   c. Recognizing the value of SPECT in the uncovering and identification of co-morbidities.
8) Understand the basics of reading and interpreting a perfusion brain SPECT scan as elaborated herein and based on the findings summarized in Part I (2).

Perfusion SPECT scans require rigorous technique and correct adjustment of the equipment. An enormous variability in SPECT images results from technical inconsistency. One of the reasons why brain SPECT imaging is not prescribed more often is that prior encounters with sub-optimal images resulting from poor technique and lack of experience, have produced unhelpful findings. These negative experiences deter further use of SPECT scans and leads to fewer referrals. In part because of this dynamic and because of the parallel academic pressure to move to PET-based procedures, the attention, experience, and interest of nuclear medicine physicians has shifted away from SPECT imaging. In addition, the wholesale bias against perfusion SPECT scans discussed heretofore has stymied the clinical growth of this inexpensive, useful, and readily available procedure. The technical aspects of correctly performing and reading these scans has been provided to rectify this situation. The recent introduction of new camera technologies has made it possible to produce images that rival FDG-PET quality with lower radiation exposure and less cost.

CONCLUSIONS

The path into the future will be paved with collaborations between neurologists, psychiatrists, and nuclear medicine physicians. Hopefully, enlightened clinicians in these fields will join together to deepen their clinical experience. Already progress has been made in identifying perfusion SPECT correlates in neurology and psychiatry as detailed in Part I (2). By applying the Food and Drug Administration's (FDA) Biomarkers, EndpointS and other Tools (BEST) glossary definition of a biomarker:

> "a defined characteristic that is measured as an indicator of normal biological processes, pathogenic processes, or responses to an exposure or intervention, including therapeutic interventions." (146).

we can see perfusion SPECT neuroimaging can serve as an objective biomarker of response to treatment (144, 145), comorbidity (30, 33, 82, 84, 133), inherently difficult symptoms to objectify, such as pain (147), and of diagnostic masqueraders as described herein and elsewhere (30, 33, 84, 133, 148).

AUTHOR CONTRIBUTIONS

DP and TH conceived the manuscript. DP and SD collaborated on initial drafts of the technical sections. TH, PC, and SD prepared the manuscript and the figures. All authors contributed to the article and approved the submitted version.

ACKNOWLEDGMENTS

We would like to acknowledge the following individuals, as well as the entire International Society of Applied Neuroimaging, for their contributions to the discussions of these matters reviewed herein: Muriel J. van Lierop, MBBS, MDPAC(M); Mary McLean, MB, ChB, FRCP; John Michael Uszler, MD, MS; John F. Rossiter-Thornton, MB, FRCPC; Daniel G. Amen MD; Yin-Hui Siow, MD, FRCPC; Howard Schneider MD, FSFP; Byron Hyde MD. We also acknowledge Taylor Tuteur for graphic art. We acknowledge Alaina M. Henderson for graphic art and assistance with the preparation of the figures.

REFERENCES

1. Report of the Therapeutics Technology Assessment Subcommittee of the American Academy of Neurology. Assessment of brain SPECT. *Neurology.* (1996) 46:278–85. doi: 10.1212/WNL.46.1.278
2. Pavel DG, Henderson TA, DeBruin S. The legacy of the TTASAAN report—premature conclusions and forgotten promises: a review of policy and practice Part I. *Front. Neurol.* 12:749579. doi: 10.3389/fneur.2021.749579
3. Henderson TA. The diagnosis and evaluation of dementia and mild cognitive impairment with emphasis on SPECT perfusion neuroimaging. *CNS Spectr.* (2012) 17:176–206. doi: 10.1017/S1092852912000636
4. Eierud C, Craddock RC, Fletcher S, Aulakh M, King-Casas B, Kuehl D, et al. Neuroimaging after mild traumatic brain injury: review and meta-analysis. *Neuroimage Clin.* (2014) 4:283–94. doi: 10.1016/j.nicl.2013.12.009
5. Asken BM, DeKosky ST, Clugston JR, Jaffee MS, Bauer RM. Diffusion tensor imaging (DTI) findings in adult civilian, military, and sport-related mild traumatic brain injury (mTBI): a systematic critical review. *Brain Imaging Behav.* (2018) 2:585–612. doi: 10.1007/s11682-017-9708-9
6. Eklund A, Nichols TE, Knutsson H. Cluster failure: why fMRI inferences for spatial extent have inflated false-positive rates. *Proc Natl Acad Sci USA.* (2016) 113:7900–5. doi: 10.1073/pnas.1602413113
7. First MB, Drevets WC, Carter C, Dickstein DP, Kasoff L, Kim KL. Clinical applications of neuroimaging in psychiatric disorders. *Am J Psychiatry.* (2018) 175:915–16. doi: 10.1176/appi.ajp.2018.1750701
8. Sadeghi MM, Glover DK, Lanza GM, Fayad ZA, Johnson LL. Imaging atherosclerosis and vulnerable plaque. *J Nucl Med.* (2010) 51:51S−65S. doi: 10.2967/jnumed.109.068163
9. Lin E Alessio A. What are the basic concepts of temporal, contrast, and spatial resolution in cardiac CT? *J Cardiovasc Comput Tomogr.* (2009) 3:403–8. doi: 10.1016/j.jcct.2009.07.003
10. Seevinck PR, Seppenwoolde JH, de Wit TC, Nijsen JF, Beekman FJ, van Het Schip AD,, et al. Factors affecting the sensitivity and detection limits of MRI CT, and SPECT for multimodal diagnostic and therapeutic agents. *Anticancer Agents Med Chem.* (2007) 7:317–34. doi: 10.2174/187152007780618153
11. Reddy SD, Younus I, Sridhar V, Reddy DS. Neuroimaging biomarkers of experimental epileptogenesis and refractory epilepsy. *Int J Mol Sci.* (2019) 20:220. doi: 10.3390/ijms20010220
12. Moreau JT, Saint-Martin C, Baillet S, Dudley RWR. MNI SISCOM: an open-source tool for computing subtraction ictal single-photon emission CT coregistered to MRI. *J Digit Imaging.* (2021) 34:357–61. doi: 10.1007/s10278-021-00422-9
13. Goffin K van Laere K. Single-photon emission tomography. *Handb Clin Neurol.* (2016) 135:241–50. doi: 10.1016/B978-0-444-53485-9.00013-1
14. Tepmongkol S, Tangtrairattanakul K, Lerdlum S, Desudchit T. Comparison of brain perfusion SPECT parameters accuracy for seizure localization in extratemporal lobe epilepsy with discordant pre-surgical data. *Ann Nucl Med.* (2015) 29:21–8. doi: 10.1007/s12149-014-0905-y
15. Jin P, Wu D, Li X, Ren L, Wang Y. Towards precision medicine in epilepsy surgery. *Ann Transl Med.* (2016) 4:24. doi: 10.3978/j.issn.2305-5839.2015.12.65
16. Jalota A, Rossi MA, Pylypyuk V, Stein M, Stoub T, Balabanov A, et al. Resecting critical nodes from an epileptogenic circuit in refractory focal-onset epilepsy patients using subtraction ictal SPECT coregistered to MRI. *J Neurosurg.* (2016) 125:1565–76. doi: 10.3171/2015.6.JNS141719
17. Chen T, Guo L. The role of SISCOM in preoperative evaluation for patients with epilepsy surgery: a meta-analysis. *Seizure.* (2016) 41:43–50. doi: 10.1016/j.seizure.2016.06.024
18. Kaur K, Garg A, Tripathi M, Chandra SP, Singh G, Viswanathan V, et al. Comparative contribution of magnetoencephalography (MEG) and single-photon emission computed tomography (SPECT) in pre-operative localization for epilepsy surgery: A prospective blinded study. *Seizure.* (2021) 86:181–8. doi: 10.1016/j.seizure.2021.02.005
19. Yassin A, El-Salem K, Al-Mistarehi AH, Momani A, Zein Alaabdin AM, Shah P, et al. Use of innovative SPECT techniques in the presurgical evaluation of patients with nonlesional extratemporal drug-resistant epilepsy. *Mol Imaging.* (2021) 2021:6614356. doi: 10.1155/2021/6614356
20. Raji CA, Willeumier K, Taylor D, Tarzwell R, Newberg A, Henderson TA, et al. Functional neuroimaging with default mode network regions distinguishes PTSD from TBI in a military veteran population. *Brain Imaging Behav.* (2015) 9:527–34. doi: 10.1007/s11682-015-9385-5
21. Amen DG, Raji CA, Willeumier K, Taylor D, Tarzwell R, Newberg A, et al. Functional neuroimaging distinguishes posttraumatic stress disorder from traumatic brain injury in focused and large community datasets. *PLoS One.* (2015) 10:e0129659. doi: 10.1371/journal.pone.0129659
22. Fellner C, Doenitz C, Finkenzeller T, Jung EM, Rennert J, Schlaier T. Improving the spatial accuracy in functional magnetic resonance imaging

(fMRI) based on the blood oxygenation level dependent (BOLD) effect: benefits from parallel imaging a 32-channel head array coil at 1.5 Tesla. *J. Clin Hemorheol Microcirc*. (2009) 43:71–82. doi: 10.3233/CH-2009-1222
23. Cherry SR, Phelps ME. "Positron emission tomography: Methods Instrumentation," In editors M.P. Sandler, R.E. Coleman J.A. Patton, F.J.Th. Wackers, A. Gottschalk, *Diagnostic Nuclear Medicine*, Fourth Edition, (Philadelphia: Lippincott Williams & Wilkins) (2003), p. 61–83.
24. Emond EC, Groves AM, Hutton BF, Thielemans K. Effect of positron range on PET quantification in diseased and normal lungs. *Phys Med Biol.* (2019) 64:205010. doi: 10.1088/1361-6560/ab469d
25. Moses WW. Fundamental limits of spatial resolution in PET. *Nucl Instrum Methods Phys Res A*. (2011) 21:S236–S240. doi: 10.1016/j.nima.2010.11.092
26. Carter LM, Kesner AL, Pratt EC, Sanders VA, Massicano AVF, Cutler CS, et al. The impact of positron range on PET resolution, evaluated with phantoms and PHITS monte carlo simulations for conventional and non-conventional radionuclides. *Mol Imaging Biol*. (2020) 22:73–84. doi: 10.1007/s11307-019-01337-2
27. Sánchez-Crespo A, Andreo P, Larsson SA. Positron flight in human tissues and its influence on PET image spatial resolution. *Eur J Nucl Med Mol Imaging*. (2004) 31:44–51. doi: 10.1007/s00259-003-1330-y
28. Herholz K, Schopphoff H, Schmidt M, Mielke R, Eschner W, Scheidhauer K, et al. Direct comparison of spatially normalized PET and SPECT scans in Alzheimer's disease. *J Nucl Med.* (2002) 43:21–6.
29. Silverman DH. Brain 18F-FDG PET in the diagnosis of neurodegenerative dementias: comparison with perfusion SPECT and with clinical evaluations lacking nuclear imaging. *J Nucl Med.* (2004) 45:594–607.
30. Cohen PF, Tarzwell R, Numerow L, Siow Y-H, Uszler JM, Pavel DG, et al. *CANM Guidelines for Brain Perfusion Single Photon Emission Computed Tomography (SPECT).* (2021). Available online at: https://www.canm-acmn.ca/guidelines. (accessed October 3, 2021),
31. Harvey HB, Brink JA, Frush DP. Informed consent for radiation risk from CT is unjustified based on the current scientific evidence. *Radiology*. (2015) 275:321–5. doi: 10.1148/radiol.2015142859
32. Raji CA, Henderson TA. PET and SPECT in Brain concussion. *Imag Concussion.* (2018) 28:67–82. doi: 10.1016/j.nic.2017.09.003
33. Henderson TA, van Lierop MJ, McLean M, Uszler JM, Thornton JF, Siow YH, et al. Functional neuroimaging in psychiatry-aiding in diagnosis and guiding treatment. what the American psychiatric association does not know. *Front Psychiatry*. (2020) 11:276. doi: 10.3389/fpsyt.2020.00276
34. Chang LT. A method for attenuation correction in radionuclide computed tomography. *IEEE Trans Nucl Sci.* (1977) 25:638–43. doi: 10.1109/TNS.1978.4329385
35. Stapleton SJ, Caldwell CB, Leonhardt CL, Ehrlich LE, Black SE, Yaffe MJ. Determination of thresholds for detection of cerebellar blood flow deficits in brain SPECT images. *J Nucl Med.* (1994) 35:1547–55.
36. Krupinski EA. The role of perception in imaging: past and future. *Semin Nucl Med.* (2011) 41:392–400. doi: 10.1053/j.semnuclmed.2011.05.002
37. Kim BJ, Kim YH, Kim YJ, Ahn SH, Lee DH, Kwon SU, et al. Color-coded fluid-attenuated inversion recovery images improve inter-rater reliability of fluid-attenuated inversion recovery signal changes within acute diffusion-weighted image lesions. *Stroke.* (2014) 45:2801–4. doi: 10.1161/STROKEAHA.114.006515
38. Ogura A, Kamakura A, Kaneko Y, Kitaoka T, Hayashi N, Taniguchi A. Comparison of grayscale and color-scale renderings of digital medical images for diagnostic interpretation. *Radiol Phys Technol.* (2017) 10:359–63. doi: 10.1007/s12194-017-0393-6
39. Darcourt J, Mena I, Cauvin J-C, Miller B. Absolute calibration of HMPAO SPECT using 133Xe rCBF values. *Alasbimn J.* (1999) 2:5. http://www.alasbimnjournal.cl/revistas/5/darcourt.htm
40. Payne JK, Trivedi MH, Devous MD Sr. Comparison of technetium-99m-HMPAO xenon-133 measurements of regional cerebral blood flow by SPECT. *J Nucl Med.* (1996) 37:1735–40.
41. Devous MD Sr, Payne JK, Lowe JL, Leroy RF. Comparison of technetium-99m-ECD to Xenon-133 SPECT in normal controls and in patients with mild to moderate regional cerebral blood flow abnormalities. *J Nucl Med.* (1993) 34:754–61.
42. Kanno I, Lassen NA. Two methods for calculating regional cerebral blood flow from emission computed tomography of inert gas concentrations. *J Comput Assist Tomogr.* (1979) 3:71–6. doi: 10.1097/00004728-197902000-00012
43. Devous MD Sr, Stokely EM, Chehabi HH, Bonte FJ. Normal distribution of regional cerebral blood flow measured by dynamic single-photon emission tomography. *J Cereb Blood Flow Metab.* (1986) 6:95–104. doi: 10.1038/jcbfm.1986.12
44. Andersen AR, Friberg HH, Schmidt JF, Hasselbalch SG. Quantitative measurements of cerebral blood flow using SPECT and [99mTc]-d,l-HM-PAO compared to xenon-133. *J Cereb Blood Flow Metab.* (1988) 8:S69–81. doi: 10.1038/jcbfm.1988.35
45. Wilkinson IM, Bull JW, Duboulay GH, Marshall J, Russell RW, Symon L. Regional blood flow in the normal cerebral hemisphere. *J Neurol Neurosurg Psychiatry.* (1969) 32:367–78. doi: 10.1136/jnnp.32.5.367
46. Obrist WD, Thompson HK Jr, Wang HS, Wilkinson WE. Regional cerebral blood flow estimated by 133-xenon inhalation. *Stroke.* (1975) 6:245–56. doi: 10.1161/01.STR.6.3.245
47. Knutsson L, Börjesson S, Larsson EM, Risberg J, Gustafson L, Passant U, et al. Absolute quantification of cerebral blood flow in normal volunteers: correlation between Xe-133 SPECT and dynamic susceptibility contrast MRI. *J Magn Reson Imaging.* (2007) 26:913–20. doi: 10.1002/jmri.21093
48. Sakai F, Gotoh F, Ebiohara S, Kitagawa Y, Hata T, Takagi Y, et al. Xenon enhances CT method for the measurement of local cerebral blood flow in man. *J Cereb Blood Flow Metabol.* (1981) 1:S29–S30.
49. Amano T, Meyer JS, Okabe T, Shaw T, Mortel KF. Stable xenon CT cerebral blood flow measurements computed by a single compartment–double integration model in normal aging and dementia. *J Comput Assist Tomogr.* (1982) 6:923–32. doi: 10.1097/00004728-198210000-00010
50. Puig O, Henriksen OM, Vestergaard MB, Hansen AE, Andersen FL, Ladefoged CN, et al. Comparison of simultaneous arterial spin labeling MRI and 15O-H2O PET measurements of regional cerebral blood flow in rest and altered perfusion states. *J Cereb Blood Flow Metab.* (2020) 40:1621–33. doi: 10.1177/0271678X19874643
51. Petersen ET, Mouridsen K, Golay X. all named co-authors of the QUASAR test-retest study. The QUASAR reproducibility study, Part II: results from a multi-center Arterial Spin Labeling test-retest study. *Neuroimage*. (2010) 49:104–13. doi: 10.1016/j.neuroimage.2009.07.068
52. Dashdorj N, Corrie K, Napolitano A, Petersen E, Mahajan RP, Auer DP. Effects of subanesthetic dose of nitrous oxide on cerebral blood flow and metabolism: a multimodal magnetic resonance imaging study in healthy volunteers. *Anesthesiology.* (2013) 118:577–86. doi: 10.1097/ALN.0b013e3182800d58
53. Darcourt J, Mena I, Cauvin J-C, Miller B. Absolute Calibration of HMPAO SPECT using 133Xe rCBF Values. *Alasbimn J.* (1999) 2:5.
54. Mena FJ, Mena I, Álamos F, Solé C, Neubauer S, de la Barra F et al. SPECT Tc99m-HMPAO brain uptake in normal children: a comparison to normal elderly subjects. *Alasbimn J.* (1998) 1:1.
55. Amen DG, Henderson TA, Newberg A. SPECT functional neuroimaging distinguishes adult attention deficit hyperactivity disorder from healthy controls in big data imaging cohorts. *Front Psychiatry.* (2021) 12:725788. doi: 10.3389/fpsyt.2021.725788
56. Amen DG, Trujillo M, Keator D, Taylor DV, Willeumier K, Meysami S, et al. Gender-based cerebral perfusion differences in 46,034 functional neuroimaging scans. *J Alzheimers Dis.* (2017) 60:605–14. doi: 10.3233/JAD-170432
57. Amen DG, Egan S, Meysami S, Raji CA, George N. Patterns of regional cerebral blood flow as a function of age throughout the lifespan. *J Alzheimers Dis.* (2018) 65:1087–92. doi: 10.3233/JAD-180598
58. Talairach J, Tournoux P. *Co-planar Stereotaxic Atlas of the Human Brain: 3-Dimensional Proportional System—an Approach to Cerebral Imaging*. New York NY: Thieme Medical Publishers (1988).
59. Fonov VS, Evans AC, McKinstry RC, Almli CR, Collins DL. Unbiased nonlinear average age-appropriate brain templates from birth to adulthood. *NeuroImage.* (2009) 47:S102. doi: 10.1016/S1053-8119(09)70884-5
60. Lassen NA, Andersen AR, Friberg L, Paulson OB. The retention of [99mTc]-d,l-HM-PAO in the human brain after intracarotid bolus injection: a kinetic analysis. *J Cereb Blood Flow Metab.* (1988) 8:S13–22. doi: 10.1038/jcbfm.1988.28

61. Andersen AR, Friberg H, Knudsen KB, Barry DI, Paulson OB, Schmidt JF, et al. Extraction of [99mTc]-d,l-HM-PAO across the blood-brain barrier. *J Cereb Blood Flow Metab.* (1988) 8:S44–51. doi: 10.1038/jcbfm.1988.32
62. Minoshima S, Koeppe RA, Frey KA, Kuhl DE. Anatomic standardization: linear scaling and nonlinear warping of functional brain images. *J Nucl Med.* (1994) 35:1528–37
63. Mena I, Correa R, Nader A, Boehme V. Bipolar affective disorders: assessment of functional brain changes by means of Tc^{99m}HMPAO neuroSPECT. *ALASBIMN J.* (2004) 6:18.
64. Mena I, Correa R, Nader A. Bipolar disorder complicated by self-mutilation: neurofunctional changes demonstrated by Tc99mHMPAO neuroSPECT. *ALASBIMN J.* (2007) 10:15.
65. Mena I. Neurospect applications in Psychiatry. *ALASBIMN J.* (2009) 11:23.
66. Soonawala D, Amin T, Ebmeier KP, Steele JD, Dougall NJ, Best J, et al. Statistical parametric mapping of (99m)Tc-HMPAO-SPECT images for the diagnosis of Alzheimer's disease: normalizing to cerebellar tracer uptake. *Neuroimage.* (2002) 17:1193–202. doi: 10.1006/nimg.2002.1259
67. Kemp PM, Hoffmann SA, Holmes C, Bolt L, Ward T, Holmes RB, et al. The contribution of statistical parametric mapping in the assessment of precuneal and medial temporal lobe perfusion by 99mTc-HMPAO SPECT in mild Alzheimer's and Lewy body dementia. *Nucl Med Commun.* (2005) 26:1099–6. doi: 10.1097/00006231-200512000-00009
68. Ishii S, Shishido F, Miyajima M, Sakuma K, Shigihara T, Tameta T, et al. Comparison of Alzheimer's disease with vascular dementia and non-dementia using specific voxel-based Z score maps. *Ann Nucl Med.* (2009) 23:25–31. doi: 10.1007/s12149-008-0210-8
69. Matsuda H, Mizumura S, Nagao T, Ota T, Iizuka T, Nemoto K, et al. Automated discrimination between very early Alzheimer disease and controls using an easy Z-score imaging system for multicenter brain perfusion single-photon emission tomography. *AJNR Am J Neuroradiol.* (2007) 28:731–6. doi: 10.1097/MNM.0b013e328013eb8b
70. Sakaguchi K, Kaida H, Yoshida S, Ishii K. Attenuation correction using deep learning for brain perfusion SPECT images. *Ann Nucl Med.* (2021) 35:589–99. doi: 10.1007/s12149-021-01600-z
71. Murata T, Yokota H, Yamato R, Horikoshi T, Tsuneda M, Kurosawa R, et al. Development of attenuation correction methods using deep learning in brain-perfusion single-photon emission computed tomography. *Med Phys.* (2021) 48:4177–90. doi: 10.1002/mp.15016
72. Chen Y, Goorden MC, Beekman FJ. Automatic attenuation map estimation from SPECT data only for brain perfusion scans using convolutional neural networks. *Phys Med Biol.* (2021) 66:065006. doi: 10.1088/1361-6560/abe557
73. Shiiba T, Arimura Y, Nagano M, Takahashi T, Takaki A. Improvement of classification performance of Parkinson's disease using shape features for machine learning on dopamine transporter single photon emission computed tomography. *PLoS ONE.* (2020) 15:e0228289. doi: 10.1371/journal.pone.0228289
74. Nazari M, Kluge A, Apostolova I, Klutmann S, Kimiaei S, Schroeder M, et al. Data-driven identification of diagnostically useful extrastriatal signal in dopamine transporter SPECT using explainable AI. *Sci Rep.* (2021) 11:22932. doi: 10.1038/s41598-021-02385-x
75. Shao W, Rowe SP, Du Y. SPECTnet: a deep learning neural network for SPECT image reconstruction. *Ann Transl Med.* (2021) 9:819. doi: 10.21037/atm-20-3345
76. Klöppel S, Abdulkadir A, Jack CR Jr, Koutsouleris N, Mourão-Miranda J, Vemuri P. Diagnostic neuroimaging across diseases. *Neuroimage.* (2012) 61:457–63. doi: 10.1016/j.neuroimage.2011.11.002
77. Chaves R, Ramírez J, Górriz JM, López M, Salas-Gonzalez D, Alvarez I, et al. SVM-based computer-aided diagnosis of the Alzheimer's disease using t-test NMSE feature selection with feature correlation weighting. *Neurosci Lett.* (2009) 461:293–7. doi: 10.1016/j.neulet.2009.06.052
78. Pagani M, Salmaso D, Rodriguez G, Nardo D, Nobili F. Principal component analysis in mild and moderate Alzheimer's disease–a novel approach to clinical diagnosis. *Psychiatry Res.* (2009) 173:8–14. doi: 10.1016/j.pscychresns.2008.07.016
79. Valotassiou V, Sifakis N, Tzavara C, Lykou E, Tsinia N, Kamtsadeli V, et al. Correlation of neuropsychiatric symptoms in dementia with brain perfusion: A 99mTc-SPECT-HMPAO Study with brodmann areas analysis. *Curr Alzheimer Res.* (2021) 18:970–83. doi: 10.2174/1567205019666211220130505
80. Rowe CC, Ng S, Ackermann U, et al. Imaging beta amyloid burden in aging and dementia. *Neurology.* (2007) 68:1718–25. doi: 10.1212/01.wnl.0000261919.22630.ea
81. Chételat G, La Joie R, Villain N, Perrotin A, de La Sayette V, Eustache F, et al. Amyloid imaging in cognitively normal individuals, at-risk populations and preclinical Alzheimer's disease. *Neuroimage Clin.* (2013) 2:356–65. doi: 10.1016/j.nicl.2013.02.006
82. Amen DG, Easton M. A new way forward: How brain SPECT imaging can improve outcomes and transform mental health care into brain health care. *Front Psychiatry.* (2021) 12:715315. doi: 10.3389/fpsyt.2021.715315
83. Geser F, Wenning GK, Poewe W, McKeith I. How to diagnose dementia with Lewy bodies: state of the art. *Mov Disord.* (2005) 20:S11–20. doi: 10.1002/mds.20535
84. Henderson TA, Uszler JM, Rossiter-Thornton JF, Siow Y-H, Pavel DG, McLean M, et al. The American Psychiatric Association fails to recognize the value of neuroimaging in psychiatry. *Interv Med Clin Imaging.* (2019) 1:1–8. doi: 10.31038/IMCI.2019212
85. La Joie R, Visani AV, Baker SL, Brown JA, Bourakova V, Cha J, et al. Prospective longitudinal atrophy in Alzheimer's disease correlates with the intensity topography of baseline tau-PET. *Sci Transl Med.* (2020) 12:eaau5732. doi: 10.1126/scitranslmed.aau5732
86. Fleisher AS, Pontecorvo MJ, Devous MD Sr, Lu M, Arora AK, Truocchio SP, et al. Positron emission tomography imaging with [18f]flortaucipir and postmortem assessment of alzheimer disease neuropathologic changes. *JAMA Neurol.* (2020) 77:829–39. doi: 10.1001/jamaneurol.2020.0528
87. Cho H, Baek MS, Lee HS, Lee JH, Ryu YH, Lyoo CH. Principal components of tau positron emission tomography and longitudinal tau accumulation in Alzheimer's disease. *Alzheimers Res Ther.* (2020) 12:114. doi: 10.1186/s13195-020-00685-4
88. Soleimani-Meigooni DN, Iaccarino L, La Joie R, Baker S, Bourakova V, Boxer AL, et al. 18F-flortaucipir PET to autopsy comparisons in Alzheimer's disease and other neurodegenerative diseases. *Brain.* (2020) 143:3477–94. doi: 10.1093/brain/awaa276
89. Mantyh WG, Spina S, Lee A, Iaccarino L, Soleimani-Meigooni D, Tsoy E, et al. Tau positron emission tomographic findings in a former US football player with pathologically confirmed chronic traumatic encephalopathy. *JAMA Neurol.* (2020) 77:517–21. doi: 10.1001/jamaneurol.2019.4509
90. Marquié M, Agüero C, Amaral AC, Villarejo-Galende A, Ramanan P, Chong MST, et al. [18F]-AV-1451 binding profile in chronic traumatic encephalopathy: a postmortem case series. *Acta Neuropathol Commun.* (2019) 7:164. doi: 10.1186/s40478-019-0808-1
91. Lesman-Segev OH, La Joie R, Stephens ML, Sonni I, Tsai R, Bourakova V, et al. Tau PET and multimodal brain imaging in patients at risk for chronic traumatic encephalopathy. *Neuroimage Clin.* (2019) 24:102025. doi: 10.1016/j.nicl.2019.102025
92. Omalu BI, DeKosky ST, Minster RL, Kamboh MI, Hamilton RL, Wecht CH. Chronic traumatic encephalopathy in a National Football League player. *Neurosurgery.* (2005) 57:128–34; discussion 128–34. doi: 10.1227/01.NEU.0000163407.92769.ED
93. Stein TD, Alvarez VE, McKee AC. Chronic traumatic encephalopathy: a spectrum of neuropathological changes following repetitive brain trauma in athletes and military personnel. *Alzheimers Res Ther.* (2014) 6:4. doi: 10.1186/alzrt234
94. McKee AC, Cairns NJ, Dickson DW, Folkerth RD, Keene CD, Litvan I, et al. The first NINDS/NIBIB consensus meeting to define neuropathological criteria for the diagnosis of chronic traumatic encephalopathy. *Acta Neuropathol.* (2016) 131:75–86. doi: 10.1007/s00401-015-1515-z
95. National Institute of Neurological Disorders and Stroke. *NIH Chronic Traumatic Encephalopathy Diagnosis Conference.* (2015). https://www.ninds.nih.gov/Current-Research/Focus-Research/Traumatic-Brain-Injury/NIH-Chronic-Traumatic-Encephalopathy (accessed December 31, 2021).
96. Hof PR, Bouras C, Buée L, Delacourte A, Perl DP, Morrison JH. Differential distribution of neurofibrillary tangles in the cerebral cortex of dementia pugilistica and Alzheimer's disease cases. *Acta Neuropathol.* (1992) 85:23–30. doi: 10.1007/BF00304630
97. Thangavel R, Sahu SK, Van Hoesen GW, Zaheer A. Modular and laminar pathology of Brodmann's area 37 in Alzheimer's disease. *Neuroscience.* (2008) 152:50–5. doi: 10.1016/j.neuroscience.2007.12.025

98. Ossenkoppele R, Iaccarino L, Schonhaut DR, Brown JA, La Joie R, O'Neil JP, et al. Tau covariance patterns in Alzheimer's disease patients match intrinsic connectivity networks in the healthy brain. *Neuroimage Clin.* (2019) 23:101848. doi: 10.1016/j.nicl.2019.101848
99. Timmers T, Ossenkoppele R, Wolters EE, Verfaillie SCJ, Visser D, Golla SSV, et al. Associations between quantitative [(18)F]flortaucipir tau PET and atrophy across the Alzheimer's disease spectrum. *Alzheimers Res Ther.* (2019) 11:60. doi: 10.1186/s13195-019-0510-3
100. Ziontz J, Bilgel M, Shafer AT, Moghekar A, Elkins W, Helphrey J, et al. Tau pathology in cognitively normal older adults. *Alzheimers Dement (Amst).* (2019) 11:637–45. doi: 10.1016/j.dadm.2019.07.007
101. Sintini I, Schwarz CG, Senjem ML, Reid RI, Botha H, Ali F, et al. Multimodal neuroimaging relationships in progressive supranuclear palsy. *Parkinsonism Relat Disord.* (2019) 66:56-61. doi: 10.1016/j.parkreldis.2019.07.001
102. Nicastro N, Rodriguez PV, Malpetti M, Bevan-Jones WR, Simon Jones P, Passamonti L, et al. 18F-AV1451 PET imaging and multimodal MRI changes in progressive supranuclear palsy. *J Neurol.* (2020) 267:341–49. doi: 10.1007/s00415-019-09566-9
103. Goodheart AE, Locascio JJ, Samore WR, Collins JA, Brickhouse M, Schultz A, et al. 18F-AV-1451 positron emission tomography in neuropathological substrates of corticobasal syndrome. *Brain.* (2021) 144:266–77. doi: 10.1093/brain/awaa383
104. Hammes J, Bischof GN, Bohn KP, Onur Ö, Schneider A, Fliessbach K, et al. One-Stop Shop: 18F-Flortaucipir PET differentiates amyloid-positive and -negative forms of neurodegenerative diseases. *J Nucl Med.* (2021) 62:240–46. doi: 10.2967/jnumed.120.244061
105. Lu M, Pontecorvo MJ, Devous MD Sr, Arora AK, Galante N, McGeehan A, et al. Aggregated tau measured by visual interpretation of flortaucipir positron emission tomography and the associated risk of clinical progression of mild cognitive impairment and alzheimer disease: results from 2 phase iii clinical trials. *JAMA Neurol.* (2021) 78:445–53.
106. Ossenkoppele R, Smith R, Mattsson-Carlgren N, Groot C, Leuzy A, Strandberg O, et al. Accuracy of tau positron emission tomography as a prognostic marker in preclinical and prodromal alzheimer disease: a head-to-head comparison against amyloid positron emission tomography and magnetic resonance imaging. *JAMA Neurol.* (2021) 78:961–71. doi: 10.1001/jamaneurol.2021.1858
107. Kahriman A, Bouley J, Smith TW, Bosco DA, Woerman AL, Henninger N. Mouse closed head traumatic brain injury replicates the histological tau pathology pattern of human disease: characterization of a novel model and systematic review of the literature. *Acta Neuropathol Commun.* (2021) 9:118. doi: 10.1186/s40478-021-01220-8
108. Djang DS, Janssen MJ, Bohnen N, Booij J, Henderson TA, Herholz K, et al. SNM practice guideline for dopamine transporter imaging with 123I-ioflupane SPECT 1.0. *J Nucl Med.* (2012) 53:154–63. doi: 10.2967/jnumed.111.100784
109. Swanson RL, Newberg AB, Acton PD, Siderowf A, Wintering N, Alavi A et al. Differences in ^{99m}Tc-TRODAT−1 SPECT binding to dopamine transporters in patients with multiple system atrophy and Parkinson's disease. *Eur J Med Mol Imaging.* (2005) 32:302–07. doi: 10.1007/s00259-004-1667-x
110. Louis ED, Levy G, Cote LT, Mejia H, Fahn S, Marder K. Diagnosing Parkinson's disease using videotaped neurological examinations: validity and factors that contribute to incorrect diagnoses. *Mov Disord.* (2002) 17:513–17. doi: 10.1002/mds.10119
111. Lee EA, Kim BJ, Lee WY. Diagnosing multiple system atrophy with greater accuracy: combined analysis of the clonidine-growth hormone test and external anal sphincter electromyography. *Mov Disord.* (2002) 17(6):1242–47. doi: 10.1002/mds.10225
112. Imon Y, Matsuda H, Ogawa M, Kogue D, Sunohara N. SPECT image analysis using statistical parametric mapping in patients with Parkinson's disease. *J Nucl Med.* (1999) 40:1583–9.
113. Feigin A, Antonini A, Fukuda M, De Notaris R, Benti R, Pezzoli G, et al. Tc-99m ethylene cysteinate dimmer SPECT in the diffrerential diagnosis of parkinsonism. *Mov Disord.* (2002) 17:1265–70. doi: 10.1002/mds.10270
114. Tachibana H, Tomino Y, Kawabata K, Sugita M, Fukuchi M. Twelve month follow-up study of regional cerebral blood flow in Parkinson's disease. *Dementia.* (1995) 6:89–93. doi: 10.1159/000106927
115. Bosman T, van Laere K, Santens P. Anatomically standardized ^{99m}Tc-ECD brain perfusion SPET allows accurate differentiation between healthy volunteers, multiple system atrophy, and idiopathic Parkinson's disease. *Eur J Nucl Med.* (2003) 30:16–24. doi: 10.1007/s00259-002-1009-9
116. Firbank MJ, Burn DJ, McKeith IG, O'Brien JT, Longitudinal study of cerebral blood flow SPECT in Parkinson's disease wth dementia, and dementia with Lewy bodies. *Int J Geriatr Psychiatr.* (2005) 20:776–82. doi: 10.1002/gps.1359
117. Otsuka M, Ichiya Y, Kuwabara Y, Hosokawa S, Sasaki M, Fukumura T et al. Glucose metabolism in the cortical and subcortical brain structures in multiple system atrophy and Parkinson's disease: a positron emission tomographic study. *J Neurol Sci.* (1996) 144:77–83. doi: 10.1016/S0022-510X(96)00172-4
118. Eckert T, Barnes A, Dhawan V, Frucht S, Gordon MF, Feigen AS et al. FDG PET in the differential diagnosis of parkinsonian disorders. *Neuroimage.* (2005) 26:912–21. doi: 10.1016/j.neuroimage.2005.03.012
119. Eidelberg D, Moeller JR, Ishikawa T, Dhawan V, Spetsieris P, Chaly T et al. Early differential diagnosis of Parkinson's disease with f18-fluorodeoxyglucose and positron emission tomography. *Neurology.* (1995) 45:1995–2004. doi: 10.1212/WNL.45.11.1995
120. Feigin A, Fukuda M, Dhawan V, Przedborski S, Jackson-Lewis V, Mentis MJ, et al. Metabolic correlate of levodopa response in Parkinson's disease. *Neurology.* (2001) 57:2083–88. doi: 10.1212/WNL.57.11.2083
121. Ghaemi M. Hilker R, Rudolf J, Sobesky J, Heis WD. Differentiating multiple system atrophy from Parkinson's disease: contribution of striatal and midbrain MRI volumetry and multi-tracer PET imaging. *J Neurol Neurosurg Psychiatry.* (2002) 73:517–23. doi: 10.1136/jnnp.73.5.517
122. Van Laere K, DeCeuninck L, Dom R, Van den Eynden J, Vanbilloen H, Cleynhens J, et al. Dopamine transporter SPECT using fast kinetic ligands: 123I-FP-beta-CIT vs. 99mTc-TRODAT-1. *Eur J Nucl Med Mol Imaging.* (2004) 31:1119–27. doi: 10.1007/s00259-004-1480-6
123. Juh R, Kim J, Moon D, Choe B, Suh T. Different metabolic patterns analysis of Parkinsonism on the ^{18}F-FDG PET. *Eur J Radiol.* (2004) 51:223–33. doi: 10.1016/S0720-048X(03)00214-6
124. Van Laere K, Casteels C, de Ceuninck L, Vanbilloen B, Maes A, Mortelmans L et al. Dual-Tracer dopamine transporter and perfusion SPECT in differential diagnosis of Parkinsonism using template-based discriminant analysis. *J Nucl Med.* (2006) 47:384–92.
125. Raji CA, Tarzwell R, Pavel D, Schneider H, Uszler M, Thornton J, et al. Clinical utility of SPECT neuroimaging in the diagnosis and treatment of traumatic brain injury: a systematic review. *PLoS One.* (2014) 9:e91088. doi: 10.1371/journal.pone.0091088
126. Lorberboym M, Lampl Y, Gerzon I, Sadeh M. Brain SPECT evaluation of amnestic ED patients after mild head trauma. *Am J Emerg Med.* (2002) 20:310–3. doi: 10.1053/ajem.2002.34201
127. Stamatakis EA, Wilson JT, Hadley DM, Wyper DJ. SPECT imaging in head injury interpreted with statistical parametric mapping. *J Nucl Med.* (2002) 43:476–83.
128. Ichise M, Chung DG, Wang P, Wortzman G, Gray BG, Franks W. Technetium-99m-HMPAO SPECT, CT and MRI in the evaluation of patients with chronic traumatic brain injury: a correlation with neuropsychological performance. *J Nucl Med.* (1994) 35:217–26.
129. Kinuya K, Kakuda K, Nobata K, Sakai S, Yamamoto K, Itoh S, et al. Role of brain perfusion single-photon emission tomography in traumatic head injury. *Nucl Med Commun.* (2004) 25:333–7. doi: 10.1097/00006231-200404000-00004
130. McLean M, Henderson TA, Pavel DG, Cohen P. SPECT neuroimaging indicates individuals at risk for bipolar disorder: a family cohort study. *Front Psychiatr.* (in press).
131. Benabarre A, Vieta E, Martínez-Arán A, Garcia-Garcia M, Martín F, Lomeña F, et al. Neuropsychological disturbances and cerebral blood flow in bipolar disorder. *Aust N Z J Psychiatry.* (2005) 39:227–34. doi: 10.1080/j.1440-1614.2004.01558.x
132. Estudillo-Guerra MA, Pacheco-Barrios K, Cardenas-Rojas A, Adame-Ocampo G, Camprodon JA, Morales-Quezada L, et al. Brain perfusion during manic episode and at 6-month follow-up period in bipolar disorder patients: Correlation with cognitive functions. *Brain Behav.* (2020) 10:e01615. doi: 10.1002/brb3.1615

133. Amen DG, Highum D, Licata R, Annibali JA, Somner L, Pigott HE, et al. Specific ways brain SPECT imaging enhances clinical psychiatric practice. *J Psychoactive Drugs.* (2012) 44:96–106. doi: 10.1080/02791072.2012.684615
134. Shroff G. Single-photon emission tomography imaging in patients with Lyme disease treated with human embryonic stem cells. *Neuroradiol J.* (2018) 31:157–67. doi: 10.1177/1971400917742470
135. Newberg A, Hassan A, Alavi A. Cerebral metabolic changes associated with Lyme disease. *Nucl Med Commun.* (2002) 23:773–7. doi: 10.1097/00006231-200208000-00011
136. Centers for Disease Control and Prevention (CDC). Recommendations for test performance and interpretation from the Second National Conference on Serologic Diagnosis of Lyme Disease.MMWR Morb Mortal Wkly Rep. (1995) 44:590–1.
137. Bransfield RC. The psychoimmunology of lyme/tick-borne diseases and its association with neuropsychiatric symptoms. *Open Neurol J.* (2012) 6:88–93. doi: 10.2174/1874205X01206010088
138. Breitschwerdt EB, Greenberg R, Maggi RG, Mozayeni BR, Lewis A, Bradley JM. Bartonella henselae bloodstream infection in a boy with pediatric acute-onset neuropsychiatric syndrome. *J Cent Nerv Syst Dis.* (2019) 11:1179573519832014. doi: 10.1177/1179573519832014
139. Lashnits E, Maggi R, Jarskog F, Bradley J, Breitschwerdt E, Frohlich F. Schizophrenia and Bartonella spp. infection: a pilot case-control study. *Vector Borne Zoonotic Dis.* (2021) 21:413–421. doi: 10.1089/vbz.2020.2729
140. Brodziński S, Nasierowski T. Psychosis in Borrelia burgdorferi infection—part II: case reports. *Psychiatr Pol.* (2019) 53:641–53. doi: 10.12740/PP/92556
141. Brodziński S, Nasierowski T. Psychosis in Borrelia burgdorferi infection—part I: epidemiology, pathogenesis, diagnosis and treatment of neuroborreliosis. *Psychiatr Pol.* (2019) 53:629–40. doi: 10.12740/PP/97336
142. Paparone PW. Neuropsychiatric manifestations of Lyme disease. *J Am Osteopath Assoc.* (1998) 98:373–8.
143. Morbelli S, Ekmekcioglu O, Barthel H, Albert NL, Boellaard R, Cecchin D, et al. COVID-19 and the brain: impact on nuclear medicine in neurology. *Eur J Nucl Med Mol Imaging.* (2020) 47:2487–92. doi: 10.1007/s00259-020-04965-x
144. Henderson TA, Morries LD. SPECT perfusion imaging demonstrates improvement of traumatic brain injury with transcranial near-infrared laser phototherapy. *Adv Mind Body Med.* (2015) 29:27–33. doi: 10.2147/NDT.S65809
145. Best SRD, Haustrup N, Pavel DG. Brain SPECT as an imaging biomarker for evaluating effects of novel treatments in psychiatry—a case series. *Front Psych.* (2022) 12:713141. doi: 10.3389/fpsyt.2021.713141
146. Food & Drug Administration. *About Biomarkers and Qualification webpage.* (2021). Available online at: *https://www.fda.gov/drugs/biomarker-qualification-program/about-biomarkers-and-qualification.* (accessed August 22, 2021).
147. Bermo M, Saqr M, Hoffman H, Patterson D, Sharar S, Minoshima S, et al. Utility of SPECT functional neuroimaging of pain. *Front Psychiatry.* (2021) 12:705242. doi: 10.3389/fpsyt.2021.705242
148. Henderson TA. Brain SPECT imaging in neuropsychiatric diagnosis and monitoring. *EPatient.* (2018) 1:40–7. Available online at: https://www.frontiersin.org/articles/10.3389/fpsyt.2020.00276/full

Conflict of Interest: All authors are members of the International Society of Applied Neuroimaging (ISAN), a volunteer organization devoted to the understanding and appropriate clinical utilization of SPECT brain imaging. All authors volunteered their time in the research and writing of this manuscript. DP was Director of PathFinder Brain SPECT which is a clinical service corporation providing SPECT functional neuroimaging and had no research funding. He is deceased. TH is the president and principal owner of the Synaptic Space, a neuroimaging consulting firm. He is also CEO and Chairman of the Board of Neuro-Luminance Corporation, a medical service company. He is also president and principal owner of Dr. Theodore Henderson, Inc., a medical service company. He is also President of the Neuro-Laser Foundation, a non-profit organization. He is a member of and a former officer of the Brain Imaging Council Board of the Society of Nuclear Medicine and Molecular Imaging (SNMMI). Since 2017, he has served in the SNMMI Brain Imaging Outreach Working Group. Currently, he serves as president of the International Society of Applied Neuroimaging. TH has no ownership in, and receives no remuneration from, any neuroimaging company. No more than 5% of his income is derived from neuroimaging. SD is President of Good Lion Imaging LLC involved in the post-processing and display of functional brain scan data. PC has no commercial or financial relationships that could be construed as a potential conflict of interest.

Publisher's Note: All claims expressed in this article are solely those of the authors and do not necessarily represent those of their affiliated organizations, or those of the publisher, the editors and the reviewers. Any product that may be evaluated in this article, or claim that may be made by its manufacturer, is not guaranteed or endorsed by the publisher.

Advantages of publishing in Frontiers

OPEN ACCESS
Articles are free to read for greatest visibility and readership

FAST PUBLICATION
Around 90 days from submission to decision

HIGH QUALITY PEER-REVIEW
Rigorous, collaborative, and constructive peer-review

TRANSPARENT PEER-REVIEW
Editors and reviewers acknowledged by name on published articles

Frontiers
Avenue du Tribunal-Fédéral 34
1005 Lausanne | Switzerland

Visit us: www.frontiersin.org
Contact us: frontiersin.org/about/contact

REPRODUCIBILITY OF RESEARCH
Support open data and methods to enhance research reproducibility

DIGITAL PUBLISHING
Articles designed for optimal readership across devices

FOLLOW US
@frontiersin

IMPACT METRICS
Advanced article metrics track visibility across digital media

EXTENSIVE PROMOTION
Marketing and promotion of impactful research

LOOP RESEARCH NETWORK
Our network increases your article's readership